



Coláiste na Tríonóide, Baile Átha Cliath  
Trinity College Dublin

Ollscoil Átha Cliath | The University of Dublin

# Human Neurodegeneration: A Spectral EEG and TMS based Approach in Amyotrophic Lateral Sclerosis

Submitted in partial fulfilment of the requirements  
for the degree of Doctor of Philosophy, 2021

By

Roisin McMackin

B.A. (Hons)

Supervised by:

Prof. Orla Hardiman, Prof. Richard Carson.

Co-advised by: Dr Nasseroleslami




## **Declaration**

I declare that this thesis has not been submitted as an exercise for a degree at this or any other university and, unless stated otherwise, it is entirely my own work. Where any of the content presented is the result of input or data from related collaborative research this is acknowledged in the text.

I agree to deposit this thesis in the University's open access institutional repository or allow the Library to do so on my behalf, subject to Irish Copyright Legislation and Trinity College Library conditions of use and acknowledgement.

I consent to the examiner retaining a copy of the thesis beyond the examining period, should they so wish (EU GDPR May 2018).

Signed:  \_\_\_\_\_

Roisin McMackin

*To Bridget McMackin*

*Who taught me to be opinionated*

## Acknowledgement

First and foremost, I would like to thank **Prof. Orla Hardiman**. Her belief in my potential when I first approached her as an undergraduate student was a springboard to what I hope will be a long and successful career in neurological research. Prof. Hardiman's career guidance and supervision has been essential to my successes in this research to date.

Second, I would like to thank **Dr Bahman Nasserolelami**, whose patience and kindness combined with expertise in motor physiology, neural engineering and statistics meant my constant questions and concerns always had answers. His support for scientific curiosity has enabled me to develop the array of skills required to perform this work.

Third, I would like to thank **Prof. Richard Carson**, who has taught me how to perform TMS, how to set up an entire TMS laboratory and many other skills in data analysis and academic writing. Prof. Carson has inspired my love of TMS-based research.

I would also like to thank **Prof. Julie Kelly, Gill Slator, Stefan Dukic and Sile Carney**, from the Academic Unit of Neurology, whose unwavering friendship, support and kindness is invaluable. They bringing brightness to even the gloomiest winter days.

I am sincerely grateful to all my colleagues at the Academic Unit of Neurology including all the students and RAs of **the Signal Analysis Strand** of the team who assisted me in data collection, as well as those who provided crucial data for the correlation analyses in this project. This includes **Emmet Costello** and **Marta Pinto-Grau** who, led by **Prof. Niall Pender**, collected the cognitive and behavioural test scores, those who collected ALSFRS-R scores at the Irish National ALS Clinic in Beaumont Hospital, including **Marie Ryan, Eoin Finnegan** and **Amina Coffey**, as well as **Mark Heverin, Colm Peelo** and **Nicola Davis**, who collected the data obtained from the Irish Registry of ALS and MND, **Prof. Russell McLaughlin, Mark Doherty** and **Ross Byrne**, who collected the genetic data required for patient subgrouping and **Prof. Peter Bede, Ranga Chipika** and **Stacey Shing**, who provided imaging data for head modelling. I thank **the Irish Research Council** and **Research Motor Neurone** for funding my PhD.

I also wish to thank my family for their support throughout this journey, especially my mom **Catherine**, my dad **Anthony**, my sisters **Ciara** and **Ailbhe** and my fiancé **Colin**. My enthusiastic and unprovoked speeches about electrophysiology and/or ALS have never fallen on deaf ears, and they have cheered me on throughout.

Finally, I am very grateful to **all the control** and **patient volunteers** who made this research possible, and were a pleasure to meet and spend time with.

## Abstract

Amyotrophic lateral sclerosis (ALS) is defined by the neurodegeneration of upper and lower motor neurons of the corticospinal tract, resulting in progressive, terminal and incurable decline in movement, speech and swallowing functions. Although motor neuron degeneration provides a unifying characteristic for this diagnosis, individual patients experience extensively heterogeneous motor and non-motor symptoms and progression rates. This not only results in distressing uncertainty for those diagnosed, but introduces unpredictable variation to patient cohorts in clinical trials, diminishing the power of these trials to detect therapeutic effects of novel drug candidates.

Extensive imaging, psychology and physiology research to date has illustrated that ALS symptoms and progression rates are driven not only by the motor neurons, but by broader cortical network dysfunction and atrophy. Quantification of the spatiotemporal patterns of cortical network dysfunction in ALS and their relationships to disease symptoms may therefore provide a basis for subcategorising patients early in disease. These physiological measurements can then be clinically implemented to facilitate more specific prediction of individual prognoses. In addition, such measures could substantially improve clinical trial design by enabling stratification of cohorts and more objective, quantitative measurement of drug effects based on fundamental ALS pathophysiology.

In this project, threshold tracking transcranial magnetic stimulation (TMS) and electroencephalography (EEG) were implemented to interrogate ALS-related cortical network pathology. Threshold tracking TMS with electromyography was used to investigate corticospinal tract function and the effects of ALS on intracortical and interhemispheric motor networks which regulate the upper motor neurons. In addition to attempting to reproduce previous reports of GABA<sub>A</sub>ergic decline as a biomarker of ALS, the effects of ALS on indices associated with the glutamatergic and GABA<sub>B</sub>ergic interneuronal and corpus callosal function in motor networks were investigated by paired pulse paradigms. Single pulse TMS was also used to investigate the latency of signal transmission from cortex to muscle, while peripheral nerve stimulation was applied to quantify lower motor neuron impairment. To interrogate the nature and location of cognitive, sensory and motor cortical dysfunction, EEG was recorded in ALS patients during performance of auditory oddball and sustained attention to response tasks. Cross-sectional and longitudinal EEG signal analyses, in addition to source analysis, were

applied to characterise changes in cortical activation using event related potentials, as well as cortical communication using event related spectral perturbations.

This work has revealed that ALS drives dynamic patterns of hypo- and hyper- activation and synchronisation in both motor and non-motor cortical circuitry. Namely, TMS and EEG studies indicate that the motor cortex is initially hyperactive in ALS, even during non-motor tasks, potentially due to loss of inhibitory interneuronal function, and that this hyperactivity wanes with disease progression. Similar patterns of early hyperactivity were observed in the dorsolateral prefrontal and posterior parietal cortices, in addition to impaired event related beta oscillation desynchronization being recorded over these areas, suggesting that GABAergic interneuronal decline also occurs in frontoparietal cognitive networks early in disease. By contrast, other sensory and cognitive areas, including the temporal and inferior frontal cortex are initially suppressed, becoming hyperactive later in the disease. Temporal regions also display alpha and beta band hypersynchrony during auditory sensation, which may reflect excessive bottom-up suppression, accounting for observed reduction in auditory cortex activation early in disease. Many of these cortical networking abnormalities correlated with impairments in associated disease symptoms, including cognitive, behavioural and motor decline at the time of recording or in future, as well as survival times.

These findings highlight the ability of threshold tracking TMS and EEG to objectively capture the pathology underpinning ALS' heterogenous symptoms. These measures might now be further developed to define clinically-relevant, network-based subphenotypes of ALS and to improve clinical trial design.

## Peer-reviewed publications from this thesis

1. **McMackin R**, Dukic S, Costello E, et al. Cognitive Network Hyperactivation and Motor Cortex Decline Correlate with ALS Prognosis. *Neurobiology of Aging*. 2021 Mar 10 (In Press)
2. **McMackin R**, Dukic S, Costello E, et al. Sustained attention to response task-related beta oscillations relate to performance and provide a functional biomarker in ALS. *Journal of Neural Engineering*. 2021 Feb 25;18(2):026006.
3. **McMackin R**, Dukic S, Costello E, et al. Localisation of Brain Networks Engaged by the Sustained Attention to Response Task Provides Quantitative Markers of Executive Impairment in Amyotrophic Lateral Sclerosis. *Cerebral Cortex* 2020;00:1–13.
4. **McMackin R**, Dukic S, Broderick M, et al. Dysfunction of attention switching networks in amyotrophic lateral sclerosis. *NeuroImage: Clinical* 2019;22:101707.
5. **McMackin R**, Muthuraman M, Groppa S, et al. Measuring network disruption in neurodegenerative diseases: New approaches using signal analysis. *J Neurol Neurosurg Psychiatry* 2019;90(9):1011–1020.
6. **McMackin R**, Bede P, Pender N, et al. Neurophysiological markers of network dysfunction in neurodegenerative diseases. *NeuroImage: Clinical* 2019;22:101706.



## **Posters and platform presentations regarding this thesis**

1. **McMackin R**, Dukic S, Broderick M, et al., Investigation of dysfunction in cognitive brain networks in ALS by localisation of the sources of mismatch negativity. Work In Progress Poster, 28th International Symposium on ALS/MND 2017.
2. **Mc Mackin R\***, Dukic S, Broderick M, et al. Investigation of dysfunction in cognitive brain networks in ALS by localisation of the sources of mismatch negativity. Platform presentation. ENCALS Meeting 2018. \*Presenter
3. **McMackin R\***, Dukic S, Broderick M, et al. Dysfunction of attention switching networks in amyotrophic lateral sclerosis correlates to impaired cognitive flexibility. Platform Communication, 29th International Symposium on ALS/MND 2018. \*Presenter.
4. **McMackin R\***, Dukic S, Chipika R, et al., Quantifying Executive Subdomain Dysfunction in ALS using EEG during the Sustained Attention to Response Task, Platform Presentation, ENCALS Meeting 2019. \*Presenter
5. **McMackin R\***, Dukic S, Costello E, et al., Onset and Decline of Cognitive and Motor Network Hyperexcitability in ALS Predict Symptomatic Progression. Platform Presentation, ENCALS Perth Satellite Meeting 2019. \*Presenter
6. **McMackin R**, Fasano A, Tadjine Y, et al., Developing biomarkers of focal network disruptions in ALS using threshold-tracking transcranial magnetic stimulation, Poster - Clinical imaging and electrophysiology, 30th International Symposium on ALS/MND 2019.
7. **McMackin R**, Dukic S, Chipika R, et al., Quantifying cognitive and motor preparatory dysfunction in ALS using EEG and electrical source imaging, Poster - Clinical imaging and electrophysiology, 30th International Symposium on ALS/MND 2019.
8. **McMackin R**, Dukic S, Costello E, et al., Cognitive and Auditory Cortical Network Oscillations are Abnormal in ALS. Poster - Clinical imaging and electrophysiology, 31st International Symposium on ALS/MND 2020.
9. **McMackin R**, Tadjine Y, Fasano A, et al., Developing Biomarkers of Focal Network Disruptions in ALS Using Threshold-Tracking Transcranial Magnetic Stimulation. Poster - Clinical imaging and electrophysiology, 31st International Symposium on ALS/MND 2020.

# Table of Contents

1. Introduction .....	5
1.1. Context .....	5
1.1.1. ALS as a motor and non-motor disease.....	5
1.1.2. ALS is a multistep process underpinned by genetic and environmental factors ...	7
1.1.3. Cellular and molecular level disruption in ALS.....	8
1.1.4. Biomarkers of ALS and their limitations .....	9
1.1.5. The Advantages of EEG and TMS for Measuring Cortical Function .....	11
1.2. Thesis Outline.....	14
2. Literature Review .....	15
Published Work List.....	15
2.1. Measuring Network Disruption in Neurodegenerative Diseases: New Approaches Using Signal Analysis .....	16
2.1.1. Introduction .....	16
2.1.2. Methods.....	16
2.1.3. Network Dysfunction in Neurodegeneration.....	33
2.1.4. Therapeutic Approaches using Network Modulation.....	43
2.1.5. Conclusion.....	45
2.2. The Application of Electrophysiology for Understanding Amyotrophic Lateral Sclerosis .....	46
2.2.1. Motor cortex .....	46
2.2.2. Prefrontal and temporal cortex .....	52
2.2.3. Parietal cortex.....	60
2.2.4. Interhemispheric networks .....	62
2.2.5. Interpreting electrophysiological measures to understand ALS pathology .....	65
2.2.6. Conclusion.....	67
3. Aims and Objectives .....	68
3.1. Aims .....	68
3.2. Objectives.....	68
3.2.1. Compare measures of cognitive and auditory cortical function evoked by the auditory oddball paradigm between ALS patients and controls.....	68
3.2.2. Characterise how cognitive and auditory cortical function changes over time in ALS .....	69

3.2.1.	Characterise the effects of ALS on cognitive regions associated with cognition and motor control.....	69
3.2.2.	Compare TT-TMS measures of short intracortical inhibition and intracortical facilitation between ALS patients and controls.....	70
3.2.3.	Compare TT-TMS measures of long intracortical inhibition and long and short interhemispheric inhibition between ALS patients and controls.....	70
3.2.4.	Determine the diagnostic and prognostic value of electrophysiological measures of cortical network function in ALS .....	71
4.	General Materials and Methods .....	72
4.1.	Electroencephalography (EEG) .....	72
4.1.1.	Hardware .....	72
4.1.2.	Software .....	73
4.1.3.	Experimental procedure .....	73
4.1.4.	Analysis.....	76
4.2.	Transcranial Magnetic Stimulation (TMS) .....	83
4.2.1.	Hardware .....	83
4.2.2.	Software .....	83
4.2.3.	Experimental procedure .....	86
4.3.	Statistics .....	86
4.4.	Participant recruitment .....	92
4.4.1.	ALS patient recruitment.....	92
4.4.2.	Healthy control recruitment .....	93
4.5.	Clinical, cognitive and behavioural measures.....	93
4.5.1.	ALS functional rating scale revised (ALSFRS-R).....	93
4.5.2.	Date of onset and survival time.....	94
4.5.3.	Cognitive and behavioural testing.....	94
4.6.	Ethical approval and informed consent.....	95
5.	Results: The Mismatch Negativity Response.....	97
	Published Work List.....	97
5.1.	Cross-sectional event related potential analysis.....	98
5.1.1.	Introduction.....	98
5.1.2.	Methods.....	99
5.1.3.	Results .....	102
5.1.4.	Discussion .....	111

5.2.	Longitudinal event-related potential analysis.....	115
5.2.1.	Introduction .....	115
5.2.2.	Methods.....	115
5.2.3.	Results .....	123
5.2.4.	Discussion .....	129
5.3.	Time-frequency analysis .....	135
5.3.1.	Introduction .....	135
5.3.2.	Methods.....	136
5.3.3.	Results .....	138
5.3.4.	Discussion .....	144
6.	Results: The Sustained Attention to Response Task .....	150
	Published Work List.....	150
6.1.	Cross-sectional event related potential analysis .....	151
6.1.1.	Introduction .....	151
6.1.2.	Methods.....	152
6.1.3.	Results .....	155
6.1.4.	Discussion .....	163
6.2.	Time-frequency analysis .....	167
6.2.1.	Introduction .....	167
6.2.2.	Methods.....	167
6.2.3.	Results .....	170
6.2.4.	Discussion .....	176
7.	Results: Transcranial Magnetic Stimulation .....	181
7.1.	Cross-sectional analysis .....	181
7.1.1.	Introduction .....	181
7.1.2.	Methods.....	183
7.1.3.	Results .....	190
7.1.4.	Discussion .....	195
7.2.	Opinion piece: Factors that limit the application of transcranial magnetic stimulation in amyotrophic lateral sclerosis patients.....	199
8.	Discussion and Conclusion .....	204
8.1.	Summary of results.....	204
8.1.1.	Auditory oddball-engaged networks .....	204

8.1.2.	SART-engaged networks .....	206
8.1.3.	TMS-engaged motor networks.....	209
8.2.	Exemplified advantages of electrophysiological measures for quantifying ALS compared to measures of symptomatic impairment.....	210
8.2.1.	Network dysfunction preceding symptomatic decline .....	210
8.2.2.	Measuring of compensatory function.....	211
8.2.3.	Sensor space vs. source space EEG measures.....	212
8.3.	Impact and future clinical applications .....	213
8.3.1.	Novel description of task-related cortical oscillation (de)synchronisations and their disruption in ALS.....	213
8.3.2.	Novel description of the cortical sources engaged by the SART and their disruption in ALS	214
8.3.3.	Novel identification of dynamic spatiotemporal patterns of cortical excitability which relate to ALS symptoms and severity measures .....	214
8.3.4.	Replication of some (but not other) previous TT-TMS-based ALS study findings in the Irish population. ....	215
8.3.5.	Novel indication that TT-TMS indices of GABA <sub>B</sub> ergic interneuronal are not uniformly affected by ALS, but may, alongside corpus callosum function, relate to disease progression. ....	216
8.3.6.	Novel identification of the utility of AP coil orientation for the detection of ALS pathology with TT-TMS. ....	216
8.3.7.	Novel biomarker candidates.....	216
8.4.	Links to genetic and molecular drivers of ALS pathogenesis.....	217
8.4.1.	Links between TDP-43 inclusions and cellular hyperexcitability and hyperactivity	218
8.4.2.	Links between RNA binding protein mutations and cellular hyperexcitability and hyperactivity.....	218
8.4.3.	Links between progressive cortical dysfunction and propagation of disease between cells to non-motor cortical areas .....	219
8.5.	Limitations .....	221
8.5.1.	Recruitment.....	221
8.5.2.	Attrition bias.....	222
8.5.3.	EEG study design and time domain analysis .....	223
8.6.	Future work.....	223
8.6.1.	Further TMS data collection .....	223

8.6.2.	Longitudinal SART and TMS studies .....	223
8.6.3.	Clustering analyses .....	224
8.7.	Overall conclusion.....	224
9.	Bibliography.....	226
10.	Appendices .....	269
10.1.	Appendix chapter 2 .....	269
10.2.	Appendix chapter 4 .....	302
10.3.	Appendix chapter 5 .....	311
10.4.	Appendix chapter 6 .....	317
10.5.	Additional publications .....	341

## List of Figures

- 2.1 The transformation of a digitised EEG signal into a frequency power spectrum.
- 2.2 EEG signal processing avenues for resting-state and task-based paradigms, the quantitative measures obtained and sample interpretations in neurodegenerative disease.
- 2.3 Schematic of a single-pulse TMS procedure and the quantitative characteristics of the resulting motor evoked potential.
- 2.4 Transcranial magnetic stimulation (TMS) can provide: (A) single-pulse measures, (B) paired-pulse measures and (C) dual-coil paired pulse measures with (D) threshold tracking can quantify network connectivity changes in the motor system.
- 5.1 Location of dipoles modelled by dipole fitting.
- 5.2 ALS patients show decreased power in both inferior frontal gyri and the left superior temporal gyrus.
- 5.3 ELORETA identified a pattern of decreased activity in the left superior temporal and inferior frontal sources, and an increase in activity in posterior areas.
- 5.4 LCMV identified a pattern of decreased activity in bilateral superior temporal and inferior frontal sources, and an increase in activity in the left hemisphere.
- 5.5 Increased activity in the left posterior parietal, central and dorsolateral prefrontal cortex in ALS is statistically significant.
- 5.6 Increased activity in the posterior parietal and dorsolateral prefrontal cortex correlates to poorer performance in cognitive switching tasks.
- 5.7 Illustration of data collection and processing pipeline for each dataset.
- 5.8 Comparison of power in each source of MMN, modelled by dipole fitting, between controls and patients at different follow-up times.
- 5.9 Modelled source activity change across EEG recording sessions in individual ALS patients.
- 5.10 Summary of median changes in normal and abnormal MMN sources in ALS patients illustrating that the activity of typical MMN generators increases over time in ALS, whereas the pathologically present activity in non-typical MMN generators declines as disease progresses.
- 5.11 Control ERSP following standard and deviant tones.
- 5.12 Top 5% of significantly active control sources of alpha band event-related oscillations 0-400ms after (A) standard tones and (B) deviant tones.

- 5.13 Area under the receiver operating characteristics curve (AUROC) values for significant deviant ERSP changes in ALS over the left temporal cortex (channel D22).
- 5.14 Source localised areas of significant differences in (A) mean alpha-band ERS 0-400ms after deviant tones and (B) slow beta-band ERS (13-18Hz, 320-420ms) after deviant tones between ALS patients and controls.
- 6.1 Mean Go (blue) and NoGo (red) trial ERPs in controls ALS patients.
- 6.2 Correlations between NoGo minus Go (NoGo-Go) N2 peak amplitude in Cz and cognitive task performance.
- 6.3 Correlations between P3 peak characteristics and SART performance.
- 6.4 Primary sources (regions with top 5% power) of N2 during Go trials, NoGo trials and NoGo trials relative to Go trials (“difference”) in controls (first rows) and patients (second rows).
- 6.5 Primary sources (regions with top 5% power) of P3 during Go trials, NoGo trials and NoGo trials relative to Go trials (“difference”) in controls (first rows) and patients (second rows).
- 6.6 P3 sources with statistically significant differences in activity in ALS compared to controls.
- 6.7 Greater behavioural inhibition in ALS is associated with increased right precuneus activity during NoGo P3 relative to Go P3.
- 7.1 Belly tendon montage employed for TMS-associated EMG.
- 7.2 Bee swarm plots illustrating control (blue) and ALS patient (red) TMS parameter values.
- 7.3 Bee swarm plots illustrating control (blue) and ALS patient (red) MEP and CMAP latency and CMAP amplitude values
- 8.1 Illustration of the proposed link between hyperexcitability spread through the cortex and TDP-43 pathology in ALS



## **List of Tables**

- 2.1 Limitations and advantages of different source localisation methods.
- 2.2 Neurophysiological biomarkers for and therapies in neurodegeneration.
- 2.3 Event related potentials, the electrode locations where they are best recorded, their associated functions and their cortical sources.
- 2.4 Summary of brain regions with motor and/or cognitive functions for which there is structural and/or neurophysiological evidence of change in ALS.
- 4.1 Paired pulse measures recorded and their associated parameters.
- 5.1 Summary of P-values and AUROCs for each source modelled by dipole fitting in ALS patients and subgroups compared to controls.
- 5.2 Comparison of the head and source models, time windows and detected source activity changes for each source localisation method used.
- 5.3 Summary of ALS patient clinical characteristics at baseline.
- 5.4 Summary of statistics for significant correlations between EEG measures and clinical characteristics in the ALS patient cohort.
- 5.5 Control cortical sources contributing top 5% of alpha ERS power across 0-400ms in deviant trials.
- 5.6 Cortical and subcortical regions with significantly increased mean alpha power (0-400ms) following deviant tones in ALS patients.
- 6.1 Characteristics of ALS patients and controls
- 6.2 Significant differences in ALS sensor level and source level measures compared to controls.
- 7.1 Summary of linear mixed effect model coefficient values of group and age effects on each paired pulse inhibition/facilitation measure.
- 7.2 Summary statistics for compound muscle action potential and single pulse TMS-associated motor evoked potential data.
- 7.3 ALS patients excluded from or of limited participation due to clinical limitations

## **Abbreviations**

$\alpha$ MRD – Alpha band movement related desynchronisation  
ACC – Anterior cingulate cortex  
AD - Alzheimer's disease  
AEP – Auditory evoked potential  
ALS – Amyotrophic lateral sclerosis  
ALSbi – ALS with behavioural impairment  
ALSci – ALS with cognitive impairment  
ALSFRS - Amyotrophic lateral sclerosis functional rating scale  
ALSFRS-R - Amyotrophic lateral sclerosis functional rating scale revised  
AP – Anteroposterior  
APB – Abductor pollicis brevis  
AUROC – Area under the receivership operating characteristics curve  
BBI - Beaumont Behavioural Inventory  
BP – Bereitschaftspotential  
 $\beta$ MRD - Movement-related beta desynchronization  
bvFTD – Behavioural variant frontotemporal dementia  
CC - Corpus callosum  
CMAP – Compound muscle action potential  
CMS – Common sense  
CNV – Contingent negative variation  
CS – Conditioning stimulus  
CTT – Conditioned target threshold  
CWIT – Colour Word Interference Test  
D-KEFS – Delis-Kaplan Executive Function System  
DLPFC – Dorsolateral prefrontal cortex  
ECAS - Edinburgh Cognitive and Behavioural ALS Screen  
EEG – Electroencephalography  
eLORETA – Exact low resolution electrical tomography  
EMG - Electromyography  
ERD – Event related desynchronization  
ERP – Event related potential  
ERS – Event related synchronization

ERSP – Event related spectral perturbation  
FA – Fractional anisotropy  
FDR – False discovery rate  
fMRI – Functional magnetic resonance imaging  
FTD – Frontotemporal dementia  
FUS – Fused in sarcoma  
GABA – Gamma aminobutyric acid  
HD - Huntington’s disease  
ICF – Intracortical facilitation  
IHI – Interhemispheric inhibition.  
ISI – Interstimulus interval  
iSP – Ipsilateral silent period  
IQR – Interquartile range  
ITV – Inter-trial variance  
LCMV – Linearly constrained minimum variance  
LICI – Long intracortical inhibition  
LIHI – Long interhemispheric inhibition  
LM – Lateromedial  
LMN – Lower motor neuron  
LORETA – Low resolution electrical tomography  
M1 – Primary motor cortex  
MCI – Mild cognitive impairment  
MD – Medial diffusivity  
MEG – Magnetoencephalography  
MEP – Motor evoked potential  
MMN – Mismatch negativity  
MRI – Magnetic resonance imaging  
MRP – Movement related potential  
MS – Multiple sclerosis  
MSO – Maximum stimulator output  
Nd – Negative difference  
NFL – Neurofilament light chain  
PA – Posteroanterior  
PD – Parkinson’s disease

PEST – Parameter estimation by sequential testing  
PET – Positron emission tomography  
PFC – Prefrontal cortex  
PN – Processing negativity  
PNFA – Progressive non-fluent aphasia  
qEEG – Quantitative electroencephalography  
RMT – Resting motor threshold  
rTMS – Repetitive TMS  
S1 – Primary somatosensory cortex  
SICI – Short intracortical inhibition  
SIHI – Short interhemispheric inhibition  
SSEP – Somatosensory evoked potentials  
SMA - Supplementary motor area  
TDP-43 - TAR DNA binding protein 43  
THT – Threshold hunting target  
TMS – Transcranial magnetic stimulation  
TT-TMS – Threshold tracking transcranial magnetic stimulation  
TS – Test stimulus  
UMN – Upper motor neuron  
WOI – Time-frequency window of interest

# 1. Introduction

## 1.1. Context

This research project was formulated in the context of increasing recognition that ALS drives pathology beyond the corticospinal tract, limitations in existing biomarkers of ALS and advancements in electrophysiological technology. This context is outlined here.

### *1.1.1. ALS as a motor and non-motor disease.*

Amyotrophic lateral sclerosis (ALS) is the most common form of motor neuron disease, and is progressive, incurable and terminal<sup>1</sup>. Half of patients do not survive past 30 months after symptom onset<sup>2</sup>. The incidence rate of ALS in Ireland (2.6 per 100,000<sup>3</sup>) is approximately half that of multiple sclerosis (~5 per 100,000<sup>4</sup>). However, the much poorer prognosis of ALS results in a much more limited living patient population at any one time<sup>5</sup>.

The underlying cause of ALS is unknown in 80-90% of cases (referred to as ‘sporadic ALS’)<sup>6</sup>, while inherited ‘familial ALS’ accounts for approximately 10-20% of cases<sup>7,8</sup>. Sufferers of the disease experience progressive motor impairment manifesting from the degeneration of both bulbar and spinal upper motor neurons (UMNs) and lower motor neurons (LMNs). Typically symptom onset is focal with deficits spreading contiguously across upper and lower motor neurons<sup>9</sup>. Degeneration of UMN controlling limb function can manifest as symptoms such as slowing of muscle contraction, weakness, spasticity and abrupt deep tendon reflexes, while degeneration of LMNs in these pathways can produce weakness, fasciculation and wasting of muscle<sup>10</sup>. Degeneration of UMNs involved in bulbar motor function can result in spastic dysarthria, while bulbar LMN degeneration can produce tongue weakening, wasting, fasciculation and flaccid dysarthria<sup>11</sup>. Respiratory failure or related respiratory infection due to degeneration of motor neurons innervating the diaphragm are the most common cause of death in ALS<sup>12,13</sup>.

ALS was originally described in the 19<sup>th</sup> Century by Charcot as a disease specific to the corticospinal tract with no cognitive impact<sup>14</sup>. Evidence of cognitive impairment in ALS began to be published in the early twentieth century<sup>15</sup> however widespread recognition of extra-motor, cognitive impairments as a major symptomatic category in ALS was delayed until the late twentieth century<sup>16</sup> for numerous reasons, including lack of investigation of such symptoms by physicians due to wide acceptance of a pure motor pathology, in

addition to the motor symptoms themselves masking the presence of such cognitive symptoms. For example, the deterioration of speech resulting from bulbar motor neuron degeneration can easily mask impairments in language expression<sup>14</sup>.

It is now established that there is a substantial overlap between ALS and frontotemporal dementia (FTD), which results from atrophy of the frontal and temporal lobes<sup>17</sup> (particularly behavioural variant-FTD, bvFTD, attributed primarily to frontal lobe degeneration<sup>18</sup>). Approximately 15% of ALS patients fulfil the criteria for FTD diagnosis (ALS-FTD)<sup>19</sup>. This degeneration results in cognitive and behavioural impairments which can vary depending on the networks affected. Symptoms of FTD include changes in executive function (such as planning and organising), in behaviour (such as disinhibition, stereotyped behaviours and apathy) and in personality as well as deterioration of language skills (such as anomia, stuttering, alexia and grammatical errors) although episodic memory is usually preserved. Patients typically are unaware of these deficits<sup>14</sup>.

While the majority of ALS patients do not meet the criteria for FTD, it is now established that behavioural and/or cognitive symptoms are present in approximately half of ALS patients. These behavioural symptoms include apathy (38% to 56%), disinhibition (18 to 46.1%)<sup>20-22</sup>, mood changes (most commonly lability and irritability) (33-63%), compulsive, ritualistic or stereotyped behaviour (19 to >50%)<sup>23</sup>, socially disinhibited behaviour (13%), selfishness (69%) and increased aggression (13%)<sup>24</sup>. Cognitive symptoms include executive dysfunction (34 to 45.7%) and impairments in attention (32%), memory and orientation (>60%)<sup>20-22,25,26</sup>. Strong and colleagues proposed the classification of patients who present with these symptoms (but only partially meet FTD criteria) as behaviourally impaired (ALSbi) and cognitively impaired (ALSci) respectively<sup>16</sup>.

Smaller numbers of ALS patients have also been found to reach the criteria for semantic dementia and progressive non-fluent aphasia (PNFA) type FTD, in which language is affected<sup>27</sup>. Language functions are largely attributed to several regions of the temporal lobe as well as the inferior frontal lobe<sup>28</sup>. Semantic dementia is associated with atrophy of the middle, inferior, and medial anterior temporal lobe while PNFA is associated with atrophy near the sylvian fissure including the inferior frontal and superior temporal regions, usually predominantly in the left hemisphere in both subtypes<sup>29,30</sup>. PNFA symptoms include language errors such impaired grammar and speech fluidity,

loss of reading and writing skills, anomia, phonemic paraphasia and oral apraxia, while semantic dementia is characterised by impaired understanding of words, faces and other sensory input as well as speech that is empty of meaning, although fluency and grammar is preserved<sup>14,31</sup>. Some symptoms of language impairment have also been identified in ALS patients in the absence of semantic dementia or PFNA, resembling the existence of a sub-threshold, language variant FTD-like syndrome in some ALS patients. These include semantic deficits and decreased verbal fluency<sup>32</sup>, although verbal fluency deficits may also be the result of impaired response generation, and therefore can also be a manifestation of executive dysfunction<sup>33</sup>. Language impairment has also been identified in writing tasks in order to overcome the obstacle of dysarthria in measuring change in language functions<sup>34</sup>.

This overlap between FTD and ALS indicates non-motor frontal and temporal pathology occurs in ALS. However, pathology in other cortical regions is also indicated by ALS' non-motor symptoms. For example, many executive functions are attributed to cortical networks with parietal nodes, such as the central executive network, which may play a role in ALS<sub>ci</sub> and ALS<sub>bi</sub>. Further, additional non-motor symptoms observed in some ALS patients include sensory symptoms such as numbness or tingling, found to occur in 32% of patients<sup>35</sup>, indicating that the primary somatosensory cortex of the parietal lobe may also be impacted.

#### *1.1.2. ALS is a multistep process underpinned by genetic and environmental factors*

The risk of developing ALS is established to be affected by both genetic and environmental risk factors (for systematic review and meta-analysis of environmental risk factors for ALS see Wang et al., 2017). A complex combination of these factors, accumulating over time, is considered to bring those who develop ALS to a threshold at which pathology begins<sup>36</sup>. However, this multistep process is shortened by the presence of certain genetic mutations, such as in *C9orf72*, *SOD1* and *TARDBP* genes<sup>37</sup>. Different genetic mutations associated with ALS also are known to contribute towards variation in ALS phenotype, such as age of onset, site of onset and emergence of cognitive impairment (although many of the underpinning mechanisms by which these genes affect ALS phenotype remain to be established)<sup>38</sup>.

### *1.1.2.1. The C9orf72 repeat expansion is a driver of ALS and its cognitive and behavioural symptoms*

Mutations in a large number of genes have been associated with ALS across the genetic ALS literature (for review see Mathis et al., 2019). However, among the most common and well-established genetic mutations associated with the Irish ALS population, is the expansion of GGGGCC hexanucleotide repeats in the *C9orf72* gene<sup>39</sup>. Hexanucleotide repeat expansion in the first intron of the *C9orf72* gene (named as an abbreviation of “Chromosome 9 Open Reading Frame 72”) was first associated with ALS and FTD in 2011 by two independent groups<sup>40,41</sup>. Typically, more than 30 repeats of this sequence are considered pathogenic, although intermediate repeat numbers (24-30) are also significantly more prevalent in ALS patient cohorts relative to controls<sup>42</sup>. Expansions of 29 or more repeats are found in 41% of familial and 5% of sporadic ALS patients in the Irish population<sup>43</sup>. The exact mechanism by which this *C9orf72* repeat expansion drives ALS and FTD pathology remains uncertain. Loss of normal *C9orf72* protein function, sequestration of toxic, bidirectionally transcribed repeat-containing RNAs and toxic dipeptide repeat protein production resulting from this mutation are, however, considered to contribute towards ALS pathogenesis<sup>44</sup>.

This mutation in *C9orf72* not only draws another connection between ALS and FTD pathology, but is associated with ALS<sub>ci</sub> and ALS<sub>bi</sub> - Those carrying this expansion showing significantly greater prevalence of cognitive and behavioural symptoms compared to those without this expansion. The pathological *C9orf72* repeat expansion is also associated with earlier age of symptom onset, shorter survival time and significantly greater grey matter atrophy in the right inferior frontal gyrus, right superior frontal gyrus, left anterior cingulate gyrus, and the right precentral gyrus<sup>45</sup>. It is, therefore, likely that those with ALS underpinned by this repeat expansion experience a more homogenous pattern of underpinning cortical network pathology than the overall ALS population, forming a cortical network disruption-based subphenotype of ALS.

### *1.1.3. Cellular and molecular level disruption in ALS*

A myriad of processes that are essential for normal neuronal function have been established to be disrupted in ALS. These include protein folding and management of misfolded proteins<sup>46</sup>, mitochondrial function and free radical neutralisation<sup>47</sup>, intracellular transport (including endoplasmic reticulum<sup>48</sup>, lysosome<sup>49</sup> and intracellular trafficking protein<sup>50</sup> function) and RNA metabolism<sup>47</sup>. The therapeutic mechanism of the only drug approved for ALS in Europe, Riluzole, is unclear, although enhancement of



gamma aminobutyric acid (GABA) function, anti-glutamatergic effects and/or blockage of voltage-gated  $\text{Ca}^{2+}$  and  $\text{Na}^{+}$  channels have been proposed<sup>51</sup>.

One of the most unifying intracellular abnormalities across ALS patients is the presence of intraneuronal deposits containing TAR DNA binding protein 43 (TDP-43) in 97% of ALS patients and 45% of FTD patients<sup>52-54</sup>. TDP-43 is an RNA-binding protein which shuttles between the cell nucleus and cytoplasm<sup>55</sup>, with TDP-43 proteinopathy considered a combination of both gain and loss of function effects<sup>56</sup>. Inclusions containing fused in sarcoma (FUS), another RNA-binding protein, are found in many of the ALS and FTD patients that do not have such TDP-43-containing deposits<sup>52</sup>. These findings, alongside the association of *TARDBP* and *FUS* mutations with ALS<sup>57</sup>, indicate that disrupted RNA metabolism is particularly pertinent to the onset of ALS pathology, and is an important mechanistic link between ALS and FTD pathology.

One theory which attempts to explain the heterogeneity of ALS symptoms and their severity is that this diagnosis includes multiple different diseases<sup>58</sup>. The prevalence of RNA binding proteinopathy across ALS patients forms a primary argument against this. However, variation in the location of TDP-43 (or other) proteinopathy within the cortex may explain this heterogeneity. This is supported by a recent study which identified that TDP-43 inclusions in the cortical regions associated with executive, language and fluency domains were predicted with 100% specificity by performance in the specific tasks of these domains within the Edinburgh Cognitive and Behavioural ALS Screen (ECAS)<sup>59</sup>.

#### *1.1.4. Biomarkers of ALS and their limitations*

Biomarkers are quantifiable changes in an individual's biology that can be used to identify the presence or characteristics of a disease. Biomarkers can be used for diagnosis (to identify that a disease is present) or prognosis (to measure how a disease will progress or is progressing)<sup>60</sup>.

##### *1.1.4.1. Diagnostic biomarkers*

Although the TDP-43 deposits identified in post-mortem tissue form a largely unifying characteristic of ALS, attempts to measure TDP-43 disruption in CSF or blood have so far failed to identify a fluid biomarker that can be used for diagnosis of living patients<sup>61</sup>. Diagnosis of ALS therefore remains predominantly contingent on the expertise of experienced neurologists, limiting early and accurate diagnosis to those with access to such experts<sup>62</sup>. According to the El Escorial revised criteria, evidence of lower motor neuron LMN degeneration ("LMN signs") captured by needle electromyography (EMG),

such as fasciculations, can be used to confirm probable diagnosis of ALS alongside the presence of clinically identified symptoms of UMN degeneration (“UMN signs”)<sup>63</sup>. An objective, quantifiable biomarker of UMN degeneration remains to be identified however, and is urgently required given observations that LMN signs can obscure the clinical identification of UMN signs<sup>64</sup>.

Neurofilament light chain (NFL), a cytoskeleton protein which normally occurs within the axons of neurons, is found to be significantly elevated in the cerebrospinal fluid and blood of ALS patients. This provides an aid for diagnosis in the context of other indicators of ALS, however this change is not specific to ALS. This is because increased NFL in blood or cerebrospinal fluid is a marker of axonal damage, rather than disease specific pathobiology<sup>65</sup>, and is therefore observed in other neurodegenerations such as FTD, Creutzfeldt-Jakob disease and multiple sclerosis (MS)<sup>66</sup>. Increased NFL does tend to be greater in the CSF of ALS compared to other neurodegenerative diseases<sup>66,67</sup> but does not assist in deciphering ALS subphenotypes<sup>68</sup> (e.g. those differing in the specific combination and severity of motor, cognitive and behavioural symptoms experienced). Additionally, the invasive nature of lumbar puncture cannot be overlooked in the development of biomarkers for routine use in clinic or for pharmaceutical testing, due to associated side effects and potential for infection<sup>69</sup>.

Threshold tracking transcranial magnetic stimulation (TT-TMS) of the primary motor cortex has been reported to sensitively capture hyperexcitability of UMNs in ALS early in disease, unlike ALS mimic diseases<sup>70,71</sup> (discussed in detail in chapter 2). It therefore has also garnered international attention as a potential diagnostic biomarker of UMN degeneration in ALS which could facilitate earlier and more objective diagnosis<sup>72</sup>. Independent replication of these findings is now required, in addition to examination of how ALS affects other potentially useful TT-TMS measures of motor cortical function.

#### *1.1.4.2. Prognostic biomarkers*

ALS patient prognoses are highly variable and unpredictable, although prognostic predictions can be slightly improved based on site of symptom onset, genetic risk factors, age at onset and gender. While these characteristics are of proven epidemiological significance<sup>73</sup>, substantial prognostic heterogeneity remains unexplained by existing ALS prognostic biomarkers. Such unknowns not only cause substantial distress to patients and their caregivers<sup>74</sup>, but also limit the ability to design clinical trials capable of demonstrating therapeutic effects of drug candidates. Currently, clinical trials depend

primarily on survival and change in ALS functional rating scale revised (ALSFERS-R) scores as outcome measures. However, the subjective nature of ALSFERS-R scoring and its specificity to motor symptoms limits the sensitivity of this measure to disease progression<sup>75</sup>. Further, survival times and ALSFERS-R decline within individuals have proven difficult to predict<sup>76,77</sup>. As a result, it can be challenging to identify significant therapeutic effects on a patient group or subgroup amidst disease heterogeneity within and between treatment groups. Attempts to avoid this effect on statistical power include reducing patient cohort variation through use of restrictive clinical trial recruitment criteria, substantially limiting patient access to and biasing any findings of these studies<sup>78</sup>. These issues could be overcome by the development of novel, objective and quantitative prognostic biomarkers of ALS.

A measurement, or combination of measurements, which captures more specific information about each individual's central nervous system dysfunction could overcome these limitations and improve understanding, explanation and prediction of the variation between individual ALS patient experiences. Structural magnetic resonance imaging (MRI) provides high spatial resolution, and can therefore pinpoint precise locations of central tissue atrophy. However, the tissue atrophy detected by volumetric MRI measures is likely to occur after an earlier stage of pre-clinical molecular, cellular and functional pathology<sup>79</sup>. These structural measures also show little progressive change from symptom onset in ALS<sup>80</sup> and have been found to be independent of disease progression rate<sup>81</sup>. While longitudinal MRI research has provided important insight into extension of ALS pathology to extra motor regions, the link between these changes and symptomatic cognitive and behavioural manifestations remains unclear. A similar phenomenon is established for MS, referred to as the "clinico-radiological paradox", wherein there is a mismatch between the number and volume of white matter lesions and concurrent disease symptoms<sup>82</sup>. As it is considered that this mismatch may be accounted for by differences in cognitive reserve and insensitivity to subtle widespread changes, it has been proposed that changes in cortical function, as opposed to structure, will align better with clinical change<sup>83</sup>. This highlights the potential application of electrophysiology for developing prognostic biomarkers of ALS.

#### *1.1.5. The Advantages of EEG and TMS for Measuring Cortical Function*

The mechanistic and physiological basis of the electrophysiological measures employed for this project, their advantages relative to alternative methods of measuring cortical

function and their use to date in quantifying ALS are discussed in detail in chapter 2. However, to provide a brief contextual introduction to the characteristics of state-of-the-art electroencephalography (EEG) and TMS in association with EMG which render them most suitable for this project, their advantages can be summarised as follows:

#### *1.1.5.1. Cost*

A complete apparatus of high density EEG hardware and software can be purchased for less than 20,000 euro, while that required for threshold tracking TMS with EMG can be purchased for approximately 50,000 euro. Running costs to employ both methodologies are minimal (tens of euro), limited to low cost (<100 euro) consumables (such as pre-gelled electrode pads and conductive gel), approximately annual replacement of electrodes (<1,500 euro) /cables (<100 euro)/electrode montage caps (<500 euro) due to wear and tear and mains electricity power for amplifiers, stimulators and data recording computers (costs cited are those of the experimental setups of this project). By contrast, other imaging methods such as MRI, computed tomography (CT) or positron emission tomography (PET), as well as magnetoencephalography (MEG), require apparatus costing millions of euro, with single recording sessions costing hundreds to thousands of euro<sup>84-88</sup>.

#### *1.1.5.2. Non-invasive*

As oppose to fluid biomarkers or needle-based electrophysiology, surface EEG and TMS do not require breach of the skin, reducing discomfort and infection risk to the participant and therefore improving their applicability in clinical research and pharmacological testing.

#### *1.1.5.3. Upright, relaxed patient stance*

A substantial limitation to the use of imaging scanners, such as those employed for functional MRI (fMRI) or PET, is that they require participants to lie flat for a single continuous period without moving. This is unsustainable for many ALS patients with respiratory system decline or excess salivation<sup>89</sup>. In addition, the enclosed nature of scanners is distressing to those who are claustrophobic<sup>90</sup>. By contrast, EEG and TMS can be performed while the participant sits upright in a chair in an open room. Further, while movement during EEG or TMS can introduce artefact to the EEG/TMS-associated EMG signal, if experiments are designed with sufficient trial repetition, short spans of contaminated signal can be identified and removed during post-session processing by an experienced data analyst/suitable algorithm<sup>91,92</sup>. Therefore, data recording does not need

to be terminated and restarted if the participant cannot continuously remain still and relaxed.

#### *1.1.5.4. Directly measuring neurons/muscle*

EEG and EMG directly capture electrical signals resulting from functioning of groups of cortical neurons and muscle fibres respectively. They do not, therefore, rely on inferences of activity based on secondary measures such as glucose metabolism or blood oxygenation changes, as is the case for PET and fMRI respectively. These factors may themselves be affected by disease or aging, affecting their relationship to neuronal activity<sup>93-95</sup> and thus any inference of neuronal activity or connectivity change.

#### *1.1.5.5. Excellent temporal resolution*

As a result of directly measuring the electrical signals produced during muscle fibre contraction or neuronal signalling, EMG and EEG have excellent temporal resolution, capturing activity at millisecond-by-millisecond scale, as oppose to the second/tens of second scale resolution of fMRI/PET respectively<sup>96</sup>. As a result, changes in neuronal/muscular activity can be precisely associated in time with the delivery of a stimulus or performance of a task. For example, the millisecond-level speed of descending signal delivery from cortex to target muscle following magnetic stimulation can be detected with EMG<sup>97</sup>. Alternatively, the successive activation of cortical network nodes can be deciphered in time using EEG during sensory stimulation or task performance<sup>98</sup>. The impact of disease on ascending or descending neural network signalling can therefore also be sensitively interrogated with these methods.

#### *1.1.5.6. Improving spatial resolution*

Despite the aforementioned advantages of EEG, this method has often been dismissed in favour of other functional imaging methods in light of its relatively poor spatial resolution (centimetre level, mapped on the scalp) compared to that of fMRI (millimetre level throughout the brain tissue)<sup>96</sup>. Advancements in source localisation algorithms have substantially improved the spatial resolution of EEG, so that it can be mapped onto the brain tissue at sub-centimetre resolution depending on the analytical pipeline (see chapter 2)<sup>99</sup>. The spatial focality of TMS of the cortex has also been refined with improvements in coil design<sup>100</sup>, and can currently provide peak stimulation intensities of approximately 1cm<sup>2</sup> area<sup>96</sup>.

## **1.2. Thesis Outline**

This thesis is composed of 8 chapters. The next chapter, chapter 2, includes a literature review of the physiological basis of the methodologies employed in this project and the current state-of-the-art in electrophysiological interrogation of network impairment in neurodegenerative disease. This is followed by a detailed review of the existing literature regarding cortical network dysfunction in ALS. Chapter 3 describes the aims and objectives of this thesis. Chapter 4 details the hardware, software and general methodologies and analyses employed in this project and the rationale for their use. Details of experiment-specific patient cohorts, analyses and results, as well as a discussion of those results specifically are described in two EEG-based results chapters, 5-6, and TMS-based results chapter 7. Each results chapter contains multiple studies/analyses. This is followed by a discussion chapter 8, which discusses the overall findings of the project, the novel insights gained, any limitations identified and future work that is planned.

## **2. Literature Review**

### **Published Work List**

An abbreviated version of section 2.1 has now been published in the peer-reviewed journal *NeuroImage: Clinical*<sup>101</sup> as:

McMackin R, Bede P, Pender N, et al. Neurophysiological markers of network dysfunction in neurodegenerative diseases. *NeuroImage: Clinical* 2019;22:101706.

The text, figures (1-3) and table (table 1) from this publication are contained in full within section 2.1.

Figure 2.4 has also been published in a separate review paper in the peer-reviewed *Journal of Neurology, Neurosurgery and Psychiatry*<sup>102</sup> as:

McMackin R, Muthuraman M, Groppa S, et al. Measuring network disruption in neurodegenerative diseases: New approaches using signal analysis. *J Neurol Neurosurg Psychiatry* 2019;90(9):1011–1020.

Table 2.1 has also been published in the peer-reviewed journal *NeuroImage: Clinical*<sup>103</sup> as:

McMackin R, Dukic S, Broderick M, et al. Dysfunction of attention switching networks in amyotrophic lateral sclerosis. *NeuroImage: Clinical* 2019;22:101707.

## **2.1. Measuring Network Disruption in Neurodegenerative Diseases: New Approaches Using Signal Analysis**

### *2.1.1. Introduction*

Modern clinical imaging, pathological<sup>104</sup> and genomic<sup>105</sup> data, support the evolving notion that neurodegenerative syndromes are best understood in terms of disrupted brain networking. Quantitative MRI and PET provide compelling evidence of widespread network changes in neurodegenerations including Alzheimer's disease (AD)<sup>106</sup>, Parkinson's disease (PD)<sup>107</sup>, ALS<sup>108</sup> and frontotemporal dementia (FTD)<sup>109</sup>. New therapeutic approaches based on network modulation are already in use for Parkinson's<sup>107</sup> and Alzheimer's Disease<sup>106</sup>.

Notwithstanding, characterizing changes in brain networking in a clinical setting remains a challenge. Structural MRI can show changes in grey and white matter integrity<sup>110</sup> and fMRI detects resting and activated states of metabolic activity. Neither modality can directly measure neuronal activity, however. Furthermore, as fMRI measurements can be confounded by vascular pathology and are limited by the requirements of the technology (including the need for the patient to remain supine)<sup>111</sup>, the use of fMRI is limited in the neurodegenerations. There remains an urgent and unmet need for user-friendly, non-invasive technologies that can rapidly and reliably detect network alteration with high temporal and spatial resolution.

Here is a review of the biology of non-invasive electrophysiology-based measurements and outline of the current state of the art in measurement of network dysfunction in the neurodegenerations. The future potential of emerging electrophysiology-based technologies in providing enhanced temporal resolution, and in using source localization that improves spatial resolution to complement structural and functional imaging is explored.

### *2.1.2. Methods*

#### *2.1.2.1. Electroencephalography and Magnetoencephalography*

Quantitative EEG (qEEG) and MEG are increasingly recognized as useful non-invasive methods to measure cortical neurophysiological activity.

MEG and EEG capture and digitise neuroelectromagnetic reflections of the synchronous generation of excitatory and inhibitory post-synaptic potentials in populations of underlying neurons. Both MEG and EEG have excellent temporal resolution but, until



recently, limited spatial resolution. Several methods, collectively referred to as source localisation methods, have now been developed that enhance the spatial resolution of both EEG and MEG to that of using fMRI<sup>112</sup>. This now allows for visualisation of brain activity at low cost, with high levels of both spatial and temporal resolution.

The physiologic basis of MEG and EEG differ. MEG sensors measure the magnetic field generated by the electrical flows in neuronal populations while EEG sensors measure the simultaneously-generated perpendicular electric field that passes through the space between the activity source and sensors<sup>113</sup>. Due to volume conduction, EEG sensors also capture electrical currents propagated between the source and sensor in the conductive human head medium. This effect of volume conduction in EEG may make MEG a more reliable measure for deeper sources. However, it must be noted that the potential advantage of MEG is reduced by the need for expensive superconductive systems<sup>114</sup> that significantly increase costs, limiting MEG's day-to-day application in clinical settings.

EEG and MEG both generate waveform data, where the x-axis represents time and the y-axis represents amplitude of electrical activity (Box 1). Quantitative M/EEG involves the digitisation of these signals and quantitative analysis of their characteristics. These analyses can be performed in time and frequency domains. Time domain analysis is the study of how brain activity changes over time<sup>115</sup> (for example at what time the intensity of neural activity peaks when performing a cognitive or motor task). Frequency domain analysis involves the use of Fourier transformation to decompose the recording into a combination of waves of different frequencies (Fig. 2.1).

**Amplitude** – The size of the electrical charge in the cerebrospinal fluid produced by the summation of neuroelectric activity such as excitatory and inhibitory post synaptic potentials in cerebral cortical neurons, typically in microvolts ( $\mu V$ )<sup>116</sup>.

**Power** – A measure of the intensity of neuronal activity, proportional to the amplitude squared<sup>116</sup>.

**Frequency** – The number of times a cycle of a wave repeats per unit time, measured in hertz (Hz)<sup>116</sup>.

**Frequency bands** – Continuous ranges of frequencies for which measurements are grouped.

**Oscillation** – Continuous, periodic neuronal activity, typically generated by feedback loops in neuronal networks<sup>117</sup>.

**Event-related potential (ERP)** – Electrical potential observed at the time that an event occurs, such as performing a motor or cognitive task or sensory stimulus<sup>118</sup>.

**Event-related (de)synchronisation (ERD/ERS)** – Relative decrease or increase in the intensity of oscillatory activity in a frequency band, caused by an event such as performing a motor or cognitive task or sensory stimulus<sup>119</sup>.

**Sensor-level** – Digitised M/EEG data analysed with respect to the position of the sensors on the scalp, providing poor spatial resolution.

**Source-level** – Digitised M/EEG data analysed using source localisation methods to determine the location of contributing sources in the brain, providing spatial resolution comparable to fMRI<sup>112</sup>.

**Box 1. Electrical and physiological characteristics defined in the context of EEG measurements.**

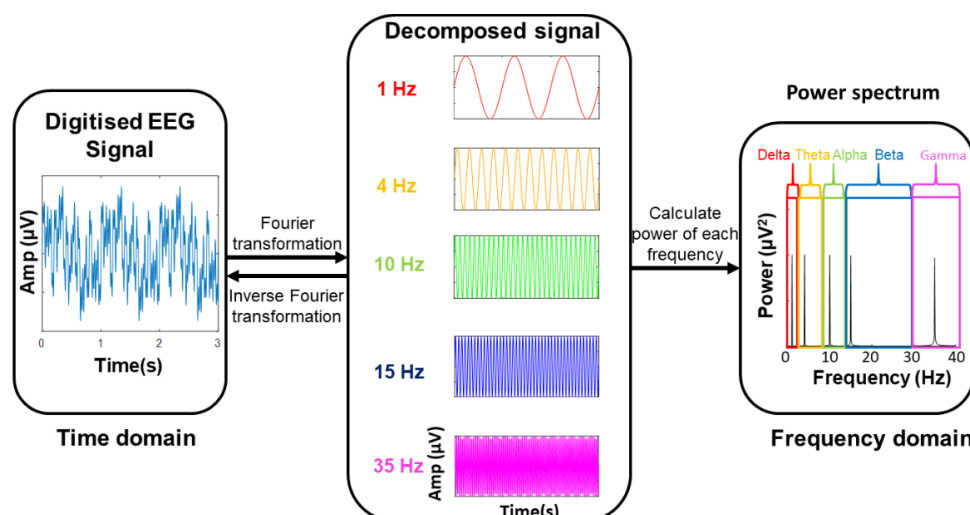


**Figure 2.1. The transformation of a digitised EEG signal into a frequency power spectrum.** This figure has been published in my paper McMackin et al 2019a (figure 1), please see appendix 2.1.

Typically, quantitative M/EEG signal frequencies are grouped into delta (0.5–3 Hz), theta (3–7 Hz), alpha (8–13 Hz), beta (14–30 Hz), and gamma (>30 Hz) frequency bands<sup>120</sup>. Oscillations in these different frequency bands have been attributed to different neuronal populations and brain activities<sup>117</sup> (Box 1). This allows for investigation of brain activity in terms of the power of oscillating network activity at different frequencies, referred to as spectral EEG<sup>121</sup>. Synchronous or time-correlated oscillations in different brain areas can also be used to infer functional connectivity between them<sup>122</sup>. The frequencies of these bands are generally negatively correlated to their amplitude (i.e. lower frequency M/EEG oscillations tend to have higher amplitude). Since amplitude is a reflection of the number of neurons contributing to a signal, lower frequency oscillations are attributed to synchronous activity of larger numbers of neurons<sup>119</sup>.

These time and frequency domain network characteristics can be examined at rest (“resting-state”) to investigate the resting activity of the brain (Fig. 2.2). M/EEG measures can also be captured during tasks such as cognition, sensation or movement, to measure the activity of brain regions contributing to the generation of the engaged function(s) (Fig. 2.2)<sup>123,124</sup>. As tasks are underpinned by integration of various distinct neural networks, the corresponding neural signatures can be marked in the frequency domain, known as event related (de)synchronisation, and/or the time domain, known as event related potentials (ERPs) (Box 1). Source localisation methods can subsequently be applied to identify the origin of these of the network components and any changes to their performance in disease. Each of these approaches allows for the study of different aspects of neural network function and can be combined to provide a well-rounded insight into the effects of disease pathology on brain network function.

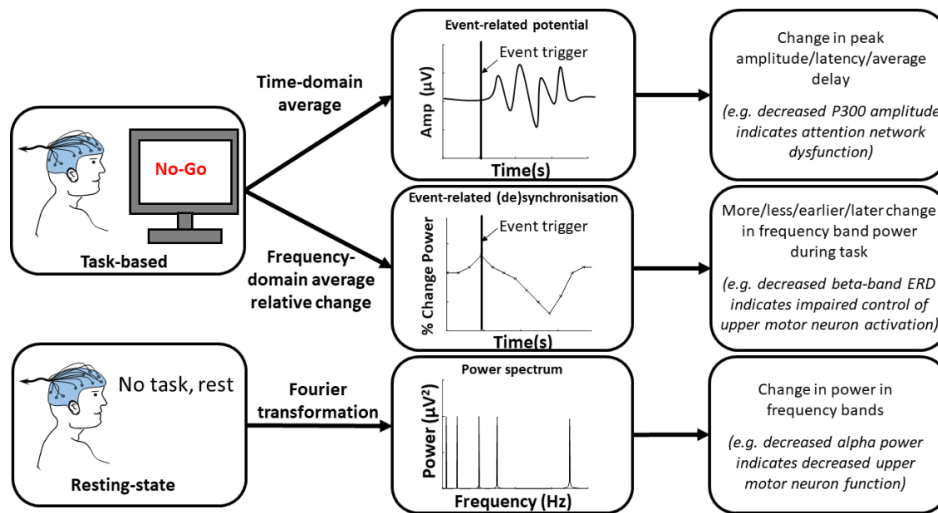


**Figure 2.2. EEG signal processing avenues for resting-state and task-based paradigms, the quantitative measures obtained and sample interpretations in neurodegenerative disease.** This figure has been published in my paper McMackin et al 2019a (figure 2), please see appendix 2.1.

### *Event related potentials*

ERPs are calculated by averaging EEG signals time locked to a stimulus or response across many trials of a task. This analysis assumes that cortical signals related to the task occur at a consistent time and phase relative to the task cues, and therefore will be maintained during averaging while task-irrelevant, background signal will be removed. The high temporal resolution of EEG means that the sequential engagement of cortical regions as a stimulus is processed, interpreted and a response is generated/inhibited can be individually quantified by characterising different peaks within the ERP. Early peaks are generated by sensory networks, followed by later peaks generated by cognitive processing domains<sup>125</sup> and motor control networks<sup>126</sup>.

Despite their common use for the study of cortical function, there are still two hypotheses about what happens within cortical networks to produce ERPs. One hypothesis is that ERPs reflect the summation of independent cortical activity in numerous sources evoked by the task. The alternative hypothesis is that tasks may cause phase resetting of ongoing oscillations in cortical networks, such that the averaging of synchronised oscillations over trials generates the ERP. However, these two options cannot yet be definitively experimentally dissected<sup>127</sup>, and both phase resetting and incoming cortical signals may contribute. It is also likely that this contribution varies between ERPs associated with different paradigms. Nonetheless, measurement of the sizes (maximum amplitudes, areas etc.) and latencies of the peaks within an ERP provide measures of the activation of

cortical networks required to perform a task, and therefore any disease-related abnormalities within these networks<sup>125</sup>.

#### *Event related spectral perturbations*

While ERPs capture valuable time and phase locked changes in signal amplitude, the assumption that non-phase locked signals are task-irrelevant is inaccurate. Averaging across trials discards information on task-related, non-phase locked changes in the amplitude of oscillations at specific frequencies. These oscillations reflect the flow of signals within and between brain regions as network nodes communicate. Therefore valuable information regarding task related changes to ongoing network communication may be lost<sup>128</sup>. This information can, however, be captured by “time-frequency” analysis, where task related changes in the power of each frequency band are calculated across the time window of interest. This can be achieved by first quantifying the power for each frequency of interest at each time point per signal epoch (segment of EEG data time locked to a stimulus/task performance) before averaging these power values across trials. The resulting average power value for each point in the time-frequency landscape is then referenced to mean baseline power for that frequency. Deviations from baseline power upon stimulation or task performance are referred to as event related spectral perturbations (ERSP), with a relative decrease referred to as event related desynchronization (ERD), and relative increase referred to as event related synchronization (ERS)<sup>119</sup>.

In motor cortical circuitry, decrease in alpha and beta band power has been associated with motor planning. This begins in the contralateral sensorimotor region approximately two seconds before movement begins and becomes bilateral immediately preceding onset of movement. This ERD has been interpreted as an electrophysiological representation of the thalamo-cortical system increasing activity of cortical areas involved in the production of a movement. Within the first second after movement ends, beta oscillations are found to be induced in the primary motor cortex (while alpha oscillations remain desynchronised). This synchrony is most prominent over the contralateral sensorimotor cortex, peaking at approximately 1s after movement termination. This beta ERS is attributed to a shift of the primary motor cortex from activation to an inactive state<sup>119,129</sup>.

ERSP related to cognitive tasks are less frequently studied, and therefore their physiological underpinnings are less clear. However, important task related oscillatory changes uncaptured by ERPs have been observed for tasks of memory<sup>130</sup>, emotional

intelligence<sup>131</sup> and attention<sup>132</sup>. Cognitive task-induced ERD in slower alpha (8-10Hz) has been associated with attention while faster alpha (10-12Hz) ERD is associated with memory<sup>133</sup>. Such oscillations may provide valuable measures of disruption to cognitive network communication in disease and aid in discrimination of diseases or their subphenotypes<sup>134</sup>.

#### *Source localisation of M/EEG*

While M/EEG directly measures neuronal function, has excellent temporal resolution and, in the case of EEG, is far more economical than other functional imaging methods, these advantages have often been considered to be negated by M/EEG's poor spatial resolution, limiting the ability to attribute findings to specific cortical regions. This is now surmountable, however, with the use of source localisation algorithms. These methods employ different physiological assumptions and mathematical models to solving the "inverse problem". That is, there is no unique solution to the level of activity in each cortical source which could lead to the generation of the signals collected by each electrode during M/EEG. This is because there are orders of magnitude more sources of electrical activity in the brain than the number of electrodes that can be used to record cortical data. These source localisation methods require a source model, which outlines the location and number of activity sources and a head model, which describes the volume of the head, its composite tissues and the tissues' electrical conductivities, and their position relative to the electrodes. The algorithm employed then determines a "forward model", that is, the activity expected in each electrode given activity in each source, based on the method's physiological assumptions. This model is inverted and employed for "inverse modelling" of the M/EEG signals recorded to determine the most probable cortical source activity pattern which produced this signal<sup>135</sup>. This provides much higher spatial resolution to the data and the ability to interrogate activity in specific cortical sources during a task or at rest.

The earliest source localisation was achieved by dipole fitting. In this method, the inverse problem is tackled through assumption that only a small number of cortical sources produce a signal. By specifying a small number of electrical dipoles, including their positions and orientations, as the sources (i.e. the source model), the inverse problem is overcome, as the number of electrodes is now much greater than the number of sources. The combination of activity in these dipoles which maximally explains the signal variance can thus provide a model of their individual activity<sup>136,137</sup>. If the sources of a signal have

not been previously determined, iterative searches employing increasing numbers of dipoles, as well as changes in dipole location, can be employed to clarify the sources. Minimisation of residual variance (the signal variance unexplained by the model) is employed to maximise model accuracy<sup>138</sup>.

Many mathematical models have subsequently been developed to facilitate “scanning” of the entire grey matter volume for sources of the EEG signal<sup>135</sup>. Two such commonly employed models are linearly constrained minimum variance (LCMV)<sup>139</sup> and exact low resolution electrical tomography (eLORETA)<sup>140</sup>. LCMV is a beamforming method, whereby a spatial filter is generated which passes the source activity from each voxel in the brain tissue of the head model while attenuating activity from other sources by minimising the power for the filter’s output, using a linear constraint. This method is attractive as it does not require a priori knowledge of underlying sources, employing a grid of all voxels in the brain tissue as a source model. It also has higher spatial resolution than LORETA methods. Its spatial filter is, however, dependent on a covariance matrix generated from the M/EEG data provided, such that localisation may be biased by correlation between the signals from simultaneously active sources. This bias has, however, been found only to occur in cases of extremely high correlation between signals<sup>141</sup>. The LORETA methods, by contrast, are based on the physiological assumption that the most probable pattern of cortical activity is that in which neighbouring dipoles have similar activity. This is mathematically expressed by minimising the Laplacian of the weighted sources, thus overcoming the inverse problem by choosing the most “smooth” spatial distribution of source activity. LORETA methods, like LCMV, do not require a priori knowledge of the source locations, but provide lower spatial resolution. Further, in some cases the assumption of correlation between neighbouring source activity may be inaccurate, such as at the interhemispheric and sylvian fissures<sup>142</sup>. While these mathematical models have been found to identify comparable source activity patterns, the aforementioned advantages and limitations (table 2.1) determine the specific methods best suited for different datasets or analytic pathways.

**Table 2.1. Limitations and advantages of different source localisation methods.** This table has been published in my paper McMackin et al 2019b (table 1), please see appendix 2.2.

<b>Method</b>	<b>Dipole fitting</b>	<b>LCMV</b>	<b>eLORETA</b>
<b>Spatial resolution</b>	Excellent	Good	Low
<b>Temporally correlated source detection</b>	No limitation	Limited	No limitation
<b>Prior knowledge required</b>	Yes	No	No
<b>Full brain map estimate</b>	No	Yes	Grey-matter



### 2.1.2.2. Transcranial Magnetic Stimulation (TMS)

TMS is the external application of a magnetic field to cortical neurons of interest, generating an electrical field around them. This electrical field will produce a charge across the membranes of the neurons in this area of the cortex, which will induce neuronal firing (e.g. the propagation of an action potential along the axon) if of sufficient magnitude<sup>143</sup>. Using an electromagnetic coil placed on the scalp this magnetic field can be delivered in focal pulses to the cortical area of interest. Therefore TMS has the major advantage of providing a method to stimulate the cortex that is both non-invasive and focal, unlike transcranial direct current stimulation<sup>144</sup>.

TMS, coupled with surface EMG of muscles of interest can measure pyramidal (i.e. corticobulbar and corticospinal) tract function, anterior horn LMN function and muscle activation (Fig. 2.3). By applying single stimulating pulses to the primary motor cortex, several commonly-used measures can be estimated, including: amplitude of the motor evoked potential (MEP, the EMG response to a stimulating pulse), the resting motor threshold (the minimum stimulation required to induce a standard motor evoked potential amplitude in 50% of electromyographic responses), cortical silent period (the period of interruption of voluntary muscle activity following stimulation of the contralateral motor cortical regions)<sup>145</sup>, ipsilateral silent period (iSP, the period of interruption of voluntary muscle activity following stimulation of the ipsilateral motor cortical regions<sup>146</sup>) and central motor conduction time (motor evoked potential latency less peripheral conduction time, measured by applying a TMS pulse at spinal level to the lower motor neurons innervating the target muscle)<sup>145</sup>.

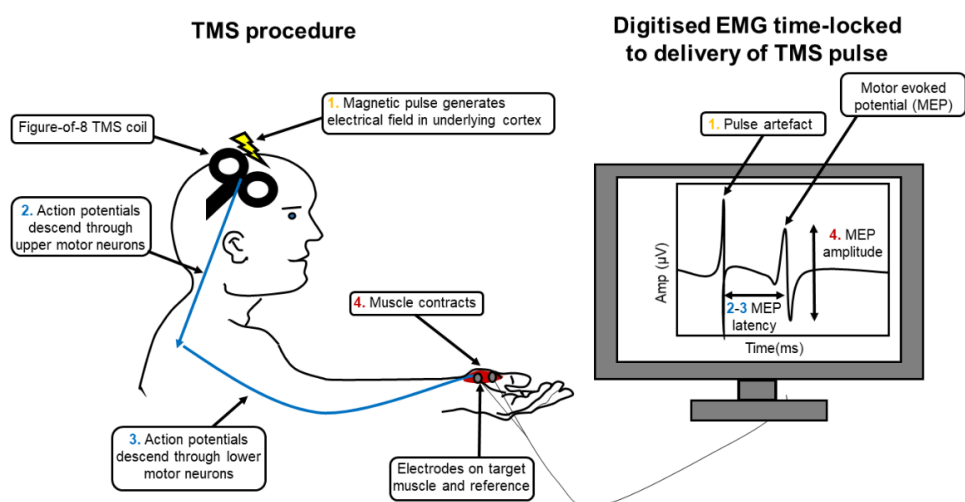


**Figure 2.3. Schematic of a single-pulse TMS procedure and the quantitative characteristics of the resulting motor evoked potential.** This figure has been published in my paper McMackin et al 2019a (figure 3), please see appendix 2.1.

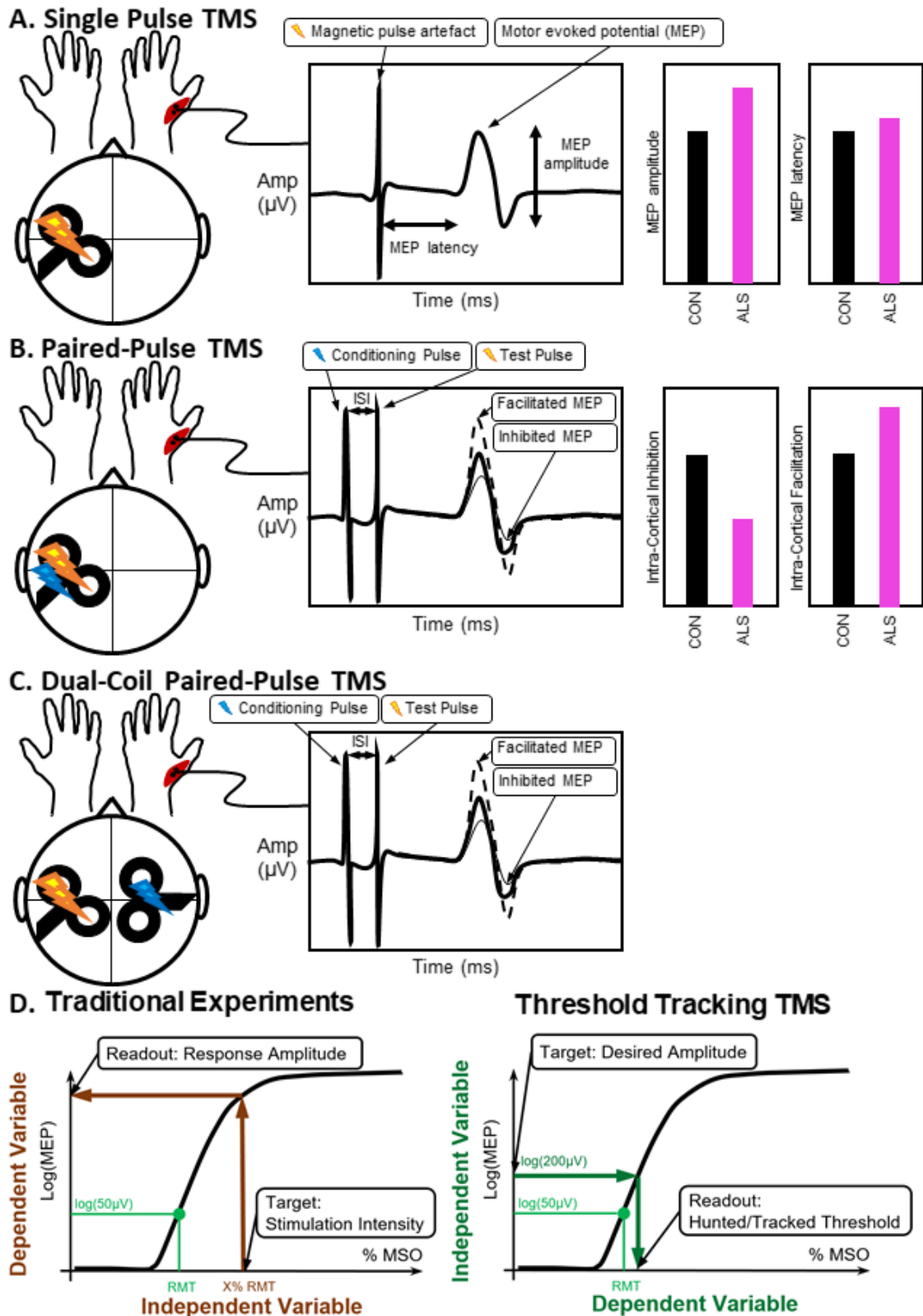


**Figure 2.4.** Transcranial magnetic stimulation (TMS) can provide: (A) single-pulse measures, (B) paired-pulse measures and (C) dual-coil paired pulse measures with (D) threshold tracking can quantify network connectivity changes in the motor system. CON – Controls. This figure has been published in my paper McMackin et al 2019c (figure 3), please see appendix 2.3.

### *Epidural spinal recording for the study of TMS measure physiology*

Evidence regarding the physiological basis of single and paired-pulse TMS is often derived from spinal electrophysiology measurements, specifically of the direct (D-waves) and indirect (I-waves) volleys recorded descending along the spinal cord via the axons of upper motor neurons. Upon sufficient cortical (electrical or magnetic) stimulation, an initial D-wave descends through the spinal cord due to direct activation of the layer 5 pyramidal UMNs of the motor cortex. This is followed by an I<sub>1</sub>-wave attributed to the activation of those layer 2 and 3 cells which monosynaptically activate the UMNs. Thereafter, a number of late I-waves are observed, which show distinct properties from the I<sub>1</sub>-wave<sup>147–149</sup>. A number of theories on the source of late I-waves exist, including the repetitive reactivation of the UMNs by one looping circuit, input from a variety of excitatory circuits and/or activation of distal dendrites of monosynaptic excitatory UMN regulators<sup>148,150</sup>.

### *Specific TMS coil orientations differentially affect descending volley components*

Variation of the orientation of the TMS coil, and therefore direction of the induced magnetic field, relative to the gyrus of interest, influences which cells are activated by the stimuli. In vitro studies indicate that those cortical axons which are bent, with the induced current directed along the axon towards the bend, have the lowest thresholds for excitation and that increasing axonal bend angle from 0 to 90° decreases this threshold<sup>151</sup>. Most TMS-based studies of the precentral gyrus position the figure-of-eight shaped coil over the hotspot of the target muscle with the coil handle pointing towards the back of the head, at a 45° angle away from the nasion-to-inion midline. Electrical current flows in a clockwise direction through the left wing of the coil, and in a counter-clockwise direction through the right wing. As a result, the current generated in the underlying gyrus flows from posterior to anterior (referred to from here onward as posteroanterior (PA) coil orientation)<sup>152</sup>. This coil orientation is typically recommended and implemented<sup>153</sup> as stimulation of the hotspot with this orientation evokes a motor response from target muscles at lower stimulation intensities than when the coil handle is oriented perpendicular to the nasion-to-inion midline (referred to from here onward as lateromedial (LM) coil orientation) or rotated 180° from PA orientation (referred to from here onward as anteroposterior (AP) coil orientation)<sup>154–156</sup>.

While use of PA orientation may facilitate use of lower stimulation intensities, epidural recordings following TMS with different coil orientations indicate that changing the angle of the coil can facilitate interrogation of different components of motor cortical networks. Application of single, monophasic TMS pulses with a PA coil orientation at ascending intensities is found to initially induce I<sub>1</sub>-waves, followed by late I-waves at higher stimulus intensities, with a D-wave only appearing at greater stimulus intensities<sup>147</sup>, indicative that perithreshold PA stimulation acts via layer 2 and 3 cell monosynaptic excitation of the motor cortex, with direct activation of the deeper UMNs only occurring at high intensity stimulation. By contrast, ascending stimulation with LM coil orientation is found to initially produce D-waves which occur later than the D-waves elicited by electrical stimulation, which may reflect more proximal activation of the UMNs, such as at the axon initial region<sup>147</sup>. AP oriented stimulation further differs from LM and PA stimulation by preferentially engaging late I-waves<sup>149</sup>.

#### *Paired pulse TMS*

Paired-pulse TMS provides the use of a conditioning stimulus (CS) at different intervals (typically) in advance of the test stimulus (TS) from either the same coil or a separate coil placed above another cortical region. The conditioning stimulus is applied at an intensity and location that will activate intracortical or interhemispheric network components which regulate motor cortex excitability. By precisely timing the interval between the CS and TS (the interstimulus interval, ISI) the CS will alter excitability of the cortex at the arrival of the TS, resulting in a change in the frequency or amplitude of descending action potential volleys via the spinal cord, ultimately dampening or heightening the amplitude of the associated MEP relative to when no CS is delivered. This can be used to study changes in inhibitory and excitatory circuits modulating motor cortical function. These measures include changes in short- and long-interval intracortical inhibition, intracortical facilitation, short- and long-interhemispheric inhibition and interhemispheric facilitation (Fig. 2.4). Each of these measures is used to interrogate regulatory inputs to the corticospinal tract<sup>157</sup>.

#### *Short intracortical inhibition*

Short intracortical inhibition (SICI), refers to the depression in amplitude of the MEP response to a suprathreshold test stimulus when preceded by 1-6ms by a subthreshold (typically 70% of resting motor threshold) CS delivered via the same coil. Typically two peaks in level of inhibition are observed across this ISI range, at 1ms and 2.5-3ms<sup>158</sup>. While any inhibition across this range is referred to as SICI, it is now acknowledged that

these two peaks in inhibition reflect, at least in part, different underlying physiology<sup>159</sup>. SICI with a 2.5ms ISI (hereafter referred to as SICI<sub>2.5ms</sub>) is elicited at lower CS intensities and is inhibited to a greater magnitude by voluntary activity compared to when a 1ms ISI is employed<sup>158</sup> (hereafter referred to as SICI<sub>1ms</sub>). Pharmacological studies have demonstrated that SICI<sub>2.5ms</sub> is dependent on  $\alpha 2$  and  $\alpha 3$  subunit-containing GABA<sub>A</sub> receptors<sup>160,161</sup>. GABA<sub>A</sub> receptors are ionotropic, facilitating rapid GABA-ergic inhibition via chloride ion influx to neurons, which in turn elevates neuronal membrane potential<sup>162</sup>. By contrast, pharmacological studies have provided less clarity regarding the mechanism of SICI<sub>1ms</sub>. It was proposed that this shorter interval inhibition was the result of delivery of the TS during the refractory period of excitatory interneurons stimulated by the CS<sup>158</sup>. This is unlikely however, as increasing TS intensity increases the amount of inhibition<sup>163</sup>, rather than decreasing or not affecting it, as this theory would predict. Magnetic resonance spectroscopy suggests instead that SICI<sub>1ms</sub> reflects extrasynaptic GABA tone<sup>164</sup>.

It is found that across the ISI range, SICI depresses the late I-waves, not the D- or I<sub>1</sub>-waves<sup>165</sup>, indicating that these inhibitory effects results from activation of inhibitory intracortical networks which indirectly regulate UMNs. Correspondingly, use of AP coil orientation, which preferentially affects late-I waves, has been found to elicit SICI<sub>3ms</sub> of greater magnitude<sup>166</sup>. This is in keeping with inhibition via GABA<sub>A</sub> receptors, whose agonists are also found to depress late I-waves<sup>167</sup>. The specific presynaptic, GABAergic cells engaged remain unclear, however, as layer 5 pyramidal neurons receive inhibitory input from a range of interneurons, including from parvalbumin-expressing interneurons at the soma and from somatostatin-expressing and neurogliaform interneurons at the distal dendrites<sup>148</sup>.

#### *Long intracortical inhibition*

Long intracortical inhibition (LICI) is the depression in amplitude of the MEP elicited by a suprathreshold test stimulus when preceded by 50-200ms by a suprathreshold (typically 120% of resting motor threshold) CS delivered via the same coil<sup>156,168,169</sup>. Like SICI, LICI is found to depress late I-waves and not the I<sub>1</sub>-wave in epidural recordings<sup>167,170</sup>, and is greater with AP, compared to PA, stimulation<sup>156</sup>. There is, however, extensive evidence that the circuitry and neurochemistry which generates inhibition at these longer ISIs is different from that which generates SICI. Pharmacological studies have identified GABA<sub>B</sub> receptors as primary vectors of LICI, while GABA<sub>A</sub> agonists (benzodiazepines) do not modulate this form of inhibition<sup>160</sup>. The GABA<sub>B</sub> receptors are metabotropic,

dampening neuronal excitability by modulating intracellular signalling, a mechanism that is of slower onset and more prolonged duration than GABA<sub>A</sub> signalling<sup>171</sup>. Accordingly, the duration of inhibitory post-synaptic potentials generated by GABA<sub>B</sub> receptors<sup>169,172</sup> are comparable to the ISIs at which LICI is achieved.

While the same presynaptic cells could generate both GABA<sub>A</sub>ergic and GABA<sub>B</sub>ergic inhibition post-synaptically, interaction studies have provided evidence of connected, but differing, underlying circuitry. Namely, SICI is found to be reduced in the presence of LICI<sup>173</sup>, as oppose to the additive or non-interactive effect that would be expected if engaging the same cells in both cases. Epidural recording has demonstrated this is not due to saturation of the circuitry and is mediated via reduction in late I-waves<sup>174</sup>. These findings instead suggest that LICI inhibits SICI-producing inhibitory cells via presynaptic GABA<sub>B</sub> receptors. Further, the fact that LICI is achieved by suprathreshold conditioning and decreases at higher TS intensities, while SICI requires a subthreshold CS and increases with higher TS intensities<sup>163,173</sup>, indicates that different, higher-threshold inhibitory cells generate LICI. In line with this evidence, the degree of SICI and LICI do not significantly correlate within individuals<sup>156,173</sup>. The specific GABAergic cells whose function is reflected by LICI are also unclear. However, neurogliaform cells have numerous characteristics which align their activation with the characteristics of LICI, reviewed extensively by Di Lazzaro, Rothwell and Capogna<sup>148</sup>.

#### *Intracortical facilitation*

Intracortical facilitation (ICF), refers to the increase in amplitude of the MEP response to a suprathreshold test stimulus when preceded by 7-25ms by a subthreshold (typically 70% of resting motor threshold) CS delivered via the same coil<sup>170,175,176</sup>. Pharmacological studies of ICF have implicated glutamatergic activity via its metabotropic NMDA receptor. GABA<sub>A</sub> receptor agonism is also found to reduce ICF, suggesting that at these ISIs some SICI also occurs, counteracting ICF somewhat. Consistently, greater CS intensity is found to increase ICF and diminish SICI<sup>175,176</sup>, while the reverse trends are found in the case of TS intensity<sup>163</sup>. In addition, ICF and SICI show similar influence by pharmacological modulation neurotransmitter systems, supporting the hypothesis that SICI contributes to the net facilitatory effect labelled as ICF<sup>160</sup>.

SICI and ICF do diverge in many of their characteristics, however. ICF is maximal when PA coil orientation is used<sup>176</sup>, while SICI is greater with AP coil orientation<sup>156</sup>. Further, the physiology basis of ICF is much less clear than that of SICI. ICF was determined to be a phenomenon of cortical origin as it did not affect H-reflexes and was

found to facilitate late I-waves when an ISI of 25ms was used. This is not found, however, for the more commonly employed 10-15ms ISI, suggesting that ICF reflects spinal excitability increase. This theory, however, has been contradicted by findings that such a cortical CS does not facilitate an electrical TS delivered to the cervical spinal cord<sup>159</sup>. An alternative hypothesis is that ICF alters the composition, but not amplitude, of descending volleys, resulting in a larger MEP<sup>177</sup>. Together these findings indicate that while ICF is observed in overlap with SICI, the two phenomena have distinct physiological underpinnings. Based on pharmacological studies, ICF has been employed as a measure of intracortical, glutamatergic motor network function<sup>178,179</sup>. However, ICF's vague pharmacological and physiological foundation, as well as poor to modest test-retest reliability<sup>180-182</sup> limits its utility and interpretability in the study of neurodegenerative diseases.

#### *Interhemispheric inhibition*

Interhemispheric inhibition (IHI) is the depression in mean MEP amplitude elicited by a suprathreshold contralateral TS when the TS is preceded by a suprathreshold (typically 120% of resting motor threshold) ipsilateral CS by 8-10ms (short IHI, SIHI) or 40-50ms (long IHI, LIHI). This CS is delivered via a different coil to the ipsilateral motor cortex, at the hotspot for evoking responses the target muscle of the other hand<sup>183-186</sup>. As callosal fibres are largely glutamatergic<sup>187,188</sup>, both SIHI and LIHI (as well as iSP) are considered to reflect glutamatergic transmission via the corpus callosum onto test hemisphere inhibitory interneurons which reduce UMN excitability upon TS arrival<sup>159</sup>. Epidural recordings have demonstrated that late I-waves are reduced by SIHI<sup>184,189</sup>, however such studies have not been performed in the case of LIHI.

Differences in the physiological foundation of long and short IHI are apparent from numerous differences in their characteristics. LIHI correlates significantly with iSP duration and can be elicited by a range of CS intensities, while SIHI does not correlate with iSP and requires higher CS intensities<sup>158,186</sup>. LIHI also has an additive effect with SICI<sup>190</sup>, while SIHI inhibits SICI<sup>163</sup>. However, neither SIHI nor LIHI are affected by the GABA<sub>A</sub> agonist midazolam<sup>191</sup>, indicative that SICI-generating intracortical networks are unlikely to be responsible for SIHI or LIHI.

Both types of IHI are suppressed by SICI or LICI but not ICF in the conditioned hemisphere<sup>192</sup> and are unaffected by conditioning coil orientation<sup>186</sup>, indicating that the same or similar interhemispheric cells are engaged by SIHI and LIHI, but different targets

are activated in the test hemisphere. Correspondingly, only LIHI is found to be enhanced by the GABA<sub>B</sub> agonist baclofen, while the pharmacology of SIHI remains less clear. SIHI decreases with target muscle activation, while LIHI<sup>183</sup> and LICI<sup>168</sup> do not. Further, LICI and LIHI are strongly correlated within individuals<sup>190</sup>. LICI and LIHI also both decrease with increasing TS intensity<sup>190</sup> (although so too does SIHI<sup>193</sup>). GABA<sub>B</sub>ergic cells which generate LICI have therefore been proposed to be engaged by LIHI following callosal transmission<sup>192</sup>. A recent study of the interaction of LICI and LIHI identified mutual inhibitory effects. LICI was, however, also found to convert LIHI to facilitation in one condition<sup>190</sup>, demonstrating that their interaction is not solely explained by inhibitory saturation or competition. Further, LICI and LIHI differ in their interactions with SICI<sup>173,190</sup> which suggests overlapping, but not identical test hemisphere circuitry.

#### *Threshold tracking*

As illustrated in Fig. 2.4D (left), paired-pulse TMS measures of inhibition and facilitation are typically quantified by calculating the mean peak-to-peak MEP amplitude following delivery of the CS and TS as a percentage of the mean peak-to-peak MEP amplitude following delivery of the TS alone. If the CS has an inhibitory effect, this will be below 100%, if it has a facilitatory effect, this will be above 100%. This methodology is susceptible to type-I and type-II error as substantial variation in MEP amplitude occurs with consecutive stimuli of the same intensity. This is due at least in part to spontaneous fluctuations in the resting threshold of neurons<sup>194</sup>. Recognition of such potential variability lead to the development of threshold tracking-TMS, in which the stimulation intensity is varied in order to obtain a specific target MEP peak-to-peak amplitude<sup>158,194</sup> (Fig. 2.4D right). In this approach, the level of inhibition or facilitation achieved is quantified as the TS intensity required to obtain the desired MEP amplitude (to within a specified degree of error) when preceded by a CS as a percentage of the TS intensity required to obtain this response amplitude when unconditioned. In this case, if the CS has an inhibitory effect the percentage is greater than 100, while if the effect is facilitatory, the percentage is less than 100.

A direct comparison of threshold tracking TMS compared to fixed-intensity TMS found that threshold tracking-elicited SICI had excellent intraday and adequate-to-excellent inter-day reproducibility, while that elicited by the classic paradigm performed poorly and poorly-to-adequately respectively<sup>195</sup>. However, as discussed further in section 4.2.2, use of appropriate, statistically accurate criteria for determining the minimum intensity



which will reliably evoke a response of the desired amplitude is important for generating such robust output measures.

### *2.1.3. Network Dysfunction in Neurodegeneration*

#### *2.1.3.1. Resting state studies*

“Resting state” EEG and MEG are used to explore brain activity and functional connectivity in the absence of specific tasks, although it must be acknowledged that the brain is continuously active with ongoing processing of both endogenous and exogenous information<sup>196</sup>. Neurodegenerative conditions exhibit changes in resting state that correlate with underlying pathogenic processes, and there is emerging evidence that resting state EEG has considerable discriminatory value in neurodegeneration.

For example, in ALS, resting state EEG can identify changes in the sensorimotor cortex, as exemplified by the presence of decreased alpha-band power<sup>108,197,198</sup>. By contrast, broadband gamma power is increased over the motor cortex in PD, a finding that also differentiates PD from dystonia and essential tremor. This difference has been attributed to PD-related changes in the spiking of pyramidal cells<sup>199</sup> and may aid in differential diagnosis. Increase in basal ganglia-cortical beta power is also consistently identified in PD<sup>112,200,201</sup>. The pathological effect of such excessive oscillations has been established using deep brain stimulation, with 5–20 Hz stimulation, but not 30-50 Hz stimulation, exacerbating bradykinesia<sup>200</sup>.

Resting state EEG can also detect changes in brain connectivity. In ALS, resting state studies have identified increased connectivity throughout the cortex including increased median absolute coherence in theta and gamma band frequencies over prefrontal areas, accompanied by decreased gamma band synchrony for some prefrontal electrodes<sup>108</sup>. Cortical gamma band oscillations have been linked to higher cognitive functions such as intermodal selective attention and perception<sup>117</sup>, therefore potentially providing a quantitative measure for detecting early cognitive impairment in ALS. In PD, decreased frontoparietal connectivity coherence in alpha band is also associated with early executive impairment<sup>202</sup>, suggesting that deterioration of frontoparietal attention networks contributes to executive dysfunction in PD.

Numerous studies have highlighted the utility of combining such resting state EEG activity and connectivity measures for differential diagnosis of neurodegenerations, particularly the dementias<sup>203</sup>. For example, using temporal high beta, parietal theta and alpha and high beta power, a stepwise discrimination function can distinguish AD and

FTD patients with 84.6% accuracy and is highly accurate in separating controls (100%) from FTD patients (84.6%)<sup>204</sup>. With increase in computational power, this methodology has been enhanced, with training support vector machine classifiers using 25 EEG parameters capable of deciphering AD, PD, dementia with Lewy bodies and bvFTD with 100% specificity and sensitivity<sup>205</sup>.

Such multidimensional biomarkers may also be enhanced by the addition of imaging and/or psychological task parameters to capture differences between broad, overlapping network pathologies. This has been demonstrated by logistic regression models combining cognitive task performance with delta and theta oscillatory activity which provide 93.3% accuracy when distinguishing AD from FTD<sup>206</sup>.

EEG measures can also quantify responses to drug therapies, for example in PD patients L-DOPA is found to induce widespread reduction in cortical delta and alpha activity, considered to reflect an excitatory effect of dopamine neuromodulation<sup>207</sup>, in addition to suppressing elevated beta oscillations in correlation with motor improvement<sup>208</sup>. Such measures therefore have potential to provide objective, quantitative measures of drug effects on neurodegenerative pathology, enhancing the power of clinical trials. This potential has already been harnessed as a dose-finding pharmacodynamic biomarker in rodents, wherein dose-dependent increase in gamma band power in rats was used to estimate therapeutically relevant concentrations of a potential antidepressant drug in humans. This effect translated to similar increases in human resting-state EEG upon drug delivery<sup>209</sup>.

Longitudinal resting-state M/EEG studies have been performed for a number of neurodegenerative conditions, but they are few in number. In AD, relative alpha and beta power is decreased, while relative theta and delta power increased longitudinally<sup>210</sup>, with changes in relative theta power capable of distinguishing between different stages of dementia. This pattern is consistent across populations<sup>211,212</sup>, demonstrating a global slowing in brain network signalling in AD.

Longitudinal increase in beta power has also been observed in PD, correlating with decline in Rey Auditory-Verbal Learning Test performance<sup>213</sup>. PD patients also show early impairment in brain network local efficiency as well as network decentralization which progress over time<sup>214</sup>.

In ALS a single longitudinal resting-state study has been reported revealing widespread, progressive increase in median coherence in theta and low gamma band frequencies<sup>108</sup>. This suggests that abnormal functional connectivity worsens throughout ALS pathology.

Network activity may increase at disease onset and decline thereafter, and accordingly future studies will also require correlation with time from disease onset, and clinical stage of disease.

These studies demonstrate the ability of resting-state EEG to characterize and quantify neurodegenerations and their progression (see table 2.2). In all cases, to attribute the recorded changes to specific networks, source localisation will be required. Moreover, future longitudinal studies will require extensive validation across large groups of well-phenotyped patients.

**Table 2.2. Neurophysiological biomarkers for and therapies in neurodegeneration.**  
 CT – Clinical trial. DLB – Dementia with Lewy Bodies, AD - Alzheimer's disease, PD – Parkinson's disease, FTD – Frontotemporal dementia, MMN – Mismatch Negativity, rTMS – Repetitive TMS, DBS – Deep brain stimulation, SICI – Short Interval Intra-Cortical Inhibition, UPDRS - Unified Parkinson's disease Rating Scale, ADAS-cog - Alzheimer's Disease Assessment Scale-Cog.

Technology	Method	Clinical application	Disease	Example	
				Biomarker/ Symptom	Reference/ Clinical Trial ID
EEG/MEG	Resting state	Differential diagnosis	FTD, AD, PDD,	Multiple	203–205
		CT outcome measure	DLB PD	Beta power	207,208
TMS	Paired pulse	Diagnostic biomarker	ALS	SICI	215,216
		CT outcome measure			NCT02450552, NCT02781454
rTMS	To leg area of motor cortex	Therapy	MS	Spasticity	217,218
			PD	Freezing of gait	219,220
	To leg area of motor cortex				NCT02850159
	To dorsolateral prefrontal cortex or motor cortex			Refractory depression	221
	To dorsolateral prefrontal cortex		FTD, AD	Language, memory, executive function	222,223
					NCT02621424

DBS	To basal ganglia	Therapy	PD	UPDRS score, mobility, activities of daily living, emotion, stigma, discomfort	224
	To nucleus basalis		AD	ADAS-cog	225

### *Source Localization of Resting State Measures*

Source-level studies using quantitative EEG can correlate pathological neuroelectric signals with anatomic locations. For example, in AD increases in delta band activity are localised to orbitofrontal and temporal cortices, while FTD patients differ, exhibiting decreases in low alpha band activity in these areas<sup>226</sup>. By contrast, reduced alpha activity in occipital sources and widespread increase in delta sources is revealed by source localisation in PD with and without cognitive impairment<sup>207</sup>.

Source localisation can also be used to enhance the spatial resolution of connectivity measures. For example, localised lagged linear connectivity in alpha band has been found to discriminate AD, dementia with Lewy bodies and PD dementia from controls with areas under the ROC curves of 0.84, 0.78 and 0.75 respectively. Source localisation of EEG resting state connectivity in ALS patients has also revealed increased functional connectivity between the posterior parietal cortices and between the posterior parietal and motor cortices, dorsolateral, dorsomedial and ventrolateral prefrontal cortices. Source analysis also reveals increases in general connectivity of the anterior and posterior cingulate cortices, frontoinsular cortex, anterior insular cortex and dorsomedial and ventrolateral prefrontal cortices to other brain areas in ALS<sup>227</sup>. Source localised EEG measures therefore provide objective evidence that ALS and FTD have overlapping pathologies<sup>228</sup>, with cognitive networks disrupted in FTD, such as the frontoparietal attention networks<sup>229</sup>, also dysfunctioning in ALS, while central and parietal activity known to be abnormal in ALS<sup>108</sup>, is found to distinguish FTD from AD<sup>226</sup>.

### *2.1.3.2. Activation Studies*

#### *Event-related M/EEG*

Network performance can also be quantified by measuring frequency or time domain characteristics of M/EEG signals generated by the performance of motor<sup>124</sup>, sensory<sup>230</sup> or cognitive<sup>118</sup> tasks designed to activate target neural networks.

#### *Motor tasks*

M/EEG can provide quantitative measures of motor network performance during movement. Movement-related alpha and beta ERD is used to quantitatively measure motor cortex dysfunction in disease. For example, in MS, latency of this ERD correlates with structural MRI T1 lesion volume and T2 lesion load<sup>231</sup>, while in PD, ERD begins closer to movement onset<sup>232</sup>, particularly in the affected hemisphere<sup>233</sup>. This difference is partially corrected by L-DOPA<sup>234</sup>.

Change in post-movement ERS has also been documented in MS, PD and ALS, providing additional quantitative measurement of motor cortex dysfunction. In MS, the latency of the ERS peak is significantly later and correlates to longer information processing speeds<sup>235</sup>, while in both ALS<sup>236</sup> and PD<sup>237</sup> post-movement ERS is reduced, even during dopaminergic treatment<sup>238</sup>. In ALS, negative correlations between this ERS and measures of structural (subcortical frontal apparent diffusion coefficient) and functional (MEP to compound muscle action potential ratio) corticospinal tract integrity have also been reported<sup>236</sup>. Decrease in post-movement ERS may therefore represent a measure of impaired inhibition or excess activity of upper motor neurons.

The time domain characteristics of M/EEG can provide additional neurophysiological correlates of motor tasks, known as movement related potentials (MRPs)<sup>118</sup>. There are three major MRPs elicited during motor anticipation. These are the Bereitschaftspotential (BP, also known as the 'readiness potential'<sup>239</sup>), the contingent negative variation (CNV), and the stimulus-preceding negativity, all long-latency negative potentials. These ERPs are distinguished based on the protocol used to generate the ERP<sup>240</sup>. CNV consists of an early, frontocentral wave and a late, centroparietal wave<sup>241</sup> and it is argued that late component of CNV is at least partially composed of the stimulus-preceding negativity and/or BP<sup>242,243</sup>. Source localisation has attributed the early BP to the supplementary motor area (SMA)<sup>239</sup>, followed by activity in the premotor cortices and then the contralateral premotor and primary motor cortices<sup>124</sup>. The contingent negative variation (CNV) has been localised in part to the premotor cortex and SMA<sup>243</sup>; however, the CNV also represents prefrontal network activity in the orbitofrontal, mesial

and dorsolateral prefrontal cortices, unlike the BP<sup>244</sup>, therefore capturing additional cognitive network components.

In PD, BP peak amplitude is not affected in patients compared with controls, although the early part of the waveform is attenuated<sup>245</sup>. Decrease in peak amplitude does, however, correlate with increasing disease severity<sup>246</sup>. This may reflect inadequate activation of the SMA by the basal ganglia<sup>245</sup> or SMA pathology in PD. Comparable findings in ALS, wherein BP amplitude is inversely correlated with spasticity<sup>247</sup>, demonstrate an overlap in the network pathology of these two neurodegenerations in the basal ganglia and/or the SMA. Such clinical correlation also points to a utility of these measures as prognostic biomarkers.

Mean amplitude of CNV is increased in ALS<sup>248</sup>, decreased in PD<sup>249</sup> and MS<sup>250,251</sup> and unaffected in AD<sup>252</sup>. Furthermore, decrease in CNV amplitude over the parietal cortex in MS correlates with neuropsychological test performance<sup>250</sup>. This suggests that CNV also captures parietal network components pertaining to movement preparation and planning. Localisation analyses have yet to identify the source(s) causing the disease-related abnormalities in MRPs. Such analyses are likely to reveal which cognitive and motor network components contribute to MRP changes in each of these neurodegenerations, highlighting any network overlap and potentially providing distinguishing biomarkers.

#### *Sensory tasks*

Somatosensory ERPs, commonly referred to as SEP or SSEP, can provide information about the involvement of primary somatosensory cortex and its inputs in neurodegenerative diseases. For example, dysfunction of thalamocortical neurons of the ascending somatosensory tracts can be shown in ALS and Huntington's disease (HD). N20, an ERP generated by median nerve stimulation, is attributed to the initial primary somatosensory cortex in somatosensation<sup>253</sup>. N20 has increased latency in HD<sup>254</sup> and ALS<sup>255</sup> patients, indicating pathological delay in transmission of stimuli to the cortex. In ALS, N20 latency increase occurs in the presence of normal peripheral conduction time, while in HD P15 latency (attributed to the brainstem<sup>230</sup>) is normal<sup>256</sup>, indicating that these impairments represent dysfunction of thalamocortical neurons of the ascending somatosensory tracts in ALS and HD pathology.

#### *Cognitive tasks*

EEG can act as a powerful, inexpensive tool in understanding the changes in the activity of cognitive networks, where the utility of single and paired pulse TMS is limited by lack

of a quantitative readout measure upon stimulation of these cortical areas. Functional imaging studies are also limited by the use of blood oxygen level as a proxy for neural activity with poor temporal resolution, limiting dissection of sensory, cognitive and other networks engaged by complex tasks. By contrast, EEG can be used to measure changes in these networks with millisecond-by-millisecond resolution during task performance<sup>118</sup>. Cognitive ERPs can be elicited during specific tasks which engage the functions of interest, providing a quantitative measure of the underlying network function with excellent temporal-resolution. These ERPs, which require little/no participation, can overcome the obstacles of measuring cognitive function using interactive tasks in motor/speech impaired patients. They may also provide a more direct, quantitative measure of pathological dysfunction compared to performance during neuropsychological tests, which have numerous limitations (as reviewed by Cullen *et al.*<sup>257</sup>).

A variety of different cognitive ERPs and ERP subcomponents have been used to objectively assess performance of different cognitive tasks in neurodegeneration. The use of an auditory oddball paradigm, where a “standard” tone is played at regular intervals, occasionally replaced by a different “deviant” tone, has frequently been used to elicit such ERPs in the study of attention. This paradigm, as well as others, can stimulate ERPs which not only reflect auditory stimulation and sensory processing but also overt (captured by the P3 peak) or covert (captured by the mismatch negativity) attention to the changing stimulus. The neural networks and functions associated with frequently employed cognitive evoked potentials are summarised in table 2.3.



**Table 2.3. Event related potentials, the electrode locations where they are best recorded, their associated functions and their cortical sources.** STG – Superior temporal gyrus. IFG – Inferior frontal gyrus. SMA – Supplementary motor area. PMC – Premotor cortex. M1 – Primary motor cortex. MMN – Mismatch negativity. CNV – Contingent negative variation, BP – Bereitschaftspotential, Nd – Negative difference, PN – Processing negativity

ERP	Timing	Sensor space peak locations	Role	Cortical sources	Change in ALS
<b>Cognitive</b>					
<b>N1</b>	+90-200ms <sup>258</sup>	Cz <sup>258</sup>	Speech and sound perception <sup>259</sup> , sensation seeking <sup>258</sup>	STG posterior to the P2 STG source <sup>260</sup>	↓Amplitude <sup>10</sup> , ↑latency <sup>11</sup>
<b>P2</b>	+100-250ms <sup>258</sup>	Cz <sup>261</sup>	Speech and sound perception <sup>259</sup> , sensation seeking <sup>258</sup>	STG anterior to the N1 STG source <sup>260</sup>	↑Latency <sup>262</sup>
<b>Nd</b>	+180-360ms <sup>261</sup>	Fz, Cz, F3, F4, C3, C4 <sup>261</sup>	Selective attention <sup>261</sup>		↓Amplitude or absent <sup>261</sup>
<b>N2a/MMN</b>	+~200ms <sup>258</sup>	Fz, F3, F4 <sup>263</sup>	Involuntary attention switching, sensory memory, discrimination <sup>263</sup>	Bilateral STG and IFG, left ACC <sup>264-266</sup>	↑Average delay <sup>267</sup>
<b>P3 (P3a+P3b)</b>	+250-700ms <sup>258,261</sup>	Fz, Cz, Pz <sup>268</sup>	Inhibition of activity to allow transmission of stimulus information from frontal (P3a) to temporal-parietal (P3b) cortex <sup>268</sup>	Fronto-parietal networks (ambiguous) <sup>264,268</sup>	↑Latency <sup>269</sup> , ↓amplitude <sup>248</sup>
<b>PN</b>	+50-500ms <sup>270,271</sup>	1 <sup>st</sup> component – Cz. 2 <sup>nd</sup> component – Fz <sup>272</sup>	Selective attention. 1 <sup>st</sup> component – Matching tone to internal template. 2 <sup>nd</sup> component – Updating the internal template <sup>272</sup>	First component – Primary auditory cortex. Second component – Deep frontal cortex. (ambiguous) <sup>272</sup>	↓Amplitude, correlation of ↓amplitude with impairment of motor function <sup>272</sup>
<b>Movement-related</b>					
<b>CNV</b>	Interval between warning and cue stimuli <sup>273</sup>	Cz, Fz <sup>248</sup>	Planning of voluntary movement <sup>274</sup> . Arousal, attention <sup>258,273</sup>	Premotor cortex <sup>243</sup> , prefrontal cortex <sup>244,275</sup>	↑Mean amplitude <sup>248</sup>

<b>BP</b>	1s or more prior to muscle activity onset <sup>276</sup>	Cz, greater over hemisphere contralateral to movement <sup>276</sup>	Planning of voluntary movement <sup>276</sup>	Early – SMA <sup>239</sup> . Late - PMC, contralateral M1 <sup>124</sup>	↓Amplitude in Cz in patients with pronounced spasticity, inverse correlation of amplitude and spasticity <sup>247</sup>
-----------	----------------------------------------------------------	----------------------------------------------------------------------	-----------------------------------------------	--------------------------------------------------------------------------	-------------------------------------------------------------------------------------------------------------------------

---

P3 is a positive peak seen in the average ERP 200-500 ms after attended ‘deviant’ stimuli are delivered in an oddball paradigm. It has been associated with inhibition of cortical networks to facilitate delivery of attention stimuli in the aftermath of an alerting signal<sup>268</sup>, and therefore can be used to quantify attention network impairment in neurodegenerative disease. For example, as P3 latency is longer for more complex stimulus evaluation and decision making tasks<sup>268</sup>, P3 latency is used to test the speed of attentional processes. P3 latency is increased in mild cognitive impairment (MCI)<sup>277</sup>, AD<sup>278</sup>, ALS<sup>269</sup> and PD<sup>279</sup> and is predicted by lesion load in MS<sup>280</sup>. P3 has been shown to be delayed or absent in 100% of a small group of cognitively impaired ALS patients<sup>281</sup> and is inversely correlated to performance in cognitive tasks globally, as well as specifically for language and attention in AD<sup>282</sup>.

Mismatch negativity (MMN, also referred to as N2a) is another cognitive ERP generated by oddball paradigms, however unlike P3, MMN has the advantage that it does not require active patient participation. MMN is a negative peak at approximately 200 ms post-stimulus seen when the average ERP following a standard stimulus is subtracted from the average response to deviant stimuli. MMN is a physiological measure of working sensory memory, involuntary attention switching and sensory accuracy, therefore capturing both cognitive and sensory networks<sup>123</sup> (see chapter 5 for more extensive review of literature regarding what physiology the MMN reflects).

MMN shows increased average delay correlating to response-inhibition task performance in ALS<sup>1</sup>, while in both PD and MS MMN is reduced in cognitively impaired patients compared to those without cognitive impairment<sup>283,284</sup>. Reduced MMN amplitude is also reported in MCI and AD (as reviewed by Horvath *et al.*)<sup>285</sup>. Such cognitive correlations to MMN impairment point to the potential of MMN as an additional quantitative measure of network dysfunction in neurodegeneration.

Few longitudinal studies of change in cognitive ERPs have been published, although in AD the P3 latency has repeatedly been shown to increase over time<sup>286</sup>, with latency increase being more substantial in those with greater cognitive decline.<sup>287</sup>

Source analysis of MMN and P3 can distinguish different degenerations with similar sensor-level ERP changes and provide more information about neurodegenerative pathology. To date however, few studies have utilised source analysis to determine the exact location of the networks producing such abnormalities, and the spatial resolution of existing findings remains to be definitively established.

#### *2.1.3.3. Transcranial Magnetic Stimulation*

It has been demonstrated that change in TMS excitability is a feature of feature of ALS, PD and HD, although the excitable characteristics of these conditions differ. For example, resting motor threshold (RMT), a TMS-based measure of upper motor neuron excitability, is lower in ALS<sup>288,289</sup> and AD<sup>290</sup> but not PD<sup>291</sup> or HD<sup>292</sup>. Conversely, PD patients show greater MEP amplitudes at low stimulus intensity<sup>293</sup> and an inverse correlation between motor impairment and RMT<sup>294</sup>. Additionally, HD, AD, PD and ALS each exhibit less SICI compared to controls<sup>288–292,295</sup>. This suggests that reduced inhibitory input to upper motor neurons contributes to corticospinal tract hyperexcitability. SICI may also capture dysfunction of dopaminergic circuitry. Dopaminergic drugs can increase SICI, while anti-dopaminergic drugs decrease SICI<sup>160</sup>. Furthermore, in PD, dopaminergic drugs and basal ganglia deep brain stimulation can partially rectify reduced SICI<sup>291,295</sup>. In AD, SICI decrease correlates with cognitive decline, and can be partially counteracted by donepezil<sup>290</sup>, also suggesting some cholinergic input to the SICI-generating circuitry. These observations point to the potential utility of TMS-based biomarkers of early neurodegeneration (see table 2.2).

#### *2.1.4. Therapeutic Approaches using Network Modulation*

##### *2.1.4.1. Electrical and Magnetic Stimulation*

Given the extensive literature of network dysfunction across the neurodegenerations, the neurophysiological modulation of these abnormalities presents a potential therapeutic target for these disorders (see table 2.2). In addition to the utility of deep brain stimulation in artificially maintaining basal ganglia function in PD, it is now known to have a separate therapeutic effect on the disease, improving motor function and emotional well-being compared to medication alone<sup>224</sup>. In a small study of AD patients, stimulation of the

nucleus basalis of Meynert stabilised or improved cognition over a year<sup>225</sup>, illustrating the potential utility of deep brain stimulation in other brain network disorders.

TMS can also be used to deliver trains of magnetic stimuli to any part of the cortex, typically at least once per second, in order to alter network activity. This is known as repetitive TMS (rTMS) and has recently been approved as a therapy for treatment-resistant depression<sup>296</sup>. rTMS has now been found to have therapeutic effects in a number of neurodegenerative diseases. Such effects include reduction of spasticity in MS<sup>217,218</sup>, improved cognition and functionality in FTD<sup>222</sup>, improved cognition and reduced cognitive decline in AD<sup>223</sup> and reduced freezing of gait in PD<sup>220</sup>. Furthermore, six out of seven studies investigating the effects of rTMS on refractory depression in PD identified significant improvement<sup>221</sup>. Larger meta analyses have indicated that low frequency TMS in PD patients significantly reduces motor symptoms compared to sham<sup>297</sup>, and that rTMS has a small, but significant positive effect on working memory<sup>297</sup>.

Some such effects are already being brought towards clinical practice. For example, rTMS is currently being investigated as a network modulating therapy for dementia in MCI or AD (NCT02621424) and spasticity in MS (NCT02747914, NCT01106365). A completed trial of rTMS in PD (NCT03219892) has also identified a significant therapeutic effect on freezing of gait as well as ambulatory and motor function<sup>219</sup>.

#### *2.1.4.2. Pharmacological network modulation*

Pharmacological intervention to rectify network dysfunction is being investigated in a number of neurodegenerations. In addition to the correction of neurophysiological measures by existing drug therapies<sup>234,290,291</sup>, novel neurotherapeutics are being investigated on the basis of their network modulating properties. For example, resting-state EEG was utilised as a secondary outcome measure in testing the nutritional aid Souvenaid as a therapy in AD, with change in delta band functional connectivity showing improved trajectory<sup>298</sup>.

A combination of multimodal TMS and EEG evoked potentials was also used as an outcome measure in a phase III trial (NCT01765361) of the recently approved drug ocrelizumab for MS.

These early studies point to a move towards therapies based on modulation of network dysfunction, allowing for earlier, and possibly presymptomatic intervention based on early changes in physiological measures.

### 2.1.5. *Conclusion*

Neurophysiological recording and neuro-electric/–magnetic signal analysis can characterize patterned changes of network function in neurodegeneration, opening up opportunities for novel biomarkers of disease progression. The attractive properties of neurophysiological measurements have often been overlooked in the past. The development of focal TMS and source localisation of M/EEG signals can now provide direct measurements of network activity with high spatiotemporal resolution. These new developments provide additional opportunities for neurophysiology-based signal analysis as an additional investigational tool in neurodegeneration.

Directly quantifying network activity can be used to objectively identify neurodegeneration without relying on subjectively-measured symptoms which manifest from network dysfunction. This can allow for earlier and potentially presymptomatic intervention, providing greater probability of therapeutic success. Such measures are already being harnessed in clinical trials, however their full potential as outcome measures is still underexploited.

Neuroelectric signalling studies have already sufficiently demonstrated the importance of network dysfunction in neurodegeneration to drive development of network modulating stimuli and drugs as the therapeutic options and suggests that other pharmacologic agents that act to modulate network dysfunction are likely to be of therapeutic benefit. Additional studies are now required to fully exploit the potential of M/EEG and TMS across the range of neurodegenerations, including additional processing and source localization that can discriminate different disease subtypes.

## 2.2. The Application of Electrophysiology for Understanding Amyotrophic Lateral Sclerosis

Recognition of non-motor symptoms and extra-motor cortical degeneration in ALS (see section 1.1.1) has inspired research of the nature of brain network deterioration in ALS beyond the motor cortex and spinal cord. Understanding which brain regions contribute to the motor and/or non-motor symptoms of the disease and investigating how the networks within and between these regions change in ALS could facilitate crucial (a) understanding the early stages of disease pathology and its spread to enhance early diagnosis and therapeutic intervention, (b) subcategorisation of the disease and their corresponding prognoses and (c) development of quantitative ALS biomarkers on the basis of changes in network structure and/or function. In this section, the literature regarding motor, prefrontal, temporal and parietal regions of cortical pathophysiology in ALS is reviewed, alongside imaging- and biochemistry-based evidence of neural network deterioration in these areas, grouped by anatomical location.

### 2.2.1. Motor cortex

#### 2.2.1.1. Upper motor neurons in the primary motor cortex (M1)

The hallmark of ALS is the degeneration of both upper and lower motor neurons of the corticospinal tract and corticobulbar tract, essential pathways in voluntary movement<sup>2,299,299</sup>, whose deterioration leads to the motor symptoms of ALS. UMNs project from the cortex of the brain to indirectly or directly synapse on bulbar or spinal lower motor neurons (both  $\alpha$  and  $\gamma$ ) which stimulate contraction of the skeletal muscles they innervate<sup>300,301</sup>. They also form many intracortical connections by which they communicate with other UMNs via axon collaterals<sup>302</sup>. The UMNs of the cortex are mostly (37%) located in the primary motor cortex (the precentral gyrus, M1)<sup>303</sup>. M1 also contains GABAergic inhibitory cells, which regulate the UMNs and help to coordinate UMN control of different muscles. These inhibitory interneurons may also, alongside excitatory UMN axon collaterals, be involved in motor learning and motor cortical remodelling. These inhibitory cells are found to account for 99.95% of cells in the macaque M1 (as reviewed by Keller *et al.*<sup>302</sup>).

There is extensive literature on the degeneration of the precentral gyrus in ALS patients, including thinning<sup>304–307</sup>, reduced number of neurons<sup>308</sup> and decreased grey matter volume<sup>309</sup>. In addition to the extensive body of information on M1 motor neurons in ALS,

there are a number of other cortical areas which contain motor neurons<sup>303</sup> and have been found to show reduced neuron number, regional cerebral blood flow, cortical thickness and/or grey matter volume in ALS. These include the primary somatosensory cortex (32%, the postcentral gyrus)<sup>308</sup>, the SMA (25%)<sup>255,305,310,311</sup> and the premotor cortex (7%)<sup>255,309,311</sup>. Corresponding to these areas of cortical degeneration, loss of integrity of their descending fibres in the corticospinal tract has also been shown by voxel-based morphometry and diffusion weighted imaging in ALS patients<sup>312–314</sup>.

These measures cannot be harnessed into a quantitative biomarker for diagnosis or prognosis of individual patients as they do not detect significant UMN degeneration in all patients due to disease heterogeneity, even though this pathology is an ALS hallmark. Therefore, according to the El Escorial criteria<sup>63</sup>, the diagnostic utility of clinical MRIs is currently restricted to the exclusion of mimic conditions. At present, clinical identification of UMN symptoms, which may be obscured by symptoms of LMN, interneuron and  $\gamma$  motor neuron degeneration (as reviewed by Swash et al., 2012) and is dependent on examiner experience and bias, is the main methodology for detecting UMN involvement<sup>315–317</sup>.

#### *2.2.1.2. Functional changes in M1*

##### *TMS measures*

While the symptoms attributed to UMN involvement are well-established, the pathophysiology driving UMN deterioration is not. TMS studies over the past 30 years consistently provide evidence that UMNs become hyperexcitable in ALS, particularly in presymptomatic/early ALS. Such evidence first emerged in 1991 with findings of lower resting motor threshold in 7 ALS patients compared to healthy controls<sup>318</sup>. This has now been replicated by numerous studies<sup>194,289,319,320</sup>. Increase in maximum MEP amplitude<sup>2,194,216,289,321</sup> and reduction in cortical silent period<sup>2,194,289,322–327</sup> have also been repetitively reported in ALS patients, consistent with hyperexcitability of UMNs. Cortical silent period and resting motor threshold have also been found to be reduced in some presymptomatic ALS patients<sup>216</sup>. These differences, particularly in presymptomatic patients, all provide evidence that hyperexcitability in UMNs is an early component of ALS pathology.

Longitudinal studies found that MEP amplitude decreases<sup>328</sup> and that both resting motor threshold<sup>328,329</sup> and cortical silent period<sup>330,331</sup> increase with progression of the disease to the point where in some patients the motor cortex cannot be stimulated<sup>332</sup>. This is

consistent with initial hyperexcitation being lost with degeneration of the motor system, leading to loss of function. This also highlights the importance of correlation of these measures to disease stage, which may account for contradictory findings identified by a smaller number of studies which found increase in motor threshold<sup>322,323,328,329</sup>, no decrease in cortical silent period<sup>331</sup> or decrease in MEP amplitude<sup>333</sup>.

Each of these contradictory studies utilised classical, fixed-intensity methods of TMS, (see section 2.1.2.2) which shows poorer reproducibility than threshold-tracking TMS<sup>195</sup>. Threshold-tracking studies in ALS patients have consistently shown decreases in motor threshold in ALS patients<sup>2,194,216,289,320,321</sup>. Paired-pulse threshold tracking has also been used to investigate facilitatory and inhibitory local networks in the motor cortex by measuring ICF and SICI respectively. Increases in ICF have been identified by many threshold tracking studies in ALS<sup>70,194,216,289,334,335</sup>, though this difference is often not found to be statistically significant<sup>194,327,336,337</sup>. SICI has consistently been shown to be reduced in ALS, both using threshold tracking<sup>70,289,321,326</sup> and classical<sup>335-337</sup> paired-pulse TMS paradigms. SICI was found to positively correlate to measures of disease progression (ALSFRS<sup>338</sup>, maximum compound muscle action potential, strength-duration time constant and neurophysiologic index<sup>194</sup>) in threshold tracking studies, although not in classical TMS studies<sup>327,339</sup>. Both increased ICF and decreased/absent SICI have also been found in three pre-symptomatic SOD-1 mutant carriers<sup>216</sup>. Longitudinal threshold tracking studies have yet to be carried out in ALS.

Early increase in ICF and decrease in SICI which reduces with disease progression provides further evidence that UMN hyperexcitability is an early pathological mechanism of ALS and suggests that loss of inhibitory control of UMNs, particularly via GABA<sub>A</sub> receptors, contributes to this. Supporting this, decreases in RMT and SICI and increases in cortical silent period and MEP amplitude are also found to be significant in the cortex contralateral to site of disease onset but not in the ipsilateral cortex in patients with relatively preserved compound muscle action potentials<sup>320</sup>. This indicates that UMN hyperexcitability is related to the location of first symptomatic presentation and is not driven by LMN dysfunction, and that the origin of the UMN dysfunction is the deterioration of cortical inhibitory interneurons.



### *Resting-state M/EEG measures*

Decreased alpha power in ALS patients at rest has repeatedly been identified over the sensorimotor cortex at sensor<sup>108,197,198,340</sup> and at source level<sup>341</sup>. Alpha frequency oscillations are attributed to the UMNs<sup>342</sup> so loss of power in this band is expected with the progression of ALS. As this decrease in low frequency power occurs at rest, and alpha power is known to decrease at movement onset (see section 2.1.2.1) it is likely that resting alpha represent the maintenance of an inactive state in these large cells by thalamocortical circuitry. Therefore loss of alpha power may be a result of the loss of interneuronal or thalamic control of the UMNs at rest or simply the loss of UMNs themselves. Correlation with TMS single and paired-pulse parameters could help to clarify how the dysfunction of interneurons and UMN individually contribute to this phenomenon.

A large, sensor-level study of over 100 ALS patients recently demonstrated decreased resting-state theta, delta and alpha power over the motor cortices, predominantly in theta band<sup>108</sup>. Subsequent source localisation identified that alpha, beta and theta band changes occur in the right precentral gyrus (as well as in non-motor areas)<sup>341</sup>. Theta band oscillations have been found to be elicited in neocortical brain slices by simultaneous muscarinic receptor activation and GABA<sub>A</sub> mediated disinhibition of neocortical inhibitory interneurons and pyramidal cells. Theta oscillations were found to be independent of GABA<sub>B</sub> receptor activation and require glutamatergic activity. Furthermore this study found current sinks in layer II and III and a current source in layer V during theta oscillations<sup>343</sup>.

These findings highlight numerous similarities to characteristics of SICI-mediating circuitry. Acetylcholine<sup>344</sup> and GABA<sub>A</sub> but not GABA<sub>B</sub> are also found to modulate SICI. Furthermore, one model of the late I-waves (see epidural section 2.1.2.2) suppressed by SICI proposes they originate from the reverberating activity of circuitry consisting of layer II and III excitatory cells and their reciprocal monosynaptic connections with layer V pyramidal tract neurons, along with the associated GABAergic connections<sup>345</sup>. This suggests that change in theta power may capture dysfunction the same or similar inhibitory interneuronal circuitry to that producing decrease in SICI in ALS.

### *Event-related M/EEG measures*

During motor tasks, movement-related beta band ERD (see section 2.1.2.1) has been found to be reduced in ALS in some studies<sup>340,346</sup>, but not others<sup>236,347</sup>. Beta ERD is found to be conserved in primary lateral sclerosis (an UMN disease)<sup>347</sup> despite patients showing

decreased amplitude movement-related potentials<sup>348</sup>. This indicates that beta ERD does not originate in the large pyramidal UMNs of M1. Therefore, if truly abnormal in ALS, this change in ERD may reflect dysfunction of UMN-regulating interneurons, ascending cells which regulate M1, or non-UMN M1 cells which receive thalamo-cortical input. Although this ERD is not specifically associated with corticobulbar circuitry, reduced movement-related alpha and beta desynchronisation in ALS has been associated with speech impairment<sup>198</sup> and bulbar scale but not upper extremity strength<sup>346</sup>. A potential explanation for this is provided by a study of ALS patients with respiratory failure which identified abnormal inspiratory neck muscle activity during spontaneous breathing<sup>349</sup>. The authors proposed that diaphragm weakness in bulbar-impaired patients can lead to compensatory cortical activity to drive breathing. Such additional activity of the motor cortex might mask or prevent observation of time-locked ERD during motor tasks. However as bulbar impairment is known to be a negative prognostic indicator<sup>350</sup>, and was shown to be negatively correlated to disease duration in one of these studies<sup>346</sup>, it is likely that there are numerous other confounding disease factors contributing to this relationship.

Beta band movement-related synchronisation has also been found to be reduced in ALS<sup>236,340</sup>. One of these studies also identified negative correlations between this beta ERS and measures of structural and functional corticospinal tract damage<sup>236</sup>. The authors noted that decreased ERS might be due to impaired inhibition or excess activity of UMNs, in line with TMS study findings. This is supported by a TMS study in healthy individuals which demonstrated reduced corticospinal tract excitability (MEP amplitude) in the first second following movement termination, the time period in which beta ERS is found to occur<sup>351</sup>, concurrent with the hypothesis that decreased beta ERS in ALS is due to impaired inactivation of UMNs. Direct comparison of these TMS and M/EEG measures has yet to be performed in ALS, however, which could draw a more definitive conclusion about the circuitry they capture.

#### *2.2.1.3. Biochemical changes in M1*

Physiological findings of impaired inhibitory network function are consistent with biochemical evidence of inhibitory interneuron loss in the motor cortex in probable and definite ALS patients. This includes reduced immunohistochemical staining of interneuron-specific proteins (parvalbumin and calbindin-D28K) in the motor cortex<sup>352,353</sup>, altered GABA<sub>A</sub> receptor subunit transcription in the motor cortex<sup>354</sup> and

decreased flumazenil (a GABA<sub>A</sub> receptor binding marker) distribution in PET scan<sup>355</sup>. Alongside the aforementioned findings of hyperexcitability in presymptomatic and early stage patients, studies of SOD-1 mutant zebrafish also indicate that this interneuron loss occurs early in pathology<sup>356</sup> while in TDP-43<sup>A315T</sup> mice, hyperactive somatostatin-expressing interneurons were found to disinhibit layer 5 pyramidal cells<sup>357</sup>. The later decrease of this reduced inhibition with disease progression is consistent with deterioration of UMNs counteracting an initial excess of excitatory activity with loss of inhibitory control.

#### 2.2.1.4. *The premotor cortex and supplementary motor area*

The premotor cortex is believed to select suitable movements for output from M1 (as reviewed by Chouinard and Paus<sup>358</sup>), while the SMA has been implicated in self-initiation of movement in response to sensory cues (as reviewed by Nachev *et al.*<sup>359</sup>). Paired-pulse TMS has not been used to study changes in connectivity between these areas in ALS, although if the obstacle of fitting two coils over these neighbouring areas can be overcome this may provide a valuable insight into any changes in their regulation of M1 in ALS. Further, it is possible to study interhemispheric premotor-M1 inhibition in a similar manner to typical IHI measures<sup>360</sup>.

EEG can, alternatively, be used to measure changes in premotor networks by examining changes in MRPs. Increased<sup>248</sup>/unchanged<sup>361</sup> CNV amplitude has been found in ALS while BP amplitude is found to be reduced over the midline in patients with pronounced spasticity. BP amplitude is also found to show an inverse correlation to Norris ALS score of spasticity in the entire ALS group<sup>247</sup>. The cognitive component of the CNV may explain the discrepancy between CNV and BP changes in ALS. CNV has also been suggested to reflect increased cortical excitability<sup>362</sup>. As increased CNV amplitude was identified in early stage patients<sup>248</sup>, this change could also represent hyperactivity in UMNs or other motor preparatory networks, which may decline later in disease progression.

The lateralised readiness potential, the difference between the BP over the left and right motor cortices, has also been shown to be significantly lower in amplitude in ALS compared to control. This decrease was associated with greater rates of failure to inhibit movement (stop trials) and smaller differences in unsuccessful and successful stop trial ERPs<sup>305,363</sup>, all indicative of deterioration in accurate motor planning due, at least

partially, to premotor cortex dysfunction. Source localisation of these abnormal ERPs in ALS is, however, warranted to directly quantify the contribution of the SMA, premotor, prefrontal and primary motor cortex to these ERP abnormalities.

#### 2.2.1.5. *The basal ganglia*

The basal ganglia have a well-established role in modulation of motor output through communication with the cortex<sup>364,365</sup>. Neuroimaging studies of ALS patients have demonstrated that atrophy of the caudate and nucleus accumbens are key elements of the disease. This circuit may play an important role in SICI based on its influence by dopaminergic drugs<sup>160,291,293,366</sup>. A comparison of structural or functional imaging of the basal ganglia with SICI measurements in ALS patients would provide a valuable insight into the extent to which basal ganglia degeneration contributes to the aforementioned reduction in SICI and might help to explain heterogeneity in SICI reduction between disease stages or within the disease population.

The basal ganglia may also represent a structure of both cognitive and motor symptomatic importance in ALS as non-human primate studies in the last 20 years have suggested additional cognitive circuits exist within these subcortical structures. These include tract tracing studies which have identified pathways linking the caudate nucleus and the dorsolateral prefrontal cortex as well as the nucleus accumbens and the cingulate and orbitofrontal cortices, suggesting roles of the basal ganglia in action selection and motivation respectively. Further neuronal recording and neuroimaging studies have provided additional evidence for such functions by demonstrated the processing of motivational information in the nucleus accumbens and cognitive aspects of action selection in the caudate (as reviewed by Trembley *et al.*<sup>367</sup>). A role of the caudate in social cognition has also been suggested based on a case study of a patient with a focal caudate lesion, in which the patient showed impairments in social cognition in the absence of any other neuropsychological symptoms<sup>368</sup>. Therefore deterioration of frontostriatal pathways may contribute to symptoms of cognitive impairment such as executive dysfunction, apathy and impaired social cognition<sup>369</sup>, however studies of the correlation between this degeneration and such cognitive symptoms are required.

#### 2.2.2. *Prefrontal and temporal cortex*

Cognitive functions are those higher mechanisms such as memory, attention, language, problem solving and planning by which we override reflexive or habitual behaviour in order to produce behaviours according to our own intentions and goals<sup>370</sup>. The

neurological networks which give rise to our cognitive functions are relatively poorly understood, however it is now well recognised that the prefrontal cortex (PFC) plays an important role in cognition and behaviour. The PFC constitutes the frontal lobe outside of the motor areas<sup>371</sup>. The different areas of the PFC have unique but overlapping connections to almost all neocortical sensory and motor areas as well as subcortical structures<sup>372,373</sup>, allowing for the integration of diverse information required to generate these higher level functions as well as for cognitive control of these areas. These connections are more prominent from visuospatial and motor areas in the posterior and dorsal portions of the lateral PFC while the ventral and anterior lateral areas of the PFC receive more input about visual form and stimulus identity. The orbitofrontal PFC receives more input from subcortical structures about one's subconscious biological state<sup>372</sup>.

Deterioration of the orbitomedial frontal and anterior temporal cortex in bvFTD patients is associated with disinhibition, distractibility, purposeless over-activity and lack of social awareness while more extended prefrontal cortex degeneration, including in the dorsolateral prefrontal cortex (DLPFC), is associated with an apathetic, unmotivated state and perseveration<sup>228</sup>. Degeneration of the frontoinsula cortex and anterior cingulate cortex (ACC) are now also recognised to contribute to social-emotional impairment in bvFTD, believed to be due to breakdown of the salience network<sup>374</sup>.

The common co-occurrence of ALS and FTD, the presence of sub-FTD cognitive, behavioural and language symptoms in some ALS patients (see section 1.1.1), the overlap in their associated intracellular pathology (see section 1.1.3) and findings that between 9 and 50% of FTD patients present with possible, probable or definite ALS<sup>375,376</sup>, provides strong evidence of a single disease continuum between ALS and FTD in which patients may suffer from one disorder or the other at either extreme, a combination of both (ALS-FTD) or one disorder predominantly with some sub-clinical expression of the other. This continuum may be a manifestation of degeneration across the frontal and temporal lobes with symptomatic presentation varying depending on the ratio of frontal to prefrontal to temporal degeneration. There is extensive evidence of prefrontal and temporal degeneration in at least some ALS patients who do not reach the symptomatic threshold for FTD diagnosis (summarised in table 2.4). MRI studies have shown grey matter loss in the PFC, including in the DLPFC, inferior and middle frontal sulci, the ACC and medial orbital sulcus<sup>377,378</sup> and the superior, middle and inferior temporal gyri<sup>310,378,379</sup>.

Grey matter atrophy in the inferior and medial temporal gyri has also been found to positively correlate with disease progression rate<sup>307</sup>. Increased mean diffusivity (MD) and decreased fractional anisotropy (FA) have also been identified in the white matter underlying the PFC including the orbitofrontal cortex<sup>313</sup> and the superior, middle and inferior frontal gyri<sup>380</sup>, while PET and single photon emission computed tomography have demonstrated reduced regional cerebral blood flow in the anterior temporal lobe<sup>381</sup> and PFC including the DLPFC<sup>382</sup>, the ACC<sup>311</sup> and the orbitofrontal region<sup>381</sup>. The ACC is also found to have a reduced N-acetyl aspartate to creatine ratio, indicative of neuronal loss<sup>16</sup> and is widely regarded as being involved in emotional regulation<sup>383</sup>.

**Table 2.4. Summary of brain regions with motor and/or cognitive functions for which there is structural and/or neurophysiological evidence of change in ALS.** M1 – Primary motor cortex, S1 – Primary somatosensory cortex, PCC – Posterior cingulate cortex, PMC – Premotor cortex, SMA – Supplementary motor area, S1 – Primary somatosensory cortex, ACC – Anterior cingulate cortex, RMT – Resting motor threshold, CSP – Cortical silent period, SICI – Short intracortical inhibition, MEP – Motor evoked potential, ICF – Intracortical facilitation, rCBF – Regional cerebral blood flow, FA - Fractional anisotropy. MD – Mean diffusivity, GM – Grey matter, IHI – Interhemispheric inhibition, ERD – Event Related Desynchronisation, ERS – Post-movement Event Related Synchronisation, GM – Grey matter, WM – White Matter, NAA - N-acetyl aspartate, Cr - Creatine.

Brain region	Attributed functions	Structural findings	Functional findings
<b>Motor</b>			
M1	Voluntary movement output <sup>384</sup>	↓ GM thickness <sup>304–307</sup> , ↓ GM volume <sup>309</sup> , ↓ neuronal number <sup>308</sup>	↑MEP amplitude, ↓RMT, ↓CSP, ↑ICF, ↓SICI <sup>194,289</sup> , ↓β ERD <sup>340,346</sup> , ↓ERS <sup>236,340</sup> , ↓α <sup>197,198,340</sup> & δ <sup>108</sup> power, ↓ mean activity during movement execution and termination in UMN-disease dominant ALS <sup>385</sup> . <b>Longitudinally:</b> ↑RMT <sup>328</sup> , ↑CSP <sup>330,331</sup> , ↓MEP amplitude <sup>328,330</sup> , ↑SICI <sup>194</sup>
PMC	Voluntary movement programming <sup>384</sup>	↓ GM thickness <sup>255</sup> , ↓ GM volume <sup>308</sup> , ↓NAA <sup>386</sup>	↓Lateralised readiness potentials <sup>305</sup> , ↑CNV amplitude <sup>248</sup> , ↓BP amplitude with spasticity <sup>247</sup> , ↓difference between successful and unsuccessful stop trial ERPs <sup>363</sup> , ipsilateral recruitment during movement execution in UMN-dominant ALS <sup>385</sup> , ipsilateral dorsal recruitment during movement termination, also during initiation and execution in UMN-disease dominant ALS <sup>385</sup> .
SMA	Self-initiated complex movements <sup>384</sup>	↓rCBF <sup>311</sup> , ↓ GM thickness <sup>255,386</sup> , ↓ GM volume <sup>310</sup> ,	↓BP amplitude with spasticity <sup>247</sup> , ↓Mean activity during movement execution, also during termination only in UMN-disease dominant ALS <sup>385</sup>

<b>Cognitive</b>			
ACC	Emotional regulation <sup>383</sup>	↓rCBF <sup>311</sup> , ↓NAA/Cr ratio in bulbar patients <sup>16</sup> , ↓GM volume <sup>378</sup>	↑Nodal degree and coherence – i.e. increased functional connectivity to rest of the cortex <sup>227</sup> .
Sup. And Mid. Frontal gyrus	Contains DLPFC <sup>387</sup> (action selection and behavioural rule performance) <sup>388</sup>	↓rCBF <sup>382</sup> , ↓GM thickness <sup>377</sup> , ↓GM volume <sup>309,310,378</sup> , ↓FA <sup>380</sup>	↑Clustering coefficient <sup>227</sup> – increased connectivity between nodes to which it is directly connected, ↓ mean activity during movement execution and termination in UMN-disease dominant ALS <sup>385</sup>
Inf. Frontal gyrus	Contains VLPFC (storage and selection of conceptual representations) <sup>389</sup>	↓GM thickness <sup>377</sup> , ↓GM volume <sup>309,310</sup> , ↓FA <sup>380</sup>	↑Clustering coefficient <sup>227</sup>
Orbitofrontal region	Uncertain <sup>390</sup> . Contains VMPFC (affective value association in decision making <sup>388</sup> )	↓rCBF <sup>381</sup> , ↓GM thickness <sup>377</sup> , ↓FA <sup>313</sup>	
Frontoinsular cortex	Social-emotional processing <sup>374</sup>		↑Nodal degree and coherence <sup>34</sup>
PCC	Regulation of attention to external stimuli as part of the default mode network <sup>391</sup> .	↓GM volume <sup>392</sup>	↑Power-based functional connectivity to temporal, parietal, motor and prefrontal cortices <sup>393</sup>

---

### **Language**

---

Inf. Temp. cortex	Visual object recognition <sup>394</sup> , face perception <sup>395</sup>	↓GM volume <sup>310,379</sup> , ↓GM thickness correlates with disease progress <sup>307</sup>
Mid. Temp. cortex	Retrieval of lexical syntactic information <sup>396</sup>	↓GM volume <sup>310</sup> , ↓GM thickness correlates with



		disease progress <sup>307</sup>	
Sup. Temp. cortex	Contains primary auditory cortex <sup>397</sup> , phonetic processing <sup>398</sup>	↓GM volume <sup>310,378</sup>	
<b>Motor and cognitive</b>			
Corpus callosum	Interhemispheric communication (see main body text)	↓FA <sup>380</sup> , ↑MD <sup>313</sup>	↓IHI <sup>399</sup> , prolonged latency or lack of iSP <sup>400-402</sup> , increased $\theta$ band interhemispheric motor cortical coherence <sup>108</sup>
Basal ganglia	Modulating motor output, action selection, motivation <sup>367</sup>	↓GM volume <sup>369</sup>	Possible contribution to ↓SICI (see main body text)
<b>Sensory processing</b>			
S1	Conscious perception of touch, temperature and pain <sup>403</sup> , contains UMNs <sup>303</sup>	↓GM thickness <sup>305</sup> , ↓GM volume <sup>310</sup> , ↓NAA <sup>386</sup> , ↓neuronal number <sup>308</sup>	↑N20 latency <sup>255,404,405</sup> , ↓N20 amplitude correlates to disease duration <sup>130</sup>
Posterior parietal cortex		Atrophy in ALSci/bi <sup>406</sup> , ↓GM thickness <sup>305,307</sup> , ↓GM thickness in ALSbi/ALSci <sup>407</sup> ↓WM thickness <sup>408</sup> more so in ALSci	↑Functional connectivity between PPCs and between hemispheres and to M1, DLPFC, DMPFC and VLPFC <sup>227,393</sup>

### 2.2.2.1. Functional change in prefrontal and temporal networks

#### Resting-state EEG

Resting-state studies using both graph theory and minimum spanning tree models<sup>409</sup> have identified increased network connectivity at rest in ALS. A study of 18 ALS patients and 17 controls identified increased connectivity and network efficiency (clustering coefficient) in frontal brain regions, including an increase in nodal degree (the number of

nodes connected to a network node) and coherence (a measure of connectivity) in the ACC and frontoinsula cortex, an increase in the clustering coefficient of the anterior insular cortex, dorsomedial and ventrolateral PFCs and increased directed transfer function (a measure of connectivity) in the anterior insular and frontal regions<sup>227</sup>. This provides objective evidence that cognitive networks disrupted in bvFTD, such as the salience network, are also affected in ALS.

Findings of increased prefrontal connectivity in ALS were subsequently shown in a larger source-space study which interrogated functional connectivity between cortical regions in terms of correlations in signal phase and signal amplitude. This study identified decreased power in the temporal and inferior prefrontal cortex, demonstrating reduced resting activity. Further, both areas show increased amplitude-based connectivity in delta, theta and gamma band and decreased phase-based connectivity in delta and beta band activity with the rest of the cortex. This demonstrates that the inferior frontal and temporal cortex tend to co-activate more with other cortical areas but with less synchronous oscillatory communication. This is consistent with aforementioned evidence of loss of inhibitory interneurons, which control neural network oscillations and activity. Increase in frontotemporal network co-activation in gamma band was also found to correlate to poorer language task performance<sup>341</sup>. Together, these studies demonstrate disruption in the activity of frontotemporal networks when not performing a specific task.

#### *Event related potentials*

While resting-state EEG is providing insights into pathological network changes in ALS, ERPs can provide further insights on how network dysfunction relates to changes in the production of cognitive functions (see table 2.3).

Changes in both overt and covert attention network functions in ALS have been demonstrated by delayed P3/P3a latency<sup>269,410</sup>, P3a and b amplitude decrease<sup>248,261</sup>, decreased processing negativity<sup>272</sup>, lacking negative difference<sup>261</sup> and increased MMN average delay<sup>267</sup>. P3 has also been found to be delayed or absent in 100% of a small group of ALS patients<sup>281</sup> and, in keeping with findings of poorer cognitive performance in bulbar ALS patients than those of spinal onset<sup>411</sup>, bulbar ALS patients demonstrate P3 peaks that are lower in amplitude and later onset compared to spinal ALS patients<sup>412</sup>. Furthermore the aforementioned increase in CNV (see section 2.2.1.4) amplitude may represent change in cortical attention generators.

Each of these ERPs has been attributed to prefrontal and/or temporal cortical activity (see table 2.3). However none of these studies utilised source analysis, therefore the spatial resolution of these findings is highly limited and source analysis is required to determine the exact location of the networks producing such abnormalities. Furthermore, source analysis may highlight changes in the function of cognitive networks even in the absence of sensor-space differences, such as in the case of compensatory network activity.

While ERPs generated during other neuropsychological tests (e.g. Stroop<sup>413</sup>, sustained attention to response<sup>414,415</sup>, and Flanker<sup>416</sup> tasks) are well established, only two studies of such ERPs have been carried out in ALS patients to date. One study using the Flanker test, a test of information processing, selective attention and response control, found no impairment in performance or difference in N2 amplitudes in ALS, although posterior negativity measured over the occipital region showed enhanced amplitude. This is indicative of disturbed modulation of visual processing by the frontoparietal attention networks, which are associated with the selection of sensory information in attentional control<sup>417</sup>. In combination with resting-state EEG findings of increased connectivity of frontoparietal networks in ALS<sup>108,227,341,393</sup> and reduced P3b amplitude, this supports the abnormal increase in frontoparietal network activity in ALS, which may contribute to attention impairments.

The other study in this area examined ERPs elicited by Stroop test in ALS. This study found that ALS patients committed significantly more errors and demonstrated increase in the latency of N1, N2, P3 and the late positive complex (peaking 600-700ms post-stimulus), indicating abnormal sensory, cortical and potentially motor cortical network engagement during this task. The latency of N4 was also found to correlate to disease duration. Using source localisation they also demonstrated that the ALS group exhibited significantly decreased activation of the left superior and middle temporal gyri compared with controls in the P2 time window and significantly reduced activation of the ACC and medial frontal gyrus in the P3 and N4 time windows compared with controls<sup>418</sup>. Unfortunately the conclusions on cognition which can be drawn from this study are limited as ERPs for each group were generated from the overall average of epochs corresponding to both congruent and non-congruent stimuli. Therefore they do not quantify network activity when responses are being inhibited compared to when they are not. The authors noted that they found no difference between separate congruent and non-congruent ERPs on preliminary examination.

#### 2.2.2.2. *Biochemistry in cognitive and language network pathology*

Physiological evidence of hyperexcitability in non-motor regions is supported by PET studies demonstrating hypermetabolism in temporal areas in ALS<sup>379,419</sup> and a range of molecular level studies. For example antibody staining of post mortem tissue samples of 13 ALS patients (compared to 8 controls) revealed a decrease in pyramidal neurons within cortical layer 5 of the DLPFC and ACC as well as calbindin-D28K+ GABAergic interneurons in cortical layers 5 and 6, changes which were also observed in M1. A trend towards decrease of parvalbumin-expressing GABAergic interneurons was also observed in layer 6 of the DLPFC<sup>352</sup>.

Decrease in benzodiazepine-binding GABA<sub>A</sub> receptors in frontal and temporal lobes has been shown by PET studies in which binding of [<sup>11</sup>C]flumazenil is found to be reduced<sup>355,420</sup>. This reduction correlated with poorer verbal fluency task performance in the right inferior frontal, superior temporal and anterior insula<sup>420</sup>. Reduced GABA<sub>A</sub> receptor  $\alpha$ 1 subunit transcription in the PFC and temporal cortex (but not the occipital or cerebellar cortices) has also been identified in post-mortem tissue, alongside upregulation of glutamic acid decarboxylase, a GABA synthesising enzyme<sup>421</sup>. This upregulation is expected as a homeostatic mechanism to increase GABA production in the case of a decrease in GABA<sub>A</sub> receptor expression. These studies, together with EEG evidence, are indicative that decreased inhibition is also present in the PFC and temporal lobes, and that the mechanisms of pathology driving network malfunction in these areas is similar to that in the corticospinal tract.

#### 2.2.3. *Parietal cortex*

Posterior to M1, the parietal lobe includes the postcentral gyrus and the posterior parietal cortex. The postcentral gyrus contains the primary somatosensory cortex (S1). In addition to the contribution of UMN's within S1 to the corticospinal tract<sup>303</sup>, S1 receives ascending somatosensory input via the thalamus and is the point of initial cortical processing of touch, temperature, vibration, pressure, proprioception and pain<sup>422</sup>. Some further somatosensory perception, such as localisation of somatic stimuli, recognising posture and understanding the arrangement of body parts has also been attributed to other areas of the parietal cortex<sup>423</sup>. In addition to its role in somatosensation, the parietal lobe receives cortical input from the visual and auditory cortices<sup>424</sup>, allowing for integration of sensory information which can be delivered to the motor cortices to refine

movement<sup>425</sup>. This sensory information is also delivered via the inversely active central executive and default mode frontoparietal networks from the posterior parietal cortex to prefrontal cognitive areas, so that relevant sensory input can be selected for attention<sup>417</sup>.

As abnormal somatosensory processing by S1 has been found to contribute to motor dysfunction in a number of motor neurological disorders<sup>425</sup> and the posterior plays important roles in executive functioning<sup>417</sup> and sensation<sup>422</sup>, parietal cortex malfunction in ALS may contribute towards motor and/or non-motor symptoms.

The impact of ALS on this region of the cortex has been investigated by a number of imaging studies. A longitudinal diffusion weighted imaging study did not initially detect parietal network disruption in ALS, but found propagation of structural network deterioration from M1 to frontal, temporal and parietal areas later in the disease. Therefore as the disease progresses, it seems that not only can pathology spread to FTD-associated networks but also posteriorly to the parietal cortex<sup>426</sup>. Structural studies have repeatedly identified cortical thinning in the inferior parietal cortex<sup>305,307,309</sup> and reduced neuron number in S1 with strong correlation to that in M1. Significant atrophy of the superior parietal gyrus and precuneus has also been found in ALSci/ALSbi patients but not/less so in ALS without this impairment<sup>406-408</sup>. This suggests a role of posterior parietal cortex degeneration in ALS cognitive pathology.

Functional measures of parietal network function may allow for early parietal pathology to be captured before the structural degeneration captured by imaging. This could allow for earlier cognitive prognosis and stratification of patients according to patterns of network pathology.

#### *2.2.3.1. Functional changes in parietal networks*

##### *Resting-state EEG*

In addition to the extensive evidence of increase in frontoparietal functional connectivity observed in ALS<sup>108,227,341,393</sup> (described in section 2.2.2), increase in interhemispheric parietal functional connectivity has also been identified from resting-state EEG<sup>227</sup>. Further, greater co-activation in frontoparietal networks at rest is found to correlate with poorer executive function<sup>341</sup>, implicating this frontoparietal network disruption in executive decline in ALS.

##### *Event-related potentials*

Median nerve SSEP studies have found normal N9 latency in ALS patients, recorded from Erb's point, indicative that afferent sensory signal transmission across the brachial

plexus is unimpinged. However, increased N20 latency in ALS patients has repeatedly been demonstrated<sup>255,404</sup>, with correlation between decreased N20 amplitude and disease duration also identified<sup>405</sup>. N20 is attributed to the initial primary somatosensory cortex in somatosensation<sup>253</sup>, as is the N1 peak evoked by lower limb-innervating nerves. N1 is often absent in ALS patients compared to controls<sup>427</sup>. This combination of N20 latency increase/N1 absence, normal peripheral conduction time and normal N9 latency indicates that thalamocortical neurons of the ascending somatosensory tracts are affected with progression of ALS pathology. A large study of 145 patients and 73 controls also recently identified larger peak-to-peak N20 to P25 amplitudes in ALS, which was associated with shorter survival. The authors concluded that this reflects sensory cortex hyperexcitability<sup>428</sup>. Therefore an initial phase of hyperexcitability followed by decline with increasing disease duration, as demonstrated in the motor cortex (see section 2.2.1) may also occur in the somatosensory cortex.

#### 2.2.4. *Interhemispheric networks*

The corpus callosum (CC) is the largest interhemispheric commissure, composed of approximately 200 million axons in the human brain<sup>188,429</sup>. Most of these tracts are homotopic (between equivalent regions of the two hemispheres) although extensive heterotopic tracts (between non-equivalent regions) are also present<sup>430</sup>. The functions of the CC include exchange and integration of information between the hemispheres, with facilitation of some cortical activities and inhibition of others. This has both motor and extra-motor roles, including bilateral motor coordination<sup>431,432</sup> and learning<sup>433</sup>, binocular visual functions<sup>434</sup>, language lateralisation<sup>435</sup> and speech comprehension<sup>436</sup> and cognitive functions such as learning, memory and executive functions<sup>437</sup>. The CC shows topographical representation of different cortical regions as homotopic tracts which connect different cortical regions travel through the CC roughly corresponding to the position of these regions along the AP axis<sup>430</sup>. Therefore focal lesions of the CC will affect communication between different cortical areas depending on the location of the lesion along the AP axis of the CC, correspondingly producing different symptomatic presentations<sup>438–440</sup>.

As a preface to review of structural imaging-based evidence of CC pathology in ALS, it should be noted that the application of the diffusion tensor model to studying the CC has inherent limitations. Specifically, this model is insufficient for the characterisation of

regions containing crossing fibres<sup>441–443</sup>. This affects interrogation of the lateral cortical projections of the CC which connect motor regions, due to the presence of crossing fibres from other bundles such as the superior longitudinal fasciculus and the corticospinal tract<sup>444</sup>. As a result, when interpreting DTI-based studies of the CC in ALS, it should be considered that many transcallosal projections are limited to the subset of fibre trajectories that can be detected using this method<sup>445</sup>.

Diffusion weighted imaging studies have repeatedly shown reduced FA and increased MD in the CC of ALS patients<sup>313,380,386,446–449</sup>, both indicative of the degeneration of these white matter tracts. In keeping with the pattern of degeneration in the cortex, deterioration of the CC in ALS is most prominent<sup>386,447,449</sup> and consistently found<sup>306,313,380,386,448</sup> in its motor-associated body. Degeneration has, however, also been repeatedly reported in the genu, containing fibres connecting the prefrontal cortices as well as in the splenium, containing fibres connecting the posterior parietal cortices, the medial occipital cortices and the medial temporal cortices<sup>313,380,446,447</sup>. In a study specifically examining the Brodmann areas associated with the homotopic fibres which degenerate in ALS, FA was found to be reduced in CC fibres connecting the motor cortex, SMA and DLPFC in ALS patients compared to controls. This was not found in homotypic fibres connecting S1, Broca's area, or the orbitofrontal cortices, suggesting that CC fibres interconnecting the motor and dorsolateral prefrontal cortices may be preferentially involved in ALS<sup>448</sup>. This preferential degeneration of CC fibres connecting motor and prefrontal areas may result in the specific deterioration of interhemispheric communication required for the production of motor and cognitive functions respectively. Therefore the contribution of corpus callosum deterioration to the aforementioned ALS upper motor neuron and cognitive symptoms should be investigated through correlation with appropriate structural and neurophysiological measures.

Several structural correlation studies link CC decline to both motor and cognitive symptoms of ALS. FA decline in fibres connecting the primary motor cortices has been shown to correlate to motor decline (ALSFRS score and the clinical extent of UMN symptoms)<sup>448</sup>, disease duration<sup>447</sup> and progression rate<sup>380</sup>. With respect to cognitive impairment, performances in tests assessing attention and executive functions correlated with diffusion tensor imaging metrics of the corpus callosum, corticospinal tract, and long association white matter tracts bilaterally, including the uncinate fasciculi. Addenbrooke's cognitive examination scores in ALS patients have also been found to

correlate positively with myelin water fraction and negatively with intra/extracellular water in the anterior CC (which contains homotypic fibres of the frontal cortices) and in frontal projections<sup>450</sup>. Reduced FA in the corpus callosum has also been related to impaired cognitive flexibility in ALS<sup>451</sup>. These studies are conducive with CC decline contributing to cognitive and motor symptoms in ALS.

#### *2.2.4.1. Functional change in the corpus callosum*

##### *TMS measured changes*

Five studies to date have used TMS-based studies to measure transcallosal activity in ALS, using the iSP and SIHI (see section 2.1.2.2). All studies of the iSP found it was reduced, delayed or totally absent in the majority of ALS patients tested, although some patients show normal measurements<sup>400–402,452–454</sup>. SIHI was also found to be significantly reduced in ALS by a small study (9 patients and 12 controls)<sup>399</sup>. Findings of reduced iSP and SIHI suggest that excessive excitatory activity of homotopic motor CC fibres and/or loss of postsynaptic inhibitory interneurons occurs in ALS. One study identified that the majority of these patients were early stage and 63% of those who showed pathological iSPs showed no UMN signs<sup>401</sup>, indicative that interhemispheric measures could be an important pre-symptomatic measure of motor circuit pathology. Notably, CC abnormalities are identified by these TMS measures before diffusion tensor imaging<sup>402</sup>, consistent with dysfunction preceding structural decline and therefore providing a basis for development of earlier biomarkers.

As impaired transcallosal communication may be an important physiological underpinning of cognitive and or motor symptoms, correlation of such measures to symptoms such as mirror movements in ALS should be explored. Mirror movements are involuntary movements contralateral to an intended movement<sup>401</sup>. A link between mirror movements and loss of CC-mediated interhemispheric inhibition has been inferred based on the observation of this phenomenon in young children before it subsides around the age of 10, coincident with the period of CC myelination. As they can occur with dys/agenesis of the CC<sup>455</sup> this is unlikely to be due to excess childhood excitatory CC function. Mean iSP latency is found to be significantly delayed in ALS patients with mirror movements compared to those without, and all those with mirror movements in this study showed pathological iSP in at least one hemisphere<sup>401</sup>. Another found mirror movements in 88% of the patient cohort showing abnormal iSP<sup>452</sup>.



However all interhemispheric TMS findings in ALS are thus-far limited by low patient numbers and the aforementioned limitations of using fixed-intensity TMS as oppose to threshold tracking. Furthermore, as these measures quantify both CC and inhibitory interneuronal function, concurrent measurement of intracortical inhibition, particularly LICI, in larger populations is needed to investigate the contribution of interneuronal dysfunction to changes in iSP and IHI.

#### *M/EEG measured changes*

Source-space EEG has identified increased theta and gamma-band and decreased alpha-band interhemispheric co-modulation and decreased beta-band synchrony between the primary motor cortices at rest<sup>456</sup>, demonstrating increased co-activation but disrupted oscillatory communication between hemispheres. These findings also indicate abnormal interhemispheric network communication, potentially by loss of inhibitory interneurons which coordinate these oscillations and regulate excitatory input<sup>341</sup>. While the spatial resolution of EEG, even at source level, does not permit the attribution of these findings to specific neuronal populations, such measures also demonstrate potential as early quantitative measures of ALS pathology.

### *2.2.5. Interpreting electrophysiological measures to understand ALS pathology*

#### *2.2.5.1. Degeneration of inhibitory networks in ALS*

There is a broadening consensus that loss of inhibitory networks plays an important role in early ALS pathology<sup>457-459</sup>. As reviewed here, electrophysiological investigation of cortical regions associated with the motor, cognitive and sensory functions in ALS have yielded evidence in support of this across the cortex. This evidence includes reduction in TMS measures of network inhibition in motor and interhemispheric networks, increase in TMS measures of network excitation in the motor cortex, reduction in EEG measures of network synchrony and co-activation and increase in ERP measures of excitability in cognitive and sensory networks. This is complemented by biochemical evidence such as reduced numbers of (parvalbumin+ or calbindin-D28K+) interneurons in motor and prefrontal regions, reduced GABA<sub>A</sub> receptor transcription and binding in motor, prefrontal and temporal regions and increased transcription of the GABA-synthesising enzyme glutamic acid decarboxylase in prefrontal and temporal regions.

A loss of the homeostatic balance between excitatory glutamatergic and inhibitory GABAergic activity can produce an excess of glutamatergic activation of cells<sup>460</sup>. This is expected to initially lead to increased excitability of networks, and perhaps

hyperconnectivity due to the role of glutamate in synaptogenesis and long term potentiation<sup>461</sup>, but ultimately have a degenerative effect on cells, due to exaggerated NMDA receptor activation causing excessive, harmful influx of Ca<sup>2+</sup> to cells<sup>462</sup>. These effects are concurrent with findings of TMS studies support the hypothesis of an initial decline in inhibitory networks (reduced RMT, cortical silent period and SICI<sup>194,289</sup>) followed by a move back towards a balance between excitation and inhibition with later loss of excitatory cells (decrease in MEP amplitude<sup>328</sup> and increase in RMT<sup>328,329</sup>, SICI<sup>194</sup> and cortical silent period<sup>330,331</sup> with disease progression).

Furthermore, resting-state EEG studies demonstrate hyperconnected functional networks in ALS patients<sup>108,227,341,393</sup>, accompanied by reduced gamma band synchrony in frontal regions<sup>108</sup>. Gamma band rhythms are believed to be entrained by inhibitory interneurons, particularly fast-spiking parvalbumin+ interneurons<sup>463</sup> which have been shown to be reduced in M1 and the PFC in ALS<sup>352,353</sup>, therefore reduced gamma band synchrony is also conducive with the hypothesis of loss of inhibitory networks in ALS. These fast-spiking inhibitory interneurons appear to consume much more energy than other types of cortical neurons, such that they are likely to be among the earliest cells affected by drivers of mitochondrial dysfunction and oxidative stress, which have been repeatedly implicated in ALS pathology<sup>464,465</sup>.

#### 2.2.5.2. *Spread of ALS pathology*

The presence of similar molecular and neurophysiological findings in different cortical networks could be the result of autonomous emergence of pathology in different regions or due to a single site of onset with spread to neighbouring regions. Support for the latter hypothesis include the fact that Onuf's, oculomotor and abducens nuclei are usually unaffected in ALS<sup>466</sup>, and evidence of a prion-like self-propagation of misfolded TDP-43 and SOD1 proteins in ALS models which can spread from cell to cell<sup>467</sup>. Furthermore a cell-to-cell form of disease spreading is fitting with the observation of initial loss of structural connectivity in ALS occurring in the motor system, later spreading to surrounding motor, prefrontal, temporal and parietal networks<sup>426</sup>. Such a mechanism of disease spread may explain the nature of the continuum between FTD and ALS pathology, whereby the initial disease presentation and might depend on the site of onset of pathology with the later onset symptomology<sup>468</sup> representing areas to which the disease spreads.

### 2.2.6. *Conclusion*

With the increasing recognition that ALS is a network disorder with pathology beyond the corticospinal tract, electrophysiological insights are necessary to understand how networks in ALS deviate from normal function. These neurophysiological methods can capture pathology in advance of structural evidence. By combining the temporal resolution of these neurophysiological measures with the spatial resolution of imaging studies and source localisation techniques, the functional changes in specific networks in ALS are becoming more apparent and helping to improve understanding of the disease. Further neurophysiological studies are required, however, including source localisation of M/EEG measures and investigation of unexplored TMS parameters, to provide greater detail of the specific networks involved, the longitudinal change in network function as the disease progresses and how these differ in relation to clinical prognosis. Such studies may pave the way for harnessing neurophysiological measures in the clinic, such as in ALS diagnostics, prognostics and clinical trials.

### 3. Aims and Objectives

In this chapter, the aims and objectives of this project are described and the rationale for the proposed approach to completing these objectives are summarised. In section 3.1, what I aimed to achieve is described. In section 3.2 the specific objectives planned in order to meet these aims, and their rationale, are outlined.

#### 3.1. Aims

Given the urgent need for more economical, accurate and objective ALS biomarkers, and the attractive properties of EEG and TMS for characterising and measuring ALS pathology, the overarching aim of my PhD was to harness these methods to improve our understanding of motor and non-motor cortical ALS pathology and to investigate their application in the development of prognostic and diagnostic ALS biomarkers. More specifically, I aimed to determine the following:

1. The nature and location of any abnormal cortical activity evoked by cognitive and cognitive-motor tasks in ALS.
2. If previously proposed TT-TMS-based biomarkers of ALS discriminate ALS patients from controls within the Irish population.
3. If measures of cortical motor network function previously unexplored by TT-TMS differ between ALS patients and controls.
4. If EEG- and TMS-linked EMG measures of cortical network function are of potential diagnostic or prognostic value and warrant further investigation as ALS biomarkers, based on measures of discrimination and effect size and correlation analyses respectively

#### 3.2. Objectives

##### *3.2.1. Compare measures of cognitive and auditory cortical function evoked by the auditory oddball paradigm between ALS patients and controls*

The primary rationale for using the MMN and the ignored auditory oddball paradigm to study non-motor network dysfunction in ALS is that it facilitates investigation of cognitive networks while not requiring active participation by the participant<sup>469</sup>. This is particularly advantageous when recording data from participants of limited motor function due to disease. Prior to the onset of this project, comparison of the MMN between ALS patients and controls already been reported at sensor level by the Academic

Unit of Neurology. Increase in the average delay of the MMN waveform in ALS was reported<sup>267</sup>, indicative of dysfunction in the cortical networks responsible for MMN generation. Due to the poor spatial resolution of this sensor space measure, however, the specific MMN generators disrupted by ALS, producing this waveform abnormality, remained unknown. Therefore, the first objective of this project was to perform source analyses of the MMN, recorded by EEG during the auditory oddball paradigm. We hypothesised that comparison of source-resolved activity underpinning the MMN between ALS patients and controls would clarify which specific cortical generators of this waveform are affected by ALS.

Following examination of the effects of ALS on MMN source activity, we hypothesised that ALS might also disrupt communication within cognitive and/or auditory networks engaged by this task, not captured by ERP analyses. Therefore, as a secondary objective, an additional study was planned to investigate changes in cortical oscillations associated with the auditory oddball task, which were not captured by the previously performed ERP sensor and source space analyses.

### *3.2.2. Characterise how cognitive and auditory cortical function changes over time in ALS*

Existing literature (reviewed throughout section 2.1) indicates that network impairment is spatiotemporally dynamic in ALS. Therefore, we wished to determine if the measures of cortical function investigated here were stationary, and if not, how change in these measures relates to ALS progression. Therefore, EEG was recorded during the auditory oddball task for up to five sessions at approximately 4-6 month intervals to facilitate longitudinal analyses of MMN source activity in ALS. Such longitudinal analysis was possible within the timeframe of this project for auditory oddball task data (but not SART or TT-TMS data) as these longitudinal data began being collected before onset of this project. Longitudinal data are being collected for all other study paradigms for future analysis.

### *3.2.1. Characterise the effects of ALS on cognitive regions associated with cognition and motor control*

We wished to investigate if/how ALS affects cortical domains associated with overt attention and motor control, which were not expected to be engaged by the auditory oddball task. We therefore chose to use a randomised SART paradigm<sup>470</sup> with concurrent EEG recording to engage these domains and compare their function between control and

ALS patient cohorts. This task was chosen as it requires minimal movement (button press by a single finger<sup>470</sup>), and therefore is well suited to performance during EEG recording, as this activity is not expected to introduce substantial movement-related artefacts to the data. Further, this task minimises the motor response required of ALS patients with declining motor function. While the ERP waveforms associated with this paradigm had previously been reported in healthy individuals<sup>126</sup>, the cortical generators of these waveforms had not. Therefore an additional objective in achieving this aim was the application of source analysis to control data to establish and report the sources of motor and cognitive performance-associated peaks in SART ERPs.

The non-phase locked oscillations associated with the randomised SART, not captured by ERP analyses, have also not been previously reported. We hypothesised that task-related motor and/or cognitive network oscillations could be identified with time-frequency analysis, and that such measures could provide additional insights into and potential biomarkers of ALS of EEG. Therefore, as an additional objective, time frequency analysis of data collected during the SART was also planned to characterise SART-related oscillation changes and if/how they are affected by ALS.

### *3.2.2. Compare TT-TMS measures of short intracortical inhibition and intracortical facilitation between ALS patients and controls*

At the onset of this project, a research team in Sydney, Australia, had published several studies demonstrating loss of SICI and increase in ICF in the motor cortex of ALS patients, using TT-TMS. These measures were shown to have with high specificity and selectivity for ALS<sup>194,216,288</sup>. Since the first of these publications in 2006, however, this change had yet to be investigated in other ALS patient populations. Therefore, another objective of this project was to establish a threshold-tracking TMS laboratory at the Academic Unit of Neurology such that SICI and ICF could be measured in Irish ALS patient and control cohorts and differences between these groups could be compared.

### *3.2.3. Compare TT-TMS measures of long intracortical inhibition and long and short interhemispheric inhibition between ALS patients and controls*

Comparisons of TT-TMS measured LICI, which is attributed to GABA<sub>B</sub>ergic motor cortex inhibition<sup>160</sup>, and long and short interhemispheric inhibition, which are associated with CC motor fibre function<sup>471</sup>, between ALS patients and controls has yet to be reported in the literature. We hypothesised that these measures of other aspects of motor network function would provide novel information on which neurotransmitters and tracts within

the motor cortex are affected by ALS. Further, we hypothesised that TT-TMS measures of interest which differ when AP and PA coil orientation are used<sup>156,166,472</sup> could provide greater information about ALS if recorded using both orientations. We therefore incorporated both AP and PA-based measurements into our TT-TMS study design.

*3.2.4. Determine the diagnostic and prognostic value of electrophysiological measures of cortical network function in ALS*

As a central hypothesis of this project is that electrophysiological measures of network disruption are of prognostic and diagnostic value in ALS, ability to discrimination between groups and correlations to clinical and cognitive scores were also planned for each EEG/TT-TMS derived measure.

## 4. General Materials and Methods

This chapter describes the general methodologies and analyses employed in this thesis. Those materials and methods employed for electroencephalography studies are described in 4.1 and the materials and methods of the experiment which utilised transcranial magnetic stimulation are described in 4.2. Statistical tests used across this project are described in 4.3. The recruitment of patient and control cohorts and their evaluation by clinical, cognitive and behavioural tests are described in 4.4 and 4.5 respectively. Ethical approval and participant written consent are described in section 4.6 and appendices 4.1-4.5. Study-specific methods, participant recruitment and demographics and inclusion and exclusion criteria are described for each study in the respective results chapters 5-7.

### 4.1. Electroencephalography (EEG)

#### 4.1.1. Hardware

All EEG was recorded using a BioSemi ActiveTwo system with 128 active sintered Ag-AgCl electrodes. These electrodes interface with the skin via an electrolyte gel bridge (SignaGel Electrode Gel, Parker Laboratories Inc., NJ, USA), positioned by input to suitably sized head caps (BioSemi B.V., Amsterdam, The Netherlands). These active electrodes contain a pre-amplification component following capture of the signal by their conductive material, such that the signal is amplified in advance of any additional noise being introduced to the signal between the electrode and the amplifier, reducing ambient noise detection<sup>473</sup>. Further, the use of wet electrodes helps to reduce noise in the presence of high inter-electrode impedance<sup>474</sup> and has been reported by participants as more comfortable than dry electrode systems<sup>475</sup>. Data were recorded in a Faraday cage-enclosed room, using a battery-powered amplifier to prevent introduction of electrical mains noise to the signal. Data were transmitted to computers in a neighbouring room by a fibre optic cable, where signals were monitored and recorded on a computer (Dell Inc., TX, USA) equipped with the Windows 7 operating system (Microsoft Corporation, WA, USA). A similar, second computer was used to deliver task stimuli to the participant within the electrically isolated room and to record responses. This task computer was plugged in via sockets in the neighbouring room to avoid introduction of electrical noise. Auditory stimuli were delivered via headphones (HD650, Sennheiser, Wedemark, Germany).



#### *4.1.2. Software*

Data were monitored during collection, filtered online (0-134Hz), digitised at 512 Hz and saved using ActiView software (BioSemi B.V., Amsterdam, The Netherlands). Tasks were delivered via Presentation software (NeuroBehavioural Systems Inc., CA, USA) as described in section 4.1.3.

#### *4.1.3. Experimental procedure*

Following discussion of the study protocol and written, informed consent, participants were led to the recording room and seated in a chair adjusted such that the participant's feet were resting on the floor and comfortably positioned. If wheelchair-bound ALS patients could not easily move to the provided chair due to motor symptoms, tasks were performed while seated in their own wheelchair. Participants were seated in front of a desk upon which a screen and mouse were positioned for delivery of visual stimuli and detection of responses. Participants' head measurements were taken to select a correctly-sized, electrode-positioning cap. Eight external reference/electro-oculography electrodes were positioned above and below the left eye and bilaterally on the earlobes, temples and mastoids. The cap was subsequently positioned with electrode A1 over the vertex (the intersection of the horizontal axis between the tragi of the ears and the vertical axis between the nasion and inion). The chin strap of the cap was closed beneath the chin of the participant to ensure secure positioning of the cap while avoiding discomfort to the patient. Correct positioning of the cap was subsequently ensured by alignment of electrode locations horizontally relative to the inter-tragus axis and rotationally and anteroposteriorly relative to the nasion-inion axis.

Conductive gel was then syringed into each electrode-holding hole in the cap, forming a bridge between the scalp and electrode. Hair was moved and the scalp was lightly abraded with the syringe tip to minimise electrode impedance. Electrodes were inserted into their assigned location in the cap, with cables attached to the back of the chair with slack to facilitate limited participant movement. Following hardware setup, direct current offset of each recording electrode relative to the common sense (CMS) electrode was checked via ActiView software, and additional abrasion/gelling was performed if necessary to ensure sufficient quality of electrode-scalp contact (i.e. all offset values were  $<25\text{mV}$  and  $>-25\text{mV}$ ). Subsequently, online signals were briefly monitored to check for artefacts in single electrodes which indicate insufficient recording quality. Following improvement

of recording from any noisy channels to the required standard, cognitive tasks were undertaken by the participant.

The recording session then started, lasting for about 1 hour and 35 minutes (from beginning of equipment setup to end of the paradigm). This included 30 minutes for head measurement, external electrode placement, cap fitting, application of gel and placement of electrodes, 10 minutes for checking and maximisation of recording quality based on online recording and electrode impedance values, 5 minutes for auditory stimulus check, silent film setup and explanation of the task to the participant, 25 minutes for the auditory oddball paradigm and (in the case of those who took part after setup of the novel protocol) 25 minutes for the SART paradigm.

#### *4.1.3.1. Cognitive tasks*

##### *Auditory oddball paradigm*

An auditory oddball paradigm was used to investigate the mismatch negativity, a signal waveform attributed to involuntary attention switching<sup>123</sup>. This paradigm was chosen in order to interrogate salience and executive networks without requiring participants to perform or actively participate in a task. This is particularly well suited to participants with response-limiting motor symptoms. Further review of the literature surrounding the physiological underpinnings of the MMN is described in section 5.1.1.2.

For this paradigm, participants were asked to direct their attention to a black and white, silent film (*The Artist*, 2011, Warner Bros. France) and to ignore any sounds they hear. Participants were also requested to relax their muscles, to focus their eyes on the centre of the screen via which the film was played and in the event of becoming uncomfortable due to their position or fatigue, to move briefly to a new comfortable position in such a way as to avoid pulling the electrode cables before resuming a relaxed, still position. Auditory tones were delivered at fixed intervals, predominantly of a single frequency (referred to as a standard tone) with occasional change in frequency (referred to as a deviant tone), eliciting a frequency mismatch to that which is entrained in sensory memory<sup>469</sup>.

The frequencies of standard and deviant tones were 720 and 800 Hz, respectively, such that deviant tones had a slightly higher pitch. Each stimulus was delivered for 150 ms at an interstimulus interval of 833ms. Deviant tones constituted approximately 10% of stimuli. Tones were mostly of fixed amplitude (i.e. loudness), set to 50% of desktop output to the headphones (except for a few participants who considered the

distractingly/uncomfortably loud, in which case the amplitude was reduced to facilitate participant comfort and correct task performance).

This paradigm was delivered as three, eight-minute sessions, during which time EEG was recorded. During each recording session the lights were turned off and experimenters left the room, monitoring data recording in the neighbouring room. Participants were provided with brief breaks between sessions. In total, 1350 standard trials and 150 deviant trials were presented.

#### *Sustained attention to response task (SART)*

Following the auditory oddball paradigm, participants undertook the SART. The SART was chosen as it tests motor and executive control networks which are not considered to be engaged by the auditory oddball task. Further, the SART requires only a simple button-press response from participants which does not introduce extensive EMG contamination to the EEG signal. In addition, behavioural performance measures can be simultaneously captured for correlation and comparison to the EEG measures<sup>126</sup>.

EEG was recorded during four, five-minute long consecutive sessions of the SART. Appropriate break times were provided between sessions to minimize fatigue. Participants were seated  $1 \pm 0.1$  m from a computer monitor where numbers one to nine in single-digit format were appearing in a random order for 250 ms. Digits were presented in light grey (RGB code: 250, 250, 250 from 255) on a black background to reduce discomfort associated with the bright light from purely white numbers, reported during protocol testing. Font size was randomized between 100, 120, 140, 160, and 180 points to avoid participants using a perceptual template of the number 3s features for target recognition and to encourage cognitive processing of the numerical value<sup>470</sup>. Each stimulus was followed by an interstimulus interval of randomized duration between 1120 and 1220 ms during which time a black screen was presented. Varied interstimulus interval was implemented to enhance detection of automated responses where attention had lapsed. Responses were registered by clicking the left button of a computer mouse with the right index finger. Each recording session contained 252 trials of which the number 3 appeared at random in 11% of trials. During these sessions lights were turned off, and experimenters were outside the room to avoid visual/auditory distractions. Five measures of task performance were captured alongside EEG: NoGo accuracy (percentage of three-digit stimuli followed by response omission), Go accuracy (percentage of non-three digit stimuli followed by a response in the permitted time window), total accuracy

(combined NoGo and Go accuracy), anticipation (clicking less than 150ms after a go stimulus), and response time.

At the beginning of the session, the task was explained to participants using the following instructions: Participants were instructed to click the left mouse button every time they saw a number except for the number 3. Participants were requested to equally prioritize speed and accuracy as both were used as measures of performance. They were asked to refrain from lifting their finger away from the mouse button between clicks as this would increase response time measures. Instructions to use their finger only to click the mouse and to avoid tension in the arm and shoulder were given to reduce EMG-related noise in the EEG signal. Participants were then given one practice round to ensure they understood the task, which had up to 45 trials (without performance being measured), performed under supervision of the experimenter.

#### *4.1.4. Analysis*

As the SART paradigm was set up and tested as part of this project, while MMN recording was ongoing in advance of this project, fewer SART datasets than MMN datasets were available for analysis.

##### *4.1.4.1. Preprocessing*

Signal preprocessing of all EEG data was performed using custom MATLAB (R2014a and R2016a, Mathworks Inc.) scripts with the EEGLAB<sup>476</sup> and FieldTrip<sup>477</sup> toolboxes. These data were filtered using a 0.3-Hz dual-pass fifth-order Butterworth high-pass filter and a 30-Hz dual-pass 117th-order equiripple finite impulse response low-pass filter, to remove slow drift noise and high frequency EMG artefacts (as gamma band signal was not being studied). Highly contaminated and nonstereotyped artefacts (e.g. EMG due to brief tension/movement/heavy breathing, sweating, cable movement, electrode ‘pops’) were removed by visual inspection of the data before segmentation of the continuous EEG recording into ‘epochs’. Epochs spanned from 200ms before the stimulus to 900ms poststimulus in the case of SART data, from 100ms before the stimulus to 500ms poststimulus in the case of MMN data. Stereotyped artefacts (e.g., eye blinks, eye movements, continuous noise in single electrodes) were then removed by independent component analysis<sup>476</sup>. Data were common average referenced, and mean baseline amplitude was subtracted. In the case of SART-EEG data, if responses occurred 150ms or less after stimulus onset, trials were rejected and counted as an “anticipation error.”

#### 4.1.4.2. *Event related potential analysis*

The ERP methodologies described here have now been published as part of complete research articles in the peer-reviewed journals *NeuroImage: Clinical*<sup>103</sup> and *Cerebral Cortex*<sup>478</sup>.

#### *Sensor space*

As sensor space analysis of the mismatch negativity ERP had been previously performed within the group<sup>267</sup>, sensor space ERP analysis was only performed for SART-related EEG data within this project. For SART ERP analysis, electrodes of primary interest were chosen based on established topographic maps of the SART N2 and P3 peaks<sup>126,479</sup>. Mean correct Go (clicking upon a non-three digit) and NoGo (not clicking upon a “3” digit), ERPs were calculated for each participant as the mean time series for each channel across trials. Due to low error number, there were an insufficient number of clean epochs for incorrect trial-associated ERP analysis. The mean number of included artefact-free correct Go/NoGo trials was 810.13/82.22 for patients and 815.42/82.79 for controls out of a maximum of 897/111. Four characteristics of the N2 and P3 peaks of each mean Go and NoGo epoch were measured in Fz, FCz, Cz, and Pz electrodes. Namely, the peak (maximal positive amplitude for P3, maximal negative amplitude for N2) amplitude and latency, mean amplitude, and area of the peak within the 220–350-ms and 350–550-ms time windows associated with N2 and P3, respectively. These time windows were chosen based on visual inspection of control group mean ERPs and the existing SART–ERP literature<sup>126,415,480,481</sup>. Time windows for quantifying peaks of interest were also limited to a maximum of 200 ms to facilitate baseline correction in source analysis (which required matching baseline and peak time windows) while using the same windows for sensor and source analysis.

For assessment of correlations with cognitive performance measures, where similarly significant correlations existed between performance measures and all peak size measures (peak amplitude, mean amplitude, and mean area), p and rho values are reported with respect to peak amplitude where describing peak size (e.g., “smaller” or “larger”).

#### *Source space*

For the first source space analysis of this project, three different methods of source localisation were used to interrogate the sources of the mismatch negativity response in controls and ALS patients due to their individual advantages and disadvantages (described in section 2.1.2.1, see table 2.1). Dipole fitting was not suitable for

interrogating SART-related EEG sources as active source locations were not previously reported. Therefore, as eLORETA provides poorer spatial resolution than LCMV, only LCMV was used to subsequently interrogate the sources of the SART ERP. The implementation of each method is described here.

In all cases, channels with continuously noisy data were excluded and data from these channels were modelled by spline interpolation of neighbouring channels. Where a cluster of electrodes (4 or more) remained continuously noisy after preprocessing (section 4.1.4.1), the participant's data were excluded from analysis as interpolated estimates of missing channel signals would be unreliable. For dipole fitting and LCMV, implemented using the FieldTrip toolbox<sup>477</sup>, boundary element head models<sup>482</sup> incorporating geometries for the brain, skull, and scalp tissues were generated using the ICBM152 MRI template<sup>483</sup> unless personalised MRI scans were available (in the case of some MMN study participants), as template-based and individualized boundary element head models are found to provide comparable localization accuracy<sup>482,484</sup>. Personal MRI data were acquired on a 3 Tesla Philips Achieva MRI platform with a maximum gradient strength of 80mT/m using an 8-channel receive-only head coil. T1-weighted images were obtained using a three-dimensional inversion recovery prepared spoiled gradient recalled echo sequence with a field of view of 256×256×160 mm, spatial resolution: 1mm<sup>3</sup>, TR/TE: 8.5/3.9ms, TI: 1060ms, flip angle: 8°, SENSE factor: 1.5<sup>485</sup>. These MRI data were collected as part of concurrently running MRI-based research of the Computational Neuroimaging Group and the Academic Unit of Neurology at Trinity College Dublin.

#### *Dipole fitting – MMN*

Dipole fitting can be used to generate least-square error models of the contributions of electrical dipoles to an EEG topographic distribution, given a-priori estimation of the number and location of contributing dipoles<sup>136</sup>. Previous studies<sup>138,265,486</sup> have repeatedly identified MMN sources in the inferior frontal gyri and superior temporal gyri. As non-linear optimisation of the dipole location repetitively produced fits at local rather than global residual variance minima, four fixed dipoles were modelled at the centroid coordinates of the bilateral superior temporal gyri and pars triangularis of the inferior frontal gyri, as determined from an AAL atlas<sup>487</sup>. Models were estimated based on the average MMN response (mean{deviant response}-mean{standard response}) for 40 ms surrounding the global field power peak between 105 and 271 ms post-stimulus, the

period for which we previously found MMN to be significant<sup>267</sup>. Subsequently, mean power for each dipole was calculated. Residual variance (the variance in the data not explained by the model) was used as a goodness-of-fit measure. The rationale for using this shorter time frame was based upon findings that these four sources better accounted for the data in this window (i.e. had smaller residual variance) than the longer time window of data 100-300 ms post-stimulus, as used for LCMV and eLORETA. A model generated using the longer 200 ms time window provided the same results (regarding ALS vs control groups) as the model reported here.

#### *eLORETA – MMN*

eLORETA<sup>140</sup> was also used to calculate mean source power maps of the average auditory evoked potential 100-300ms after standard and deviant cues to match the data input to LCMV. LORETA-KEY software was used to implement eLORETA. This software models sources at 5 mm resolution within the brain volume of a boundary-element headmodel based on the Colin27 average brain<sup>488</sup>, excluding sources located within white matter. For statistical comparison and comparability to the head model employed for dipole fitting and LCMV, grid resolution was reduced to 10 mm in advance of statistical analysis to avoid the loss of discriminatory power that may result from correction of over 6000 comparisons. Regularisation was implemented for a signal to noise ratio of 10.

#### *LCMV*

LCMV beamforming was performed using custom MATLAB scripts and the FieldTrip toolbox. In all cases, regularization of the covariance matrices was implemented at 5% of the average variance of EEG electrodes for each subject separately. Sources within the brain volume were modelled by a grid with 10mm resolution. The leadfield matrix was normalized to avoid potential norm artifacts<sup>489</sup>.

#### *MMN*

LCMV was used to calculate brain maps of mean power for the average auditory evoked potential (AEP) 100-300ms after standard and deviant cues, based on a common spatial filter. A time window of 100-300ms was utilised to ensure accurate calculation of the covariance matrix from which the spatial filter is calculated and avoid high functional correlation between the sources which would hinder localisation of such distinct sources. Covariance matrices were also calculated for individual trials to minimise such correlations. Sources of MMN activity were identified by the locations of the maximal logarithm of the power ratio between deviant and standard maps. As standard and deviant

AEPs alone were not of interest, baseline correction was not required as inter-trial comparison facilitated correction for centre-of-head bias.

#### *SART*

LCMV was used to estimate brain power maps for the Go and NoGo trials during two time windows, 220–350ms and 350–550ms poststimulus onset, to localize sources of the N2 and P3 ERPs, respectively, as well as of the corresponding baseline windows of equal duration (N2: –130 to 0 ms, P3: –200 to 0 ms). Source localizations of baseline and peak windows were performed using common spatial filters (estimated separately for N2 and P3) calculated from epoched data spanning the start of the peak’s baseline window to the end of that peak’s time window. Use of a common spatial filter based on appended peak and baseline data produced negligible difference in source location. These common spatial filters were then used to source localize baseline and peak time windows separately. Covariance matrices, used by LCMV, were calculated for individual trials and then mean averaged. Go and NoGo source activities are reported with baseline correction as  $10 \cdot \log_{10}(\text{Power}_{\text{peak}}/\text{Power}_{\text{baseline}})$  to correct for centre-of-head bias, with the difference between Go and NoGo source activity reported as  $10 \cdot \log_{10}(\text{Power}_{\text{NoGo}}/\text{Power}_{\text{Go}})$ .

#### *Longitudinal analysis*

As longitudinal analyses are specific to section 5.2, these methods are described in full in section 5.2.2.

#### *4.1.4.3. Time-frequency analysis*

The methodologies described here have now been published in the peer-reviewed Journal of Neural Engineering.

#### *Sensor space*

Preprocessed trial epochs (generated as described in 4.1.4.1) obtained from auditory oddball task and SART associated EEG subsequently underwent separate time frequency analyses. Trial epochs consisted of 307 (i.e. 600ms of data recorded at 512Hz) data points ( $d$ ) in the case of auditory oddball data and 563 (i.e. 1100ms of data recorded at 512Hz) data points in the case of SART data, per channel. A random subset of standard/correct Go trials was chosen to match the number of deviant/correct NoGo trials for auditory oddball/SART time frequency analysis respectively. Complex Morlet wavelets were chosen for time-frequency analysis as they have a sinusoidal basis with symmetric Gaussian envelopes and their width can be adjusted for the desired number of oscillations. For each channel, data were padded to facilitate complex Morlet wavelet



convolution by applying  $d$  repetitions of the first data point at the start of each epoch and  $d$  repetitions of the last data point at the end of each epoch. Padded epochs were then concatenated to form a single time series per channel. As data were low-pass filtered at 35Hz during pre-processing designed for previous time-domain analysis, calculation of wavelet moduli was performed for a range of 1 to 35Hz. The complex coefficients of transform (W) data were subsequently re-epoched with removal of zero padding. Mean inter-trial variance (ITV) across epochs ( $e$ ) was calculated per time point ( $t$ ) and frequency ( $f$ ) to provide a measure of non-phase locked (i.e. not captured by ERP analysis) oscillatory activity<sup>490</sup> as:

$$ITV(f, t) = \frac{\sum_1^{N_e} |W_{f,t,e} - \bar{W}_{f,t}|^2}{N_e - 1}$$

Where  $\bar{W}$  denotes mean value of W across epochs. ITV were calculated for the Fz, Cz and Pz, D22 and B25 channels for auditory oddball data analysis, and for Fz, Cz and Pz channels for SART data analysis, in order to capture oscillations over major cognition-associated cortical regions as well as to examine those areas known to contribute to the evoked time locked potentials<sup>126,138,372,478,486</sup>. Baseline values were calculated per frequency as mean ITV across the -100ms to 0 ms window in the case of auditory oddball analysis, and -200ms to 0 ms window in the case of SART analysis. Event related spectral perturbation values for each time and frequency were subsequently calculated as:

$$ERSP(f, t) = 100 * \frac{ITV_{f,t} - \overline{ITV}_{f,baseline}}{\overline{ITV}_{f,baseline}}$$

for  $t=1-500$ ms (auditory oddball epochs) or  $1-900$ ms (SART epochs). Time-frequency analysis was performed separately for different trial types and ERSP values for the difference between trial types were calculated by subtracting standard/correct Go trial ERSP values from deviant/correct NoGo trial ERSP values for auditory oddball/SART analyses respectively. Delta and theta band frequencies were not examined for auditory oddball data, and delta band frequencies were not examined for SART data, as one complete oscillation cycle could not be achieved within the limited baseline durations.

#### *Source space - MMN*

ERSP within time-frequency windows of interest (WOIs), determined by sensor level analysis, were source localised using LCMV beamforming for MMN data, as the lack of spatial specificity of oscillations observed at sensor level limited interpretation of these findings alone. Source analysis of SART-related ERSP is ongoing, and is beyond the

extent of this project. The phase-locked, ERP activity we have previously localised were removed by subtracting the mean waveform across trials from each epoch of that trial type (e.g. mean of standard trial epochs subtracted from all standard epochs, mean of deviant trial epochs subtracted from all deviant epochs), the time-domain equivalent to the implementation of inter-trial variance in frequency domain employed in sensor space. For each time-frequency window of interest, a common spatial filter was generated for beamforming based on the covariance of appended baseline and post-stimulus window of interest data of standard and deviant trials. The relatively short, 100ms baseline (chosen based on originally planned ERP analysis), restricted the WOIs which could be localised in a single analysis to this length, in order to match timespans for source space baseline correction. Long ROIs (>2\*baseline length) were analysed in baseline length segments, followed by averaging of power values for each source across segments. Shorter WOIs that were greater than baseline length were analysed by taking the central time frame within the region that was equivalent to baseline length. Separated standard and deviant baseline and post-stimulus time window of interest signals then underwent LCMV beamforming with a common spatial filter, implemented as described in our source localised ERP studies<sup>103,478</sup> (see section 4.1.4.2).

The beginning and end of the time domain signals localised to each of the 3744 points within the 10mm grid in the brain tissue of the head model were zero padded by 200ms. The resulting 0.5s signals were Fourier transformed to determine the spectral power composition of the signal at each source at a resolution of 2 Hz (i.e. 1/0.5s). Power values were summed across frequencies within the window of interest (e.g. 8, 10 and 12Hz where the window of interest was 8-12Hz). Percentage change from baseline in power (P) at each source (s) was then calculated as:

$$\frac{P_{s,window\ of\ interest} - P_{s,baseline}}{P_{s,baseline}} \times 100$$

for standard and deviant trials, and the “mismatch” between deviant and standard power was calculated as the difference between deviant and standard trial percentage change values.

## **4.2. Transcranial Magnetic Stimulation (TMS)**

### *4.2.1. Hardware*

In order to perform paired-pulse TMS, hardware was ordered and assembled. A Deymed DuoMag MP Dual stimulator (BrainBox Ltd., Cardiff, UK) was chosen based on its output parameters being superior to those of competitor stimulators while at a comparable cost. Further, the presence of a stimulation intensity changing wheel and trigger button on the Deymed coil handles (not present on competitor coils) removed the requirement for an additional research assistant typically required to control the device settings and triggers using controls on the stimulator unit. EMG was recorded via Cleartrace pre-gelled (1.5cm diameter) electrode pads (Aquilant Medical Ltd., Dublin, Ireland) connected to clip leads (Biopac Systems Inc., CA, USA). These data were amplified (gain = 1000) and band-pass filtered (10-500Hz) via EMG100C amplifiers (Biopac Systems Inc., CA, USA) and electrical mains noise was subsequently removed by a HumBug Noise Eliminator (Digitimer Ltd., Hertfordshire, UK). The Humbug device was employed as it records the ambient electrical noise, generates a template noise signal that is continuously updated to match the current environment, and subtracts this signal from the incoming data to eliminate noise while leaving true EMG data unaffected. This is superior to the use of high-pass or notch filters which are less specific and can eliminate or alter true biological signals.

Following output from the HumBug, the data were delivered (via a T-connector) to a Tektronix TBS1000 oscilloscope (IMEX Instruments, Louth, Ireland) for live readout to the experimenter to monitor noise levels and motor responses, and to a Micro1401 (CED Ltd., Cambridge, UK) from which signals (digitised at a sampling rate of 10kHz) were recorded on a Dell Inspiron 5559 laptop (Dell Inc., Dublin, Ireland) with Signal software (Signal 7.01, CED, Cambridge, UK).

To record compound muscle action potentials, a Digitimer DS7A electrical stimulator (Digitimer Ltd., Hertfordshire, UK) was used to apply electrical stimulation via a bipolar electrode with felt pads soaked in saline solution. The associated muscle responses were recorded by the same hardware pathway described above for TMS-associated responses.

### *4.2.2. Software*

Digitised data were recorded via Signal 7 software (CED Ltd., Cambridge, UK) as the software has many inbuilt functions for coding personalised scripts for automated

hardware control (see section 4.2.2.1), a graphic user interface for basic protocol and online data collection and analysis functions for real-time feedback of peak-to-peak amplitudes to the experimenter.

#### *4.2.2.1. Threshold tracking*

As described in section 2.1.2.2, the original and typical application of TMS, whereby stimulus intensity is the independent, fixed variable and response signal amplitude is the dependent output variable, has given rise to variable, unreproducible results in the study of ALS and more generally. As TMS literature investigating ALS pathology with a “threshold tracking” methodology has shown more consistent findings than that with a fixed-intensity approach, this method was also implemented here. In this approach, the signal amplitude is considered a fixed independent variable, while the output dependent variable is the stimulus intensity required to obtain this fixed amplitude (to within a specified margin of error which varies among existing TT-TMS literature<sup>156,194</sup>) in response to 50% of pulses delivered (referred to as the threshold). Therefore a more complex online analysis is required, as the signal amplitude of interest must be consistently monitored and used to inform whether the next stimulus intensity delivered should be greater or lesser than the previous and to what magnitude. Further, an algorithm which determines when the desired signal output has been determined to the experimenter’s certainty criteria must be applied online during data collection.

Upon initiation of experiment design and apparatus setup there were two approaches to TT-TMS reported multiple times by two separate teams in the literature. In one of these, a manual approach is taken, which involves one experimenter holding the coil over the participant while another reads the peak-to-peak signal amplitude from a computer screen, interprets if it is above or below threshold, and inputs this decision into a parameter estimation by sequential testing (PEST) software graphic user interface (MTAT PEST 2.0). This software in turn informs the experimenter of the next stimulus intensity to deliver to increase the probability of obtaining the desired amplitude. The experimenter then alters the stimulator settings and trigger delivery of the next TMS pulse. This cycle continues for each TMS trial (pulse delivered and response recorded) until the PEST algorithm determines a threshold stimulus intensity which is predicted to elicit a signal of target amplitude in 50% of trials, with a 95% confidence interval acceptable according to the guidelines of Rossi et al.<sup>491</sup>, i.e. for a subject with true threshold  $X$ , an estimate of the threshold,  $eX$ , is acceptable<sup>492</sup> if:

$$0.95 X < eX < 1.05X$$

While this methodology is statistically robust and facilitates disregard of trials wherein there is excessive background noise, it is liable to human error, requires an additional researcher and limits control of the interval between delivery of single/pairs of pulses.

The other reported approach involves an automated programme whereby the intensity of the stimulator is automatically increased and decreased for each trial to move the signal amplitude towards the threshold of interest, with the stimulus intensity chosen where it can elicit three consecutive response amplitudes within 20% of the threshold, or two either side of the threshold amplitude consecutively. This implementation requires fewer pulses to be delivered and is automated, reducing the number of experimenters required, however the output is decided based on subjectively chosen criteria, may not meet the aforementioned criteria for threshold estimation, and the methodology does not allow for online rejection of trials with background noise.

For this project we wished to implement TT-TMS with the advantages of both of these approaches. To do so, novel scripts were generated in Signal 7 and MATLAB software. These scripts automated a procedure whereby Signal 7 records the response signal and delivers it to a script running in MATLAB with which the peak-to-peak amplitude of the response signal within the time window of interest is determined. This is added to a list of stimulus intensity and response amplitude paired data input to the PEST algorithm, which determines the next stimulus intensity to be delivered. This stimulus intensity recommendation is then delivered back to Signal 7, which (via the Micro1401) adjusts the intensity setting of the stimulator before delivery of the next pulse. This cycle continues until, on the basis of the PEST algorithm, it is determined that the required stimulus intensity has been estimated with sufficient confidence. This decision having been reached, a stop signal is delivered to Signal 7 to terminate pulse delivery and data sampling. This implementation facilitated completely automated, statistically robust threshold tracking with controlled interstimulus intervals. Further, for each trial a MATLAB script calculated the baseline signal root mean square amplitude and, if this value was above a predetermined noise threshold, the trial was rejected such that the response was not input to the PEST algorithm. Such trials were then repeated. This facilitates fully automated rejection of noisy trials. Therefore the protocol can be run completely in the presence of only one experimenter who is required to hold the TMS coil. Each measurement requires 20 pulses/pairs of pulses to be delivered, excluding any

trials on which the baseline root mean square amplitude value was above the rejection threshold criterion.

#### *4.2.3. Experimental procedure*

The experimental procedure and analysis pipelines for the TMS aspect of this project are described in full in chapter 7.

### **4.3. Statistics**

Specific statistical analyses are described for each analysis in the result subsections of chapters 5-7. Here, this section describes more generally the statistics employed during this project and the rationale for their use. Statistical analyses were performed with MATLAB R2016a (MathWorks Inc., MA, USA).

#### *4.3.1.1. Non-parametric statistics*

Many commonly employed tests employed to identify statistically significant differences between groups/conditions are “parametric”, so-named as they require the estimation of parameters which characterise the data distribution, such as the standard deviation and mean. These parametric tests, such as t-tests, require that a number of fundamental assumptions are valid, including the assumption that the data are normally distributed. While this is true for measurements of many biological phenomena, or can be achieved through correct transformation of the data, in some cases these tests remain unsuitable for the data being analysed due to violation of underpinning assumptions (both due to physiological complexities, and the presence of outliers or artefactual effects). By contrast, non-parametric tests make little-to-no assumptions about the statistical characteristics of data, and can therefore be better suited to the interrogation of data where the distribution of the population data is unknown or skewed.

One commonly employed non-parametric alternative to the t-test in the comparison of data between independent two groups is the Mann-Whitney U test, also named the Wilcoxon rank sum test<sup>493-495</sup>. This test is performed as follows:

1. Data are ranked in order of increasing magnitude irrespective of their group, with matching values both assigned a rank of the midpoint of the unadjusted ranks.
2. The ranks of the smaller group, or either of the groups if matched in size, are then summated.
3. The test statistic,  $U$ , is calculated as follows:

$$U_1 = R_1 - \frac{n_1(n_1 + 1)}{2}$$

where  $n_1$  is the sample size for the smaller sample, and  $R_1$  is the sum of the ranks in that sample.

4. The probability of the null hypothesis being true ( $p$ ) can then be ascertained from this  $U$  statistic based on tabulated values.

Another frequently employed non-parametric test is the Wilcoxon sign rank test<sup>495</sup>, which can be used to determine the probability of a measured value or the difference between paired measured values (not) being a hypothesised value, such as zero. This test is therefore comparable in its applications to those of the parametric one sample and paired t-tests, with this test also requiring each sample/pair of samples to be independent from one another. To calculate the test statistic for comparison of the data to zero the following steps are taken:

1. If investigating paired data, the absolute value of the difference between pairs are calculated and used in the remaining steps. Otherwise, single data samples are used.
2. Data values equal to zero are excluded.
3. The absolute values of the remaining data are ranked from smallest to largest. Matching values are ranked to the average of the ranks over which they range.
4. The test statistics  $W_+$  and  $W_-$  are calculated as follows<sup>495</sup>:

$$W_+ = \sum_{i+=1}^{N-} R_{i+}$$

$$W_- = \sum_{i=-1}^{N-} R_{i-}$$

where  $N_+$  is the number of data points greater than 0 and  $R_{i+}$  is the rank of the  $i$ th (single or difference between pairs) data value greater than 0,  $N_-$  is the number of data points less than 0 and  $R_{i-}$  is the rank of the  $i$ th (single or difference between pairs) data value less than 0.

5. The probability of the null hypothesis being true ( $p$ ) can then be ascertained from these  $W$  statistics based on tabulated values.

The use of ranks in these tests limits the effect of outliers on the test statistic, which can be particularly influential over parametric test statistics. The disadvantage of using non-parametric tests compared to their parametric counterparts is that they may have lesser statistical power where the assumption of normality is valid<sup>493</sup>. However, given the sample sizes employed for each experiment within this project (tens of subjects per group), the use of non-parametric testing was deemed to be more robust and suitable for the required EEG data testing. In the case of TMS data, where approximately 10 ALS patient datasets per comparison were available, parametric testing (i.e. t-tests) were used where the data met the assumptions of the test, and non-parametric testing was used otherwise.

#### *4.3.1.2. Controlling the false discovery rate*

Typically for a single hypothesis test, researchers require the probability of the null hypothesis being true ( $p$ ) to be less than 5% (i.e.  $p < 0.05$ ) to have sufficient confidence that the null hypothesis can be rejected and the difference/change observed to be “statistically significant”.

Such a statistical test may be performed numerous times to test a hypothesis separately for numerous variables measured collected within an experiment, for example, the hypothesis that ALS patients and controls differ in activity at source  $j$ , where  $j = (1, 2, \dots, n)$ . In such cases, the number of false positive findings (type I error,  $\alpha$ ) within this family of tests increases. Accordingly, additional steps, typically referred to as “multiple comparison correction” must be taken to counteract this phenomenon. One of the most mathematically straightforward methods of such correction is the Bonferroni method. In this method, the threshold  $p$  value, below which a difference/change is deemed “statistically significant”, is divided by the number of comparisons. While this method is suitable for small numbers of comparisons, this correction is increasingly stringent with increasing size of the comparison family. Statistical power is accordingly limited, resulting in high type II error ( $\beta$ , false negative findings)<sup>496</sup>.

Such multiple comparison correction tests aim to limit the familywise error rate, defined as “the probability of making any error in a given family of inferences”<sup>497</sup> but typically considered specifically with respect to type I error.

An alternative method of accounting for this multiplicity problem with greater statistical power is to control the false discovery rate (FDR), “the proportion of errors committed by falsely rejecting null hypotheses”. A method to do so was proposed in 1995 by



Benjamini and Hochberg, accordingly referred to as the Benjamini-Hochberg method<sup>498</sup>. This method aims to define an alternative criterion based on  $q$  (as FDR), which is the ratio of the falsely-discovered values among all of the detections from the family of  $p$ -values in multiple tests. Therefore, a criterion such as  $p < 0.05$ , is substituted with a similar (but not exactly the same) criterion  $q = 0.05$ . The  $p$ -values that pass this  $q$  threshold represent differences that match the FDR criterion at the chosen  $q$ . In the procedure for FDR correction, the  $p$ -values are adjusted to an increased value so that those which remain below the critical  $p$  value (typically 0.05) will only incorrectly reject the null-hypothesis at the desired FDR (typically 0.05 or 0.1). This is achieved as follows:

1. The  $p$  values are ranked ( $i$ ) from smallest ( $i=1$ ) to largest ( $i=n$ ).
2. In order of descending rank, each  $p$  value is adjusted so that the adjusted  $p$  value is either the adjusted  $P$  value of rank  $i+1$ , or  $n/i$ , whichever is smallest.
3. Those adjusted  $P$  values that are smaller than the chosen FDR are considered to be significant with the FDR controlled to the desired rate.

This method typically provides greater statistical power relative to the aforementioned Bonferroni method<sup>498</sup>. This method was therefore employed for multiple comparison correction in this project. Following the FDR procedure, it is possible to report the corrected  $p$ -values at the specified  $q$ , or report the original  $p$ -values and indicate the  $p$ -values that pass the  $q$  threshold.

#### 4.3.1.3. Empirical Bayesian Inference (EBI)

Bayesian inference is a form of statistical interference (i.e. assuming information about the population distribution based on analysis of a representative sample). Bayesian inference involves the application of Bayes' theorem to update the probability of a hypothesis as more information comes to be known. Bayes' theorem describes the probability of an occurrence, based on prior knowledge related to that occurrence. This allows the probability of an occurrence for a given individual to be more accurately estimated than by assuming that the individual is typical of the population. The theorem is stated by the following equation:

$$P(A|B) = \frac{P(B|A) \cdot P(A)}{P(B)}$$

Where  $A$  and  $B$  are occurrences,  $P(A|B)$  is the conditional probability of  $A$  occurring given that  $B$  is true (or has happened), also referred to as the posterior probability,  $P(B|A)$  is the conditional probability of  $B$  occurring given that  $A$  is true, also referred to as the

likelihood,  $P(A)$  is the probability of  $A$  being true, referred to as the prior probability, and  $P(B)$  is the probability of  $B$  being true<sup>497</sup>.

Bayesian inference involves the following central components:

- i. Obtain the likelihood,  $P(B/A)$ , which describes how the data  $B$  arises given unknown parameter  $A$ .
- ii. Determine the prior distribution,  $P(A)$ , describing what is known about  $A$  before observing the data
- iii. Apply Bayes' theorem to determine the posterior distribution,  $P(A/B)$ , describing what is known about  $A$  having observed the data
- iv. Derive appropriate inferences from the posterior distribution such as point estimates, interval estimates or probabilities of a hypothesis based on the posterior distribution.

The term “empirical” refers to the inference being made based on an estimate of the prior probability from current numerical (typically multivariate) observations, as opposed to from laws, theories or previous knowledge or studies. Therefore empirical Bayesian inference, or EBI, is a procedure in which the prior distribution required for Bayesian inference is identified by empirical multivariate evidence, and specifically, the same data from which the posterior distribution will be determined<sup>497</sup>. Such posterior probabilities not only details the probability of an event of interest (such as a participant having ALS) given the data but can also be related to frequentist measures such as the FDR and statistical power. These additional measures provide a more informative statistical inference of the nature and extent to which groups differ by large scale multivariable measures beyond typically cited p values, which solely describe the probability of the null hypothesis being true<sup>498</sup>.

EBI is a useful method where the number of variables being measured per individual is high enough that allows the empirical estimation of the prior probability. This can be much greater than the number of individuals being measured, which is often the case in modern clinical research and renders the data unsuitable for other classic predictor methods<sup>499</sup>. In the case of this project, the number of sources modelled in the brain tissue (>1000) following source localisation of EEG data, is at least an order of magnitude greater than the number of subjects studied. One of the frequently employed mitigations for this issue is cluster-based permutation<sup>500</sup>, however this has 3 main limitations:

- i. The fundamental assumption that significant effects/changes are spatially clustered is not always valid, limiting power to detect small clusters across the spatial plane.
- ii. The definition of a cluster is arbitrary
- iii. This method does not provide posterior probability or statistical power estimates.

Therefore, EBI was employed here, using z-transformed non-parametric test statistics, to generate descriptive, detailed inferences regarding the differences in cortical activity between baseline and post-stimulus time windows (test statistic: rank sum  $W^{495}$ ) and between ALS patients and healthy controls (test statistic: area under the receivership operating characteristic curve, AUROC, the probability of the data in one group being larger than the other<sup>501</sup>) while accounting for multiple comparisons.

In brief (described in detail by Nasserolelami et al.<sup>502</sup>) the following steps the following steps take place in the EBI toolbox employed for this analysis (<https://github.com/NeuroMotor-org/EBI>):

- i. The z-transformed test statistic ( $z$ ) was calculated for each variable (for example each source defined within the brain).
- ii. Gaussian mixed model analysis is then employed to determine the probability density function  $f(z)$  from the pooled  $z$  statistics, with the Akaike Information Criteria informing the decision of optimal model fit.
- iii. Bootstrapping was implemented by resampling the data with substitution  $B_0$  times and used to calculate  $z_j$  values at each iteration as in step 2. The data from all bootstraps and all source power variables were pooled to estimate the null distribution  $f_0(z)$ .
- iv. Prior probability  $p_0$  was estimated based on the assumption that at the maximum value of  $f_0(z)$ ,  $f_1(z)=0$ . Using the previous estimates of  $f(z)$  and  $f_0(z)$ ,  $p_0$  was calculated as follows:

$$p_0 = \frac{f(z)}{f_0(z)}$$

where  $z$  is the  $z$  statistic for the median of the null data.

- v. The posterior probability of the null and alternative hypothesis being true given the data,  $P_0$  and  $P_1$  respectively, were estimated from the null distribution and pooled probability density function according to Bayes' theorem as follows:

$$P_0(z) = \frac{p_0 \cdot f_0(z)}{f(z)}$$

$$P_1(z) = 1 - P_0(z)$$

- vi. Type I error ( $\alpha$ ), II error ( $\beta$ ) and FDR (see section 4.3.1.2) were calculated from the afore-estimated posterior probabilities and functions by integration.
- vii. To account for multiple comparisons, a chosen FDR (0.05 or 0.1 depending on the nature of the comparison) was used as a frequentist method to determine significant differences in source activity. A mask of logical values for each source is generated which is only true (i.e. equal to 1) for those values deemed significant at this FDR. This mask is applied to the test statistic values of all sources and plotted onto the corresponding source coordinates within the head model cortex/model MRI scan. As a result, the significant sources, for whom the test statistic is illustrated, can be considered to be significant with a type I error rate of, at most, the chosen FDR.

#### **4.4. Participant recruitment**

As inclusion and exclusion criteria for participants varied between studies, these criteria are defined for each study across chapters 5-7. All participants took part on a voluntary basis. All participants were capable of giving informed consent. Some control and ALS patient volunteers took part in more than one study as part of this project, however cohorts differed overall across each study. The specific demographics of each cohort included per analysis are detailed in chapters 5-7.

##### *4.4.1. ALS patient recruitment*

Throughout the project, individuals diagnosed with possible, probable or definite ALS according to the El Escorial Criteria Revised<sup>63</sup> were recruited from the Irish National ALS Clinic, at Beaumont Hospital Dublin. Patients were approached, if appropriate, by a member of the Academic Unit of Neurology, to ask if they were interested in hearing about ongoing research of ALS at a future time. If the patient consented, they were contacted by the experimenter after at least one week by phone or email to discuss specific information about the study/studies of interest and any questions regarding participation from the patient were answered. If the participant was then willing to take part and deemed suitable according to the study's inclusion and exclusion criteria, they were scheduled for a research session appointment at their earliest convenience. Patient participants were informed at recruitment that the study is longitudinal (up to five

sessions, T1-T5, approximately every four to six months), but were not required to commit to all follow up sessions in order to take part, as high dropout was expected by session four and five (>1 year after baseline recording) due to disease progression. Participant drop out was due to inability to attend the hospital and/or sit upright, relaxed and still due to motor disability.

#### *4.4.2. Healthy control recruitment*

Throughout the project, individuals without any neurological, psychiatric or muscular disease diagnoses were recruited to each EEG- and TMS-based study. Those with a first degree relative with ALS were also not eligible, to avoid potential inclusion of individuals with premorbid familial ALS pathology or ALS-related, subthreshold pathobiology. Control participants were recruited via advertisement of the study and call for volunteers to spouses and friends of ALS patients and through public advertising of the Academic Unit of Neurology's research studies. In order to maintain age-matched patient and control cohorts, recruitment of control volunteers between the ages of eighteen and thirty years old was limited to match the low frequency of ALS patient participants of this age bracket within each study.

### **4.5. Clinical, cognitive and behavioural measures**

Clinical, behavioural and cognitive scores collected by the Academic Unit of Neurology and the National ALS Clinic, independently of this research project, were obtained for correlation analyses with measures collected as part of this thesis. If time-sensitive (e.g. tests of symptom severity), data measured at suitable times relative to study participation was used for correlation analyses (further information on permitted time intervals are described in chapters 5-7).

#### *4.5.1. ALS functional rating scale revised (ALSFRS-R)*

The ALSFRS-R is a 48 point semi-quantitative scoring scale for the measurement of ALS motor symptom severity. The ALSFRS-R is a revision of the original, 40 point ALS functional rating scale, which consists of 10 subscores ranging from 0 to 4 (4 being normal function). These subscores address impairments of daily living due to motor symptoms of ALS<sup>503</sup>. The ALSFRS-R replaces one of these subscores, regarding breathing, with three respiratory subscores regarding dyspnoea, orthopnoea and use of

mechanical respiratory aids, such that the total score range is 0 to 48 (48 being normal function)<sup>504</sup>.

The ALSFRS-R was recorded for most ALS patients who took part in the studies of this project at least once, independently of study participation. Scores were determined by a neurologist or suitably trained member of the Academic Unit of Neurology research team, during patient attendance of the Irish National ALS Clinic.

#### *4.5.2. Date of onset and survival time*

All ALS patients who took part in this research consented to be listed in the Irish Registry of Amyotrophic Lateral Sclerosis and Motor Neurone Disease. As part of their enrolment to the Registry by Register Managers, patients were asked to recall the date of first symptom onset, which was recorded as the date of onset of ALS symptoms. If the specific date could not be recalled, the first day of that month was noted as the date of onset. In the event of death, the date of death was obtained for ALS patients enrol on the register via contact from patient relatives/carers and monitoring of public death notices. Survival time was subsequently calculated as the time between date of death and reported date of onset for deceased individuals.

#### *4.5.3. Cognitive and behavioural testing*

ECAS, Beaumont Behavioural Inventory (BBI) and Delis-Kaplan Executive Function System (D-KEFS) Colour Word Interference Test (CWIT) scores were collected by trained members of the Psychology Strand of the Academic Unit of Neurology as part of concurrent psychological ALS research projects.

##### *4.5.3.1. Beaumont Behavioural Inventory (BBI)*

The BBI is a 41-item behavioural, self-explanatory questionnaire for caregivers of ALS patients (higher 'since the onset of MND' scores indicate greater behavioural impairment since symptom onset). This inventory was designed to measure changes in behaviour associated with ALS while accounting for the influence of motor symptoms. The BBI is demonstrated to be sensitive and specific in assessing the entire behavioural spectrum of ALS<sup>505</sup>.

##### *4.5.3.2. Edinburgh Cognitive and Behavioural Assessment Scale (ECAS)*

The ECAS is a screening tool designed to detect the profile of cognition and behaviour changes in ALS and to differentiate this profile from other disorders. The ECAS takes approximately 15 to 20 minutes to complete, enabling screening of ALS patients for

cognitive and behavioural impairment during clinic visits. The Screen includes an ALS-specific score, incorporating executive functions, social cognition, verbal fluency and language tasks, an ALS non-specific score, incorporating memory and visuospatial tasks<sup>506,507</sup>. Larger scores indicate better task performance. Those who were flagged as having abnormally poor ECAS scores, based on established cut-off scores, underwent a detailed (2-3 hour long) battery of psychological tests as part of a concurrently running psychological research project, which included the D-KEFS CWIT<sup>508</sup>. Those assessed cross-sectionally via the ECAS were tested using version A of the ECAS. Those who provided subsequent further ECAS measurements were assessed via version B and C at follow up times to avoid practice effects influencing these measures<sup>509</sup>.

#### *4.5.3.3. Delis-Kaplan Executive Function System (D-KEFS) Colour Word Interference Test (CWIT)*

The CWIT is one of a nine standalone tests that compose the D-KEFS<sup>508</sup>. The CWIT tests language and executive skills via its subscores. The subject is first presented with a panel of different coloured squares and timed as they name all their colours (Colour Naming subscore), then presented with a panel of written names of colours in black ink and timed as they read the words (Word Reading subscore). Then, the same list of colour names, printed in ink of the colours shown in the colour naming task, is presented. For the Inhibition subscore they are required to name the colours of the ink, and not read the words written in that colour ink, and for the Inhibition Switching subscore, the participant is required to alternate between reading the word and naming the ink colour. The inhibition subscore tests the ability to inhibit the overlearned response of reading the printed word in order to produce the conflicting response of naming the unmatching ink colour that the word is printed in, while the inhibition/switching subscore measures both inhibition and cognitive flexibility<sup>510</sup>. The CWIT was measured only in those who were flagged as cognitively impaired by the ECAS, and volunteered to take part in a concurrently running psychological research study, which was undertaken in participant's homes<sup>511</sup>.

## **4.6. Ethical approval and informed consent**

Ethical approval was obtained from the ethics committee of Beaumont Hospital (REC reference: 13/102) for the collection of EEG data recorded before the onset of this project (which contributed towards the dataset utilised in MMN analyses), and from the St.

James's Hospital (REC reference: 2017-02, see appendix 4.1) for the collection of all EEG and TMS data recorded during this project. All participants provided written informed consent before participation (see consent forms in appendices 4.2-4.5). All work was performed in accordance with the Declaration of Helsinki.



## **5. Results: The Mismatch Negativity Response**

### **Published Work List**

The work described in section 5.1 has been published in the peer-reviewed journal *NeuroImage: Clinical*<sup>103</sup> as:

McMackin R, Dukic S, Broderick M, et al. Dysfunction of attention switching networks in amyotrophic lateral sclerosis. *NeuroImage: Clinical* 2019;22:101707.

Section 5.1 contains all figures (1-6) and tables 2 and 3 as well as the results and discussion section text in full from this publication. Introduction and methods section text from this publication have been abbreviated in this chapter to avoid repetition of the contents of chapters 1-4.

## 5.1. Cross-sectional event related potential analysis

### 5.1.1. Introduction

#### 5.1.1.1. MMN an Index of Cognitive Decline

Multiple hypotheses have been proposed regarding the cortical function(s) measured by MMN, including both sensory and cognitive components of auditory processing. MMN was first described by Näätänen et al. in 1978, who hypothesised that the waveform resulted from comparison of a deviant input to a sensory memory template. It was also suggested that MMN might represent recognition of target criteria fulfilment<sup>512</sup>, however such a “relevance effect” was considered unlikely as attention to the stimulus did not affect the waveform<sup>513</sup>. This was subsequently supported by multiple studies demonstrating MMN in the absence of attention<sup>514</sup>, including in sleeping infants<sup>515</sup> or those in a vegetative state<sup>516</sup>. The MMN was therefore proposed to reflect an automatic detection of sensory change and modification of the physiological model of the environment to incorporate this new stimulus, referred to as the model adjustment hypothesis<sup>514</sup>.

An additional automatic attention-switching process related to the frontal generators was then proposed to occur on the basis that right frontal sources were activated irrespective of the ear detecting the stimulus change<sup>266,517</sup>. This is believed to reflect the call to switch attention to changes in the unattended environment<sup>514</sup>, the occurrence of which is supported by autonomic responses such as heart rate and skin conductance changes following MMN<sup>518</sup> as well as many other studies<sup>519-521</sup>. An alternative adaptation hypothesis, first proposed by May et al. in 1999<sup>522-524</sup>, hypothesised that the MMN response results from cortical adaptation to monotonous stimuli, with MMN reflecting the difference between N1 to a novel sound and a lower amplitude, higher latency N1 generated by repetitive standard tones. This hypothesis has been supported by later studies, such as those of Jääskeläinen et al.<sup>525</sup> and Ulanovsky et al.,<sup>526</sup> (for review see<sup>527</sup>). However, an exclusively auditory hypotheses cannot account for the established prefrontal activation during MMN.

Indeed, source localisation of PET, EEG, fMRI and MEG-derived MMN has reliably highlighted both the superior temporal and inferior frontal gyri as important sources of this signal<sup>266,528-530</sup>, demonstrating that volume conduction alone does not account for frontal MMN. Furthermore, those with lesions of the dorsolateral prefrontal cortex have also been found to have reduced MMN amplitudes<sup>531</sup>. Source localisation across the

MMN timeframe has additionally revealed two subcomponents, an early, sensory component that is maximal in the late N1 range (105-125ms post-stimulus) generated by temporal sources and a later, cognitive component (170-200ms post-stimulus), generated by frontal and temporal sources<sup>266,517,532</sup>. These temporal sources are attributed to sensory memory and change detection while the later active, frontal sources are attributed to involuntary attention switching in response to change<sup>266,517,533,534</sup>.

Hence, source-localised MMN affords the benefit of separately interrogating each of these functions and the neural network which generate them, both in healthy individuals and those with neurological diseases. This is supported by several previous studies in different neurological and neuropsychiatric diseases, where MMN has been used as an index of abnormal auditory perception, involuntary attention switching, pathological brain excitability and cognitive and functional decline (see <sup>535-539</sup> for reviews).

#### *5.1.1.2. Identifying the Sources of MMN Change in ALS*

Using qEEG to measure MMN, we have recently shown a functional change in the underlying networks in ALS, with MMN being significant in healthy controls from 105-271ms post-stimulus and having an increased average delay within the 100-300ms post-stimulus window in ALS<sup>267</sup>. Due to the limited spatial resolution of sensor space studies, however, the specific sources contributing to MMN change and the nature of their dysfunction in ALS remains unclear. We therefore were unable to specify which network components indexed by MMN are affected by ALS pathology.

In this study we have used high-density qEEG in combination with each of three source localisation methods to determine and cross-validate the locations of MMN generators, and to measure differences in their activity between ALS patients and healthy controls. Here we show how the dysfunction of each source of MMN is affected by ALS, characterised by both under-active and over-active sources contributing to the abnormal response.

### *5.1.2. Methods*

#### *5.1.2.1. Ethical Approval*

Ethical approval was obtained from the ethics committee of Beaumont Hospital (REC reference: 13/102) and the St. James's Hospital (REC reference: 2017-02) as described in section 4.6

#### 5.1.2.2. Inclusion Criteria

Patients were over 18 years of age and diagnosed within the previous 18 months with Possible, Probable or Definite ALS in accordance with the El Escorial Revised Diagnostic Criteria.

#### 5.1.2.3. Exclusion Criteria

Patients with Transient Ischemic Attack, Multiple Sclerosis, stroke, seizure disorders, brain tumours, structural brain diseases and other comorbidities were excluded. Those currently taking neuro- or myo-modulatory medications other than riluzole (e.g. muscle relaxants, antidepressants, antipsychotics, benzodiazepines or other anxiolytics) were excluded.

#### 5.1.2.1. Clinical and psychological scores

A contemporaneous ALSFRS-R<sup>504</sup> score was available in 51 patients. 27 patients also undertook the D-KEFS CWIT<sup>508</sup>, which is a test of attention shift, inhibitory control, error monitoring and cognitive flexibility (see section 4.5).

#### 5.1.2.2. Demographics of Patients and Controls

A total of 95 ALS patients and 43 controls underwent recording. 58 ALS patients (f/m: 20/38; age: 59.2 years, range: 29-81 years) and 39 healthy controls (f/m: 28/11; age: 58.9 years, range: 36-78 years) were included in final analyses. Data with poor recording quality (determined by the lack of auditory evoked potentials), were excluded. Eight controls and 44 patients were also included in our previous sensor-space analysis<sup>267</sup>.

Within the ALS group, 44 patients had spinal onset, 12 bulbar, and 2 thoracic onset. All patients were tested for the hexanucleotide repeat expansion in *C9orf72*, of whom 7 were positive (*C9orf72*+). Twelve patients had a known family history of at least one first or second degree relative with ALS, 3 of whom carried the *C9orf72* repeat expansion. One additional patient had a known family history of at least one first or second degree relative with frontotemporal dementia<sup>540</sup>. Mean ALSFRS-R was 37.8 with an interquartile range (IQR) of 33.5-42. Mean disease duration was 1.83 years (IQR: 0.89-2.09) from estimated symptom onset.

#### 5.1.2.3. EEG Acquisition Experimental Paradigm

EEG acquisition and the employed experimental paradigm (auditory oddball paradigm) are described in section 4.1.3.

#### *5.1.2.4. Data Analysis*

EEG data were preprocessed as described in section 4.1.4.1. Source analysis was performed by LCMV, eLORETA and dipole fitting. Sensor and source space analysis pipelines are described in section 4.1.4.2. Mean number of included artefact-free standard/deviant trials was 1267/144 for patients and 1223/146 for controls. For source analyses the number of standard trials was matched to that of deviant trials by random selection. Channels with continuously noisy data after pre-processing were excluded (mean excluded channels  $\pm$  standard deviation in controls:  $1.59\pm 1.65$ , patients:  $1.52\pm 1.55$ ) and data from these channels were modelled by spline interpolation of neighbouring channels for source analysis. Three different source localisation methods were used to circumvent the limitations imposed by different mathematical assumptions for finding a unique solution to the ‘inverse problem’ by each single method<sup>541</sup> (table 2.1).

#### *5.1.2.5. Statistics*

##### *LCMV and eLORETA*

A 10 mm grid in the brain volume yields 733 sources excluding white matter (as modelled by eLORETA) and 1726 sources including white matter (as modelled by LCMV). To analyse these high-dimensional data, 10% FDR<sup>498</sup> was used as a frequentist methods for preliminary screening. Subsequently, EBI<sup>499</sup> was used to find Bayesian posterior probabilities, as well as achieved statistical power and AUROC. AUROC is a measure of how well the test separates patient and control groups<sup>501</sup> which ranges from 0 to 1, where if the null hypothesis of no separation is true, AUROC equals 0.5. Therefore, the further the value of AUROC from 0.5, the greater the separation.

##### *Dipole fitting*

Dipole power for each of the four modelled dipoles in the complete ALS group as well as *C9orf72+*, *C9orf72-*, bulbar-onset and spinal-onset subgroups were compared by Mann-Whitney U test<sup>494</sup>. Bonferroni correction for multiple comparisons established a significance threshold of  $p < 0.0025$ . AUROC and statistics were also calculated for each dipole by empirical bootstrapping-based inference<sup>502</sup>.

##### *Neuropsychology correlation*

Spearman's rank partial correlation<sup>542</sup> (which is inherently robust to outliers) was used to individually compare changes in EEG source power to CWIT performance (colour naming, word reading, inhibition and inhibition switching times in seconds) while

correcting for speech impairment (ALS-FRS speech score on the day of testing) and age. CWIT was investigated on the basis of a previously identified correlation between sensor-level MMN average delay and performance in this task<sup>267</sup>. Correlations were performed for power in each fitted dipoles and for the mean power in the left superior and medial frontal gyri (combined), primary motor cortex and posterior parietal cortex, according to the AAL atlas<sup>487</sup>. Multiple comparison correction was by Bonferroni correction. BBI<sup>505</sup> and ECAS<sup>511</sup> data were also available, however the main scores of these measures showed no significant correlation to source activity and were, therefore, not investigated further.

### 5.1.3. Results

#### 5.1.3.1. Dipole fitting

Locations of dipole fits are illustrated in Fig. 5.1. Control and patient groups showed similar goodness of fit (median (IQR) residual variance in patients: 23.32% (15.24-30.2%), controls: 24.39% (15.55-35.49%)). P-values obtained by Mann-Whitney U-test comparison of dipole power between ALS patients and healthy controls are summarised in table 5.1.

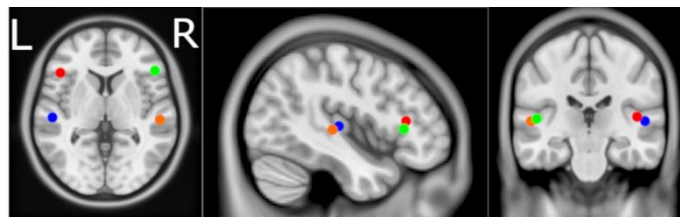


**Figure 5.1. Location of dipoles modelled by dipole fitting.** Centroids of the left (blue) and right (orange) superior temporal gyri and left (red) and right (green) inferior frontal pars triangularis were used to seed dipoles for dipole fitting. Axial MRI view is from above (L-Left, R-Right). This figure has been published in my paper McMackin et al. 2019b (figure 1), please see appendix 2.2.

Power was significantly lower in the IFG bilaterally as well as the left STG. AUROC demonstrated that power in each of these three dipoles has good group discrimination ability (table 5.1, Fig. 5.2). No differences were found between male and female patients for any dipole ( $p=0.27-0.75$ , AUROC=0.42-0.58). The discrepancy from complete fit indicated the presence of additional sources, which were subsequently aggregated by eLORETA and LCMV.

**Table 5.1. Summary of P-values and AUROCs for each source modelled by dipole fitting in ALS patients and subgroups compared to controls.** All subgroups show decreased power in inferior frontal and left temporal dipoles compared to controls. Inferior frontal activity has excellent discrimination ability between *C9orf72+* patients and controls and good discriminating ability in other groups. P-values were obtained by Mann-Whitney U test. AUROC given in parentheses. Bold indicates statistical significance ( $p < 0.0025$ ). This table has been published in my paper McMackin et al. 2019b (table 2), please see appendix 2.2

Dipole Location	All	<i>C9orf72+</i>	<i>C9orf72-</i>	Bulbar-onset	Spinal-onset
Left IFG	<b>5.16*10<sup>-6</sup></b> (0.7741)	<b>6.87*10<sup>-4</sup></b> (0.9084)	<b>1.98*10<sup>-5</sup></b> (0.7637)	<b>1.22*10<sup>-3</sup></b> (0.802)	<b>1.22*10<sup>-3</sup></b> (0.769)
Right IFG	<b>1.07*10<sup>-5</sup></b> (0.7648)	<b>2.15*10<sup>-4</sup></b> (0.9451)	<b>9.29 *10<sup>-5</sup></b> (0.7416)	<b>2.37*10<sup>-5</sup></b> (0.895)	<b>1.74*10<sup>-4</sup></b> (0.74)
Left STG	<b>9.30*10<sup>-6</sup></b> (0.7666)	0.016 (0.7912)	<b>2.30*10<sup>-6</sup></b> (0.761)	2.64*10 <sup>-3</sup> (0.795)	<b>2.40*10<sup>-4</sup></b> (0.738)
Right STG	0.081 (0.6052)	0.39 (0.6044)	0.118 (0.5968)	0.035 (0.698)	0.23 (0.576)

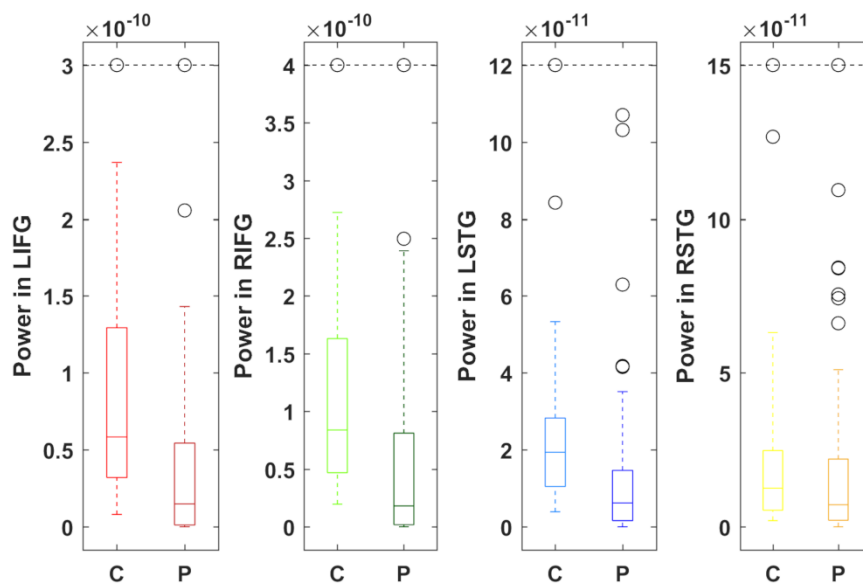


**Figure 5.2 ALS patients show decreased power in both inferior frontal gyri and the left superior temporal gyrus.** Boxes illustrate the interquartile range with whiskers illustrating the maximum and minimum power (A-m) within twice the interquartile range for ALS patients (P) and controls (C), determined by dipole fitting. Outliers are illustrated in black. Dashed line caps up to two outliers beyond this value. L – Left, R – Right, IFG – Inferior frontal gyrus, STG – Superior Temporal Gyrus. This figure has been published in my paper McMackin et al. 2019b (figure 2), please see appendix 2.2.

### 5.1.3.2. eLORETA

ELORETA identified maximal intensity of neural activity during MMN in the left IFG and bilateral STG and middle temporal gyri in controls (Fig. 5.3A), confirming the localisation of major sources to those previously established, with the exception of the

right IFG<sup>138,265,486</sup>. ALS patients showed a pattern of reduced activity in these sources, consistent with the results of dipole fitting, as well as an increase in activity in posterior sources (Fig. 5.3B). While the eLORETA estimated the general distribution pattern of activity, the method's low spatial resolution prevented the effects reaching statistical significance.



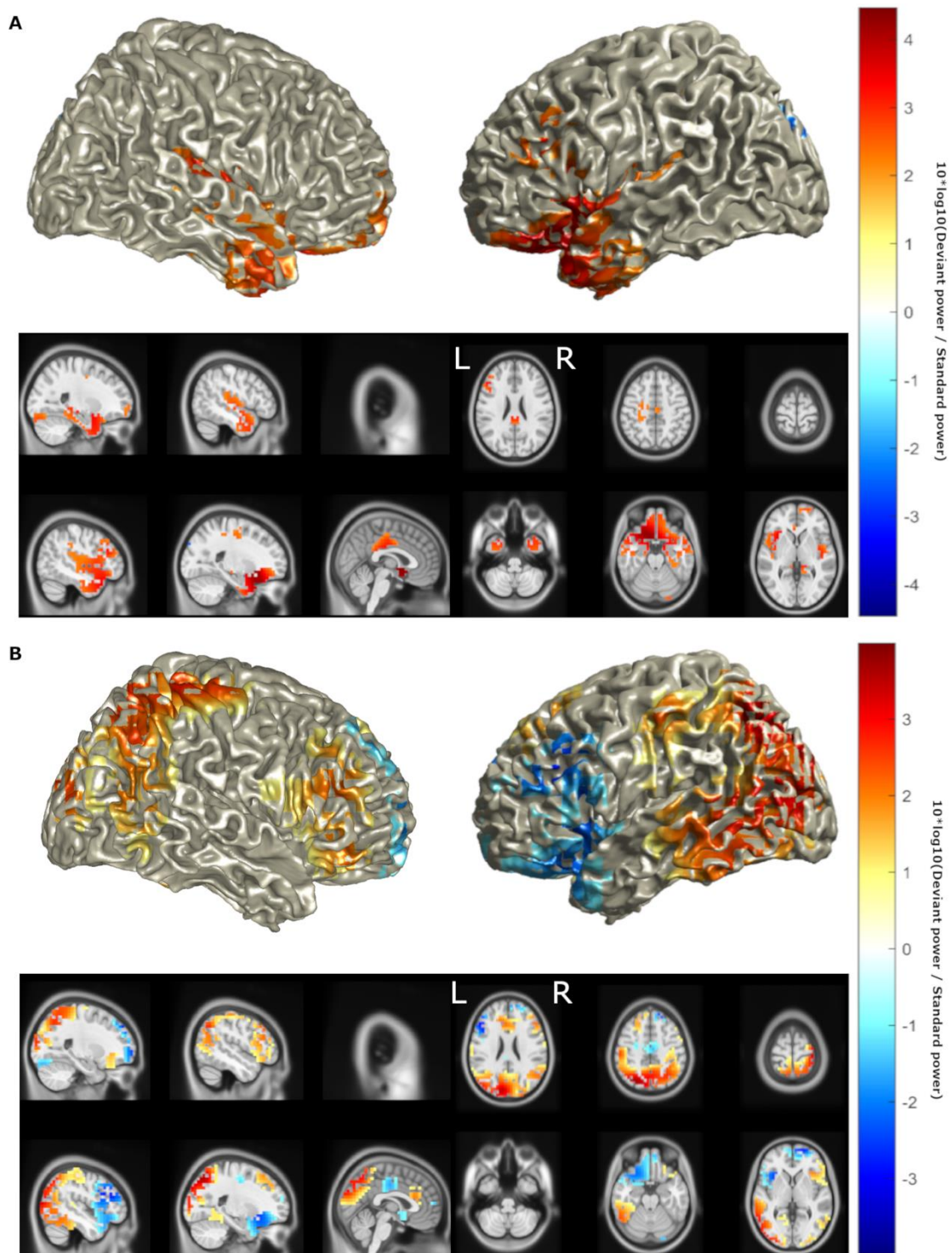


**Figure 5.3. ELORETA identified a pattern of decreased activity in the left superior temporal and inferior frontal sources, and an increase in activity in posterior areas.** Location of MMN sources with (A) top 50% of power ( $10 \cdot \log_{10}(\text{Deviant power} / \text{Standard power})$ ) in healthy controls and (B) power differences  $>25\%$  of maximum between ALS patients and healthy controls as determined by eLORETA. Red denotes increase in power, blue denotes decrease in power. Axial MRI views are from above (L-Left, R-Right). This figure has been published in my paper McMackin et al. 2019b (figure 3), please see appendix 2.2.

### 5.1.3.3. LCMV

LCMV identified sources of MMN similar to the findings of eLORETA (Fig. 5.4A) but also identifying the right IFG as a source, as identified by previous studies<sup>138,265,486</sup>. LCMV also detected a trend of reduced activity in these sources bilaterally, in keeping with the results of dipole fitting and eLORETA, as well as an increase in activity in the left parietal, central and dorsolateral prefrontal cortex (Fig 5.4B).

No significant differences were found between male and female patient sources ( $\alpha_{\text{global}}=0.92$ ,  $\beta_{\text{global}}=0.075$ ) or mean power of the left posterior parietal, motor or inferior frontal cortices ( $p=0.56-0.89$ ).

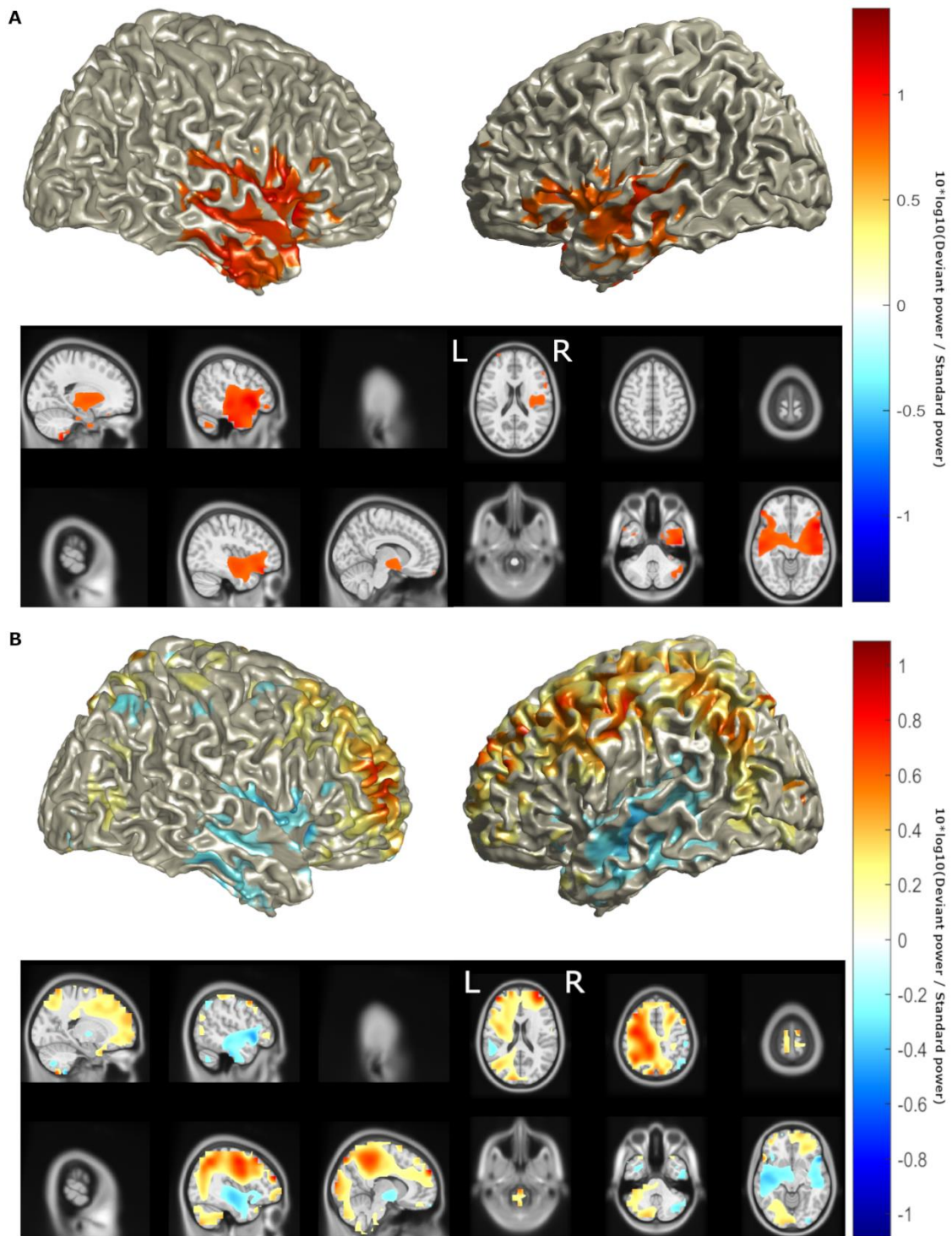


**Figure 5.4. LCMV identified a pattern of decreased activity in bilateral superior temporal and inferior frontal sources, and an increase in activity in the left hemisphere.** Location of MMN sources with (A) top 25% of power ( $10 \cdot \log_{10}(\text{Deviant power} / \text{Standard power})$ ) in healthy controls and (B) power differences  $>25\%$  of maximum between ALS patients and healthy controls as determined by LCMV beamforming. Red denotes increase in power, blue denotes decrease in power. Axial MRI views are from above (L-Left, R-Right). This figure has been published in my paper McMackin et al. 2019b (figure 4), please see appendix 2.2.

This increase reached statistical significance (Fig. 5.5, FDR=10%, statistical power=0.58). Based on interpolation with an AAL atlas, sources with significantly increased activity included the superior parietal lobe and precuneus, motor structures including the primary motor cortex, supplementary motor area and mid cingulum, as well as the mid frontal gyrus of the left hemisphere (table 5.2).

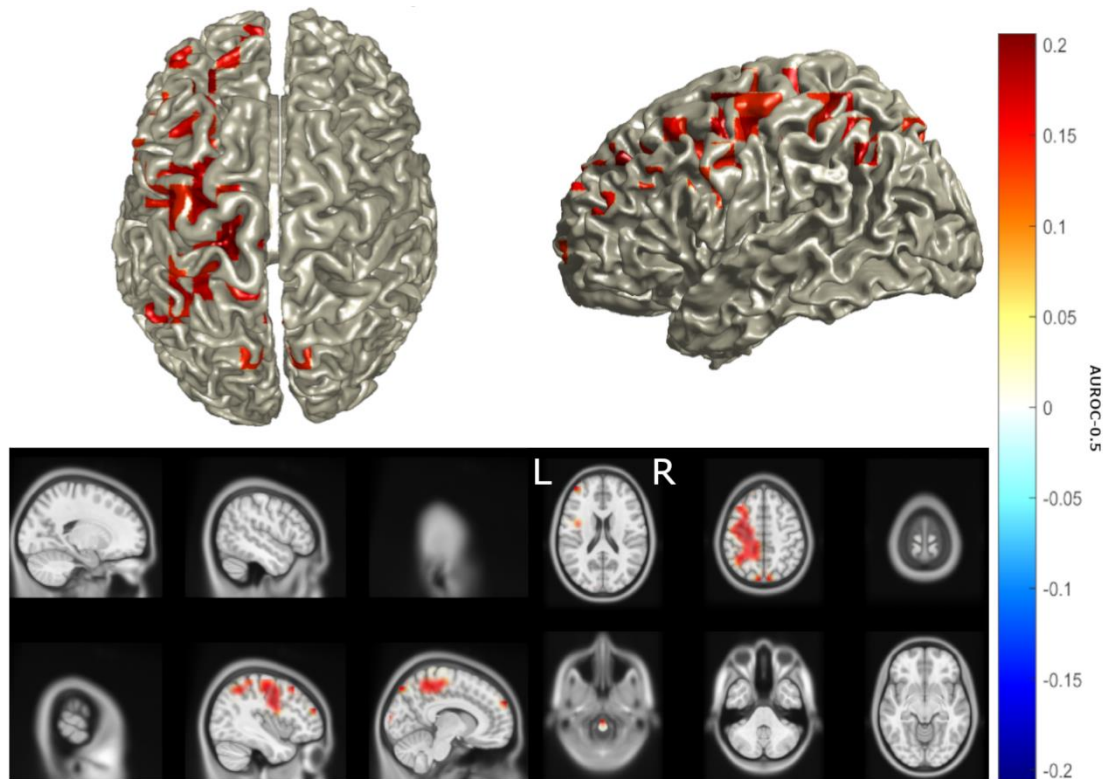


**Figure 5.5. Increased activity in the left posterior parietal, central and dorsolateral prefrontal cortex in ALS is statistically significant.** Statistically significant (false discovery rate=10%) differences in power between ALS patients and healthy controls as determined by LCMV. Heat map values are AUROC-0.5. Red denotes AUROC>0.5 (i.e. values higher in ALS than controls), blue denotes decrease in AUROC<0.5 (i.e. values lower in ALS than controls). Axial MRI views are from above (L-Left, R-Right). This figure has been published in my paper McMackin et al. 2019b (figure 5), please see appendix 2.2.

Positive correlations (Fig. 5.6) were found between CWIT inhibition-switching time (but not other CWIT scores) and mean power in the left primary motor cortex ( $\rho=0.45$ ,  $p=0.055$ ), the superior and middle frontal gyri combined ( $\rho=0.47$ ,  $p=0.031$ ) and the posterior parietal cortex ( $\rho=0.45$ ,  $p=0.042$ ), where greater inhibition-switching score indicates more impaired cognitive flexibility and verbal inhibition<sup>510</sup>. P-values below 0.05

in the prefrontal and parietal cortices did not survive multiple comparison correction, likely due to the low number of CWIT scores available.

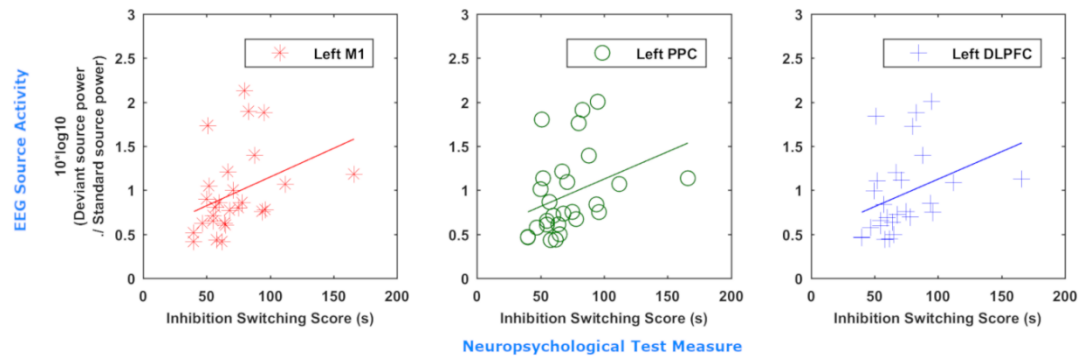


**Figure 5.6. Increased activity in the posterior parietal and dorsolateral prefrontal cortex correlates to poorer performance in cognitive switching tasks.** Correlation of inhibition/switching score (in seconds) for 27 patients with mean power in the left primary motor cortex (red), posterior parietal cortex (PPC, green), and middle and superior frontal gyri (M/SFG, blue) illustrated by scatterplot with line of best fit. This figure has been published in my paper McMackin et al. 2019b (figure 6), please see appendix 2.2.

**Table 5.2. Comparison of the head and source models, time windows and detected source activity changes for each source localisation method used.** L – left, R – right, IFG – inferior frontal gyrus, STG – superior temporal gyrus. Arrows represent direction of change in power. \*Statistically significant ( $p < 0.0025$ ). BEM – Boundary element model. This table has been published in my paper McMackin et al. 2019b (table 3), please see appendix 2.2.

Method	Head/source model	Time (ms)	L IFG	R IFG	L STG	R STG	Other significant source changes
LCMV	ICBM152/personal MRI BEM, 10mm grid	100-300	↓	↓	↓	↓	↑* Left superior parietal lobe, precuneus, primary motor cortex, supplementary motor area, mid cingulum, mid frontal gyrus
eLORETA	Colin27 MRI BEM, 10mm grid excl. white matter	100-300	↓	↑	↓	↓	None
Dipole fitting	ICBM152/personal MRI BEM, 4 dipoles	105-271 & 100-300	↓*	↓*	↓*	↓	N/A

#### 5.1.3.4. Differences between ALS Subgroups

*C9orf72*<sup>+</sup> patients were not distinguished from *C9orf72*<sup>-</sup> patients by any localisation method, nor were bulbar-onset from spinal-onset patients. This was likely due to insufficient sample size. *C9orf72*<sup>-</sup> and spinal subgroups individually showed similar patterns of significant difference to the full patient group across each localisation method. Bulbar and *C9orf72*<sup>+</sup> subgroups significantly differed from controls with respect to bilateral IFG dipole activity, and exhibited better discrimination ability (summarised in table 5.1). The discrimination ability of this difference was excellent for *C9orf72*<sup>+</sup> patients (AUROC > 0.9). CWIT and speech score data were insufficient (*C9orf72*<sup>+</sup> n=0, bulbar-onset n=3) for correlation analyses.

#### 5.1.4. Discussion

This study demonstrates that source localization of cognitive ERPs measured by EEG reliably distinguishes attentional network changes in ALS patients compared to controls, particularly in subgroups with higher prevalence of cognitive impairment<sup>45,411</sup>. Furthermore, this study indicates for the first time a correlation between the activities of specific sources underlying cognitive event-related potentials and cognitive performance in a neurodegenerative disease. Compared with controls, ALS patients show decreased activity in both inferior frontal gyri and the left superior temporal gyrus and increased left posterior parietal and dorsolateral prefrontal activity. ALS patients also show significantly increased activity in the left motor cortex.

##### 5.1.4.1. Imbalance of Attention-Regulating Network Activity during Sensory Processing in ALS

The superior temporal and inferior frontal gyri are well established sources of MMN activity<sup>138,532,543</sup>. In this study, decreased activity in these regions was identified independently using each of the methods, however, dipole fitting allowed for a more temporally and spatially precise interrogation of these sources.

Repetitive TMS<sup>544</sup> and non-word rhyming task studies<sup>545</sup> have demonstrated the role of the IFG in phonological working memory, where information about one stimulus is stored for later comparison to a second. The IFG is also known to be active when ignoring stimuli<sup>546</sup> and is functionally connected to the default mode network<sup>547</sup>. This network is active when directed attention is not required and is deactivated by goal-directed activity, as defined by resting-state fMRI<sup>548</sup>. The activity of the default mode network is anti-correlated with that of the central executive network, where attention needs to be directed to a task<sup>549</sup>. Inferior frontal source activity during the MMN is therefore consistent with calling for a switch of attention to changes in the unattended environment (i.e. involuntary attention switching), to which prefrontal MMN sources have previously been attributed<sup>266,514,517</sup>.

The observed substantial reduction in IFG activity in ALS is correspondingly expected to parallel impairments in these cognitive functions. As posterior parietal and dorsolateral prefrontal cortices are nodes of the central executive network<sup>550</sup>, their abnormal activation in combination with IFG dysfunction during MMN in ALS may represent a loss of

balance between the activity of these attention-regulating networks<sup>417</sup> resulting in dysregulation of involuntary attention switching.

As participants were asked to ignore and not respond to stimuli in this study, attention regulation could not be behaviourally measured during MMN recording. This hypothesis is, however, supported by our preliminary findings of a positive correlation between increases in left posterior parietal and dorsolateral prefrontal activity during MMN, and the inhibition/switching score of the CWIT (and not other subscores of the CWIT). This indicates that abnormal increase in the activity of this network conveys cognitive inflexibility and disinhibition<sup>510</sup>. Such behavioural inflexibility and disinhibition is consistent with incorrect orientation to irrelevant stimuli and is expected in those with abnormal central executive network activation. Correspondingly, change in bilateral IFG activity was shown to be an excellent discriminator of *C9orf72+* and bulbar-onset ALS subgroups, which are more prone to cognitive impairment<sup>45,411</sup>.

This imbalance hypothesis is also evidenced by data from previously reported functional connectivity studies in ALS. For example, resting-state MEG has identified increased functional connectivity between the left posterior cingulate and prefrontal cortices, as well as within and between posterior parietal cortices, in addition to increased overall parietal connectivity (e.g. node weight)<sup>393</sup>. Furthermore, resting state fMRI has demonstrated increased left precuneus, posterior parietal and mid cingulate cortex connectivity in addition to decreased inferior frontal connectivity<sup>551</sup> in ALS. Accordingly, the frontoparietal hyperactivity and inferior frontal depression observed in our study may reflect a spread in pathological hyperactivity into cognitive networks, which in turn alters the balance in normal network activity. Activation of the central cortex in addition to cognitive network nodes during MMN in ALS may correspondingly represent abnormal activation of networks connecting motor and cognitive areas. This is consistent with previous physiological studies which have consistently identified hyperactivity in upper motor neurons in ALS<sup>194</sup> and loss of inhibitory control<sup>289</sup>.

ALSFRS-R total score showed no correlation to source activity - this is likely a reflection of the relatively low burden disease in the majority of patients, and the study being underpowered to explore the subscores of ALSFRS-R. However, previous studies have shown that functional connectivity is increased with ALS and correlates with disease severity<sup>552</sup>. A reduction in MMN in healthy individuals is also found to parallel increased connectivity and decreased inhibitory control between underlying sources, particularly in frontal nodes<sup>553</sup>. The recently demonstrated relationship between cognitive impairment



and disease stage in ALS<sup>468</sup> is therefore likely to reflect the spread of hyperactivity from motor to cognitive networks.

#### *5.1.4.2. Potentially Abnormal Function of Auditory Network in ALS*

Temporal source activity has been attributed predominantly to sensory memory and change detection in early MMN<sup>266,517,533,534</sup>; however, it has also been found to contribute to MMN's later attention switching component<sup>532</sup>. Furthermore, as the difference wave early in the 100-300ms studied may also capture changes in N1<sup>527</sup>, temporal activity may include sensory detection.

As STG contains the primary auditory cortex<sup>397</sup> and has been shown to be active during attention control<sup>554</sup>, the decrease in left STG activity identified here in ALS may represent impairment in either auditory or cognitive networks. These findings, in addition to the greater number of (excluded) patients lacking clear AEPs compared to controls, suggest the additional presence of auditory network dysfunction in ALS. An additional investigation of AEPs generated during a solely auditory task is required to investigate this network further in ALS.

#### *5.1.4.3. Harnessing the Advantages of Quantitative EEG*

The detected changes in ALS reflect the additive benefits of physiological investigation to those of structural imaging. The discriminative ability of these changes, determined by the AUROC (up to 0.95 here) was comparable to, or better than, that achieved by fMRI (AUROC=0.714)<sup>555</sup> and sensor space qEEG (AUROC=0.69)<sup>267</sup>. This methodology therefore has the potential to provide neurodegenerative disease markers prior to the onset of discernible structural degeneration, allowing for earlier and more sensitive monitoring of potential interventions.

#### *5.1.4.4. Limitations*

A sample size of 58 patients and limited availability of psychological and clinical test scores restricted exploration of the relationship between cognitive symptoms and source activity within subgroups of this heterogeneous condition. Further studies of larger sample size are therefore warranted to explore such relationships and ALS inter-subgroup differences with greater statistical power.

#### *5.1.4.5. Conclusion*

In conclusion, combining multiple localisation methods to determine the sources of ERPs provides high spatial resolution to complement qEEGs' excellent temporal resolution in

the investigation of ALS-related network dysfunction. The use of this approach to localise activity during other cognitive, motor and sensory tasks allows for detailed interrogation of the location and nature of brain network disruption in neurodegenerative disorders, with the potential to provide early, non-invasive and inexpensive biomarkers of neurodegenerations or their subtypes.

## **5.2. Longitudinal event-related potential analysis**

The work described in section 5.3 has been accepted for publication in the peer-reviewed journal *Neurobiology of Aging* as:

McMackin R, Dukic S, Costello E, et al. Cognitive Network Hyperactivation and Motor Cortex Decline Correlate with ALS Prognosis. *Neurobiology of Aging*. 2021 Mar 10 (In Press).

Section 5.3 contains all figures (1-4) and tables (1-2) as well as the results and discussion section text in full from this publication. Introduction and methods section text from this publication have been abbreviated in this chapter to avoid repetition of the contents of chapters 1-4.

### *5.2.1. Introduction*

As ALS is highly heterogeneous in its progression between patients, the cross-sectional analysis described in section 5.1 could not determine the temporal profile of the identified cortical activity changes with respect to disease progression or determine whether such changes can act as a marker of disease progression. In this section, the tracking of MMN source activity changes in ALS over time is described. We sought to determine whether progressive changes occur in cortical sources of neuro-electric activity that are abnormal at baseline in ALS. We also aimed to investigate the relationship between any progressive changes in network function and survival times and disease progression as measured by functional (ALSF<sub>RS</sub>-R) and cognitive-behavioural scores (ECAS<sup>506</sup> and BBI<sup>505</sup>). Finally, to probe the prognostic utility of these electrophysiological measures and the relevance of non-motor cortical pathology to ALS prognosis, we have investigated whether cortical baseline activity and activity changes are predictive of ALS symptom progression after one year and whether changes in non-motor function associated network hubs relate to survival times.

### *5.2.2. Methods*

#### *5.2.2.1. Ethical Approval*

Ethical approval and participant written consent were obtained as described in section 4.6.

#### 5.2.2.2. *Inclusion Criteria*

All participants were over 18 years of age and able to give informed written or verbal (in the presence of two witnesses) consent. Patients were diagnosed with Possible, Probable or Definite ALS in accordance with the El Escorial Revised Diagnostic Criteria<sup>556</sup>.

#### 5.2.2.3. *Exclusion Criteria*

Exclusion criteria included multiple sclerosis, stroke, seizure disorders, brain tumours, psychological and structural brain diseases and other relevant neuromuscular comorbidities were excluded. Those currently taking neuro- or myo-modulatory medications other than riluzole (e.g. muscle relaxants, antidepressants, antipsychotics, benzodiazepines or other anxiolytics) were excluded.

#### 5.2.2.4. *Clinical and psychological scores*

Longitudinal ALSFRS-R<sup>504</sup>, ECAS<sup>506,507</sup>, BBI<sup>505</sup> and CWIT<sup>508</sup> data (at least two data points, collected at least 6 months apart) were only collected for those patients who attended the National ALS Clinic/took part in concurrent psychology research (see section 4.5) with frequency and timing which sufficiently overlapped with the patient's participation in this study (see section 5.2.3.1). Survival was calculated for deceased patients as the number of months between symptom onset and death.

#### 5.2.2.5. *Participant demographics*

A total of 71 ALS patients underwent longitudinal recording while 71 healthy controls underwent a single recording session. Of those who underwent recording, 60 patients (17 female; age mean: 60.56 years, range: 32-81 years, standard deviation: 11.49 years) and 62 controls (42 female; age mean: 60.25 years, range: 36-82 years, standard deviation: 10.70 years) were included in final analyses as data lacking clear AEPs were excluded (one participant, who did not report hearing issues, showed no AEP over three separate recordings. Remaining excluded participants took part in two or three recordings, showing AEPs in one recording, but no clear AEP in the other(s), due to similar baseline and post-stimulus signal amplitudes. Due to lack of longitudinal data of sufficient quality, they were therefore excluded). Patients and controls were age matched ( $p=0.14$ ) but not gender matched ( $p=3.00 \times 10^{-5}$ ,  $\chi^2=17.42$ ), however we previously established no significant difference between genders for these measures<sup>103</sup>, and we have included gender as a factor in our statistical analysis. Controls did not undergo longitudinal assessment (primarily driven by recruitment difficulty due to hesitation to enrol in longitudinal studies). Significant individual test-retest stability has, however, been

previously demonstrated for the MMN<sup>557</sup>, supporting the stability of measures in controls as baseline.

ALSFRS-R data were available for 50 patients (n range: 2-20 data points, mean: 10.66). Cognitive-behavioural data were available for 45 (ECAS n range: 2-5, mean: 3.48), 19 (BBI n range: 2-4, mean: 3.1) and 19 patients (CWIT n range: 3-4, mean: 3.84, one lacking an inhibition switching subscore). The timespan of this data collection overlapped with that of EEG data collection for all but 5 patients, who had a baseline EEG within 6 months after final ECAS follow-up and had either 3 or 4 ECAS data points each spanning at least 14 months, facilitating reliable modelling. Time in months (median [range]) between baseline EEG and nearest data point collection was 0.53 [0-4.11] for ALSFRS-R, 1.74 [0-6.74] for ECAS, 0.20 [0.03-2.10] for CWIT and 1.59 [0.19-5.36] for BBI. Survival data (median: 49.93 months, interquartile range: 35.73-69.69 months) were available for 38 patients, who were deceased by the time of analysis. Patient clinical characteristics at baseline (EEG T1) are summarised in table 5.3. Overlap in cohort with those included in our previous cross-sectional analysis<sup>103</sup> includes 34 patients (including all five *C9orf72*+ patients and six of those of bulbar onset) and 39 controls included in this study.

**Table 5.3. Summary of ALS patient clinical characteristics at baseline.** IQR – Interquartile range. Symptom onset date is determined by patient reported estimate.

Site of onset (spinal/bulbar/thoracic)	50/9/1
<i>C9orf72</i> expansion carrier (n)	5
Comorbid FTD diagnosis	3
ALSFRS-R (median [IQR])	37.76 [35.80-41.42]
Months since symptom onset (median [IQR])	21.10 [12.26-40.30]
BBI (median [IQR])	4.23 [1.4-7.15]
ECAS total (median [IQR])	113.26 [105.81-118.76]
ECAS ALS specific (median [IQR])	85.30 [77.26-88.11]
ECAS ALS non-specific (median [IQR])	29.25 [26.75-31.89]

#### 5.2.2.6. EEG Acquisition and Experimental paradigm

The experimental paradigm and data processing pipeline are illustrated (simplified) in Fig. 5.7. EEG acquisition and the employed experimental paradigm (auditory oddball paradigm) are described in section 4.1.3.

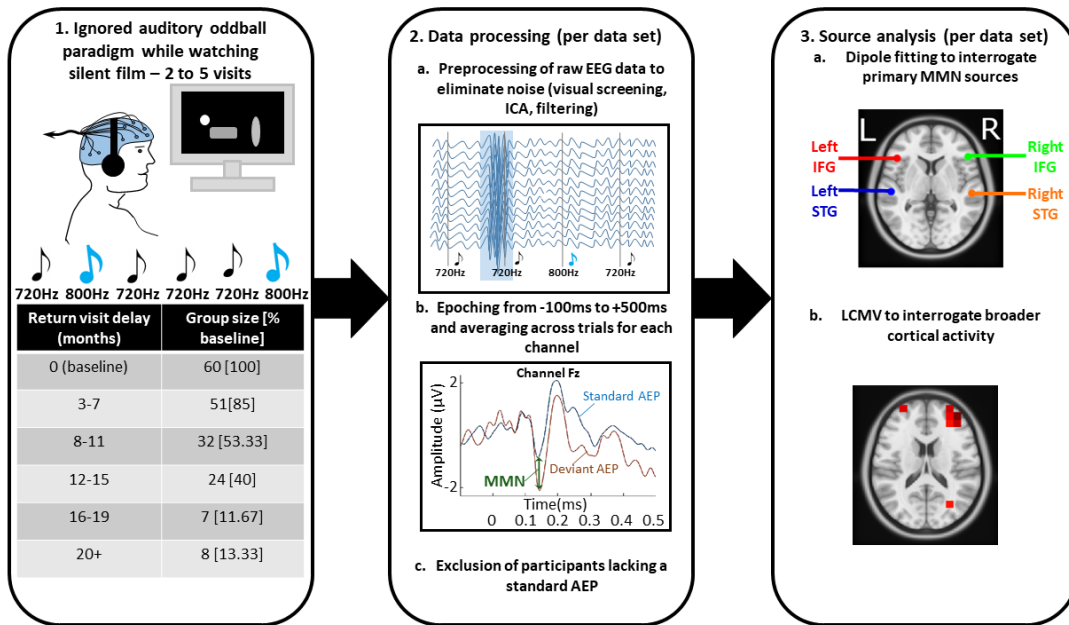


**Figure 5.7. Illustration of data collection and processing pipeline for each dataset.** Frequencies cited refer to the pitch of tones delivered (720Hz – Standard tone, 800Hz – Deviant tone). AEP – Auditory evoked potential. MMN – Mismatch negativity. LCMV – Linearly constrained minimum variance (beamforming). IFG – Inferior frontal gyrus. STG – Superior temporal gyrus. L – Left, R – Right

#### 5.2.2.7. Data Analysis

##### *EEG signal processing*

In total, Mean number of included artefact-free standard/deviant trials for controls was 1230/144 and for patients was 1274/145 at T1, 1230/141 at T2, 1182/136 at T3, 1195/136 at T4 and 1137/131 at T5. Therefore, following matching of standard trial numbers (e.g. approximately 140 trials) clear individual AEPs were still obtained from trial means, in alignment with trial numbers of other auditory EEG studies<sup>558–560</sup>. Preprocessing is described in section 4.1.4.1.

##### *Source analysis*

Channels with continuously noisy data were excluded (controls mean [range]: 1.56 [1-7], patients mean [range]: T1: 1.15 [0-5], T2: 1.38 [1-7], T3: 1.29 [1-4], T4: 1.23 [1-3], T5: 1.5 [1-4]) and modelled by spline interpolation of surrounding channels.

Brain, skull and scalp tissues were modelled using boundary element models. Personal models were generated for 45 patients, using T1-weighted images from MRI (see section 4.1.4.2). These MRI were collected on the same day as baseline EEG recording, at the Centre of Advanced Medical Imaging, St. James' Hospital. A ICBM152-based<sup>1483</sup> head model was used for remaining patients and controls who declined to/were unsuitable to undergo MRI. Comparable localization accuracy has been demonstrated for template-

based and individualised boundary-element head models<sup>482,484</sup>, indicating that personalised MRI scans were not essential for modelling. Further, as a single model was used across timepoints for each individual, change in head tissue modelling was not a confounding factor to change in source activity. For group level analyses, source position coordinate vectors of personal MRI-based head models were warped to those of the ICBM152-based headmodels to ensure matching sources were compared.

As we previously identified that the spatial precision of dipole fitting was best suited to the study of the most consistently reported four sources of the MMN while LCMV identified excessive activity of other cortical sources in ALS with better spatial resolution than exact LORETA<sup>103</sup> we have again used dipole fitting and LCMV for common and uncommon MMN source analysis respectively (as described in section 4.1.4.2) in keeping with our previous, cross-sectional protocol (section 5.1).

#### 5.2.2.8. *Statistics*

##### *Comparison of patient and control power*

In order to investigate how ALS patient data varied over time relative to control baseline (for example, to investigate if initially underactive sources become normally active or hyperactive), longitudinal data were grouped for comparison to controls. Due to variable intervals between EEG data collection (due to practical aspects and availability of participants), patient longitudinal data were grouped according to months since first EEG: 0 months (i.e. T1, n=60), 3-7 months (n=51), 8-11 months (n=32), 12-15 months (n=24), 16-19 months (n=7) and 20-57 months (n=8) for comparison to control data. Each ALS patient had a maximum of one data point per time group.

##### *LCMV*

For LCMV, a 10mm grid in the brain volume (including white matter regions) yielding 1726 modelled sources was implemented. In order to compare power between patients within each time group to control values for all voxels throughout brain simultaneously, a 10% False Discovery Rate<sup>562</sup> was used as a frequentist method for preliminary screening of significant activity difference, corrected across the 1726 source model voxels. Subsequently, EBI<sup>499</sup> was used to find Bayesian posterior probabilities, as well as achieved statistical power and AUROC.

##### *Dipole fitting*

For lower dimensional comparison of dipole power for each of the four modelled dipoles, data from the control and ALS patient groups were compared by Mann-Whitney U-test<sup>494</sup>.

A 5% FDR was implemented using the Benjamini and Hochberg (1995) method<sup>498</sup> to account and correct for multiple comparisons, following the significance testing at  $p < 0.05$ . Specifically, this FDR was applied across the six time group power values compared to controls power values across all 4 sources of interest (i.e. correction across 24 p-values).

#### *Models of longitudinal change in source power*

To investigate change in power over time within ALS patients, the fixed effect of time since T1 and the random effects of delay from symptom onset, gender and age at baseline were simultaneously investigated for each source by linear mixed effects models with the following Wilkinson-style<sup>563</sup> model description formula:

$$\text{Power} = \text{Time since T1} + (1/\text{Delay from symptom onset}) + (1/\text{Sex}) + (1/\text{Age at baseline}) + (\text{Time since T1} | \text{Patient})$$

Intercept and slope (to account for the repeated nature of the analysis) was permitted to vary randomly per patient in all models. Group effect (i.e. patient or control) was not incorporated into this analysis the main purpose is to test for longitudinal changes in patients (not measured in controls). For source activity models of the LPPC, LDLPFC and LM1, power was calculated from the mean activity of voxels within the region demonstrating significant hyper activation in cross-sectional analysis. Power values were normalised for linear mixed modelling by inverse normal transformation<sup>564</sup> as residuals were not normally distributed for IFG and STG models without transformation. The null hypothesis of model residuals being normally distributed was accepted by Shapiro Wilks tests for each model ( $p > 0.05$ ).

Linear regression models with time since T1 as the fixed variable and power at source of interest as the dependent variable were also fitted for each source per individual. Robust estimation was used where 3 or more data points were available. Linear regression modelling facilitated clear illustration of the change in individual source activity over time and allowed for assignment of rate of change values to each individual for correlation analyses. Furthermore, these models allowed for estimation of power values for each individual at common time points relative to baseline despite variation across and within datasets in number of data points and intervals between data points and intervals (e.g. power at one year after baseline). Second order models (curves) were calculated for all 7



sources per individual, however no quadratic components were deemed significant by sign rank testing<sup>495</sup> (comparing the coefficient value to zero), so further analyses were based on first order models.

Longitudinal analysis was performed with respect to baseline, rather than with respect to patient reported disease onset (table 5.3) or time of diagnosis as timing of symptom onset relative to underlying pathophysiology is highly variable in neurodegenerative disease, patient reported disease onset may or may not represent true first disease symptoms as early symptoms may be missed or unrelated events may attributed to the disease, and ALS diagnosis occurs with substantial variation relative to symptom onset and initial clinical presentation. While baseline referencing has similar limitations, it provides a basis for the alignment of individual participation timelines.

#### *Modelling functional and cognitive-behavioural scores for correlation analysis*

As intervals between EEG collection and psychological/motor test score collection varied across individuals, linear regression models (robust estimation method used where 3 or more data points were available) were generated for functional or cognitive-behavioural measures (CWIT colour naming, word reading, inhibition and inhibition-switching subscores, ECAS total, ECAS ALS-specific, ECAS ALS-nonspecific, ALSFRS-R and BBI scores) for those individuals where two data points collected more than 6 months apart were available. In these models, the functional/cognitive-behavioural measure was the dependent variable and time since baseline EEG was the independent variable. Second order models (curves) were also calculated for all measurements, however no quadratic components were deemed significant by sign rank testing<sup>495</sup> (comparing the coefficient value to zero). Therefore, the slope (1<sup>st</sup> order coordinates) of each linear model was used to quantify the rate of change for each measure per individual. Based on these models, the values of each variable (e.g. motor and cognitive-behavioural test scores) at baseline EEG (T1, i.e. 0 months) and after 12 months were calculated.

#### *Correlations*

Spearman's non-parametric rank correlation<sup>542</sup>, which is robust to outliers<sup>565</sup>, was used to investigate relationships between source activity changes, and between source activity and psychological/motor test scores. Confidence intervals (95%) of rho values were determined by bootstrapping of the rho statistic using 1000 bootstrap samples of the patient dataset with the required clinical scores. Partial correlation was implemented for

investigating relationships to CWIT scores, to account for ALSFRS-R speech score at time of CWIT testing, as performance in this task is affected by speech impairment. Multiple comparison correction across the 7 sources of interest, separately for ALS total score (7 comparisons), ECAS total score (7 comparisons), survival (7 comparisons), CWIT scores (4×7 comparisons) and BBI post MND score (7 comparisons) was implemented using a 5% FDR, implemented using the Benjamini and Hochberg method<sup>498</sup>.

#### *Age and gender matching*

The differences between age and gender in the patient and control groups were tested by Mann-Whitney U test<sup>494</sup> and chi-squared proportions test respectively.

### 5.2.3. Results

#### 5.2.3.1. Cross-sectional analysis

Baseline cross-sectional analysis in this cohort confirms the presence of previously observed abnormal cognitive and motor cortical function. Subgroup cross-sectional analysis was not repeated due to the high overlap of *C9orf72+* and bulbar-onset patients with our previous publication<sup>103</sup> (reported in section 5.1).

At baseline, both IFG showed significantly reduced power (Fig. 5.8, left:  $p=0.0157$ , right:  $p=0.0022$ ) compared to controls, as we previously observed<sup>103</sup>. While the left STG showed a trend of decreased activity in line with our previous findings, this difference was not statistically significant ( $p=0.24$ ). Baseline hyperactivity in left motor, posterior parietal, dorsolateral prefrontal and mid cingulate cortices was again identified in T1 (baseline time point) recordings (appendix 5.3), consistent with our previous findings<sup>103</sup>. Significantly increased activity was also observed within the left medial occipital and right dorsolateral prefrontal cortices. Maximum AUROC was 0.67, in the right middle frontal gyrus.

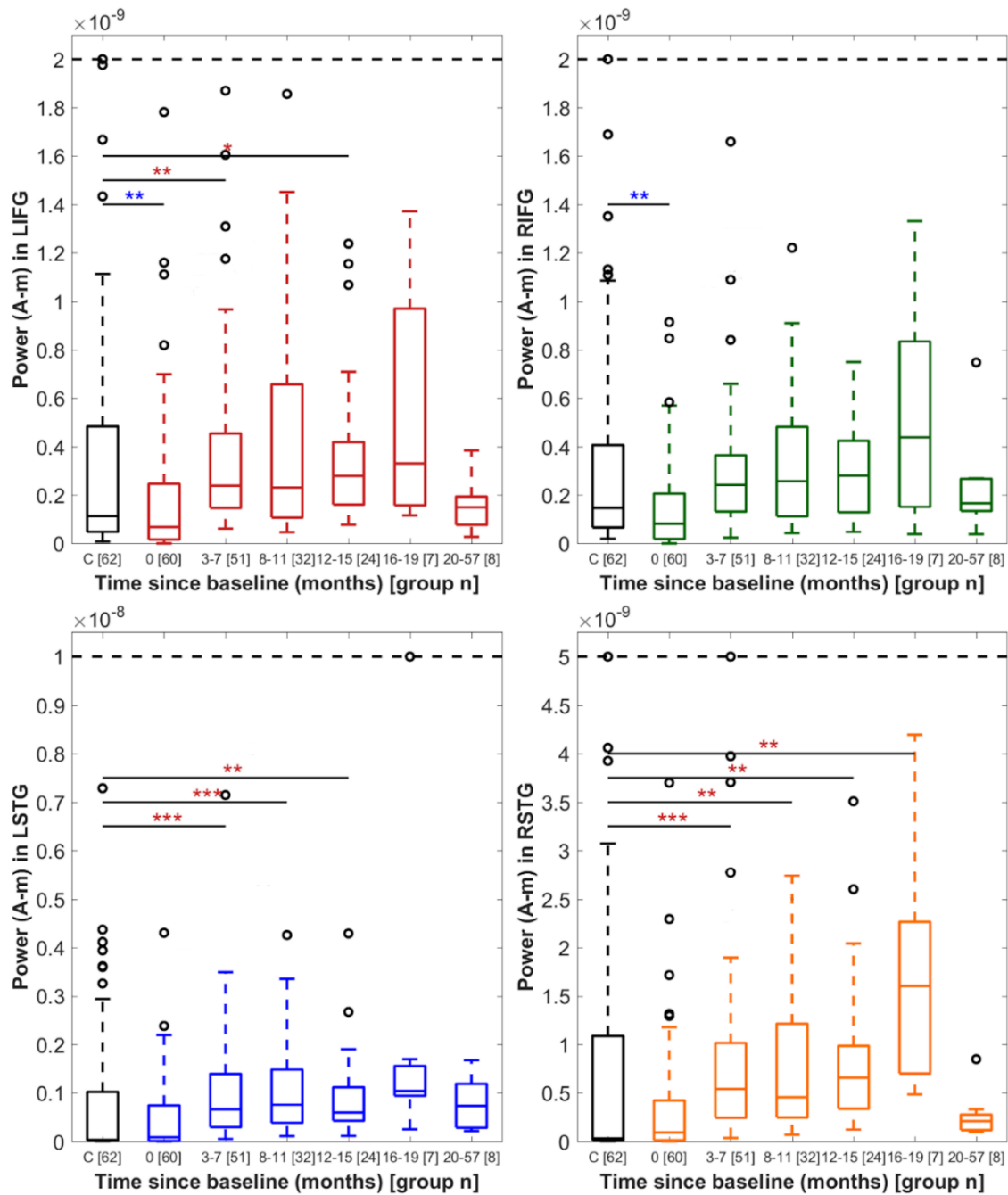


**Figure 5.8. Comparison of power in each source of MMN, modelled by dipole fitting, between controls and patients at different follow-up times.** Significant differences (false discovery rate = 5%) are highlighted by asterisk(s). Red asterisks - Significant increase in patient longitudinal time group power relative to controls. Blue asterisks - Significant decrease in patient longitudinal time group power relative to controls. \* $p < 0.05$ , \*\* $p < 0.01$ , \*\*\* $p < 0.001$ , X axis label shows the time range of the data (in months) in each bin and [group n] values represent data points per bin. L/RIFG – Left/right inferior frontal gyrus. L/RSTG – Left/right superior temporal gyrus. C – Controls.

#### 5.2.3.2. Longitudinal analysis

Patients took part in a mean of 3.05 sessions (total recording number  $\times$  number of patients:  $2 \times 25$ ,  $3 \times 14$ ,  $4 \times 14$ ,  $5 \times 7$ ), with no more than one visit per time point group but potential

absence of data in an intermediate time group (for example, data grouped into 0 months, 3-7 and 12-15 months due to delay in return for third recording). Longitudinally, mean residual variance of dipole fitting models was consistent across timepoints and groups (controls: 22%, ALS baseline: 21%, ALS follow up: 3-7 months - 21%, 8-11 months - 25%, 12-15 months - 21%, 16-19 months – 21%, 20-57 months - 18%), demonstrating consistent goodness of fit. At follow up times the left IFG and STG (3-15 months post-baseline) and the right STG (3-19 months post-baseline) showed significantly greater activity than controls, indicating a transition from decreased activity to a state of hyperactivation (Fig. 5.8). By contrast, the initial hyperactivity observed in the left M1, PPC and DLPFC returned to control levels of inactivity thereafter (no significant voxel differences to be illustrated). Linear mixed effects modelling demonstrated significant longitudinal decrease in bilateral IFG and STG power and significant longitudinal increase in LDLPFC and LM1 (but not LPPC) power within patients with increasing time from baseline (coefficient p-values reported in Fig. 5.9).

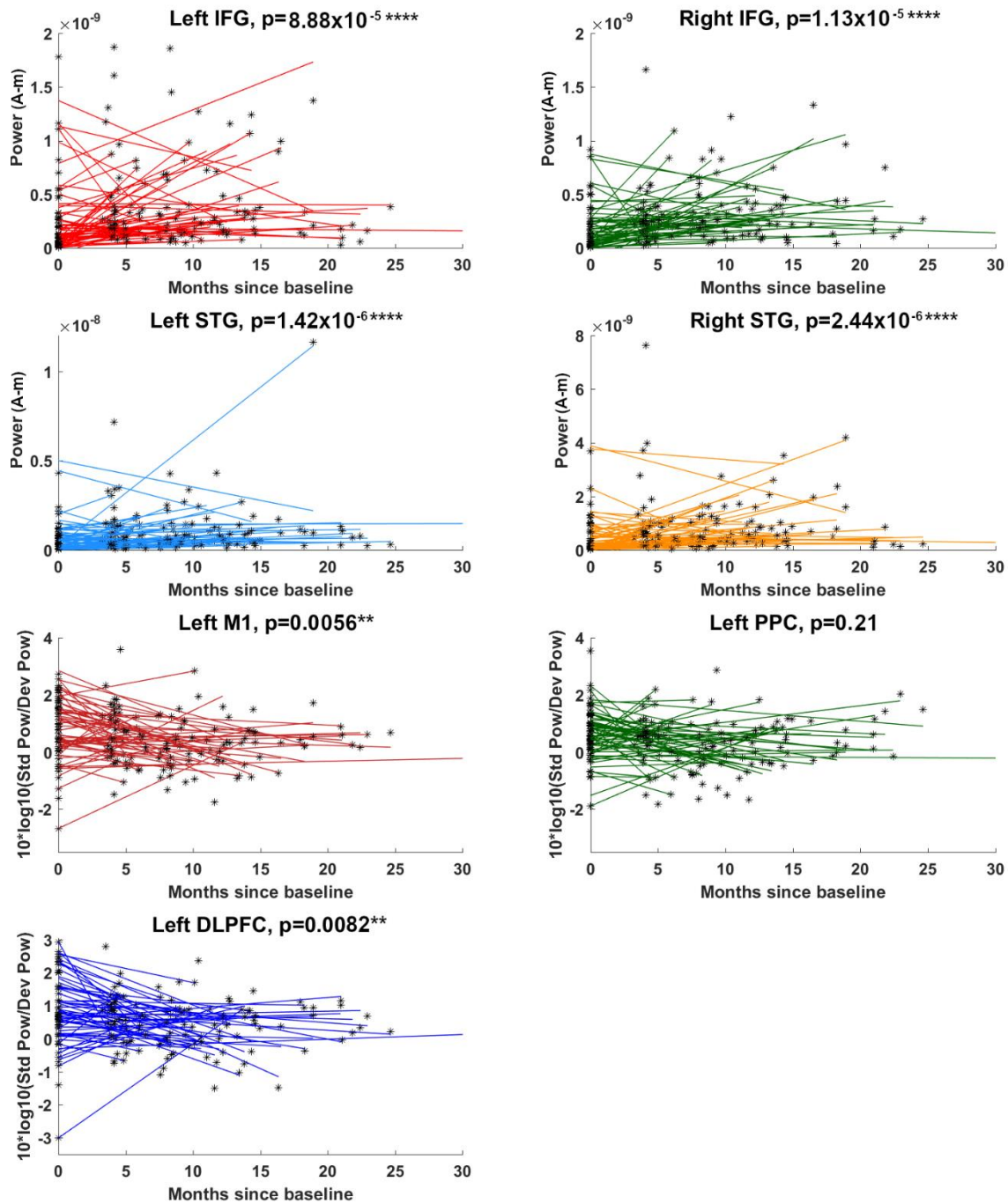


**Figure 5.9. Modelled source activity change across EEG recording sessions in individual ALS patients.** Asterisks indicate individual datapoints while lines represent first order models of data change per participant. P-values listed are the uncorrected values associated with the effect of time since baseline on power in these sources ascertained by linear mixed effects modelling. Asterisks denote values deemed statistically significant at a 5% FDR. \*\* $p < 0.01$ , \*\*\*\* $p < 0.0001$  X-axes have been limited to 30 months for clarity (e.g. a single data point at 57 months is not shown). Power – Power determined by dipole fitting in A-m, Std Pow – Standard power determined by LCMV, Dev Pow – Deviant power determined by LCMV, M1 – Primary motor cortex, PPC – Posterior parietal cortex, DLPFC – Dorsolateral prefrontal cortex

#### 5.2.3.3. *Correlation with clinical scores*

Significant correlations between electrophysiological baseline measures or their rate of change over time and clinical scores are summarised in table 5.4. Correlations not deemed significant (corrected  $p > 0.05$ ) are not reported due to the extensive number of correlations performed. All correlations deemed significant by Spearman rank correlation were also deemed significant upon omission of extreme outliers and had a rho value 95% confidence interval that did not cross zero.

**Table 5.4. Summary of statistics for significant correlations between EEG measures and clinical characteristics in the ALS patient cohort.** Confidence intervals are determined by bootstrapping of the rho statistic using 1000 bootstrap samples of the patient dataset with the required clinical scores (n). DLPFC – Left dorsolateral prefrontal cortex, M1 – Left primary motor cortex, L/R – Left/right, STG – Superior temporal gyrus. IFG – Inferior frontal gyrus. ECAS – Edinburgh Cognitive and Behavioural ALS Screen, BBI – Beaumont Behavioural Inventory, CWIT - Delis-Kaplan Executive Function System Colour-Word Interference Test. ALSFRS-R – Revised ALS Functional Rating Scale

<b>Clinical characteristic</b>	EEG measure	n	Source	Rho	p	Bootstrapping-derived rho confidence interval
<b>Motor</b>						
ALSFRS-R slope	Slope	50	RSTG	-0.40	0.0042	[-0.62,-0.14]
	Power at baseline		LIFG	0.43	0.0022	[0.14,0.61]
			RIFG	0.47	0.00058	[0.20, 0.67]
ALSFRS-R at baseline			LSTG	-0.37	0.0087	[-0.59, -0.06]
			RSTG	-0.39	0.0058	[-0.61, -0.10]
<b>Survival</b>						
Survival time (months)		38	LIFG	0.49	0.0016	[0.17, 0.69]
			RIFG	0.48	0.0023	[0.21, 0.67]
			LSTG	0.47	0.0032	[0.15, 0.68]
			RSTG	0.48	0.0025	[0.24, 0.68]
<b>Behavioural</b>						
BBI score 1 year after baseline		19	DLPFC	-0.68	0.0017	[-0.84, -0.39]
<b>Cognitive</b>						
ECAS total score 1 year after baseline		46	DLPFC	-0.41	0.0056	[-0.60, -0.12]
CWIT word reading score slope		18	LSTG	0.60	0.0088	[0.13, 0.88]
			RSTG	0.60	0.0086	[0.19, 0.85]
CWIT inhibition switching score slope			LIFG	0.61	0.0098	[0.17, 0.84]
			LSTG	0.73	0.00094	[0.35, 0.92]
			RSTG	0.66	0.0037	[0.27, 0.86]



### *Survival*

Both IFG and STG baseline activity values correlated with survival, illustrating that those with more severely decreased activity at baseline had a poorer outcome.

### *ALSFRS-R*

The mean slope of ALSFRS-R change was 0.57 points per month (range=-1.83-0.074,  $p=1.02*10^{-9}$ ). Strong significant positive correlations were identified between ALSFRS-R slope and baseline left and right IFG activity. This illustrates that those with lower baseline IFG activity progressed more rapidly (i.e. have a faster rate of ALSFRS-R decline). Further, a significant negative correlation between slope of right STG engagement over time and ALSFRS-R slope was observed (i.e. those whose right STG became more rapidly hyperactive experienced faster ALSFRS-R decline). A significant negative correlation between ALSFRS-R score at baseline recording and STG power at baseline recording was also identified.

### *Cognitive and behavioural tasks*

Slope in word reading score positively correlated with baseline STG activation (i.e. those patients with higher STG engagement at baseline had a faster rate of decline in language function). Rate of change in CWIT inhibition-switching score also correlated with baseline LIFG and bilateral STG activity (i.e. more rapid decline in cognitive flexibility correlates with higher baseline activity in these sources). LDLPFC activity at baseline was negatively correlated with model-interpolated total BBI score (higher score indicates greater behavioural impairment) and ECAS total score (lower score indicates greater cognitive impairment) 12 months later. DLPFC correlations to concurrent BBI and ECAS total scores were not significant with multiple comparison correction.

### *Correlation between sources*

No significant correlations were found between individual model slopes for left M1/DLPFC/PPC and those for the left and right IFG or STG (n=60 per correlation, 8 correlations performed, all  $p > 0.39$ , all  $|\rho| < 0.12$ ).

### *5.2.4. Discussion*

This study demonstrates that source localized EEG can detect impairments in different regions (nodes) of cortical networks related to ALS progression and may provide useful insight on how the diseases progression takes place. We have identified the emergence of

progressive cognitive network hyperactivation in ALS which precedes clinical decline. In addition, we have demonstrated that by directly measuring cortical activity, EEG can detect early pathophysiology that predicts current and later cognitive and behavioural symptoms, as well as functional decline measured by ALSFRS-R, and survival.

#### *5.2.4.1. Initial Suppression and Subsequent Hyperactivation of the IFG and STG*

We previously postulated that decrease in power in IFG and STG sources of MMN reflected an early imbalance between activity in the attentional control networks, with the central executive network being overactive and these nodes suppressed<sup>103</sup>. Our longitudinal data now show that previously observed suppressed nodes become progressively more active to the point of hyperactivation by attention-demanding stimuli with disease progression, as evidenced by significantly greater activity at follow up time points relative to controls as well as relative to baseline. Significant negative correlation between ALSFRS-R score at baseline and STG activation at baseline also highlights that STG suppression is associated with early stages of ALS. These data support the hypothesis that as ALS progresses, initially hyperactive nodes subsequently decline, while hyperactivity spreads to other areas, such as the IFG and STG.

Baseline IFG and STG suppression correlates with shorter survival time, with baseline IFG suppression also correlating to more rapid motor decline. However, greater STG activation at baseline correlates with more rapid deterioration in performance in the CWIT word reading task, indicating that hyperactivation of the STG may have pathogenic effects on language functions, known to be affected in some ALS patients<sup>566</sup>. This is in keeping with previous evidence that the STG contributes to language impairment in ALS (for review see Pinto-Grau et al., 2018). A similar correlation was identified between baseline STG and left IFG activity and CWIT inhibition switching score slope. In the case of the STG, this is likely to reflect the aforementioned relationship to language impairment. However in the case of the left IFG, as no significant correlations to colour naming or word reading scores were identified, this correlation indicates a relationship between hyperactivation of the IFG and impaired response inhibition, for which the left IFG has previously been deemed ‘critical’<sup>567</sup>. Taken together, these correlations indicate that those with strong baseline suppression of the IFG and STG experience a fast progressing form of ALS, while those who demonstrated higher IFG and STG activation at baseline may experience a slower progressing form of ALS wherein pathological

hyperactivity has time to spread to cognitive and language regions, driving extramotor impairment.

#### 5.2.4.2. Initial Hyperactivation and Progressive Inactivity of the Motor and Dorsolateral Prefrontal Cortex

Our data show that initial hyperactivity occurs in the primary motor cortex and neighbouring DLPFC, a finding supported by fMRI and other electrical source imaging studies<sup>341,568</sup>. As MMN is a non-motor task, motor cortex hyperactivity may reflect dysregulated inhibitory and/or excitatory input to the upper motor neurons from networks that are activated by the task.

Hyperexcitability of upper motor neurons has also been consistently identified by TMS studies, which demonstrate a reduction in the stimulation required to elicit a motor response. These studies have attributed motor cortical hyperexcitability to loss of GABA<sub>A</sub> inhibitory interneuron function<sup>71</sup>.

It is likely that this dysfunction characterized in the motor cortex subsequently emerges in the prefrontal and temporal cortex, driving the longitudinal pattern of progressive cortical hyperactivation identified here (Fig. 5.10).

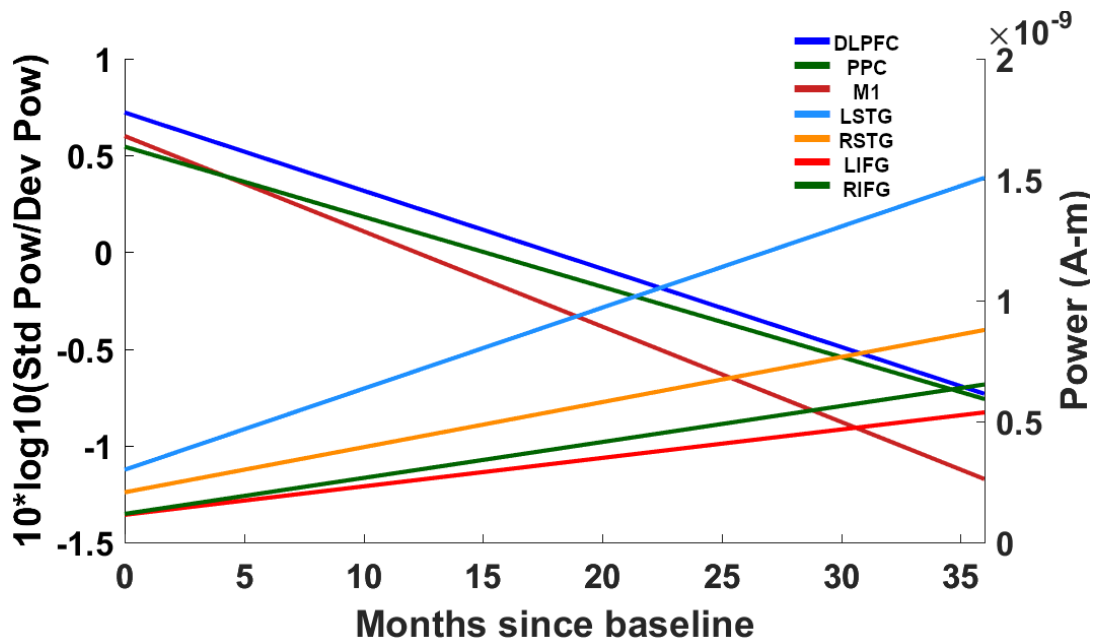


**Figure 5.10. Summary of median changes in normal and abnormal MMN sources in ALS patients illustrating that the activity of typical MMN generators increases over time in ALS, whereas the pathologically present activity in non-typical MMN generators declines as disease progresses.** Lines represent median slope and intercept of patient models. M1, PPC and DLPFC lines are plotted according to the left-hand y-axis. IFG and STG lines are plotted according to the right-hand y-axis. L/RIFG – Left/right inferior frontal gyrus. L/RSTG – Left/right superior temporal gyrus. DLPFC – Left dorsolateral prefrontal cortex. M1 – Left primary motor cortex, PPC – Left posterior parietal cortex.

Given that ALS is characterized by loss of motor neurons, it is to be expected that early motor hyperexcitability wanes with disease progression. This was previously supported by TMS studies which demonstrate elevated motor thresholds or inexcitable motor cortices in some ALS patients<sup>71</sup>. Our EEG work has now definitively demonstrated an initial abnormal activation of the motor cortex which declines longitudinally within individuals which also occurs in the dorsolateral prefrontal cortex. As controls show normal inactivity in the motor cortex during MMN, identification of ‘below normal’ motor activity is unlikely with this paradigm. The observed changes in ALS patients did not correlate with ALSFRS-R or survival measures<sup>569</sup>.

#### *5.2.4.3. Distinct Prefrontal Pathology Relates to Cognitive and Behavioural Impairment in ALS*

Left DLPFC activity demonstrated distinct relationships with cognitive and behavioural symptoms. Lower DLPFC activity was associated with greater behavioural impairment, while greater DLPFC activity correlated with greater cognitive impairment. These differing correlations indicate separate cortical pathology underlying ALSbi and ALSci, which often present clinically independently of one another<sup>570</sup>. Furthermore, the strengthening of these correlations for future task performance measures, compared to measures of performance at the time of EEG recording, supports our hypothesis that EEG measures of cortical network component dysfunction can predict later symptomatic changes.

#### *5.2.4.4. Cortical Hyperactivity Spread in ALS*

The progressive emergence of frontotemporal dementia-like cortical pathology<sup>571</sup> is in keeping with the consensus that ALS and FTD are extremes of a single disease spectrum<sup>572</sup>, with symptoms of one often emerging following a primary diagnosis of the other<sup>468,573</sup>. The IFG and STG specifically have been identified as predominant areas of grey matter loss in those with frontotemporal dementia and a *C9orf72* expansion<sup>571</sup>, which is associated with both diseases. Our work shows that early measures of activity in these areas relate to poorer executive and language symptom prognoses, indicating that these changes warrant further investigation as markers of ALS-FTD progression.

#### *5.2.4.5. The Importance of Wider Cortical Pathology in ALS Prognosis*

Taken together, our findings demonstrate that symptomatic deterioration in ALS is preceded by changes in indices that capture the spread of pathology through the cortex,

rather than indices of motor cortex function alone. While motor cortical dysfunction characterized during this task did not correlate with survival or motor decline, IFG and STG activation at baseline showed highly significant correlations with survival, highlighting the importance of considering pathology beyond the motor cortex in generating effective prognostic biomarkers of ALS. The absence of correlation between motor cortical functional decline and survival, in addition to epidemiological evidence of poorer prognosis in patients with cognitive<sup>574</sup> or behavioural<sup>21</sup> symptoms, and the much slower progression of the upper motor neuron-localised primary lateral sclerosis<sup>575</sup>, indicates that spread of cortical pathology beyond the motor cortex has greater relevance to ALS prognosis than primary motor cortex decline alone.

We have previously shown that patient subgroups with poorer prognoses and greater susceptibility to cognitive impairment (i.e. *C9orf72*+ and bulbar-onset patients) exhibited greater IFG impairment than the cohort as a whole<sup>103</sup>. Using neuroelectric signal analysis to quantify this more widespread pathology may therefore not only dramatically improve the development of prognostic tools, but also has the potential to provide more personalized and objective measures of the impacts of novel therapeutics on disease progression in clinical trials.

Our study is limited by the availability of psychological task scores, which restricted our exploration of the relationship between cognitive/behavioural symptoms and source activity. Further, due to small numbers of clinically defined subgroups (e.g. bulbar/thoracic onset) and the prevalence of *C9orf72* expansion-associated ALS in the Irish population, we were limited to performing group-level analysis on ALS patients as a single disease group. Disease heterogeneity was, however examined via modelling and correlation analyses. Additional studies of broader cortical networks, risk gene carriers and larger patient groups, supported by other methods of characterising hyperexcitability (such as single- and paired-pulse TMS-based measures in the case of the motor cortex) are now required to disentangle if patient subcategorization based on spatiotemporal patterns of cortical network malfunction overlap with genetically/clinically defined patient subphenotypes. As this study was not designed or intended to interrogate non-contrasted AEPs, variation in auditory stimulus amplitude was not strictly prohibited to avoid participant discomfort. Going forward, stimulus amplitude should be recorded for each individual or, if possible, fixed, to facilitate coincident study of early AEP peak characteristics. Finally, the disease progression-related dropout which occurred between return visits is likely to have inflated the proportion of long surviving patients represented

in datasets with more return visits. This bias is likely to have affected the sign-rank and Mann-Whitney U test-based group-level longitudinal analysis. Specifically, this bias is likely to have contributed to the lack of statistically significant differences between controls/baseline patient power measurements and patient power measurements 16-19 months or 20-57 months after baseline, despite clear, significant differences at all previous follow up times. This bias should not, however, substantially affect the linear models which were used to determine the rate of change in power in each individual for each source for correlation analysis and which also determined the significant patterns of change longitudinally that were indicated at group level. Should such longitudinal measures be implemented as clinical tools, our modelling indicates that 2-3 recordings is sufficient to capture this change.

Nonetheless, our data demonstrate that the high spatiotemporal resolution of EEG can provide insights into distinct patterns of dysfunction in specific cortical network nodes in ALS. Using this approach, we have identified previously unknown dynamic patterns of cortical dysfunction that relate to ALS progression. EEG with source localization has potential to provide an inexpensive set of objective prognostic biomarkers and clinical trial outcome measures that are feasible for clinical implementation. Going forward, additional longitudinal investigation is now required to formally quantify the ability of these patterns to predict ALS symptoms as prognostic biomarkers.

## 5.3. Time-frequency analysis

### 5.3.1. Introduction

In the analyses described in sections 5.2 and 5.3, we used the auditory oddball paradigm to elicit the MMN, a time- and phase-locked ERP<sup>103,267</sup> (see section 5.1.1.2 for detailed discussion of the MMN). ERPs are calculated by averaging many trials of EEG which are time-locked to the delivery of a stimulus<sup>119</sup>. This isolates a waveform which reflects temporally consistent cortical activation elicited by the stimulus while removing remaining activity not phase-locked to delivery of the stimulus (and therefore presumed task irrelevant). By characterising this ERP, we have demonstrated spatially and temporally precise dysfunction in cognitive and motor cortical activity in ALS cross-sectionally<sup>103,267</sup> and longitudinally (see section 5.2), and highlighted the importance of quantifying non-motor pathology in predicting ALS prognosis.

In addition to eliciting ERPs, however, sensory input and cognitive/motor tasks also alter communication within the cortex and between cortical and subcortical regions, captured as changes in signal oscillation magnitude (e.g. power) at specific frequencies. This may be observed as an increase (event related synchronisation) or decrease (event related desynchronisation) in oscillations during task performance or following sensory input. In ERP analysis, such as our previous MMN study, any ERD/ERS which is not phase-locked (i.e. the oscillation peaks and troughs do not occur at the same time relative to a stimulus in every trial) is lost through averaging<sup>119</sup>. Such oscillations may provide important information on disturbances to intracortical<sup>576</sup> and corticothalamic<sup>577</sup> communication (see Pfurtscheller (2003)<sup>578</sup> for discussion on the physiological basis of ERD/ERS) in ALS and have been found to provide better diagnostic utility than ERP measures in mild cognitive impairment and Alzheimer's disease<sup>130</sup>.

Here, we have examined the cortical oscillations induced by the auditory oddball paradigm at sensor level using time-frequency analysis, and have localised the observed changes in EEG to the potential underlying brain sources. We sought to determine whether these measures of network communication are perturbed in ALS and whether such perturbations relate to cognitive-behavioural symptoms, motor symptoms or survival times.

### 5.3.2. *Methods*

#### 5.3.2.1. *Ethical Approval*

Ethical approval and participant written consent were obtained as described in section 4.6.

#### 5.3.2.2. *Inclusion Criteria*

All participants were over 18 years of age and able to give informed written consent, or in the presence of two witnesses, verbal consent. Patients were diagnosed with Possible, Probable or Definite ALS in accordance with the El Escorial Revised Diagnostic Criteria.

#### 5.3.2.3. *Exclusion Criteria*

Those with neurological (e.g. functional, structural and psychological, but not comorbid frontotemporal dementia) or muscular disorders other than ALS and those currently taking neuro- or myo-modulatory medications other than riluzole (e.g. muscle relaxants, antidepressants, antipsychotics, benzodiazepines or other anxiolytics) were excluded.

#### 5.3.2.4. *EEG Acquisition and Experimental Paradigm*

EEG acquisition and the employed experimental paradigm (auditory oddball paradigm) are described in section 4.1.3.

#### 5.3.2.5. *Clinical, cognitive and behavioural measures*

ALSFRS-R, ECAS, BBI and D-KEFS CWIT data were acquired for each participant (see section 4.5). Scores were used if collected within 90 days of EEG. If scores were collected before and after EEG, but not within 90 days, score at the EEG recording day was estimated by linear interpolation. Survival was calculated for deceased patients as the number of months between patient-reported symptom onset and death.

#### 5.3.2.1. *Participant demographics*

94 patients (21 female; age median: 61.50 years, range: 29-81 years) and 62 controls (43 female; age median: 60.35 years, range: 36-82 years) underwent analysis. Groups were age-matched ( $p=0.93$ ) but not gender matched. However, comparison of male and female controls for oscillations of interest revealed no gender-related differences. Ten patients carried the *C9orf72* gene expansion, five were diagnosed with comorbid FTD and 22 patients had bulbar onset disease. This cohort overlaps to varying extent with our previously reported MMN analyses<sup>103</sup>. ALSFRS-R scores collected within 90 days of EEG were available for 74 patients and were estimated by linear interpolation for an additional 12 for whom scores were available before and after EEG, but not within 90 days. ECAS, BBI and CWIT data were available for 71, 32 and 33 patients respectively.



Linearly interpolated scores for these tasks were generated for an additional 10, 8 and 0 patients respectively based on pre- and post-EEG scoring. Survival data were available for 58 patients, who were deceased by the time of data analysis.

#### 5.3.2.2. Data Analysis

Mean number of included artefact-free standard/deviant trials for controls was 1230/144 and for patients was 1265/144. Signal preprocessing steps are described in section 4.1.4.1. In addition to those ITV-based ERSP sensor space analyses on preselected electrodes Fz, Cz, Pz, D22 and B25 and source space analyses (described in detail in section 4.1.4.3), spectral perturbations associated with the average time signals across trials (i.e. the AEPs) following standard and deviant tones were calculated as follows:

$$ERP\ ERSP(f, t) = 100 * \frac{|(W_{f,t})^2| - \overline{|(W_{f,baseline})^2|}}{\overline{|(W_{f,baseline})^2|}}$$

Where  $W$  denotes the complex wavelet coefficients ( $W$ ) of the signal averaged across epochs (i.e. the ERP) per time point ( $t$ ) and frequency ( $f$ ). This served as an additional checkpoint that the observed ERSP were not characteristic of the phase locked AEPs. Delta and theta band frequencies were not examined as one complete oscillation cycle could not be captured within the limited baseline duration.

#### 5.3.2.3. Statistics

##### *Oscillation analysis*

For three-dimensional, complete time-frequency spectrum statistical analysis, data were down sampled to 34Hz (i.e. 1/15 datapoints). Sign rank testing<sup>495</sup> was employed to identify significant, non-zero ERSP for standard and deviant trials and significant differences in paired deviant and standard ERSP (i.e. mismatch ERSP). At each source, the difference between patients and controls were determined based on Z-transformed AUROC values at each time-frequency-space voxel as the test statistic. A FDR<sup>562</sup> of  $q = 0.05$  was implemented as a frequentist method for determining significant ERSP differences in the multivariate data (voxels). Subsequently, EBI<sup>499</sup> was used to find Bayesian posterior probabilities ( $P_1$ ) and achieved statistical power ( $1-\beta$ ). As this EBI approach is less reliable for smaller group numbers such as those with *C9orf72* expansions (*C9orf72+*) or those of bulbar disease site onset, specific time-frequency windows were defined as WOIs based on oscillations present in control means. Mean ERSP values (without down sampling) within these WOIs were compared between

controls and all patients, between controls and those with *C9orf72* expansions or those of bulbar onset, between those with and without *C9orf72* expansions (*C9orf72*-) and between those of spinal and bulbar disease onset. Significant differences in WOIs were defined as those with a p value < 0.05 when corrected at a 5% FDR, implemented using the Benjamini and Hochberg method<sup>498</sup>.

#### *Source space analysis*

The 10 mm grid applied across the brain volume of the ICBM152 MRI template yields 1726 sources including white matter. To analyse these high-dimensional data, a 10% FDR threshold was applied to the p-values of the Wilcoxon sign rank test<sup>495</sup>, to determining significant activity at sources in controls. Furthermore, for determining significant source activity differences between patients and controls based on Z-transformed AUROC values at each source as the test statistic. EBI was used to find  $P_1$  and achieved statistical power.

#### *Correlations*

Spearman's non-parametric rank correlation<sup>542</sup> was used to investigate relationships between WOI ERSP values and survival, psychological and motor test scores. Partial correlation was implemented for investigating relationships to CWIT scores, to account for ALSFRS-R speech score at time of CWIT testing, as speech impairment can affect performance. Multiple comparison correction was implemented using a 5% FDR, using the Benjamini and Hochberg method<sup>498</sup>.

#### *Age and gender matching*

Mann-Whitney U-test<sup>494</sup> and chi-squared proportion tests were used to compare age and gender respectively between groups, with significant differences determined where  $p < 0.05$ .

### *5.3.3. Results*

#### *5.3.3.1. Standard and Deviant Tone Related Spectral Perturbations*

Both standard (Fig. 5.11, left) and deviant (Fig. 5.11, right) trials elicited significant, broadband ERS, peaking in alpha band (8-12Hz) from 0-400ms post-stimulus. This window was investigated further for both standard and deviant trials as WOIs. Inter trial variance-based event related spectral perturbation (reflecting the changes in non-phase-locked oscillations) differed from that associated with the standard and deviant tone AEPs (i.e. the phase-locked components). Specifically, AEPs were associated with strong, distinct and spatially specific alpha and beta band synchronisation between 100 and

200ms post stimulus (appendix 5.4), the time window in which the high amplitude N1 and P2 peaks of AEPs are observed<sup>579</sup>. No significant difference between standard and deviant (i.e. mismatch) ITV-based ERSP was identified by sign-rank tests.

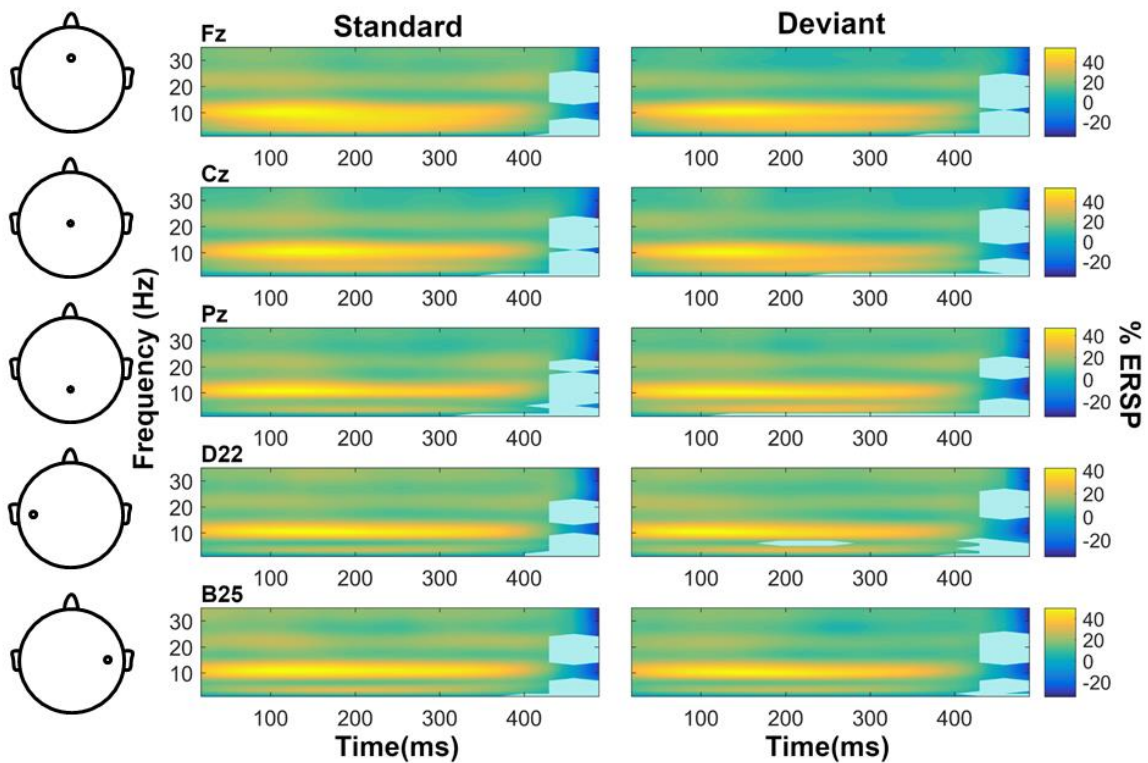


**Figure 5.11. Control ERSP following standard and deviant tones.** Colour bar values illustrate percentage spectral perturbation relative to baseline. Values are masked such that non-significant values (sign rank  $p > 0.05$  corrected at a false discovery rate of 5%) are blocked out in light blue.

#### 5.3.3.2. Source analysis

Alpha ERS was found to be significantly greater than zero across the cortex upon source localisation for both deviant and standard tones during all four 100ms time windows interrogated (0-100ms, 100-200ms, 200-300ms and 300-400ms). Those areas with the greatest ERS (top 5%, summarised in table 5.5 for deviant trials) were mostly consistent across time windows, namely the medial and dorsolateral prefrontal, premotor, orbitofrontal and sensorimotor cortices and superior parietal lobule. Mean source activity 0-400ms post-deviant stimulus (averaged first across time windows within individuals, then across individuals) is shown in Fig. 5.12 (figures for each time window are shown in appendices 5.5 and 5.6). No significant differences between standard and deviant tone alpha-band source activity were identified for any of these four time windows.

**Table 5.5. Control cortical sources contributing top 5% of alpha ERS power across 0-400ms in deviant trials.**

Time (ms post-stimulus)	Lobe	Source
0-100	Frontal	Bilateral superior frontal gyri, left precentral, superior medial, inferior and middle frontal and anterior cingulate gyri and paracentral lobule, right orbitofrontal cortex.
	Parietal	Right postcentral gyrus, bilateral superior parietal lobule
	Occipital	Left middle occipital
100-200	Frontal	Bilateral superior medial gyri, left precentral, superior, middle and inferior frontal gyri and supplementary motor area
	Parietal	Right postcentral gyrus and superior parietal area
200-300	Frontal	Bilateral superior frontal gyri, right orbitofrontal cortex, left precentral, superior medial, middle and inferior and frontal gyri,
	Parietal	Right postcentral gyrus and superior parietal area
300-400	Frontal	Bilateral anterior cingulate, superior medial, superior and middle frontal gyri, left precentral and inferior frontal gyri and supplementary motor area, right orbitofrontal cortex
	Parietal	Left postcentral gyrus, right superior parietal lobule

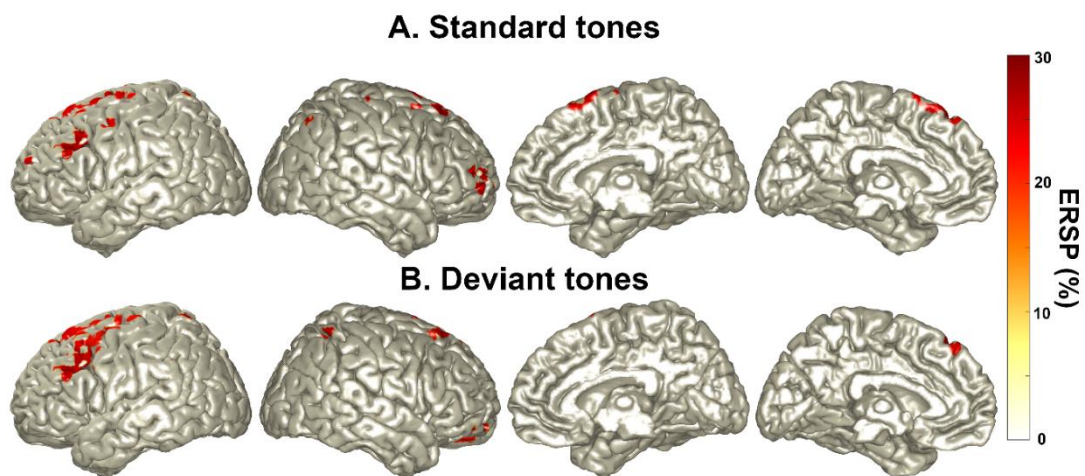


**Figure 5.12. Top 5% of significantly active control sources of alpha band event-related oscillations 0-400ms after (A) standard tones and (B) deviant tones.** All sources highlighted show significant increase in alpha band oscillatory power relative to baseline, determined by sign rank testing at a false discovery rate of 10%. Heat map values are area under the receiver operating characteristics curve values minus 0.5 for each voxel.

### 5.3.3.3. Differences between ALS patients and controls Event related spectral perturbations

Analysis of the entire time-frequency landscape identified significantly greater oscillatory activity across numerous time-frequency bands in electrode D22 (Fig. 5.13), over the left

temporal cortex during deviant trials. Greatest AUROC values (0.7) were associated with increased alpha, early fast beta and late slow beta band ERS. As a result, changes in activity of sources of deviant tone-elicited beta ERS (20-26Hz 140-240ms post-stimulus and 13-18Hz, 320-420ms post-stimulus) in ALS patients were also investigated as WOIs for correlation analysis. Source analysis was also employed to investigate the sources generating these time-frequency regions of excess ERS.

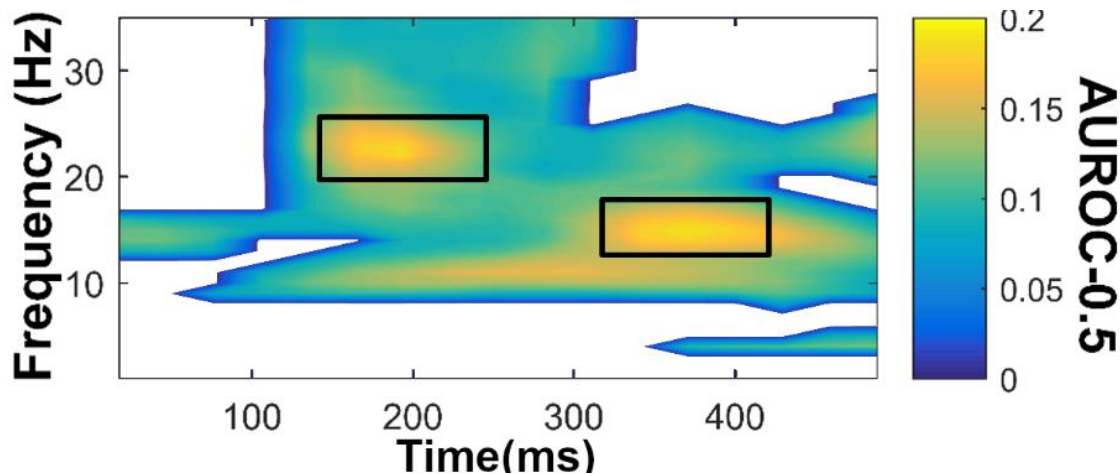


**Figure 5.13.** Area under the receiver operating characteristics curve (AUROC) values for significant deviant ERSP changes in ALS over the left temporal cortex (channel D22). Non-zero values plotted are those deemed significant based on a 5% false discovery rate (deviant  $P_i=0.87$ ,  $1-\beta=0.68$ ). Colour represents AUROC-0.5 values. Areas outlined by black boxes (20-26Hz 140-240ms post-stimulus and 13-18Hz, 320-420ms post-stimulus) underwent source analysis in addition to alpha ERS. Non-significant (FDR of 5%) differences are blocked out in white.

#### *Subgroup analysis*

No significant ERSP differences were identified between *C9orf72+* and *C9orf72-* patients, or between bulbar-onset and spinal-onset ALS patients. When compared to controls, bulbar patients alone also exhibited significantly increased alpha band deviant ERS in D22 ( $p=0.0049$ , AUROC=0.70).

#### *Source analysis*

In keeping with sensor level findings, ALS patients did not show significant differences in standard tone-elicited alpha ERS source activity compared to controls but did show widespread significantly increased alpha ERS in both cortical and subcortical regions following deviant tones compared to controls across. This increase in alpha ERS was present across all four 100ms time windows interrogated between 0 and 400ms post-stimulus (maximum AUROC=0.69-0.71). Sources of significant differences in mean (across time windows) power from 0 to 400ms post-stimulus (table 5.6), which are similar

to those for each individual time window were predominant (>95<sup>th</sup> percentile source AUROC values) in the bilateral medial and lateral temporal cortices and right insula (Fig. 5.14A).

**Table 5.6. Cortical and subcortical regions with significantly increased mean alpha power (0-400ms) following deviant tones in ALS patients.** Those sources most discriminant between ALS and controls (>95<sup>th</sup> percentile of AUROC values) are bolded. L or R in brackets refers to a specific hemisphere (left or right respectively) being above the 95<sup>th</sup> percentile of AUROC values

<b>Lobe</b>	<b>Sources of increased alpha oscillations in ALS</b>
Frontal	Bilateral precentral, middle frontal and posterior cingulate gyri, <b>insula (R)</b> and paracentral lobules, left superior and inferior gyri and lateral orbitofrontal cortex, <b>right rolandic operculum</b> and supplementary motor area
Parietal	Bilateral superior parietal lobule, supramarginal gyrus, precuneus and cuneus, left angular gyrus and inferior parietal lobule, <b>right postcentral gyrus</b>
Temporal	<b>Bilateral hippocampus and parahippocampal and fusiform gyri</b> , right amygdala, bilateral <b>superior (R), middle (L)</b> and inferior temporal gyri and superior pole, <b>right mid temporal pole</b>
Occipital	Bilateral lingual gyri, left superior, middle and inferior gyri
Subcortical	Bilateral thalamus, caudate and putamen and left pallidum

Increased slow beta ERS (13-18Hz, 320-420Hz) observed in ALS patients in electrode D22 was predominantly (>95<sup>th</sup> percentile source AUROC values) localised to the left medial and lateral posterior parietal cortex and middle occipital gyrus (Fig. 5.14B). Increased fast beta ERS (20-26Hz, 140-240ms post-stimulus) was not attributable to significant change in the activity of any specific source locations.

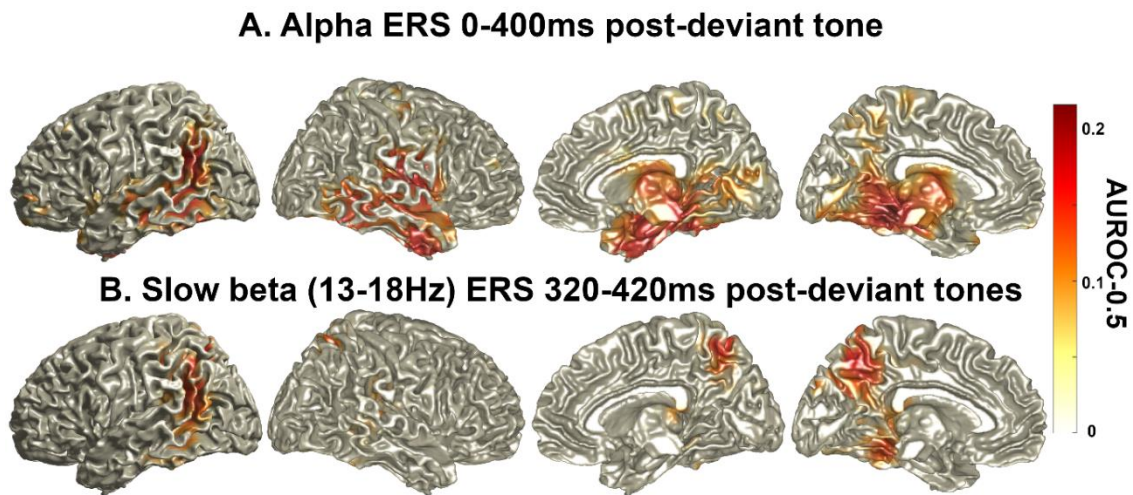


**Figure 5.14. Source localised areas of significant differences in (A) mean alpha-band ERS 0-400ms after deviant tones and (B) slow beta-band ERS (13-18Hz, 320-420ms) after deviant tones between ALS patients and controls. Red colour indicates significant discrimination of groups by measures in the highlighted voxels. Localised windows of interest correspond to time-frequency ranges deemed to show significantly increased ERSP at sensor level (see Fig. 5.13).**

#### 5.3.3.4. Correlation with clinical scores

At sensor level, no significant correlations were identified between standard or deviant trial ERSP and survival, ALSFRS-R, CWIT or BBI score. Alpha ERS following deviant tones over the temporal lobes showed significant negative correlation to disease duration (electrode D22  $p=0.0038$ ,  $\rho=-0.30$ , electrode B25  $p=0.021$ ,  $\rho=-0.24$ ). Alpha ERS following standard tones over the sensorimotor cortex showed significant negative correlation to ECAS total score ( $p=0.0023$ ,  $\rho=-0.36$ ).

At source level, a significant negative correlation was observed between early fast beta ERS in the right dorsolateral prefrontal cortex and disease duration ( $p=9.19 \times 10^{-4}$ ,  $\rho=-0.34$ ). No significant correlations were identified between these clinical measures and mean alpha ERSP in the thalamus, caudate, putamen, hippocampus, left dorsolateral prefrontal cortex, left/right insula, left/right occipital cortex, left/right primary motor cortex, left/right posterior parietal cortex, left/right orbitofrontal cortex, left/right ACC, left/right superior temporal cortex or left/right inferior frontal cortex.

#### 5.3.4. Discussion

Here we have identified the sources of alpha ERS evoked by the auditory oddball task, that are distinct from auditory evoked potentials. Further, we demonstrate that ALS patients display excessive deviant tone-elicited alpha ERS, as well as deviant-elicited cortical beta ERS. Additionally, some auditory evoked spectral perturbations show correlation to disease duration and cognitive impairment in ALS.



#### 5.3.4.1. *Physiological basis of alpha band oscillations*

Alpha oscillations have been recorded from an array of cortical regions in addition to subcortical sources including the thalamus, hippocampus and reticular formation<sup>580</sup>. Cortical alpha rhythms are attributed to layer 5 pyramidal neurons<sup>581</sup>, and considered to be predominantly coordinated by the thalamus through thalamocortical loops<sup>582,583</sup>. Decrease in alpha power in Huntington's disease<sup>584-587</sup>, reduced alpha power in healthy individuals<sup>584</sup> and slowed alpha with lesions of the globus pallidus<sup>588</sup> have also implicated the basal ganglia in alpha oscillation regulation.

Increase in alpha rhythms, evident during closed-eye relaxation (first in the thalamus, and then in the cortex)<sup>589</sup>, has been attributed to cortical idling<sup>590</sup>. However, changes in alpha oscillations are also associated with movement, attention, memory and lexical processing<sup>580</sup>. In such contexts, alpha ERD is considered to reflect thalamocortical network excitation<sup>578</sup> and the activation of cortical areas involved in processing task information<sup>591</sup>, while ERS has been associated with inhibitory control of other cortical regions<sup>592</sup>. Such observations have led to the formation of the alpha suppression hypothesis, whereby alpha ERS is considered to reflect active suppression of task-irrelevant cortical regions as a method of selective attention<sup>593</sup>.

Whether suppression of alpha causes or reflects cortical activity suppression remains unclear<sup>594</sup>. Nonetheless, these studies have provided a basis for the use of resting-state alpha power and alpha ERD/ERS as markers of corticothalamic network function in disease<sup>582,595-597</sup>. For example, increase in thalamic resting low alpha power and increasing directed transmission of alpha from thalamus to cortex has been found in those with amnesic mild cognitive impairment at high risk of developing Alzheimer's disease, considered to reflect preclinical corticothalamic network pathophysiology<sup>597</sup>.

#### 5.3.4.2. *Auditory stimulus associated ERSP*

Non-phase locked oscillatory changes related to the auditory oddball paradigm are less established than associated ERPs, particularly in the case of ignored auditory stimuli. Most existing studies report solely on the difference between standard and deviant tone ERSP, focus on delta to alpha oscillations and/or do not deduct phase locked oscillations in time-frequency analysis, such that a frequency-domain representations of MMN and P3 ERPs are included with non-phase locked information<sup>598-603</sup>.

While the phase-locked mismatch negativity induced by this passive paradigm is found to capture involuntary attention switching<sup>123,521</sup>, the non-phase locked alpha ERS we measure here does not significantly differ with tone pitch. This ERS is most prominent over frontoparietal cognitive and motor regions following both standard and deviant tones.

A previous study of attended oddball tasks identified that both target and non-target tones elicit frontocentral alpha band ERS from 0-500ms post-stimulus, followed by alpha ERD only in the case of target, attended tones. This alpha ERD in Pz was positively correlated with reaction time while in Cz this ERD correlated to P3 amplitude, an ERP associated with attention<sup>133</sup>. Beta ERD has also been identified to be evoked specifically in response to discriminable, attended stimuli within an auditory oddball paradigm, while delta to alpha ERS were reported to be common across auditory stimuli<sup>604</sup>. This delta to alpha ERS, ranging from approximately 0-400ms post-stimulus, has also been identified in another unattended auditory oddball paradigm, albeit including both phase and non-phase locked oscillations<sup>605</sup>. These studies, alongside the lack of significant difference between standard and deviant ERSP observed here, suggests that the alpha ERS we have identified reflects thalamocortical gating of processing of ignored sensory input, rather executive performance. These findings may also explain why, in this unattended oddball paradigm, no ERD was identified.

Although this paradigm is established to evoke auditory processing and involuntary attention switching and engage associated temporal and prefrontal networks<sup>103,138,486</sup>, the passive nature of this paradigm prevents interrogation the relationship of ERSP observed here to task performance.

#### *5.3.4.3. Abnormal alpha oscillation in ALS*

Here we have identified increased event related synchronization of alpha and beta oscillations, specifically in response to deviant tones, in ALS. Source localisation attributes this excess synchronization to the thalamus, basal ganglia and predominantly temporal cortical regions. Atrophy of the thalamus, basal ganglia, amygdala and hippocampus in ALS has been previously demonstrated by structural imaging studies<sup>369,606</sup>, however atrophy-preceding dysfunction in these areas in ALS remains to be elucidated. Our finding of heightened synchronisation of alpha in these areas and much of the cortex indicates a general excess in dampening of temporal cortical excitation by

excessively active thalamocortical and corticobasal networks during the sensation of sound. The engagement of the hippocampus by an attended auditory oddball task has previously been demonstrated in line with its role in memory and novelty processing, with delta to alpha ERS being reduced in those with hippocampal lesions<sup>598</sup>. Therefore our findings of excessive alpha ERS in the hippocampus of ALS suggests the medial temporal cortex is also excessively engaged by this paradigm. Such patterns of early hyperactivation preceding progressive decline and atrophy has been demonstrated already in other cortical areas in ALS and in other neurodegenerations<sup>607-610</sup>.

While we did not find significant differences between standard and deviant tone elicited oscillations in controls, or differences in the “mismatch” between deviant and standard ERSP between ALS patients and controls, the specificity of this abnormality to deviant tone elicited oscillations suggests that such heightened synchrony in ALS does not represent a general impairment of bottom-up sensory processing of any auditory input, but represents an excessive suppression of novelty detection, or excessive “ignoring” of novel input. This may explain our previous findings of depressed auditory and inferior frontal cortex activation during the mismatch negativity response in ALS<sup>103</sup>. Furthermore, deviant (and not standard) tone-related alpha synchronization over the temporal lobes was negatively correlated with disease duration (i.e. greater alpha synchronization was measured in those closer to first symptom onset). This is in line with our previous findings of the primary auditory cortex being underactivated during the MMN early in disease, but becoming progressively hyperactivated later in disease (see section 5.1-5.2).

In addition to disruption of deviant-evoked synchronization of alpha in ALS, standard tone-evoked alpha synchronization was found to correlate negatively with ECAS score (i.e., those with greater cognitive performance display less alpha synchronization over the motor cortex). The physiology of this relationship is unclear, but may become apparent with future, longitudinal study.

#### *5.3.4.4. Abnormal beta oscillations in ALS*

In addition to excessive alpha ERS, ALS patients displayed greater synchronisation of beta in electrode D22 following deviant tones, particularly of early, fast beta and late, slow beta oscillations. Change in the former at sensor level was not attributable to a specific region of cortical dysfunction, and therefore likely represents spatial summation of mild dysfunction across a number of sources. Late, slow beta

hypersynchrony was predominantly attributed to the left medial and lateral posterior parietal cortex and middle occipital gyrus.

Beta oscillations are more spatially restricted within cortical regions compared to the slower (delta to alpha) oscillations associated with longer intracortical and cortico-subcortical network communication<sup>119</sup>. Studies of these faster oscillations typically employ motor tasks which, have demonstrated that beta and alpha ERD/ERS are functionally distinct phenomena<sup>611</sup>. Slow beta (12-20Hz) in the parietal cortex specifically has, however, been proposed to reflect the “episodic buffer” component of working memory, which combines sensory stimuli with executive commands to form task relevant representations of the input for later use<sup>612</sup>. The location of excess slow beta synchrony in ALS patients, its later timing (>150ms post-stimulus) and its specificity to rare deviant tones in this task suggests that this oscillation also represent abnormal hyperactivity in working memory centres which compare deviant tones to the expected standard tone template.

Excess fast beta synchrony in the right dorsolateral prefrontal cortex, while not significantly different in ALS, was found to negatively correlate to disease duration. This may reflect this abnormality being present in early ALS, or greater robustness of the dorsolateral prefrontal cortex in those of longer disease duration (who are well enough to partake in EEG later in disease), however the physiological basis of right dorsolateral prefrontal beta oscillations are unclear and will require further investigation before further inference is made.

#### *5.3.4.5. Clinical applicability*

While the AUROC values identified here are insufficient for diagnostic utility alone, these measures may provide additional discriminative power in the development of a multimodal, quantitative biomarker of ALS or its subphenotypes based on patterns of cortical network pathology.

#### *5.3.4.6. Limitations*

Our study is limited by the relatively short pre-stimulus baseline time window. As a result, the findings for frequencies below alpha band may be unreliable and have not been examined in detail here. The limited availability of psychological task scores also restricted our exploration of the relationship between cognitive symptoms and oscillatory activity, and as sensory task scores were not collected, the relationship between these measures and auditory function could not be measured.

#### *5.3.4.7. Conclusion*

Our data demonstrate that an ignored auditory oddball paradigm evokes broad alpha ERS, particularly in frontoparietal and motor regions in healthy individuals. This paradigm evokes significantly greater cortical and subcortical alpha and beta synchronization in ALS patients, indicative of abnormal corticobasal and thalamocortical regulation of cortical engagement following auditory stimulation and excess communication within parietal working memory hubs.

## **6. Results: The Sustained Attention to Response Task**

### **Published Work List**

The work described in section 6.1 has been published in the peer-reviewed journal *Cerebral Cortex*<sup>478</sup> as:

McMackin R, Dukic S, Costello E, et al. Localization of Brain Networks Engaged by the Sustained Attention to Response Task Provides Quantitative Markers of Executive Impairment in Amyotrophic Lateral Sclerosis. *Cerebral Cortex* 2020;00:1–13.

Section 6.1 contains all figures (1-7) and tables (1-2) as well as the results and discussion section text in full from this publication. Introduction and methods section text from this publication have been abbreviated in this chapter to avoid repetition of the contents of chapters 1-4.

The work described in section 6.2 has been published in the peer-reviewed *Journal of Neural Engineering* as:

McMackin R, Dukic S, Costello E, et al. Sustained attention to response task-related beta oscillations relate to performance and provide a functional biomarker in ALS. *Journal of Neural Engineering*. 2021 Feb 25;18(2):026006.

Section 6.2 contains all figures (1-4) and tables (1-2) as well as the results and discussion section text in full from this publication. Introduction and methods section text from this publication have been abbreviated in this chapter to avoid repetition of the contents of chapters 1-4.

## 6.1. Cross-sectional event related potential analysis

### 6.1.1. Introduction

The SART has been developed to detect clinically relevant lapses in attention. It represents a simple and quantitative task of executive functions that has been used to capture attentional impairments in different neurodegenerative diseases<sup>470,613–615</sup>. Drifts in attention are captured by a failure to inhibit motor responses to targets (i.e. commission errors). As the task requires only button press responses it is suitable for performing during EEG recording with little to no electromyographic artefacts. Recently, SART-generated ERPs time-locked to Go and NoGo trials have been interrogated in healthy individuals using quantitative EEG. These ERPs have individual peaks which relate to sensory detection ('P1' and 'N1')<sup>616</sup>, motor control ('N2') and attentional engagement ('P3'). The latter two peaks are typically larger during correct response withholding<sup>126</sup>. By combining SART with EEG, distinct indices of the neural network activities required for different aspects of task performance can be determined. This facilitates specific interrogation of the sequentially engaged sensory, motor and cognitive networks on a millisecond-by-millisecond basis in a quantitative, economical manner. Further, by requiring both motor and cognitive performance, the SART is expected to engage networks that bridge cognitive and motor functions, as oppose to tasks that demand only the individual functions. This suggest that SART has potential as an instrument to assess the neurophysiological substrates underpinning motor and executive decline in conditions such as ALS, Huntington's disease and Parkinson's disease<sup>617</sup>.

Despite these advantages, the cortical regions engaged by the SART remain unclear. Low-resolution sensor-level topographies have indicated frontoparietal engagement during the task<sup>126,479</sup> and dorsolateral prefrontal and anterior cingulate malfunctioning during SART has been reported in Huntington's disease<sup>618</sup>. However, the sources of the SART ERPs in healthy individuals have yet to be reported in high spatial and temporal resolution.

Such source-resolved measures could provide important insights into and biomarkers of different cognitive and/or motor neurodegenerations, such as occurs in the neurodegenerative condition ALS.

Detailed neuropsychological assessment with appropriate adjustments for motor impairment has provided information on the nature and frequency of different cognitive domain impairments in ALS<sup>19</sup>. However, these types of assessments are excessively time

consuming for clinical trials, in some instances are subject to learning effects, and are insensitive to early, presymptomatic network deterioration. Screening tools, such as the ECAS for ALS, are useful in a clinical setting but have limited utility in clinical trials and are not sufficiently sensitive for a detailed assessment of cognitive/behavioural change<sup>511</sup>. PET and fMRI have been used to measure cortical activity during specific tasks, but these technologies are limited by cost<sup>619</sup>, low temporal resolution and variance across different scanners<sup>102</sup>.

By contrast, we and others have recently demonstrated how the source localisation of EEG facilitates spatially and temporally precise functional imaging of ALS cortical pathology<sup>102,341</sup>. Therefore, given the motor and cognitive pathology of ALS, measurement of SART-associated ERPs using source-resolved EEG provides an opportunity to simultaneously interrogate motor and cognitive network functions and investigate their relationship to symptomatic impairments.

Here, we have spatially resolved the sources of these cognitive indices in healthy individuals and patients with ALS by LCMV-based source imaging. We demonstrate how quantifying changes in SART-ERP indices and their relation to cognitive and motor symptoms facilitates investigation of neurophysiological changes associated with cognitive impairment in ALS.

### *6.1.2. Methods*

#### *6.1.2.1. Ethical Approval*

Ethical approval and participant written consent were obtained as described in section 4.6.

#### *6.1.2.2. Inclusion Criteria*

Patients were over 18 years of age and diagnosed within the previous 18 months with Possible, Probable or Definite ALS in accordance with the El Escorial Revised Diagnostic Criteria<sup>63</sup>.

#### *6.1.2.3. Exclusion Criteria*

Exclusion criteria included any diagnosed psychological, neurological or muscular disease other than ALS, use of central nervous system medications (e.g. antidepressants, anti-seizure medication) except riluzole, inability to participate due to ALS-related motor decline (e.g. inability to sit in the chair for the required time or click the mouse to respond), or evidence of significant respiratory insufficiency. Participants were also



rescheduled if they slept two or more hours below normal the night before the session and were asked to abstain from consuming alcohol the night before the recording.

#### *6.1.2.4. EEG Acquisition and Experimental Paradigm*

EEG acquisition and the employed experimental paradigm (sustained attention to response task) are described in section 4.1.3. Electrodes of primary interest (Fz, FCz, Cz and Pz) were chosen based on established topographic maps of the SART N2 and P3 peaks<sup>126,479</sup>.

#### *6.1.2.5. Clinical and psychological scores*

Fifteen patients underwent psychological assessment using the ECAS within 4 weeks of the EEG recording. Additionally, ALSFRS-R was collected longitudinally by neurologists at the Irish National ALS specialty clinic in Beaumont Hospital (see section 4.5).

#### *Participant demographics*

Patient and control characteristics are summarised in table 6.1. None of the participants met the criteria for FTD diagnosis. One patient was using non-invasive ventilation at night time but had ALSFRS-R orthopnoea and dyspnoea scores of 3 (out of 4). Total and ALS specific ECAS scores within 30 days of EEG data collection were available for 15 patients, while ALS non-specific scores were available for 17 patients and ALSFRS-R scores were available for 14 patients. Three additional patients had ALSFRS-R data within three months before and after the EEG recording date. Using the data from these two time points, ALSFRS-R scores for these three patients were estimated by interpolation assuming linear decline such that ALSFRS-R scores were available for 17 patients in total. Scores are summarised in table 6.1. Of those patient who performed abnormally in the ECAS, two had abnormal ALS non-specific scores but not total or ALS-specific scores, one had an abnormal ALS non-specific score but could not complete the language, fluency and spelling tasks to provide remaining scores and one performed abnormally in total and ALS-specific scores but not in their ALS non-specific score.

**Table 6.1. Characteristics of ALS patients and controls.** Handedness was determined by the Edinburgh Handedness Index. ECAS scores are out of a maximum total score of 136, ALS non-specific score of 36 and ALS specific score of 100. *C9orf72*+ - Carrying a repeat expansion of the *C9orf72* gene. ECAS – Edinburgh Cognitive and Behavioural Assessment Scale. N abnormal – Number of participants scoring below the abnormality cut off score, accounting for years of education. This table has been published in my paper McMackin et al. 2020 (table 1), please see appendix 6.1.

	<b>Patients</b>	<b>Controls</b>
N	23	33
Mean age at EEG [range] (years)	63 [32-78]	63.21 [46-82]
Gender (f/m)	3/20	17/16
Site of onset (spinal/bulbar/thoracic)	17/5/1	N/A
Mean disease duration [range] (months)	20.01 [4-42]	N/A
Handedness (right/left/ambidextrous)	22/0/1	31/2/0
<i>C9orf72</i> +	3	Untested
Mean ALSFRS-R score [range]	38.24 [24-43]	N/A
Mean ECAS total score [n abnormal]	105.33 [3]	Untested
Mean ECAS ALS specific score [n abnormal]	78.47 [3]	Untested
Mean ECAS ALS non-specific score [n abnormal]	26.65 [2]	Untested

#### 6.1.2.6. Data Analysis

EEG data were preprocessed as described in section 4.1.4.1. Source analysis was performed by LCMV beamforming. Sensor and source space analysis pipelines are described in section 4.1.4.2.

#### 6.1.2.7. Statistics

##### *Behavioural analysis*

Group level comparisons of performance during the SART were implemented with Mann-Whitney U test<sup>494</sup>. A FDR of 5% was implemented to correct for multiple comparisons, calculated by the Benjamini Hochberg method<sup>498</sup>. P-values are reported as uncorrected values where significant (determined by a corrected p-value is <0.05).

##### *Sensor space analysis*

A four factor ANOVA was performed for each of the four peak characteristics for both N2 and P3, resulting in eight ANOVA. For each ANOVA the variables included were sex (male or female, accounting for gender imbalance), trial type (Go or NoGo), electrode (Fz, FCz, Cz or Pz) and group (ALS patient or control). Post-hoc analysis was implemented by Tukey's honestly significant difference<sup>620</sup>. A 5% FDR was implemented to correct post-hoc p-values for multiple comparisons as described for behavioural analysis.

### *Source space analysis*

A 10 mm grid in the brain volume yields 1726 sources including white matter. To analyse these high-dimensional data, a 10% FDR was used as a frequentist method for determining significant source activity differences. Discrimination ability between patients and controls is quantified by AUROC<sup>501</sup>. EBI<sup>499</sup> was used to calculate the Bayesian Posterior probability and statistical power.

### *Neuropsychology correlation*

Spearman's rank correlation<sup>542</sup> was used to test the association of the changes in EEG measures (peak characteristics or mean power within a cortical region) and cognitive and functional measures based on inter-individual differences. These measures were: Performance in the SART task during EEG collection, performance in the D-KEFS CWIT<sup>621</sup>, ECAS scores and ALSFRS-R scores. Multiple comparison correction was implemented using a FDR<sup>498</sup> set to 5%. For source level correlation analysis, mean power was calculated for brain regions identified as major sources of peak activity, defined by the Automated Anatomical Labelling atlas<sup>487</sup>. Where significant correlations are reported regarding Go and NoGo combination measures, for example total (Go and NoGo) performance accuracy or the difference between NoGo and Go ERP measures, the relationship was verified not to be due to only Go or NoGo trials.

## *6.1.3. Results*

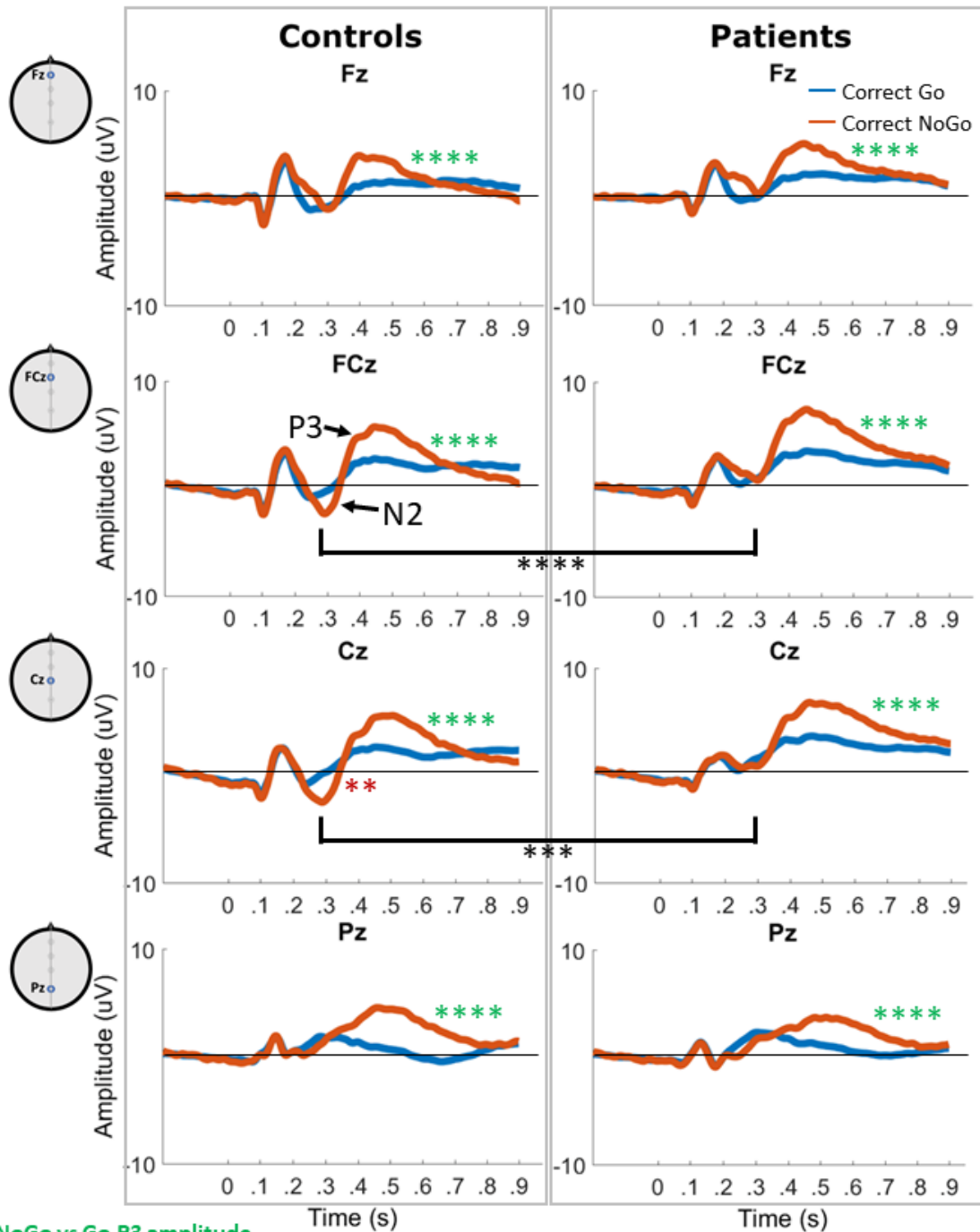
### *6.1.3.1. Performance*

Patients (n=23) and controls (n=33) did not differ significantly in response time or accuracy. However, patients committed significantly more anticipation errors (patient mean [standard deviation]: 8.73% [13.85%], control mean [standard deviation]: 1.01% [3.26%], p=0.0031).

### *6.1.3.2. Control characteristics*

#### *Sensor space*

Mean patient and control Go and NoGo ERPs in electrodes of interest are shown in Fig. 6.1. ANOVAs did not reveal any significant gender effects on waveform features.



\*NoGo vs Go P3 amplitude

\*NoGo vs Go N2 amplitude

\*ALS vs CON NoGo-Go N2 amplitude

**Figure 6.1.** Mean Go (blue) and NoGo (red) trial ERPs in controls ALS patients. N2 peaks are visible in the NoGo trial ERP in Fz and Cz in the 220-350ms window. P3 peaks are present in the 350-550ms window in both Go and NoGo trial ERPs in all electrodes. Green asterisks represent significantly larger P3 peak amplitudes in NoGo vs Go trials. Red asterisks represent significantly larger (more negative) N2 peak amplitudes in NoGo vs Go trials. Black asterisks represent significant differences in NoGo-Go N2 peak amplitude between ALS patients and controls. \*\* $p < 0.01$ , \*\*\*\*  $p < 0.0001$ . CON – Controls. This figure has been published in my paper McMackin et al. 2020 (figure 1), please see appendix 6.1.

*N2*: *N2* in Cz was significantly smaller in Go trials than NoGo trials in controls (peak area  $p=0.018$ , peak amplitude  $p=0.006$ ). This *N2* difference significantly correlated with faster response times ( $p=8.08 \times 10^{-6}$ ,  $\rho=0.69$ ) and poorer NoGo accuracy ( $p=0.0086$ ,  $\rho=0.45$ ) in controls (Fig. 6.2A).

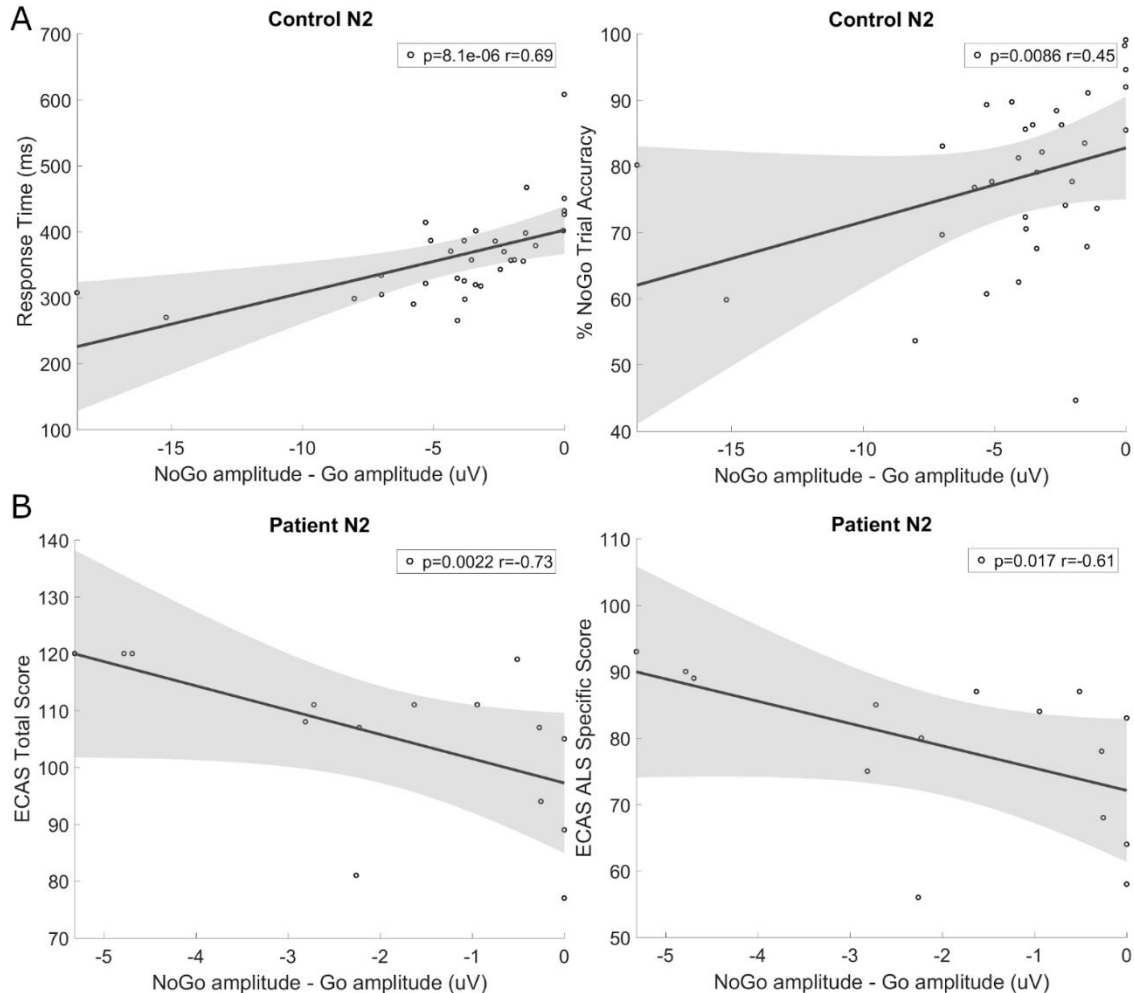


**Figure 6.2. Correlations between NoGo minus Go (NoGo-Go) *N2* peak amplitude in Cz and cognitive task performance.** (A) Correlation with response time and NoGo trial accuracy in controls demonstrates that those with smaller NoGo versus Go *N2* peak differences had significantly faster response times and better NoGo accuracy. (B) Correlation with patient ECAS total and ALS specific score demonstrates that those with smaller (less negative) *N2* peak differences had lower ECAS scores.  $r$  – Rho. This figure has been published in my paper McMackin et al. 2020 (figure 2), please see appendix 6.1.

*P3*: *P3* was significantly smaller for Go trials compared to NoGo trials in all four electrodes of interest (Fig. 6.1, Tukey's post-hoc  $p=3.50 \times 10^{-5}$ - $8.15 \times 10^{-7}$ ). *P3* peak latency in the Pz electrodes was also significantly greater in NoGo trials compared to Go trials ( $p=5.12 \times 10^{-7}$ ). Controls with later responses had later NoGo *P3* peaks in Fz ( $p=0.0020$ ,  $\rho=0.52$ ) while those with better NoGo accuracy had smaller Go *P3* peaks in Cz ( $p=0.011$ ,  $\rho=-0.43$ ) and FCz ( $p=0.0034$ ,  $\rho=-0.50$ ) and those with better Go accuracy

had larger NoGo P3 peaks in Pz ( $p=0.0070$ ,  $\rho=0.46$ ). Better overall accuracy also correlated significantly with smaller NoGo P3 peaks in Fz ( $p=1.26 \times 10^{-4}$ ,  $\rho=-0.62$ ). Correlations are illustrated in Fig. 6.3A-D.

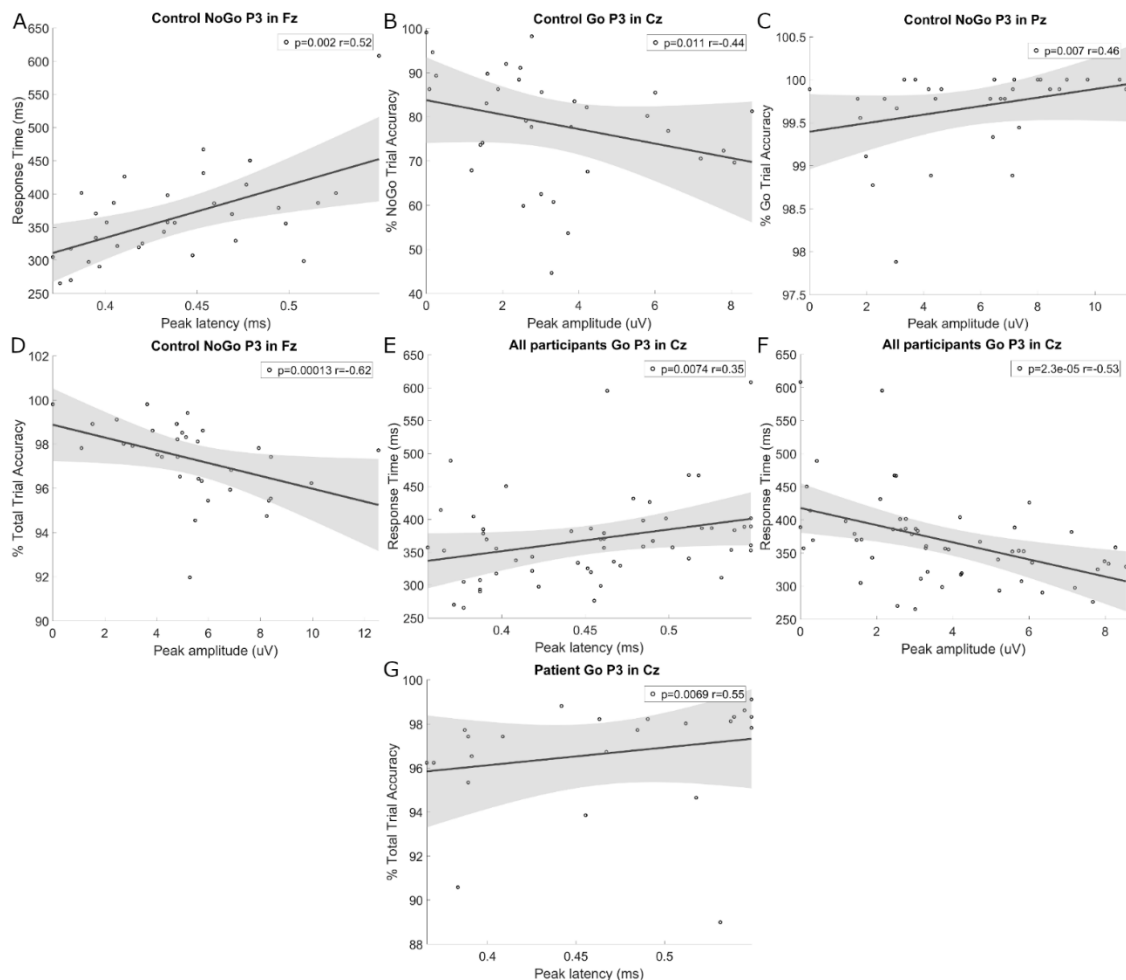


**Figure 6.3. Correlations between P3 peak characteristics and SART performance.** In controls, (A) later responses correlate with later P3 peaks in Fz during NoGo trials, (B) better NoGo accuracy inversely correlates with Go P3 peak size in Cz, (C) Go accuracy positively correlates with NoGo P3 peak amplitude in Pz and (D) overall accuracy inversely correlates with NoGo P3 peak amplitude in Fz. In all participants, (E) later response correlate with longer peak latency and (F) smaller peak amplitude during Go trials in Cz. In patients, (G) greater overall accuracy correlates with longer Go P3 peak latency in Cz. This figure has been published in my paper McMackin et al. 2020 (figure 3), please see appendix 6.1.

#### *Source space*

*N2*: The left primary motor cortex and bilateral DLPFC and lateral PPC were identified as primary mean sources of both Go and NoGo *N2*, with greater bilateral precuneus activation during NoGo trials (Fig. 6.4).

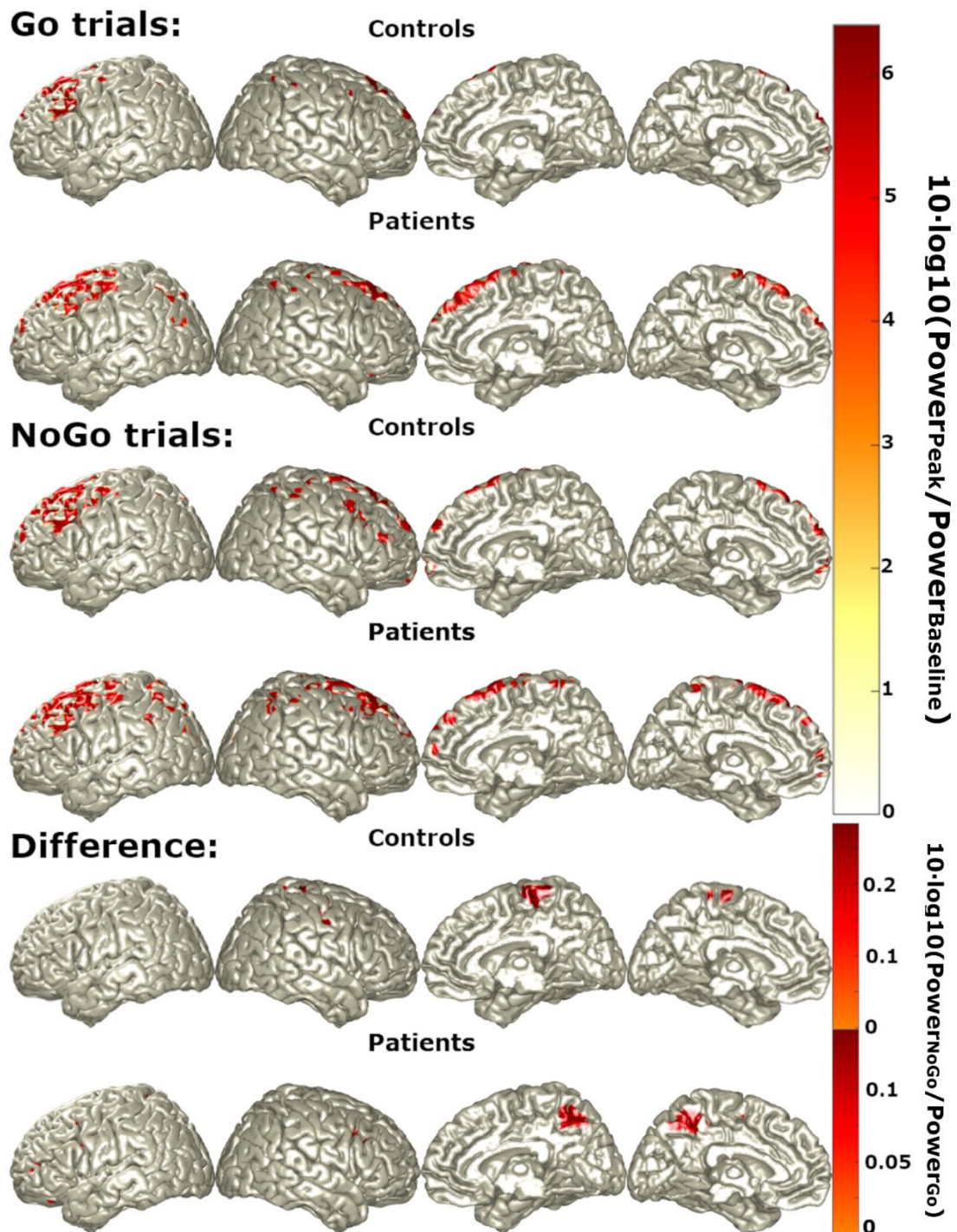


**Figure 6.4. Primary sources (regions with top 5% power) of N2 during Go trials, NoGo trials and NoGo trials relative to Go trials (“difference”) in controls (first rows) and patients (second rows).** This figure has been published in my paper McMackin et al. 2020 (figure 4), please see appendix 6.1.

*P3*: Mean P3 sources were similar to those of N2 for Go and NoGo trials, although controls showed decreased left insular, PPC and DLPFC activity during NoGo trials relative to Go trials (Fig. 6.5).

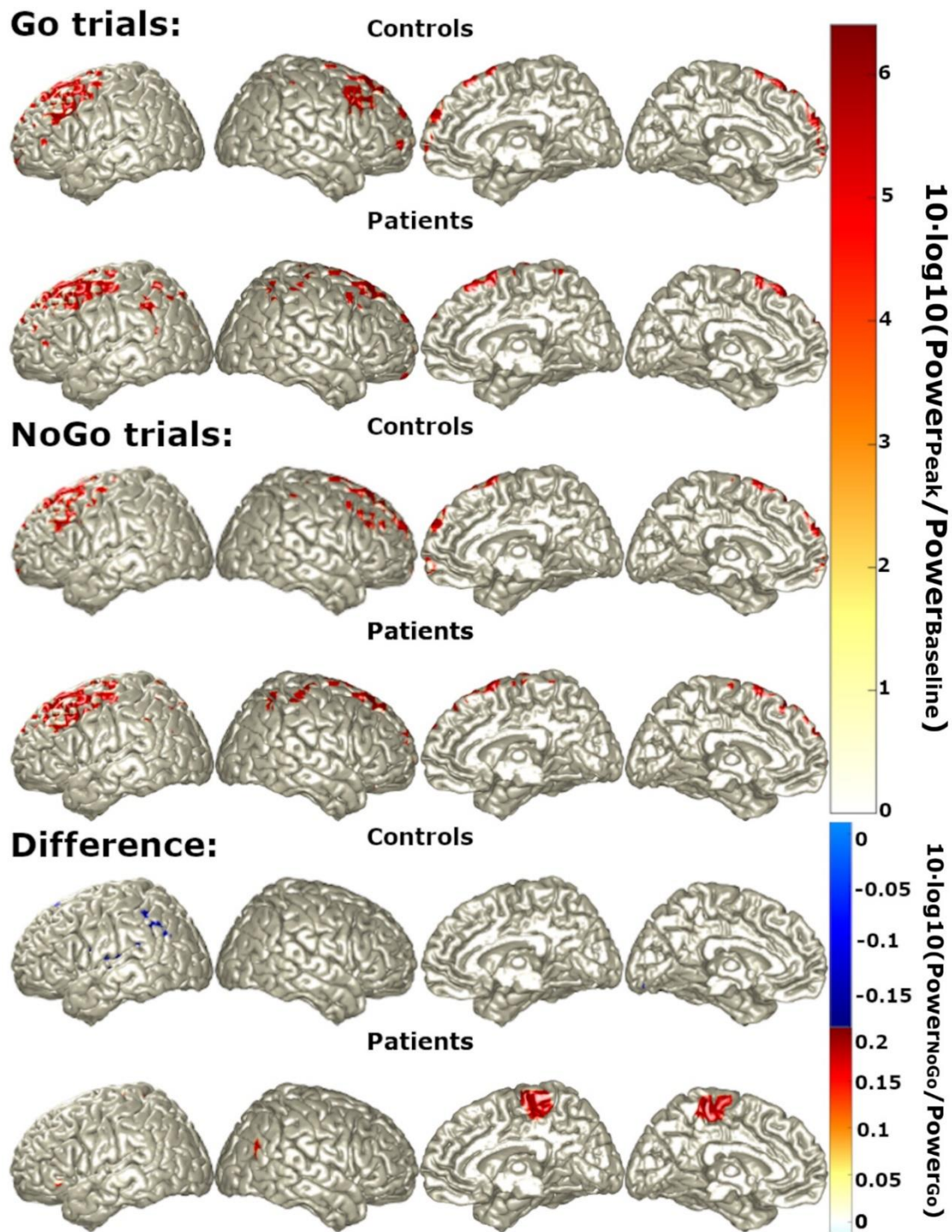


**Figure 6.5.** Primary sources (regions with 5% power) of P3 during Go trials, NoGo trials and NoGo trials relative to Go trials in controls (first rows) and patients (second rows). This figure has been published in my paper McMackin et al. 2020 (figure 5), please see appendix 6.1.

#### 6.1.3.3. ALS patient differences

Differences in peak and source measures between patients and controls are summarised in table 6.2.



*Sensor space (ERP) differences*

**N2:** Patients did not show a significant difference in the N2 peak between Go and NoGo trials. Correspondingly, N2 was significantly smaller for NoGo trials in ALS patients compared to controls in FCz ( $p=5.08 \times 10^{-4}$ ) and Cz ( $p=0.001$ ). Unlike controls, the difference in N2 between Go and NoGo trials did not correlate with SART performance, however those patients with greater N2 NoGo-Go differences in Cz had higher ECAS total ( $p=0.0022$ ,  $\rho=-0.73$ ) and ALS-specific ( $p=0.017$ ,  $\rho=-0.61$ ) scores, indicating better cognitive performance, particularly in tasks of executive function and language (Fig. 6.2B).

**P3:** The P3 peak did not differ significantly between patients and controls for any trial type or characteristic. Patients and control with longer response times had later ( $p=0.0074$ ,  $\rho=0.35$ ), smaller ( $p=2.31 \times 10^{-5}$ ,  $\rho=-0.53$ ) Go P3 peaks in Cz (Fig. 6.3E-F). Otherwise, patients did not display the correlations between their P3 peak characteristics and task performance that were observed for controls. Overall accuracy was found to significantly correlate with later Go P3 peaks in Cz in patients ( $p=0.0069$ ,  $\rho=0.54$ , Fig. 6.3G).

**Table 6.2. Significant differences in ALS sensor level and source level measures compared to controls.** This table has been published in my paper McMackin et al. 2020 (table 2), please see appendix 6.1.

<b>Sensor level (ERP peaks)</b>			
<b>Peak</b>	<b>Trial</b>	<b>Electrode</b>	<b>Change in ALS</b>
N2	NoGo	Cz	↓ Peak amplitude
		FCz	↓ Peak amplitude
	NoGo-Go	Cz	No correlation to task performance
P3	Go	Cz	Later peak positively correlates with greater overall accuracy, no correlation between peak amplitude and accuracy.
	NoGo	Fz, Pz	No correlation between amplitude or latency to performance
<b>Source level</b>			
<b>Peak</b>	<b>Trial</b>	<b>Source</b>	<b>Change in ALS</b>
P3	NoGo-Go	Left posterior parietal and insular cortex	↑ Activation, area under receivership operating characteristics curve >0.75

### Source space differences

*N2*: Patients showed similar patterns of source activity to controls during N2 (Fig. 6.4).

*P3*: While similar locations of source activity were observed in patients and controls during Go and NoGo trials, ALS patients showed similar differences between NoGo and Go source differences to N2 during P3 (Fig. 6.5), unlike controls. Correspondingly, ALS patients displayed widespread, significantly increased activity during NoGo trials relative to Go trials when compared to controls, with the most discriminant differences (AUROC>0.75) being in the left inferior parietal lobule and left insula (Fig. 6.6).

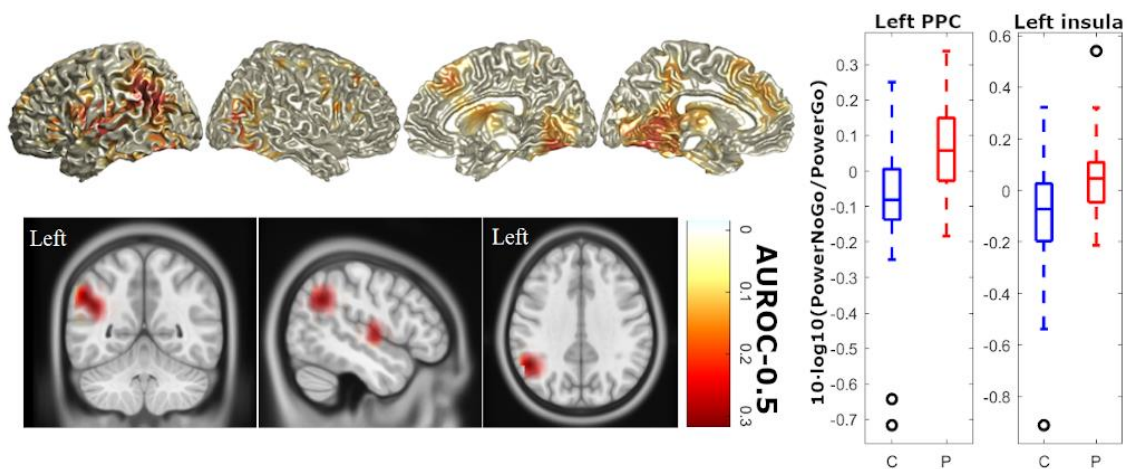


**Figure 6.6. P3 sources with statistically significant differences in activity in ALS compared to controls.** Differences between NoGo and Go trial source activity during the P3 peak were compared between ALS patients and controls. All highlighted areas represent significant (FDR=10%, type II error=0.38, Bayesian Posterior probability=0.87) increases in power with heat map values representing AUROC-0.5 (i.e. perfect discrimination=0.5). Orthogonal MRI scans show only those differences with an AUROC>0.75, i.e. very good discriminators. AUROC – Area Under the Receivership Operating Characteristics Curve. This figure has been published in my paper McMackin et al. 2020 (figure 6), please see appendix 6.1.

### Source space correlations in ALS patients

Greater right precuneus power during P3 in NoGo relative to Go trials negatively correlates with CWIT inhibition score ( $p=0.0015$ ,  $\rho=-0.91$ , Fig. 6.7). As greater scores in this task indicated poorer behavioural inhibition, this relationship demonstrated that the abnormal activation of this area was associated with greater preservation of this executive function.

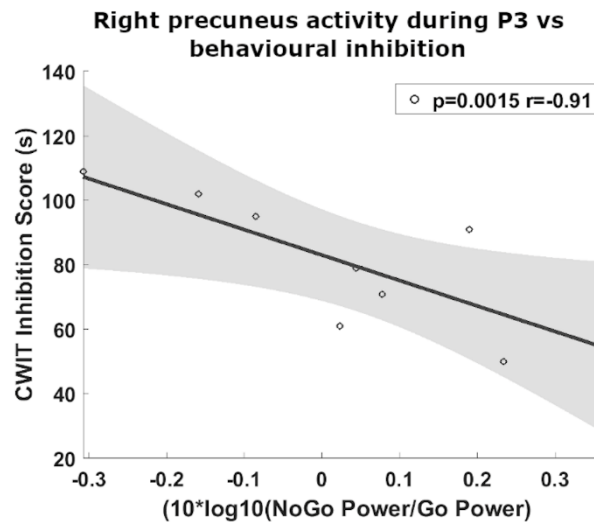


**Figure 6.7. Greater behavioural inhibition in ALS is associated with increased right precuneus activity during NoGo P3 relative to Go P3.** Higher CWIT inhibition score indicates poorer behavioural inhibition. This figure has been published in my paper McMackin et al. 2020 (figure 7), please see appendix 6.1.

#### 6.1.4. Discussion

This study demonstrates for the first time the specific cortical structures that contribute to performance of the SART and quantifies the relationship between SART performance measures and underlying cognitive performance. Furthermore, we have identified abnormalities in cortical function which strongly correlate with executive impairment in ALS.

##### 6.1.4.1. ERP peak characteristics

At sensor level, our control findings were consistent with the literature, demonstrating the robustness of SART-associated ERPs. N2 and P3 peaks were present in the anticipated time windows and, as expected, larger for healthy individuals during correct response omission.

##### Central N2

NoGo N2 was maximal in Cz, as previously established. We identified that smaller differences in N2 size between NoGo and Go trials was associated with faster reaction times. We also identified a correlation between smaller NoGo N2 peaks and better NoGo trial accuracy. As the N2 peak has been association with automated motor response control<sup>126</sup>, this may reflect greater ability to withhold and greater response speed where less cortical resources are required to inhibit upper motor neurons.

Notably, these correlations were not present for ALS patients, which may represent the compensatory engagement of alternative cortical resources. Alternatively, the established malfunction of inhibitory cells of the motor system<sup>569</sup> in addition to upper motor neurons may lead to reduction in NoGo N2 in combination with slowing reaction times.

#### *Frontal and Parietal P3*

The P3 peak was present across the frontoparietal axis of sensors during NoGo trials in keeping with the SART ERP literature<sup>126,415,479</sup>. Such spatially distributed P3 peaks associated with other cognitive tasks have been shown to consist of two distinct entities, namely the frontal and parietal P3. Frontal P3 peaks have been associated with orientation to novel stimuli, declining over task duration although remaining elevated in distractible children<sup>622</sup> and those with panic disorder<sup>623</sup>. By contrast, parietal P3 peaks are associated with working memory and attention to target stimuli<sup>622,623</sup>.

Here we have identified similarly distinct behaviours in the frontal and parietal SART-associated P3 peaks. In frontocentral electrodes, P3 latency related to response timing and is likely to provide an index of orientation speed. Smaller frontocentral P3 peaks were associated with more accurate performance in the opposite trial type (i.e. better Go performance with smaller NoGo peaks and vice versa). By contrast, larger NoGo parietal P3 was associated with better Go trial performance. This is in keeping with the cognitive resources required for accurate Go and NoGo SART performance. The engagement of working memory and attentional control was indicated by a large NoGo parietal P3, and quick orientation to the task was indicated by earlier, smaller frontal P3 peaks<sup>622,623</sup>.

The orienting frontal P3 is typically earlier than the parietal P3, however it has been hypothesised that frontal P3 peaks may also encompass compensatory prefrontal engagement due to parietal decline<sup>624</sup>. This may explain why ALS patients, but not in controls, demonstrated greater Cz P3 peak latencies during Go trials in those with better accuracy.

#### *6.1.4.2. Cortical source imaging*

At source level both Go and NoGo N2 and P3 peaks were associated with extensive prefrontal and motor cortex engagement, particularly in the left cortex, in keeping with use of the right hand for task performance. Such widespread cortical engagement is expected, given the numerous cognitive and motor domains required for accurate task performance. The medial PPC (i.e. the precuneus) was additionally engaged during NoGo trials relative to Go trials during N2, in keeping with its role in both voluntary attention

shifting and movement control<sup>625</sup>. By contrast, the left insula and inferior parietal lobule show lower power in NoGo trials relative to Go trials during P3, in keeping with role of the left insula in the salience network<sup>626</sup> and goal directed behaviour<sup>627</sup>. The left inferior parietal lobule has been attributed numerous functions, among which are object-directed action<sup>628</sup> and expectancy violation<sup>629</sup>. This engagement of numerous cortical structures by different elements of the SART highlights the range of cortical pathologies that could contribute to decline in SART performance measures. While SART ERP analysis can temporally dissect the cause of such performance decline, it is clear from source imaging that a specific peak abnormality could also result from dysfunction in several different cortical structures. Source imaging can therefore not only inform on source contributing to cognitive and motor symptoms but could also discriminate between psychiatric or neurodegenerative syndromes with similar symptoms driven by differing cortical pathologies.

#### *6.1.4.3. Quantifying cortical pathology driving cognitive impairment in ALS*

ALS patients maintained similar Go and NoGo accuracy but were more likely to attempt to complete trials rapidly clicking before cognitively processing the presented digit, resulting in greater anticipation error. Despite sensor level differences, patients and control activity did not differ significantly at a specific N2 source. This is likely to be a function of spatially distributed differences in activity which summate in signals captured by individual electrodes at source level. Patients did, however, demonstrate very similar elevation in precuneus activity during NoGo relative to Go trials in both N2 and P3. As this elevation in right precuneus activity during P3 was associated with greater behavioural inhibitory function, this may represent a compensatory recruitment of this region. Indeed, this exemplifies the utility of source localised EEG during task performance for quantifying cognitive pathology during presymptomatic phases of compensatory cortical activity that are more amenable to clinical intervention.

ALS patients demonstrated additional widespread cortical activity elevation during NoGo relative to Go trials during P3, particularly in the left insula and inferior parietal lobule, which showed very good discrimination between patients and controls (AUROC>0.75). Such posterior parietal hyper-engagement has previously observed during involuntary attention switching<sup>103</sup> and at rest<sup>341,393</sup>, and may provide additional discriminatory power in the development of cortical diagnostic biomarkers. A previous study in Huntington's

disease identified reduced activity in the left DLPFC<sup>618</sup>, right medial frontal and anterior cingulate cortex during the NoGo P3, while we find hyperactivity in these areas in ALS, highlighting the ability of this task to identify differing underlying cortical pathologies in neurodegenerations with overlapping cognitive and behavioural symptoms.

We acknowledge that while these cross-sectional data serve well to characterization of ALS disease heterogeneity, these measure demand larger-scale studies for adequately-powered subgroup analysis. Additional larger, longitudinal studies will be required to further evaluate the application of this technology in clinical trials and disease prognostics.

In conclusion, here we have provided a spatially and temporally precise description of the cortical activity which underlies the N2 and P3 peaks of the randomised SART-ERP in healthy adults and illustrated the applications of this methodology for interrogating cognitive and motor malfunction in a complex neurodegenerative disease. While larger patient recruitment is required for further investigation of the use of SART as an ALS biomarker, we have established that the SART-ERP and its underlying source activity can provide objective, quantitative, early markers of cognitive and motor pathology. The localisation of EEG recorded during a wider battery of cognitive, motor and sensory tasks has considerable potential to provide patient-specific profiles of cortical network disturbance which could in turn provide biomarkers that improve patient subgrouping, clinical trial stratification and prognostic accuracy.

## **6.2. Time-frequency analysis**

### *6.2.1. Introduction*

Following demonstration of the locations of cortical activation by SART through ERP analysis and demonstration of ALS-related abnormalities in cortical network activation<sup>478</sup>, we investigated the changes in cortical oscillations during the SART that are not captured in our ERP analysis by quantifying non-phase locked ERS. We sought to establish whether these oscillations are disrupted in ALS using time-frequency domain EEG analysis, and to determine whether such oscillations predict task performance measures in controls and in ALS patients. We hypothesised that these measures will provide additional insight into the nature of dysfunction in cortical networks which bridge motor and cognitive function in ALS.

### *6.2.2. Methods*

#### *6.2.2.1. Ethical Approval*

Ethical approval and participant written consent were obtained as described in section 4.6.

#### *6.2.2.2. Inclusion Criteria*

All participants were over 18 years of age and able to give informed written consent, or in the presence of two witnesses, verbal consent. Patients were diagnosed with Possible, Probable or Definite ALS in accordance with the El Escorial Revised Diagnostic Criteria.

#### *6.2.2.3. Exclusion Criteria*

Those with neurological functional/structural, psychological or muscular disorders other than ALS (including those with comorbid FTD) and those currently taking neuromodulatory or myomodulatory medications (e.g. antidepressants, anti-epileptics, GABA antagonists) that could affect recordings were excluded, except for riluzole.

#### *6.2.2.4. Clinical and behavioural scores*

ALSFRS-R data were recorded at the Irish National ALS specialty clinic for each participant. Scores were included in analysis if collected within  $\pm 90$  days of EEG.

ALSFRS-R, ECAS and Delis-Kaplan CWIT<sup>508</sup> data (see section 4.6) were included if collected within  $\pm 90$  days of EEG. Disease duration was quantified as the number of months between patient-reported date of first symptom onset and date of EEG recording.

#### *6.2.2.1. Participant demographics*

The same ALS patient and control datasets were employed as in our previous time-domain study<sup>478</sup>, with one additional patient dataset analysed here. Therefore, a total of 24 ALS patients (3 female, age median [interquartile range]: 69 [59-72] years) and 33 controls (17 female, age median [interquartile range]: 64 [57-69] years) were included in this analysis. Groups were age-matched but not gender matched, as previous comparison of male and female controls for parameters of interest revealed no gender-related differences<sup>478</sup>. ANOVA found significant group effects for some WOI (described below) but no significant gender effects. The ALS cohort included three patients with a *C9orf72* gene expansion, with the remainder of patients not carrying or not tested for this pathogenic expansion. Site of onset of disease symptoms was spinal in 18 patients, bulbar in five patients, and thoracic in one patient. Disease duration and time since diagnosis median [interquartile range] of patients was 17.65 [10.15-23.92] months and 4.42 [2.98-9.71] respectively. ALSFRS-R, ECAS and CWIT scores collected within 90 days of EEG were available for 18, 15 and 9 patients respectively. Survival data were not analysed as only 2 patients were deceased at time of analysis.

#### *6.2.2.1. EEG Acquisition and Experimental paradigm*

EEG acquisition and the employed experimental paradigm (sustained attention to response task) are described in section 4.1.3. Electrodes of primary interest (Fz, Cz and Pz) were chosen based on established topographic maps of the SART N2 and P3 peaks<sup>126,479</sup>.

#### *6.2.2.2. Data Analysis*

##### *EEG signal pre-processing*

Signal pre-processing procedures are described in section 4.1.4.1. Sensor and source space analysis of ITV-based ERSP are described in section 4.1.4.3.

#### *6.2.2.3. Statistics*

##### *Oscillation analysis*

To check for gender effect, ANOVA were performed separately for each Go and NoGo WOI, using electrode, gender and group (patient or control) as independent variables, to determine the significance and gender and group effects on WOI power (dependent variable). A FDR of 5% was applied to p-value families across ANOVA, implemented using the Benjamini and Hochberg method<sup>498</sup>, to account for multiple comparisons. Tukey's post hoc analysis was also implemented for each ANOVA to identify individual



electrodes which significantly differed between groups. For time-frequency plane statistical analysis of each electrode, data were down sampled to 34Hz (i.e. 1/15 data points). To identify significant (i.e. significantly different from zero) ERSP in controls, Wilcoxon's (paired) Sign-Rank W-statistic<sup>495</sup>, transformed to Z scores, was used as a test statistic. To identify significant differences between control and patient ERSP, AUROC<sup>501</sup> was used as a test statistic. In both cases, a 5% false discovery rate<sup>498</sup> was used as a frequentist method for determining significant power differences amidst these high-dimensional data. EBI<sup>499</sup> provided Bayesian posterior probabilities, as well as the achieved statistical power and AUROC.

#### *Effect sizes and correlations*

Specific time-frequency areas were defined as WOI based on significant oscillation patterns identified in the control group (without inclusion of, or comparison to the patient group) as ERD/ERS elicited by the SART in controls has not previously been reported. These WOI were defined in order to determine effect size of differences between patients and controls and investigate clinical correlations in patients, based on mean ERSP values (without down sampling) within these WOIs. Cohen's d was used as an index of effect size, where  $d > 0.8$  indicates a large effect size<sup>630</sup>.

Spearman's non-parametric rank correlation<sup>542</sup> was used to investigate relationships between mean ERSP values in the WOIs and neuropsychological and motor test scores. Partial correlation was implemented for investigating relationships to CWIT inhibition and inhibition-switching subscores, to control for the effects of decline in speech function (quantified by the ALSFRS-R speech score) at time of CWIT testing. Multiple comparisons were accounted for using a 5% FDR, implemented using the Benjamini and Hochberg method<sup>498</sup>.

#### *Gender and age matching*

Mann-Whitney U testing<sup>494</sup> and chi-squared proportion testing were used to compare age and gender respectively between groups, with significant differences determined where  $q = 0.05$  (corresponding to the  $p < 0.05$  for individual testing).

#### *Selected measures for reporting the main findings*

For reporting the results of statistical analyses, we use the p-values as a first stage screening for significant findings. We then report the effect sizes (e.g. Cohen's d), which reflect how strong the changes in the brain are (as a patho-physiological phenomenon). Finally, to show how much discrimination between controls and ALS patients is afforded

by each measure, we use the AUROC as a measure commonly used in medical statistics<sup>631</sup>.

### 6.2.3. Results

#### 6.2.3.1. Task Performance

Mean response time was 364ms in controls and 375ms in patients. Mean  $\pm$  standard deviation trial accuracy (Go and NoGo) was  $99.67 \pm 0.48$  and  $78.31 \pm 12.73\%$  in controls and  $98.96 \pm 1.60$  and  $77.90 \pm 12.53\%$  in patients respectively. Control and patient accuracy and response time measures were not significantly different. Patients had significantly ( $p=0.0042$ ) greater anticipation errors than controls (patient mean  $\pm$  standard deviation:  $0.084 \pm 0.14\%$ , control:  $0.01 \pm 0.03\%$ ).

#### 6.2.3.2. Event Related Spectral Perturbations

##### *Go trials*

During Go trials, theta-band (4-7Hz) ERS (i.e. increase in power relative to baseline), alpha-band (8-12Hz) ERD (i.e. decrease in power relative to baseline) and beta-band (13-30Hz) ERD were present across the frontoparietal axis. Beta ERD was followed by ERS, predominantly in Fz and Cz. These ERSP patterns in healthy controls, as informed by sign rank<sup>495</sup> statistical analysis, were examined further as windows of interest for comparing ALS patients against controls and when performing correlation analyses in 100-700ms, 250-600ms, 200-500ms and 650-850ms post-stimulus time windows respectively (Fig. 6.8A).

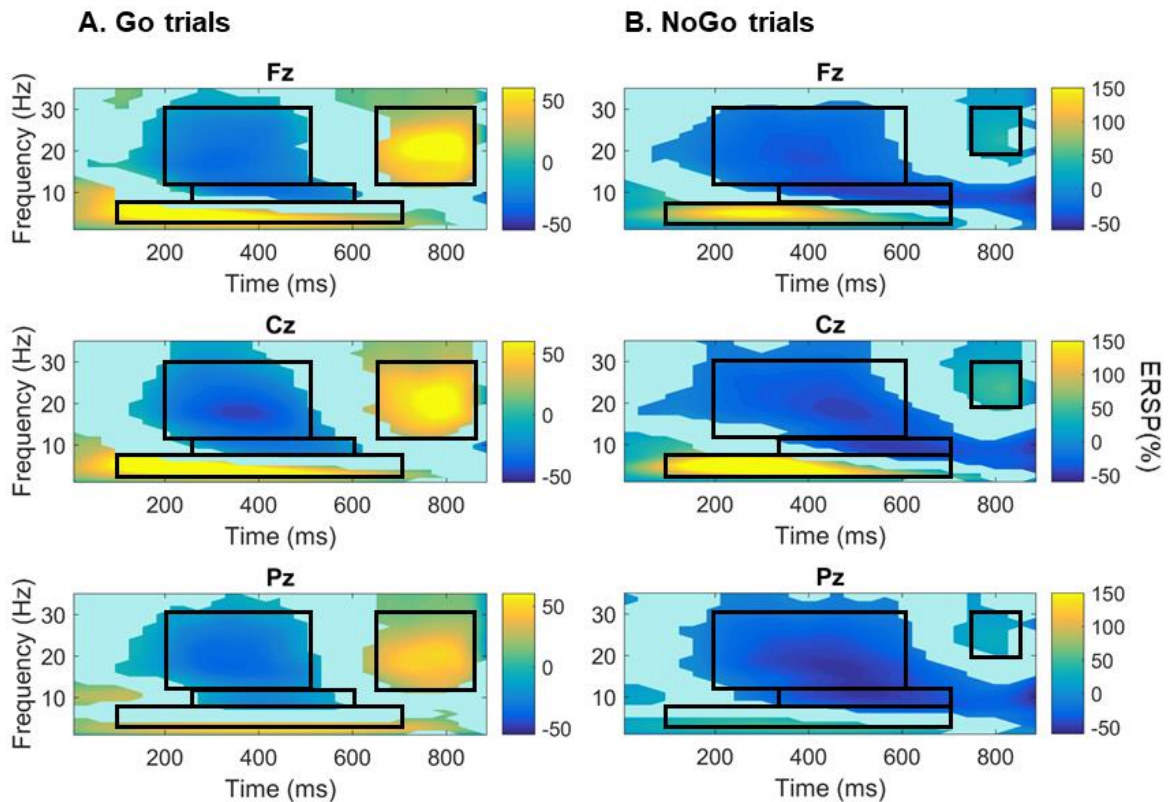


**Figure 6.8. Significant (A) Go and (B) NoGo trial related spectral perturbations in controls.** Heat maps illustrate mean ERSP values for significant (sign rank  $p_{\text{corr}} < 0.05$ , at  $q = 0.05$ ) ERSP. Regions of interest are demarcated by black boxes. Light blue areas are those of no significant spectral perturbation relative to baseline. Colour bar limits are set according to the maximum and minimum values observed for that trial type in any electrode of interest. This figure has been published in my paper McMackin et al. (In Press) (figure 1), please see appendix 6.2.

#### *NoGo trials*

Theta-band ERS, alpha-band ERD and beta-band ERD were also present across the frontoparietal axis during NoGo trials. A significant synchronization was also present in upper beta band (20-30Hz). These ERSP were examined further as windows of interest (when comparing ALS patients and controls and when performing correlation analyses) in 100-700ms, 350-700ms, 200-600ms and 750-850ms post-stimulus time windows respectively (Fig. 6.8B).

#### *The difference between NoGo and Go trials*

NoGo trials differed from Go trials by greater theta band ERS over Fz and Cz, greater alpha ERD (i.e. greater event-related reduction in oscillatory power in NoGo trials relative to Go trials) and reduced slow beta (13-22Hz) ERS (i.e. less event-related increase in oscillatory power in NoGo trials relative to Go trials) in all three electrodes.

These ERSP differences in the control group were in the 150-450ms, 500-900ms and 600-850ms post-stimulus time windows respectively (Fig. 6.9), and were defined as additional windows of interest (for comparing ALS patients against controls and when performing correlation analyses).

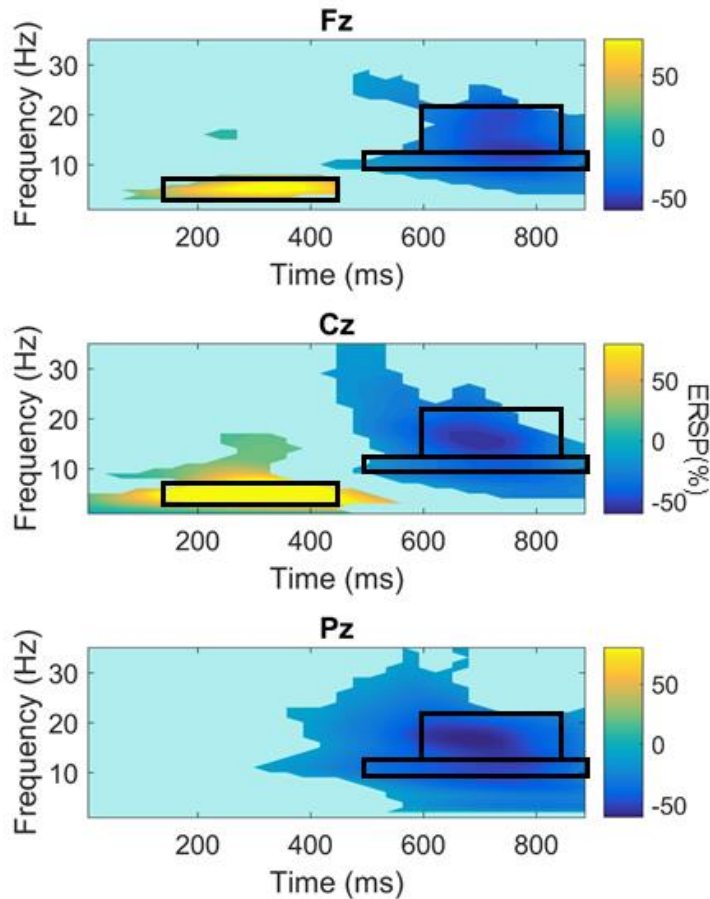


**Figure 6.9. Significant differences between NoGo and Go trial related spectral perturbations in controls.** Heat maps illustrate mean ERSP NoGo-Go values for significant (sign rank  $p_{\text{corr}} < 0.05$ , at  $q = 0.05$ ) trial differences in ERSP. Regions of interest are demarcated by black boxes. Colour bar limits are set according to the maximum and minimum values observed for that trial type in any electrode of interest. This figure has been published in my paper McMackin et al. (In Press) (figure 2), please see appendix 6.2.

#### 6.2.3.3. Event Related Spectral Perturbations in ALS compared to controls

Analysis of the entire time-frequency plane identified significantly reduced beta-band ERD in Fz and Pz during Go and NoGo trials in ALS compared to controls (AUROC values illustrated in Fig. 6.10, effect sizes and AUROC values listed in table 6.3). These findings are in keeping with the findings of ANOVA, which identified significant group effect (across electrodes) on beta-band power in this window ( $p$  values listed in table 6.3). This ANOVA also identified significant reduction in Go trial beta ERS (650-850ms,  $p=7.72 \times 10^{-4}$ ) across electrodes, which was predominantly accounted for by Fz, the only

individual electrode to show significant difference between groups at post hoc testing (Tukey's  $p=0.048$ ). No significant differences between patients and controls were found for the difference between NoGo and Go trial ERSP.

**Table 6.3. Summary of statistics for significant changes in SART-associated ERD/ERS in ALS patients compared to controls.** ANOVA group effect  $p$  values are the effect of group on this windows of interest for this trial type, across electrodes. Difference between ALS and controls pertains to ANOVA and individual electrode analyses. Cohen's  $d$  quantifies effect size ( $>0.8$  denotes large effect size,  $>1$  denotes very large effect size), area under the receivership operating characteristic curve (AUROC) quantifies discrimination between ALS and controls by this measure ( $>0.8$  denotes very good discrimination). This table has been published in my paper McMackin et al. (In Press) (table 1), please see appendix 6.2.

Frequency range (Hz)	Trial	Time range (ms post stimulus)	Difference between ALS and controls	ANOVA group effect $p$	Electrode	AUROC	Cohen's $d$
13-30	Go	200-500	Less ERD in ALS	$5.18 \cdot 10^{-4}$	Fz	$>0.8$	0.97
					Pz	$>0.82$	0.92
	NoGo	200-600	Less ERD in ALS	$9.71 \cdot 10^{-4}$	Fz	$>0.8$	0.89
					Pz	$>0.82$	1.12

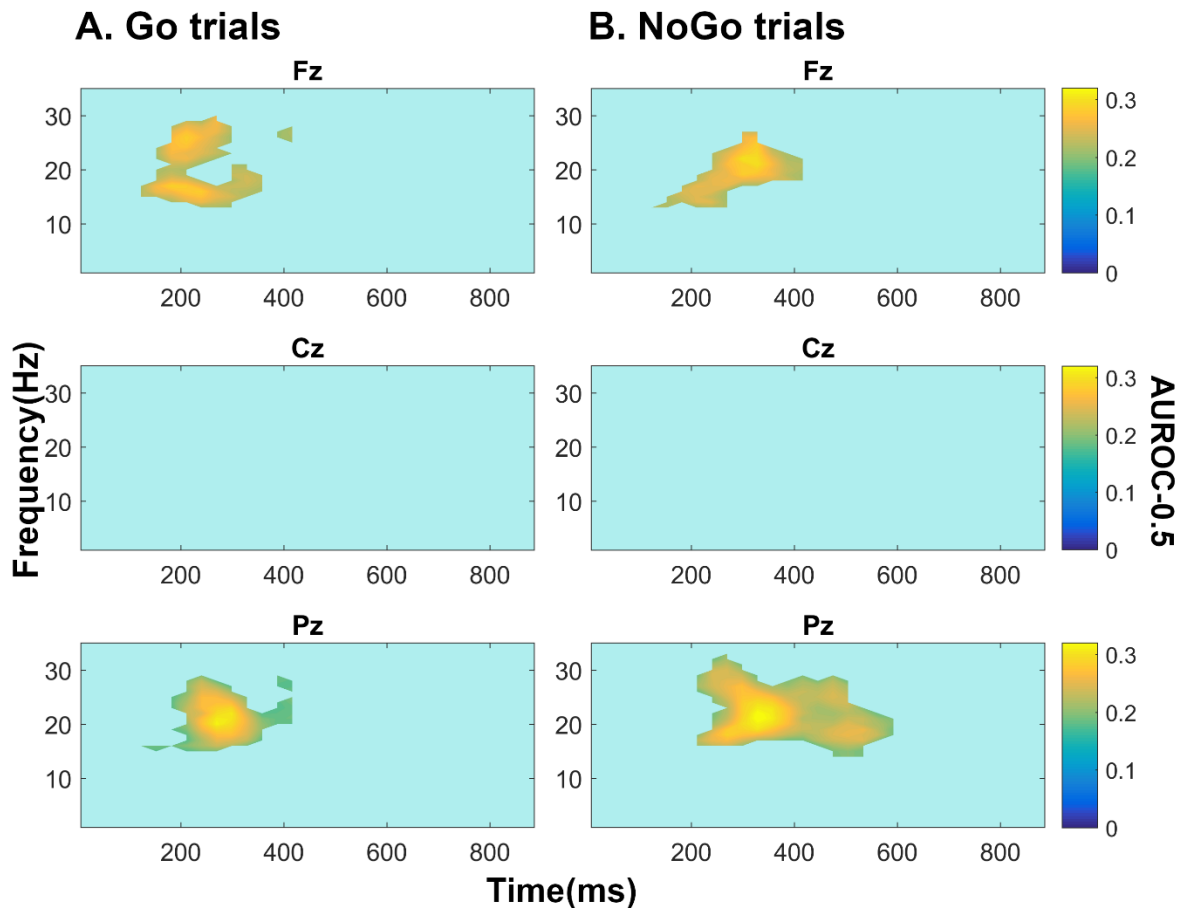


**Figure 6.10.** Area under the receiver operating characteristic curve minus 0.5 values for significant ERSP changes in ALS (versus controls) for (A) Go and (B) NoGo trials. All significant findings were of increased power (i.e. ERS) in ALS patients relative to controls. Fz and Pz power  $(1-\beta) = 0.32$  and  $0.31$  and Bayesian Posterior probability  $(P_1) = 0.92$  and  $0.88$  respectively during Go trials and power= $0.18/0.27$  and  $P_1=0.90/0.88$  respectively during NoGo trials. Non-zero values plotted are those deemed significant based on a 5% false discovery rate by testing the full time-frequency plane using empirical Bayesian inference. Colour bar illustrates area under the receivership operating characteristic curve centred around zero (i.e. AUROC-0.5). This figure has been published in my paper McMackin et al. (In Press) (figure 3), please see appendix 6.2.

#### 6.2.3.4. Correlation with task performance

Correlations between late beta-band ERS in Go (650-850ms post stimulus) and NoGo (750-850ms post stimulus) trials and task performance measures are summarised in table 6.4. Significant negative correlation was identified between response accuracy and late beta band ERS in Pz during Go trials (i.e. poorer accuracy with greater beta ERS) for controls but not patients.

Significant negative correlations between response time and beta-band late ERS in patients and the overall group (i.e. faster response time with greater beta ERS) across the electrodes of interest were present in controls alone as a trend but were not significant

following multiple comparison correction. Theta band ERS in Pz during Go trials showed significant negative correlation with response time in the total group ( $p=0.010$ ,  $\rho=-0.34$ ) with similar trends when patients and controls were considered separately (patients:  $p=0.055$ ,  $\rho=-0.39$ , controls:  $p=0.052$ ,  $\rho=-0.34$ ). Patient, but not control, response times also negatively correlated with Cz alpha band ERSP in NoGo trials (i.e. greater alpha ERD was associated slower response times,  $p=0.013$ ,  $\rho=-0.5$ ). Patient ECAS ALS-specific score was correlated with beta ERS (750-850ms post stimulus,  $p=0.0024$ ,  $\rho=0.72$ ) over Cz during NoGo trials (i.e. greater executive performance with greater beta ERS, Fig. 6.11). No significant correlations were identified for other regions of interest, disease duration or ALSFRS-R or CWIT scores.

**Table 6.4. Significant correlations between beta-band (13-30Hz) ERS (%) and SART performance measures.** Negative rho values reflect less ERS with larger behavioural measure value (longer reaction time or greater accuracy). Go trials time window - 650-850ms post stimulus, NoGo trials time window - 750-850ms post stimulus. Uncorrected p-values (p) remained significant when corrected at FDR  $q = 0.05$ . This table has been published in my paper McMackin et al. (In Press) (table 2), please see appendix 6.2.

EEG trial	Channel	Behavioural measure	Participant	p	Rho
Go	Fz	Response time	All	$1.18 \times 10^{-4}$	-0.49
			Patient	$1.12 \times 10^{-4}$	-0.72
	Cz		All	$9.22 \times 10^{-6}$	-0.56
			Patient	$6.19 \times 10^{-5}$	-0.74
	Pz		All	$9.30 \times 10^{-4}$	-0.43
			Patient	$9.97 \times 10^{-5}$	-0.72
	Total accuracy (%)	Control	0.011	-0.44	
NoGo accuracy (%)			0.008	-0.45	
NoGo	Cz	Response time	All	0.0036	-0.38
			Patient	0.0052	-0.56

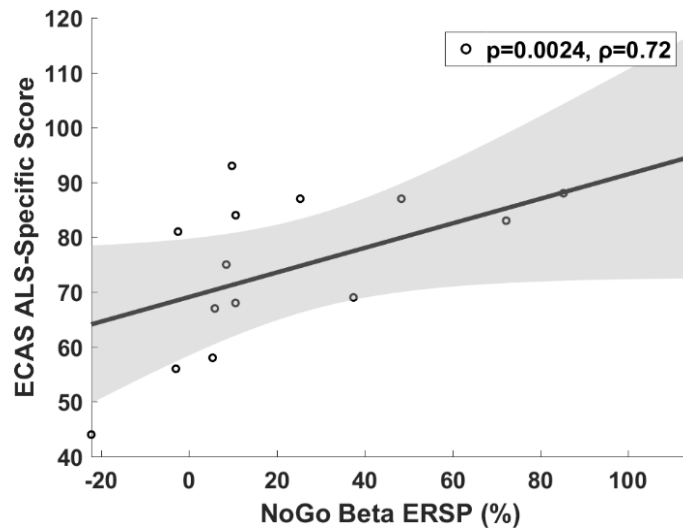


**Figure 6.11. Correlations between ECAS ALS-specific score and ERS over Cz in beta band 750-850ms post stimulus during NoGo trials.** P-value (uncorrected) and rho ( $\rho$ ) pertains to non-parametric Spearman’s correlation test and was significant at FDR  $q = 0.05$ . This figure has been published in my paper McMackin et al. (In Press) (figure 4), please see appendix 6.2.

#### 6.2.4. Discussion

We have characterized SART-evoked cortical oscillation changes at sensor level along the frontoparietal axis and have correlated these with task performance. These oscillations relate to the speed and accuracy with which a participant performs the task, and are disrupted in ALS patients.

##### 6.2.4.1. SART related spectral perturbations in controls

Beginning at approximately 150ms post-stimulus, alpha and beta band ERD were observed during both Go and NoGo trials across the frontoparietal axis, in addition to theta band ERS over the frontal lobe (in Fz and Cz), which was greater during correct response withholding. Beta ERD was followed by ERS, which was significantly reduced during correct response withholding.

##### *Beta oscillations (13-30Hz)*

Motor tasks evoke well-characterized movement-related beta desynchronization ( $\beta$ MRD), beginning in the second before movement onset and peaking during movement performance, followed by movement-related synchronization ( $\beta$ MRS) during movement termination<sup>632,633</sup>.  $\beta$ MRD is associated with motor planning and execution, while  $\beta$ MRS reflects inhibition of the motor networks to terminate the motor program<sup>634</sup>. Like SART-related beta ERS observed here,  $\beta$ MRS is maximal in Cz and larger in Go trials than NoGo trials, and reaches significance at approximately 800ms post-stimulus<sup>634</sup>. Similar



to the SART, a Go/NoGo task not designed to test sustained attention is also found to elicit beta ERD/ERS during Go and NoGo trials, with Go trial ERS inversely correlating with response time<sup>635</sup>. These similarities indicate that the SART captures this measure of motor cortical activation and inactivation in addition to those of attention and response control.

#### *Alpha oscillations (8-12Hz)*

Alpha ERD/ERS did not correlate with control task performance in this study, such that the ability to determine the role of this ERD in SART performance is limited. Alpha ERD is associated with thalamocortical network excitation<sup>578</sup> and release of the task-engaged cortical regions from inhibition<sup>636</sup>. This measure has been captured during a number of other attention and memory tasks, and is considered to reflect retrieval of task-relevant information from one's "knowledge system"<sup>636,637</sup>.

Peri-movement alpha ERD is also observed in Go/NoGo tasks not designed to test attention or memory, and represents a general disinhibition of the motor networks to facilitate movement. In keeping with our observations, this movement-related alpha band ERD ( $\alpha$ MRD) generally persists for longer than  $\beta$ MRD and does not typically rebound to synchronization<sup>638</sup>. However,  $\alpha$ MRD is not found to be greater during NoGo trials of these tasks<sup>635,638,639</sup>, as we observed here, while cognitive alpha ERD increases with task complexity. Therefore, this alpha change may not be a purely motor cortical phenomenon and requires further characterization by larger, source level studies to differentiate potential cognitive and motor underpinnings.

#### *Theta oscillations (4-7Hz)*

Theta band ERS showed significant correlation with SART response time in the overall group, with similar trends within the individual groups that were probably underpowered to detect this effect in each single group. An n-back task study, which also identified frontocentral-predominant theta ERS peaking approximately 250ms after stimulus delivery, demonstrated association of this ERS with attention allocation, rather than working memory<sup>640</sup>. Further, frontal midline theta, a focal increase in theta power induced by numerous cognitive tasks and localized to the dorsal anterior cingulate and medial prefrontal cortex<sup>641</sup>, reflects attentional processing<sup>642</sup>. This is consistent with the presence of theta ERS for all trial types, with greater magnitude during NoGo trials.

#### *6.2.4.2. Increasing SART specificity and understanding the speed-accuracy trade-off*

Utility of the SART as a test of sustained attention has been criticized due to the extent of performance variation within healthy populations, which has been attributed to the speed-accuracy trade-off<sup>643</sup>. Task performance requires sufficient working memory, attention, response inhibition and motor control, among other functions. Therefore, differences in performance measures such as response time and accuracy may reflect normal or abnormal differences in an array of cortical functions. However, this lack of specificity is advantageous when EEG is recorded simultaneously, as a battery of measures which individually interrogate each of these functions, differentiated by their spatial, temporal and frequency characteristics, can be measured from a single paradigm. We have previously demonstrated how time-domain analysis of SART-EEG provides individual measures of response control and attention, facilitating identification of specific cognitive and motor functions affected in ALS<sup>478</sup>. Here we have extracted non-phase locked cortical oscillatory changes across time and frequency domains, capturing additional measures of specific network activity and communication that were lost through averaging in our previous analysis and which are not frequency-domain reflections of event related potentials. We have demonstrated that individuals who prioritize speed over accuracy display greater beta ERS during Go trials, potentially reflecting greater post-movement motor cortical inhibition in these individuals. While the causative relationship between this measure of motor cortical deactivation and task approach warrants further investigation, the specificity of this correlation to this WOI within the time-frequency plane facilitates separation of this variation in speed-accuracy trade-off observed in healthy cohorts<sup>643</sup> from other, pathological, changes in cortical networking captured at other times and frequencies, such as those we have identified in ALS.

#### *6.2.4.3. Dysfunctional network communication in ALS during the SART*

ALS patients showed significant reduction in frontal and parietal beta ERD.  $\beta$ MRD elicited by motor preparation-specific paradigms<sup>128</sup> has previously been shown to be reduced in ALS. This has been proposed to reflect upper motor neuron degeneration, although motor function of the upper extremities does not correlate with  $\beta$ MRD<sup>346,596</sup>. SART-elicited beta ERD similarly did not correlate with task performance, in alignment with the lack of difference in task response time or accuracy between patients and

controls. The lack of significant change in Cz beta ERD in ALS patients observed here also indicates measurement of broader motor network dysfunction beyond the precentral gyrus, such as in the premotor, supplementary motor and posterior parietal cortices. Therefore, while the similarity of this ERD to  $\beta$ MRD suggests that they are of similar (or the same) motor physiological basis, source localisation is required to clarify the specific generators of these oscillations.

Regardless of its physiological origin, the large effect size (Cohen's  $d=1.12$ ) and good discrimination ( $AUC=0.82$ ) of ALS patients from controls by beta ERD highlights the need for further exploration of this promising measure as a biomarker of ALS and ALS subphenotypes. Further, as the symptoms of neurodegenerative diseases such as ALS can limit the duration of data collection sessions, the ability of SART to simultaneously elicit a number of distinct measures of motor, motor preparatory and executive function could maximise the efficiency with which cognitive and motor networks are interrogated in both research and clinical settings.

As a group, ALS patients also showed reduced Go trial beta ERS, predominantly over the prefrontal cortex. While the correlation between Go trial beta ERS and poorer response accuracy observed in controls was absent, strong correlations were observed between NoGo trial beta ERS over the motor cortex and executive performance in patients. This correlation, alongside existing literature (described above), may reflect ALS patients with sufficient executive function exerting increased prefrontal control over motor cortex activation to sustain task performance. Patient (but not control) response times were also longer in those with more central alpha ERD in NoGo trials. Together, these findings indicate that sustained performance in patients is achieved through balancing pathological dysfunction with compensatory engagement in cognitive and motor networks. These findings exemplify the utility of EEG in capturing cortical network (dys)function in disease with greater sensitivity and source specificity than task performance measures, which do not emerge until cognitive reserve and alternative neural networks can no longer compensate<sup>644</sup>. However, larger dataset collection is now required to perform comparisons of these measures between clinical, genetic and disease stage ALS subcohorts and facilitate further interrogation of the relationship between this cortical pathophysiology and cognitive and motor symptom severity with higher statistical power.

Further, the pathological or compensatory roles of ERSP in ALS require further elucidation through longitudinal and source level analyses.

#### *6.2.4.4. Limitations*

This analysis focussed on three electrodes of interest across the frontoparietal axis in order to simultaneously investigate previously unexamined SART-associated cortical oscillations and perform preliminary screening for potential ALS biomarkers. Spatial resolution of these findings is poor. Therefore, while they capture the activity of important generators of SART response across primary motor, pre-motor and supplementary motor areas (in the motor domain) and prefrontal and parietal generators (in the cognitive domain), our ability to attribute different ERSP to specific cortical regions is limited. Source-localised analysis will be needed in a future study to elucidate the sources of abnormalities in cognitive oscillations across the cortex, informed by a dense electrode montage, and potentially increase the discriminative ability of these measures in detecting ALS. Expansion of the datasets shall facilitate further interrogation of the relationships between these measures of cortical pathophysiology and disease stage, rate of progression and symptom severity.

#### *6.2.4.5. Conclusion*

Our data demonstrate that time-frequency analysis of EEG during SART, in addition to event related potential analysis, provide measures of cognitive and motor network function that may not be captured by behavioural performance or by other neuropsychological testing. These measures help to dissect the summated complex interactions within and between the cortical networks which regulate task performance, including speed-accuracy trade-off strategy and compensation for pathology. Moreover, we demonstrate that cortical oscillation abnormalities not captured by task performance measures have large effect sizes and show good discrimination between ALS patients and controls. Such discrete measurements may provide informative, sensitive biomarkers of disease-related network dysfunction and warrant further investigation.

## 7. Results: Transcranial Magnetic Stimulation

Results chapter 7 comprises the TMS aspects of this project. An analysis of the collected data has been presented in section 7.1. Section 7.2 contains an opinion piece submitted to the editor of *Clinical Neurophysiology* in October 2020.

### 7.1. Cross-sectional analysis

#### 7.1.1. Introduction

TMS has been employed as a tool by which to quantitatively measure ALS-related upper motor neuron decline in numerous previous studies. However lack of reproducibility across both single and paired pulse TMS studies of ALS has previously led to this methodology falling out of favour.

While some of this variation is likely to be due to heterogeneity in ALS motor network pathology, the use of typically employed “fixed-intensity” paired pulse TMS protocol is also known to exhibit poor reproducibility within individuals<sup>195</sup>. In order to improve paired pulse TMS reproducibility, TT-TMS (also referred to as “threshold-hunting”) protocols have been developed<sup>158</sup>. These protocols are based on reversal of the traditional assignment of input and output variables, such that stimulation intensity is varied in order to obtain a specified target MEP peak-to-peak amplitude. In these studies, a variation (i.e. between groups of individuals) or a change (e.g. prior to and following an intervention) in the state of intracortical circuits with projections on to upper motor neurons (which could be interpreted as the degree to which these circuits exert a facilitatory or inhibitory effect) is inferred by comparison of the TS intensities required to obtain the desired MEP amplitude when preceded by a CS compared to when unconditioned. Comparison of TT-TMS to fixed-intensity TMS has demonstrated that threshold tracking-elicited intracortical inhibition has excellent intraday and adequate-to-excellent interday reproducibility, while equivalent fixed intensity protocol produce poorly-to-adequately reproducible intracortical inhibition measures<sup>195</sup>.

Adoption of TT-TMS in the study of ALS has brought the application of TMS in the development of ALS biomarkers back into favour. All TT-TMS studies in ALS to date have been generated from a single laboratory investigating Australian patient cohorts. Lower SICI in ALS has repeatedly and consistently been reported from TT-TMS studies, with greater ICF in ALS being intermittently observed<sup>194,569,645</sup>. The first of these studies

reported “completely absent” SICI at ISIs  $\leq 1$ ms, with SICI with a 3ms ISI also being reported as significantly lower than in controls<sup>194</sup>. Most studies thereafter report averaged SICI measures across a 1-7ms ISI range when investigating the use of this measure as an ALS biomarker<sup>645</sup>, which showed better sensitivity and specificity balance for diagnosing ALS compared to measures at specific ISIs. An inter-session reliability analysis by this group also deemed that measurement of averaged SICI reduces variability of individual measurements<sup>646</sup>.

These findings warrant replication in another ALS population, which may be characterised by distinct genetic/environmental ALS risk factors which are known to vary geographically<sup>647</sup>. The more general aim is to determine the broader applicability of these potential biomarkers. As SICI recorded with a 1ms ISI (SICI<sub>1ms</sub>) is attributed to GABAergic tone, while SICI recorded with a 3ms ISI (SICI<sub>3ms</sub>) is attributed to GABA<sub>A</sub>ergic interneuronal inhibition, investigating averaged SICI only, without consideration of individual ISI measures could lead to valuable prognostic/subphenotype biomarkers being missed. Therefore unaveraged measures were investigated here. The effect of ALS on LICI, SIHI and LIHI have also yet to be reported in ALS using TT-TMS, such that their utility for investigating GABA<sub>B</sub>ergic interneuronal and corpus callosal pathophysiology (see section 2.1.2.2) in ALS has yet to be exploited. These measures now warrant investigation alongside SICI and ICF. Notably, some of these paired pulse measures can be evoked by the same interstimulus interval, but differ by the required conditioning stimulus location, for example LICI and LIHI both require a suprathreshold CS with a 40-50ms, but differ by CS location (the contralateral and ipsilateral motor hotspot respectively). Therefore, a focal, figure of eight coil must be used for these measures, as the large circular coil used in previous TT-TMS studies of ALS can simultaneously activate both motor cortices (and therefore both intracortical and interhemispheric networks simultaneously<sup>100</sup>) when positioned over the vertex.

Finally, all studies of SICI in ALS to date have used (typically employed) PA coil orientation (i.e. that which delivers a magnetic field across the precentral gyrus in a posterior to anterior direction, see section 2.1.2.2<sup>152</sup>), which preferentially induce motor cortical output via early (I<sub>1</sub>) waves<sup>149</sup>. However, SICI, LICI and SIHI reduce corticospinal tract output via indirect, late I waves (I<sub>2</sub> and I<sub>3</sub>-waves)<sup>165,170,184,189</sup>, which are preferentially engaged by stimulation with AP coil orientation<sup>149</sup> (i.e. that which delivers a magnetic field across the precentral gyrus in an anterior to posterior direction, see section 2.1.2.2<sup>152</sup>). Correspondingly, SICI<sub>3ms</sub> is found to be of greater magnitude when

AP coil orientation is used ( $SICI_{AP}$ ), and the extent of  $SICI_{AP-3ms}$  is found to correlate with the difference between AP and LM-induced MEP latency, a proxy measure of late I wave engagement. By contrast,  $SICI_{PA-3ms}$  is not found to correlate with the difference between PA and LM-induced MEP latency, a proxy measure of early I wave engagement. Considering this evidence that late I wave-generating inhibitory interneurons are more sensitive to stimulation with AP orientation, and that  $SICI_{AP}$  relates to the extent of late I wave engagement, it has been proposed that  $SICI_{AP}$  could provide a better measure for the detection of pathology in such intracortical motor networks, such as in ALS, compared to  $SICI_{PA}$ <sup>156</sup>.

The aim of this study was to investigate if the previously reported changes in TT-TMS measures of ICF and SICI in ALS could be replicated in a cohort from the Irish ALS population, to investigate if SIHI, LIHI and/or LICI are affected by ALS using TT-TMS, to investigate if TT-TMS measures of specific aspects of intracortical and interhemispheric motor network function show statistically significant correlations to ALS motor symptoms and progression, and to investigate if implementing AP coil orientation with TT-TMS provides greater sensitivity to/more information regarding ALS pathology.

### *7.1.2. Methods*

#### *7.1.2.1. Ethical Approval*

Ethical approval and participant written consent were obtained as described in section 4.6.

#### *7.1.2.2. Inclusion Criteria*

All participants were over 18 years of age and able to give informed written or verbal (in the presence of two witnesses) consent. Patients were diagnosed with Possible, Probable or Definite ALS in accordance with the El Escorial Revised Diagnostic Criteria.

#### *7.1.2.3. Exclusion Criteria*

Participants were prescreened during recruitment according to the 13-question TMS screening questionnaire of Rossi et al.<sup>648</sup> and excluded if any contraindications to TMS were identified or if they reported currently/in the last month using neuro-modulatory drugs which affect central nervous system neurotransmission (via GABA, glutamate, serotonin, dopamine or noradrenaline) with the exception of riluzole, prescribed for ALS (see section 7.2 for discussion on the effects of riluzole on paired pulse TMS measures,

which do not mirror those identified in ALS patients here). Prescreening was repeated and acute screening was also undertaken on the day of TMS recording in advance of formal written consenting to ensure the participant had reported any potential contraindications and to ensure the participant had slept “normally” (no more than 2 hours below average), had eaten that morning and had not taken any illicit drugs or had drunk alcohol in the 24 hours prior to recording.

#### *7.1.2.4. Demographics*

Healthy controls included neurologically normal, age-matched individuals recruited from an existing cohort of population-based controls. A total of 17 ALS patients and 24 healthy controls were recruited, following exclusion of those taking neuromodulatory medications known to influence neurotransmitters which influence the paired-pulse TMS measures of interest (i.e. baclofen, beta-blockers, SSRIs, benzodiazepines) or who did not meet the safety criteria outlined by Rossi et al., (2009).

#### *7.1.2.5. Clinical scores*

ALSFRS-R score recorded within 90 days of participation and disease duration data were acquired for each participant as described in section 4.6. In the case of two participants, last ALSFRS-R available was >90 before recording due to slow disease progression limiting clinic attendance, however, a representative mean of ALSFRS-R score recorded over 2.5/3.8 years (within which time both participants experienced a total score decrease of 2 points) was used.

#### *7.1.2.6. Experimental paradigm*

##### *Handedness*

Handedness was recorded via the Edinburgh Handedness Scale<sup>649</sup>. One ALS patient and two controls were determined to be left handed. Test stimuli of paired pulse TMS protocol were applied to the hemisphere contralateral to the muscle of the dominant hand.

##### *Electromyography*

Participants were seated upright in a sofa-style chair with wide arm rests and asked to sit with their arms in their lap or on the arm rest in such a way that was most comfortable and maintained a baseline EMG amplitude below the maximum acceptable limit (root mean squared amplitude of 10 $\mu$ V). EMG activity was recorded from left and right abductor pollicis brevis (APB) via pairs of pre-gelled electrode pads connected to clip leads (see section 4.2 for recording hardware and software details) spaced approximately 2cm apart in a belly-tendon montage (Fig. 7.1).



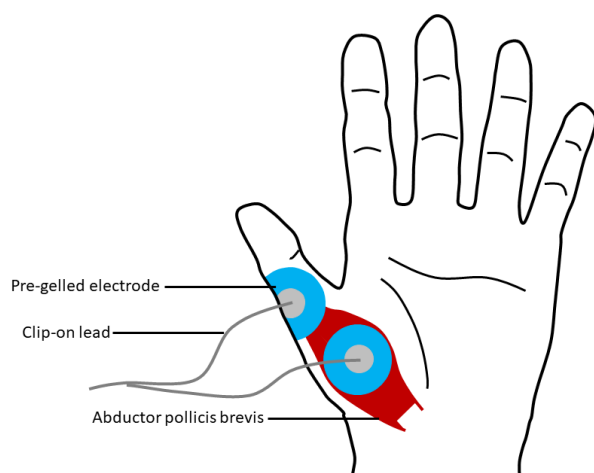


**Figure 7.1. Belly-tendon montage employed for TMS-associated EMG.**

In some early participants (3 ALS patients, 6 controls) where signals were amplified with 1000 gain, amplifier saturation was identified by the tips of the positive/negative compound muscle action potential (CMAP) peak flat-lining at  $\pm 5V$  respectively. In such cases, peaks were repaired by spline interpolation prior to maximum CMAP peak-to-peak amplitude calculation. Following identification of this issue, amplifier gain was reduced to 500 during CMAP recording to avoid amplifier saturation (at  $\pm 5V$ ). This reduction in gain was accounted for by subsequently accounting for the multiplication of all CMAP signal amplitudes by two in these individuals. The accuracy of peak-to-peak amplitude calculation following this repair method was validated using 15 CMAPs where 500 gain was applied and positive or negative peak was greater than 5mV (i.e values which would have been lost due to amplifier saturation were gain set to 1000). In these data, peak amplitude values above 5mV were artificially removed and recalculated by spline interpolation, with the resulting peak-to-peak amplitude being compared to that calculated from the true signal. Lin's concordance correlation coefficient was 0.997, demonstrating almost perfect agreement ( $>0.99$ )<sup>650</sup> between real signal and interpolation-based signal CMAP amplitude measurements.

#### *Transcranial magnetic stimulation*

Participants wore a fitted cloth cap upon which landmarks aligning with markings on the TMS coils were illustrated to maximise consistency of coil positioning. Monophasic magnetic stimuli were delivered via a DuoMag MP Dual stimulator (Deymed Diagnostics

s.r.o., Hronov, Czech Republic), equipped with 50mm mid-diameter figure-of-eight coils. The non-dominant APB “hotspot”, the optimal position of stimulation to elicit an MEP in APB of the non-dominant hand was determined first. The axis of intersection between the two loops was oriented at 90° to the sagittal to induce LM current flow across M1 of the hemisphere contralateral to the non-dominant hand. Stimulator output was gradually increased in 10 percent of maximum stimulator output (% MSO) increments 2cm anterior and 5cm lateral from the vertex, until an MEP was elicited in the target muscle, or until 70% MSO was reached. Thereafter, the coil was moved in ~1cm increments along either the anteroposterior or mediolateral axis from this point and the stimulus intensity increased or reduced until the position which elicited an MEP at lowest stimulation was identified. This coil position was illustrated on the head by drawing four reference points to which the coil must be aligned in this position on the cloth cap. Resting motor threshold (the % MSO at which 50% of stimuli elicit an MEP of 50µV) was then measured. The hotspotting procedure was then repeated over the hemisphere contralateral to the dominant hand with the axis of intersection between the two loops of the coil oriented at 45° to the sagittal plane to induce PA current flow across the motor strip of M1. Thereafter RMT and threshold hunting target (THT, the % MSO at which 50% of stimuli elicit an MEP of 200µV) were measured using a fully automated PEST protocol (see section 4.2.2.1) with PA current flow, followed by rotation of the coil by 180° to achieve AP current flow across M1 and remeasurement of the RMT and THT in the same position. Once RMT and THT values were determined, the following paired pulse protocol were delivered in random order. In order to limit the session duration to three hours, to avoid participant fatigue and discomfort, PA coil orientation was used for all paired pulse measures of interest, while AP coil orientation was only implemented for measures demonstrated to be significantly different between AP and PA applications using threshold hunting protocol<sup>156,166,472</sup>. Additionally, specific ISIs were chosen based on existing literature. Namely, four ISIs were used to investigate LICI as this measure was not previously investigated using threshold tracking in ALS and peaks at varied ISIs between individuals. A single, 10ms ISI was used to measure ICF, based on the ICF ISI which previously demonstrated maximal difference between ALS patients and controls<sup>194</sup>, as previous ICF findings are variable<sup>70,194,216,289,334,335</sup> and the physiological underpinnings of ICF remain uncertain. As SICI is established to peak at 1ms and 3ms ISIs, and these peaks are attributed to distinct aspects of motor network function, SICI was measured at 1 and 3ms ISIs. Therefore the protocol measured with a single coil using

PA orientation were:  $SICI_{PA-1ms}$ ,  $SICI_{PA-3ms}$ , LICI with 50ms, 100ms, 150ms and 200ms ISIs ( $LICI_{PA-50-200ms}$ ) and ICF with 10ms ISI ( $ICF_{10ms}$ ). The protocol measured with a single coil using AP coil orientation were:  $SICI_{AP-3ms}$ , LICI with 150ms and 200ms ISI ( $LICI_{AP-150-200ms}$ ). The protocol measured with two coils (the conditioning coil placed over the ipsilateral hemisphere motor hotspot with LM orientation and the test coil placed over the contralateral hemisphere motor hotspot) were: IHI with 10ms ISI ( $SIHI_{PA}$ ), IHI with 40ms ISI ( $LIHI_{PA}$ ) when the test coil was at PA orientation and IHI with 10ms ISI ( $SIHI_{AP}$ ) when the test coil was at AP orientation.

#### *Adaptive threshold hunting*

An adaptive threshold hunting protocol was applied to obtain all single-pulse (i.e. RMT and THT) and paired-pulse measures, using maximum likelihood protocol PEST (Awiszus and Borckardt, 2011). This procedure utilises a sigmoid-shaped logistic function to determine the stimulation intensity at which there exists a 50% probability of eliciting a MEP with the peak-to-peak amplitude that has been defined (i.e.  $50\mu V$  for RMT,  $200\mu V$  for THT and all paired pulse protocols). This function and its implementation via manual interface with the commonly used MTAT 2.0 programme are described by Prof. Friedemann Awiszus<sup>651</sup>. Here and in our previous publication<sup>652</sup>, however, we have fully automated the procedure using Signal (CED Ltd., Cambridge UK) and MATLAB (MathWorks Inc., MA, USA) scripts to reduce probability of human error (for example by misreading response amplitudes or incorrectly setting the recommended stimulation intensity), to reduce required experimenter presence and to facilitate automated baseline amplitude screening and trial rejection. The experimenter also visually monitored the EMG during data collection to identify where lower motor neuron-associated EMG abnormalities (e.g. fasciculations, fibrillations) occurred within the MEP-peak search window and not in the baseline, which could mislead the PEST algorithm. In such cases the protocol was terminated and restarted. Following collection of 4 patient and 9 control datasets, the baseline window was expanded from 50ms to 200ms to improve automated detection of these artefacts, however experimenter monitoring of signal input was maintained.

#### *Maximum compound muscle action potential*

Maximum compound muscle action potential in the dominant hand APB was determined using electrical stimulation via a Digitimer DS7A stimulator (Digitimer Ltd., Welwyn Garden City, UK) at the elbow over the median nerve. A bar electrode containing two

steel electrodes (0.8cm diameter) holding saline-soaked felt pads with a fixed distance of 3cm between the cathode and anode was used to deliver stimuli. Stimulation was initiated at 10mA and increased in 10mA increments until CMAP peak-to-peak amplitude no longer increased, followed by increase in stimulus amplitude by 20% to ensure supramaximal threshold stimulation. Maximal electrical stimulator output was 99.99mA. Participant comfort was continuously monitored between stimuli. Participation in electrical nerve stimulation was not mandatory for participation in the magnetic stimulation study. CMAP trials with a 200ms pre-stimulus baseline root mean square amplitude  $>50\mu\text{V}$  were rejected.

#### *7.1.2.7. Data analysis*

For all TMS-associated signal analyses, MEP peak to peak amplitudes were measured within the 15-50ms window following test stimulation.

#### *Mean MEP and CMAP latency*

To determine mean AP and PA-orientation associated MEP latencies, EMG data collected during AP and PA THT measurement by PEST were employed from those from whom both measures were successfully recorded. Each stimulus trial was baseline corrected using a baseline window 200ms pre-stimulus. Onset of each MEP was searched for 15-50ms post-stimulus. For CMAP data, peaks were evaluated in the 5-30ms post-stimulus signal. Onset thresholds were defined for each MEP/CMAP as the mean baseline window amplitude plus/minus two standard deviations of baseline window amplitude. Latency of the MEP/CMAP was then defined as the first time point at which signal amplitude at this time and the four following data points crossed one of these onset thresholds. Mean latency was then calculated across those trials containing MEPs with a peak to peak amplitude  $>50\mu\text{V}$  and root mean square amplitude below  $10\mu\text{V}$  in the baseline window for AP MEPs, PA MEPs and CMAPs (all EMG data recorded was saved for potential offline analyses, while EMG frames with noisy baseline data were not passed to the PEST algorithm during the TMS session).

#### *Paired pulse TMS*

Facilitation/inhibition was defined as the percentage change in test stimulator output necessary to evoke a MEP of target amplitude ( $200\mu\text{V}$ ) in the presence of the conditioning stimulus (i.e. the conditioned threshold target, CTT) compared to in its absence (i.e. the THT) as follows:

$$\text{Inhibition/Facilitation (\%)} = \left( \frac{\text{CTT} - \text{THT}}{\text{THT}} \times 100\% \right) - 100$$

with positive values indicating inhibition and negative values indicating facilitation of upper motor neurons via the network components engaged by the conditioning stimulus. As a proxy measure of the steepness of the stimulus-response curve slope, THT was compared to RMT for AP and PA coil orientation as follows:

$$\text{THT as a \% of RMT} = \left( \frac{\text{THT} - \text{RMT}}{\text{THT}} \times 100\% \right) - 100$$

This measure was compared between ALS patients and controls alongside paired pulse measures and RMT values.

#### *7.1.2.8. Statistics*

##### *Group differences*

Wilcoxon sign rank tests<sup>495</sup> were used to compare control values for each paired pulse measure to zero, to determine if significant facilitation or inhibition was identified in the control cohort. Two-tailed t-tests were used to compare paired pulse measures, MEP/CMAP latencies and mCMAP amplitude between ALS patients and controls. Mann Whitney U tests<sup>494</sup> were employed in place of t-tests where values for that measure were determined to have a non-normal distribution. Data values were deemed to have a normal distribution based on Shapiro-Wilk<sup>653</sup> testing. To account for multiple comparisons, only those p values with a positive FDR below 5% (determined by the Benjamini Hochberg method) were considered significant. These FDR were calculated across parameter families (e.g. across the 13 sign rank test p values for each paired pulse parameter and across the 17 group comparison-associated p values for each RMT, THT (as a percentage of RMT) and paired pulse parameter).

##### *Discrimination ability and effect size*

In order to quantify the ability of paired pulse TMS measures to discriminate ALS patients from controls, the AUROC was calculated for each inhibition/facilitation parameter for each ISI and coil orientation used. AUROC values were used to index how well each of these paired pulse TMS measures separated patient and control groups<sup>501</sup> where if the null hypothesis of no separation is true, AUROC equals 0.5, and values closer to 0 or 1 indicate greater separation. Effect size was measured by Cohen's d, where absolute d>0.2 indicates a small effect size, absolute d>0.5 indicates a medium effect size and absolute d>0.8 indicates a large effect size<sup>630</sup> and sign indicates direction of the effect (positive

represents larger value in ALS patients, negative represents smaller values in ALS patients).

### *Correlations*

Spearman's partial rank correlation<sup>542</sup> analysis was used to investigate the relationships of single and paired pulse TMS and CMAP measures with disease duration and ALSFRS-R score while accounting for the effect of age. To account for multiple comparisons across correlations, only those p values with a positive FDR below 5% (determined by the Benjamini Hochberg method) were considered significant. These FDR were calculated across the 17 paired pulse, RMT and THT measures, as described for group difference analysis.

### *7.1.3. Results*

#### *7.1.3.1. Data collection*

Of the 17 ALS patients and 24 healthy controls recruited only 11 ALS patients (2 female, age median [range]: 69 [41-79]) and 23 healthy controls (5 female, age median [range]: 61 [37-76] years) underwent paired-pulse TMS recording upon session attendance. This was due to the following unforeseeable factors: One control and two ALS patients were unable to contribute data as they could not relax the target muscles to below acceptable baseline EMG amplitude. Four patients could not contribute paired pulse data due to inability to achieve MEPs of 200 $\mu$ V in the dominant target muscle at maximum stimulator output, and therefore it was not possible to employ THT. Three patients and three controls were unable to contribute paired pulse data with AP coil orientation due to inability to elicit MEPs of 200 $\mu$ V in the dominant target muscle at maximum stimulator output. One patient and one control were unable to contribute interhemispheric measures due to inability to elicit MEPs of 200 $\mu$ V in the non-dominant target muscle at maximum stimulator output. Those patient and control groups who underwent paired-pulse recording were age ( $p=0.11$ ) and gender ( $\chi^2=0.58$ ,  $p=0.81$ ) matched.

Maximum CMAP data were collected in 13 ALS patients (4 female, age median [range]: 69 [41-79] years) and 17 controls (4 female, age median [range]: 59 [37-76] years). Those patient and control groups who underwent CMAP were age ( $p=0.12$ ) and gender ( $\chi^2=0.66$ ,  $p=0.20$ ) matched. One patient and one control, who contributed both paired pulse TMS and CMAP data, were determined to be left handed, the remainder of participants were right handed. These 20 controls (3 female, median [range] age: 62.5 [34-76]) and 8 ALS

patients (0 female, median [range] age: 70 [41-79] from whom AP and PA MEP latency measures were obtained were also age ( $p=0.15$ ) and gender ( $\chi^2=0.13$ ,  $p=0.25$ ) matched.

#### *7.1.3.2. Differences between ALS patients and controls*

##### *Paired pulse TMS*

Sign rank test (examining the difference between control values and zero) and group comparison p values for each inhibition/facilitation parameter measured are reported in table 7.1. Significant sign rank p values for all measures except for ICF at a 5% FDR demonstrate that significant inhibition was achieved in controls by all inhibitory protocol, while ICF was not significant. Differences from zero and differences between ALS patient and control group values are illustrated in Fig 7.2.

##### *SICI*

When PA orientation was implemented, only  $SICI_{1ms}$  was found to be of a different magnitude in ALS patients with respect to controls with less inhibition occurring in ALS. While trends towards lower  $SICI_{3ms}$  in ALS patients were observed, these differences were not found to be significant in this analysis. When an AP coil orientation was used, however,  $SICI_{3ms}$  was reliably lower in ALS compared to controls.

##### *ICF*

Intracortical facilitation was not different in ALS patients and controls.

##### *LICI*

Irrespective of coil orientation or ISI, LICI was not found to be significantly different in ALS patients compared to controls.

##### *IHI*

While trends of lower interhemispheric inhibition were observed in ALS patients were observed, most evident for SIHI with AP test coil orientation, these differences were not found to be statistically significant at a false discovery rate of 5%.

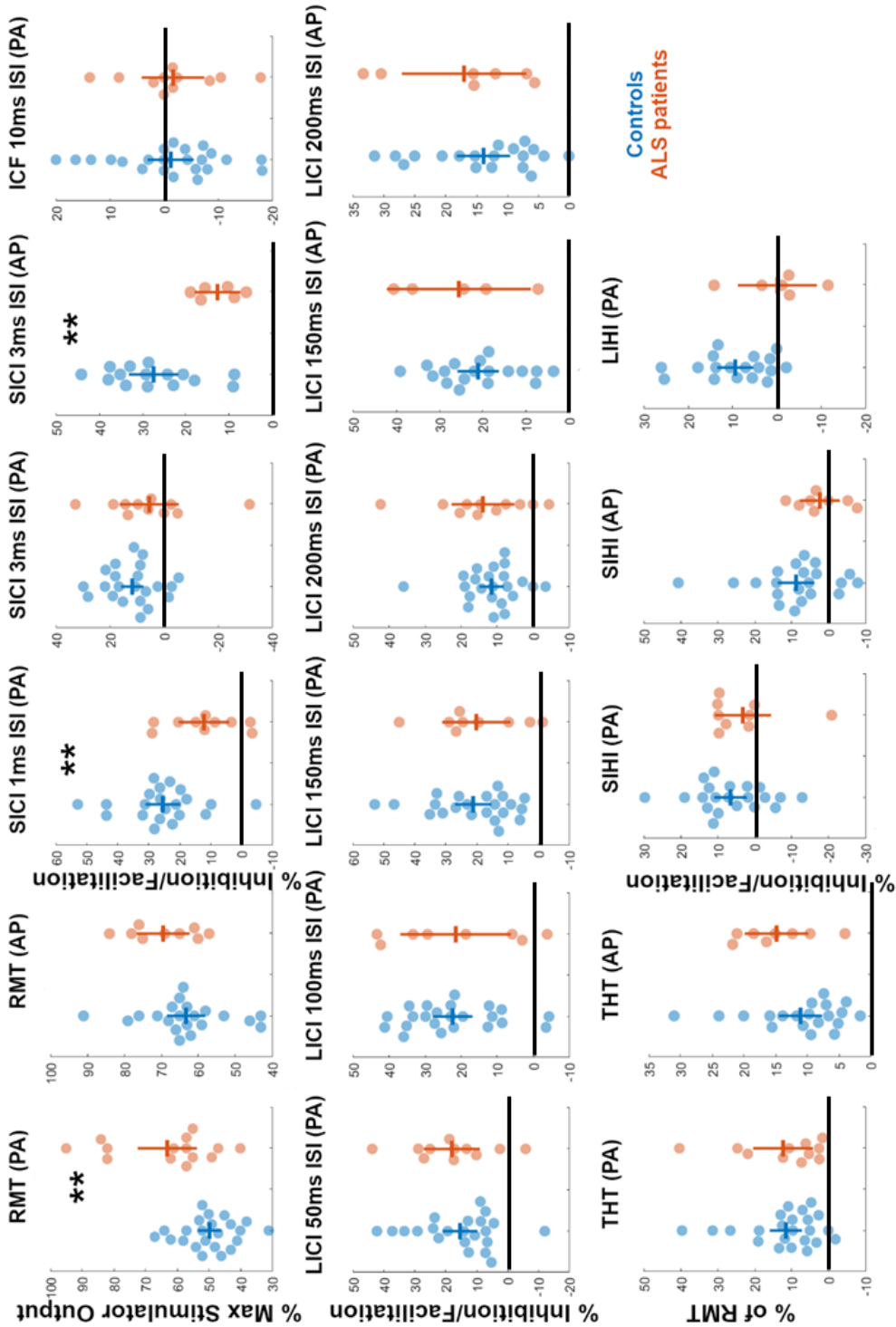


**Figure 7.2. Bee swarm plots illustrating control (blue) and ALS patient (red) TMS parameter values.** Black lines highlight zero (i.e. where no inhibition/facilitation is observed). Horizontal coloured lines denote group mean, vertical coloured lines denote 95% confidence interval of the mean. Threshold hunting target (THT) values are expressed as a percentage of resting motor threshold (RMT) values (i.e. the percentage difference in intensity required to achieve 50% of MEP peak to peak amplitudes >200uV vs percentage difference in intensity required to achieve 50% of MEP peak to peak amplitudes >50uV) PA – Posteroanterior coil test orientation used. AP – Anteroposterior test coil orientation used. \*\* -  $p_{uncorr} < 0.01$  and statistically significant at a false discovery rate of 5%.



**Table 7.1. Summary of statistics for each paired pulse inhibition/facilitation measure.** Numbers of patient and control datasets recorded are listed under Cn and Pn respectively. Numbers of patient and control datasets excluded due to CTT>100% MSO are listed under C>100 and P>100 respectively. Tests used to compare controls and ALS patients (MWU – Mann Whitney-U, TT – two tailed t-test) are listed under “ALS vs. control test”. All p values are listed are uncorrected. Those coefficient values with corrected p values (at 5% false discovery rate) < 0.05 are emboldened. Ori – Orientation AUROC – Area under the receivership operating characteristic curve, ISI – Interstimulus interval. PA – Posteroanterior. AP – Anteroposterior, ppTMS – Paired pulse TMS measure.

pp TMS	Test coil ori	ISI	C n	C >100	P n	P >100	AU ROC	Cohen's d	Sign rank p value	ALS vs. control test	ALS vs. control p value
SICI	PA	1ms	21	2	10	1	0.77	-1.10	<b>6.88*</b> <b>10<sup>-5</sup></b>	TT	<b>0.0077</b>
		3ms	22	1	11	0	0.63	-0.52	<b>1.19*</b> <b>10<sup>-4</sup></b>	TT	0.17
	AP	3ms	15	4	6	1	0.89	-1.60	<b>6.10*</b> <b>10<sup>-5</sup></b>	TT	<b>0.0036</b>
ICF	PA	10ms	23	0	11	0	0.51	-0.047	0.48	TT	0.90
LICI	PA	50ms	22	1	11	0	0.58	0.20	<b>1.55*</b> <b>10<sup>-4</sup></b>	TT	0.58
		100ms	23	0	8	2	0.51	0.059	<b>4.02*</b> <b>10<sup>-5</sup></b>	TT	0.89
		150ms	22	1	9	2	0.52	-0.075	<b>4.01*</b> <b>10<sup>-5</sup></b>	TT	0.85
		200ms	23	0	11	0	0.55	0.24	<b>5.27*</b> <b>10<sup>-5</sup></b>	TT	0.51
	AP	150ms	18	2	5	2	0.61	0.43	<b>1.96*</b> <b>10<sup>-4</sup></b>	TT	0.41
		200ms	19	0	7	0	0.59	0.33	<b>1.96*</b> <b>10<sup>-4</sup></b>	TT	0.46
IHI	PA	10ms	21	0	8	1	0.7	-0.65	<b>0.0012</b>	TT	0.13
		40ms	21	0	9	1	0.61	-0.34	<b>0.0095</b>	MWU	0.35
	AP	10ms	18	0	6	0	0.81	-1.15	<b>5.99*</b> <b>10<sup>-4</sup></b>	TT	0.024

*Single pulse TMS and peripheral nerve stimulation*

Single pulse associated MEP- and CMAP- associated statistics are summarised in table 7.2. Recorded values are illustrated in Fig. 7.3. RMT (Fig 7.2) was greater in ALS patients

where PA coil orientation was applied (Cohen's  $d=1.12$ ,  $t$ -test  $p=0.0023$ ), but not where AP coil orientation was applied (Cohen's  $d=0.58$ ,  $t$ -test  $p=0.16$ ).

*MEP and CMAP latency*

Patients showed significantly shorter MEP latency compared to controls when AP but not PA coil orientation was used. No significant difference in CMAP latency was observed between ALS patients and controls.

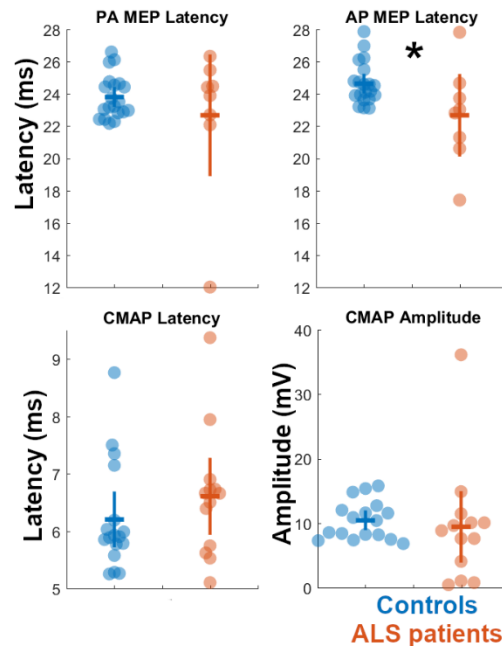


**Figure 7.3. Bee swarm plots illustrating control (blue) and ALS patient (red) MEP and CMAP latency and CMAP amplitude values.** Horizontal coloured lines denote group mean, vertical coloured lines denote 95% confidence interval of the mean. \* -  $p_{\text{uncorr}} < 0.05$  and statistically significant at a false discovery rate of 5%. PA – Posteroanterior coil orientation used. AP – Anteroposterior coil orientation used. MEP – Motor evoked potential. CMAP – Compound muscle action potential.

**Table 7.2. Summary statistics for compound muscle action potential and single pulse TMS-associated motor evoked potential data.** All measures were recorded in dominant hand abductor pollicis brevis. Numbers of patient and control datasets recorded are listed under Cn and Pn respectively. Mann Whitney U-associated p values are listed under ‘p’ as Shapiro-Wilks testing rejected the hypothesis of normality for all measures. PA – Posteroanterior. AP – Anteroposterior. MEP – Motor evoked potential. CMAP – Compound muscle action potential.

Parameter	Summary value	TMS coil orientation	Cn	Pn	Control mean	Patient mean	p
MEP	Mean latency	PA	20	8	23.81 ms	22.67 ms	0.94
		AP	20	8	24.64 ms	22.67 ms	<b>0.031</b>
CMAP	Maximum amplitude	N/A	17	13	10.43 mV	9.42 mV	0.24
	Mean latency	N/A	17	13	6.20 ms	6.60 ms	0.32

### 7.1.3.3. Clinical correlations

No correlation associated p values were deemed significant at a FDR of 5%. However a number of strong ( $\rho > 0.6$ ) and very strong ( $\rho > 0.7$ ) trends ( $p_{\text{uncorr}} < 0.05$ ,  $p_{\text{corr}} > 0.05$ ) were identified. Namely, ALSFRS-R score negatively correlated with  $\text{RMT}_{\text{PA}}$  ( $p = 0.033$ ,  $\rho = -0.67$ ) and positively correlated with  $\text{LICI}_{150\text{PA}}$  ( $p = 0.040$ ,  $\rho = 0.89$ ), SIHI ( $p = 0.035$ ,  $\rho = 0.90$ ) and LIHI ( $p = 0.049$ ,  $\rho = 0.81$ ). Further, disease duration negatively correlated with  $\text{LICI}_{150\text{PA}}$  ( $p = 0.049$ ,  $\rho = -0.63$ ).

### 7.1.4. Discussion

Due to the COVID-19 pandemic, data collection to date has been limited and therefore some group differences and correlations deemed non-significant at a 5% FDR in this analysis may be underpowered to detect truly significant differences. As addressed in section 7.2, a variety of unforeseen and previously unreported challenges in the recording of paired pulse TMS in ALS patients were encountered, further limiting the patient cohort suitable for this research study. Additional data collection is required before definitive conclusion are drawn and published, to ensure the heterogeneity of ALS patients is captured in these analyses. However, these preliminary results have provided important findings about ALS effects of large size on motor network function, demonstrated replicability of previous  $\text{SICI}_{\text{PA}}$ -based findings in ALS and highlighted additional TMS measures which capture ALS pathology and relate to motor decline. Further, strong/very strong correlations identified here highlight measures which warrant further examination upon expansion of the dataset in order to draw more definitive conclusions regarding ALS pathophysiology and to determine their utility as prognostic biomarkers.

### *Replication of previously reported findings in ALS*

This study confirms the previously reported findings of reduction in  $SICI_{PA}$ , particularly  $SICI_{PA-1ms}$ . While a trend of decrease in  $SICI_{PA-3ms}$  was observed, this was not deemed statistically significant in this analysis, likely due to insufficient statistical power resulting from recruitment limitations. By contrast, ICF was not found to differ between ALS patients and controls. Although a facilitatory effect of this paired pulse paradigm in controls is indicated by mean control group values, ICF values were not deemed statistically significant. Therefore,  $ICF_{10ms}$  appears to be of low effect size, among healthy individuals. This may explain previous inconsistent findings of ALS-related change in  $ICF^{194,645}$ . As ICF is an inconsistent phenomenon, is established to be confounded by SICI, and has uncertain physiological underpinnings<sup>177,654</sup>, this measure is unlikely to provide clear and consistent insights into ALS pathology or robust biomarkers of the disease.

Previous studies of  $RMT_{PA}$  in ALS have reported lower values in ALS in some cases<sup>288,289</sup> and higher values in ALS in others<sup>328,329</sup>. As RMT is influenced by both upper and lower motor neuron degeneration, it is an imprecise measure of underpinning pathophysiology. However, as no significant difference in CMAP was identified between the groups studied here, the greater  $RMT_{PA}$  we have observed in ALS is likely to reflect UMN deterioration not yet evident in those cells preferentially engaged by AP coil orientation (as  $RMT_{AP}$  was not significantly different). As RMT is considered to be lower in early ALS pathology due to UMN disinhibition<sup>288,289</sup>, and is shown to increase longitudinally in ALS<sup>328</sup>, likely due to declining corticospinal tract function, heterogeneity among studies may reflect variation in disease progression between study cohorts. This is supported by the strong negative correlation between  $RMT_{PA}$  and ALSFRS-R score (i.e. those with greater motor impairment had a higher  $RMT_{PA}$ ). While this correlation was not deemed significant in this dataset, potentially due to the limited cohort size, it aligns with previously findings of increase in RMT with ALS progression<sup>328,329</sup>.

### *Long intracortical inhibition*

This study is the first to employ the more reproducible TT-TMS methodology to measure the effect of ALS on LICI. Irrespective of coil orientation or ISI, no significant effect of ALS on LICI was observed. This finding indicates that LICI, and therefore its underpinning  $GABA_B$ ergic interneuronal networks, are not consistently affected early in ALS, or that such an effect is of very low effect size. However, this finding does not dismiss the value of future investigation of LICI in ALS, for example, for investigation

of network disruption-based subphenotypes. Further, the strong negative correlation between  $LICI_{PA150}$  and disease duration and very strong positive correlation between  $LICI_{PA150}$  and ALSFRS-R also indicate that LICI (and its generating  $GABA_B$ ergic networks) may be affected later in ALS progression. This correlation and the relationship between LICI and other disease characteristics require further examination upon expansion of the dataset, where sufficient statistical power can be achieved.

#### *Interhemispheric inhibition*

While no statistically significant group effect on IHI was identified in this analysis, effect size measures, particularly in the case of  $SIHI_{AP}$  (Cohen's  $d=-1.15$ ) suggest that the trend of lower IHI in ALS may be deemed statistically significant when measured in a larger cohort. Further, the very strong positive correlation between long and short  $IHI_{PA}$  and ALSFRS-R score indicates that progressive corpus callosum malfunction relates to disease progression, and that such measures of corpus callosum function warrant further investigation as prognostic biomarkers of ALS.

#### *The value of anteroposterior coil orientation for capturing ALS pathology*

Most TMS studies apply stimulation with PA coil orientation as it evokes a response at lower stimulation intensities than when LM or AP orientation is used. Use of PA orientation is accordingly recommended for diagnostic TMS applications<sup>153</sup>. Epidural studies of the descending volleys in the spinal cord from the motor cortex have, however, demonstrated that these different orientations preferentially engage different aspects of motor cortical networks. Namely, lateromedial stimulation preferentially elicits the D-wave, the earliest component of these volleys, which correspond to direct depolarisation of the upper motor neurons' initial segment. By contrast, PA stimulation preferentially engages the first 'indirect'  $I_1$ -wave following the D-wave, attributed to engagement of axons of more superficial facilitatory cells which monosynaptically engage the upper motor neurons. Finally, AP stimulation preferentially engages the later indirect  $I_2$ - and  $I_3$ -waves. These waves have been attributed to engagement of axons which depolarise excitatory interneurons, which synapse both with the upper motor neurons and  $GABA_A$ ergic interneurons<sup>150</sup>.

This differential engagement of D- and early and late I-waves is reflected in the difference in latency of MEPs evoked by these orientations, with LM orientation evoking MEPs at shorter latency than PA orientation, which in turn evokes MEPs earlier than AP orientation. On this basis, PA minus LM and AP minus LM MEP latency values have

been used as proxy measures of early and late I wave engagement respectively<sup>156</sup>. In this study, while LM latency measures were not recorded, we have demonstrated that AP-induced MEP latency is significantly lower in ALS, while PA-induced MEP latency is not significantly different. This may reflect impaired late I wave recruitment in ALS, however analysis of measures specifically designed to investigate I wave recruitment in ALS is required going forward to address this hypothesis.

Greater latency of AP-induced MEPs has previously been found to correlate with greater  $SICI_{AP-3ms}$ . In this study ALS was found to have a much larger effect on  $SICI_{AP-3ms}$  (Cohen's  $d=-1.60$ ) than  $SICI_{PA-3ms}$  (Cohen's  $d=-0.52$ ), to the extent that at this preliminary cohort size, a significant difference in this measure was detected by  $SICI_{3ms}$  only when AP orientation was applied. SIHI is also established to inhibit late I-waves<sup>184,189</sup> and to be greater with AP test stimulation compared to PA stimulation<sup>472</sup>. Alongside SICI, SIHI was found to be lower in ALS with greater effect size using AP stimulation (Cohen's  $d=-1.15$ ) compared to PA stimulation (Cohen's  $d=-0.65$ ). These findings support the inclusion of AP stimulation protocol in further studies of ALS pathology, particularly small studies, as well in the newly proposed application of TMS in providing supportive evidence of ALS diagnosis<sup>72</sup>, as this orientation can provide greater sensitivity to ALS. It is, however, important to note that as AP stimulation typically requires higher intensity to evoke MEPs than for PA orientation, AP stimulation may not be possible for some ALS patients who exhibit high  $RMT_{PA}$  due to muscle wasting/cortical inexcitability.

#### *7.1.4.1. Conclusion*

These preliminary results have provided important findings about ALS effects of large size on motor network function and demonstrated replicability of previously reported effects of ALS on SICI, but not ICF. Additionally, this preliminary analysis has revealed that the effect of ALS on the GABA<sub>B</sub>ergic network function captured by LICI, if any, is of low power, or occurs later in disease progression. Further, impaired function of callosal inhibitory motor fibres, captured by IHI, may relate to motor decline in ALS and warrants further investigation to determine its prognostic and diagnostic utility. Finally, these data support the use of AP coil orientation for generating diagnostic supportive evidence and for providing additional and more sensitive insights into ALS motor network pathology than those measured with typically applied PA test coil orientation.

## **7.2. Opinion piece: Factors that limit the application of transcranial magnetic stimulation in amyotrophic lateral sclerosis patients**

TMS has been identified as a potentially useful method for the objective identification of upper motor neuron dysfunction in ALS. It has been reported that paired-pulse measures of upper motor neuron disinhibition and hyperexcitability, such as SICI and ICF - recorded using threshold-tracking TMS, offer particular promise in the diagnosis of ALS<sup>71</sup>. The use of threshold-tracking methods is viewed as being critical, as it provides more robust and reliable measurements than traditional assessments of variations in MEP amplitude<sup>195</sup>.

We have attempted to replicate recent empirical findings in an independent population of well-characterized ALS patients. In our pursuit of accurate, reliable measurements, we were confronted by numerous practical challenges, such that no data or only limited data could be acquired from 12 of 19 ALS patient volunteers (table 7.3). Although one might suppose that specific challenges could be circumvented through further refinement of data collection protocols, our experience illustrates that in the context of ALS, the widespread clinical deployment of paired-pulse TMS is not yet feasible.

Specifically, while in some cases it has been reported that ALS patients (i.e. as a group) have lower motor thresholds than controls<sup>71</sup>, many individuals in our cohort presented with wasting of the target muscles (abductor pollicis brevis) to the extent that MEPs of 50 $\mu$ V peak-to-peak amplitude could not be obtained. This precluded the designation of a RMT, even at maximum stimulator output (using a DuoMAG MP-Dual stimulator (Deymed Diagnostic s.r.o., Hronov, Czech Republic)). In other instances, extremely high TMS intensities were required to elicit MEPs of an amplitude sufficient to record a RMT (50 $\mu$ V) or permit threshold tracking (200 $\mu$ V). While this phenomenon may be clinically informative, it precludes the recording of paired-pulse measures of interhemispheric and intracortical inhibition or facilitation. This can be due either to failure to elicit an unconditioned MEP of sufficient amplitude, or an inability to deliver conditioning stimuli of sufficient intensity to generate the paired-pulse effect under consideration. In the case of threshold-tracking, if the unconditioned MEP is obtained using an intensity close to the maximum output of the stimulator, the addition of an inhibitory conditioning stimulus may lead to responses that cannot be restored to the designated threshold, even by applying the largest available magnetic field. These issues are most prominent when using

a coil orientation that induces AP current flow, due to the higher threshold stimulation intensities required to evoke target MEP amplitudes compared to PA current flow<sup>166,652</sup>. We also encountered high levels of background EMG activity “at rest” in some ALS patients, associated with symptoms of stiffness, cramping or other discomforts<sup>11</sup>. In spite of postural support, and extensive efforts to ensure the comfort and relaxation of the patients, background EMG levels were of higher amplitude than those obtained for control participants. This was reflected in a significantly greater number of rejected trials due to excessive prestimulus EMG amplitude (root mean squared  $>10\mu\text{V}$ ) in ALS patients compared to controls, even during successful RMT measurement (mean number of rejected trials in ALS patient=4, in controls=0.52, Mann Whitney U-test  $p=0.024$ , alongside the required 20 accepted trials). The presence of EMG activity indicates that some spinal motor neurons are discharging action potentials, while others are close to firing threshold and will thus discharge upon receipt of minimal excitatory input (i.e. the descending corticospinal volley evoked by TMS). For a descending corticospinal volley of a given magnitude, the MEP recorded in a target muscle will be larger in the presence of EMG, than in its absence<sup>655</sup>. If not accounted for, elevated baseline EMG introduces a confound when comparing MEP amplitude or threshold measures between ALS patients and controls.

While the distorting effect of spinal motor neuron excitability on estimates of cortical states can be dealt with by excluding trials with elevated pre-stimulus EMG, special consideration must be made in the case of ALS patients displaying fasciculations and/or fibrillations in the target muscle. These symptoms of lower motor neuron degeneration<sup>11</sup> can appear similar to MEPs in EMG records. If they occur during the time window following TMS in which the evoked responses are resolved, they can result in erroneous estimates of MEP amplitude. Furthermore, if the time window employed for background EMG measurement is narrower than the interval between these repetitive spikes, a trial in which fasciculations and fibrillations begin before the delivery of TMS may go undetected and contaminate MEP amplitude measurements. Sufficient experience is required in the rapid identification of these artefacts through inspection of the EMG recordings during data collection to permit accurate recordings. In the case of threshold tracking procedures, a wide background EMG estimation window and stringent amplitude criteria must be employed in order to exclude such erroneous data before it is entered into the tracking algorithm to minimise potential misdirection of the algorithm<sup>652</sup>. For patients who are capable of intermittently achieving an acceptable level of muscle



relaxation, the consequence of applying this method is prolonged data collection and increased patient burden. Some ALS patients, however, are simply unable to maintain the necessary muscle quiescence.

The widespread use of Riluzole for ALS treatment introduces an additional variable in the comparison of ALS patients and controls. Riluzole has been shown to reduce ICF and, to a lesser extent, enhance SICI<sup>160</sup>. While these effects will tend to reduce, rather than to accentuate the reported differences between ALS patients and controls, the prescription of this drug should be considered. Additional pharmacological agents are also often prescribed for the treatment of symptoms and the psychiatric burden caused by the disease. For example baclofen, used for the treatment of spasms in ALS<sup>656</sup>, Gabapentin, prescribed to alleviate muscle cramping<sup>656</sup>, selective serotonin reuptake inhibitors, prescribed for pseudobulbar affect<sup>657</sup>, depression and anxiety<sup>658</sup>, and some benzodiazepines, used for the treatment of anxiety and to support initiation of non-invasive ventilation<sup>659</sup> can alter single and paired pulse TMS measures of the motor cortex<sup>160,660</sup>. These specific medications, which were being taken by patients encountered during recruitment to our study (table 7.3), represent examples of numerous neuromodulatory medications prescribed for ALS symptoms which influence paired-pulse TMS measures. Excluding patients on such medications to remove this covariation imposes further limitations on sample size, and distorts the representation of the ALS population. The alternative of including the type and dose of medications as covariates would, in order to be effective, require the recruitment of very large samples.

**Table 7.3. ALS patients excluded from or of limited participation due to clinical limitations.** Patients unsuitable for TMS due to metallic implants, migraines or seizure disorders were excluded before consideration of these limitations. “Too high” refers to a resting motor threshold (RMT) > 83% stimulator output, such that suprathreshold (120% of RMT) conditioning stimuli were unobtainable or test stimulation > 100% of stimulator output was required. Disease duration is time in months from self-reported first disease symptom to date of recording or exclusion. The target muscle was abductor pollicis brevis. \*-X to -Y months – These participants had last ALSFRS-R recorded Y months before recording, due to slow disease progression (2 points decline in 2.5/3.8 years) limiting clinic attendance, therefore a representative mean of ALSFRS-R score recorded between -X and -Y months before recording is listed. AP – Using anterior-posterior coil orientation. M – Male. F – Female. SSRI – Selective serotonin reuptake inhibitor. ALSFRS-R – ALS functional rating scale revised.

Sex	Age (years)	Disease duration (months)	Diagnostic delay (months)	ALS FRS-R	Days from ALS FRS-R to recording	Clinical/ pharma limitation	Missing data
M	76.33	11	5	37	4	SSRI	Excluded
F	72.83	24	10	36	13	MEP response to PA and AP stimulation <50uV	No data collected
M	67.42	8	3	38	35	Upper arm stiffness	No data collection
M	67.75	32	3	N/A	N/A	Baclofen	Excluded
M	61.33	20	3	33	36	GABApentin	Excluded
M	72.08	20	2	40	27	MEP response to PA and AP stimulation <50uV	No data collected
F	72.41	19	5	38	22	Benzo-diazepine	Excluded
M	59.75	33	17	39	13	MEP response to AP stimulation <50uV	No AP data collected
F	75.58	96	80	34.9 2*	-63 to -17 months	MEP response to AP stimulation <50uV	No AP data collected

F	72.83	24	10	36	13	MEP response to AP stimulation <50uV, PA threshold too high	No paired-pulse data collected
F	61.25	91	43	34*	-41 to -11 months	AP threshold too high	No AP data collected
M	66	29	5	38	37	AP threshold too high	No paired-pulse data collected

In summary, clinical and research protocols must be devised with the impact of these factors in mind. The diagnostic/prognostic application of TMS is not uniformly practical in ALS, and the potential impact of pharmacological agents must be considered in patients for whom it can feasibly be employed. Particular attention should also be given to features of the EMG that arise from disruption to lower motor neurons, which must be monitored assiduously during data collection. Methodologies such as magneto- or electroencephalography may, in some cases, facilitate interrogation of the central neurophysiology of interest with fewer limitations. These practical considerations do not preclude the use of TMS as a research instrument in the study of neurodegenerative diseases, nor do they detract from the significance of the TMS-based studies in ALS conducted to date. They do however impose constraints on realisable sample sizes and introduce potential sources of bias. Such limitations should be considered carefully in the design and interpretation of TMS protocols for the clinical assessment of ALS.

## 8. Discussion and Conclusion

In this chapter an overall summary and interpretation of the project's results, a discussion of the relevance of results to understanding and quantifying ALS pathophysiology, a consideration of the limitations of the project and the future research that is called for are described. An overall summary of the project results is given in section 8.1. The advantages of using the employed electrophysiological paradigms for characterising ALS are described in Section 8.2. The potential impact and clinical applications of this work are considered in section 8.3 and links between these electrophysiological findings and genetic and molecular drivers of ALS pathogenesis are considered in section 8.4. The limitations of this work are summarised in section 8.5. Future work that can build upon this project to bring these results towards real world applications are described in section 8.6. Finally, section 8.7 contains a brief conclusion with regards to the entire thesis.

### 8.1. Summary of results

#### 8.1.1. Auditory oddball-engaged networks

In this project, the time domain ERPs and time-frequency domain ERD/ERS associated with the ignored auditory oddball paradigm were recorded using high-density EEG. As abnormalities in the MMN in ALS patients had already been characterised at sensor level by this team, this project commenced with source analyses of the MMN. Thereafter, ERD/ERS associated with this paradigm were analysed at sensor and source level.

##### 8.1.1.1. Cortical activation during the mismatch negativity

The ignored auditory oddball task was first used to determine the effects of ALS on the sources of the MMN, in order to investigate if ALS-related cognitive network impairment could be detected using a passive task that is well suited to those unable to perform attended/motor tasks. Using source analyses, we identified that during the MMN, the activation of the IFG and STG observed in healthy controls here and elsewhere<sup>264–266</sup> was lower in ALS patients, significantly so in both IFG and the left STG. Baseline activity levels in both STG and IFG were positively correlated with survival times (i.e. those with lower baseline STG and IFG activity had worse prognoses), while baseline activity in both IFG correlated with the rate of decline in ALSFRS-R score (i.e. those with lower baseline IFG activity showed more rapid decline in motor symptoms). This illustrated that such non-motor pathology in ALS is relevant to disease progression. Activity in the

IFG and STG underpinning the MMN significantly increased longitudinally within ALS patients. The left IFG and bilateral STG in ALS patients at later time points in disease were also found to be hyperactive relative to controls. However, those with greater baseline left IFG activity showed greater deterioration in inhibition-switching score and those with greater STG power at baseline showed more rapid deterioration in word reading score. This indicates that hyperactivation of these non-motor regions are relevant to cognitive and language decline in ALS.

By contrast, the DLPFCs and left motor and posterior parietal cortices were found to be hyperactive during MMN at baseline recordings. The activation of the left motor and dorsolateral prefrontal cortices during the MMN were found to significantly decline over time in ALS patients, such that they no longer significantly differed from control group levels of activation at follow up recording sessions. Left DLPFC activity at baseline was significantly correlated with behavioural and cognitive scores one year after EEG recording (but not at the time of EEG recording). These findings illustrated that poorer cognitive and behavioural impairment both relate to dorsolateral prefrontal pathophysiology, but in distinct ways, highlighting differences in the pathophysiology driving ALSbi and ALSci. Further, we have demonstrated that such measures can predict future disease symptoms.

#### 8.1.1.2. *Auditory-associated spectral perturbations*

Investigation of the MMN involves investigation of signals that are phase-locked to performance of the auditory oddball paradigm. We next sought to investigate if ALS-related network pathology was captured in cortical signals that are not phase-locked to the stimuli. Such signals are lost through averaging during ERP analysis. We analysed the changes in non-phase locked cortical oscillations associated with standard and deviant tones, as well as the difference between deviant and standard tone-related spectral perturbations. Significant task-related spectral perturbations were then compared between ALS patients and controls. Both standard and deviant tones evoked significant synchronisation of alpha band oscillations, observed across the frontoparietal axis and over the temporal cortices. No significant difference between deviant and standard evoked oscillatory changes were present in controls or ALS patients. ALS patients showed greater alpha and beta ERS over the left temporal lobe following deviant, but not standard, tones. Deviant tone-related alpha ERS over the temporal lobes showed significant negative correlation to disease duration (i.e. greater alpha ERS was measured

in those closer to first symptom onset). This correlation, alongside our previous findings of the primary auditory cortex being underactivated during the MMN early in disease, supports our hypothesis that this excessive deviant-tone related alpha ERS reflects excessive thalamocortical suppression.

Source analysis was subsequently employed to determine the sources generating standard and deviant tone-associated alpha ERS and excess deviant tone-associated alpha and beta ERS in ALS patients. In keeping with sensor level findings, ALS patients did not show abnormal standard tone-elicited alpha ERS source activity but did show widespread significantly greater alpha ERS in both cortical and subcortical regions following deviant tones compared to controls across, predominant in the bilateral medial and lateral temporal cortices and right insula. Greater deviant tone-evoked slow beta ERS observed in ALS patients was predominantly localised to the left medial and lateral posterior parietal cortex and middle occipital gyrus. This excessive beta ERS is likely to represent hyperactivity in working memory centres which compare deviant tones to the expected standard tone template.

In addition to these abnormal cortical oscillations identified across the ALS group compared to controls, standard tone-related alpha ERS over the sensorimotor cortex showed significant negative correlation to ECAS total score (i.e. those with greater cognitive performance had less alpha ERS over the motor cortex after standard tones). Excess fast beta synchrony in the right DLPFC, while also not significantly different in ALS, was found to negatively correlate to disease duration. The physiology underpinning these relationships is unclear, however such correlations to clinical progression demonstrates that measures which do not significantly differ between ALS patients and controls overall may still contribute predictive information in the development of prognostic ALS biomarkers.

### *8.1.2. SART-engaged networks*

Both the time domain ERPs and time-frequency domain ERD/ERS associated with the sustained attention to response task were recorded using high-density EEG and analysed separately at sensor and source level.

#### *8.1.2.1. SART related potentials*

Previous studies in healthy individuals have characterised the randomised SART-evoked potentials. The two waveforms typically studied are those associated with correct NoGo

and Go responses to cues. Two of the peaks in these waveforms were employed to investigate different aspects of the cortical network pathophysiology. Namely, N2, which peaks over the motor cortex and is attributed to motor control, and P3, which is most prevalent over the prefrontal cortex (attributed to orientation to novel stimuli<sup>622,661</sup>) and parietal cortex (attribute to working memory and attention control<sup>622,623</sup>). Both N2 and P3 peaks are larger during NoGo trials than Go trials<sup>126</sup>.

The SART evoked potentials measured in controls this project were characteristic of those previously described. Sources underpinning the N2 and P3 peaks in healthy individuals had not previously been reported, and therefore were investigated as part of this project. The left primary motor cortex and both DLPFCs and lateral PPCs were identified as primary mean sources of both Go and NoGo N2, with greater bilateral precuneus activation during NoGo trials. Mean P3 sources were similar to those of N2 for Go and NoGo trials, although left insular, PPC and DLPFC activity was lower during NoGo trials relative to Go trials.

In ALS, a significantly smaller N2 peak was evoked over the frontal lobe during NoGo trials. Those patients with greater N2 NoGo-Go differences over the sensorimotor cortex had higher ECAS scores (i.e. those of better cognitive performance, particularly in tasks of executive function and language, showed greater difference in N2 between correct withholding and responding trials), indicative that this N2 peak decline relates to impaired cognitive network function.

At source level, patients conversely showed similar patterns of source activity to controls during N2, while during P3, ALS patients displayed widespread, significantly increased activity during NoGo trials relative to Go trials when compared to controls, with the most discriminant differences being in the left inferior parietal lobule and left insula. Abnormal precuneus activation was also associated with greater preservation of this executive function in ALS. These sensor and source level findings highlight the advantage of employing both sensor and source space analyses, as in some cases differences at source level are not detected as significant at sensor level. In others, clinically informative differences in sensor level ERP characteristics may not relate to a significant abnormality in a single/small number of underpinning sources but represent the summation of broader pathophysiology.

#### *8.1.2.2. SART related spectral perturbations*

As SART induced spectral perturbations had not previously been reported in the literature, this analysis was the first to describe the ERD/ERS associated with this task in healthy individuals, as well as in ALS. During Go trials, theta-band ERS and alpha and beta band ERD were present across the frontoparietal axis. Beta ERD was followed by ERS, predominantly recorded over the frontal lobe. Based on comparison to the existing literature regarding movement related beta desynchronization and synchronization, our findings indicated that the SART captures these oscillatory indices of motor cortical activation and inactivation in addition to those of attention and response control. Correct withholding during NoGo trials induced greater theta band ERS over the frontal lobe, as well as greater alpha ERD and less beta ERS across the frontoparietal axis compared to correct responding during Go trials. Theta band ERS was deemed likely to reflect attention allocation<sup>640,642</sup>, while the physiological basis of SART-related alpha desynchronization is potentially underpinned by cognitive and motor components. Based on correlation analyses, we also identified that these oscillations relate to the speed-accuracy trade-off, with those who prioritized speed over accuracy displaying greater beta ERS during Go trials. This speed accuracy trade-off introduces variation to behavioural measures of SART performance in healthy individuals, reducing the ability of these measures to detect pathological impairments<sup>643</sup>. These objective and quantitative measures might therefore help to account for this variation such that disease related impairments can be deciphered.

ALS patients displayed lower beta-band ERD in over the prefrontal and parietal cortices during Go and NoGo trials in ALS compared to controls. Go trial-induced beta ERS was also reduced in ALS, predominantly over the prefrontal cortex.

#### *8.1.2.3. Disrupted correlations between SART-associated EEG measures and task performance*

Some of the correlations between SART-related ERP/ERD/ERS characteristics and task performance measures identified in controls were not present in ALS patients, while other significant correlations identified between these measures existed in ALS patients but not controls. These correlations indicate that the network disruption identified in ALS from these SART studies is likely to be a combination of both pathophysiological and compensatory change. Such measures of compensatory activity which sustains performance in task/functional measures may facilitate detection of presymptomatic ALS pathology.



### 8.1.3. TMS-engaged motor networks

In addition to using EEG to investigate ALS cortical pathology beyond the corticospinal tract, TMS was employed to interrogate disruption of subcomponents of the cortical motor networks. In order to investigate the reproducibility of previous TT-TMS study findings, we measured SICI and ICF in ALS patients and controls. As SICI is known to include two physiologically distinct measures, peaking at 1 and 3ms ISIs, both measures were investigated separately.

#### 8.1.3.1. Comparison to previous TT-TMS studies in ALS

In this study, we found no significant ICF in the control cohort. This aligns with previous reports that ICF is not consistent in healthy young adults, and is absent/overridden by concurrent SICI in older adults<sup>662</sup>. We also identified no differences in ICF between ALS patients and controls. While greater ICF has previously been reported in ALS, this finding is inconsistent<sup>194,645</sup> and is likely to be confounded by SICI changes, and has uncertain physiological underpinnings<sup>177,654</sup>. ICF is therefore unlikely to be substantially informative with respect to ALS pathology or the development of ALS biomarkers compared to other electrophysiological measures.

When PA coil orientation was implemented, only  $SICI_{PA-1ms}$  was found to be of a different magnitude in ALS patients with respect to controls with less inhibition occurring in ALS. While trends towards lower  $SICI_{3ms}$  in ALS patients were observed, these differences were not found to be significant in this analysis. These findings are consistent with previous TT-TMS studies in ALS, where  $SICI_{PA-1ms}$  is found to be largely absent in ALS patients, while  $SICI_{PA-3ms}$  has been reported to be lower in ALS compared to controls, but to a lesser extent than  $SICI_{PA-1ms}$ <sup>194</sup>. The consistently distinct effects of ALS on  $SICI_{PA-1ms}$  and  $SICI_{PA-3ms}$  indicate that these measures are capturing distinct aspects of ALS pathophysiology which should be individually considered in future studies designed to investigate ALS-related cortical dysfunction or ALS subphenotype characterisation.

#### 8.1.3.2. Measures of motor cortical network function previously unexplored by TT-TMS in ALS

In order to measure the effect of ALS on GABA<sub>B</sub>ergic intracortical and motor callosal tract function in ALS, LICI, SIHI and LIHI were measured in controls and ALS patients. Irrespective of coil orientation or ISI, LICI was not found to be different in ALS patients compared to controls, indicative that GABA<sub>B</sub>ergic function is not uniformly affected across time and individuals by ALS. While trends of lower interhemispheric inhibition

were observed in ALS patients were observed, these were not significant upon multiple comparison correction. This may be due to insufficient statistical power, as lower SIHI<sup>399</sup> and abnormal iSP<sup>400,401,453</sup> have previously been reported in ALS, albeit not with TT-TMS protocol. However, strong correlations between these measures and measures of ALS progression, albeit not deemed statistically significant in this preliminary cohort, indicate that these measures warrant further examination upon expansion of this dataset.

### *8.1.3.3. Novel application of AP coil orientation in ALS*

When an AP coil orientation was used, SICI<sub>AP-3ms</sub> was reliably lower in ALS compared to controls. Both effect size and AUROC measures demonstrate that SICI<sub>AP-3ms</sub> is more sensitive to ALS pathology than SICI<sub>PA-3ms</sub>. While the lack of statistical significance pertaining to decreased SICI<sub>PA-3ms</sub> described here is likely to reflect insufficient statistical power due to boundaries to patient recruitment, such limitations help to exemplify the benefit of implementing AP coil orientation when attempting to sensitively quantify ALS pathophysiology via some SICI in small cohorts/individuals. Similarly, lower SIHI in ALS compared to controls was more evident when AP stimulation was used versus when PA stimulation was applied, indicating that this orientation can also provide greater sensitivity to callosal malfunction in ALS. Further, ALS patients showed significantly shorter MEP latency compared to controls when AP but not PA coil orientation was used. This indicated that cortical circuitry impaired by ALS is more sensitively interrogated by AP stimulation, perhaps due to preferential engagement of circuits affected by ALS. In some individuals, AP orientation-based TMS measures are inaccessible due to reduced cortical combined with the higher intensities required to evoke responses with TMS with AP orientation, compared to PA orientation<sup>472</sup>. However, these findings indicate that AP orientation-based TMS should be employed where possible, alongside/in preference to PA orientation, when gathering TMS-based supportive evidence for ALS diagnosis (recommended in the most recently published diagnostic criteria for ALS<sup>72</sup>).

## **8.2. Exemplified advantages of electrophysiological measures for quantifying ALS compared to measures of symptomatic impairment**

### *8.2.1. Network dysfunction preceding symptomatic decline*

Throughout this project, a number of measures have been identified which indicate that ALS pathology can be objectively detected presymptomatically. For example, left DLPFC hyperactivation during the MMN predicts cognitive decline one year later, but

does not significantly correlate to simultaneously-measured cognitive performance. Additionally, those who display greater STG activity during the MMN early in disease have poorer language prognoses. Furthermore, despite ALS patients showing comparable accuracy and response time measures in the SART to controls, electrophysiology revealed hyperactivation of the left PPC and insula and excessive beta oscillation synchronisation during task performance. Notably, each of these examples (among others listed above) identify excess motor and/or cognitive cortical network function. Presymptomatic hyperexcitability of upper motor neurons has previously been identified in ALS via TMS studies in a small number of pathogenic SOD1 mutation carriers<sup>288</sup>. This project's findings have now demonstrated that over activity also occurs in non-motor networks, and relates to impairment in their associated cognitive and language functions. Such measures may, with further refinement, facilitate detection of those who will develop cognitive and/or behavioural impairment in advance of this decline.

#### 8.2.2. *Measuring of compensatory function*

Lack of correlation, especially where established to exist for healthy populations, or lesser symptoms in the presence of abnormal cortical functioning, may reflect capture of compensatory cortical physiology. Such compensatory function is expected (and demonstrated<sup>663,664</sup>) to occur in neurological disease, especially at presymptomatic/early symptomatic stages, due to the plastic nature of neural networks. Such compensatory ability forms the basis of many post-stroke rehabilitation strategies<sup>665</sup>. Further, the reserve capacity of neuronal networks can sustain function in the context of substantial neurodegeneration, exemplified in Parkinson's disease, where at least 40% nigral cell loss and striatal dopamine depletion occurs in presymptomatically<sup>666</sup>. A number of the abnormal SART-associated cortical signals identified in ALS in this project are likely to be compensatory. This reasoning is based on observed discrepancies between groups in correlations between task performance and electrophysiological indices. For example, the significant negative correlation between response accuracy and Go trial-related beta synchronisation identified in controls was not observed in patients. By contrast, greater alpha ERD was associated slower response times in patients but not controls. Additionally, a number of correlations between N2 and P3 peak characteristics in SART-related potentials and response time/accuracy performance measures in controls were not observed in ALS patients. These disrupted correlations were observed in the context of comparable accuracy and response times between ALS patients and controls. This

indicates that performance in the SART can be sustained in ALS by a combination of neural network activity in ALS patients that differs from that which dictates performance in healthy controls. This highlights the utility of EEG for detecting ALS pathology in those who do not appear abnormal based on measures of symptomatic impairment.

### 8.2.3. *Sensor space vs. source space EEG measures*

With the development of source analysis algorithms for the improvement of M/EEG spatial resolution, research of sensor space measures might be presumed redundant. The results of this project have highlighted the advantages and disadvantages of both source and sensor space measures of pathophysiology. In the case of sensor space measures, spatial resolution is poor due to conduction of electrical signals to the electrode from both adjacent and distant cortical sources<sup>101</sup>. This limits the ability to prescribe detected abnormalities to specific anatomical regions unless source analysis is performed. For example, in this project we identified spatially diffuse audition-associated alpha ERS at sensor level and required source analysis to determine its underpinning sources.

However, the spatial summation of cortical activity which gives rise to ERP peaks may be advantageous in the quantification or investigation of disease. In this project, for example, the SART-evoked potential N2 peak, an index of inhibition of the motor response attributed to prefrontal and motor networks was significantly reduced in ALS. However, at source level, a specific region within these sources was not deemed to underpin the abnormality, indicative that a summation of low level disruption across these sources is responsible. Had sensor level analysis been skipped in this investigation in favour of source level analysis alone, this diffuse pathophysiology would have remained undetected due to insufficient statistical power. Such sensor level analysis is relatively simple to perform alongside source analysis as its most methodologically and mathematically challenging components (signal preprocessing and noise removal) are also required in advance of source analysis.

SART-related potential analysis also exemplified the opposing advantage of employing source analysis, rather than sensor space analysis alone. In the case of the P3 peak, at sensor level the peak was not detected to differ between ALS patients and controls. However, a number of cortical regions were identified to be hyperactive in ALS patients upon source analysis of the P3 signal. This may represent compensatory activity, or may reflect pathophysiology masked amidst the activity of other sources which contribute to the P3 peak measured at sensor level. Therefore, it is ideal that event related cortical

signals be investigated at both source and sensor level both in healthy population studies and in the investigation of disease-related pathology.

### **8.3. Impact and future clinical applications**

The significance of this project to the understanding of normal and ALS-related cortical (dys)function and the potential applications of the findings of this project to the medical field are summarised in this section.

#### *8.3.1. Novel description of task-related cortical oscillation (de)synchronisations and their disruption in ALS*

While motor task-related changes in cortical oscillations are well established and have been examined in ALS by many studies, sensation- and cognition-associated cortical oscillations are less frequently examined in healthy individuals, and, to the best of the author's knowledge, have not previously been examined in ALS. The time-frequency analyses of SART-related oscillations as part of this thesis is the first to describe the synchronization and desynchronization of cortical oscillations associated with SART performance and their relationship to performance speed and accuracy. Further, the utility of these measures for capturing and quantifying neurodegenerative disease cognitive network pathology was exemplified by a comparison of these measures between ALS patients and controls. Not only has this study (now accepted for publication in Journal of Neural Engineering) highlighted potential biomarkers of ALS, but the description of these measures in healthy individuals will facilitate their application for the investigation of other neurodegenerative and psychiatric diseases where the cognitive network disruption underpinning cognitive symptoms remains unclear (such as Huntington's disease and multiple sclerosis<sup>102</sup>). The identified correlations between SART-related (de)synchronisation and task performance measures also indicates that these measures can help to explain variation in speed vs. accuracy strategies between individuals.

While time-frequency analyses of auditory oddball task-related spectral perturbations have previously been reported<sup>605,667</sup>, such studies included both phase-locked and non-phase locked oscillation changes, and therefore did not specifically report the oscillation ERD/ERS evoked by the task that are distinct from those captured in time-domain (i.e. as waveforms) by ERP analyses. Therefore the time-frequency analyses of auditory oddball task-related oscillations within this thesis is the first to describe the synchronization and

desynchronization of non-phase locked cortical oscillations associated with auditory sensation at sensor and source level, as well as the lack of difference between these oscillations evoked by standard and deviant tones in controls. Additionally, the utility of these measures to identify thalamocortical pathophysiology in neurodegenerative and psychiatric disease was exemplified by a comparison of these measures between ALS patients and controls. Novel identification of disrupted auditory task-associated oscillation (de)synchronisation in ALS by this component of the project has also unveiled that excessive bottom-up inhibition by overactive thalamocortical networking is a potential mechanisms for early hypoactivity preceding hyperactivity in non-motor cortical regions.

### *8.3.2. Novel description of the cortical sources engaged by the SART and their disruption in ALS*

While randomised SART-related cortical potentials have previously been described<sup>126</sup>, the sources underpinning generation of the N2 and P3 peaks of these waveforms had not. The source analyses of SART ERPs during this thesis (now published in *Cerebral Cortex*<sup>478</sup>) is the first to describe the location and nature of SART-evoked cortical activity and the relationship between this activity and task performance measures. This study is also the first to describe changes in SART ERPs and their underlying cortical activity in ALS, revealing that electrophysiological measures of movement and attention control are disrupted in the absence of abnormal speed or accuracy performance measures. Such findings exemplify the rationale for further investigation of EEG-based measures as early/presymptomatic biomarkers of cognitive impairment in ALS.

### *8.3.3. Novel identification of dynamic spatiotemporal patterns of cortical excitability which relate to ALS symptoms and severity measures*

To the best of the author's knowledge, the MMN ERP analyses performed within this study is the first to identify progressive decline in motor cortical function within individuals with ALS via direct measurement of neuronal activity. Further, this study has identified for the first time that this pattern of early hyperactivity followed by progressive decline also occurs in the DLPFC. Further, correlation analysis with measures of cognitive and behavioural impairment revealed that levels of DLPFC engagement during the MMN can predict levels of cognitive and behavioural impairment after one year. This correlation analysis reveals that DLPFC activity correlates better with future symptoms associated with this region than concurrent symptoms, and, as these correlations differed

in direction between behavioural and cognitive impairment measures, that distinct DLPFC pathophysiology is associated with ALS<sub>bi</sub> compared to ALS<sub>sci</sub>. Such a distinction is in keeping with ALS<sub>bi</sub> and ALS<sub>sci</sub> often clinically presenting independently of one another<sup>570</sup>.

This longitudinal analysis has also demonstrate that some cognitive (i.e. the IFG) and auditory/language (i.e. the STG) network hubs are suppressed early in ALS pathology, and become progressively hyperactive. This early suppression in non-motor cortical activity showed strong correlations to shorter survival times and faster decline in ALSFRS-R score. These correlations indicate that non-motor pathology is pertinent when accounting for variation in rates of ALS progression, and that measures of cortical function both inside and outside the primary motor cortex should be considered in the development of ALS prognostic biomarkers. Finally, this study also highlighted that greater activity in the STG (which is associated with language function<sup>566</sup>) during the MMN at baseline related to poorer performance in the CWIT word reading subscore. Therefore, MMN-related cortical activity measurements may also be useful in the early detection of temporal lobe language pathology in ALS.

#### *8.3.4. Replication of some (but not other) previous TT-TMS-based ALS study findings in the Irish population.*

Previous findings of decrease in both SICI<sub>1ms</sub> and SICI<sub>3ms</sub>, which is of greater effect size for SICI<sub>1ms</sub> (associated with extracellular GABAergic tone<sup>164</sup>) than for SICI<sub>3ms</sub> (associated with GABA<sub>A</sub>ergic interneuronal function<sup>160</sup>)<sup>194,216,288</sup> were replicated in this study of Irish ALS patient cohorts. However, previous findings of increase in ICF in the motor cortex of ALS patients<sup>70,194,216,289,334,335</sup> were not. Further, ICF values were highly similar between ALS patients and controls, demonstrating that lack of statistical power relative to previous studies was not responsible for this difference in findings. These findings support the use of TT-TMS-measured SICI as a diagnostic biomarker of ALS, but do not support the use of ICF as a biomarker of ALS. Further, as ICF was not significant within the control cohort, our findings do not support the measurement of ICF as a reliable phenomenon of normal network function against which to compare ALS patients.

*8.3.5. Novel indication that TT-TMS indices of GABA<sub>B</sub>ergic interneuronal are not uniformly affected by ALS, but may, alongside corpus callosum function, relate to disease progression.*

The TT-TMS study of this project is the first to characterise TT-TMS measured LICI, SIHI and LIHI in ALS. This study has demonstrated that ALS does not homogeneously affect LICI or IHI. This indicates that their underpinning network generators, such as GABA<sub>B</sub>ergic interneurons and the corpus callosum components of cortical motor networks are not consistently disrupted across ALS patients. Nonetheless, as these measures were reliably evoked across the control cohort, this measure may be of value in future research of the motor network dysfunction underpinning ALS symptom heterogeneity and disease progression. This is indicated by correlations between these measures and ALSFRS-R scores, although these correlations require confirmation in a larger dataset. Similarly, while comparisons of SIHI values between ALS patients and controls were not deemed significant upon correction for multiple comparisons, this may reflect insufficient statistical power due to limitations to ALS patient recruitment (see sections 7.2 and 8.5.2). Therefore, these measures should not be discounted in design of future TT-TMS studies as their utility for quantifying ALS progression warrants further investigation, following additional data collection.

*8.3.6. Novel identification of the utility of AP coil orientation for the detection of ALS pathology with TT-TMS.*

The TT-TMS study of this project is the first to investigate the utility of AP coil orientation-based TT-TMS measures compared to PA orientation based measures for measuring ALS pathology. As described in section 8.1.3.3, the findings of this study indicate that TT-TMS measures of MEP latency, SIHI and SICI are more sensitive to ALS pathology when AP coil orientation is used than when PA orientation is used. Therefore, future TT-TMS based research of ALS should incorporate AP coil orientation and AP orientation-based measures should be considered further in the clinical development of TT-TMS measures as biomarkers of ALS.

*8.3.7. Novel biomarker candidates*

*8.3.7.1. Diagnostic biomarker candidates*

Based on AUROC measures, a number of electrophysiological parameters have been identified which display excellent discrimination of ALS patients from controls.



Specifically, SART-related beta ERD, left inferior parietal lobule and insula engagement during the SART-evoked P3 and SICI<sub>AP-3ms</sub> showed very good (AUROC=0.8-0.9) discrimination of these groups. Such measures warrant further investigation as ALS biomarkers, and should be considered as secondary outcome measures of ALS clinical trials as they may capture therapeutic effects on ALS pathology undetected by measures of disease symptoms.

Baseline IFG activity during the MMN, which showed good (AUROC=0.7-0.8) discrimination of these groups, showed excellent (AUROC>0.9) discrimination of bulbar-onset and *C9orf72*+ subcohorts of ALS patients from to controls, in line with these subgroups being more prone to cognitive impairment<sup>45,411</sup>. Such elevation of the discriminative ability in cognitively impaired ALS subcohorts is supportive of the hypothesis that those diagnosed with ALS include numerous overlapping subphenotypes which are individually more homogenous<sup>317</sup>, and therefore, more similar in underpinning pathophysiology and prognosis.

#### 8.3.7.2. Prognostic biomarker candidates

While a number of cognitive and motor cortical hubs were deemed to be reliably disrupted across the ALS cohorts studied as a whole, many measures which did not differ significantly between ALS patients and controls at group level showed significant correlation to measures of disease progression and/or cognitive, language or motor symptom severity. Given the extensive variation of symptoms experienced and progression rate between individual ALS patients, such measures may be highly valuable for developing prognostic biomarkers of ALS, as well as for stratification of clinical trial cohorts. Those measures which showed very strong correlation to symptom measures (absolute  $\rho > 0.8$ , e.g. positive correlation of IHI<sub>PA</sub> with ALSFRS-R score, negative correlation of right precuneus power during P3 in SART NoGo relative to Go trials with behavioural inhibition) represent obvious candidates. However, those which show weaker correlations, when combined with other electrophysiological/structural/psychological/functional measures into multidimensional biomarkers, may facilitate the subcategorization of ALS patients into network-based subphenotypes for which prognosis can be more reliably predicted.

### 8.4. Links to genetic and molecular drivers of ALS pathogenesis

A core theme across the results of this thesis, and prevalent in the existing ALS literature, is evidence which supports the presence of hyperactivity and hyperexcitability as well as

loss of GABAergic inhibition in the motor cortex, with hyperactivity declining progressively. Building upon the theory of pathogenic motor cortical hyperactivity in ALS, the findings of this project indicate that such hyperactivity progressively emerges in non-motor cortical regions and this non-motor dysfunction relates to the heterogeneity of ALS non-motor symptoms (see sections 5.1-6.2). However, this network-focussed approach to understanding ALS pathogenesis must be considered in the context of intracellular level changes relating to ALS onset, including the role of TDP-43 proteinopathies (see section 1.1.3) and underpinning genetic mutations (see section 1.1.2), and prevailing views on how ALS spreads at a cellular level.

#### *8.4.1. Links between TDP-43 inclusions and cellular hyperexcitability and hyperactivity*

Upper motor neuron hyperexcitability in ALS is considered to result from early loss of vulnerable interneurons which control their responsiveness to excitatory input<sup>321,327,668</sup>. In keeping with this theory, ALS patient cohorts studied in this study showed reduced intracortical inhibition measures attributed to GABA<sub>A</sub>ergic interneurons (see section 7.1), as well as abnormal activation during non-motor tasks, in the primary motor cortex (see sections 5.1 and 5.2).

Despite the extensive literature evidencing motor cortical hyperexcitability/hyperactivity at a network level and at a cellular level, the relationship between motor neuron excitability and the TDP-43 containing inclusions which are found in almost all ALS patients has only begun to be probed. A study which used induced pluripotent stem cell (iPSC)-derived neurons recently found that hyperexcitability (induced by potassium channel blockade) drives TDP-43 pathology via upregulated transcription of a shortened form of TDP-43 which is exported from the nucleus. This short isoform forms cytoplasmic inclusions which sequester full-length TDP-43. In support of a toxic role of this short isoform, increased expression of shortened TDP-43 was toxic to neurons, and shortened TDP-43 was found to be accumulated in neurons and glia from ALS patients<sup>669</sup>.

#### *8.4.2. Links between RNA binding protein mutations and cellular hyperexcitability and hyperactivity*

The above *in vitro* evidence suggests that hyperexcitability may occur upstream of TDP-43 pathology. However, this does not explain the observation of hyperexcitability in

iPSC-derived cultures of motor neurons derived from *C9orf72* and *FUS* mutation associated ALS patients<sup>670</sup>. Reduction in GABAergic interneurons have also been identified in TDP-43 knock-in mice and prefrontal cortex tissue from *C9orf72*-ALS<sup>671</sup>. These findings suggests that mutated RNA-binding proteins can drive motor neuronal hyperexcitability.

Hyperexcitability in iPSC-derived cultures of motor neurons derived from ALS patients carrying ALS-causing *TARDBP* or *C9orf72* mutations is found to progressively decline to loss of synaptic activity and action potential output<sup>672</sup>. This is in keeping with the progressive decline in early motor hyperactivity observed here, and previous TMS-based evidence of progressively declining UMN hyperexcitability in ALS<sup>328–331</sup>. Further, a study of mouse cortical neurons over-expressing mutant TDP-43<sup>A315T</sup> (generated by an ALS-linked mutation in *TARDBP*<sup>53</sup>) identified reduced dendritic spine density and localisation of the glutamate AMPA receptor subunit GluR1 to dendritic spines, compared to wild-type cells. Action potential generation was also found to be lower in TDP-43<sup>A315T</sup> mouse pyramidal neurons<sup>673</sup>. Therefore, mutant RNA-binding proteins may drive initial hyperexcitability in UMNs via early toxicity to vulnerable interneurons, followed by hypoexcitability due to disruption of glutamatergic signalling and toxicity to the UMNs themselves.

#### *8.4.3. Links between progressive cortical dysfunction and propagation of disease between cells to non-motor cortical areas*

The studies discussed in sections 8.4.1 and 8.4.2 indicate that upper motor neuron hyperexcitability/hyperactivity and TDP-43 proteinopathy perpetuate one another, with ultimately toxic effects on the function of neurons which become hypoactive before cell death. However, this does not explain the heterogeneity of ALS non-motor symptoms and the dynamic patterns of hypo- and hyperactivation in non-motor networks observed in this project (see section 5.2).

The mechanism by which ALS pathology spreads between cells (if at all) remains uncertain, and may vary between subphenotypes based on the characteristics of the pathogenic protein. Predominant hypotheses which propose independent pathogenesis within individual cells, rather than spread between them include the multifocal hit hypothesis and the ubiquitous change hypothesis. The multifocal hit hypothesis proposes that pathogenic processes occur randomly in each cell and converge to initiate the disease, while the ubiquitous change hypothesis proposes that molecular abnormalities emerge in

individual cells, with some cells having no defects<sup>674</sup>. By contrast, one of the proposed mechanisms of ALS pathology spread is the release of pathogenic protein oligomers from cells, which, upon uptake into neighbouring cells, drives nucleation of cytoplasmic inclusions in the recipient (referred to as “prion-like propagation”<sup>674</sup>). This is supported by presence of TDP-43 oligomers in exosomes<sup>675</sup>, observed exchange of TDP-43 between cell somata and uptake of microvesicular TDP-43 into cells where it has toxic effects. TDP-43 oligomer seeding in cultured primary motor cortical mouse neurons has also been demonstrated by introduction of TDP-43 containing ALS patient brain lysate<sup>676</sup>. Similarly, CSF from ALS patients (but not from controls) into mice expressing human wild-type TDP-43, developed motor and cognitive impairment alongside TDP-43 proteinopathy<sup>677</sup>.

Our findings of early hyperactivity in the motor cortex-neighbouring DLPFC and PPC which progressively declines, contrasted by later progressive hyperactivation of the IFG and STG (section 5.2), may represent gradual spread of TDP-43 pathology from early-affected motor and motor-neighbouring regions to more distal cognitive, sensory and language-associated regions, where hyperactivity subsequently emerges. In theory, spread of glutamate induced excitotoxicity along cortical networks<sup>678,679</sup> could alternatively drive spread of upregulation of shortened TDP-43 and toxic TDP-43 nucleation to non-motor cortical network hubs.

Regardless of the specific causative relationship(s) between TDP-43 and neuronal hyperactivity/hyperexcitability, these studies indicate that hyperexcitability and TDP-43 co-spread across the cortex, driving non-motor ALS symptoms such as cognitive and language impairment. This hypothesis (illustrated in Fig. 8.1) is supported by our electrophysiological findings that greater early hyperactivity in the DLPFC predicts greater cognitive impairment (measured by ECAS total score,) after one year (see section 5.2) and the previously reported association between executive dysfunction (measured by ECAS executive scores) and TDP-43 pathology in the orbitofrontal cortex ventral anterior cingulate, DLPFC and medial prefrontal cortex<sup>59</sup>.

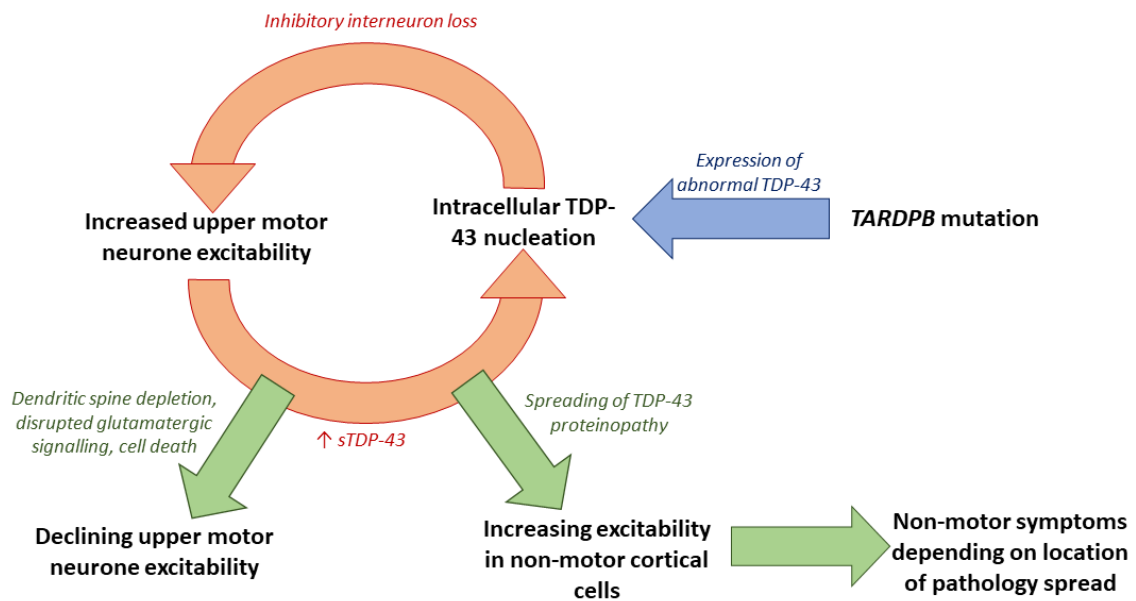


**Figure 8.1. Illustration of the proposed link between hyperexcitability spread through the cortex and TDP-43 pathology in ALS.** Arrows indicate passage of time, with direction of arrows indicating directionality of the link between proposed steps in ALS pathology onset and progression. Evidence in support of this hypothesis from this thesis and existing literature are described in section 8.4. Italicised, non-bolded text refer to linking mechanisms between proposed key steps in ALS pathology stated in bold text. Blue coloured text and arrows refer to genetic risk factors, red coloured arrows and text refer to ALS onset and green text and arrows refers to disease progression. sTDP-43 – Shortened isoform of TDP-43

## 8.5. Limitations

In this section, general limitations which influenced the design of this project or limited the analyses/interpretation of results within this project are discussed. Limitations pertaining specifically to each analysis performed within this project are described within chapters 5-7.

### 8.5.1. Recruitment

The typically rapid rate of ALS progression<sup>2</sup> presented a challenge in the recruitment of patients to this hospital-based research. Participants had to be sufficiently mobile (at minimum, by wheelchair) to attend the research facility, and in the case of those no longer able to take public transport or drive due to decline in motor function, participants needed to be accompanied by someone who could transport them to and from the research location. Further, in the case of motor tasks (e.g. button press during the SART), participants require sufficient motor function to respond.

Recruitment is further limited by the exclusion criteria of the studies performed here. Each study required that participants not have any co-morbid neuromuscular or psychiatric diagnosis which might influence the electrophysiological measures under investigation, a typical exclusion criteria in such studies<sup>108,156,207,680</sup>. Participants were also excluded in some circumstances due to the use of certain medications which influence the central nervous system or, in the case of TMS research, due to potentially increased risk of adverse response to the study protocol (see section 7.2).

As 2.1-3.8 people per 100,000 are diagnosed per year in European populations<sup>73</sup>, and a portion of these patients are uninterested in, excluded from or at too late a disease stage to take part in such research, sufficient time windows must be allowed for recruitment and data collection of ALS patients as they are newly diagnosed. This limitation was accounted for during the design of this project, and recruitment and data collection was continuously performed across a window of at least one year in the case of all studies in this project. Nonetheless, in the case of the TMS arm of this project, unforeseen limitations to data collection (e.g. inexcitability, noisy baseline EMG data) and the pausing of data collection during much of 2020 due to the COVID-19 pandemic, resulted in further slowing of the participant recruitment rate. Therefore while a preliminary analysis was performed and described in chapter 7, the current dataset is likely underpowered to detect some disease-related abnormalities in the investigated measurements. TMS data collection remains ongoing for further analysis.

#### 8.5.2. Attrition bias

Longitudinal research is advantageous over the correlation of cross-sectional findings to measures of disease progression, as changes which occur with disease progression can be definitively demonstrated. However, such studies of ALS can be biased by the drop out of those more severely affected by disease at earlier time points in the study<sup>81,681,682</sup>. Such drop out can inflate representation of those with milder disease at later time points in longitudinal studies, where dropout is allowed. If only those who contribute to all time points are examined, this final cohort may not be representative of the full disease population. In the case of this project, such bias is likely to have influenced comparisons between time-grouped patient and control data (see section 5.2.3.1). In this analysis, some later data time groups which represented relatively small proportions of the complete participant cohort due to drop out between return visits diverged from significant trends of hyperactivation/reduced activation observed across earlier time points. In order to

minimise the influence of such bias on this study's findings, measures of change in cortical activity were prescribed to each individual, irrespective of number of return visits or disease duration, based on linear modelling. The potential influence of such bias was also considered in the discussion of our longitudinal findings.

### *8.5.3. EEG study design and time domain analysis*

The intervals between delivery of stimuli/cues of the auditory oddball paradigm and SART were based on previous ERP studies, allowing for the complete ERP to be recorded between each stimulus, in addition to 100/200ms of baseline data for correction of the oncoming ERP. Following the majority of data collection and completion of ERP analyses, time-frequency domain analyses were undertaken to maximise the information which could be derived from the recorded signals. Such analyses were not planned during study design. While the implemented study designs and collected datasets are suitable for accurate time-frequency analysis, ERSP at some slow frequencies were not interpreted where the baseline data windows were shorter than one full cycle of this oscillation. This limitation has been described in detail in sections 5.3 and 6.2.

## **8.6. Future work**

### *8.6.1. Further TMS data collection*

As described in sections 7.1 and 8.4, a number of factors slowed and limited the recruitment of ALS patients to the TMS study within this project. Data collection is ongoing in order to gain sufficient statistical power to definitively determine if those trends which did not reach statistical significance here are abnormal in ALS patients. Additional TT-TMS work is now also starting to be undertaken in ALS patients to determine if the motor cortex is abnormally regulated by the IFG, premotor and supplementary motor cortices, wherein abnormal functionality was identified in this project. This novel study aims to bridge our understanding of the EEG-based cognitive and TT-TMS-based motor findings regarding ALS pathology gained this project.

### *8.6.2. Longitudinal SART and TMS studies*

As demonstrated by our longitudinal MMN study, longitudinal capture of electrophysiological measures can provide important insight into the dynamic nature of network dysfunction in ALS and how this progressive pathology relates to disease

progression. Such studies are now required to build upon the SART and TMS cross-sectional analyses described here, in order to determine if the cortical pathophysiology is stable or relate to a specific stage of ALS pathology. Collection of this longitudinal data has been ongoing throughout this project and analysis will be performed in 2021.

### *8.6.3. Clustering analyses*

It is clear from the established array of variably prevalent non-motor symptoms in ALS patients<sup>19,428,566</sup>, as well as the correlations between non-motor cortical dysfunction and non-motor symptoms and survival times identified here, that ALS heterogeneity relates to the pattern of cortical impairment which occurs within individuals. Therefore, a combination of the measures identified here (and others) which together predict sensory, cognitive, behavioural, language and motor impairment in ALS could provide a basis for objective, quantitative grouping of ALS patients into network-based subphenotypes via clustering analyses. This additional measure development and clustering analysis is now being undertaken. Such clusters will be compared to existing criteria for ALS subcategorization (e.g. genetic risk factors, site of motor symptom onset) in order to determine the clinical utility of such clusters for improving predictability of individual patient prognoses.

## **8.7. Overall conclusion**

This project has uncovered complex spatio-temporal patterns of hypo- and hyper-activity across the cortex in ALS. Many of these patterns show strong correlations to measures of concurrent or future cognitive, behavioural and motor symptoms, survival times and disease progression. These findings definitively demonstrate that ALS pathology does not solely affect motor-associated cortical regions and does not uniformly influence all areas of the cortex.

While some of these measures individually demonstrate excellent ability to discriminate ALS patients from controls, the combined findings of this project, in the context of existing literature regarding cortical network dysfunction in ALS, indicate that ALS patients with similar patterns of cortical network disruption will experience more similar disease symptoms and progression rates.

These patterns can be readily and economically quantified by combination of EEG and TT-TMS-linked EMG measures which capture different aspects of ALS pathophysiology. Therefore, going forward, I intend to refine understanding of the impact of ALS on these measures of motor, cognitive, language and sensory cortical function through longitudinal



analyses and analyses of larger patient cohorts which capture more of the heterogeneity present in the ALS population. In addition, measures of cortical regions/connections not interrogated here (e.g. activity in regions associated with vision, somatosensory and a number of language functions and connections linking cognitive and motor network hubs) will also be investigated in ALS. I will then analyse these measures in combination using clustering analyses to determine if network-based subphenotypes of ALS can facilitate improved prediction of ALS motor and non-motor prognoses. Such improved subphenotyping could facilitate improved stratification of patients enrolled to clinical trials, enabling less restrictive inclusion criteria to be employed and rendering such trials more accessible to ALS patients eager to participate in such trials. Additionally, measures of different aspects of ALS pathophysiology will be refined in consultation with the pharmaceutical industry for use as secondary clinical trial outcome measures in future ALS clinical trials.

## 9. Bibliography

1. Talbott EO, Malek AM, Lacomis D. The epidemiology of amyotrophic lateral sclerosis. *Handb Clin Neurol* 2016;138:225–238.
2. Kiernan MC, Vucic S, Cheah BC, et al. Amyotrophic lateral sclerosis. *Lancet* 2011;377(9769):942–955.
3. O’Toole O, Traynor BJ, Brennan P, et al. Epidemiology and clinical features of amyotrophic lateral sclerosis in Ireland between 1995 and 2004. *Journal of Neurology, Neurosurgery & Psychiatry* 2008;79(1):30–32.
4. McGuigan C, McCarthy A, Quigley C, et al. Latitudinal variation in the prevalence of multiple sclerosis in Ireland, an effect of genetic diversity. *J Neurol Neurosurg Psychiatry* 2004;75(4):572–576.
5. Martin S, Al Khleifat A, Al-Chalabi A. What causes amyotrophic lateral sclerosis? *F1000Res* 2017;6:371–371.
6. van Es MA, Hardiman O, Chio A, et al. Amyotrophic lateral sclerosis. *The Lancet* 2017;390(10107):2084–2098.
7. Ryan M, Heverin M, Doherty MA, et al. Determining the incidence of familiarity in ALS: A study of temporal trends in Ireland from 1994 to 2016. *Neurology Genetics* 2018;4(3)
8. Siddique T, Ajroud-Driss S. Familial amyotrophic lateral sclerosis, a historical perspective. *Acta Myol* 2011;30(2):117–120.
9. Ravits JM, La Spada AR. ALS motor phenotype heterogeneity, focality, and spread. *Neurology* 2009;73(10):805–811.
10. Kent-Braun JA, Walker CH, Weiner MW, Miller RG. Functional significance of upper and lower motor neuron impairment in amyotrophic lateral sclerosis. *Muscle & nerve* 1998;21(6):762–768.
11. Zarei S, Carr K, Reiley L, et al. A comprehensive review of amyotrophic lateral sclerosis. *Surgical neurology international* 2015;6
12. Corcia P, Pradat P-F, Salachas F, et al. Causes of death in a post-mortem series of ALS patients. *Amyotrophic Lateral Sclerosis* 2008;9(1):59–62.
13. Wolf J, Safer A, Wöhrle JC, et al. Causes of death in amyotrophic lateral sclerosis : Results from the Rhineland-Palatinate ALS registry. *Nervenarzt* 2017;88(8):911–918.
14. Achi EY, Rudnicki SA. ALS and frontotemporal dysfunction: a review. *Neurology research international* 2012;2012
15. Neary D, Snowden JS, Mann DM. Cognitive change in motor neurone disease/amyotrophic lateral sclerosis (MND/ALS). *J. Neurol. Sci.* 2000;180(1–2):15–20.
16. Strong MJ, Grace GM, Orange JB, et al. A prospective study of cognitive impairment in ALS. *Neurology* 1999;53(8):1665–1670.
17. Warren JD, Rohrer JD, Rossor MN. Frontotemporal dementia. *BMJ* 2013;347:f4827.
18. Perry RJ, Graham A, Williams G, et al. Patterns of frontal lobe atrophy in frontotemporal

- dementia: a volumetric MRI study. *Dement Geriatr Cogn Disord* 2006;22(4):278–287.
19. Phukan J, Elamin M, Bede P, et al. The syndrome of cognitive impairment in amyotrophic lateral sclerosis: a population-based study. *J. Neurol. Neurosurg. Psychiatry* 2012;83(1):102–108.
  20. Chiò A, Vignola A, Mastro E, et al. Neurobehavioral symptoms in ALS are negatively related to caregivers' burden and quality of life. *European journal of neurology* 2010;17(10):1298–1303.
  21. Chio A, Ilardi A, Cammarosano S, et al. Neurobehavioral dysfunction in ALS has a negative effect on outcome and use of PEG and NIV. *Neurology* 2012;78(14):1085–1089.
  22. Tsujimoto M, Senda J, Ishihara T, et al. Behavioral changes in early ALS correlate with voxel-based morphometry and diffusion tensor imaging. *J. Neurol. Sci.* 2011;307(1–2):34–40.
  23. Lillo P, Mioshi E, Zoing MC, et al. How common are behavioural changes in amyotrophic lateral sclerosis? *Amyotroph Lateral Scler* 2011;12(1):45–51.
  24. Gibbons ZC, Richardson A, Neary D, Snowden JS. Behaviour in amyotrophic lateral sclerosis. *Amyotroph Lateral Scler* 2008;9(2):67–74.
  25. Machts J, Bittner V, Kasper E, et al. Memory deficits in amyotrophic lateral sclerosis are not exclusively caused by executive dysfunction: a comparative neuropsychological study of amnesic mild cognitive impairment. *BMC Neurosci* 2014;15:83.
  26. Massman PJ, Sims J, Cooke N, et al. Prevalence and correlates of neuropsychological deficits in amyotrophic lateral sclerosis. *J. Neurol. Neurosurg. Psychiatry* 1996;61(5):450–455.
  27. Saxon JA, Harris JM, Thompson JC, et al. Semantic dementia, progressive non-fluent aphasia and their association with amyotrophic lateral sclerosis. *J Neurol Neurosurg Psychiatry* 2017;88(8):711–712.
  28. Ardila A, Bernal B, Rosselli M. How Localized are Language Brain Areas? A Review of Brodmann Areas Involvement in Oral Language. *Arch Clin Neuropsychol* 2016;31(1):112–122.
  29. Mohandas E, Rajmohan V. Frontotemporal dementia: An updated overview. *Indian J Psychiatry* 2009;51 Suppl 1:S65-69.
  30. Rohrer JD, Warren JD, Modat M, et al. Patterns of cortical thinning in the language variants of frontotemporal lobar degeneration. *Neurology* 2009;72(18):1562–1569.
  31. Mann D, Snowden JS. Frontotemporal lobar degeneration: Pathogenesis, pathology and pathways to phenotype. *Brain Pathology* 2017;
  32. Leslie FV, Hsieh S, Caga J, et al. Semantic deficits in amyotrophic lateral sclerosis. *Amyotrophic Lateral Sclerosis and Frontotemporal Degeneration* 2015;16(1–2):46–53.
  33. Abrahams S, Leigh PN, Harvey A, et al. Verbal fluency and executive dysfunction in amyotrophic lateral sclerosis (ALS). *Neuropsychologia* 2000;38(6):734–747.
  34. Ichikawa H, Kawamura M. Language impairment in amyotrophic lateral sclerosis. *Brain Nerve* 2010;62(4):435–440.

35. Hammad M, Silva A, Glass J, et al. Clinical, electrophysiologic, and pathologic evidence for sensory abnormalities in ALS. *Neurology* 2007;69(24):2236–2242.
36. Al-Chalabi A, Hardiman O. The epidemiology of ALS: a conspiracy of genes, environment and time. *Nature Reviews Neurology* 2013;9(11):617–628.
37. Chiò A, Mazzini L, D’Alfonso S, et al. The multistep hypothesis of ALS revisited: The role of genetic mutations. *Neurology* 2018;91(7):e635–e642.
38. Connolly O, Le Gall L, McCluskey G, et al. A Systematic Review of Genotype–Phenotype Correlation across Cohorts Having Causal Mutations of Different Genes in ALS. *Journal of Personalized Medicine* 2020;10(3):58.
39. Ryan M, Zaldívar Vaillant T, McLaughlin RL, et al. Comparison of the clinical and genetic features of amyotrophic lateral sclerosis across Cuban, Uruguayan and Irish clinic-based populations. *J Neurol Neurosurg Psychiatry* 2019;90(6):659–665.
40. DeJesus-Hernandez M, Mackenzie IR, Boeve BF, et al. Expanded GGGGCC hexanucleotide repeat in non-coding region of C9ORF72 causes chromosome 9p-linked frontotemporal dementia and amyotrophic lateral sclerosis. *Neuron* 2011;72(2):245–256.
41. Renton AE, Majounie E, Waite A, et al. A hexanucleotide repeat expansion in C9ORF72 is the cause of chromosome 9p21-linked ALS-FTD. *Neuron* 2011;72(2):257–268.
42. Iacoangeli A, Al Khleifat A, Jones AR, et al. C9orf72 intermediate expansions of 24–30 repeats are associated with ALS. *Acta Neuropathologica Communications* 2019;7(1):115.
43. van Blitterswijk M, DeJesus-Hernandez M, Rademakers R. How do C9ORF72 repeat expansions cause ALS and FTD: can we learn from other non-coding repeat expansion disorders? *Curr Opin Neurol* 2012;25(6):689–700.
44. Jiang J, Ravits J. Pathogenic Mechanisms and Therapy Development for C9orf72 Amyotrophic Lateral Sclerosis/Frontotemporal Dementia. *Neurotherapeutics* 2019;16(4):1115–1132.
45. Byrne S, Elamin M, Bede P, et al. Cognitive and clinical characteristics of patients with amyotrophic lateral sclerosis carrying a C9orf72 repeat expansion: a population-based cohort study. *Lancet Neurol* 2012;11(3):232–240.
46. Webster CP, Smith EF, Shaw PJ, De Vos KJ. Protein homeostasis in amyotrophic lateral sclerosis: therapeutic opportunities? *Frontiers in molecular neuroscience* 2017;10:123.
47. Bozzo F, Mirra A, Carrì MT. Oxidative stress and mitochondrial damage in the pathogenesis of ALS: New perspectives. *Neurosci Lett* 2017;636:3–8.
48. Sasaki S. Endoplasmic reticulum stress in motor neurons of the spinal cord in sporadic amyotrophic lateral sclerosis. *J Neuropathol Exp Neurol* 2010;69(4):346–355.
49. Sullivan PM, Zhou X, Hu F. Autophagy-lysosome dysfunction in amyotrophic lateral sclerosis and frontotemporal lobar degeneration. *Lysosomes: Associated Diseases and Methods to Study Their Function* 2017;63.
50. Soo KY, Farg M, Atkin JD. Molecular Motor Proteins and Amyotrophic Lateral Sclerosis. *Int J Mol Sci* 2011;12(12):9057–9082.
51. Cheah BC, Vucic S, Krishnan AV, Kiernan MC. Riluzole, Neuroprotection and

- Amyotrophic Lateral Sclerosis. *Current Medicinal Chemistry* 2010;17(18):1942–1959.
52. Ling S-C, Polymenidou M, Cleveland DW. Converging mechanisms in ALS and FTD: disrupted RNA and protein homeostasis. *Neuron* 2013;79(3):416–438.
  53. Neumann M, Sampathu DM, Kwong LK, et al. Ubiquitinated TDP-43 in Frontotemporal Lobar Degeneration and Amyotrophic Lateral Sclerosis. *Science* 2006;314(5796):130–133.
  54. Mackenzie IRA, Bigio EH, Ince PG, et al. Pathological TDP-43 distinguishes sporadic amyotrophic lateral sclerosis from amyotrophic lateral sclerosis with SOD1 mutations. *Ann Neurol* 2007;61(5):427–434.
  55. Ayala YM, Zago P, D'Ambrogio A, et al. Structural determinants of the cellular localization and shuttling of TDP-43. *J Cell Sci* 2008;121(Pt 22):3778–3785.
  56. Scotter EL, Chen H-J, Shaw CE. TDP-43 Proteinopathy and ALS: Insights into Disease Mechanisms and Therapeutic Targets. *Neurotherapeutics* 2015;12(2):352–363.
  57. Mathis S, Goizet C, Soulages A, et al. Genetics of amyotrophic lateral sclerosis: A review. *Journal of the Neurological Sciences* 2019;399:217–226.
  58. Grad LI, Rouleau GA, Ravits J, Cashman NR. Clinical spectrum of amyotrophic lateral sclerosis (ALS). *Cold Spring Harbor perspectives in medicine* 2017;7(8):a024117.
  59. Gregory JM, McDade K, Bak TH, et al. Executive, language and fluency dysfunction are markers of localised TDP-43 cerebral pathology in non-demented ALS. *J Neurol Neurosurg Psychiatry* 2020;91(2):149–157.
  60. Verber NS, Shephard SR, Sassani M, et al. Biomarkers in motor neuron disease: a state of the art review. *Frontiers in neurology* 2019;10:291.
  61. Feneberg E, Gray E, Ansorge O, et al. Towards a TDP-43-Based Biomarker for ALS and FTL. *Mol Neurobiol* 2018;55(10):7789–7801.
  62. Galvin M, Ryan P, Maguire S, et al. The path to specialist multidisciplinary care in amyotrophic lateral sclerosis: a population-based study of consultations, interventions and costs. *PLoS one* 2017;12(6):e0179796.
  63. Ludolph A, Drory V, Hardiman O, et al. A revision of the El Escorial criteria - 2015. *Amyotroph Lateral Scler Frontotemporal Degener* 2015;16(5–6):291–292.
  64. Swash M. Why are upper motor neuron signs difficult to elicit in amyotrophic lateral sclerosis? *J. Neurol. Neurosurg. Psychiatry* 2012;83(6):659–662.
  65. Gagliardi D, Meneri M, Saccomanno D, et al. Diagnostic and prognostic role of blood and cerebrospinal fluid and blood neurofilaments in amyotrophic lateral sclerosis: a review of the literature. *International journal of molecular sciences* 2019;20(17):4152.
  66. Gaetani L, Blennow K, Calabresi P, et al. Neurofilament light chain as a biomarker in neurological disorders. *J Neurol Neurosurg Psychiatry* 2019;90(8):870–881.
  67. Xu Z, Henderson RD, David M, McCombe PA. Neurofilaments as Biomarkers for Amyotrophic Lateral Sclerosis: A Systematic Review and Meta-Analysis. *PLOS ONE* 2016;11(10):e0164625.

68. Poesen K, Van Damme P. Diagnostic and prognostic performance of neurofilaments in ALS. *Frontiers in neurology* 2019;9:1167.
69. Evans RW. Complications of Lumbar Puncture. *Neurologic Clinics* 1998;16(1):83–105.
70. Vucic S, Cheah BC, Yiannikas C, Kiernan MC. Cortical excitability distinguishes ALS from mimic disorders. *Clin Neurophysiol* 2011;122(9):1860–1866.
71. Vucic S, van den Bos M, Menon P, et al. Utility of threshold tracking transcranial magnetic stimulation in ALS. *Clin Neurophysiol Pract* 2018;3:164–172.
72. Shefner JM, Al-Chalabi A, Baker MR, et al. A proposal for new diagnostic criteria for ALS. *Clinical Neurophysiology* 2020;131(8):1975–1978.
73. Longinetti E, Fang F. Epidemiology of amyotrophic lateral sclerosis: an update of recent literature. *Curr Opin Neurol* 2019;32(5):771–776.
74. Galvin M, Corr B, Madden C, et al. Caregiving in ALS – a mixed methods approach to the study of Burden. *BMC Palliative Care* 2016;15(1):81.
75. Rutkove SB. Clinical Measures of Disease Progression in Amyotrophic Lateral Sclerosis. *Neurotherapeutics* 2015;12(2):384–393.
76. van Eijk RP, Eijkemans MJ, Rizopoulos D, et al. Comparing methods to combine functional loss and mortality in clinical trials for amyotrophic lateral sclerosis. *Clin Epidemiol* 2018;10:333–341.
77. Westeneng H-J, Debray TPA, Visser AE, et al. Prognosis for patients with amyotrophic lateral sclerosis: development and validation of a personalised prediction model. *The Lancet Neurology* 2018;17(5):423–433.
78. van Eijk RPA, Westeneng H-J, Nikolakopoulos S, et al. Refining eligibility criteria for amyotrophic lateral sclerosis clinical trials. *Neurology* 2019;92(5):e451–e460.
79. Eisen A, Kiernan M, Mitsumoto H, Swash M. Amyotrophic lateral sclerosis: a long preclinical period? *Journal of Neurology, Neurosurgery & Psychiatry* 2014;85(11):1232–1238.
80. Bede P, Hardiman O. Longitudinal structural changes in ALS: a three time-point imaging study of white and gray matter degeneration. *Amyotrophic Lateral Sclerosis and Frontotemporal Degeneration* 2018;19(3–4):232–241.
81. van der Burgh HK, Westeneng H-J, Walhout R, et al. Multimodal longitudinal study of structural brain involvement in amyotrophic lateral sclerosis. *Neurology* 2020;94(24):e2592–e2604.
82. Chard D, Trip SA. Resolving the clinico-radiological paradox in multiple sclerosis. *F1000Research* 2017;6
83. Van Schependom J, Nagels G. Targeting cognitive impairment in multiple sclerosis—the road toward an imaging-based biomarker. *Frontiers in Neuroscience* 2017;11:380.
84. Crease RP. Images of conflict: MEG vs. EEG (magnetoencephalography vs electroencephalography). *Science* 1991;253(5018):374–376.
85. Berger M, Gould MK, Barnett PG. The Cost of Positron Emission Tomography in Six

- United States Veterans Affairs Hospitals and Two Academic Medical Centers. *American Journal of Roentgenology* 2003;181(2):359–365.
86. Singh SP. Magnetoencephalography: Basic principles. *Ann Indian Acad Neurol* 2014;17(Suppl 1):S107–S112.
  87. Mayerhoefer ME, Prosch H, Beer L, et al. PET/MRI versus PET/CT in oncology: a prospective single-center study of 330 examinations focusing on implications for patient management and cost considerations. *Eur J Nucl Med Mol Imaging* 2020;47(1):51–60.
  88. DellaBadia Jr J, Bell WL, Keyes Jr JW, et al. Assessment and cost comparison of sleep-deprived EEG, MRI and PET in the prediction of surgical treatment for epilepsy. *Seizure* 2002;11(5):303–309.
  89. Antonescu F, Adam M, Popa C, Tuță S. A review of cervical spine MRI in ALS patients. *Journal of medicine and life* 2018;11(2):123.
  90. Munn Z, Moola S, Lisy K, et al. Claustrophobia in magnetic resonance imaging: A systematic review and meta-analysis. *Radiography* 2015;21(2):e59–e63.
  91. Liu Q, Liu A, Zhang X, et al. Removal of EMG Artifacts from Multichannel EEG Signals Using Combined Singular Spectrum Analysis and Canonical Correlation Analysis. *Journal of Healthcare Engineering* 2019;2019
  92. Mucarquer JA, Prado P, Escobar M-J, et al. Improving EEG muscle artifact removal with an EMG array. *IEEE Transactions on Instrumentation and Measurement* 2020;69(3):815–824.
  93. Girouard H, Iadecola C. Neurovascular coupling in the normal brain and in hypertension, stroke, and Alzheimer disease. *Journal of Applied Physiology* 2006;100(1):328–335.
  94. Mosconi L. Glucose metabolism in normal aging and Alzheimer’s disease: methodological and physiological considerations for PET studies. *Clinical and translational imaging* 2013;1(4):217–233.
  95. Hock C, Müller-Spahn F, Schuh-Hofer S, et al. Age dependency of changes in cerebral hemoglobin oxygenation during brain activation: a near-infrared spectroscopy study. *Journal of Cerebral Blood Flow & Metabolism* 1995;15(6):1103–1108.
  96. Crosson B, Ford A, McGregor KM, et al. Functional Imaging and Related Techniques: An Introduction for Rehabilitation Researchers. *J Rehabil Res Dev* 2010;47(2):vii–xxxiv.
  97. Booth KR, Streletz LJ, Raab JJ, et al. Motor evoked potentials and central motor conduction: studies of transcranial magnetic stimulation with recording from the leg. *Electroencephalography and Clinical Neurophysiology/Evoked Potentials Section* 1991;81(1):57–62.
  98. Odom JV, Bach M, Brigell M, et al. ISCEV standard for clinical visual evoked potentials: (2016 update). *Doc Ophthalmol* 2016;133(1):1–9.
  99. Michel CM, Murray MM, Lantz G, et al. EEG source imaging. *Clin Neurophysiol* 2004;115(10):2195–2222.
  100. Gomez LJ, Goetz SM, Peterchev AV. Design of transcranial magnetic stimulation coils with optimal trade-off between depth, focality, and energy. *J Neural Eng* 2018;15(4):046033.

101. McMackin R, Bede P, Pender N, et al. Neurophysiological markers of network dysfunction in neurodegenerative diseases. *NeuroImage: Clinical* 2019;22:101706.
102. McMackin R, Muthuraman M, Groppa S, et al. Measuring network disruption in neurodegenerative diseases: New approaches using signal analysis. *J Neurol Neurosurg Psychiatry* 2019;90(9):1011–1020.
103. McMackin R, Dukic S, Broderick M, et al. Dysfunction of attention switching networks in amyotrophic lateral sclerosis. *NeuroImage: Clinical* 2019;22:101707.
104. Yates D. Neurodegenerative disease: Neurodegenerative networking. *Nature Reviews Neuroscience* 2012;13(5):288.
105. Saura CA, Parra-Damas A, Enriquez-Barreto L. Gene expression parallels synaptic excitability and plasticity changes in Alzheimer's disease. *Frontiers in cellular neuroscience* 2015;9:318.
106. Canter RG, Penney J, Tsai L-H. The road to restoring neural circuits for the treatment of Alzheimer's disease. *Nature* 2016;539(7628):187–196.
107. Gratwicke J, Jahanshahi M, Foltynie T. Parkinson's disease dementia: a neural networks perspective. *Brain* 2015;138(Pt 6):1454–1476.
108. Nasserolelami B, Dukic S, Broderick M, et al. Characteristic Increases in EEG Connectivity Correlate With Changes of Structural MRI in Amyotrophic Lateral Sclerosis. *Cereb Cortex* 2017;1–15.
109. Bede P, Omer T, Finegan E, et al. Connectivity-based characterisation of subcortical grey matter pathology in frontotemporal dementia and ALS: a multimodal neuroimaging study. *Brain Imaging Behav* 2018;1–12.
110. Symms M, Jäger HR, Schmierer K, Yousry TA. A review of structural magnetic resonance neuroimaging. *Journal of Neurology, Neurosurgery & Psychiatry* 2004;75(9):1235–1244.
111. Glover GH. Overview of Functional Magnetic Resonance Imaging. *Neurosurg Clin N Am* 2011;22(2):133–139.
112. Moeller F, Muthuraman M, Stephani U, et al. Representation and propagation of epileptic activity in absences and generalized photoparoxysmal responses. *Human brain mapping* 2013;34(8):1896–1909.
113. da Silva FL. EEG and MEG: relevance to neuroscience. *Neuron* 2013;80(5):1112–1128.
114. Wendel K, Väisänen O, Malmivuo J, et al. EEG/MEG source imaging: methods, challenges, and open issues. *Computational intelligence and neuroscience* 2009;2009
115. Nuwer M. Assessment of digital EEG, quantitative EEG, and EEG brain mapping: report of the American Academy of Neurology and the American Clinical Neurophysiology Society. *Neurology* 1997;49(1):277–292.
116. Cohen MX. *Analyzing Neural Time Series Data: Theory and Practice*. Cambridge, MA: MIT press; 2014.
117. Herrmann CS, Strüber D, Helfrich RF, Engel AK. EEG oscillations: From correlation to causality. *International Journal of Psychophysiology* 2016;103:12–21.



118. Luck SJ, Woodman GF, Vogel EK. Event-related potential studies of attention. *Trends in cognitive sciences* 2000;4(11):432–440.
119. Pfurtscheller G, Lopes da Silva FH. Event-related EEG/MEG synchronization and desynchronization: basic principles. *Clin Neurophysiol* 1999;110(11):1842–1857.
120. Başar E, Schürmann M, Demiralp T, et al. Event-related oscillations are 'real brain responses'--wavelet analysis and new strategies. *Int J Psychophysiol* 2001;39(2–3):91–127.
121. Kaiser DA. Basic Principles of Quantitative EEG. *J Adult Dev* 2005;12(2–3):99–104.
122. Stam CJ, Nolte G, Daffertshofer A. Phase lag index: Assessment of functional connectivity from multi channel EEG and MEG with diminished bias from common sources. *Human Brain Mapping* 2007;28(11):1178–1193.
123. Garrido MI, Kilner JM, Stephan KE, Friston KJ. The mismatch negativity: A review of underlying mechanisms. *Clin Neurophysiol* 2009;120(3):453–463.
124. Shibasaki H, Hallett M. What is the Bereitschaftspotential? *Clinical neurophysiology* 2006;117(11):2341–2356.
125. Landa L, Krpoun Z, Kolarova M, Kasperek T. Event-related Potentials and Their Applications. *Act Nerv Super* 2014;56(1):17–23.
126. Zordan L, Sarlo M, Stablum F. ERP components activated by the “GO!” and “WITHHOLD!” conflict in the random Sustained Attention to Response Task. *Brain Cogn* 2008;66(1):57–64.
127. Sauseng P, Klimesch W, Gruber WR, et al. Are event-related potential components generated by phase resetting of brain oscillations? A critical discussion. *Neuroscience* 2007;146(4):1435–1444.
128. Neuper C, Pfurtscheller G. Event-related dynamics of cortical rhythms: frequency-specific features and functional correlates. *International Journal of Psychophysiology* 2001;43(1):41–58.
129. Neuper C, Wörtz M, Pfurtscheller G. ERD/ERS patterns reflecting sensorimotor activation and deactivation. *Prog. Brain Res.* 2006;159:211–222.
130. Fraga FJ, Mamani GQ, Johns E, et al. Early diagnosis of mild cognitive impairment and Alzheimer's with event-related potentials and event-related desynchronization in N-back working memory tasks. *Comput Methods Programs Biomed* 2018;164:1–13.
131. Jaušovec N, Jaušovec K, Gerlič I. Differences in event-related and induced EEG patterns in the theta and alpha frequency bands related to human emotional intelligence. *Neuroscience Letters* 2001;311(2):93–96.
132. Peng W, Hu L, Zhang Z, Hu Y. Causality in the Association between P300 and Alpha Event-Related Desynchronization. *PLOS ONE* 2012;7(4):e34163.
133. Yordanova J, Kolev V, Polich J. P300 and alpha event-related desynchronization (ERD). *Psychophysiology* 2001;38(1):143–152.
134. Fraga FJ, Ferreira LA, Falk TH, et al. Event-related synchronisation responses to N-back memory tasks discriminate between healthy ageing, mild cognitive impairment, and mild

- Alzheimer's disease. In: 2017 IEEE International Conference on Acoustics, Speech and Signal Processing (ICASSP). 2017 p. 964–968.
135. Grech R, Cassar T, Muscat J, et al. Review on solving the inverse problem in EEG source analysis. *Journal of neuroengineering and rehabilitation* 2008;5(1):25.
  136. Scherg M, Berg P. Use of prior knowledge in brain electromagnetic source analysis. *Brain Topogr* 1991;4(2):143–150.
  137. Kavanagh RN, Darcey TM, Lehmann D, Fender DH. Evaluation of Methods for Three-Dimensional Localization of Electrical Sources in the Human Brain. *IEEE Transactions on Biomedical Engineering* 1978;BME-25(5):421–429.
  138. Jemel B, Achenbach C, Müller BW, et al. Mismatch negativity results from bilateral asymmetric dipole sources in the frontal and temporal lobes. *Brain Topogr* 2002;15(1):13–27.
  139. Van Veen BD, van Drongelen W, Yuchtman M, Suzuki A. Localization of brain electrical activity via linearly constrained minimum variance spatial filtering. *IEEE Trans Biomed Eng* 1997;44(9):867–880.
  140. Pascual-Marqui RD, Lehmann D, Koukkou M, et al. Assessing interactions in the brain with exact low-resolution electromagnetic tomography. *Philos Trans A Math Phys Eng Sci* 2011;369(1952):3768–3784.
  141. Belardinelli P, Ortiz E, Braun C. Source activity correlation effects on LCMV beamformers in a realistic measurement environment. *Computational and mathematical methods in medicine* 2012;2012
  142. *Clinical Neurophysiology: Basis and Technical Aspects: Handbook of Clinical Neurology Series*. Elsevier; 2019.
  143. Grunhaus L, Dannon PN, Gershon AA. Transcranial magnetic stimulation: a new tool in the fight against depression. *Dialogues Clin Neurosci* 2002;4(1):93–103.
  144. Elder GJ, Taylor J-P. Transcranial magnetic stimulation and transcranial direct current stimulation: treatments for cognitive and neuropsychiatric symptoms in the neurodegenerative dementias? *Alzheimers Res Ther* 2014;6(9):74.
  145. Rossini PM, Burke D, Chen R, et al. Non-invasive electrical and magnetic stimulation of the brain, spinal cord, roots and peripheral nerves: Basic principles and procedures for routine clinical and research application. An updated report from an I.F.C.N. Committee. *Clin Neurophysiol* 2015;126(6):1071–1107.
  146. Meyer B-U, Röricht S, Von Einsiedel HG, et al. Inhibitory and excitatory interhemispheric transfers between motor cortical areas in normal humans and patients with abnormalities of the corpus callosum. *Brain* 1995;118(2):429–440.
  147. Di Lazzaro V, Oliviero A, Pilato F, et al. Comparison of descending volleys evoked by transcranial and epidural motor cortex stimulation in a conscious patient with bulbar pain. *Clinical neurophysiology* 2004;115(4):834–838.
  148. Di Lazzaro V, Rothwell J, Capogna M. Noninvasive stimulation of the human brain: activation of multiple cortical circuits. *The Neuroscientist* 2018;24(3):246–260.
  149. Di Lazzaro V, Oliviero A, Saturno E, et al. The effect on corticospinal volleys of reversing

- the direction of current induced in the motor cortex by transcranial magnetic stimulation. *Experimental brain research* 2001;138(2):268–273.
150. Di Lazzaro V, Ziemann U. The contribution of transcranial magnetic stimulation in the functional evaluation of microcircuits in human motor cortex. *Frontiers in neural circuits* 2013;7:18.
  151. Maccabee PJ, Amassian VE, Eberle LP, Cracco RQ. Magnetic coil stimulation of straight and bent amphibian and mammalian peripheral nerve in vitro: locus of excitation. *J Physiol* 1993;460:201–219.
  152. Derosiere G, Vassiliadis P, Duque J. Advanced TMS approaches to probe corticospinal excitability during action preparation. *NeuroImage* 2020;213:116746.
  153. Groppa S, Oliviero A, Eisen A, et al. A practical guide to diagnostic transcranial magnetic stimulation: report of an IFCN committee. *Clin Neurophysiol* 2012;123(5):858–882.
  154. Hannah R, Rothwell JC. Pulse Duration as Well as Current Direction Determines the Specificity of Transcranial Magnetic Stimulation of Motor Cortex during Contraction. *Brain Stimul* 2017;10(1):106–115.
  155. Wassermann E, Epstein C, Ziemann U, Walsh V. *Oxford Handbook of Transcranial Stimulation*. Oxford,: OUP Oxford; 2008.
  156. Cirillo J, Byblow WD. Threshold tracking primary motor cortex inhibition: the influence of current direction. *European Journal of Neuroscience* 2016;44(8):2614–2621.
  157. Goss DA, Hoffman RL, Clark BC. Utilizing transcranial magnetic stimulation to study the human neuromuscular system. *JoVE (Journal of Visualized Experiments)* 2012;(59):e3387.
  158. Fisher RJ, Nakamura Y, Bestmann S, et al. Two phases of intracortical inhibition revealed by transcranial magnetic threshold tracking. *Exp Brain Res* 2002;143(2):240–248.
  159. Reis J, Swayne OB, Vandermeeren Y, et al. Contribution of transcranial magnetic stimulation to the understanding of cortical mechanisms involved in motor control. *J Physiol* 2008;586(2):325–351.
  160. Ziemann U, Reis J, Schwenkreis P, et al. TMS and drugs revisited 2014. *Clin Neurophysiol* 2015;126(10):1847–1868.
  161. Di Lazzaro V, Pilato F, Dileone M, et al. GABAA receptor subtype specific enhancement of inhibition in human motor cortex. *J Physiol* 2006;575(Pt 3):721–726.
  162. Farrant M, Kaila K. The cellular, molecular and ionic basis of GABAA receptor signalling. *Progress in brain research* 2007;160:59–87.
  163. Daskalakis ZJ, Christensen BK, Fitzgerald PB, et al. The mechanisms of interhemispheric inhibition in the human motor cortex. *J Physiol* 2002;543(Pt 1):317–326.
  164. Stagg CJ, Bestmann S, Constantinescu AO, et al. Relationship between physiological measures of excitability and levels of glutamate and GABA in the human motor cortex. *J. Physiol. (Lond.)* 2011;589(Pt 23):5845–5855.
  165. Di Lazzaro V, Restuccia D, Oliviero A, et al. Magnetic transcranial stimulation at intensities below active motor threshold activates intracortical inhibitory circuits.

Experimental Brain Research 1998;119(2):265–268.

166. Cirillo J, Semmler JG, Mooney RA, Byblow WD. Conventional or threshold-hunting TMS? A tale of two SICIs. *Brain Stimul* 2018;11(6):1296–1305.
167. Di Lazzaro V, Oliviero A, Meglio M, et al. Direct demonstration of the effect of lorazepam on the excitability of the human motor cortex. *Clin Neurophysiol* 2000;111(5):794–799.
168. Valls-Solé J, Pascual-Leone A, Wassermann EM, Hallett M. Human motor evoked responses to paired transcranial magnetic stimuli. *Electroencephalography and Clinical Neurophysiology/Evoked Potentials Section* 1992;85(6):355–364.
169. Werhahn KJ, Kunesch E, Noachtar S, et al. Differential effects on motorcortical inhibition induced by blockade of GABA uptake in humans. *The Journal of Physiology* 1999;517(2):591–597.
170. Nakamura H, Kitagawa H, Kawaguchi Y, Tsuji H. Intracortical facilitation and inhibition after transcranial magnetic stimulation in conscious humans. *J Physiol* 1997;498(Pt 3):817–823.
171. Terunuma M. Diversity of structure and function of GABAB receptors: a complexity of GABAB-mediated signaling. *Proc Jpn Acad Ser B Phys Biol Sci* 2018;94(10):390–411.
172. McCormick DA, Williamson A. Convergence and divergence of neurotransmitter action in human cerebral cortex. *PNAS* 1989;86(20):8098–8102.
173. Sanger TD, Garg RR, Chen R. Interactions between two different inhibitory systems in the human motor cortex. *J. Physiol. (Lond.)* 2001;530(Pt 2):307–317.
174. Ni Z, Gunraj C, Wagle-Shukla A, et al. Direct demonstration of inhibitory interactions between long interval intracortical inhibition and short interval intracortical inhibition. *J Physiol* 2011;589(Pt 12):2955–2962.
175. Kujirai T, Caramia MD, Rothwell JC, et al. Corticocortical inhibition in human motor cortex. *J. Physiol. (Lond.)* 1993;471:501–519.
176. Ziemann U, Rothwell JC, Ridding MC. Interaction between intracortical inhibition and facilitation in human motor cortex. *J. Physiol. (Lond.)* 1996;496 ( Pt 3):873–881.
177. Di Lazzaro V, Pilato F, Oliviero A, et al. Origin of Facilitation of Motor-Evoked Potentials After Paired Magnetic Stimulation: Direct Recording of Epidural Activity in Conscious Humans. *Journal of Neurophysiology* 2006;96(4):1765–1771.
178. Li C-T, Yang K-C, Lin W-C. Glutamatergic dysfunction and glutamatergic compounds for major psychiatric disorders: evidence from clinical neuroimaging studies. *Frontiers in psychiatry* 2019;9:767.
179. Benussi A, Alberici A, Buratti E, et al. Toward a glutamate hypothesis of frontotemporal dementia. *Frontiers in neuroscience* 2019;13:304.
180. Du X, Hong LE. Test-retest reliability of short-interval intracortical inhibition and intracortical facilitation in patients with schizophrenia. *Psychiatry Res* 2018;267:575–581.
181. Hermsen AM, Haag A, Duddek C, et al. Test–retest reliability of single and paired pulse transcranial magnetic stimulation parameters in healthy subjects. *Journal of the Neurological Sciences* 2016;362:209–216.

182. Orth M, Snijders AH, Rothwell JC. The variability of intracortical inhibition and facilitation. *Clinical Neurophysiology* 2003;114(12):2362–2369.
183. Chen R, Yung D, Li J-Y. Organization of Ipsilateral Excitatory and Inhibitory Pathways in the Human Motor Cortex. *Journal of Neurophysiology* 2003;89(3):1256–1264.
184. Hanajima R, Ugawa Y, Machii K, et al. Interhemispheric facilitation of the hand motor area in humans. *J. Physiol. (Lond.)* 2001;531(Pt 3):849–859.
185. Gerloff C, Cohen LG, Floeter MK, et al. Inhibitory influence of the ipsilateral motor cortex on responses to stimulation of the human cortex and pyramidal tract. *J. Physiol. (Lond.)* 1998;510 ( Pt 1):249–259.
186. Ni Z, Gunraj C, Nelson AJ, et al. Two Phases of Interhemispheric Inhibition between Motor Related Cortical Areas and the Primary Motor Cortex in Human. *Cereb Cortex* 2009;19(7):1654–1665.
187. Conti F, Manzoni T. The neurotransmitters and postsynaptic actions of callosally projecting neurons. *Behav. Brain Res.* 1994;64(1–2):37–53.
188. Innocenti GM. General organization of callosal connections in the cerebral cortex. In: *Sensory-motor areas and aspects of cortical connectivity*. Springer; 1986 p. 291–353.
189. Di Lazzaro V, Oliviero A, Profice P, et al. Direct demonstration of interhemispheric inhibition of the human motor cortex produced by transcranial magnetic stimulation. *Exp Brain Res* 1999;124(4):520–524.
190. Udupa K, Ni Z, Gunraj C, Chen R. Effect of long interval interhemispheric inhibition on intracortical inhibitory and facilitatory circuits. *J Physiol* 2010;588(Pt 14):2633–2641.
191. Irlbacher K, Brocke J, Mechow J v., Brandt SA. Effects of GABAA and GABAB agonists on interhemispheric inhibition in man. *Clinical Neurophysiology* 2007;118(2):308–316.
192. Lee H, Gunraj C, Chen R. The effects of inhibitory and facilitatory intracortical circuits on interhemispheric inhibition in the human motor cortex. *J Physiol* 2007;580(Pt 3):1021–1032.
193. Ferbert A, Priori A, Rothwell JC, et al. Interhemispheric inhibition of the human motor cortex. *The Journal of physiology* 1992;453(1):525–546.
194. Vucic S, Kiernan MC. Novel threshold tracking techniques suggest that cortical hyperexcitability is an early feature of motor neuron disease. *Brain* 2006;129(Pt 9):2436–2446.
195. Samusyte G, Bostock H, Rothwell J, Koltzenburg M. Short-interval intracortical inhibition: Comparison between conventional and threshold-tracking techniques. *Brain Stimul* 2018;11(4):806–817.
196. Khanna A, Pascual-Leone A, Michel CM, Farzan F. Microstates in resting-state EEG: Current status and future directions. *Neuroscience & Biobehavioral Reviews* 2015;49:105–113.
197. Mai R, Facchetti D, Micheli A, Poloni M. Quantitative electroencephalography in amyotrophic lateral sclerosis. *Electroencephalogr Clin Neurophysiol* 1998;106(4):383–386.

198. Santhosh J, Bhatia M, Sahu S, Anand S. Decreased electroencephalogram alpha band [8-13 Hz] power in amyotrophic lateral sclerosis patients: a study of alpha activity in an awake relaxed state. *Neurol India* 2005;53(1):99–101.
199. Crowell AL, Ryapolova-Webb ES, Ostrem JL, et al. Oscillations in sensorimotor cortex in movement disorders: an electrocorticography study. *Brain* 2012;135(2):615–630.
200. Jenkinson N, Brown P. New insights into the relationship between dopamine, beta oscillations and motor function. *Trends Neurosci.* 2011;34(12):611–618.
201. Pollok B, Krause V, Martsch W, et al. Motor-cortical oscillations in early stages of Parkinson's disease. *J. Physiol. (Lond.)* 2012;590(13):3203–3212.
202. Teramoto H, Morita A, Ninomiya S, et al. Relation between resting state front-parietal EEG coherence and executive function in parkinson's disease. *BioMed research international* 2016;2016
203. Nardone R, Sebastianelli L, Versace V, et al. Usefulness of EEG techniques in distinguishing frontotemporal dementia from alzheimer's disease and other dementias. *Disease markers* 2018;2018
204. Yener GG, Leuchter AF, Jenden D, et al. Quantitative EEG in frontotemporal dementia. *Clin Electroencephalogr* 1996;27(2):61–68.
205. Garn H, Coronel C, Waser M, et al. Differential diagnosis between patients with probable Alzheimer's disease, Parkinson's disease dementia, or dementia with Lewy bodies and frontotemporal dementia, behavioral variant, using quantitative electroencephalographic features. *J Neural Transm (Vienna)* 2017;124(5):569–581.
206. Lindau M, Jelic V, Johansson S-E, et al. Quantitative EEG abnormalities and cognitive dysfunctions in frontotemporal dementia and Alzheimer's disease. *Dement Geriatr Cogn Disord* 2003;15(2):106–114.
207. Babiloni C, Del Percio C, Lizio R, et al. Levodopa may affect cortical excitability in Parkinson's disease patients with cognitive deficits as revealed by reduced activity of cortical sources of resting state electroencephalographic rhythms. *Neurobiol. Aging* 2019;73:9–20.
208. Muthuraman M, Koirala N, Ciolac D, et al. Deep brain stimulation and L-dopa therapy: concepts of action and clinical applications in Parkinson's disease. *Frontiers in neurology* 2018;9:711.
209. Sanacora G, Smith MA, Pathak S, et al. Lanicemine: a low-trapping NMDA channel blocker produces sustained antidepressant efficacy with minimal psychotomimetic adverse effects. *Mol Psychiatry* 2014;19(9):978–985.
210. Coben LA, Danziger W, Storandt M. A longitudinal EEG study of mild senile dementia of Alzheimer type: changes at 1 year and at 2.5 years. *Electroencephalogr Clin Neurophysiol* 1985;61(2):101–112.
211. Verdoorn TA, McCarten JR, Arciniegas DB, et al. Evaluation and tracking of Alzheimer's disease severity using resting-state magnetoencephalography. *J. Alzheimers Dis.* 2011;26 Suppl 3:239–255.
212. Kwak YT. Quantitative EEG findings in different stages of Alzheimer's disease. *J Clin Neurophysiol* 2006;23(5):456–461.

213. Caviness JN, Hentz JG, Belden CM, et al. Longitudinal EEG changes correlate with cognitive measure deterioration in Parkinson's disease. *J Parkinsons Dis* 2015;5(1):117–124.
214. Dubbelink O, E KT, Hillebrand A, et al. Disrupted brain network topology in Parkinson's disease: a longitudinal magnetoencephalography study. *Brain* 2014;137(1):197–207.
215. Menon P, Geevasinga N, Yiannikas C, et al. Sensitivity and specificity of threshold tracking transcranial magnetic stimulation for diagnosis of amyotrophic lateral sclerosis: a prospective study. *Lancet Neurol* 2015;14(5):478–484.
216. Vucic S, Kiernan MC. Cortical excitability testing distinguishes Kennedy's disease from amyotrophic lateral sclerosis. *Clin Neurophysiol* 2008;119(5):1088–1096.
217. Mori F, Codecà C, Kusayanagi H, et al. Effects of intermittent theta burst stimulation on spasticity in patients with multiple sclerosis. *Eur. J. Neurol.* 2010;17(2):295–300.
218. Mori F, Ljoka C, Magni E, et al. Transcranial magnetic stimulation primes the effects of exercise therapy in multiple sclerosis. *J. Neurol.* 2011;258(7):1281–1287.
219. Chang WH, Kim MS, Park E, et al. Effect of Dual-Mode and Dual-Site Noninvasive Brain Stimulation on Freezing of Gait in Patients With Parkinson Disease. *Arch Phys Med Rehabil* 2017;98(7):1283–1290.
220. Kim MS, Chang WH, Cho JW, et al. Efficacy of cumulative high-frequency rTMS on freezing of gait in Parkinson's disease. *Restor. Neurol. Neurosci.* 2015;33(4):521–530.
221. Lesenskyj AM, Samples MP, Farmer JM, Maxwell CR. Treating refractory depression in Parkinson's disease: a meta-analysis of transcranial magnetic stimulation. *Translational Neurodegeneration* 2018;7(1):8.
222. Antczak J, Kowalska K, Klimkowicz-Mrowiec A, et al. Repetitive transcranial magnetic stimulation for the treatment of cognitive impairment in frontotemporal dementia: an open-label pilot study. *Neuropsychiatr Dis Treat* 2018;14:749–755.
223. Rutherford G, Lithgow B, Moussavi Z. Short and Long-term Effects of rTMS Treatment on Alzheimer's Disease at Different Stages: A Pilot Study. *J Exp Neurosci* 2015;9:43–51.
224. Deuschl G, Schade-Brittinger C, Krack P, et al. A randomized trial of deep-brain stimulation for Parkinson's disease. *N. Engl. J. Med.* 2006;355(9):896–908.
225. Kuhn J, Hardenacke K, Lenartz D, et al. Deep brain stimulation of the nucleus basalis of Meynert in Alzheimer's dementia. *Molecular Psychiatry* 2015;20(3):353–360.
226. Nishida K, Yoshimura M, Isotani T, et al. Differences in quantitative EEG between frontotemporal dementia and Alzheimer's disease as revealed by LORETA. *Clin Neurophysiol* 2011;122(9):1718–1725.
227. Iyer PM, Egan C, Pinto-Grau M, et al. Functional Connectivity Changes in Resting-State EEG as Potential Biomarker for Amyotrophic Lateral Sclerosis. *PLoS ONE* 2015;10(6):e0128682.
228. Phukan J, Pender NP, Hardiman O. Cognitive impairment in amyotrophic lateral sclerosis. *The Lancet Neurology* 2007;6(11):994–1003.
229. Zhou J, Greicius MD, Gennatas ED, et al. Divergent network connectivity changes in

- behavioural variant frontotemporal dementia and Alzheimer's disease. *Brain* 2010;133(5):1352–1367.
230. Momma F, Tsutsui T, Symon L, Ono M. The clinical significance of the P15 wave of the somatosensory evoked potential in tentorial herniation. *Neurol. Res.* 1987;9(3):154–158.
  231. Leocani L, Rovaris M, Martinelli-Boneschi F, et al. Movement preparation is affected by tissue damage in multiple sclerosis: Evidence from EEG event-related desynchronization. *Clinical Neurophysiology* 2005;116(7):1515–1519.
  232. Defebvre L, Bourriez J-L, Dujardin K, et al. Spatiotemporal study of Bereitschaftspotential and Event-Related Desynchronization during voluntary movement in Parkinson's disease. *Brain Topogr* 1994;6(3):237–244.
  233. Defebvre L, Bourriez JL, Destee A, Guieu JD. Movement related desynchronisation pattern preceding voluntary movement in untreated Parkinson's disease. *Journal of Neurology, Neurosurgery & Psychiatry* 1996;60(3):307–312.
  234. Defebvre L, Bourriez JL, Derambure P, et al. Influence of chronic administration of L-DOPA on event-related desynchronization of mu rhythm preceding voluntary movement in Parkinson's disease. *Electroencephalography and Clinical Neurophysiology/Electromyography and Motor Control* 1998;109(2):161–167.
  235. Barratt EL, Tewarie PK, Clarke MA, et al. Abnormal task driven neural oscillations in multiple sclerosis: A visuomotor MEG study. *Hum Brain Mapp* 2017;38(5):2441–2453.
  236. Riva N, Falini A, Inuggi A, et al. Cortical activation to voluntary movement in amyotrophic lateral sclerosis is related to corticospinal damage: electrophysiological evidence. *Clin Neurophysiol* 2012;123(8):1586–1592.
  237. Diez null, Ortmayr B, Pichler-Zalaudek K, et al. Ereignisbezogene EEG-Desynchronisation und Synchronisation (ERD und ERS) bei idiopathischem Parkinson-Syndrom. *Klin Neurophysiol* 1999;30(1):15–21.
  238. Pfurtscheller G, Pichler-Zalaudek K, Ortmayr B, et al. Postmovement beta synchronization in patients with Parkinson's disease. *J Clin Neurophysiol* 1998;15(3):243–250.
  239. Deecke L. Bereitschaftspotential as an indicator of movement preparation in supplementary motor area and motor cortex. *Ciba Found. Symp.* 1987;132:231–250.
  240. Brunia CH, van Boxtel GJ, Böcker KB. Negative slow waves as indices of anticipation: the Bereitschaftspotential, the contingent negative variation, and the stimulus-preceding negativity. In: *The Oxford handbook of event-related potential components*. 2012
  241. Leuthold H, Jentzsch I. Neural correlates of advance movement preparation: a dipole source analysis approach. *Cognitive Brain Research* 2001;12(2):207–224.
  242. Brunia CHM. Movement and stimulus preceding negativity. *Biological Psychology* 1988;26(1):165–178.
  243. Hultin L, Rossini P, Romani GL, et al. Neuromagnetic localization of the late component of the contingent negative variation. *Electroencephalography and clinical Neurophysiology* 1996;98(6):435–448.
  244. Ikeda A, Lüders HO, Collura TF, et al. Subdural potentials at orbitofrontal and mesial prefrontal areas accompanying anticipation and decision making in humans: a comparison



- with Bereitschaftspotential. *Electroencephalography and clinical Neurophysiology* 1996;98(3):206–212.
245. Dick JP, Rothwell JC, Day BL, et al. The Bereitschaftspotential is abnormal in Parkinson's disease. *Brain* 1989;112 ( Pt 1):233–244.
  246. Patil AL, Sood SK, Goyal V, Kochhar KP. Cortical Potentials Prior to Movement in Parkinson's Disease. *J Clin Diagn Res* 2017;11(3):CC13–CC16.
  247. Westphal KP, Heinemann HA, Grözinger B, et al. Bereitschaftspotential in amyotrophic lateral sclerosis (ALS): lower amplitudes in patients with hyperreflexia (spasticity). *Acta neurologica scandinavica* 1998;98(1):15–21.
  248. Hanagasi HA, Gurvit IH, Ermutlu N, et al. Cognitive impairment in amyotrophic lateral sclerosis: evidence from neuropsychological investigation and event-related potentials. *Brain Res Cogn Brain Res* 2002;14(2):234–244.
  249. Pulvermüller F, Lutzenberger W, Müller V, et al. P3 and contingent negative variation in Parkinson's disease. *Electroencephalography and Clinical Neurophysiology* 1996;98(6):456–467.
  250. Uysal U, Idiman F, Idiman E, et al. Contingent negative variation is associated with cognitive dysfunction and secondary progressive disease course in multiple sclerosis. *J Clin Neurol* 2014;10(4):296–303.
  251. Praamstra P, Meyer AS, Cools AR, et al. Movement preparation in Parkinson's disease Time course and distribution of movement-related potentials in a movement precueing task. *Brain* 1996;119(5):1689–1704.
  252. van Deursen JA, Vuurman EFPM, Smits LL, et al. Response speed, contingent negative variation and P300 in Alzheimer's disease and MCI. *Brain Cogn* 2009;69(3):592–599.
  253. Banoub M, Tetzlaff JE, Schubert A. Pharmacologic and Physiologic Influences Affecting Sensory Evoked Potentials Implications for Perioperative Monitoring. *Anesthes* 2003;99(3):716–737.
  254. Abbruzzese G, Dall'Agata D, Morena M, et al. Abnormalities of parietal and prerolandic somatosensory evoked potentials in Huntington's disease. *Electroencephalography and Clinical Neurophysiology/Evoked Potentials Section* 1990;77(5):340–346.
  255. Zhang J, Yin X, Zhao L, et al. Regional alterations in cortical thickness and white matter integrity in amyotrophic lateral sclerosis. *J. Neurol.* 2014;261(2):412–421.
  256. Josiassen RC, Shagass C, Mancall EL, Roemer RA. Somatosensory evoked potentials in Huntington's disease. *Electroencephalography and Clinical Neurophysiology* 1982;54(5):483–493.
  257. Cullen B, O'Neill B, Evans JJ, et al. A review of screening tests for cognitive impairment. *J. Neurol. Neurosurg. Psychiatry* 2007;78(8):790–799.
  258. Sur S, Sinha VK. Event-related potential: An overview. *Ind Psychiatry J* 2009;18(1):70–73.
  259. Alain C, Tremblay K. The role of event-related brain potentials in assessing central auditory processing. *J Am Acad Audiol* 2007;18(7):573–589.

260. Papanicolaou AC, Baumann S, Rogers RL, et al. Localization of auditory response sources using magnetoencephalography and magnetic resonance imaging. *Arch Neurol* 1990;47(1):33–37.
261. Pinkhardt EH, Jürgens R, Becker W, et al. Signs of impaired selective attention in patients with amyotrophic lateral sclerosis. *J. Neurol.* 2008;255(4):532–538.
262. Volpato C, Piccione F, Silvoni S, et al. Working memory in amyotrophic lateral sclerosis: auditory event-related potentials and neuropsychological evidence. *J Clin Neurophysiol* 2010;27(3):198–206.
263. Kujala T, Tervaniemi M, Schröger E. The mismatch negativity in cognitive and clinical neuroscience: theoretical and methodological considerations. *Biol Psychol* 2007;74(1):1–19.
264. Dietz MJ, Friston KJ, Mattingley JB, et al. Effective Connectivity Reveals Right-Hemisphere Dominance in Audiospatial Perception: Implications for Models of Spatial Neglect. *J Neurosci* 2014;34(14):5003–5011.
265. Oades RD, Wild-Wall N, Juran SA, et al. Auditory change detection in schizophrenia: sources of activity, related neuropsychological function and symptoms in patients with a first episode in adolescence, and patients 14 years after an adolescent illness-onset. *BMC Psychiatry* 2006;6:7.
266. Rinne T, Alho K, Ilmoniemi RJ, et al. Separate time behaviors of the temporal and frontal mismatch negativity sources. *Neuroimage* 2000;12(1):14–19.
267. Iyer PM, Mohr K, Broderick M, et al. Mismatch negativity as an indicator of cognitive sub-domain dysfunction in amyotrophic lateral sclerosis. *Frontiers in neurology* 2017;8:395.
268. Polich J. Updating P300: an integrative theory of P3a and P3b. *Clinical neurophysiology* 2007;118(10):2128–2148.
269. Gil R, Neau JP, Dary-Auriol M, et al. Event-related auditory evoked potentials and amyotrophic lateral sclerosis. *Arch. Neurol.* 1995;52(9):890–896.
270. Näätänen R. Processing negativity: An evoked-potential reflection. *Psychological bulletin* 1982;92(3):605.
271. Näätänen R. The role of attention in auditory information processing as revealed by event-related potentials and other brain measures of cognitive function. *Behavioral and Brain Sciences* 1990;13(2):201–233.
272. Vieregge P, Wauschkuhn B, Heberlein I, et al. Selective attention is impaired in amyotrophic lateral sclerosis—a study of event-related EEG potentials. *Cognitive Brain Research* 1999;8(1):27–35.
273. Walter WG, Cooper R, Aldridge VJ, et al. Contingent Negative Variation: An Electric Sign of Sensorimotor Association and Expectancy in The Human Brain. *Nature* 1964;203:380–384.
274. Brunia CHM, Damen EJP. Distribution of slow brain potentials related to motor preparation and stimulus anticipation in a time estimation task. *Electroencephalography and Clinical Neurophysiology* 1988;69(3):234–243.

275. Rosahl SK, Knight RT. Role of Prefrontal Cortex in Generation of the Contingent Negative Variation. *Cereb Cortex* 1995;5(2):123–134.
276. Colebatch JG. Bereitschaftspotential and movement-related potentials: Origin, significance, and application in disorders of human movement. *Mov. Disord.* 2007;22(5):601–610.
277. Lai C-L, Lin R-T, Liou L-M, Liu C-K. The role of event-related potentials in cognitive decline in Alzheimer's disease. *Clinical Neurophysiology* 2010;121(2):194–199.
278. Pedroso RV, Fraga FJ, Corazza DI, et al. P300 latency and amplitude in Alzheimer's disease: a systematic review. *Brazilian Journal of Otorhinolaryngology* 2012;78(4):126–132.
279. Tokic K, Titlic M, Beganovic-Petrovic A, et al. P300 Wave Changes in Patients with Parkinson's Disease. *Med Arch* 2016;70(6):453–456.
280. Kimiskidis VK, Papaliagkas V, Sotirakoglou K, et al. Cognitive event-related potentials in multiple sclerosis: Correlation with MRI and neuropsychological findings. *Mult Scler Relat Disord* 2016;10:192–197.
281. Portet F, Cadilhac C, Touchon J, Camu W. Cognitive impairment in motor neuron disease with bulbar onset. *Amyotrophic Lateral Sclerosis and Other Motor Neuron Disorders* 2001;2(1):23–29.
282. Lee M-S, Lee S-H, Moon E-O, et al. Neuropsychological correlates of the P300 in patients with Alzheimer's disease. *Prog. Neuropsychopharmacol. Biol. Psychiatry* 2013;40:62–69.
283. Brønneck KS, Nordby H, Larsen JP, Aarsland D. Disturbance of automatic auditory change detection in dementia associated with Parkinson's disease: A mismatch negativity study. *Neurobiology of Aging* 2010;31(1):104–113.
284. Jung J, Morlet D, Mercier B, et al. Mismatch negativity (MMN) in multiple sclerosis: an event-related potentials study in 46 patients. *Clin Neurophysiol* 2006;117(1):85–93.
285. Horvath A, Szucs A, Csukly G, et al. EEG and ERP biomarkers of Alzheimer's disease: a critical review. *Front Biosci (Landmark Ed)* 2018;23:183–220.
286. Ball SS, Marsh JT, Schubarth G, et al. Longitudinal P300 latency changes in Alzheimer's disease. *J Gerontol* 1989;44(6):M195-200.
287. St Clair D, Blackburn I, Blackwood D, Tyrer G. Measuring the course of Alzheimer's disease. A longitudinal study of neuropsychological function and changes in P3 event-related potential. *Br J Psychiatry* 1988;152:48–54.
288. Vucic S, Nicholson GA, Kiernan MC. Cortical hyperexcitability may precede the onset of familial amyotrophic lateral sclerosis. *Brain* 2008;131(6):1540–1550.
289. Grieve SM, Menon P, Korgaonkar MS, et al. Potential structural and functional biomarkers of upper motor neuron dysfunction in ALS. *Amyotroph Lateral Scler Frontotemporal Degener* 2015;17(1–2):85–92.
290. Liepert J, Bär KJ, Meske U, Weiller C. Motor cortex disinhibition in Alzheimer's disease. *Clin Neurophysiol* 2001;112(8):1436–1441.
291. Ni Z, Bahl N, Gunraj CA, et al. Increased motor cortical facilitation and decreased

- inhibition in Parkinson disease. *Neurology* 2013;80(19):1746–1753.
292. Abbruzzese G, Buccolieri A, Marchese R, et al. Intracortical inhibition and facilitation are abnormal in Huntington's disease: a paired magnetic stimulation study. *Neurosci. Lett.* 1997;228(2):87–90.
  293. Leon-Sarmiento FE, Rizzo-Sierra CV, Bayona EA, et al. Novel mechanisms underlying inhibitory and facilitatory transcranial magnetic stimulation abnormalities in Parkinson's disease. *Arch. Med. Res.* 2013;44(3):221–228.
  294. Park J, Chang WH, Cho JW, et al. Usefulness of Transcranial Magnetic Stimulation to Assess Motor Function in Patients With Parkinsonism. *Ann Rehabil Med* 2016;40(1):81–87.
  295. Pierantozzi M, Palmieri MG, Mazzone P, et al. Deep brain stimulation of both subthalamic nucleus and internal globus pallidus restores intracortical inhibition in Parkinson's disease paralleling apomorphine effects: a paired magnetic stimulation study. *Clin Neurophysiol* 2002;113(1):108–113.
  296. George MS, Taylor JJ, Short EB. The Expanding Evidence Base for rTMS Treatment of Depression. *Curr Opin Psychiatry* 2013;26(1):13–18.
  297. Zhu H, Lu Z, Jin Y, et al. Low-frequency repetitive transcranial magnetic stimulation on Parkinson motor function: a meta-analysis of randomised controlled trials. *Acta Neuropsychiatr* 2015;27(2):82–89.
  298. Scheltens P, Twisk JW, Blesa R, et al. Efficacy of Souvenaid in mild Alzheimer's disease: results from a randomized, controlled trial. *Journal of Alzheimer's Disease* 2012;31(1):225–236.
  299. Jang SH. The corticospinal tract from the viewpoint of brain rehabilitation. *J Rehabil Med* 2014;46(3):193–199.
  300. Ahmed Z. Modulation of gamma and alpha spinal motor neurons activity by trans-spinal direct current stimulation: effects on reflexive actions and locomotor activity. *Physiol Rep* 2016;4(3):e12696.
  301. Harvey L. Chapter 1 - Background information. In: *Management of Spinal Cord Injuries*. Edinburgh: Churchill Livingstone; 2008 p. 3–33.
  302. Keller A, Asanuma H. Synaptic relationships involving local axon collaterals of pyramidal neurons in the cat motor cortex. *J. Comp. Neurol.* 1993;336(2):229–242.
  303. Seo JP, Jang SH. Different characteristics of the corticospinal tract according to the cerebral origin: DTI study. *AJNR Am J Neuroradiol* 2013;34(7):1359–1363.
  304. Roccatagliata L, Bonzano L, Mancardi G, et al. Detection of motor cortex thinning and corticospinal tract involvement by quantitative MRI in amyotrophic lateral sclerosis. *Amyotroph Lateral Scler* 2009;10(1):47–52.
  305. Thorns J, Jansma H, Peschel T, et al. Extent of cortical involvement in amyotrophic lateral sclerosis--an analysis based on cortical thickness. *BMC Neurol* 2013;13:148.
  306. Verstraete E, van den Heuvel MP, Veldink JH, et al. Motor network degeneration in amyotrophic lateral sclerosis: a structural and functional connectivity study. *PLoS ONE* 2010;5(10):e13664.

307. Verstraete E, Veldink JH, Hendrikse J, et al. Structural MRI reveals cortical thinning in amyotrophic lateral sclerosis. *J. Neurol. Neurosurg. Psychiatry* 2012;83(4):383–388.
308. Mochizuki Y, Mizutani T, Shimizu T, Kawata A. Proportional neuronal loss between the primary motor and sensory cortex in amyotrophic lateral sclerosis. *Neurosci. Lett.* 2011;503(1):73–75.
309. Grosskreutz J, Kaufmann J, Frädrieh J, et al. Widespread sensorimotor and frontal cortical atrophy in Amyotrophic Lateral Sclerosis. *BMC Neurol* 2006;6:17.
310. Cosottini M, Cecchi P, Piazza S, et al. Mapping Cortical Degeneration in ALS with Magnetization Transfer Ratio and Voxel-Based Morphometry. *PLOS ONE* 2013;8(7):e68279.
311. Kew JJ, Leigh PN, Playford ED, et al. Cortical function in amyotrophic lateral sclerosis. A positron emission tomography study. *Brain* 1993;116 ( Pt 3):655–680.
312. Huynh W, Simon NG, Grosskreutz J, et al. Assessment of the upper motor neuron in amyotrophic lateral sclerosis. *Clin Neurophysiol* 2016;127(7):2643–2660.
313. Sage CA, Van Hecke W, Peeters R, et al. Quantitative diffusion tensor imaging in amyotrophic lateral sclerosis: revisited. *Human brain mapping* 2009;30(11):3657–3675.
314. Sarica A, Cerasa A, Valentino P, et al. The corticospinal tract profile in amyotrophic lateral sclerosis. *Hum. Brain Mapp.* 2017;38(2):727–739.
315. Agosta F, Al-Chalabi A, Filippi M, et al. The El Escorial criteria: strengths and weaknesses. *Amyotroph Lateral Scler Frontotemporal Degener* 2015;16(1–2):1–7.
316. Kaufmann P, Mitsumoto H. Amyotrophic lateral sclerosis: objective upper motor neuron markers. *Curr Neurol Neurosci Rep* 2002;2(1):55–60.
317. Al-Chalabi A, Hardiman O, Kiernan MC, et al. Amyotrophic lateral sclerosis: moving towards a new classification system. *Lancet Neurol* 2016;15(11):1182–1194.
318. Caramia MD, Cicinelli P, Paradiso C, et al. 'Excitability changes of muscular responses to magnetic brain stimulation in patients with central motor disorders. *Electroencephalogr Clin Neurophysiol* 1991;81(4):243–250.
319. Mills KR, Nithi KA. Corticomotor threshold to magnetic stimulation: normal values and repeatability. *Muscle & nerve* 1997;20(5):570–576.
320. Menon P, Geevasinga N, van den Bos M, et al. Cortical hyperexcitability and disease spread in amyotrophic lateral sclerosis. *Eur. J. Neurol.* 2017;24(6):816–824.
321. Vucic S, Ziemann U, Eisen A, et al. Transcranial magnetic stimulation and amyotrophic lateral sclerosis: pathophysiological insights. *J Neurol Neurosurg Psychiatry* 2013;84(10):1161–1170.
322. Attarian S, Azulay J-P, Lardillier D, et al. Transcranial magnetic stimulation in lower motor neuron diseases. *Clinical Neurophysiology* 2005;116(1):35–42.
323. Desiato MT, Caramia MD. Towards a neurophysiological marker of amyotrophic lateral sclerosis as revealed by changes in cortical excitability. *Electroencephalogr Clin Neurophysiol* 1997;105(1):1–7.

324. Desiato MT, Bernardi G, Hagi A, et al. Transcranial magnetic stimulation of motor pathways directed to muscles supplied by cranial nerves in amyotrophic lateral sclerosis. *Clinical Neurophysiology* 2002;113(1):132–140.
325. Siciliano G, Manca ML, Saggiocco L, et al. Cortical silent period in patients with amyotrophic lateral sclerosis. *J. Neurol. Sci.* 1999;169(1–2):93–97.
326. Vucic S, Cheah BC, Yiannikas C, et al. Corticomotoneuronal function and hyperexcitability in acquired neuromyotonia. *Brain* 2010;133(9):2727–2733.
327. Zanette G, Tamburin S, Manganotti P, et al. Changes in motor cortex inhibition over time in patients with amyotrophic lateral sclerosis. *J. Neurol.* 2002;249(12):1723–1728.
328. Floyd AG, Yu QP, Piboolnurak P, et al. Transcranial magnetic stimulation in ALS: utility of central motor conduction tests. *Neurology* 2009;72(6):498–504.
329. Triggs WJ, Menkes D, Onorato J, et al. Transcranial magnetic stimulation identifies upper motor neuron involvement in motor neuron disease. *Neurology* 1999;53(3):605–611.
330. Mills KR. The natural history of central motor abnormalities in amyotrophic lateral sclerosis. *Brain* 2003;126(11):2558–2566.
331. Prout AJ, Eisen AA. The cortical silent period and amyotrophic lateral sclerosis. *Muscle Nerve* 1994;17(2):217–223.
332. Eisen A, Pant B, Stewart H. Cortical excitability in amyotrophic lateral sclerosis: a clue to pathogenesis. *Canadian journal of neurological sciences* 1993;20(1):11–16.
333. Eisen A, Shytbel W, Murphy K, Hoirsch M. Cortical magnetic stimulation in amyotrophic lateral sclerosis. *Muscle Nerve* 1990;13(2):146–151.
334. Bos MAV den, Geevasinga N, Menon P, et al. Imbalance in cortical inhibition-excitation networks underlies als. *J Neurol Neurosurg Psychiatry* 2017;88(5):e1–e1.
335. Stefan K, Kunesch E, Benecke R, Classen J. Effects of riluzole on cortical excitability in patients with amyotrophic lateral sclerosis. *Ann. Neurol.* 2001;49(4):536–539.
336. Yokota T, Yoshino A, Inaba A, Saito Y. Double cortical stimulation in amyotrophic lateral sclerosis. *J. Neurol. Neurosurg. Psychiatry* 1996;61(6):596–600.
337. Ziemann U, Winter M, Reimers CD, et al. Impaired motor cortex inhibition in patients with amyotrophic lateral sclerosis. Evidence from paired transcranial magnetic stimulation. *Neurology* 1997;49(5):1292–1298.
338. Agarwal S, Highton-Williamson E, Caga J, et al. Primary lateral sclerosis and the amyotrophic lateral sclerosis-frontotemporal dementia spectrum. *J. Neurol.* 2018;265(8):1819–1828.
339. Sommer M, Tergau F, Wischer S, et al. Riluzole does not have an acute effect on motor thresholds and the intracortical excitability in amyotrophic lateral sclerosis. *J. Neurol.* 1999;246 Suppl 3:III22–III26.
340. Bizovičar N, Koritnik B, Zidar I, et al. Movement-related cortical potentials in ALS increase at lower and decrease at higher upper motor neuron burden scores. *Amyotroph Lateral Scler Frontotemporal Degener* 2013;14(5–6):380–389.

341. Dukic S, McMackin R, Buxo T, et al. Patterned functional network disruption in amyotrophic lateral sclerosis. *Human brain mapping* 2019;40(16):4827–4842.
342. Jones SR, Pinto DJ, Kaper TJ, Kopell N. Alpha-frequency rhythms desynchronize over long cortical distances: a modeling study. *J Comput Neurosci* 2000;9(3):271–291.
343. Lukatch HS, MacIver MB. Physiology, pharmacology, and topography of cholinergic neocortical oscillations in vitro. *J. Neurophysiol.* 1997;77(5):2427–2445.
344. Ziemann U. Pharmacology of TMS measures. Wassermann EM, ZU, Walsh, V., Paus, T., Lisanby, S.(Eds.), *The Oxford Handbook of Transcranial Stimulation*. Oxford University Press Inc, New York 2008;135–151.
345. Di Lazzaro V, Profice P, Ranieri F, et al. I-wave origin and modulation. *Brain Stimul* 2012;5(4):512–525.
346. Kasahara T, Terasaki K, Ogawa Y, et al. The correlation between motor impairments and event-related desynchronization during motor imagery in ALS patients. *BMC Neurosci* 2012;13:66.
347. Proudfoot M, Rohenkohl G, Quinn A, et al. Altered cortical beta-band oscillations reflect motor system degeneration in amyotrophic lateral sclerosis. *Human brain mapping* 2017;38(1):237–254.
348. Bai O, Vorbach S, Hallett M, Floeter MK. Movement-related cortical potentials in primary lateral sclerosis. *Annals of neurology* 2006;59(4):682–690.
349. Georges M, Moraviec E, Raux M, et al. Cortical drive to breathe in amyotrophic lateral sclerosis: a dyspnoea-worsening defence? *Eur. Respir. J.* 2016;47(6):1818–1828.
350. Del Aguila MA, Longstreth WT, McGuire V, et al. Prognosis in amyotrophic lateral sclerosis A population-based study. *Neurology* 2003;60(5):813–819.
351. Chen R, Yaseen Z, Cohen LG, Hallett M. Time course of corticospinal excitability in reaction time and self-paced movements. *Ann. Neurol.* 1998;44(3):317–325.
352. Maekawa S, Al-Sarraj S, Kibble M, et al. Cortical selective vulnerability in motor neuron disease: a morphometric study. *Brain* 2004;127(Pt 6):1237–1251.
353. Nihei K, Kowall NW. Involvement of NPY-immunoreactive neurons in the cerebral cortex of amyotrophic lateral sclerosis patients. *Neurosci. Lett.* 1993;159(1–2):67–70.
354. Petri S, Krampfl K, Hashemi F, et al. Distribution of GABAA receptor mRNA in the motor cortex of ALS patients. *Journal of Neuropathology & Experimental Neurology* 2003;62(10):1041–1051.
355. Lloyd CM, Richardson MP, Brooks DJ, et al. Extramotor involvement in ALS: PET studies with the GABAA ligand [11C] flumazenil. *Brain* 2000;123(11):2289–2296.
356. McGown A, McDearmid JR, Panagiotaki N, et al. Early interneuron dysfunction in ALS: insights from a mutant *sod1* zebrafish model. *Annals of neurology* 2013;73(2):246–258.
357. Zhang W, Zhang L, Liang B, et al. Hyperactive Somatostatin Interneurons Contribute to Excitotoxicity in Neurodegenerative Disorders. *Nat Neurosci* 2016;19(4):557–559.
358. Chouinard PA, Paus T. The primary motor and premotor areas of the human cerebral

- cortex. *Neuroscientist* 2006;12(2):143–152.
359. Nachev P, Kennard C, Husain M. Functional role of the supplementary and pre-supplementary motor areas. *Nat. Rev. Neurosci.* 2008;9(11):856–869.
  360. Mochizuki H, Huang Y-Z, Rothwell JC. Interhemispheric interaction between human dorsal premotor and contralateral primary motor cortex. *J. Physiol. (Lond.)* 2004;561(Pt 1):331–338.
  361. Mannarelli D, Pauletti C, Locuratolo N, et al. Attentional processing in bulbar- and spinal-onset amyotrophic lateral sclerosis: insights from event-related potentials. *Amyotroph Lateral Scler Frontotemporal Degener* 2014;15(1–2):30–38.
  362. Rockstroh B, Müller M, Wagner M, et al. “Probing” the nature of the CNV. *Electroencephalography and clinical Neurophysiology* 1993;87(4):235–241.
  363. Thorns J, Wieringa BM, Mohammadi B, et al. Movement initiation and inhibition are impaired in amyotrophic lateral sclerosis. *Experimental neurology* 2010;224(2):389–394.
  364. Alexander GE, DeLong MR, Strick PL. Parallel organization of functionally segregated circuits linking basal ganglia and cortex. *Annu. Rev. Neurosci.* 1986;9:357–381.
  365. Groenewegen HJ. The basal ganglia and motor control. *Neural Plast.* 2003;10(1–2):107–120.
  366. Barbin L, Leux C, Sauleau P, et al. Non-homogeneous effect of levodopa on inhibitory circuits in Parkinson’s disease and dyskinesia. *Parkinsonism Relat. Disord.* 2013;19(2):165–170.
  367. Tremblay L, Worbe Y, Thobois S, et al. Selective dysfunction of basal ganglia subterritories: From movement to behavioral disorders. *Mov. Disord.* 2015;30(9):1155–1170.
  368. Kemp J, Berthel M-C, Dufour A, et al. Caudate nucleus and social cognition: neuropsychological and SPECT evidence from a patient with focal caudate lesion. *Cortex* 2013;49(2):559–571.
  369. Bede P, Elamin M, Byrne S, et al. Basal ganglia involvement in amyotrophic lateral sclerosis. *Neurology* 2013;81(24):2107–2115.
  370. Pessoa L. On the relationship between emotion and cognition. *Nature reviews neuroscience* 2008;9(2):148.
  371. Fuster JM. Prefrontal cortex. In: *Comparative neuroscience and neurobiology*. Springer; 1988 p. 107–109.
  372. Miller EK. The prefrontal cortex and cognitive control. *Nat. Rev. Neurosci.* 2000;1(1):59–65.
  373. Miller EK, Wallis JD. Executive function and higher-order cognition: definition and neural substrates. *Encyclopedia of neuroscience* 2009;4(99–104)
  374. Seeley WW, Merkle FT, Gaus SE, et al. Distinctive neurons of the anterior cingulate and frontoinsula cortex: a historical perspective. *Cerebral Cortex* 2011;22(2):245–250.
  375. Johnson JK, Diehl J, Mendez MF, et al. Frontotemporal lobar degeneration: demographic



- characteristics of 353 patients. *Archives of neurology* 2005;62(6):925–930.
376. Lomen-Hoerth C, Anderson T, Miller B. The overlap of amyotrophic lateral sclerosis and frontotemporal dementia. *Neurology* 2002;59(7):1077–1079.
  377. Agosta F, Valsasina P, Riva N, et al. The cortical signature of amyotrophic lateral sclerosis. *PLoS One* 2012;7(8):e42816.
  378. Grossman M, Anderson C, Khan A, et al. Impaired action knowledge in amyotrophic lateral sclerosis. *Neurology* 2008;71(18):1396–1401.
  379. Buhour M-S, Doidy F, Mondou A, et al. Voxel-based mapping of grey matter volume and glucose metabolism profiles in amyotrophic lateral sclerosis. *EJNMMI research* 2017;7(1):21.
  380. Ciccarelli O, Behrens TE, Johansen-Berg H, et al. Investigation of white matter pathology in ALS and PLS using tract-based spatial statistics. *Human brain mapping* 2009;30(2):615–624.
  381. Talbot PR, Goulding PJ, Lloyd JJ, et al. Inter-relation between " classic" motor neuron disease and frontotemporal dementia: neuropsychological and single photon emission computed tomography study. *Journal of Neurology, Neurosurgery & Psychiatry* 1995;58(5):541–547.
  382. Abrahams S, Leigh PN, Kew JJM, et al. A positron emission tomography study of frontal lobe function (verbal fluency) in amyotrophic lateral sclerosis. *Journal of the neurological sciences* 1995;129:44–46.
  383. Stevens FL, Hurley RA, Taber KH. Anterior cingulate cortex: unique role in cognition and emotion. *The Journal of neuropsychiatry and clinical neurosciences* 2011;23(2):121–125.
  384. Cheney PD. Role of cerebral cortex in voluntary movements. A review. *Phys Ther* 1985;65(5):624–635.
  385. Inuggi A, Riva N, González-Rosa JJ, et al. Compensatory movement-related recruitment in amyotrophic lateral sclerosis patients with dominant upper motor neuron signs: an EEG source analysis study. *Brain Res.* 2011;1425:37–46.
  386. Agosta F, Chio A, Cosottini M, et al. The present and the future of neuroimaging in amyotrophic lateral sclerosis. *American Journal of Neuroradiology* 2010;31(10):1769–1777.
  387. Petrides M, Pandya DN. Dorsolateral prefrontal cortex: comparative cytoarchitectonic analysis in the human and the macaque brain and corticocortical connection patterns. *European Journal of Neuroscience* 1999;11(3):1011–1036.
  388. O'Reilly RC. The what and how of prefrontal cortical organization. *Trends in neurosciences* 2010;33(8):355–361.
  389. Badre D, Wagner AD. Left ventrolateral prefrontal cortex and the cognitive control of memory. *Neuropsychologia* 2007;45(13):2883–2901.
  390. Stalnaker TA, Cooch NK, Schoenbaum G. What the orbitofrontal cortex does not do. *Nature neuroscience* 2015;18(5):620.
  391. Leech R, Braga R, Sharp DJ. Echoes of the brain within the posterior cingulate cortex. *J.*

- Neurosci. 2012;32(1):215–222.
392. Menke RAL, Proudfoot M, Talbot K, Turner MR. The two-year progression of structural and functional cerebral MRI in amyotrophic lateral sclerosis. *NeuroImage: Clinical* 2018;17:953–961.
  393. Proudfoot M, Colclough GL, Quinn A, et al. Increased cerebral functional connectivity in ALS: A resting-state magnetoencephalography study. *Neurology* 2018;90(16):e1418–e1424.
  394. Creem SH, Proffitt DR. Defining the cortical visual systems: “what”, “where”, and “how.” *Acta psychologica* 2001;107(1–3):43–68.
  395. Haxby JV, Gobbini MI, Furey ML, et al. Distributed and overlapping representations of faces and objects in ventral temporal cortex. *Science* 2001;293(5539):2425–2430.
  396. Acheson DJ, Hagoort P. Stimulating the brain’s language network: syntactic ambiguity resolution after TMS to the inferior frontal gyrus and middle temporal gyrus. *J Cogn Neurosci* 2013;25(10):1664–1677.
  397. Howard MA, Volkov IO, Mirsky R, et al. Auditory cortex on the human posterior superior temporal gyrus. *J. Comp. Neurol.* 2000;416(1):79–92.
  398. Chang EF, Rieger JW, Johnson K, et al. Categorical speech representation in human superior temporal gyrus. *Nat. Neurosci.* 2010;13(11):1428–1432.
  399. Hübers A, Boeckler B, Abaei A, et al. Functional and structural impairment of transcallosal motor fibres in ALS: a study using transcranial magnetic stimulation, diffusion tensor imaging, and diffusion weighted spectroscopy. *Brain imaging and behavior* 2020;
  400. Karandreas N, Papadopoulou M, Kokotis P, et al. Impaired interhemispheric inhibition in amyotrophic lateral sclerosis. *Amyotroph Lateral Scler* 2007;8(2):112–118.
  401. Wittstock M, Wolters A, Benecke R. Transcallosal inhibition in amyotrophic lateral sclerosis. *Clin Neurophysiol* 2007;118(2):301–307.
  402. Wittstock M, Wilde N, Grossmann A, et al. Mirror Movements in Amyotrophic Lateral Sclerosis: A Combined Study Using Diffusion Tensor Imaging and Transcranial Magnetic Stimulation. *Front Neurol* 2020;11:164.
  403. McGlone F, Reilly D. The cutaneous sensory system. *Neurosci Biobehav Rev* 2010;34(2):148–159.
  404. Cosi V, Poloni M, Mazzini L, Callieco R. Somatosensory evoked potentials in amyotrophic lateral sclerosis. *Journal of Neurology, Neurosurgery & Psychiatry* 1984;47(8):857–861.
  405. Iglesias C, Sangari S, El Mendili M-M, et al. Electrophysiological and spinal imaging evidences for sensory dysfunction in amyotrophic lateral sclerosis. *BMJ open* 2015;5(2):e007659.
  406. Mioshi E, Lillo P, Yew B, et al. Cortical atrophy in ALS is critically associated with neuropsychiatric and cognitive changes. *Neurology* 2013;80(12):1117–1123.
  407. Schuster C, Kasper E, Dyrba M, et al. Cortical thinning and its relation to cognition in

- amyotrophic lateral sclerosis. *Neurobiol. Aging* 2014;35(1):240–246.
408. Abrahams S, Goldstein LH, Suckling J, et al. Frontotemporal white matter changes in amyotrophic lateral sclerosis. *Journal of neurology* 2005;252(3):321–331.
  409. Stam CJ, Tewarie P, Van Dellen E, et al. The trees and the forest: Characterization of complex brain networks with minimum spanning trees. *Int J Psychophysiol* 2014;92(3):129–138.
  410. Paulus KS, Magnano I, Piras MR, et al. Visual and auditory event-related potentials in sporadic amyotrophic lateral sclerosis. *Clinical neurophysiology* 2002;113(6):853–861.
  411. Schreiber H, Gaigalat T, Wiedemuth-Catrinescu U, et al. Cognitive function in bulbar- and spinal-onset amyotrophic lateral sclerosis. A longitudinal study in 52 patients. *J. Neurol.* 2005;252(7):772–781.
  412. Ogawa T, Tanaka H, Hirata K. Cognitive deficits in amyotrophic lateral sclerosis evaluated by event-related potentials. *Clin Neurophysiol* 2009;120(4):659–664.
  413. Sahinoglu B, Dogan G. Event-Related Potentials and the Stroop Effect. *Eurasian J Med* 2016;48(1):53–57.
  414. Datta A, Cusack R, Hawkins K, et al. The P300 as a marker of waning attention and error propensity. *Computational intelligence and neuroscience* 2007;2007
  415. Hart EP, Dumas EM, Reijntjes RHAM, et al. Deficient sustained attention to response task and P300 characteristics in early Huntington’s disease. *J Neurol* 2012;259(6):1191–1198.
  416. Sokhadze E, Stewart C, Hollifield M, Tasman A. Event-Related Potential Study of Executive Dysfunctions in a Speeded Reaction Task in Cocaine Addiction. *J Neurother* 2008;12(4):185–204.
  417. Menon V, Uddin LQ. Saliency, switching, attention and control: a network model of insula function. *Brain Structure and Function* 2010;214(5–6):655–667.
  418. Amato N, Riva N, Cursi M, et al. Different frontal involvement in ALS and PLS revealed by Stroop event-related potentials and reaction times. *Frontiers in Aging Neuroscience* 2013;5:82.
  419. Pagani M, Chiò A, Valentini MC, et al. Functional pattern of brain FDG-PET in amyotrophic lateral sclerosis. *Neurology* 2014;83(12):1067–1074.
  420. Wicks P, Turner MR, Abrahams S, et al. Neuronal loss associated with cognitive performance in amyotrophic lateral sclerosis: an (11C)-flumazenil PET study. *Amyotroph Lateral Scler* 2008;9(1):43–49.
  421. Petri S, Kollewe K, Grothe C, et al. GABA(A)-receptor mRNA expression in the prefrontal and temporal cortex of ALS patients. *J. Neurol. Sci.* 2006;250(1–2):124–132.
  422. Wickremaratchi MM, Llewelyn JG. Effects of ageing on touch. *Postgrad Med J* 2006;82(967):301–304.
  423. Longo MR, Azañón E, Haggard P. More than skin deep: Body representation beyond primary somatosensory cortex. *Neuropsychologia* 2010;48(3):655–668.
  424. Cohen YE. Multimodal activity in the parietal cortex. *Hear Res* 2009;258(1–2):100–105.

425. Borich MR, Brodie SM, Gray WA, et al. Understanding the role of the primary somatosensory cortex: Opportunities for rehabilitation. *Neuropsychologia* 2015;79(Pt B):246–255.
426. Verstraete E, Veldink JH, van den Berg LH, van den Heuvel MP. Structural brain network imaging shows expanding disconnection of the motor system in amyotrophic lateral sclerosis. *Hum Brain Mapp* 2014;35(4):1351–1361.
427. Georgesco M, Salerno A, Camu W. Somatosensory evoked potentials elicited by stimulation of lower-limb nerves in amyotrophic lateral sclerosis. *Electroencephalography and Clinical Neurophysiology/Evoked Potentials Section* 1997;104(4):333–342.
428. Shimizu T, Bokuda K, Kimura H, et al. Sensory cortex hyperexcitability predicts short survival in amyotrophic lateral sclerosis. *Neurology* 2018;90(18):e1578–e1587.
429. van Meer N, Houtman AC, Van Schuerbeek P, et al. Interhemispheric Connections between the Primary Visual Cortical Areas via the Anterior Commissure in Human Callosal Agenesis. *Front Syst Neurosci* 2016;10:101.
430. Aboitiz F, Montiel J. One hundred million years of interhemispheric communication: the history of the corpus callosum. *Braz. J. Med. Biol. Res.* 2003;36(4):409–420.
431. van der Knaap LJ, van der Ham IJM. How does the corpus callosum mediate interhemispheric transfer? A review. *Behav. Brain Res.* 2011;223(1):211–221.
432. Carson RG. What is the function of inter-hemispheric inhibition? *J Physiol* 2020;598(21):4781–4802.
433. Andres FG, Mima T, Schulman AE, et al. Functional coupling of human cortical sensorimotor areas during bimanual skill acquisition. *Brain* 1999;122 ( Pt 5):855–870.
434. Berlucchi G. Visual interhemispheric communication and callosal connections of the occipital lobes. *Cortex* 2014;56:1–13.
435. Hinkley LBN, Marco EJ, Brown EG, et al. The Contribution of the Corpus Callosum to Language Lateralization. *J. Neurosci.* 2016;36(16):4522–4533.
436. Sammler D, Kotz SA, Eckstein K, et al. Prosody meets syntax: the role of the corpus callosum. *Brain* 2010;133(9):2643–2655.
437. Huang X, Du X, Song H, et al. Cognitive impairments associated with corpus callosum infarction: a ten cases study. *International journal of clinical and experimental medicine* 2015;8(11):21991.
438. Arguin M, Lassonde M, Quattrini A, et al. Divided visuo-spatial attention systems with total and anterior callosotomy. *Neuropsychologia* 2000;38(3):283–291.
439. Ihori N, Kawamura M, Fukuzawa K, Kamaki M. Somesthetic disconnection syndromes in patients with callosal lesions. *Eur. Neurol.* 2000;44(2):65–71.
440. Risse GL, Gates J, Lund G, et al. Interhemispheric transfer in patients with incomplete section of the corpus callosum. Anatomic verification with magnetic resonance imaging. *Arch. Neurol.* 1989;46(4):437–443.
441. Jeurissen B, Leemans A, Tournier J-D, et al. Investigating the prevalence of complex fiber configurations in white matter tissue with diffusion magnetic resonance imaging. *Hum*

Brain Mapp 2013;34(11):2747–2766.

442. Tuch DS, Reese TG, Wiegell MR, et al. High angular resolution diffusion imaging reveals intravoxel white matter fiber heterogeneity. *Magnetic Resonance in Medicine: An Official Journal of the International Society for Magnetic Resonance in Medicine* 2002;48(4):577–582.
443. Alexander DC, Pierpaoli C, Basser PJ, Gee JC. Spatial transformations of diffusion tensor magnetic resonance images. *IEEE transactions on medical imaging* 2001;20(11):1131–1139.
444. Jeurissen B, Leemans A, Jones DK, et al. Probabilistic fiber tracking using the residual bootstrap with constrained spherical deconvolution. *Hum Brain Mapp* 2011;32(3):461–479.
445. Ruddy KL, Leemans A, Woolley DG, et al. Structural and Functional Cortical Connectivity Mediating Cross Education of Motor Function. *J Neurosci* 2017;37(10):2555–2564.
446. Agosta F, Pagani E, Rocca MA, et al. Voxel-based morphometry study of brain volumetry and diffusivity in amyotrophic lateral sclerosis patients with mild disability. *Hum Brain Mapp* 2007;28(12):1430–1438.
447. Chapman MC, Jelsone-Swain L, Johnson TD, et al. Diffusion tensor MRI of the corpus callosum in amyotrophic lateral sclerosis. *J Magn Reson Imaging* 2014;39(3):641–647.
448. Kim J-E, Oh JS, Sung J-J, et al. Diffusion tensor tractography analysis of the corpus callosum fibers in amyotrophic lateral sclerosis. *Journal of Clinical Neurology* 2014;10(3):249–256.
449. Rose S, Pannek K, Bell C, et al. Direct evidence of intra- and interhemispheric corticomotor network degeneration in amyotrophic lateral sclerosis: an automated MRI structural connectivity study. *Neuroimage* 2012;59(3):2661–2669.
450. Kolind S, Sharma R, Knight S, et al. Myelin imaging in amyotrophic and primary lateral sclerosis. *Amyotroph Lateral Scler Frontotemporal Degener* 2013;14(7–8):562–573.
451. Evans J, Olm C, McCluskey L, et al. Impaired cognitive flexibility in amyotrophic lateral sclerosis. *Cognitive and behavioral neurology: official journal of the Society for Behavioral and Cognitive Neurology* 2015;28(1):17.
452. Hubers A, Bockler B, Kammer T, et al. Functional involvement of the motor corpus callosum in amyotrophic lateral sclerosis. *Amyotrophic Lateral Sclerosis and Frontotemporal Degeneration* 2017;18(Suppl. S2):201.
453. Wittstock M, Meister S, Walter U, et al. Mirror movements in amyotrophic lateral sclerosis. *Amyotroph Lateral Scler* 2011;12(6):393–397.
454. Salerno A, Georgesco M. Double magnetic stimulation of the motor cortex in amyotrophic lateral sclerosis. *Electroencephalogr Clin Neurophysiol* 1998;107(2):133–139.
455. Nadkarni NA, Deshmukh SS. Mirror movements. *Ann Indian Acad Neurol* 2012;15(1):13–14.
456. Fraschini M, Lai M, Demuru M, et al. Functional brain connectivity analysis in amyotrophic lateral sclerosis: an EEG source-space study. *Biomedical Physics &*

- Engineering Express 2017;4(3):037004.
457. Clark R, Blizzard C, Dickson T. Inhibitory dysfunction in amyotrophic lateral sclerosis: future therapeutic opportunities. *Neurodegener Dis Manag* 2015;5(6):511–525.
  458. Foerster BR, Callaghan BC, Petrou M, et al. Decreased motor cortex  $\gamma$ -aminobutyric acid in amyotrophic lateral sclerosis. *Neurology* 2012;78(20):1596–1600.
  459. Turner MR, Kiernan MC. Does interneuronal dysfunction contribute to neurodegeneration in amyotrophic lateral sclerosis? *Amyotrophic Lateral Sclerosis* 2012;13(3):245–250.
  460. Guerriero RM, Giza CC, Rotenberg A. Glutamate and GABA imbalance following traumatic brain injury. *Curr Neurol Neurosci Rep* 2015;15(5):27.
  461. Lüscher C, Malenka RC. NMDA receptor-dependent long-term potentiation and long-term depression (LTP/LTD). *Cold Spring Harb Perspect Biol* 2012;4(6):a005710.
  462. McEachern JC, Shaw CA. The plasticity–pathology continuum: Defining a role for the LTP phenomenon. *J. Neurosci. Res.* 1999;58(1):42–61.
  463. Bartos M, Vida I, Jonas P. Synaptic mechanisms of synchronized gamma oscillations in inhibitory interneuron networks. *Nature Reviews Neuroscience* 2007;8(1):45–56.
  464. Barber SC, Shaw PJ. Oxidative stress in ALS: key role in motor neuron injury and therapeutic target. *Free Radic. Biol. Med.* 2010;48(5):629–641.
  465. Turner MR, Bowser R, Buijijn L, et al. Mechanisms, models and biomarkers in amyotrophic lateral sclerosis. *Amyotroph Lateral Scler Frontotemporal Degener* 2013;14 Suppl 1:19–32.
  466. Eisen A, Kim S, Pant B. Amyotrophic lateral sclerosis (ALS): A phylogenetic disease of the corticomotoneuron? *Muscle Nerve* 1992;15(2):219–224.
  467. Lee S, Kim H-J. Prion-like Mechanism in Amyotrophic Lateral Sclerosis: are Protein Aggregates the Key? *Exp Neurobiol* 2015;24(1):1–7.
  468. Crockford C, Newton J, Lonergan K, et al. ALS-specific cognitive and behavior changes associated with advancing disease stage in ALS. *Neurology* 2018;91(15):e1370–e1380.
  469. Näätänen R, Pakarinen S, Rinne T, Takegata R. The mismatch negativity (MMN): towards the optimal paradigm. *Clinical Neurophysiology* 2004;115(1):140–144.
  470. Robertson IH, Manly T, Andrade J, et al. Oops!': performance correlates of everyday attentional failures in traumatic brain injured and normal subjects. *Neuropsychologia* 1997;35(6):747–758.
  471. Boroojerdi B, Diefenbach K, Ferbert A. Transcallosal inhibition in cortical and subcortical cerebral vascular lesions. *J Neurol Sci* 1996;144(1–2):160–170.
  472. Mooney RA, Cirillo J, Byblow WD. Adaptive threshold hunting reveals differences in interhemispheric inhibition between young and older adults. *Eur. J. Neurosci.* 2018;48(5):2247–2258.
  473. Laszlo S, Ruiz-Blondet M, Khalifian N, et al. A direct comparison of active and passive amplification electrodes in the same amplifier system. *J. Neurosci. Methods* 2014;235:298–307.

474. Mathewson KE, Harrison TJL, Kizuk SAD. High and dry? Comparing active dry EEG electrodes to active and passive wet electrodes. *Psychophysiology* 2017;54(1):74–82.
475. Oliveira AS, Schlink BR, Hairston WD, et al. Proposing metrics for benchmarking novel EEG technologies towards real-world measurements. *Frontiers in human neuroscience* 2016;10:188.
476. Delorme A, Makeig S. EEGLAB: an open source toolbox for analysis of single-trial EEG dynamics including independent component analysis. *Journal of Neuroscience Methods* 2004;134(1):9–21.
477. Oostenveld R, Fries P, Maris E, Schoffelen J-M. FieldTrip: Open Source Software for Advanced Analysis of MEG, EEG, and Invasive Electrophysiological Data. *Computational Intelligence and Neuroscience* 2011;2011
478. McMackin R, Dukic S, Costello E, et al. Localisation of Brain Networks Engaged by the Sustained Attention to Response Task Provides Quantitative Markers of Executive Impairment in Amyotrophic Lateral Sclerosis. *Cerebral Cortex* 2020;00:1–13.
479. Staub B, Doignon-Camus N, Marques-Carneiro JE, et al. Age-related differences in the use of automatic and controlled processes in a situation of sustained attention. *Neuropsychologia* 2015;75:607–616.
480. Jurgens CK, van der Hiele K, Reijntjes RH a. M, et al. Basal ganglia volume is strongly related to P3 event-related potential in premanifest Huntington’s disease. *Eur. J. Neurol.* 2011;18(8):1105–1108.
481. Kam JW, Mickleborough MJ, Eades C, Handy TC. Migraine and attention to visual events during mind wandering. *Experimental brain research* 2015;233(5):1503–1510.
482. Fuchs M, Kastner J, Wagner M, et al. A standardized boundary element method volume conductor model. *Clinical Neurophysiology* 2002;113(5):702–712.
483. Fonov V, Evans AC, Botteron K, et al. Unbiased Average Age-Appropriate Atlases for Pediatric Studies. *Neuroimage* 2011;54(1):313–327.
484. Douw L, Nieboer D, Stam CJ, et al. Consistency of magnetoencephalographic functional connectivity and network reconstruction using a template versus native MRI for co-registration. *Human Brain Mapping* 2018;39(1):104–119.
485. Schuster C, Hardiman O, Bede P. Survival prediction in Amyotrophic lateral sclerosis based on MRI measures and clinical characteristics. *BMC Neurol* 2017;17(1):1–10.
486. Oknina LB, Wild-Wall N, Oades RD, et al. Frontal and temporal sources of mismatch negativity in healthy controls, patients at onset of schizophrenia in adolescence and others at 15 years after onset. *Schizophr. Res.* 2005;76(1):25–41.
487. Tzourio-Mazoyer N, Landeau B, Papathanassiou D, et al. Automated anatomical labeling of activations in SPM using a macroscopic anatomical parcellation of the MNI MRI single-subject brain. *Neuroimage* 2002;15(1):273–289.
488. Holmes CJ, Hoge R, Collins L, et al. Enhancement of Mr Images Using Registration for Signal Averaging. *Journal of Computer Assisted Tomography* 1998;22(2):324–333.
489. Jonmohamadi Y, Poudel G, Innes C, et al. Comparison of beamformers for EEG source signal reconstruction. *Biomedical Signal Processing and Control* 2014;14:175–188.

490. Kalcher J, Pfurtscheller G. Discrimination between phase-locked and non-phase-locked event-related EEG activity. *Electroencephalogr Clin Neurophysiol* 1995;94(5):381–384.
491. Rossi S, Hallett M, Rossini PM, et al. Safety, ethical considerations, and application guidelines for the use of transcranial magnetic stimulation in clinical practice and research. *Clin Neurophysiol* 2009;120(12):2008–2039.
492. Awiszus F. Fast estimation of transcranial magnetic stimulation motor threshold: is it safe? *Brain Stimul* 2011;4(1):58–59; discussion 60–63.
493. Whitley E, Ball J. Statistics review 6: Nonparametric methods. *Critical Care* 2002;6(6):509.
494. Mann HB, Whitney DR. On a test of whether one of two random variables is stochastically larger than the other. *Annals of Mathematical Statistics* 1947;18:50–60.
495. Wilcoxon F. Individual Comparisons by Ranking Methods. *Biometrics Bulletin* 1945;1(6):80–83.
496. Williams VSL, Jones LV, Tukey JW. Controlling Error in Multiple Comparisons, with Examples from State-to-State Differences in Educational Achievement. *Journal of Educational and Behavioral Statistics* 1999;24(1):42–69.
497. Everitt B, Skrondal A. *The Cambridge Dictionary of Statistics, Fourth Edition*. Cambridge University Press; 2010.
498. Benjamini Y, Hochberg Y. Controlling the false discovery rate: a practical and powerful approach to multiple testing. *Journal of the Royal statistical society: series B (Methodological)* 1995;57(1):289–300.
499. Efron B. Empirical Bayes estimates for large-scale prediction problems. *Journal of the American Statistical Association* 2009;104(487):1015–1028.
500. Jas M, Larson E, Engemann DA, et al. A reproducible MEG/EEG group study with the MNE software: recommendations, quality assessments, and good practices. *Frontiers in neuroscience* 2018;12:530.
501. Hajian-Tilaki K. Receiver Operating Characteristic (ROC) Curve Analysis for Medical Diagnostic Test Evaluation. *Caspian J Intern Med* 2013;4(2):627–635.
502. Nasserolelami B. An Implementation of Empirical Bayesian Inference and Non-Null Bootstrapping for Threshold Selection and Power Estimation in Multiple and Single Statistical Testing. *bioRxiv* 2018;342964.
503. Brooks BR, Sanjak M, Ringel S, et al. The amyotrophic lateral sclerosis functional rating scale-Assessment of activities of daily living in patients with amyotrophic lateral sclerosis. *Archives of neurology* 1996;53(2):141–147.
504. Cedarbaum JM, Stambler N, Malta E, et al. The ALSFRS-R: a revised ALS functional rating scale that incorporates assessments of respiratory function. *Journal of the neurological sciences* 1999;169(1–2):13–21.
505. Elamin M, Pinto-Grau M, Burke T, et al. Identifying behavioural changes in ALS: Validation of the Beaumont Behavioural Inventory (BBI). *Amyotroph Lateral Scler Frontotemporal Degener* 2017;18(1–2):68–73.



506. Abrahams S, Newton J, Niven E, et al. Screening for cognition and behaviour changes in ALS. *Amyotrophic Lateral Sclerosis and Frontotemporal Degeneration* 2014;15(1–2):9–14.
507. Niven E, Newton J, Foley J, et al. Validation of the Edinburgh Cognitive and Behavioural Amyotrophic Lateral Sclerosis Screen (ECAS): A cognitive tool for motor disorders. *Amyotroph Lateral Scler Frontotemporal Degener* 2015;16(3–4):172–179.
508. Delis DC, Kaplan E, Kramer JH. Delis-Kaplan executive function system (D-KEFS). San Antonio TX: Psychological Corporation. 2001;
509. Crockford CJ, Kleynhans M, Wilton E, et al. ECAS A-B-C: alternate forms of the Edinburgh Cognitive and Behavioural ALS Screen. *Amyotrophic Lateral Sclerosis and Frontotemporal Degeneration* 2018;19(1–2):57–64.
510. Swanson J. The Delis-Kaplan Executive Function System: A Review. *Canadian Journal of School Psychology* 2005;20(1–2):117–128.
511. Pinto-Grau M, Burke T, Lonergan K, et al. Screening for cognitive dysfunction in ALS: validation of the Edinburgh Cognitive and Behavioural ALS Screen (ECAS) using age and education adjusted normative data. *Amyotrophic Lateral Sclerosis and Frontotemporal Degeneration* 2017;18(1–2):99–106.
512. Näätänen R, Gaillard AWK, Mäntysalo S. Early selective-attention effect on evoked potential reinterpreted. *Acta Psychologica* 1978;42(4):313–329.
513. Naatanen R. The Mismatch Negativity: A Powerful Tool for Cognitive Neuroscience. *Ear & Hearing* 1995;16(1):6–18.
514. Winkler I, Karmos G, Näätänen R. Adaptive modeling of the unattended acoustic environment reflected in the mismatch negativity event-related potential. *Brain Res.* 1996;742(1–2):239–252.
515. Ruusuvirta T, Huotilainen M, Fellman V, Näätänen R. Numerical discrimination in newborn infants as revealed by event-related potentials to tone sequences. *European Journal of Neuroscience* 2009;30(8):1620–1624.
516. Wijnen VJM, van Boxtel GJM, Eilander HJ, de Gelder B. Mismatch negativity predicts recovery from the vegetative state. *Clin Neurophysiol* 2007;118(3):597–605.
517. Giard M-H, Perrin F, Pernier J, Bouchet P. Brain generators implicated in the processing of auditory stimulus deviance: a topographic event-related potential study. *Psychophysiology* 1990;27(6):627–640.
518. Lyytinen H, Blomberg AP, Näätänen R. Event-related potentials and autonomic responses to a change in unattended auditory stimuli. *Psychophysiology* 1992;29(5):523–534.
519. Escera C, Yago E, Alho K. Electrical responses reveal the temporal dynamics of brain events during involuntary attention switching. *Eur. J. Neurosci.* 2001;14(5):877–883.
520. Escera C, Yago E, Corral M-J, et al. Attention capture by auditory significant stimuli: semantic analysis follows attention switching. *Eur. J. Neurosci.* 2003;18(8):2408–2412.
521. Schröger E. A neural mechanism for involuntary attention shifts to changes in auditory stimulation. *J Cogn Neurosci* 1996;8(6):527–539.

522. May P, Tiitinen H, Ilmoniemi RJ, et al. Frequency change detection in human auditory cortex. *J Comput Neurosci* 1999;6(2):99–120.
523. May P, Tiitinen H. Human cortical processing of auditory events over time. *Neuroreport* 2001;12(3):573–577.
524. May PJC, Tiitinen H. The MMN is a derivative of the auditory N100 response. *Neurol Clin Neurophysiol* 2004;2004:1–5.
525. Jääskeläinen IP, Ahveninen J, Bonmassar G, et al. Human posterior auditory cortex gates novel sounds to consciousness. *Proc. Natl. Acad. Sci. U.S.A.* 2004;101(17):6809–6814.
526. Ulanovsky N, Las L, Nelken I. Processing of low-probability sounds by cortical neurons. *Nature Neuroscience* 2003;6(4):391–398.
527. May PJC, Tiitinen H. Mismatch negativity (MMN), the deviance-elicited auditory deflection, explained. *Psychophysiology* 2010;47(1):66–122.
528. Opitz B, Rinne T, Mecklinger A, et al. Differential contribution of frontal and temporal cortices to auditory change detection: fMRI and ERP results. *Neuroimage* 2002;15(1):167–174.
529. Yago E, Escera C, Alho K, Giard MH. Cerebral mechanisms underlying orienting of attention towards auditory frequency changes. *Neuroreport* 2001;12(11):2583–2587.
530. Müller BW, Jüptner M, Jentzen W, Müller SP. Cortical activation to auditory mismatch elicited by frequency deviant and complex novel sounds: a PET study. *Neuroimage* 2002;17(1):231–239.
531. Alho K, Woods DL, Algazi A, et al. Lesions of frontal cortex diminish the auditory mismatch negativity. *Electroencephalography and clinical neurophysiology* 1994;91(5):353–362.
532. Maess B, Jacobsen T, Schröger E, Friederici AD. Localizing pre-attentive auditory memory-based comparison: magnetic mismatch negativity to pitch change. *Neuroimage* 2007;37(2):561–571.
533. Alho K. Cerebral generators of mismatch negativity (MMN) and its magnetic counterpart (MMNm) elicited by sound changes. *Ear Hear* 1995;16(1):38–51.
534. Näätänen R, Michie PT. Early selective-attention effects on the evoked potential: a critical review and reinterpretation. *Biol Psychol* 1979;8(2):81–136.
535. Näätänen R, Kujala T, Escera C, et al. The mismatch negativity (MMN)--a unique window to disturbed central auditory processing in ageing and different clinical conditions. *Clin Neurophysiol* 2012;123(3):424–458.
536. Schall U. Is it time to move mismatch negativity into the clinic? *Biol Psychol* 2016;116:41–46.
537. Näätänen R, Sussman ES, Salisbury D, Shafer VL. Mismatch negativity (MMN) as an index of cognitive dysfunction. *Brain Topogr* 2014;27(4):451–466.
538. Kujala T, Leminen M. Low-level neural auditory discrimination dysfunctions in specific language impairment-A review on mismatch negativity findings. *Dev Cogn Neurosci* 2017;28:65–75.

539. Todd J, Harms L, Michie P, Schall U. Mismatch negativity: translating the potential. *Frontiers in psychiatry* 2013;4:171.
540. Byrne S, Elamin M, Bede P, Hardiman O. Absence of consensus in diagnostic criteria for familial neurodegenerative diseases. *J Neurol Neurosurg Psychiatry* 2012;83(4):365–367.
541. Darvas F, Pantazis D, Kucukaltun-Yildirim E, Leahy RM. Mapping human brain function with MEG and EEG: methods and validation. *NeuroImage* 2004;23:S289–S299.
542. Lovie AD. Who discovered Spearman’s rank correlation? *British Journal of Mathematical and Statistical Psychology* 1995;48(2):255–269.
543. MacLean SE, Blundon EG, Ward LM. Brain regional networks active during the mismatch negativity vary with paradigm. *Neuropsychologia* 2015;75:242–251.
544. Nixon P, Lazarova J, Hodinott-Hill I, et al. The inferior frontal gyrus and phonological processing: an investigation using rTMS. *J Cogn Neurosci* 2004;16(2):289–300.
545. Burton MW. The role of inferior frontal cortex in phonological processing. *Cognitive Science* 2001;25(5):695–709.
546. Bunge SA, Ochsner KN, Desmond JE, et al. Prefrontal regions involved in keeping information in and out of mind. *Brain* 2001;124(10):2074–2086.
547. Beaty RE, Benedek M, Wilkins RW, et al. Creativity and the default network: A functional connectivity analysis of the creative brain at rest. *Neuropsychologia* 2014;64:92–98.
548. Raichle ME, MacLeod AM, Snyder AZ, et al. A default mode of brain function. *Proc Natl Acad Sci U S A* 2001;98(2):676–682.
549. Nekovarova T, Fajnerova I, Horacek J, Spaniel F. Bridging disparate symptoms of schizophrenia: a triple network dysfunction theory. *Frontiers in behavioral neuroscience* 2014;8:171.
550. Seeley WW, Menon V, Schatzberg AF, et al. Dissociable intrinsic connectivity networks for salience processing and executive control. *J. Neurosci.* 2007;27(9):2349–2356.
551. Agosta F, Canu E, Valsasina P, et al. Divergent brain network connectivity in amyotrophic lateral sclerosis. *Neurobiol. Aging* 2013;34(2):419–427.
552. Sorrentino P, Rucco R, Jacini F, et al. Brain functional networks become more connected as amyotrophic lateral sclerosis progresses: a source level magnetoencephalographic study. *Neuroimage Clin* 2018;20:564–571.
553. Cooray G, Garrido MI, Hyllienmark L, Brismar T. A mechanistic model of mismatch negativity in the ageing brain. *Clin Neurophysiol* 2014;125(9):1774–1782.
554. Hopfinger JB, Buonocore MH, Mangun GR. The neural mechanisms of top-down attentional control. *Nature Neuroscience* 2000;3(3):284–291.
555. Welsh RC, Jelsone-Swain LM, Foerster BR. The utility of independent component analysis and machine learning in the identification of the amyotrophic lateral sclerosis diseased brain. *Frontiers in human neuroscience* 2013;7:251.
556. Brooks BR, Miller RG, Swash M, et al. El Escorial revisited: revised criteria for the diagnosis of amyotrophic lateral sclerosis. *Amyotroph. Lateral Scler. Other Motor Neuron*

- Disord. 2000;1(5):293–299.
557. Pekkonen E, Rinne T, Näätänen R. Variability and replicability of the mismatch negativity. *Electroencephalography and Clinical Neurophysiology/Evoked Potentials Section* 1995;96(6):546–554.
558. De Beer NA, Van Hooff JC, Brunia CH, et al. Midlatency auditory evoked potentials as indicators of perceptual processing during general anaesthesia. *British journal of anaesthesia* 1996;77(5):617–624.
559. Ethridge LE, White SP, Mosconi MW, et al. Reduced habituation of auditory evoked potentials indicate cortical hyper-excitability in Fragile X Syndrome. *Translational Psychiatry* 2016;6(4):e787–e787.
560. Kaneshiro S, Hiraumi H, Sato H. Central processing of speech sounds and non-speech sounds with similar spectral distribution: An auditory evoked potential study. *Auris Nasus Larynx* 2020;
561. Schuster C, Hardiman O, Bede P. Development of an Automated MRI-Based Diagnostic Protocol for Amyotrophic Lateral Sclerosis Using Disease-Specific Pathognomonic Features: A Quantitative Disease-State Classification Study. *PLoS ONE* 2016;11(12):e0167331.
562. Benjamini Y. Discovering the false discovery rate. *Journal of the Royal Statistical Society: series B (statistical methodology)* 2010;72(4):405–416.
563. Wilkinson GN, Rogers CE. Symbolic Description of Factorial Models for Analysis of Variance. *Journal of the Royal Statistical Society: Series C (Applied Statistics)* 1973;22(3):392–399.
564. Beasley TM, Erickson S, Allison DB. Rank-Based Inverse Normal Transformations are Increasingly Used, But are They Merited? *Behav Genet* 2009;39(5):580–595.
565. de Winter JC, Gosling SD, Potter J. Comparing the Pearson and Spearman correlation coefficients across distributions and sample sizes: A tutorial using simulations and empirical data. *Psychological methods* 2016;21(3):273.
566. Pinto-Grau M, Hardiman O, Pender N. The Study of Language in the Amyotrophic Lateral Sclerosis - Frontotemporal Spectrum Disorder: a Systematic Review of Findings and New Perspectives. *Neuropsychol Rev* 2018;28(2):251–268.
567. Swick D, Ashley V, Turken AU. Left inferior frontal gyrus is critical for response inhibition. *BMC Neuroscience* 2008;9(1):102.
568. Shen D, Cui L, Cui B, et al. A systematic review and meta-analysis of the functional MRI investigation of motor neuron disease. *Frontiers in neurology* 2015;6:246.
569. Menon P, Yiannikas C, Kiernan MC, Vucic S. Regional motor cortex dysfunction in amyotrophic lateral sclerosis. *Ann Clin Transl Neurol* 2019;6(8):1373–1382.
570. Burke T, Pinto-Grau M, Lonergan K, et al. A Cross-sectional population-based investigation into behavioral change in amyotrophic lateral sclerosis: subphenotypes, staging, cognitive predictors, and survival. *Ann Clin Transl Neurol* 2017;4(5):305–317.
571. Cash DM, Bocchetta M, Thomas DL, et al. Patterns of gray matter atrophy in genetic frontotemporal dementia: results from the GENFI study. *Neurobiology of Aging*

2018;62:191–196.

572. Strong MJ, Abrahams S, Goldstein LH, et al. Amyotrophic lateral sclerosis - frontotemporal spectrum disorder (ALS-FTSD): Revised diagnostic criteria. *Amyotroph Lateral Scler Frontotemporal Degener* 2017;18(3–4):153–174.
573. Hu WT, Seelaar H, Josephs KA, et al. Survival Profiles of Patients With Frontotemporal Dementia and Motor Neuron Disease. *Arch Neurol* 2009;66(11):1359–1364.
574. Elamin M, Phukan J, Bede P, et al. Executive dysfunction is a negative prognostic indicator in patients with ALS without dementia. *Neurology* 2011;76(14):1263–1269.
575. Tartaglia MC, Rowe A, Findlater K, et al. Differentiation between primary lateral sclerosis and amyotrophic lateral sclerosis: examination of symptoms and signs at disease onset and during follow-up. *Arch. Neurol.* 2007;64(2):232–236.
576. Clayton MS, Yeung N, Cohen Kadosh R. The roles of cortical oscillations in sustained attention. *Trends Cogn Sci* 2015;19(4):188–195.
577. Hari R, Salmelin R, Mäkelä JP, et al. Magnetoencephalographic cortical rhythms. *International Journal of Psychophysiology* 1997;26(1):51–62.
578. Pfurtscheller G. Induced Oscillations in the Alpha Band: Functional Meaning. *Epilepsia* 2003;44(s12):2–8.
579. Picton TW, Hillyard SA, Krausz HI, Galambos R. Human auditory evoked potentials. I: Evaluation of components. *Electroencephalography and Clinical Neurophysiology* 1974;36:179–190.
580. Kolev V, Yordanova J, Schürmann M, Baţar E. Event-related alpha oscillations in task processing. *Clinical Neurophysiology* 1999;110(10):1784–1792.
581. Silva LR, Amitai Y, Connors BW. Intrinsic oscillations of neocortex generated by layer 5 pyramidal neurons. *Science* 1991;251(4992):432–435.
582. Hughes SW, Crunelli V. Thalamic mechanisms of EEG alpha rhythms and their pathological implications. *Neuroscientist* 2005;11(4):357–372.
583. Schreckenberger M, Lange-Asschenfeld C, Lochmann M, et al. The thalamus as the generator and modulator of EEG alpha rhythm: a combined PET/EEG study with lorazepam challenge in humans. *NeuroImage* 2004;22(2):637–644.
584. Sazonova OB, Lukashevich IP. [The EEG characteristics in a lesion of different sections of the human caudate nucleus]. *Zh Vyssh Nerv Deiat Im I P Pavlova* 1995;45(5):886–893.
585. Pokrovskaja ZA, Insarova NG. [The EEG characteristics of patients with Huntington's chorea and their clinically healthy relatives]. *Zh Nevropatol Psikhiatr Im S S Korsakova* 1988;88(3):22–26.
586. Odish OFF, Johnsen K, van Someren P, et al. EEG may serve as a biomarker in Huntington's disease using machine learning automatic classification. *Scientific Reports* 2018;8(1):16090.
587. Bylsma FW, Peyser CE, Folstein SE, et al. EEG power spectra in huntington's disease: Clinical and neuropsychological correlates. *Neuropsychologia* 1994;32(2):137–150.

588. Petrovic J, Milosevic V, Zivkovic M, et al. Slower EEG alpha generation, synchronization and “flow”-possible biomarkers of cognitive impairment and neuropathology of minor stroke. *PeerJ* 2017;5:e3839.
589. de Munck JC, Gonçalves SI, Huijboom L, et al. The hemodynamic response of the alpha rhythm: an EEG/fMRI study. *Neuroimage* 2007;35(3):1142–1151.
590. Pfurtscheller G, Stancák A, Neuper Ch. Event-related synchronization (ERS) in the alpha band — an electrophysiological correlate of cortical idling: A review. *International Journal of Psychophysiology* 1996;24(1):39–46.
591. Pfurtscheller G. EEG event-related desynchronization (ERD) and synchronization (ERS). *Electroencephalography and Clinical Neurophysiology* 1997;1(103):26.
592. Klimesch W, Sauseng P, Hanslmayr S. EEG alpha oscillations: The inhibition–timing hypothesis. *Brain Research Reviews* 2007;53(1):63–88.
593. Kelly SP, Lalor EC, Reilly RB, Foxe JJ. Increases in alpha oscillatory power reflect an active retinotopic mechanism for distracter suppression during sustained visuospatial attention. *J. Neurophysiol.* 2006;95(6):3844–3851.
594. Antonov PA, Chakravarthi R, Andersen SK. Too little, too late, and in the wrong place: Alpha band activity does not reflect an active mechanism of selective attention. *NeuroImage* 2020;2020:117006.
595. Dushanova J, Philipova D, Nikolova G. Event-Related Desynchronization/Synchronization During Discrimination Task Conditions in Patients with Parkinson’s Disease. *Cell Mol Neurobiol* 2009;29(6):971–980.
596. Bizovičar N, Dreo J, Koritnik B, Zidar J. Decreased movement-related beta desynchronization and impaired post-movement beta rebound in amyotrophic lateral sclerosis. *Clinical Neurophysiology* 2014;125(8):1689–1699.
597. Cantero JL, Atienza M, Gomez-Herrero G, et al. Functional integrity of thalamocortical circuits differentiates normal aging from mild cognitive impairment. *Human Brain Mapping* 2009;30(12):3944–3957.
598. Vilà-Balló A, François C, Cucurell D, et al. Auditory Target and Novelty Processing in Patients with Unilateral Hippocampal Sclerosis: A Current-Source Density Study. *Scientific Reports* 2017;7(1):1612.
599. Bishop DVM, Hardiman MJ, Barry JG. Lower-Frequency Event-Related Desynchronization: A Signature of Late Mismatch Responses to Sounds, Which Is Reduced or Absent in Children with Specific Language Impairment. *J. Neurosci.* 2010;30(46):15578–15584.
600. Fuentemilla L, Marco-Pallarés J, Münte TF, Grau C. Theta EEG oscillatory activity and auditory change detection. *Brain Res.* 2008;1220:93–101.
601. Bishop DVM, Hardiman MJ. Measurement of mismatch negativity in individuals: A study using single-trial analysis. *Psychophysiology* 2010;47(4):697–705.
602. Halliday LF, Barry JG, Hardiman MJ, Bishop DV. Late, not early mismatch responses to changes in frequency are reduced or deviant in children with dyslexia: an event-related potential study. *Journal of Neurodevelopmental Disorders* 2014;6(1):21.

603. Kaser M, Soltesz F, Lawrence P, et al. Oscillatory Underpinnings of Mismatch Negativity and Their Relationship with Cognitive Function in Patients with Schizophrenia. *PLOS ONE* 2013;8(12):e83255.
604. Cacace AT, McFarland DJ. Spectral dynamics of electroencephalographic activity during auditory information processing. *Hear. Res.* 2003;176(1–2):25–41.
605. Cahn BR, Delorme A, Polich J. Event-related delta, theta, alpha and gamma correlates to auditory oddball processing during Vipassana meditation. *Soc Cogn Affect Neurosci* 2013;8(1):100–111.
606. Finegan E, Shing SLH, Chipika RH, et al. Thalamic, hippocampal and basal ganglia pathology in primary lateral sclerosis and amyotrophic lateral sclerosis: Evidence from quantitative imaging data. *Data in brief* 2020;29:105115.
607. Yu H, Sternad D, Corcos DM, Vaillancourt DE. Role of hyperactive cerebellum and motor cortex in Parkinson’s disease. *NeuroImage* 2007;35(1):222–233.
608. Geevasinga N, Menon P, Özdinler PH, et al. Pathophysiological and diagnostic implications of cortical dysfunction in ALS. *Nature Reviews Neurology* 2016;12(11):651–661.
609. Blandini F, Nappi G, Tassorelli C, Martignoni E. Functional changes of the basal ganglia circuitry in Parkinson’s disease. *Progress in Neurobiology* 2000;62(1):63–88.
610. Busche MA, Konnerth A. Neuronal hyperactivity – A key defect in Alzheimer’s disease? *BioEssays* 2015;37(6):624–632.
611. Hari R, Salmelin R. Human cortical oscillations: a neuromagnetic view through the skull. *Trends Neurosci.* 1997;20(1):44–49.
612. Gelastopoulos A, Whittington MA, Kopell NJ. Parietal low beta rhythm provides a dynamical substrate for a working memory buffer. *PNAS* 2019;116(33):16613–16620.
613. Bellgrove MA, Hawi Z, Gill M, Robertson IH. The cognitive genetics of attention deficit hyperactivity disorder (ADHD): sustained attention as a candidate phenotype. *Cortex* 2006;42(6):838–845.
614. Huntley JD, Hampshire A, Bor D, et al. The importance of sustained attention in early Alzheimer’s disease. *International journal of geriatric psychiatry* 2017;32(8):860–867.
615. O’Gráda C, Barry S, McGlade N, et al. Does the ability to sustain attention underlie symptom severity in schizophrenia? *Schizophrenia research* 2009;107(2–3):319–323.
616. Jin CY, Borst JP, van Vugt MK. Predicting task-general mind-wandering with EEG. *Cognitive, Affective, & Behavioral Neuroscience* 2019;19(4):1059–1073.
617. Gan L, Cookson MR, Petrucelli L, La Spada AR. Converging pathways in neurodegeneration, from genetics to mechanisms. *Nat Neurosci* 2018;21(10):1300–1309.
618. Beste C, Saft C, Andrich J, et al. Response inhibition in Huntington’s disease—a study using ERPs and sLORETA. *Neuropsychologia* 2008;46(5):1290–1297.
619. Lulé D, Ludolph AC, Kassubek J. MRI-based functional neuroimaging in ALS: an update. *Amyotrophic Lateral Scler* 2009;10(5–6):258–268.

620. Kim H-Y. Statistical notes for clinical researchers: post-hoc multiple comparisons. *Restor Dent Endod* 2015;40(2):172–176.
621. Delis DC, Kramer JH, Kaplan E, Holdnack J. Reliability and validity of the Delis-Kaplan Executive Function System: An update. *Journal of the International Neuropsychological Society* 2004;10(2):301–303.
622. Kilpeläinen R, Luoma L, Herrgård E, et al. Persistent frontal P300 brain potential suggests abnormal processing of auditory information in distractible children. *Neuroreport* 1999;10(16):3405–3410.
623. Richard Clark C, McFarlane AC, Weber DL, Battersby M. Enlarged frontal P300 to stimulus change in panic disorder. *Biological Psychiatry* 1996;39(10):845–856.
624. van Dinteren R, Arns M, Jongsma MLA, Kessels RPC. Combined frontal and parietal P300 amplitudes indicate compensated cognitive processing across the lifespan. *Front Aging Neurosci* 2014;6:294.
625. Cavanna AE, Trimble MR. The precuneus: a review of its functional anatomy and behavioural correlates. *Brain* 2006;129(3):564–583.
626. Uddin LQ, Nomi JS, Hebert-Seropian B, et al. Structure and function of the human insula. *J Clin Neurophysiol* 2017;34(4):300–306.
627. Varjačić A, Mantini D, Levenstein J, et al. The role of left insula in executive set-switching: Lesion evidence from an acute stroke cohort. *Cortex* 2018;107:92–101.
628. Chen Q, Garcea FE, Jacobs RA, Mahon BZ. Abstract Representations of Object-Directed Action in the Left Inferior Parietal Lobule. *Cereb Cortex* 2018;28(6):2162–2174.
629. O'Connor AR, Han S, Dobbins IG. The Inferior Parietal Lobule and Recognition Memory: Expectancy Violation or Successful Retrieval? *J. Neurosci.* 2010;30(8):2924–2934.
630. Cohen J. *Statistical Power Analysis for the Behavioral Sciences* (2nd edition). Hillsdale, NJ: Lawrence Erlbaum Associates; 1988.
631. Zhou X-H, McClish DK, Obuchowski NA. *Statistical methods in diagnostic medicine*. John Wiley & Sons; 2009.
632. Vinding MC, Tsitsi P, Piitulainen H, et al. Attenuated beta rebound to proprioceptive afferent feedback in Parkinson's disease. *Scientific Reports* 2019;9(1):1–11.
633. Alegre M, Gurtubay IG, Labarga A, et al. Frontal and central oscillatory changes related to different aspects of the motor process: a study in go/no-go paradigms. *Exp Brain Res* 2004;159(1):14–22.
634. Solis-Escalante T, Müller-Putz GR, Pfurtscheller G, Neuper C. Cue-induced beta rebound during withholding of overt and covert foot movement. *Clinical Neurophysiology* 2012;123(6):1182–1190.
635. Wu H-M, Hsiao F-J, Chen R-S, et al. Attenuated NoGo-related beta desynchronisation and synchronisation in Parkinson's disease revealed by magnetoencephalographic recording. *Scientific reports* 2019;9(1):1–12.
636. Klimesch W. Alpha-band oscillations, attention, and controlled access to stored information. *Trends Cogn Sci* 2012;16(12):606–617.



637. Klimesch W. EEG alpha and theta oscillations reflect cognitive and memory performance: a review and analysis. *Brain Res. Brain Res. Rev.* 1999;29(2–3):169–195.
638. Schmiedt-Fehr C, Mathes B, Kedilaya S, et al. Aging differentially affects alpha and beta sensorimotor rhythms in a go/nogo task. *Clin Neurophysiol* 2016;127(10):3234–3242.
639. Funderud I, Lindgren M, Løvstad M, et al. Differential Go/NoGo Activity in Both Contingent Negative Variation and Spectral Power. *PLOS ONE* 2012;7(10):e48504.
640. Missonnier P, Deiber M-P, Gold G, et al. Frontal theta event-related synchronization: comparison of directed attention and working memory load effects. *J Neural Transm (Vienna)* 2006;113(10):1477–1486.
641. Ishii R, Canuet L, Aoki Y, et al. Non-parametric permutation thresholding for adaptive nonlinear beamformer analysis on MEG revealed oscillatory neuronal dynamics in human brain. In: 2013 35th Annual International Conference of the IEEE Engineering in Medicine and Biology Society (EMBC). 2013 p. 4807–4810.
642. Ishii R, Canuet L, Ishihara T, et al. Frontal midline theta rhythm and gamma power changes during focused attention on mental calculation: an MEG beamformer analysis. *Frontiers in human neuroscience* 2014;8:406.
643. Dang JS, Figueroa IJ, Helton WS. You are measuring the decision to be fast, not inattention: the Sustained Attention to Response Task does not measure sustained attention. *Exp Brain Res* 2018;236(8):2255–2262.
644. Anthony M, Lin F. A Systematic Review for Functional Neuroimaging Studies of Cognitive Reserve Across the Cognitive Aging Spectrum. *Arch Clin Neuropsychol* 2018;33(8):937–948.
645. Geevasinga N, Menon P, Yiannikas C, et al. Diagnostic utility of cortical excitability studies in amyotrophic lateral sclerosis. *European Journal of Neurology* 2014;21(12):1451–1457.
646. Matamala JM, Howells J, Dharmadasa T, et al. Inter-session reliability of short-interval intracortical inhibition measured by threshold tracking TMS. *Neuroscience Letters* 2018;674:18–23.
647. Logroscino G, Piccininni M. Amyotrophic Lateral Sclerosis Descriptive Epidemiology: The Origin of Geographic Difference. *NED* 2019;52(1–2):93–103.
648. Rossi S, Hallett M, Rossini PM, Pascual-Leone A. Screening questionnaire before TMS: An update. *Clinical Neurophysiology* 2011;122(8):1686.
649. Oldfield RC. The assessment and analysis of handedness: The Edinburgh inventory. *Neuropsychologia* 1971;9(1):97–113.
650. Akoglu H. User's guide to correlation coefficients. *Turkish Journal of Emergency Medicine* 2018;18(3):91–93.
651. Awiszus F. TMS and threshold hunting. *Suppl Clin Neurophysiol* 2003;56:13–23.
652. Calvert GHM, McMackin R, Carson RG. Probing interhemispheric dorsal premotor-primary motor cortex interactions with threshold hunting transcranial magnetic stimulation. *Clinical Neurophysiology* 2020;131(11):2551–2560.

653. Shapiro SS, Wilk MB. An analysis of variance test for normality (complete samples). *Biometrika* 1965;52(3/4):591–611.
654. Wiegel P, Niemann N, Rothwell JC, Leukel C. Evidence for a subcortical contribution to intracortical facilitation. *European Journal of Neuroscience* 2018;47(11):1311–1319.
655. Hanajima R, Wang R, Nakatani-Enomoto S, et al. Comparison of different methods for estimating motor threshold with transcranial magnetic stimulation. *Clinical Neurophysiology* 2007;118(9):2120–2122.
656. Diana A, Pillai R, Bongioanni P, et al. Gamma aminobutyric acid (GABA) modulators for amyotrophic lateral sclerosis/motor neuron disease. *Cochrane Database of Systematic Reviews* 2017;(1)
657. Ahmed A, Simmons Z. Pseudobulbar affect: prevalence and management. *Ther Clin Risk Manag* 2013;9:483–489.
658. Kurt A, Nijboer F, Matuz T, Kübler A. Depression and anxiety in individuals with amyotrophic lateral sclerosis: epidemiology and management. *CNS Drugs* 2007;21(4):279–291.
659. Devlin JW, Nava S, Fong JJ, et al. Survey of sedation practices during noninvasive positive-pressure ventilation to treat acute respiratory failure. *Crit. Care Med.* 2007;35(10):2298–2302.
660. Caipa A, Alomar M, Bashir S. TMS as tool to investigate the effect of pharmacological medications on cortical plasticity. *Eur Rev Med Pharmacol Sci* 2018;22(3):844–852.
661. Clark CR, McFarlane AC, Weber DL, Battersby M. Enlarged frontal P300 to stimulus change in panic disorder. *Biol Psychiatry* 1996;39(10):845–856.
662. McGinley M, Hoffman RL, Russ DW, et al. Older adults exhibit more intracortical inhibition and less intracortical facilitation than young adults. *Experimental Gerontology* 2010;45(9):671–678.
663. Bobkova N, Vorobyov V. The brain compensatory mechanisms and Alzheimer’s disease progression: a new protective strategy. *Neural Regen Res* 2015;10(5):696–697.
664. Nuenen BFL van, Helmich RC, Buenen N, et al. Compensatory Activity in the Extrastriate Body Area of Parkinson’s Disease Patients. *J. Neurosci.* 2012;32(28):9546–9553.
665. Takeuchi N, Izumi S-I. Rehabilitation with poststroke motor recovery: a review with a focus on neural plasticity. *Stroke research and treatment* 2013;2013
666. Mahlknecht P, Seppi K, Poewe W. The Concept of Prodromal Parkinson’s Disease. *J Parkinsons Dis* [date unknown];5(4):681–697.
667. Granados-Ramos DE, Zamora-Lugo S, Torres-Morales P, et al. Time-frequency analysis of Mismatch Negativity (MMN) in healthy Mexican preschool children. *Rev Mex Neuroci* 2018;19(3):21–39.
668. Enterzari-Taher M, Eisen A, Stewart H, Nakajima M. Abnormalities of cortical inhibitory neurons in amyotrophic lateral sclerosis. *Muscle Nerve* 1997;20(1):65–71.
669. Weskamp K, Tank EM, Miguez R, et al. Shortened TDP43 isoforms upregulated by neuronal hyperactivity drive TDP43 pathology in ALS. *J Clin Invest* 2020;130(3):1139–

1155.

670. Wainger BJ, Kiskinis E, Mellin C, et al. Intrinsic membrane hyperexcitability of amyotrophic lateral sclerosis patient-derived motor neurons. *Cell Rep* 2014;7(1):1–11.
671. Lin Z, Kim E, Ahmed M, et al. MRI-guided histology of TDP-43 knock-in mice implicates parvalbumin interneuron loss, impaired neurogenesis and aberrant neurodevelopment in ALS-FTD. *bioRxiv* 2020;2020.05.24.107177.
672. Devlin A-C, Burr K, Boroah S, et al. Human iPSC-derived motoneurons harbouring TARDBP or C9ORF72 ALS mutations are dysfunctional despite maintaining viability. *Nature communications* 2015;6(1):1–12.
673. Jiang T, Handley E, Brizuela M, et al. Amyotrophic lateral sclerosis mutant TDP-43 may cause synaptic dysfunction through altered dendritic spine function. *Disease Models & Mechanisms* 2019;12(5)
674. Kanouchi T, Ohkubo T, Yokota T. Can regional spreading of amyotrophic lateral sclerosis motor symptoms be explained by prion-like propagation? *J Neurol Neurosurg Psychiatry* 2012;83(7):739–745.
675. Iguchi Y, Eid L, Parent M, et al. Exosome secretion is a key pathway for clearance of pathological TDP-43. *Brain* 2016;139(Pt 12):3187–3201.
676. Feiler MS, Strobel B, Freischmidt A, et al. TDP-43 is intercellularly transmitted across axon terminals. *J Cell Biol* 2015;211(4):897–911.
677. Mishra PS, Boutej H, Soucy G, et al. Transmission of ALS pathogenesis by the cerebrospinal fluid. *Acta neuropathologica communications* 2020;8:1–21.
678. Deleglise B, Lassus B, Soubeyre V, et al. Dysregulated Neurotransmission induces Trans-synaptic degeneration in reconstructed Neuronal Networks. *Scientific Reports* 2018;8(1):11596.
679. Rovegno M, Soto PA, Sáez JC, von Bernhardt R. Biological mechanisms involved in the spread of traumatic brain damage. *Medicina Intensiva (English Edition)* 2012;36(1):37–44.
680. Muthuraman M, Raethjen J, Koirala N, et al. Cerebello-cortical network fingerprints differ between essential, Parkinson’s and mimicked tremors. *Brain* 2018;141(6):1770–1781.
681. Schuster C, Elamin M, Hardiman O, Bede P. Presymptomatic and longitudinal neuroimaging in neurodegeneration—from snapshots to motion picture: a systematic review. *J Neurol Neurosurg Psychiatry* 2015;86(10):1089–1096.
682. Roberts-South A, Findlater K, Strong MJ, Orange JB. Longitudinal changes in discourse production in amyotrophic lateral sclerosis. In: *Seminars in Speech and Language*. New York, NY; 2012 p. 79.
683. Mutanen T, Mäki H, Ilmoniemi RJ. The effect of stimulus parameters on TMS–EEG muscle artifacts. *Brain stimulation* 2013;6(3):371–376.
684. Ruddy KL, Woolley DG, Mantini D, et al. Improving the quality of combined EEG-TMS neural recordings: Introducing the coil spacer. *Journal of Neuroscience Methods* 2018;294:34–39.

685. Borckardt JJ, Smith AR, Hutcherson K, et al. Reducing Pain and Unpleasantness During Repetitive Transcranial Magnetic Stimulation. *The Journal of ECT* 2006;22(4):259–264.
686. Croarkin PE, Wall CA, King JD, et al. Pain During Transcranial Magnetic Stimulation in Youth. *Innov Clin Neurosci* 2011;8(12):18–23.
687. Di Flumeri G, Aricò P, Borghini G, et al. The dry revolution: evaluation of three different EEG dry electrode types in terms of signal spectral features, mental states classification and usability. *Sensors* 2019;19(6):1365.

# 10. Appendices

## 10.1. Appendix chapter 2

### Appendix 2.1. McMackin et al., 2019a

NeuroImage: Clinical 22 (2019) 101706



Contents lists available at ScienceDirect

NeuroImage: Clinical

journal homepage: [www.elsevier.com/locate/ynicl](http://www.elsevier.com/locate/ynicl)



## Neurophysiological markers of network dysfunction in neurodegenerative diseases



Roisin McMackin<sup>a</sup>, Peter Bede<sup>a,b</sup>, Niall Pender<sup>a,c</sup>, Orla Hardiman<sup>a,d,e,1</sup>, Bahman Nasserroleslami<sup>a,1</sup>

<sup>a</sup> Academic Unit of Neurology, Trinity Biomedical Sciences Institute, 152-160 Pearse St., Trinity College Dublin, The University of Dublin, Ireland

<sup>b</sup> Computational Neuroimaging Group, Trinity Biomedical Sciences Institute, 152-160 Pearse St., Trinity College Dublin, The University of Dublin, Ireland

<sup>c</sup> Beaumont Hospital Dublin, Department of Psychology, Beaumont Road, Beaumont, Dublin 9, Ireland

<sup>d</sup> Beaumont Hospital Dublin, Department of Neurology, Beaumont Road, Beaumont, Dublin 9, Ireland

### ARTICLE INFO

#### Keywords:

MEG  
TMS  
EEG  
Neurodegeneration  
Network  
Biomarker

### ABSTRACT

There is strong clinical, imaging and pathological evidence that neurodegeneration is associated with altered brain connectivity. While functional imaging (fMRI) can detect resting and activated states of metabolic activity, its use is limited by poor temporal resolution, cost and confounding vascular parameters. By contrast, electrophysiological (e.g. EEG/MEG) recordings provide direct measures of neural activity with excellent temporal resolution, and source localization methodologies can address problems of spatial resolution, permitting measurement of functional activity of brain networks with a spatial resolution similar to that of fMRI. This opens an exciting therapeutic approach focussed on pharmacological and physiological modulation of brain network activity.

This review describes current neurophysiological approaches towards evaluating cortical network dysfunction in common neurodegenerative disorders. It explores how modern neurophysiologic tools can provide markers for diagnosis, prognosis, subcategorization and clinical trial outcome measures, and how modulation of brain networks can contribute to new therapeutic approaches.

### 1. Introduction

Modern clinical imaging, pathological (Yates, 2012) and genomic (Saura et al., 2015) data, support the evolving notion that neurodegenerative syndromes are best understood in terms of disrupted brain networking. Quantitative Magnetic Resonance Imaging (MRI) and Positron Emission Tomography (PET) provide compelling evidence of widespread network changes in neurodegenerations including Alzheimer's disease (AD) (Canter et al., 2016), Parkinson's disease (PD) (Gratwicke et al., 2015), amyotrophic lateral sclerosis (ALS) (Nasserroleslami et al., 2017) and frontotemporal dementia (FTD) (Bede et al., 2018). New therapeutic approaches based on network modulation are already in use for Parkinson's (Gratwicke et al., 2015) and Alzheimer's Disease (Canter et al., 2016).

Notwithstanding, characterizing changes in brain networking in a clinical setting remains a challenge. Structural MR imaging can show changes in grey and white matter integrity (Symms et al., 2004) and

functional imaging (fMRI) detects resting and activated states of metabolic activity. Neither modality can directly measure neuronal activity, however. Furthermore, as fMRI measurements can be confounded by vascular pathology and are limited by the requirements of the technology (including the need for the patient to remain supine) (Glover, 2011), the use of fMRI is limited in the neurodegenerations. There remains an urgent and unmet need for user-friendly, non-invasive technologies that can rapidly and reliably detect network alteration with high temporal and spatial resolution.

Here we review the biology of non-invasive electrophysiology-based measurements and outline the current state of the art in measurement of network dysfunction in the neurodegenerations. We explore the future potential of emerging electrophysiology-based technologies in providing enhanced temporal resolution, and in using source localization that improves spatial resolution to complement structural and functional imaging.

<sup>\*</sup> Corresponding author at: Academic Unit of Neurology, Trinity College Dublin, The University of Dublin, Room 5.43, Trinity Biomedical Sciences Institute, 152-160 Pearse Street, Dublin D02 R590, Ireland.

E-mail addresses: [mcmackr@tcd.ie](mailto:mcmackr@tcd.ie) (R. McMackin), [bedep@tcd.ie](mailto:bedep@tcd.ie) (P. Bede), [niallpender@beaumont.ie](mailto:niallpender@beaumont.ie) (N. Pender), [hardimao@tcd.ie](mailto:hardimao@tcd.ie) (O. Hardiman), [Bahman.Nasserroleslami@tcd.ie](mailto:Bahman.Nasserroleslami@tcd.ie) (B. Nasserroleslami).

<sup>1</sup> Joint Last Author.

<https://doi.org/10.1016/j.nicl.2019.101706>

Received 12 September 2018; Received in revised form 28 January 2019; Accepted 31 January 2019

Available online 02 February 2019

2213-1582/ © 2019 The Authors. Published by Elsevier Inc. This is an open access article under the CC BY license (<http://creativecommons.org/licenses/by/4.0/>).

## 2. Methods

### 2.1. Electroencephalography and magnetoencephalography

Quantitative EEG (qEEG) and magnetoencephalography (MEG) are increasingly recognized as useful non-invasive methods to measure cortical neurophysiological activity.

MEG and qEEG capture and digitise neuroelectromagnetic reflections of the synchronous generation of excitatory and inhibitory post-synaptic potentials in populations of underlying neurons. Both MEG and qEEG have excellent temporal but, until recently, limited spatial resolution. Several methods, collectively referred to as source localisation methods, have now been developed that enhance the spatial resolution of both EEG and MEG to that of using fMRI (Moeller et al., 2013). This now allows for visualisation of brain activity at low cost, with high levels of both spatial and temporal resolution.

The physiologic basis of MEG and EEG differ. MEG sensors measure the magnetic field generated by the electrical flows in neuronal populations while EEG sensors measure the simultaneously-generated perpendicular electric field that passes through the space between the activity source and sensors (da Silva, 2013). Due to volume conduction, EEG sensors also capture electrical currents propagated between the source and sensor in the conductive human head medium. This effect of volume conduction in EEG may make MEG a more reliable measure for deeper sources.

However, it must be noted that the potential advantage of MEG is reduced by the need for expensive superconductive systems (Wendel et al., 2009) that significantly increase costs, limiting MEG's day-to-day application in clinical settings.

EEG and MEG both generate waveform data, where the x-axis represents time and the y-axis represents amplitude of electrical activity (Box 1). Quantitative M/EEG involves the digitisation of these signals and quantitative analysis of their characteristics (Fig. 1). These analyses can be performed in time and frequency domains. Time domain analysis is the study of how brain activity changes over time (Nuwer, 1997) (for example at what time the intensity of neural activity peaks when performing a cognitive or motor task). Frequency domain analysis involves the use of Fourier transformation to decompose the recording into a combination of waves of different frequencies.

Typically, quantitative M/EEG signal frequencies are grouped into delta (0.5–3 Hz), theta (3–7 Hz), alpha (8–13 Hz), beta (14–30 Hz), and gamma (> 30 Hz) frequency bands (Başar et al., 2001, p.). Oscillations in these different frequency bands have been attributed to different neuronal populations and brain activities (Herrmann et al., 2016) (Box 1). This allows for investigation of brain activity in terms of the power of oscillating network activity at different frequencies, referred to as spectral EEG (Kaiser, 2005). Synchronous or time-correlated

oscillations in different brain areas can also be used to infer functional connectivity between them (Stam et al., 2007). The frequencies of these bands are generally negatively correlated to their amplitude (i.e. lower frequency M/EEG oscillations tend to have higher amplitude). Since amplitude is a reflection of the number of neurons contributing to a signal, lower frequency oscillations are attributed to synchronous activity of larger numbers of neurons (Pfurtscheller and Lopes da Silva, 1999).

These time and frequency domain network characteristics can be examined at rest ("resting-state") to investigate the resting activity of the brain (Fig. 2). M/EEG measures can also be captured during tasks such as cognition, sensation or movement, to measure the activity of brain regions contributing to the generation of that function (Fig. 2) (Garrido et al., 2009; Shibasaki and Hallett, 2006). As tasks are underpinned by integration of various distinct neural networks, the corresponding neural signatures can be marked in the frequency domain, known as event-related (de)synchronisation (ERD/S), and/or the time domain, known as event-related potentials (ERPs) (Box 1). Source localisation methods can subsequently be applied to identify the origin of these of the network components and any changes to their performance in disease. Each of these approaches allows for the study of different aspects of neural network function and can be combined to provide a well-rounded insight into the effects of disease pathology on brain network function.

### 2.2. Transcranial magnetic stimulation (TMS)

TMS is the external application of a magnetic field to cortical neurons of interest, generating an electrical field around them. This electrical field will produce a charge across the membranes of the neurons in this area of the cortex, which will induce neuronal firing (e.g. the proliferation of an action potential along the axon) if of sufficient magnitude (Grunhaus et al., 2002). Using an electromagnetic coil placed on the scalp this magnetic field can be delivered in focal pulses to the cortical area of interest. Therefore TMS has the major advantage of providing a method to stimulate the cortex that is both non-invasive and focal, unlike transcranial electrical stimulation (Elder and Taylor, 2014).

TMS, coupled with surface electromyography (EMG) of muscles of interest can measure pyramidal tract function, anterior horn cell function and muscle activation (Fig. 3). By applying single stimulating pulses to the primary motor cortex, several commonly-used measures can be estimated, including: amplitude of the motor evoked potential (the EMG response to a stimulating pulse), the resting motor threshold (the minimum stimulation required to induce a standard motor evoked potential amplitude in 50% of electromyographic responses), cortical silent period (the period of interruption of voluntary muscle activity

#### Box 1

Electrical and physiological characteristics defined in the context of EEG measurements.

**Amplitude** – The size of the electrical charge in the cerebrospinal fluid produced by the summation of neuroelectric activity such as excitatory and inhibitory post synaptic potentials in cerebral cortical neurons, typically in microvolts ( $\mu\text{V}$ ) (Cohen, 2014).

**Power** – A measure of the intensity of neuronal activity, proportional to the amplitude squared (Cohen, 2014).

**Frequency** – The number of times a cycle of a wave repeats per unit time, measured in hertz (Hz) (Cohen, 2014).

**Frequency bands** – Continuous ranges of frequencies for which measurements are grouped.

**Oscillation** – Continuous, periodic neuronal activity, typically generated by feedback loops in neuronal networks (Herrmann et al., 2016)

**Event-related potential (ERP)** – Electrical potential observed at the time that an event occurs, such as performing a motor or cognitive task or sensory stimulus (Luck et al., 2000, p.).

**Event-related (de)synchronisation (ERD/ERS)** – Relative decrease or increase in the intensity of oscillatory activity in a frequency band, caused by an event such as performing a motor or cognitive task or sensory stimulus (Pfurtscheller and Lopes da Silva, 1999).

**Sensor-level** – Digitised M/EEG data analysed with respect to the position of the sensors on the scalp, providing poor spatial resolution.

**Source-level** – Digitised M/EEG data analysed using source localisation methods to determine the location of contributing sources in the brain, providing spatial resolution comparable to fMRI (Moeller et al., 2013).

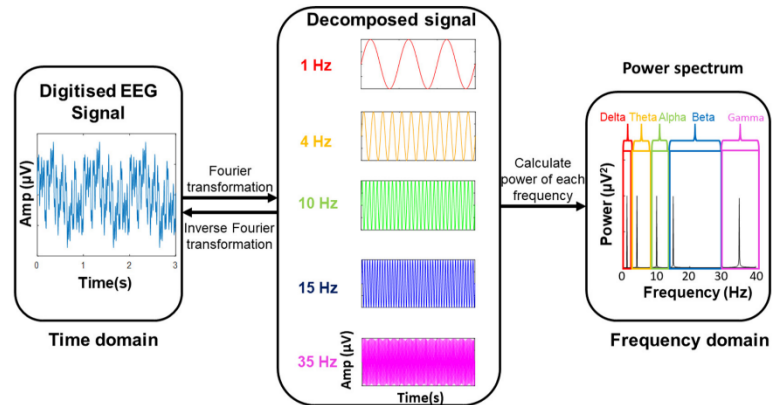


Fig. 1. The transformation of a digitised EEG signal into a frequency power spectrum.

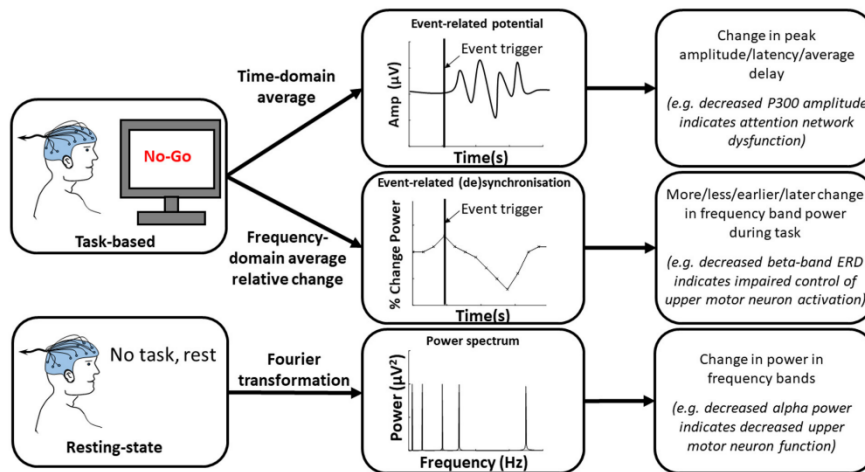


Fig. 2. EEG signal processing avenues for resting-state and task-based paradigms, the quantitative measures obtained and sample interpretations in neurodegenerative disease.

following stimulation of the corresponding motor cortical regions) and central motor conduction time (motor evoked potential latency less peripheral conduction time, measured by applying a TMS pulse at spinal level to the lower motor neurons innervating the target muscle) (Rossini et al., 2015).

Paired-pulse TMS provides the use of a conditioning stimulus (CS) at different intervals in advance of the test stimulus (TS) from either the same coil or a separate coil placed above another cortical region, usually over the opposite hemisphere. This can be used to study changes in inhibitory and excitatory circuits modulating motor cortical function. These measures include changes in short- and long-interval intracortical inhibition, intracortical facilitation, short- and long-interhemispheric inhibition and interhemispheric facilitation. Each of these measures is used to interrogate regulatory inputs to the corticospinal tract (Goss et al., 2012).

### 3. Network dysfunction in neurodegeneration

#### 3.1. Resting state studies

“Resting state” EEG and MEG are used to explore brain activity and functional connectivity in the absence of specific tasks, although it must be acknowledged that the brain is continuously active with ongoing processing of both endogenous and exogenous information (Khanna et al., 2015). Neurodegenerative conditions exhibit changes in resting state that correlate with underlying pathogenic processes, and there is emerging evidence that resting state EEG has considerable discriminatory value in neurodegeneration.

In ALS, resting state EEG can identify changes in the sensorimotor cortex, as exemplified by the presence of decreased alpha-band power (Mai et al., 1998; Nasserolelami et al., 2017; Santhosh et al., 2005).

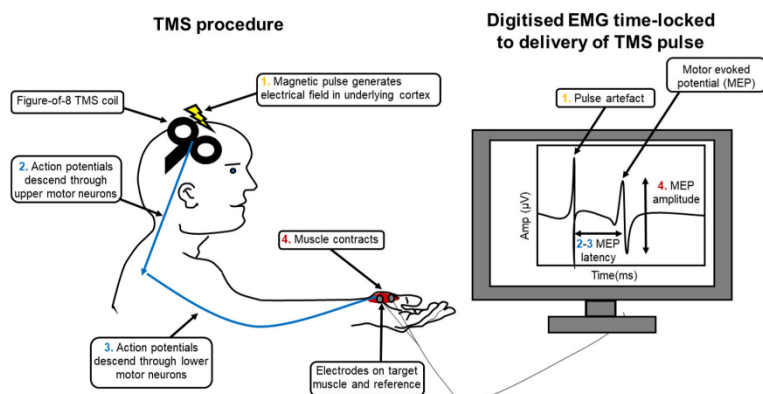


Fig. 3. Schematic of a single-pulse TMS procedure and the quantitative characteristics of the resulting motor evoked potential.

Alpha frequency oscillations over the sensorimotor cortex are attributed to the layer V pyramidal upper motor neurons (Jones et al., 2000), and as alpha power is known to decrease at movement onset (Pfurtscheller and Lopes da Silva, 1999) it is likely to represent the inactive state in these large cells. Loss of power in this band is therefore likely due to loss of cell bodies in this region, and possibly loss of inter-neuronal or thalamic control of the upper motor neurons at rest.

By contrast, broadband gamma power is increased over the motor cortex in PD, a finding that also differentiates PD from dystonia and essential tremor. This difference has been attributed to PD-related changes in the spiking of pyramidal cells (Crowell et al., 2012) and may aid in differential diagnosis. Increase in basal ganglia-cortical beta power is also consistently identified in PD (Giannicola et al., 2010; Jenkinson and Brown, 2011; Pollok et al., 2012). The pathological effect of such excessive oscillations has been established using deep brain stimulation, with 5–20 Hz stimulation, but not 30–50 Hz stimulation, exacerbating bradykinesia (Jenkinson and Brown, 2011).

Resting state EEG can also detect changes in brain connectivity. In ALS, resting state studies have identified increased connectivity throughout the cortex including increased median absolute coherence in theta and gamma band frequencies over prefrontal areas, accompanied by decreased gamma band synchrony for some prefrontal electrodes (Nasserolelami et al., 2017). Cortical gamma band oscillations have been linked to higher cognitive functions such as intermodal selective attention and perception (Herrmann et al., 2016), providing a quantitative measure for detecting early cognitive impairment in ALS. In PD, decreased frontoparietal connectivity coherence in alpha band is also associated with early executive impairment (Teramoto et al., 2016), suggesting that deterioration of frontoparietal attention networks contributes to executive dysfunction in PD.

Numerous studies have highlighted the utility of combining such resting state EEG activity and connectivity measures for differential diagnosis of neurodegenerations, particularly the dementias (Nardone et al., 2018). For example, using temporal high beta, parietal theta and alpha and high beta power, a stepwise discrimination function can distinguish AD and FTD patients with 84.6% accuracy and is highly accurate in separating controls (100%) from FTD patients (84.6%) (Yener et al., 1996). With increase in computational power, this methodology has been enhanced, with training support vector machine classifiers using 25 EEG parameters capable of deciphering AD, PD, LBD and bvFTD with 100% specificity and sensitivity (Garn et al., 2017).

Such multidimensional biomarkers may also be enhanced by the addition of imaging and/or psychological task parameters to capture

differences between broad, overlapping network pathologies. This has been demonstrated by logistic regression models combining cognitive task performance with delta and theta oscillatory activity which provide 93.3% accuracy when distinguishing AD from FTD (Lindau et al., 2003).

EEG measures can also quantify responses to drug therapies, for example in PD patients L-DOPA is found to induce widespread reduction in cortical delta and alpha activity, considered to reflect an excitatory effect of dopamine neuromodulation (Babiloni et al., 2019), in addition to suppressing elevated beta oscillations in correlation with motor improvement (Muthuraman et al., 2018). Such measures therefore have potential to provide objective, quantitative measures of drug effects on neurodegenerative pathology, enhancing the power of clinical trials. This potential has already been harnessed as a dose-finding pharmacodynamic biomarker in rodents, wherein dose-dependent increase in gamma band power in rats was used to estimate therapeutically relevant concentrations of a potential antidepressant drug in humans. This effect translated to similar increases in human resting-state EEG upon drug delivery (Sanacora et al., 2014).

Longitudinal resting-state M/EEG studies have been performed for a number of neurodegenerative conditions, but they are few in number. In AD, relative alpha and beta power is decreased, while relative theta and delta power increased longitudinally (Coben et al., 1985), with changes in relative theta power capable of distinguishing between different stages of dementia. This pattern is consistent across populations (Kwak, 2006; Verdoorn et al., 2011), demonstrating a global slowing in brain network signalling in AD.

Longitudinal increase in beta power has also been observed in PD, correlating with decline in Rey Auditory-Verbal Learning Test performance (Caviness et al., 2015), consistent with increasing delta power capturing progressive decline of specific cognitive networks. PD patients also show early impairment in brain network local efficiency as well as network decentralization which progress over time (Dubbink et al., 2014).

In ALS a single longitudinal resting-state study has been reported revealing widespread, progressive increase in median coherence in theta and low gamma band frequencies (Nasserolelami et al., 2017). This suggests that abnormal functional connectivity worsens throughout ALS pathology. Network activity may increase at disease onset and decline thereafter, and accordingly future studies will also require correlation with time from disease onset, and clinical stage of disease.

These studies demonstrate the ability of resting-state EEG to



**Table 1**  
Neurophysiological biomarkers for and therapies in neurodegeneration.

Technology	Method	Clinical application		Biomarker/symptom	Reference
		Example	Disease		
EEG/MEG	Resting state	Differential diagnosis	FTD, AD, PDD, DLB	Multiple	(Garr et al., 2017; Nardone et al., 2018; Yener et al., 1996)
TMS	Paired pulse	CT outcome measure	PD	Beta power	(Babiloni et al., 2019; Muthuraman et al., 2018)
rTMS	To leg area of motor cortex To leg area of motor cortex	Diagnostic biomarker	ALS	SICI	(Memon et al., 2015; Vučić et al., 2008)
		Therapy	MS	Spasticity	(NCI02450552, NCT02781454)
			PD	Freezing of gait	(Mori et al., 2010, 2011)
				Refractory depression	(Chang et al., 2017; Kim et al., 2015)
					(NCT02850159)
					(Lesenský et al., 2018)
			FTD, AD	Language, memory, executive function	(Antczak et al., 2018; Rutherford et al., 2015)
					(NCT02621424)
DBS	To basal ganglia	Therapy	PD	UPDRS score, mobility, activities of daily living, emotion, stigma, discomfort	(Deuschl et al., 2006)
			AD	ADAS-cog	(Kuhn et al., 2015)

CT – Clinical trial, DLB – Dementia with Lewy Bodies, AD – Alzheimer's disease, PD – Parkinson's disease, FTD – Frontotemporal dementia, MMN – Mismatch Negativity, rTMS – Repetitive TMS, DBS – Deep brain stimulation, SICI – Short Interval Intra-Cortical Inhibition, UPDRS – Unified Parkinson's disease Rating Scale, ADAS-cog – Alzheimer's Disease Assessment Scale-Cog.

characterize and quantify neurodegenerations and their progression (see Table 1). In all cases, to attribute the recorded changes to specific networks, source localisation will be required. Moreover, future longitudinal studies will require extensive validation across large groups of well-phenotyped patients.

### 3.1.1. Source localization studies

Source-level studies using quantitative EEG can correlate pathological neuroelectric signals with anatomic locations. For example, in AD increases in delta band activity are localised to orbitofrontal and temporal cortices, while frontotemporal dementia (FTD) patients differ, exhibiting decreases in low alpha band activity in these areas (Nishida et al., 2011). By contrast, reduced alpha activity in occipital sources and widespread increase in delta sources is revealed by source localisation in PD with and without cognitive impairment (Babiloni et al., 2019).

Source localisation can also be used to enhance the spatial resolution of connectivity measures. For example, localised lagged linear connectivity in alpha band has been found to discriminate AD, Dementia with Lewy Bodies and PD dementia from controls with areas under the ROC curves of 0.84, 0.78 and 0.75 respectively. Source localisation of EEG resting state connectivity in ALS patients has also revealed increased functional connectivity between the posterior parietal cortices (PPCs) and between the PPC and the motor cortex, dorsolateral, dorsomedial and ventrolateral prefrontal cortices. Source analysis also reveals increases in general connectivity of the anterior and posterior cingulate cortices, fronto-insular cortex, anterior insular cortex and dorsomedial and ventrolateral prefrontal cortices to other brain areas in ALS (Iyer et al., 2015). Source localised EEG measures therefore provide objective evidence that ALS and FTD have overlapping pathologies (Phukan et al., 2007), with cognitive networks disrupted in FTD, such as the frontoparietal attention networks (Zhou et al., 2010), also dysfunctioning in ALS, while central and parietal activity known to be abnormal in ALS (Nasser-oleslami et al., 2017), is found to distinguish FTD from AD (Nishida et al., 2011).

### 3.2. Activation studies

#### 3.2.1. Event-related M/EEG

Network performance can also be quantified by measuring frequency or time domain characteristics of M/EEG signals generated by the performance of motor (Shibasaki and Hallett, 2006), sensory (Momma et al., 1987) or cognitive (Luck et al., 2000) tasks designed to activate target neural networks.

**3.2.1.1. Motor tasks.** M/EEG can provide quantitative measures of motor network performance during movement. Movements are preceded by decrease in alpha and beta band oscillation power in the primary motor cortex. This is referred to as event-related desynchronisation (ERD). ERD is interpreted as an electrophysiological correlate of increasing activity in cortical areas involved in the movement (Pfurtscheller and Lopes da Silva, 1999). ERD is therefore used to quantitatively measure motor cortex dysfunction in disease. For example, in multiple sclerosis (MS), latency of ERD correlates with structural MRI T1 lesion volume and T2 lesion load (Leocani et al., 2005), while in PD, ERD begins closer to movement onset (Defebvre et al., 1994), particularly in the affected hemisphere (Defebvre et al., 1996). This difference is partially corrected by L-DOPA (Defebvre et al., 1998). By contrast, ERD is conserved in the upper motor neuron syndrome of Primary Lateral Sclerosis, despite the presence of decreased amplitude in movement-related potentials (Bai et al., 2006), suggesting that changes in ERD may quantify dysfunction of cells that regulate the primary motor cortex or non-upper motor neuron cells that receive thalamo-cortical input.

Following ERD, in the first second after movement ends, increased beta-band oscillations are recorded in the primary motor cortex, most

prominent over the contralateral sensorimotor cortex. This is referred to as beta event related synchronisation (ERS) and is attributed to a shift of the primary motor cortex from activation back to an inactive state (Pfurtscheller and Lopes da Silva, 1999). Change in post-movement ERS has also been documented in MS, PD and ALS, providing additional quantitative measurement of motor cortex dysfunction. In MS, the latency of the ERS peak is significantly later and correlates to longer information processing speeds (Barratt et al., 2017), while in both ALS (Riva et al., 2012) and PD (Diez et al., 1999) ERS is reduced, even during dopaminergic treatment (Pfurtscheller et al., 1998). In ALS, negative correlations between ERS and measures of structural (sub-cortical frontal apparent diffusion coefficient) and functional (MEP to compound muscle action potential ratio) corticospinal tract integrity have also been reported (Riva et al., 2012). Increase in ERS may therefore represent a measure of impaired inhibition or excess activity of upper motor neurons.

The time domain characteristics of M/EEG can provide additional neurophysiological correlates of motor tasks, known as movement related potentials (MRPs) (Luck et al., 2000). Two major MRPs are elicited during motor planning. These are the Bereitschaftspotential (BP) (Shibasaki and Hallett, 2006) and the contingent negative variation (Rockstroh et al., 1993), providing measures of contributing motor preparatory and planning networks' function.

Source localisation has attributed the early BP to the supplementary motor area and premotor cortex bilaterally, followed by activity in the contralateral premotor and primary motor cortices (Shibasaki and Hallett, 2006). In PD, BP peak amplitude is not affected in patients compared with controls, but the early part of the waveform is attenuated (Dick et al., 1989). Decrease in peak amplitude does, however, correlate with increasing disease severity (Patil et al., 2017). This may reflect inadequate activation of the supplementary motor area by the basal ganglia (Dick et al., 1989) or supplementary motor area pathology in PD. Comparable findings in ALS, wherein BP amplitude is inversely correlated with spasticity (Westphal et al., 1998), demonstrate an overlap in the network pathology of these two neurodegenerations in the basal ganglia and/or the supplementary motor area. Such clinical correlation also points to a utility of these measures as prognostic biomarkers.

The contingent negative variation (CNV) has been localised in part to the premotor cortex and supplementary motor area (Hultin et al., 1996); however, CNV also represents prefrontal network activity in the orbitofrontal, mesial and dorsolateral prefrontal cortices, unlike the BP (Ikeda et al., 1996), therefore capturing additional motor preparatory network components. Mean amplitude of CNV is increased in ALS (Hanagasi et al., 2002), decreased in PD (Pulvermüller et al., 1996) and MS (Praagstra et al., 1996; Uysal et al., 2014) and unaffected in Alzheimer's disease (AD) (van Deursen et al., 2009). The discrepancy between ALS-related BP and CNV abnormalities suggests that prefrontal network decline makes an important contribution to changes in this ERP, consistent with the now-well established cognitive component of ALS pathology (Phukan et al., 2007). Furthermore, decrease in CNV amplitude over the parietal cortex in MS correlates with neuropsychological test performance (Uysal et al., 2014). This suggests that CNV also captures parietal network components pertaining to movement preparation and planning.

Localisation analyses have yet to identify the source(s) causing the disease-related abnormalities in MRPs. Such analyses are likely to reveal which cognitive and motor network components contribute to MRP changes in each of these neurodegenerations, highlighting any network overlap and potentially providing distinguishing biomarkers.

**3.2.1.2. Sensory tasks.** Somatosensory ERPs, commonly referred to as SEP or SSEP, can provide information about the involvement of primary somatosensory cortex and its inputs in neurodegenerative diseases. For example, dysfunction of thalamocortical neurons of the ascending somatosensory tracts can be shown in ALS and HD. N20, an ERP

generated by median nerve stimulation, is attributed to the initial primary somatosensory cortex in somatosensation (Banoub et al., 2003). N20 has increased latency in HD (Abbruzzese et al., 1990) and ALS (Zhang et al., 2014) patients, indicating pathological delay in transmission of stimuli to the cortex. In ALS, N20 latency increase occurs in the presence of normal peripheral conduction time, while in HD P15 latency (attributed to the brainstem (Momma et al., 1987) is normal (Josiasen et al., 1982), indicating that these impairments represent dysfunction of thalamocortical neurons of the ascending somatosensory tracts in ALS and HD pathology. Decrease in N20 amplitude also correlates to disease duration in ALS (Iglesias et al., 2015), which may reflect spread of pathology from the motor cortex to the primary somatosensory with disease progression.

**3.2.1.3. Cognitive tasks.** A variety of different cognitive ERPs and ERP subcomponents have been used to objectively assess performance of different cognitive tasks in neurodegeneration, including P3 and mismatch negativity.

P3 is a positive peak seen in the average ERP 200-500 ms after an infrequent 'deviant' stimulus is delivered in a train of attended 'standard' stimuli, known as an oddball paradigm. It has been associated with inhibition of cortical networks to facilitate delivery of attention stimuli in the aftermath of an alerting signal (Polich, 2007), and therefore can be used to quantify attention network impairment in neurodegenerative disease. For example, as P3 latency is longer for more complex stimulus evaluation and decision making tasks (Polich, 2007), P3 latency is used to test the speed of attentional processes.

P3 latency is increased in MCI (Lai et al., 2010), AD (Pedroso et al., 2012), ALS (Gil et al., 1995) and PD (Tokic et al., 2016) and is predicted by lesion load in MS (Kimiskidis et al., 2016). P3 has been shown to be delayed or absent in 100% of a small group of cognitively impaired ALS patients (Portet et al., 2001) and is inversely correlated to performance in cognitive tasks globally, as well as specifically for language and attention in AD (Lee et al., 2013).

Mismatch negativity (MMN), also referred to as N2a) is another cognitive ERP generated by oddball paradigms, however unlike P3, MMN has the advantage that it does not require active patient participation. MMN is a negative peak at approximately 200 ms post-stimulus seen when the average ERP following a standard stimulus is subtracted from the average response to deviant stimuli. MMN is a physiological measure of working sensory memory, involuntary attention switching and sensory accuracy, therefore capturing both cognitive and sensory networks (Garrido et al., 2009).

MMN shows increased average delay correlating to response-inhibition task performance in ALS (Iyer et al., 2017), while in both PD and MS MMN is reduced in cognitively impaired patients compared to those without cognitive impairment (Brönnick et al., 2010; Jung et al., 2006). Reduced MMN amplitude is also reported in MCI and AD as reviewed by Horvath et al. (2018). Such cognitive correlations to MMN impairment point to the potential of MMN an additional quantitative measure of network dysfunction in neurodegeneration.

Few longitudinal studies of change in cognitive ERPs have been published, although in AD the P3 latency has repeatedly been shown to increase over time (Ball et al., 1989), with latency increase being more substantial in those with greater cognitive decline (St Clair et al., 1988). In ALS, correlation studies have found that P3 amplitude is related to disease duration (Volpato et al., 2010) and that P3a latency correlates to months from disease onset and symptoms severity (Raggi et al., 2008), consistent with progressive network decline with disease progression.

Source analysis of MMN and P3 can distinguish different degenerations with similar sensor-level ERP changes and provide more information about neurodegenerative pathology. To date however, few studies have utilised source analysis to determine the exact location of the networks producing such abnormalities, and the spatial resolution of existing findings remains to be definitively established.

### 3.2.2. Transcranial magnetic stimulation

TMS has been established for three decades as a useful tool that interrogates cortical and potentially subcortical motor networks (Rossini et al., 2015). TMS can interrogate motor cortical excitability and has demonstrated that hyperexcitability is a feature of feature of ALS, PD and HD, although the excitable characteristics of these conditions differ (discussed below).

Resting motor threshold (RMT), a TMS-based measure of upper motor neuron excitability, is decreased in ALS (Grieve et al., 2015; Vucic et al., 2008) and AD (Liepert et al., 2001) but not in PD (Ni et al., 2013) or HD (Abbruzzese et al., 1997). Conversely, PD patients show greater motor evoked potential (MEP) amplitudes at low stimulus intensity (Leon-Sarmiento et al., 2013) and an inverse correlation between motor impairment and RMT (Park et al., 2016).

TMS can also interrogate the function of intracortical circuits regulating the corticospinal tract. SICI is a measure of the increase in muscle response to cortical magnetic stimulation due to a preceding conditioning stimulus from the same coil and is a measure of inhibitory interneuron function (Ziemann et al., 1996). Huntington's disease (HD), AD, PD and ALS each exhibit reduced short intracortical inhibition (SICI) (Abbruzzese et al., 1997; Grieve et al., 2015; Liepert et al., 2001; Ni et al., 2013; Pierantozzi et al., 2002; Vucic et al., 2008). This suggests that reduced inhibitory input to upper motor neurons contributes to corticospinal tract hyperexcitability. SICI may also capture dysfunction of dopaminergic circuitry. Dopaminergic drugs can increase SICI, while anti-dopaminergic drugs decrease SICI (Ziemann et al., 2015). Furthermore, in PD, dopaminergic drugs and BG deep brain stimulation can partially rectify reduced SICI (Ni et al., 2013; Pierantozzi et al., 2002). In AD, SICI decrease correlates with cognitive decline, and can be partially counteracted by donepezil (Liepert et al., 2001), also suggesting some cholinergic input to the SICI-generating circuitry.

Intracortical facilitation (ICF) is the increase in muscle response to cortical magnetic stimulation due to a preceding conditioning stimulus from the same coil. The interstimulus interval values giving rise to ICF are higher than those for SICI. ICF is increased in HD (Abbruzzese et al., 1997), ALS (Grieve et al., 2015; Vucic et al., 2008) and PD (Ni et al., 2013). The circuitry underlying ICF is relatively poorly understood, although novel investigation using the threshold tracking method indicates that short and long ICF measures of different circuitry exist, which differ in underlying circuitry from each other and that of SICI (Van den Bos et al., 2018). Pharmacological studies suggest ICF also involves GABAergic and dopaminergic circuitry (Ziemann et al., 2015). Consistent with this hypothesis, the ICF increase in PD can be partially counteracted by dopaminergic treatment (Ni et al., 2013).

Both increased ICF and decreased/absent SICI have been reported in three pre-symptomatic SOD-1 mutant carriers who later developed ALS (Vucic et al., 2008), while increased RMT has been found in preclinical and very early HD (Schippling et al., 2009).

These observations point to the potential utility of TMS-based biomarkers of early neurodegeneration (see Table 1).

Longitudinal TMS studies in ALS show decreases in MEP amplitude and increases in RMT (Floyd et al., 2009) and cortical silent period (Mills, 2003) with progression of the disease. SICI also correlates with measures of disease progression (compound muscle action potential, strength-duration time constant and neurophysiologic index) (Vucic and Kiernan, 2006) in TT-TMS studies. This is consistent with early excess excitation which later declines with degeneration of the motor system, leading to loss of function. In keeping with this hypothesis, RMT is decreased in patients who do not exhibit a weakness, wasting or upper motor neuron symptoms, but increased in those with lower and upper motor neuron symptoms (Mills and Nithi, 1997).

## 4. Therapeutic approaches using network modulation

### 4.1. Electrical and magnetic stimulation

Given the extensive literature of network dysfunction across the neurodegenerations, the neurophysiological modulation of these abnormalities presents a potential therapeutic target for these disorders (see Table 1). In addition to the utility of deep brain stimulation in artificially maintaining basal ganglia function in PD, it is now known to have a separate therapeutic effect on the disease, improving motor function and emotional well-being compared to medication alone (Deuschl et al., 2006). In a small study of AD patients stimulation of the nucleus basalis of Meynert stabilises or improves cognition over a year (Kuhn et al., 2015), illustrating the potential utility of deep brain stimulation in other brain network disorders.

TMS can also be used to deliver trains of magnetic stimuli to any part of the cortex, typically at least once per second, in order to alter network activity. This is known as repetitive TMS (rTMS) and has recently been approved as a therapy for treatment-resistant depression (George et al., 2013). rTMS has now been found to have therapeutic effects in a number of neurodegenerative diseases. Such effects include reduction of spasticity in MS (Mori et al., 2010, 2011), improved cognition and functionality in FTD (Antczak et al., 2018), improved cognition and reduced cognitive decline in AD (Rutherford et al., 2015) and reduced freezing of gait in PD (Kim et al., 2015). Furthermore, six out of seven studies investigating the effects of rTMS on refractory depression in PD identified significant improvement (Lesenskyj et al., 2018).

Some such effects are already being brought towards clinical practice. For example, rTMS is currently being investigated as a network modulating therapy for dementia in MCI or AD (NCT02621424) and spasticity in MS (NCT02747914, NCT01106365). A completed trial of rTMS in PD (NCT03219892) has also identified a significant therapeutic effect on freezing of gait as well as ambulatory and motor function (Chang et al., 2017).

### 4.2. Pharmacological network modulation

Pharmacological intervention to rectify network dysfunction is being investigated in a number of neurodegenerations. In addition to the correction of neurophysiological measures by existing drug therapies (Defebvre et al., 1998; Liepert et al., 2001; Ni et al., 2013), novel neurotherapeutics are being investigated on the basis of their network modulating properties. In ALS, a recent retigabine trial has used decrease in SICI as a recruitment criterion (NCT02450552) while a trial of mexiletine (NCT02781454) is now using change in RMT and SICI as primary and secondary outcome measures respectively. Resting-state EEG was also utilised as a secondary outcome measure in testing the nutritional aid Souvenaid as a therapy in AD, with change in delta band functional connectivity showing improved trajectory (Scheltens et al., 2012).

A combination of multimodal evoked potentials was also used an outcome measure in a phase III trial (NCT01765361) of the recently approved drug ocrelizumab for MS.

These early studies point to a move towards therapies based on modulation of network dysfunction, allowing for earlier, and possibly presymptomatic intervention based on early changes in physiological measures.

## 5. Conclusion

Neurophysiological recording and neuro-electric/–magnetic signal analysis can characterize patterned changes of network function in neurodegeneration, opening up opportunities for novel biomarkers of disease progression. The attractive properties of neurophysiological measurements have often been overlooked in the past. The

development of focal TMS and source localisation of M/EEG signals can now provide direct measurements of network activity with high spatiotemporal resolution. These new developments provide additional opportunities for neurophysiology-based signal analysis as an additional investigational tool in neurodegeneration.

Directly quantifying network activity can be used to objectively identify neurodegeneration without relying on subjectively-measured symptoms which manifest from network dysfunction. This can allow for earlier and potentially presymptomatic intervention, providing greater probability of therapeutic success. Such measures are already being harnessed in clinical trials, however their full potential as outcome measures is still underexploited.

Neuroelectric signalling studies have already sufficiently demonstrated the importance of network dysfunction in neurodegeneration to drive development of network modulating stimuli and drugs as the therapeutic options and suggests that other pharmacologic agents that act to modulate network dysfunction are likely to be of therapeutic benefit. Additional studies are now required to fully exploit the potential of M/EEG and TMS across the range of neurodegenerations, including additional processing and source localization that can discriminate different disease subtypes.

#### Acknowledgments

Funding sources include the Irish Health Research Board (OH, BN, PB) [grant numbers: EIA-2017-019, HRB-MRCG-2018-02, HRB-JPND-2017-1], the Irish Research Council (RM, BN) [grant numbers: GOIPG/2017/1014, GOIPD/2015/213], Science Foundation Ireland [grant number: 16/ERC/D/3854], the American ALS Association (OH) [grant number: ALS18-CM-396], Research Motor Neurone (OH, RM), the Irish Institute of Clinical Neuroscience (IICN) – Novartis Ireland Research grant (PB) and the Iris O'Brien Foundation (PB). Funding sources had no involvement in the writing of this review.

#### Search strategy and selection criteria

References for this Review were identified by searches of PubMed, Google Scholar and ScienceDirect with no time or language restrictions. Primary search terms included the methodologies ('transcranial magnetic stimulation', 'electroencephalography', 'magnetoencephalography', 'fMRI', 'PET') and neurodegenerations ('frontotemporal dementia', 'Alzheimer's disease', 'Parkinson's disease', 'multiple sclerosis', 'amyotrophic lateral sclerosis', 'Huntington's disease') under review, with follow up secondary searches of any neural networks, electrophysiological methodologies or anatomy deemed relevant from the primary search. The only anatomical limitation was the exclusion of occipital electrophysiology to due to relatively limited literature.

#### Declaration of interest

OH has consulted for ONO Pharmaceuticals and KNOPP Pharmaceuticals, and has received research support from Sanofi-Aventis and Serono Pharmaceuticals. OH has received advisory board fees from Novartis, Biogen, and Merck Sorono, and has received travel and accommodation sponsorship from Merck Sorono. She is the inventor of a patent held by the Royal College of Surgeons in Ireland for the use of angiogenin as a therapeutic in ALS. PB receives a Novartis Research Grant from the Irish Institute of Clinical Neuroscience. NP was Speaker Honorarium for Biogen (Feb 2018).

#### References

Abbruzzese, G., Dall'Agata, D., Morena, M., Reni, L., Favale, E., 1990. Abnormalities of parietal and prerolandic somatosensory evoked potentials in Huntington's disease. *Electroencephalogr. Clin. Neurophysiol. Potentials Sect.* 77, 340–346. [https://doi.org/10.1016/0168-5597\(90\)90055-1](https://doi.org/10.1016/0168-5597(90)90055-1).

Abbruzzese, G., Buccolieri, A., Marchese, R., Trompetto, C., Mandich, P., Schieppati, M., 1997. Intracortical inhibition and facilitation are abnormal in Huntington's disease: a paired magnetic stimulation study. *Neurosci. Lett.* 228, 87–90.

Antczak, J., Kowalska, K., Klimkiewicz-Mrowiec, A., Wach, B., Kasprzyk, K., Banach, M., Rzeźnicka-Brzegowy, K., Kubica, J., Slowik, A., 2018. Repetitive transcranial magnetic stimulation for the treatment of cognitive impairment in frontotemporal dementia: an open-label pilot study. *Neuropsychiatr. Dis. Treat.* 14, 749–755. <https://doi.org/10.2147/NDT.S153213>.

Babiloni, C., Del Percio, C., Lizio, R., Noce, G., Lopez, S., Soricelli, A., Ferri, R., Pascarelli, M.T., Catania, V., Nobili, F., Arnaldi, D., Famà, F., Orzi, F., Buttinelli, C., Giubilei, F., Bonanni, L., Franciotti, R., Onofri, M., Stirpe, P., Fuhr, P., Gschwandtner, U., Ransmayr, G., Fraioli, L., Parnetti, L., Farotti, L., Pievani, M., D'Antonio, F., De Lena, C., Güntekin, B., Hanoğlu, L., Yener, G., Emek-Savas, D.D., Triggiani, A.L., Taylor, J.P., McKeith, I., Stocchi, F., Vacca, L., Frisoni, G.B., De Pandis, M.F., 2019. Levodopa may affect cortical excitability in Parkinson's disease patients with cognitive deficits as revealed by reduced activity of cortical sources of resting state electroencephalographic rhythms. *Neurobiol. Aging* 73, 9–20. <https://doi.org/10.1016/j.neurobiolaging.2018.08.010>.

Bai, O., Vorbach, S., Hallett, M., Floeter, M.K., 2006. Movement-related cortical potentials in primary lateral sclerosis. *Ann. Neurol.* 59, 682–690.

Ball, S.S., Marsh, J.T., Schubarth, G., Brown, W.S., Strandburg, R., 1989. Longitudinal P300 latency changes in Alzheimer's disease. *J. Gerontol.* 44, M195–M200.

Banoub, M., Tetzlaff, J.E., Schubert, A., 2003. Pharmacologic and physiologic influences affecting sensory evoked potentials: implications for perioperative monitoring. *Anesthesiol. J. Am. Soc. Anesthesiol.* 99, 716–737.

Barratt, E.L., Tewarie, P.K., Clarke, M.A., Hall, E.L., Gowland, P.A., Morris, P.G., Francis, S.T., Evangelou, N., Brooks, M.J., 2017. Abnormal task driven neural oscillations in multiple sclerosis: a visuomotor MEG study. *Hum. Brain Mapp.* 38, 2441–2453. <https://doi.org/10.1002/hbm.23531>.

Başar, E., Schürmann, M., Demiralp, T., Başar-Eroglu, C., Ademoglu, A., 2001. Event-related oscillations are 'real brain responses'—wavelet analysis and new strategies. *Int. J. Psychophysiol. Off. J. Int. Organ. Psychophysiol.* 39, 91–127.

Bede, P., Omer, T., Finegan, E., Chipika, R.H., Iyer, P.M., Doherty, M.A., Vajda, A., Pender, N., McLaughlin, R.L., Hutchinson, S., Hardiman, O., 2018. Connectivity-based characterisation of subcortical grey matter pathology in frontotemporal dementia and ALS: a multimodal neuroimaging study. *Brain Imaging Behav.* 1 (12). <https://doi.org/10.1007/s11682-018-9837-9>.

Brønneck, K.S., Nordby, H., Larsen, J.P., Aarsland, D., 2010. Disturbance of automatic auditory change detection in dementia associated with Parkinson's disease: a mismatch negativity study. *Neurobiol. Aging* 31, 104–113. <https://doi.org/10.1016/j.neurobiolaging.2008.02.021>.

Canter, R.G., Penney, J., Tsai, L.-H., 2016. The road to restoring neural circuits for the treatment of Alzheimer's disease. *Nature* 539, 187–196. <https://doi.org/10.1038/nature20412>.

Caviness, J.N., Hentz, J.G., Belden, C.M., Shill, H.A., Driver-Dunckley, E.D., Sabbagh, M.N., Powell, J.J., Adler, C.H., 2015. Longitudinal EEG changes correlate with cognitive measure deterioration in Parkinson's disease. *J. Park. Dis.* 5, 117–124. <https://doi.org/10.3233/JPD-140480>.

Chang, W.H., Kim, M.S., Park, E., Cho, J.W., Youn, J., Kim, Y.K., Kim, Y.-H., 2017. Effect of dual-mode and dual-site noninvasive brain stimulation on freezing of gait in patients with Parkinson disease. *Arch. Phys. Med. Rehabil.* 98, 1283–1290. <https://doi.org/10.1016/j.apmr.2017.01.011>.

Cohen, L.A., Danziger, W., Storandt, M., 1985. A longitudinal EEG study of mild senile dementia of Alzheimer type: changes at 1 year and at 2.5 years. *Electroencephalogr. Clin. Neurophysiol.* 61, 101–112.

Cohen, M.X., 2014. *Analyzing Neural Time Series Data: Theory and Practice*. MIT Press.

Crowell, A.L., Ryapolova-Webb, E.S., Ostrem, J.L., Galifianakis, N.B., Shimamoto, S., Lim, D.A., Starr, P.A., 2012. Oscillations in sensorimotor cortex in movement disorders: an electrocorticography study. *Brain* 135, 615–630. <https://doi.org/10.1093/brain/awr332>.

da Silva, F.L., 2013. EEG and MEG: relevance to neuroscience. *Neuron* 80, 1112–1128.

Defebvre, L., Bourriez, J.-L., Dujeardin, K., Derambure, P., Destee, A., Guieu, J.-D., 1994. Spatiotemporal study of Bereitschaftspotential and Event-Related Desynchronization during voluntary movement in Parkinson's disease. *Brain Topogr.* 6, 237–244. <https://doi.org/10.1007/BF01187715>.

Defebvre, L., Bourriez, J.L., Destee, A., Guieu, J.D., 1996. Movement related desynchronization pattern preceding voluntary movement in untreated Parkinson's disease. *J. Neurol. Neurosurg. Psychiatry* 60, 307–312.

Defebvre, L., Bourriez, J.L., Derambure, P., Duhamel, A., Guieu, J.D., Destee, A., 1998. Influence of chronic administration of l-DOPA on event-related desynchronization of mu rhythm preceding voluntary movement in Parkinson's disease. *Electroencephalogr. Clin. Neurophysiol. Mot. Control* 109, 161–167. [https://doi.org/10.1016/S0924-980X\(97\)00085-4](https://doi.org/10.1016/S0924-980X(97)00085-4).

Deuschl, G., Schade-Brittinger, C., Krack, P., Volkmann, J., Schäfer, H., Bötzel, K., Daniels, C., Deuschländer, A., Dillmann, U., Eisner, W., Gruber, D., Hamel, W., Herzog, J., Hilker, R., Klebe, S., Kloss, M., Koy, J., Krause, M., Pusch, A., Lorenz, D., Lorenz, S., Mehndorn, H.M., Moringlane, J.R., Oertel, W., Pinski, M.O., Reichmann, H., Reuss, A., Schneider, G.-H., Schnitzler, A., Steude, U., Sturm, V., Timmermann, L., Tronnier, V., Trottenberg, T., Wojtecki, L., Wolf, E., Poewe, W., Voges, J., German Parkinson Study Group, Section, Neurostimulation, 2006. A randomized trial of deep-brain stimulation for Parkinson's disease. *N. Engl. J. Med.* 355, 896–908. <https://doi.org/10.1056/NEJMoa060281>.

Dick, J.P., Rothwell, J.C., Day, B.L., Cantello, R., Buruma, O., Gioux, M., Benecke, R., Berardelli, A., Thompson, P.D., Marsden, C.D., 1989. The Bereitschaftspotential is abnormal in Parkinson's disease. *Brain J. Neurol.* 112 (Pt 1), 233–244.

Diez, null, Ortmayr, B., Pichler-Zalaudek, K., Reisecker, F., Pfurtscheller, G., 1999.

- Ergebnisbezogene EEG-desynchronisation und synchronisation (ERD und ERS) bei idiopathischem Parkinson-Syndrom. *Klin. Neurophysiol.* 30, 15–21. <https://doi.org/10.1055/s-2008-1066081>.
- Dubbelink, O., E, K.T., Hillebrand, A., Stoffers, D., Deijen, J.B., Twisk, J.W.R., Stam, C.J., Berendse, H.W., 2014. Disrupted brain network topology in Parkinson's disease: a longitudinal magnetoencephalography study. *Brain* 137, 197–207. <https://doi.org/10.1093/brain/awt316>.
- Elder, G.J., Taylor, J.-P., 2014. Transcranial magnetic stimulation and transcranial direct current stimulation: treatments for cognitive and neuropsychiatric symptoms in the neurodegenerative dementias? *Alzheimers Res. Ther.* 6 (74). <https://doi.org/10.1186/s13195-014-0074-1>.
- Floyd, A.G., Yu, Q.P., Fiboolorak, P., Tang, M.X., Fang, Y., Smith, W.A., Yim, J., Rowland, L.P., Mitsunoto, H., Pullman, S.L., 2009. Transcranial magnetic stimulation in ALS: utility of central motor conduction tests. *Neurology* 72, 498–504. <https://doi.org/10.1212/01.wnl.0000341933.97883.a4>.
- Garn, H., Coronel, C., Waser, M., Caravias, G., Ransmayr, G., 2017. Differential diagnosis between patients with probable Alzheimer's disease, Parkinson's disease dementia, or dementia with Lewy bodies and frontotemporal dementia, behavioral variant, using quantitative electroencephalographic features. *J. Neural Transm.* 124, 569–581. <https://doi.org/10.1007/s00702-017-1699-6>.
- Garrido, M.L., Kilner, J.M., Stephan, K.E., Friston, K.J., 2009. The mismatch negativity: a review of underlying mechanisms. *Clin. Neurophysiol.* 120, 453–463. <https://doi.org/10.1016/j.clinph.2008.11.029>.
- George, M.S., Taylor, J., Short, E.B., 2013. The expanding evidence base for rTMS treatment of depression. *Curr. Opin. Psychiatry* 26, 13–18. <https://doi.org/10.1097/YCO.0b013e32835ab84d>.
- Giannicola, G., Mareglia, S., Rossi, L., Mrakie-Spota, S., Rampini, P., Tamma, F., Cogliamanian, F., Barbieri, S., Priori, A., 2010. The effects of levodopa and ongoing deep brain stimulation on subthalamic beta oscillations in Parkinson's disease. *Exp. Neurol.* 226, 120–127. <https://doi.org/10.1016/j.expneurol.2010.08.011>.
- Gil, R., Neau, J.P., Dary-Auriol, M., Agbo, C., Tantom, A.M., Ingrand, P., 1995. Event-related auditory evoked potentials and amyotrophic lateral sclerosis. *Arch. Neurol.* 52, 890–896.
- Glover, G.H., 2011. Overview of functional magnetic resonance imaging. *Neurosurg. Clin. N. Am.* 22, 133–139. <https://doi.org/10.1016/j.nec.2010.11.001>.
- Goss, D.A., Hoffman, R.L., Clark, B.C., 2012. Utilizing transcranial magnetic stimulation to study the human neuromuscular system. *J. Vis. Exp. JoVE*. <https://doi.org/10.3791/3387>.
- Gratwicke, J., Jahanshahi, M., Foltynie, T., 2015. Parkinson's disease dementia: a neural networks perspective. *Brain J. Neurol.* 138, 1454–1476. <https://doi.org/10.1093/brain/awv104>.
- Grève, S.M., Menon, P., Korgaonkar, M.S., Gomes, L., Foster, S., Kiernan, M.C., Vucic, S., 2015. Potential structural and functional biomarkers of upper motor neuron dysfunction in ALS. *Amyotroph. Lateral Scler. Front. Degener.* 17, 85–92. <https://doi.org/10.3109/21678421.2015.1074707>.
- Grunhaus, L., Dannon, P.N., Gershon, A.A., 2002. Transcranial magnetic stimulation: a new tool in the fight against depression. *Dialogues Clin. Neurosci.* 4, 93–103.
- Hanagasi, H.A., Gurvit, I.H., Ermutlu, N., Kaptanoglu, G., Karamursel, S., Idrisoglu, H.A., Emre, M., Demiralp, T., 2002. Cognitive impairment in amyotrophic lateral sclerosis: evidence from neuropsychological investigation and event-related potentials. *Brain Res. Cogn. Brain Res.* 14, 234–244.
- Herrmann, C.S., Strüber, D., Helfrich, R.F., Engel, A.K., 2016. EEG oscillations: from correlation to causality. *Int. J. Psychophysiol.* 103, 12–21. <https://doi.org/10.1016/j.ijpsycho.2015.02.003>. Research on Brain Oscillations and Connectivity in A New Take-Off State.
- Horvath, A., Szucs, A., Csukly, G., Sakovics, A., Stefanics, G., Kamondi, A., 2018. EEG and ERP biomarkers of Alzheimer's disease: a critical review. *Front. Biosci. Landmark Ed.* 23, 183–220.
- Hultin, L., Rossini, P., Romani, G.L., Höglstedt, P., Tecchio, F., Pizzella, V., 1996. Neuronavigation localization of the late component of the contingent negative variation. *Electroencephalogr. Clin. Neurophysiol.* 98, 435–448.
- Iglesias, C., Sangari, S., El Mendili, M.-M., Benali, H., Marchand-Pauvert, V., Pradat, P.-F., 2015. Electrophysiological and spinal imaging evidences for sensory dysfunction in amyotrophic lateral sclerosis. *BMJ Open* 5, e007659.
- Ikeda, A., Lüders, H.O., Collura, T.F., Burgess, R.C., Morris, H.H., Hamano, T., Shibusaki, H., 1996. Subdural potentials at orbitofrontal and mesial prefrontal areas accompanying anticipation and decision making in humans: a comparison with Bereitschaftspotential. *Electroencephalogr. Clin. Neurophysiol.* 98, 206–212.
- Iyer, P.M., Egan, C., Pinto-Grau, M., Burke, T., Elamin, M., Nasserolelami, B., Pender, N., Lalor, E.C., Hardiman, O., 2015. Functional connectivity changes in resting-state EEG as potential biomarker for amyotrophic lateral sclerosis. *PLoS One* 10, e0128682. <https://doi.org/10.1371/journal.pone.0128682>.
- Iyer, P.M., Mohr, K., Broderick, M., Gavin, B., Burke, T., Bede, P., Pinto-Grau, M., Pender, N.P., McLaughlin, R., Vajda, A., Heverin, M., Lalor, E.C., Hardiman, O., Nasserolelami, B., 2017. Mismatch negativity as an indicator of cognitive sub-domain dysfunction in amyotrophic lateral sclerosis. *Front. Neurol.* 8. <https://doi.org/10.3389/fneur.2017.00395>.
- Jenkinson, N., Brown, P., 2011. New insights into the relationship between dopamine, beta oscillations and motor function. *Trends Neurosci.* 34, 611–618. <https://doi.org/10.1016/j.tins.2011.09.003>.
- Jones, S.R., Pinto, D.J., Kaper, T.J., Kopell, N., 2000. Alpha-frequency rhythms desynchronize over long cortical distances: a modeling study. *J. Comput. Neurosci.* 9, 271–291.
- Josiassen, R.C., Shagass, C., Mancall, E.L., Roemer, R.A., 1982. Somatosensory evoked potentials in Huntington's disease. *Electroencephalogr. Clin. Neurophysiol.* 54, 483–493. [https://doi.org/10.1016/0013-4694\(82\)90033-5](https://doi.org/10.1016/0013-4694(82)90033-5).
- Jung, J., Morlet, D., Mercier, B., Confavreux, C., Fischer, C., 2006. Mismatch negativity (MMN) in multiple sclerosis: an event-related potentials study in 46 patients. *Clin. Neurophysiol. Off. J. Int. Fed. Clin. Neurophysiol.* 117, 85–93. <https://doi.org/10.1016/j.clinph.2005.09.013>.
- Kaiser, D.A., 2005. Basic principles of quantitative EEG. *J. Adult Dev.* 12, 99–104. <https://doi.org/10.1007/s10804-005-7025-9>.
- Khanna, A., Pascual-Leone, A., Michel, C.M., Farzan, F., 2015. Microstates in resting-state EEG: current status and future directions. *Neurosci. Biobehav. Rev.* 49, 105–113. <https://doi.org/10.1016/j.neubiorev.2014.12.010>.
- Kim, M.S., Chang, W.H., Cho, J.W., Youn, J., Kim, Y.K., Kim, S.W., Kim, Y.-H., 2015. Efficacy of cumulative high-frequency rTMS on freezing of gait in Parkinson's disease. *Restor. Neurol. Neurosci.* 33, 521–530. <https://doi.org/10.3233/RNN-140489>.
- Kimiskidis, V.K., Papaliagkas, V., Sotirakoglou, K., Kouvatou, Z.K., Kapina, V.K., Papadaki, E., Tsimourou, V., Masoura, E., Kazis, D.A., Papayiannopoulos, S., Geroukis, T., Bostanjopoulou, S., 2016. Cognitive event-related potentials in multiple sclerosis: Correlation with MRI and neuropsychological findings. *Mult. Scler. Relat. Disord.* 10, 192–197. <https://doi.org/10.1016/j.msard.2016.10.006>.
- Kuhn, J., Hardenacke, K., Lenartz, D., Gruender, T., Ullsperger, M., Bartsch, C., Mai, J.K., Zilles, K., Bauer, A., Matusch, A., Schulz, R.-J., Noreik, M., Bührle, C.P., Maintz, D., Wopen, C., Häussermann, P., Hellmich, M., Klosterkötter, J., Wiltfang, J., Maarouf, M., Freund, H.-J., Sturm, V., 2015. Deep brain stimulation of the nucleus basalis of Meynert in Alzheimer's dementia. *Mol. Psychiatry* 20, 353–360. <https://doi.org/10.1038/mp.2014.32>.
- Kwak, Y.T., 2006. Quantitative EEG findings in different stages of Alzheimer's disease. *J. Clin. Neurophysiol. Off. Publ. Am. Electroencephalogr. Soc.* 23, 456–461. <https://doi.org/10.1097/01.wmp.0000223453.47663.63>.
- Lai, C.-L., Lin, R.-T., Liou, L.-M., Liu, C.-K., 2010. The role of event-related potentials in cognitive decline in Alzheimer's disease. *Clin. Neurophysiol.* 121, 194–199. <https://doi.org/10.1016/j.clinph.2009.11.001>.
- Lee, M.-S., Lee, S.-H., Moon, E.-O., Moon, Y.-J., Kim, S., Kim, S.-H., Jung, I.-K., 2013. Neuropsychological correlates of the P300 in patients with Alzheimer's disease. *Prog. Neuro-Psychopharmacol. Biol. Psychiatry* 40, 62–69. <https://doi.org/10.1016/j.pnpbp.2012.08.009>.
- Leocani, L., Rovaris, M., Martinelli-Boneschi, F., Annovazzi, P., Filippi, M., Colombo, B., Martinelli, V., Comi, G., 2005. Movement preparation is affected by tissue damage in multiple sclerosis: evidence from EEG event-related desynchronization. *Clin. Neurophysiol.* 116, 1515–1519. <https://doi.org/10.1016/j.clinph.2005.02.026>.
- Leon-Sarmiento, F.E., Rizzo-Sierra, C.V., Bayona, E.A., Bayona-Prieto, J., Doty, R.L., Bara-Jimenez, W., 2013. Novel mechanisms underlying inhibitory and facilitatory transcranial magnetic stimulation abnormalities in Parkinson's disease. *Arch. Med. Res.* 44, 221–228. <https://doi.org/10.1016/j.arcmed.2013.03.003>.
- Lesenskyj, A.M., Samples, M.P., Farmer, J.M., Maxwell, C.R., 2018. Treating refractory depression in Parkinson's disease: a meta-analysis of transcranial magnetic stimulation. *Trans. Neurodegener.* 7 (8). <https://doi.org/10.1186/s40035-018-0113-0>.
- Liepert, J., Bär, K.J., Meske, U., Weiller, C., 2001. Motor cortex disinhibition in Alzheimer's disease. *Clin. Neurophysiol. Off. J. Int. Fed. Clin. Neurophysiol.* 112, 1436–1441.
- Lindau, M., Jelic, V., Johansson, S.-E., Andersen, C., Wahlund, L.-O., Almkvist, O., 2003. Quantitative EEG abnormalities and cognitive dysfunctions in frontotemporal dementia and Alzheimer's disease. *Dement. Geriatr. Cogn. Disord.* 15, 106–114. <https://doi.org/10.1159/000067973>.
- Luck, S.J., Woodman, G.F., Vogel, E.K., 2000. Event-related potential studies of attention. *Trends Cogn. Sci.* 4, 432–440.
- Mai, R., Facchetti, D., Micheli, A., Poloni, M., 1998. Quantitative electroencephalography in amyotrophic lateral sclerosis. *Electroencephalogr. Clin. Neurophysiol.* 106, 383–386.
- Menon, P., Geveasinga, N., Yiannikas, C., Howells, J., Kiernan, M.C., Vucic, S., 2015. Sensitivity and specificity of threshold tracking transcranial magnetic stimulation for diagnosis of amyotrophic lateral sclerosis: a prospective study. *Lancet Neurol.* 14, 478–484. [https://doi.org/10.1016/S1474-4422\(15\)00014-9](https://doi.org/10.1016/S1474-4422(15)00014-9).
- Mills, K.R., 2003. The natural history of central motor abnormalities in amyotrophic lateral sclerosis. *Brain* 126, 2558–2566.
- Mills, K.R., Nihi, K.A., 1997. Corticospinal threshold is reduced in early sporadic amyotrophic lateral sclerosis. *Muscle Nerve* 20, 1137–1141.
- Moeller, F., Muthuraman, M., Stephani, U., Deuschl, G., Raethjen, J., Siniatchkin, M., 2013. Representation and propagation of epileptic activity in absences and generalized photoparoxysmal responses. *Hum. Brain Mapp.* 34, 1896–1909. <https://doi.org/10.1002/hbm.22026>.
- Momma, F., Tsutsui, T., Symon, L., Ono, M., 1987. The clinical significance of the P15 wave of the somatosensory evoked potential in tentorial herniation. *Neurol. Res.* 9, 154–158.
- Mori, F., Codecà, C., Kusayanaqi, H., Monteleone, F., Boffa, L., Rimano, A., Bernardi, G., Koch, G., Centonze, D., 2010. Effects of intermittent theta burst stimulation on spasticity in patients with multiple sclerosis. *Eur. J. Neurol.* 17, 295–300. <https://doi.org/10.1111/j.1468-1331.2009.02806.x>.
- Mori, F., Ljoka, C., Magni, E., Codecà, C., Kusayanaqi, H., Monteleone, F., Sancesario, A., Bernardi, G., Koch, G., Foti, C., Centonze, D., 2011. Transcranial magnetic stimulation primes the effects of exercise therapy in multiple sclerosis. *J. Neurol.* 258, 1281–1287. <https://doi.org/10.1007/s00415-011-5924-1>.
- Muthuraman, M., Koirala, N., Giolac, D., Pintea, B., Glaser, M., Groppa, Stanislav, Tamás, G., Groppa, Sergio, 2018. Deep brain stimulation and L-DOPA therapy: concepts of action and clinical applications in Parkinson's disease. *Front. Neurol.* 9. <https://doi.org/10.3389/fneur.2018.00711>.
- Nardone, R., Sebastianelli, L., Versace, V., Saluati, L., Lochner, P., Frey, V., Golaszewski, S., Brigo, F., Trinka, E., Höller, Y., 2018. Usefulness of EEG techniques in distinguishing frontotemporal dementia from Alzheimer's disease and other dementias

- [WWW document]. Dis. Markers. <https://doi.org/10.1155/2018/6581490>.
- Nasserolami, B., Dukie, S., Broderick, M., Mohr, K., Schuster, C., Gavin, B., McLaughlin, R., Heverin, M., Vajda, A., Iyer, P.M., Pender, N., Bede, P., Lalor, E.C., Hardiman, O., 2017. Characteristic increases in EEG connectivity correlate with changes of structural MRI in amyotrophic lateral sclerosis. *Cereb. Cortex* 1–15. <https://doi.org/10.1093/cercor/bbx301>.
- Ni, Z., Bahl, N., Gunraj, C.A., Mazzeo, F., Chen, R., 2013. Increased motor cortical facilitation and decreased inhibition in Parkinson disease. *Neurology* 80, 1746–1753.
- Nishida, K., Yoshimura, M., Isotani, T., Yoshida, T., Kitaura, Y., Saito, A., Mii, H., Kato, M., Takekita, Y., Suwa, A., Morita, S., Kinoshita, T., 2011. Differences in quantitative EEG between frontotemporal dementia and Alzheimer's disease as revealed by LORETA. *Clin. Neurophysiol. Off. J. Int. Fed. Clin. Neurophysiol.* 122, 1718–1725. <https://doi.org/10.1016/j.clinph.2011.02.011>.
- Nuwer, M., 1997. Assessment of digital EEG, quantitative EEG, and EEG brain mapping: report of the American Academy of Neurology and the American Clinical Neurophysiology Society. *Neurology* 49, 277–292.
- Park, J., Chang, W.H., Cho, J.W., Youn, J., Kim, Y.K., Kim, S.W., Kim, Y.-H., 2016. Usefulness of transcranial magnetic stimulation to assess motor function in patients with Parkinsonism. *Ann. Rehabil. Med.* 40, 81–87. <https://doi.org/10.5535/arm.2016.40.1.81>.
- Patil, A.L., Sood, S.K., Goyal, V., Kochhar, K.P., 2017. Cortical potentials prior to movement in Parkinson's disease. *J. Clin. Diagn. Res. JCDR* 11, OC13–OC16. <https://doi.org/10.7860/JCDR/2017/25520.9598>.
- Pedross, R.V., Fraga, F.J., Corazza, D.L., Andreatto, C.A.A., de Melo Coelho, F.G., Costa, J.L.R., Santos Galduróz, R.F., 2012. P300 latency and amplitude in Alzheimer's disease: a systematic review. *Braz. J. Otorhinolaryngol.* 78, 126–132. <https://doi.org/10.1590/S1808-8694201200040023>.
- Plurtscheller, G., Lopes da Silva, F.H., 1999. Event-related EEG/MEG synchronization and desynchronization: basic principles. *Clin. Neurophysiol. Off. J. Int. Fed. Clin. Neurophysiol.* 110, 1842–1857.
- Plurtscheller, G., Pichler-Zalaudek, K., Ortmayr, B., Diez, J., Reisecker, F., 1998. Postmovement beta synchronization in patients with Parkinson's disease. *J. Clin. Neurophysiol. Off. Publ. Am. Electroencephalogr. Soc.* 15, 243–250.
- Phukan, J., Pender, N.P., Hardiman, O., 2007. Cognitive impairment in amyotrophic lateral sclerosis. *Lancet Neurol.* 6, 994–1003. [https://doi.org/10.1016/S1474-4422\(07\)0265-X](https://doi.org/10.1016/S1474-4422(07)0265-X).
- Pierantozzi, M., Palmieri, M.G., Mazzone, P., Marciari, M.G., Rossini, P.M., Stefani, A., Giacomini, P., Peppe, A., Stanzione, P., 2002. Deep brain stimulation of both subthalamic nucleus and internal globus pallidus restores intracortical inhibition in Parkinson's disease paralleling amorphine effects: a paired magnetic stimulation study. *Clin. Neurophysiol. Off. J. Int. Fed. Clin. Neurophysiol.* 113, 108–113.
- Polich, J., 2007. Updating P300: an integrative theory of P3a and P3b. *Clin. Neurophysiol.* 118, 2128–2148. <https://doi.org/10.1016/j.clinph.2007.04.019>.
- Pollok, B., Krause, V., Marsch, W., Waech, C., Schmitzler, A., Südmeyer, M., 2012. Motor-cortical oscillations in early stages of Parkinson's disease. *J. Physiol.* 590, 3203–3212. <https://doi.org/10.1113/jphysiol.2012.231316>.
- Portet, F., Cadilhac, C., Touchon, J., Camu, W., 2001. Cognitive impairment in motor neuron disease with bulbar onset. *Neurology. Lateral Scler. Other Motor Neuron Disord.* 2, 23–29.
- Praamstra, P., Meyer, A.S., Cools, A.R., Horstink, M.W.L.M., Stegeman, D.F., 1996. Movement preparation in Parkinson's disease: Time course and distribution of movement-related potentials in a movement pre-cueing task. *Brain* 119, 1689–1704. <https://doi.org/10.1093/brain/119.5.1689>.
- Pulvermüller, F., Lutzenberger, W., Müller, V., Mohr, B., Dichgans, J., Birbaumer, N., 1996. P3 and contingent negative variation in Parkinson's disease. *Electroencephalogr. Clin. Neurophysiol.* 98, 456–467. [https://doi.org/10.1016/0013-4694\(96\)95537-6](https://doi.org/10.1016/0013-4694(96)95537-6).
- Raggi, A., Consonni, M., Iannaccone, S., Perani, D., Zamboni, M., Sferazza, B., Cappa, S.F., 2008. Auditory event-related potentials in non-demented patients with sporadic amyotrophic lateral sclerosis. *Clin. Neurophysiol.* 119, 342–350. <https://doi.org/10.1016/j.clinph.2007.10.010>.
- Riva, N., Falini, A., Inuggi, A., Gonzalez-Rosa, J.J., Amadio, S., Cerri, F., Fazio, R., Del Carro, U., Comola, M., Comi, G., Leocani, L., 2012. Cortical activation to voluntary movement in amyotrophic lateral sclerosis is related to corticospinal damage: electrophysiological evidence. *Clin. Neurophysiol. Off. J. Int. Fed. Clin. Neurophysiol.* 123, 1586–1592. <https://doi.org/10.1016/j.clinph.2011.12.013>.
- Rockstroh, B., Müller, M., Wagner, M., Cohen, R., Elbert, T., 1993. "Probing" the nature of the CNV. *Electroencephalogr. Clin. Neurophysiol.* 87, 235–241.
- Rossini, P.M., Burke, D., Chen, R., Cohen, L.G., Daskalakis, Z., Di Iorio, R., Di Lazzaro, V., Ferreri, F., Fitzgerald, P.B., George, M.S., Hallett, M., Lefaucheur, J.P., Langguth, B., Matsumoto, H., Miniussi, C., Nitsche, M.A., Pascual-Leone, A., Paulus, W., Rossi, S., Rothwell, J.C., Siebner, H.R., Ugawa, Y., Walsh, V., Ziemann, U., 2015. Non-invasive electrical and magnetic stimulation of the brain, spinal cord, roots and peripheral nerves: basic principles and procedures for routine clinical and research application. An updated report from an I.F.C.N. Committee. *Clin. Neurophysiol. Off. J. Int. Fed. Clin. Neurophysiol.* 126, 1071–1107. <https://doi.org/10.1016/j.clinph.2015.02.001>.
- Rutherford, G., Lithgow, B., Moussavi, Z., 2015. Short and long-term effects of rTMS treatment on Alzheimer's Disease at different stages: a pilot study. *J. Exp. Neurosci.* 9, 43–51. <https://doi.org/10.4137/JEN.S24004>.
- Sanacora, G., Smith, M.A., Pathak, S., Su, H.-L., Boeijinga, P.H., McCarthy, D.J., Quirk, M.C., 2014. Lamicemine: a low-trapping NMDA channel blocker produces sustained antidepressant efficacy with minimal psychotomimetic adverse effects. *Mol. Psychiatry* 19, 978–985. <https://doi.org/10.1038/mp.2013.130>.
- Santhosh, J., Bhatia, M., Sahu, S., Anand, S., 2005. Decreased electroencephalogram alpha band [8–13 Hz] power in amyotrophic lateral sclerosis patients: a study of alpha activity in an awake relaxed state. *Neurol. India* 53, 99–101.
- Saura, C.A., Parra-Damas, A., Enriquez-Barreto, L., 2015. Gene expression parallels synaptic excitability and plasticity changes in Alzheimer's disease. *Front. Cell. Neurosci.* 9. <https://doi.org/10.3389/fncel.2015.00318>.
- Scheele, P., Twisk, J.W., Blesa, R., Scarpini, E., von Arnim, C.A., Bongers, A., Harrison, J., Swinkels, S.H., Stam, C.J., de Waal, H., 2012. Efficacy of Souvenaid in mild Alzheimer's disease: results from a randomized, controlled trial. *J. Alzheimers Dis.* 31, 225–236.
- Schipling, S., Schneider, S., Bhatia, K., Münch, A., Rothwell, J., Tabrizi, S., Orth, M., 2009. Abnormal motor cortex excitability in preclinical and very early Huntington's disease. *Biol. Psychiatry* 65, 959–965. <https://doi.org/10.1016/j.biopsych.2008.12.026>.
- Shibasaki, H., Hallett, M., 2006. What is the Bereitschaftspotential? *Clin. Neurophysiol.* 117, 2341–2356.
- St Clair, D., Blackburn, I., Blackwood, D., Tyrer, G., 1988. Measuring the course of Alzheimer's disease. A longitudinal study of neuropsychological function and changes in P3 event-related potential. *Br. J. Psychiatry J. Ment. Sci.* 152, 48–54.
- Stam, C.J., Nolte, G., Daffertshofer, A., 2007. Phase lag index: assessment of functional connectivity from multi channel EEG and MEG with diminished bias from common sources. *Hum. Brain Mapp.* 28, 1178–1193. <https://doi.org/10.1002/hbm.20346>.
- Symms, M., Jäger, H.R., Schmierer, K., Yousry, T.A., 2004. A review of structural magnetic resonance neuroimaging. *J. Neurol. Neurosurg. Psychiatry* 75, 1235–1244. <https://doi.org/10.1136/jnnp.2003.032714>.
- Teramoto, H., Morita, A., Niinomiya, S., Akinoto, T., Shiota, H., Kamei, S., 2016. Relation between resting state frontoparietal EEG coherence and executive function in Parkinson's disease. *Biomed. Res. Int.* 2016. <https://doi.org/10.1155/2016/2845754>.
- Tokic, K., Titlic, M., Beganovic-Petrovic, A., Suljic, E., Romac, R., Silic, S., 2016. P300 wave changes in patients with Parkinson's disease. *Med. Arch.* 70, 453–456. <https://doi.org/10.5455/medarh.2016.70.453-456>.
- Uysal, U., Idiman, F., Idiman, E., Ozakbas, S., Karakas, S., Bruce, J., 2014. Contingent negative variation is associated with cognitive dysfunction and secondary progressive disease course in multiple sclerosis. *J. Clin. Neurosci.* 17, 296–303. <https://doi.org/10.3988/jcn.2014.10.4.296>.
- Van den Bos, J.M.A., Menon, P., Howells, J., Geevasinga, N., Kiernan, M.C., Vucic, S., 2018. Physiological processes underlying short interval intracortical facilitation in the human motor cortex. *Front. Neurosci.* 12. <https://doi.org/10.3389/fnins.2018.00240>.
- van Deursen, J.A., Vuurman, E.F.P.M., Smits, L.L., Verhey, F.R.J., Riedel, W.J., 2009. Response speed, contingent negative variation and P300 in Alzheimer's disease and MCI. *Brain Cogn.* 69, 592–599. <https://doi.org/10.1016/j.bandc.2008.12.007>.
- Verdoorn, T.A., McCarten, J.R., Arciniegas, D.B., Golden, R., Moldauer, L., Georgopoulos, A., Lewis, S., Cassano, M., Hemmy, L., Orr, W., Rojas, D.C., 2011. Evaluation and tracking of Alzheimer's disease severity using resting-state magnetoencephalography. *J. Alzheimers Dis. JAD* 26 (Suppl. 3), 239–255. <https://doi.org/10.3233/JAD-2011-0056>.
- Volpato, C., Piccione, F., Silvoni, S., Cavinato, M., Palmieri, A., Meneghelli, F., Birbaumer, N., 2010. Working memory in amyotrophic lateral sclerosis: auditory event-related potentials and neuropsychological evidence. *J. Clin. Neurophysiol. Off. Publ. Am. Electroencephalogr. Soc.* 27, 198–206. <https://doi.org/10.1097/WNP.0b013e3181e0aa14>.
- Vucic, S., Kiernan, M.C., 2006. Novel threshold tracking techniques suggest that cortical hyperexcitability is an early feature of motor neuron disease. *Brain J. Neurol.* 129, 2436–2446. <https://doi.org/10.1093/brain/awl172>.
- Vucic, S., Nicholson, G.A., Kiernan, M.C., 2008. Cortical hyperexcitability may precede the onset of familial amyotrophic lateral sclerosis. *Brain* 131, 1540–1550. <https://doi.org/10.1093/brain/awn071>.
- Wendel, K., Väisänen, O., Malmivuo, J., Gencer, N.G., Vanrumste, B., Durka, P., Magjarić, R., Supek, S., Pascu, M.L., Fontenelle, H., Grave de Peralta Menendez, R., 2009. EEG/MEG source imaging: methods, challenges, and open issues [WWW Document]. *Comput. Intell. Neurosci.* <https://doi.org/10.1155/2009/656092>.
- Westphal, K.P., Heinenmann, H.A., Grözinger, B., Ketschoubey, B.J., Diekmann, V., Becker, W., Kornhuber, H.H., 1998. Bereitschaftspotential in amyotrophic lateral sclerosis (ALS): lower amplitudes in patients with hyperreflexia (spasticity). *Acta Neurol. Scand.* 98, 15–21.
- Yates, D., 2012. Neurodegenerative disease: Neurodegenerative networking. *Nat. Rev. Neurosci.* 13, 288.
- Yener, G.G., Leuchter, A.F., Jenden, D., Read, S.L., Cummings, J.L., Miller, B.L., 1996. Quantitative EEG in frontotemporal dementia. *Clin. EEG Electroencephalogr.* 27, 61–68.
- Zhang, J., Yin, X., Zhao, L., Evans, A.C., Song, L., Xie, B., Li, H., Luo, C., Wang, J., 2014. Regional alterations in cortical thickness and white matter integrity in amyotrophic lateral sclerosis. *J. Neurol.* 261, 412–421. <https://doi.org/10.1007/s00415-013-7215-5>.
- Zhou, J., Greicius, M.D., Gennatas, E.D., Growdon, M.E., Jang, J.Y., Rabinovici, G.D., Kramer, J.H., Weiner, M., Miller, B.L., Seeley, W.W., 2010. Divergent network connectivity changes in behavioural variant frontotemporal dementia and Alzheimer's disease. *Brain* 133, 1352–1367. <https://doi.org/10.1093/brain/awq075>.
- Ziemann, U., Rothwell, J.C., Ridding, M.C., 1996. Interaction between intracortical inhibition and facilitation in human motor cortex. *J. Physiol.* 496 (Pt 3), 873–881.
- Ziemann, U., Reis, J., Schwenkreis, P., Rosanova, M., Strafella, A., Badawy, R., Müller-Dahlhaus, F., 2015. TMS and drugs revisited 2014. *Clin. Neurophysiol. Off. J. Int. Fed. Clin. Neurophysiol.* 126, 1847–1868. <https://doi.org/10.1016/j.clinph.2014.08.028>.



## Dysfunction of attention switching networks in amyotrophic lateral sclerosis



Roisin McMackin<sup>a</sup>, Stefan Dukic<sup>a</sup>, Michael Broderick<sup>a,b</sup>, Parameswaran M. Iyer<sup>a,c</sup>,  
Marta Pinto-Grau<sup>a,d</sup>, Kieran Mohr<sup>a</sup>, Rangaririyashe Chipika<sup>a,e</sup>, Amina Coffey<sup>a,c</sup>, Teresa Buxo<sup>a</sup>,  
Christina Schuster<sup>a,c</sup>, Brigid Gavin<sup>a</sup>, Mark Heverin<sup>a</sup>, Peter Bede<sup>a,e</sup>, Niall Pender<sup>a,c</sup>,  
Edmund C. Lalor<sup>a,f,g</sup>, Muthuraman Muthuraman<sup>h</sup>, Orla Hardiman<sup>a,c,e,\*</sup>,  
Bahman Nasseroleslami<sup>a,1</sup>

<sup>a</sup>Academic Unit of Neurology, Trinity College Dublin, The University of Dublin, Ireland

<sup>b</sup>Trinity Centre for Bioengineering, Trinity College Dublin, The University of Dublin, Ireland

<sup>c</sup>Beaumont Hospital Dublin, Department of Neurology, Dublin, Ireland

<sup>d</sup>Beaumont Hospital Dublin, Department of Psychology, Dublin, Ireland

<sup>e</sup>Computational Neuroimaging Group, Trinity College Dublin, The University of Dublin, Ireland.

<sup>f</sup>Trinity College Institute of Neuroscience, Trinity College Dublin, The University of Dublin, Ireland.

<sup>g</sup>Department of Biomedical Engineering, University of Rochester, Rochester, New York, USA.

<sup>h</sup>Movement Disorders and Neurostimulation, Biomedical Statistics and Multimodal Signal Processing Unit, Department of Neurology, Johannes-Gutenberg-University Hospital, Mainz, Germany

## ARTICLE INFO

## Keywords:

Amyotrophic lateral sclerosis  
Network  
EEG  
Cognition  
Source localisation  
Mismatch negativity

## ABSTRACT

**Objective:** To localise and characterise changes in cognitive networks in Amyotrophic Lateral Sclerosis (ALS) using source analysis of mismatch negativity (MMN) waveforms.

**Rationale:** The MMN waveform has an increased average delay in ALS. MMN has been attributed to change detection and involuntary attention switching. This therefore indicates pathological impairment of the neural network components which generate these functions. Source localisation can mitigate the poor spatial resolution of sensor-level EEG analysis by associating the sensor-level signals to the contributing brain sources. The functional activity in each generating source can therefore be individually measured and investigated as a quantitative biomarker of impairment in ALS or its sub-phenotypes.

**Methods:** MMN responses from 128-channel electroencephalography (EEG) recordings in 58 ALS patients and 39 healthy controls were localised to source by three separate localisation methods, including beamforming, dipole fitting and exact low resolution brain electromagnetic tomography.

**Results:** Compared with controls, ALS patients showed significant increase in power of the left posterior parietal, central and dorsolateral prefrontal cortices (false discovery rate = 0.1). This change correlated with impaired cognitive flexibility ( $\rho = 0.45, 0.45, 0.47, p = .042, .055, .031$  respectively). ALS patients also exhibited a decrease in the power of dipoles representing activity in the inferior frontal (left:  $p = 5.16 \times 10^{-6}$ , right:  $p = 1.07 \times 10^{-5}$ ) and left superior temporal gyri ( $p = 9.30 \times 10^{-6}$ ). These patterns were detected across three source localisation methods. Decrease in right inferior frontal gyrus activity was a good discriminator of ALS patients from controls (AUROC = 0.77) and an excellent discriminator of C9ORF72 expansion-positive patients

**Abbreviation:** LS, Amyotrophic Lateral Sclerosis; fMRI, Functional magnetic resonance imaging; MMN, Mismatch negativity; EEG, Electroencephalography; qEEG, Quantitative EEG; MEG, Magnetoencephalography; PET, Positron emission tomography; IFG, Inferior frontal gyrus; MTG, Mid temporal gyrus; STG, Superior temporal gyrus; CWIT, Colour-word interference test; IQR, Interquartile range; AEP, Auditory evoked potential; LCMV, Linearly constrained minimum variance; eLORETA, Exact low-resolution brain electromagnetic tomography; AAL, Automated Anatomical Labelling; AUROC, Area under receiver operating characteristic curve; DLPFC, Dorsolateral prefrontal cortex

\* Corresponding author at: Academic Unit of Neurology, Trinity College Dublin, The University of Dublin, Room 5.43, Trinity Biomedical Sciences Institute, 152-160 Pearse Street, Dublin D02 R590, Ireland.

**E-mail addresses:** [mcmackr@tcd.ie](mailto:mcmackr@tcd.ie) (R. McMackin), [dukics@tcd.ie](mailto:dukics@tcd.ie) (S. Dukic), [brodermi@tcd.ie](mailto:brodermi@tcd.ie) (M. Broderick), [parameswaranier@beaumont.ie](mailto:parameswaranier@beaumont.ie) (P.M. Iyer), [pintogrm@tcd.ie](mailto:pintogrm@tcd.ie) (M. Pinto-Grau), [mohrk@tcd.ie](mailto:mohrk@tcd.ie) (K. Mohr), [chipikar@tcd.ie](mailto:chipikar@tcd.ie) (R. Chipika), [coffey1@tcd.ie](mailto:coffey1@tcd.ie) (A. Coffey), [buxhernt@tcd.ie](mailto:buxhernt@tcd.ie) (T. Buxo), [schuster@tcd.ie](mailto:schuster@tcd.ie) (C. Schuster), [mark.heverin@tcd.ie](mailto:mark.heverin@tcd.ie) (M. Heverin), [bedep@tcd.ie](mailto:bedep@tcd.ie) (P. Bede), [edlalar@tcd.ie](mailto:edlalar@tcd.ie) (E.C. Lalor), [mmuthura@uni-mainz.de](mailto:mmuthura@uni-mainz.de) (M. Muthuraman), [hardimao@tcd.ie](mailto:hardimao@tcd.ie) (O. Hardiman), [nasserob@tcd.ie](mailto:nasserob@tcd.ie) (B. Nasseroleslami).

<sup>1</sup> Joint Last Authorship.

<https://doi.org/10.1016/j.nicl.2019.101707>

Received 25 October 2018; Received in revised form 28 January 2019; Accepted 31 January 2019

Available online 02 February 2019

2213-1582/ © 2019 The Authors. Published by Elsevier Inc. This is an open access article under the CC BY license (<http://creativecommons.org/licenses/by/4.0/>).

from controls (AUROC = 0.95).

**Interpretation:** Source localization of evoked potentials can reliably discriminate patterns of functional network impairment in ALS and ALS subgroups during involuntary attention switching. The discriminative ability of the detected cognitive changes in specific brain regions are comparable to those of functional magnetic resonance imaging (fMRI).

Source analysis of high-density EEG patterns has excellent potential to provide non-invasive, data-driven quantitative biomarkers of network disruption that could be harnessed as novel neurophysiology-based outcome measures in clinical trials.

## 1. Introduction

Amyotrophic lateral sclerosis is a progressive neurodegenerative condition characterized by upper and lower motor neuron degeneration (Kiernan et al., 2011). Extra-motor behavioural and cognitive symptoms are common in ALS (Phukan et al., 2007), and imaging technologies have provided early evidence of broader network disruption (Bede et al., 2015, 2018).

Although structural imaging can reliably record changes in grey and white matter integrity (Schuster et al., 2016) and functional imaging detects resting and activated states of metabolic activity (Erdoğan et al., 2016), there remains an unmet need for real-time measurement of different patterns of network disruption.

### 1.1. EEG for assessing neural function

Electrophysiological measurement of network activity during cognitive performance allows for direct objective quantification of dysfunction (Katada et al., 2004) with excellent temporal resolution (Teplan, 2002). These measures, captured by EEG or MEG, are distinct from secondary blood flow or oxygen content measures upon which fMRI is based (Erdoğan et al., 2016). EEG measures the electrical dipoles produced by transmembrane ion flow in large numbers of simultaneously-active, aligned cortical neurons, while MEG measures the concurrently generated magnetic fields (da Silva, 2013). EEG/MEG measurements have traditionally been limited by noise from extracerebral (such as facial muscles, ocular, and cardiac) artefacts, in addition to poor spatial resolution (Reis et al., 2014). However, the use of improved recording instrumentation with up to 256 sensors, combined with digitized data processing (Dukic et al., 2017; Muthuraman et al., 2018; Nasserrolesami et al., 2017), has substantially improved the signal to noise ratio.

Due to volume conduction, EEG sensors capture electrical currents propagated from both adjacent and distant sources in the conductive human head medium. However, source localisation of EEG sensor recordings localises the activity underlying these signals with spatial resolution comparable to fMRI (Moeller et al., 2013) and source localised MEG (Muthuraman et al., 2014). Furthermore, as EEG does not require expensive superconductive systems needed for MEG (Wendel et al., 2009), it is more cost effective and therefore more suited to day-to-day clinical application.

As EEG/MEG directly measure the functional neuronal activity at a network level, they can capture cognitive network dysfunction in the absence of cognitive symptoms (Döring et al., 2016), and therefore may provide greater sensitivity to cognitive pathology than psychological (behavioural) task parameters. Correlating these measures with specific domains of cognitive impairment could provide quantifiable cognitive biomarkers to improve neurodegenerative disease diagnostics, and additional outcome measures for clinical trials.

### 1.2. MMN an index of cognitive decline

MMN is a measure typically elicited and recorded during an auditory oddball task, wherein the participant receives series of auditory stimuli (tones). These tones are of one pitch, except for a fraction of

cases (e.g. 10% in this study) which are of higher “deviant” frequency (pitch). The MMN is a negative waveform, found by the difference between the auditory evoked potentials generated by these deviant and standard tones at 100-300 ms post-stimulus (Iyer et al., 2017; Näätänen et al., 2007; Naatanen, 1995).

Multiple hypotheses have been proposed regarding the cortical function(s) measured by MMN, including both sensory and cognitive components of auditory processing. MMN was first described by Näätänen et al. in 1978, who hypothesised that the waveform resulted from comparison of a deviant input to a sensory memory template. It was also suggested that MMN might represent recognition of target criteria fulfilment (Näätänen et al., 1978), however such a “relevance effect” was considered unlikely as attention to the stimulus did not affect the waveform (Näätänen, 1995). This was subsequently supported by multiple studies demonstrating MMN in the absence of attention (Winkler et al., 1996), including in sleeping infants (Ruusuvirta et al., 2009) or those in a vegetative state (Wijnen et al., 2007). The MMN was therefore proposed to reflect an automatic detection of sensory change and modification of the physiological model of the environment to incorporate this new stimulus, referred to as the *model adjustment hypothesis* (Winkler et al., 1996).

An additional automatic attention-switching process related to the frontal generators was then proposed to occur on the basis that right frontal sources were activated irrespective of the ear detecting the stimulus change (Giard et al., 1990). This is believed to reflect the call to switch attention to changes in the unattended environment (Winkler et al., 1996), the occurrence of which is supported by autonomic responses such as heart rate and skin conductance changes following MMN (Lyytinen et al., 1992) as well as many other studies (Escera et al., 2001, 2003; Schröger, 1996).

An alternative *adaptation hypothesis*, first proposed by May et al. in 1999 (May et al., 1999; May and Tiitinen, 2001, 2004), proposes that the MMN response results from cortical adaptation to monotonous stimuli, with MMN reflecting the difference between N1 to a novel sound and a lower amplitude, higher latency N1 generated by repetitive standard tones. This hypothesis was supported by later studies, such as those of Jääskeläinen et al. (Jääskeläinen et al., 2004) and Ulanovsky et al., (Ulanovsky et al., 2003) (for review see (May and Tiitinen, 2010)). However, an exclusively auditory hypotheses cannot account for the established prefrontal activation during MMN. Indeed, source localisation of PET, EEG, fMRI and MEG-derived MMN has reliably highlighted both the superior temporal and inferior frontal gyri as important sources of this signal (Rinne et al., 2000; Opitz et al., 2002; Yago et al., 2001; Müller et al., 2002), demonstrating that volume conduction alone does not account for frontal MMN. Furthermore, those with lesions of the dorsolateral prefrontal cortex have also been found to have reduced MMN amplitudes (Alho et al., 1994).

Source localisation across the MMN timeframe has additionally revealed two subcomponents, an early, sensory component that is maximal in the late N1 range (105-125 ms post-stimulus) generated by temporal sources and a later, cognitive component (170-200 ms post-stimulus), generated by frontal and temporal sources (Giard et al., 1990; Rinne et al., 2000; Maess et al., 2007). These temporal sources are attributed to sensory memory and change detection while the later active, frontal sources are attributed to involuntary attention switching



in response to change (Giard et al., 1990; Rinne et al., 2000; Alho, 1995; Näätänen and Michie, 1979). As this early component overlaps with the N1 range, temporal activity may also represent sensory detection (May and Tiitinen, 2010).

Hence, source-localised MMN affords the benefit of separately interrogating each of these functions and the neural network which generate them, both in healthy individuals and those with neurological diseases. This is supported by several previous studies in different neurological and neuropsychiatric diseases, where MMN has been used as an index of abnormal auditory perception, involuntary attention switching, pathological brain excitability and cognitive and functional decline (see (Näätänen et al., 2012, 2014; Schall, 2016; Todd et al., 2013; Kujala and Leminen, 2017) for reviews).

### 1.3. Identifying the sources of MMN change in ALS

Using qEEG to measure MMN, we recently have shown a functional change in the underlying networks in ALS, with MMN being significant in healthy controls from 105 to 271 ms post-stimulus and having an increased average delay within the 100-300 ms post-stimulus window in ALS (Iyer et al., 2017). Due to the limited spatial resolution of sensor space studies, however, the specific sources contributing to MMN change and the nature of their dysfunction in ALS remains unclear. We therefore were unable to specify which network components indexed by MMN are affected by ALS pathology.

In this study we have used high-density qEEG in combination with each of three source localisation methods to determine and cross-validate the locations of MMN generators, and to measure differences in their activity between ALS patients and healthy controls. Here we show how the dysfunction of each source of MMN is affected by ALS, characterized by both under-active and over-active sources contributing to the abnormal response.

## 2. Methods

### 2.1. Ethical approval

Ethical approval was obtained from the ethics committee of Beaumont Hospital (REC reference: (Nasserolelami et al., 2017)/102) and the St. James's Hospital (REC reference: 2017-02). All participants provided written informed consent before participation. All work was performed in accordance with the Declaration of Helsinki.

### 2.2. Participants

#### 2.2.1. Recruitment

Patient recruitment was undertaken from the National ALS specialty clinic in Beaumont Hospital. Healthy controls included neurologically-normal spouses of ALS patients and neurologically-normal, age- and sex-matched individuals recruited from an existing cohort of population-based controls.

#### 2.2.2. Inclusion criteria

Patients were over 18 years of age and diagnosed within the previous 18 months with Possible, Probable or Definite ALS in accordance with the El Escorial Revised Diagnostic Criteria.

#### 2.2.3. Exclusion criteria

Patients with Transient Ischemic Attack, Multiple Sclerosis, stroke, seizure disorders, brain tumours, structural brain diseases and other comorbidities were excluded.

#### 2.2.4. Demographics of patients and controls

A total of 95 ALS patients and 43 controls underwent recording. 58 ALS patients (f/m: 20/38; age: 59.2 years, range: 29–81 years) and 39 healthy controls (f/m: 28/11; age: 58.9 years, range: 36–78 years) were

included in final analyses. Data with poor recording quality (determined by the lack of auditory evoked potentials), were excluded. Eight controls and 44 patients were also included in our previous sensor-space analysis (Iyer et al., 2017).

### 2.2.5. Medical profile

Within the ALS group, 44 patients had spinal onset, 12 bulbar, and 2 thoracic onset. All patients were tested for the hexanucleotide repeat expansion in *C9ORF72*, of whom 7 were positive (*C9ORF72+*). Twelve patients had a known family history of at least one first or second degree relative with ALS, 3 of whom carried the *C9ORF72* repeat expansion. One additional patient had a known family history of at least one first or second degree relative with frontotemporal dementia (Byrne et al., 2012a). A contemporaneous ALSFRS-R score was available in 51 patients. Mean ALSFRS-R was 37.8 with an IQR of 33.5–42. Mean disease duration was 1.83 years (IQR: 0.89–2.09) from estimated symptom onset.

### 2.3. Experimental paradigm

EEG was recorded across 128-channels in 3 consecutive, 8 min sessions, during which an auditory frequency-mismatch oddball paradigm was delivered as described in our previously reported methods (Iyer et al., 2017). In total, 1350 standard trials and 150 deviant trials were presented.

### 2.4. Data acquisition

EEG recordings were conducted in the Clinical Research Facility at St. James's Hospital, Dublin using a BioSemi® ActiveTwo system (BioSemi B.V., Amsterdam, The Netherlands) within a Faraday cage. Subjects were measured with an appropriately-sized EEG cap. Data were online filtered to a bandwidth of 0–134 Hz and digitized at 512 Hz. Common average referencing was used. 27 patients also undertook the Colour-Word Interference Test from the Delis-Kaplan Executive Function System (Delis et al., 2001), which is a test of attention shift, inhibitory control, error monitoring and cognitive flexibility.

### 2.5. Data analysis

Data were preprocessed as described in our previous sensor space analysis (Iyer et al., 2017) using custom MATLAB (version R2014a and R2016a, Mathworks Inc., Natick, MA, USA) scripts and the FieldTrip Toolbox (Oostenveld et al., 2011). Mean number of included artefact-free standard/deviant trials was 1267/144 for patients and 1223/146 for controls. For source analyses the number of standard trials was matched to that of deviant trials by random selection.

### 2.6. EEG signal processing

The mean standard and deviant auditory evoked potentials were calculated for each participant from 100 ms before the stimulus to 500 ms post-stimulus as previously reported (Iyer et al., 2017). MMN waveforms were calculated for each electrode in each individual as the difference between mean deviant and standard AEPs. Channels with continuously noisy data were excluded (mean excluded channels  $\pm$  standard deviation in controls:  $1.59 \pm 1.65$ , patients:  $1.52 \pm 1.55$ ) and data from these channels were modelled by spline interpolation of neighbouring channels.

### 2.7. Source localisation and analysis

Source localisation was implemented using custom MATLAB (version R2016a) scripts and the FieldTrip Toolbox for linearly constrained minimum variance (Van Veen et al., 1997) beamforming and dipole

fitting, as well as LORETA-KEY software (version 20170220, The KEY Institute for Brain-Mind Research, Zurich, Switzerland) for exact low-resolution electrotopography (Pascual-Marqui et al., 2011). Three different source localisation methods were used to circumvent the limitations imposed by different mathematical assumptions for finding a unique solution to the 'inverse problem' by each single method (Darvas et al., 2004) (Table 1). Head models incorporating individual geometries for the brain, skull and scalp tissues were constructed for 41 patients. Boundary-element head models (Fuchs et al., 2002) were generated using T1 images from contemporaneous MRI (3-Tesla Philips Achieva scanner, Best, The Netherlands), acquired at the Centre of Advanced Medical Imaging, St. James' Hospital (Schuster et al., 2016). For other subjects with no personal MRI, the ICBM152 head model (Fonov et al., 2011) was used, as template-based and individualised boundary-element head models are found to provide comparable localisation accuracy (Fuchs et al., 2002; Douw et al., 2018).

#### 2.7.1. Linearly constrained minimum variance (LCMV)

LCMV is a beamforming source localisation method wherein the covariance of the signals recorded from the electrodes is used to generate a spatial filter formed by a linear combination of electrode weights, for each grid point in the brain. The identified solution is that which affords minimum experimental variance of data when projected to the source, thus minimising the amount of activity from other sources (Van Veen et al., 1997). LCMV was used to calculate brain maps of mean power for the average AEP 100-300 ms after standard and deviant cues, based on a common spatial filter. A time window of 100-300 ms was utilised to ensure accurate calculation of the covariance matrix from which the spatial filter is calculated and avoid high functional correlation between the sources which would hinder localisation of such distinct sources. Covariance matrices were also calculated for individual trials to minimise such correlations. Regularisation of the covariance matrix was implemented at 5% of the average variance of EEG electrodes to account for reduced dimensionality caused by independent component analysis during preprocessing. Sources within the brain volume were modelled by a grid with 10 mm resolution. The leadfield matrix was normalised to avoid potential norm artefacts. Sources of MMN activity were identified by the locations of the maximal logarithm of the power ratio between deviant and standard maps.

#### 2.7.2. Exact low resolution brain electromagnetic tomography (eLORETA)

ELORETA (Pascual-Marqui et al., 2011) identifies a unique source power map based on the implicit assumption that neighbouring dipoles have similar activity (low spatial resolution). This is achieved by identifying the solution with the least activity norm, subject to minimising the Laplacian (spatial gradient or derivative) of the sources. This assumption yields solutions with a relatively low spatial resolution. ELORETA was also used to calculate mean source power maps of the average auditory evoked potential 100-300 ms after standard and deviant cues to match the data input to LCMV. LORETA-KEY software models sources at 5 mm resolution within the brain volume of a boundary-element headmodel based on the Colin27 average brain (Holmes et al., 1998), excluding sources located within white matter. For statistical comparison, grid resolution was reduced to 10 mm to avoid the loss of discriminatory power that may result from correction of over 6000 comparisons. Regularisation was implemented for a signal to noise ratio of 10. Sources of MMN activity were identified as described for LCMV.

#### 2.7.3. Dipole fitting

Dipole fitting can be used to generate least-square error models of the contributions of electrical dipoles to an EEG topographic distribution, given a-priori estimation of the number and location of contributing dipoles (Scherg and Berg, 1991). Residual variance (the variance in the data not explained by the model) is used as a goodness-of-fit measure. Previous studies (Jemel et al., 2002; Oknina et al., 2005;

Oades et al., 2006) have repeatedly identified MMN sources in the inferior frontal gyri and superior temporal gyri. As non-linear optimisation of the dipole location repetitively produced fits at local rather than global residual variance minima, four fixed dipoles were modelled at the centroid coordinates of the bilateral superior temporal gyri and pars triangularis of the inferior frontal gyri, as determined from an AAL atlas (Tzourio-Mazoyer et al., 2002). Models were estimated based on the average MMN response (mean(deviant response)-mean(standard response)) for 40 ms surrounding the global field power peak between 105 and 271 ms post-stimulus, the period for which we previously found MMN to be significant (Iyer et al., 2017). Subsequently, mean power for each dipole was calculated. The rationale for using this shorter time frame was based upon findings that these four sources better accounted for the data in this window (i.e. had smaller residual variance) than the longer time window of data 100-300 ms post-stimulus, as used for LCMV and eLORETA. A model generated using the longer 200 ms time window provided the same results as the model reported here.

## 2.8. Statistics

### 2.8.1. LCMV and eLORETA

A 10 mm grid in the brain volume yields 733 sources excluding white matter (as modelled by eLORETA) and 1726 sources including white matter (as modelled by LCMV). To analyse these high-dimensional data, 10% False Discovery Rate (Benjamini, 2010) was used as a frequentist methods for preliminary screening. Subsequently, Empirical Bayesian Inference (EBI) (Efron, 2009) was used to find Bayesian posterior probabilities, as well as achieved statistical power and AUROC. AUROC is a measure of how well the test separates patient and control groups (Hajian-Tilaki, 2013) which ranges from 0 to 1, where if the null hypothesis of no separation is true, AUROC equals 0.5. Therefore, the further the value of AUROC from 0.5, the greater the separation.

### 2.8.2. Dipole fitting

Dipole power for each of the four modelled dipoles in the complete ALS group as well as C9ORF72+, C9ORF72-, bulbar-onset and spinal-onset subgroups were compared by Mann-Whitney *U* test. Bonferroni correction for multiple comparisons established a significance threshold of  $p < .0025$ . AUROC and statistics were also calculated for each dipole by empirical bootstrapping-based inference (Nasserolelami, 2018).

### 2.8.3. Neuropsychology correlation

Spearman's rank partial correlation (which is inherently robust to outliers) was used to individually compare changes in EEG source power to CWIT performance (colour naming, word reading, inhibition and inhibition switching times in seconds) while correcting for speech impairment (ALS-FRS speech score on the day of testing) and age. CWIT was investigated on the basis of a previously identified correlation between sensor-level MMN average delay and performance in this task (Iyer et al., 2017). Correlations were performed for power in each fitted dipoles and for the mean power in the left superior and medial frontal gyri (combined), primary motor cortex and posterior parietal cortex, according to the AAL atlas (Tzourio-Mazoyer et al., 2002). Multiple comparison correction was by Bonferroni correction. Beaumont

**Table 1**  
Limitations and advantages of different source localisation methods.

Method	Dipole fitting	LCMV	eLORETA
Spatial resolution	Excellent	Good	Low
Temporally correlated source detection	No limitation	Limited	No limitation
Prior knowledge required	Yes	No	No
Full brain map estimate	No	Yes	Grey-matter

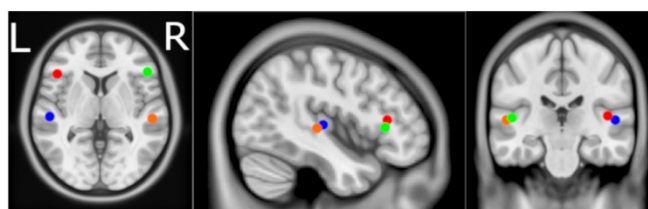


**Fig. 1.** Location of dipoles modelled by dipole fitting. Centroids of the left (blue) and right (orange) superior temporal gyri and left (red) and right (green) inferior frontal pars triangularis were used to seed dipoles for dipole fitting. Axial MRI view is from above (L-Left, R-Right).

**Table 2**

Summary of P-values and AUROCs for each source modelled by dipole fitting in ALS patients and subgroups compared to controls. All subgroups show decreased power in inferior frontal and left temporal dipoles compared to controls. Inferior frontal activity has excellent discrimination ability between *C9orf72* + patients and controls and good discriminating ability in other groups. P-values were obtained by Mann-Whitney U test. AUROC given in parentheses. Bold indicates statistical significance ( $p < .0025$ ).

Dipole Location	All	<i>C9orf72</i> +	<i>C9orf72</i> -	Bulbar-onset	Spinal-onset
Left IFG	<b><math>5.16 \times 10^{-6}</math></b> (0.7741)	<b><math>6.87 \times 10^{-4}</math></b> (0.9084)	<b><math>1.98 \times 10^{-5}</math></b> (0.7637)	<b><math>1.22 \times 10^{-3}</math></b> (0.802)	<b><math>1.22 \times 10^{-3}</math></b> (0.769)
Right IFG	<b><math>1.07 \times 10^{-5}</math></b> (0.7648)	<b><math>2.15 \times 10^{-4}</math></b> (0.9451)	<b><math>9.29 \times 10^{-5}</math></b> (0.7416)	<b><math>2.37 \times 10^{-5}</math></b> (0.895)	<b><math>1.74 \times 10^{-4}</math></b> (0.74)
Left STG	<b><math>9.30 \times 10^{-6}</math></b> (0.7666)	0.016 (0.7912)	<b><math>2.30 \times 10^{-6}</math></b> (0.761)	<b><math>2.64 \times 10^{-3}</math></b> (0.795)	<b><math>2.40 \times 10^{-4}</math></b> (0.738)
Right STG	0.081 (0.6052)	0.39 (0.6044)	0.118 (0.5968)	0.035 (0.698)	0.23 (0.576)

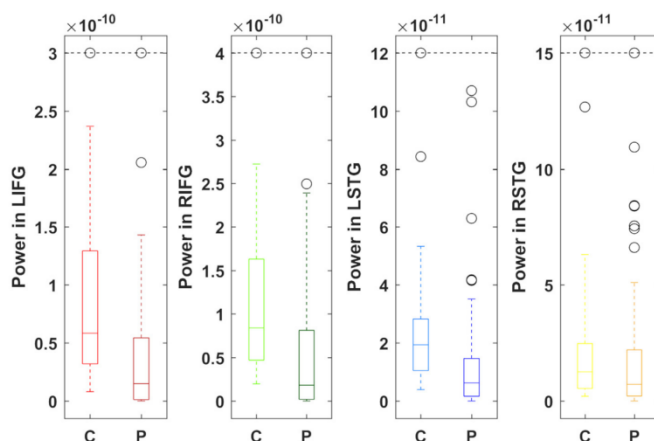


**Fig. 2.** ALS patients show decreased power in both inferior frontal gyri and the left superior temporal gyrus. Boxes illustrate the interquartile range with whiskers illustrating the maximum and minimum power (A-m) within twice the interquartile range for ALS patients (P) and controls (C), determined by dipole fitting. Outliers are illustrated in black. Dashed line caps up to two outliers beyond this value. L – Left, R – Right, IFG – Inferior frontal gyrus, STG – Superior Temporal Gyrus.

Behavioural Inventory (Elamin et al., 2017) and Edinburgh Cognitive Assessment Score (Pinto-Grau et al., 2017) data were also available, however the main scores of these measures showed no significant correlation to source activity and were, therefore, not investigated further.

### 3. Results

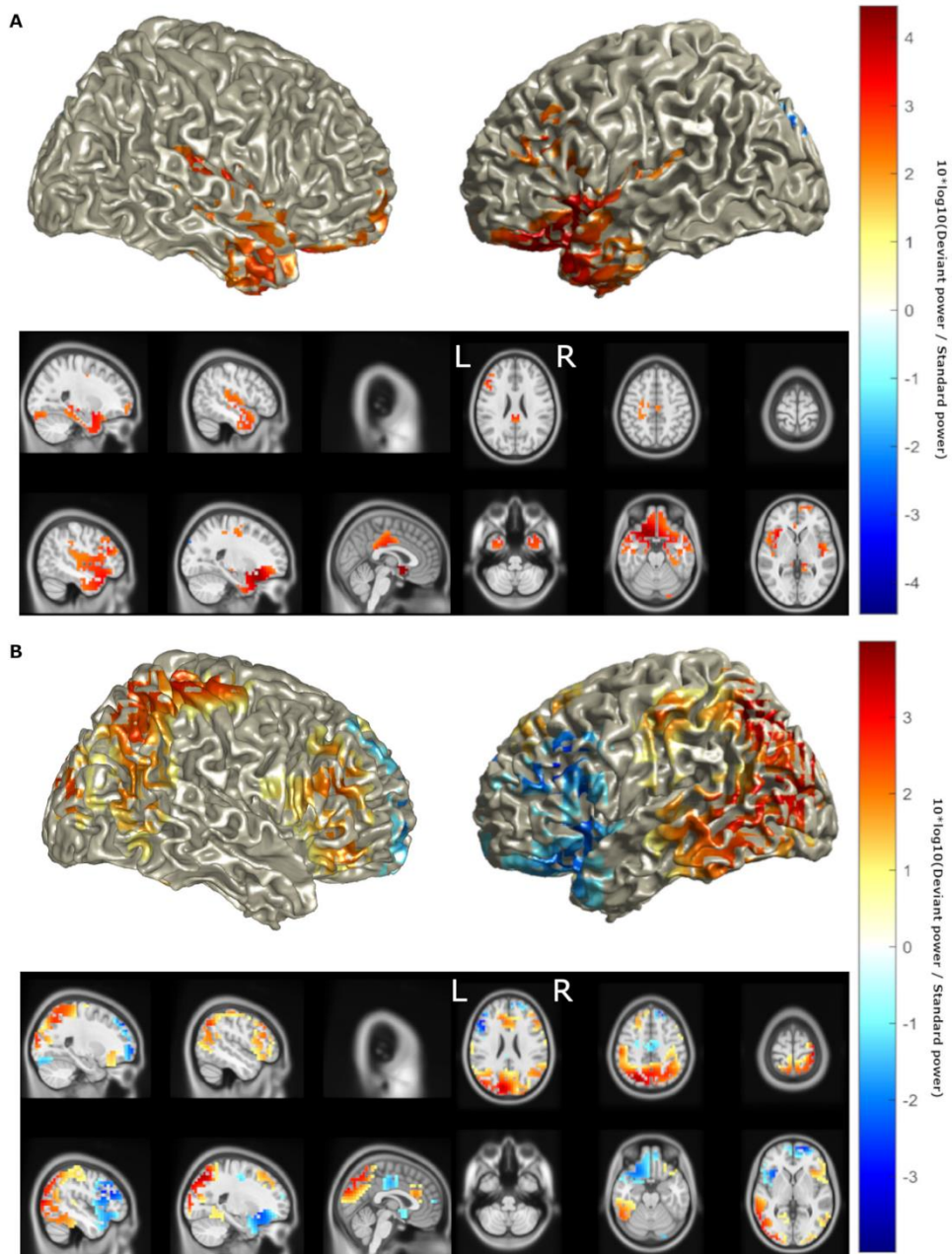
#### 3.1. Dipole fitting

Locations of dipole fits are illustrated in Fig. 1. Control and patient groups showed similar goodness of fit (median (IQR): patients: 23.32% (15.24–30.2%), controls: 24.39% (15.55–35.49%)). P-values obtained

by Mann-Whitney U test comparison of dipole power between ALS patients and healthy controls are summarised in Table 2. Power was significantly lower in the IFG bilaterally as well as the left STG. AUROC demonstrated that power in each of these three dipoles has good group discrimination ability (Table 2, Fig. 2). No differences were found between male and female patients for any dipole ( $p = .27$ – $.75$ , AUROC = 0.42–0.58). The discrepancy from complete fit indicated the presence of additional sources, which were subsequently aggregated by eLORETA and LCMV.

#### 3.2. eLORETA

eLORETA identified maximal intensity of neural activity during



(caption on next page)

**Fig. 3.** eLORETA identified a pattern of decreased activity in the left superior temporal and inferior frontal sources, and an increase in activity in posterior areas. Location of MMN sources with (a) top 50% of power ( $10 \cdot \log_{10}(\text{Deviant power} / \text{Standard power})$ ) in healthy controls and (b) power differences > 25% of maximum between ALS patients and healthy controls as determined by eLORETA. Red denotes increase in power, blue denotes decrease in power. Axial MRI views are from above (L-Left, R-Right).

MMN in the left IFG and bilateral STG and MTG in controls (Fig. 3a), confirming the localisation of major sources to those previously established, with the exception of the right IFG (Jemel et al., 2002; Oknina et al., 2005; Oades et al., 2006). ALS patients showed a pattern of reduced activity in these sources, consistent with the results of dipole fitting, as well as an increase in activity in posterior sources (Fig. 3b). While the eLORETA estimated the general distribution pattern of activity, the method's low spatial resolution prevented the effects reaching statistical significance.

### 3.3. LCMV

LCMV identified sources of MMN similar to the findings of eLORETA (Fig. 4a) but also identifying the right IFG as a source, as identified by previous studies (Jemel et al., 2002; Oknina et al., 2005; Oades et al., 2006). LCMV also detected a trend of reduced activity in these sources bilaterally, in keeping with the results of dipole fitting and eLORETA, as well as an increase in activity in the left parietal, central and dorsolateral prefrontal cortex (Fig. 4b). This increase reached statistical significance (Fig. 5, FDR = 10%, statistical power = 0.58). Based on interpolation with an AAL atlas, sources with significantly increased activity included the superior parietal lobe and precuneus, left motor structures including the primary motor cortex, supplementary motor area and mid cingulum, as well as the mid frontal gyrus (Table 3). Positive correlations (Fig. 6) were found between CWIT inhibition-switching time (but not other CWIT scores) and mean power in the left primary motor cortex ( $\rho = 0.45$ ,  $p = .055$ ), the superior and middle frontal gyri combined ( $\rho = 0.47$ ,  $p = .031$ ) and the posterior parietal cortex ( $\rho = 0.45$ ,  $p = .042$ ), where greater inhibition-switching score indicates more impaired cognitive flexibility and verbal inhibition (Swanson, 2005).  $P$ -values below 0.05 in the prefrontal and parietal cortices did not survive multiple comparison correction, likely due to the low number of CWIT scores available. No significant differences were found between male and female patient sources ( $\alpha_{\text{global}} = 0.92$ ,  $\beta_{\text{global}} = 0.075$ ) or mean power of the left posterior parietal, motor or inferior frontal cortices ( $p = .56-.89$ ).

### 3.4. Differences between ALS subgroups

C9ORF72+ patients were not distinguished from C9ORF72- patients by any localisation method, nor were bulbar-onset from spinal-onset patients. This was likely due to insufficient sample size. C9ORF72- and spinal subgroups individually showed similar patterns of significant difference to the full patient group across each localisation method. Bulbar and C9ORF72+ subgroups significantly differed from controls with respect to bilateral IFG dipole activity, and exhibited better discrimination ability (summarised in Table 2). The discrimination ability of this difference was excellent for C9ORF72+ patients (AUROC > 0.9) with low AUROC variation (0.002 bilaterally). CWIT and speech score data were insufficient (C9ORF72+  $n = 0$ , bulbar-onset  $n = 3$ ) for correlation analyses.

## 4. Discussion

This study demonstrates that source localization of cognitive event-related potentials measured by EEG reliably distinguishes attentional network changes in ALS patients compared to controls, particularly in subgroups with higher prevalence of cognitive impairment (Byrne et al., 2012b; Schreiber et al., 2005). Furthermore, this study indicates for the first time a correlation between the activities of specific sources

underlying cognitive event-related potentials and cognitive performance in a neurodegenerative disease. Compared with controls, ALS patients show decreased activity in both inferior frontal gyri and the left superior temporal gyrus and increased left posterior parietal and dorsolateral prefrontal activity. ALS patients also show significantly increased activity in the left motor cortex.

### 4.1. Imbalance of attention-regulating network activity during sensory processing in ALS

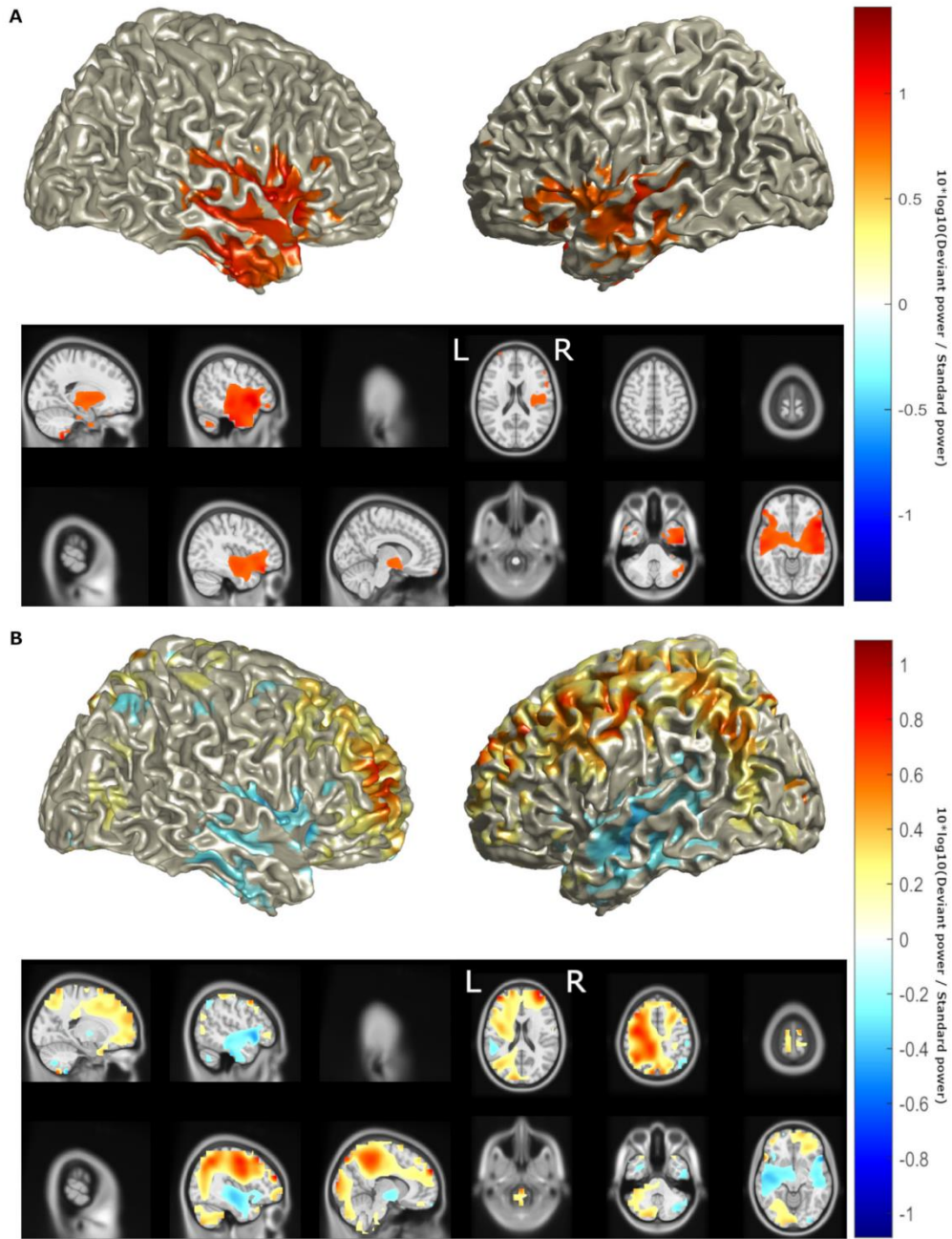
The superior temporal and inferior frontal gyri are well established sources of MMN activity (Maess et al., 2007; Jemel et al., 2002; MacLean et al., 2015). In this study, decreased activity in these regions was identified independently using each of the methods, however, dipole fitting allowed for a more temporally and spatially precise interrogation of these sources.

Repetitive TMS (Nixon et al., 2004) and nonword rhyming task studies (Burton, 2001) have demonstrated the role of the IFG in phonological working memory, where information about one stimulus is stored for later comparison to a second. The IFG is also known to be active when ignoring stimuli (Bunge et al., 2001) and is functionally connected to the default mode network (Beatty et al., 2014). This network is active when directed attention is not required and is deactivated by goal-directed activity, as defined by resting-state fMRI (Raichle et al., 2001). The activity of the default mode network is anti-correlated with that of the central executive network, where attention needs to be directed to a task (Nekovarova et al., 2014). Inferior frontal source activity during the MMN is therefore consistent with calling for a switch of attention to changes in the unattended environment (i.e. involuntary attention switching), to which prefrontal MMN sources have previously been attributed (Winkler et al., 1996; Giard et al., 1990).

The observed substantial reduction in IFG activity in ALS is correspondingly expected to parallel impairments in these cognitive functions. As posterior parietal and dorsolateral prefrontal cortices are nodes of the central executive network (Seeley et al., 2007), their abnormal activation in combination with IFG dysfunction during MMN in ALS may represent a loss of balance between the activity of these attention-regulating networks (Menon and Uddin, 2010) resulting in dysregulation of involuntary attention switching.

As participants were asked to ignore and not respond to stimuli in this study, attention regulation could not be behaviourally measured during MMN recording. This hypothesis is, however, supported by our preliminary findings of a positive correlation between increases in left posterior parietal and dorsolateral prefrontal activity during MMN, and the inhibition/switching score of the CWIT (and not other subscores of the CWIT). This indicates that abnormal increase in the activity of this network conveys cognitive inflexibility and disinhibition (Swanson, 2005). Such behavioural inflexibility and disinhibition is consistent with incorrect orientation to irrelevant stimuli and is expected in those with abnormal central executive network activation. Correspondingly, change in bilateral IFG activity was shown to be an excellent discriminator of C9ORF72+ and bulbar-onset ALS subgroups, which are more prone to cognitive impairment (Byrne et al., 2012b; Schreiber et al., 2005).

This imbalance hypothesis is also evidenced by data from previously reported functional connectivity studies in ALS. For example, resting-state MEG has identified increased functional connectivity between the left posterior cingulate and prefrontal cortices, as well as within and between posterior parietal cortices, in addition to increased overall parietal connectivity (e.g. node weight) (Proudfoot et al., 2018).



(caption on next page)

Fig. 4. LCMV identified a pattern of decreased activity in bilateral superior temporal and inferior frontal sources, and an increase in activity in the left hemisphere. Location of MMN sources with (a) top 25% of power ( $10 \cdot \log_{10}(\text{Deviant power} / \text{Standard power})$ ) in healthy controls and (b) power differences > 25% of maximum between ALS patients and healthy controls as determined by LCMV beamforming. Red denotes increase in power, blue denotes decrease in power. Axial MRI views are from above (L-Left, R-Right).

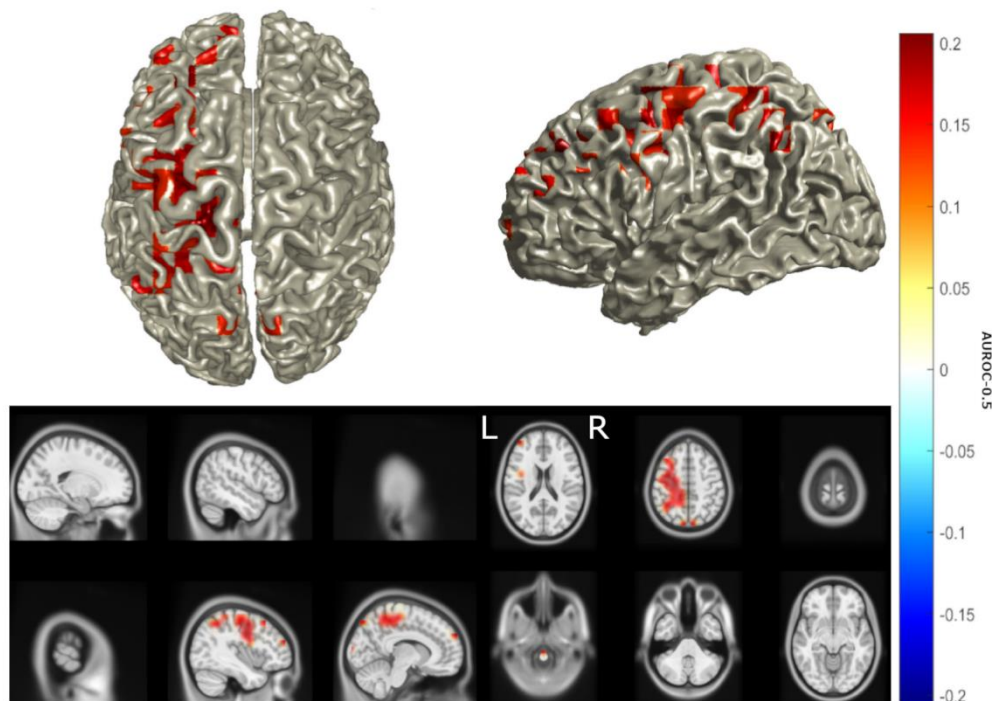


Fig. 5. Increased activity in the left posterior parietal, central and dorsolateral prefrontal cortex in ALS is statistically significant. Statistically significant (false discovery rate = 10%) differences in power between ALS patients and healthy controls as determined by LCMV. Heat map values are AUROC-0.5. Red denotes AUROC > 0.5, blue denotes decrease in AUROC < 0.5. Axial MRI views are from above (L-Left, R-Right).

Furthermore, resting state fMRI has demonstrated increased left precuneus, posterior parietal and mid cingulate cortex connectivity in addition to decreased inferior frontal connectivity (Agosta et al., 2013) in ALS. Accordingly, the frontoparietal hyperactivity and inferior frontal depression observed in our study may reflect a spread in pathological hyperactivity into cognitive networks, which in turn alters the balance in normal network activity. Activation of the central cortex in addition to cognitive network nodes during MMN in ALS may correspondingly represent abnormal activation of networks connecting motor and cognitive areas. This is consistent with previous physiological studies which have consistently identified hyperactivity in upper motor neurons in ALS (Vucic and Kiernan, 2006) and loss of inhibitory control (Grieve et al., 2015).

ALS-FRS-R total score showed no correlation to source activity - this is likely a reflection of the relatively low burden disease in the majority of patients, and the study being underpowered to explore the subscores of ALSFRS-R. However, previous studies have shown that functional connectivity is increased with ALS and correlates with disease severity (Sorrentino et al., 2018). A reduction in MMN in healthy individuals is also found to parallel increased connectivity and decreased inhibitory

control between underlying sources, particularly in frontal nodes (Cooray et al., 2014). The recently demonstrated relationship between cognitive impairment and disease stage in ALS (Crockford et al., 2018) is therefore likely to reflect the spread of hyperactivity from motor to cognitive networks.

#### 4.2. Potentially abnormal function of auditory network in ALS

Temporal source activity has been attributed predominantly to sensory memory and change detection in early MMN (Giard et al., 1990; Rinne et al., 2000; Alho, 1995; Näätänen and Michie, 1979); however, it has also been found to contribute to MMN's later attention switching component (Maess et al., 2007). Furthermore, as the difference wave early in the 100-300 ms studied may also capture changes in N1 (May and Tiitinen, 2010), temporal activity may include sensory detection.

As STG contains the primary auditory cortex (Howard et al., 2000) and has been shown to be active during attention control (Hopfinger et al., 2000), the decrease in left STG activity identified here in ALS may represent impairment in either auditory or cognitive networks. These

**Table 3**  
Comparison of the head and source models, time windows and detected source activity changes for each source localisation method used. L – left, R – right, IFG – inferior frontal gyrus, STG – superior temporal gyrus. Arrows represent direction of change in power. \*Statistically significant ( $p < .0025$ ), BEM – Boundary element model.

Method	Head/source model	Time (ms)	Other significant source changes					
			L IFG	R IFG	L STG	R STG	Other significant source changes	
LCMV	ICBM152/personal MRI BEM, 10 mm grid	100-300	↓	↓	↓	↓	†* Left superior parietal lobe, precuneus, primary motor cortex, supplementary motor area, mid cingulum, mid frontal gyrus	
eLORETA	Colin27 MRI BEM, 10 mm grid excl. white matter	100-300	↓	↑	↓	↓	None	
Dipole fitting	ICBM152/personal MRI BEM, 4 dipoles	105-271 & 100-300	↓*	↓*	↓*	↓	N/A	

findings, in addition to the greater number of (excluded) patients lacking clear AEPs compared to controls, suggest the additional presence of auditory network dysfunction in ALS. An additional investigation of AEPs generated during a solely auditory task is required to investigate this network further in ALS.

4.3. Harnessing the advantages of quantitative EEG

The detected changes in ALS reflect the additive benefits of physiological investigation to those of structural imaging. The discriminative ability of these changes, determined by the AUROC (up to 0.95 here) was comparable to, or better than, that achieved by fMRI (AUROC = 0.714) (Welsh et al., 2013) and sensor space qEEG (AUROC = 0.69) (Iyer et al., 2017). This methodology therefore has the potential to provide neurodegenerative disease markers prior to the onset of discernible structural degeneration, allowing for earlier and more sensitive monitoring of potential interventions.

4.4. Limitations

A sample size of 58 patients and limited availability of psychological and clinical test scores restricted exploration of the relationship between cognitive symptoms and source activity within subgroups of this heterogeneous condition. Further studies of larger sample size are therefore warranted to explore such relationships and ALS inter-subgroup differences with greater statistical power.

4.5. Conclusion

In conclusion, combining multiple localisation methods to determine the sources of ERPs provides high spatial resolution to complement qEEGs' excellent temporal resolution in the investigation of ALS-related network dysfunction. The use of this approach to localise activity during other cognitive, motor and sensory tasks allows for detailed interrogation of the location and nature of brain network disruption in neurodegenerative disorders, with the potential to provide early, non-invasive and inexpensive biomarkers of neurodegenerations or their subtypes.

Acknowledgements

This study was funded by the Irish Research Council [IRC, grant numbers: GOIPG/2017/1014, GOIPD/2015/213], the Health Research Board [HRB, grant numbers: HRA-POR-2013-246, MRCG-2018-02], Science Foundation Ireland [SFI, grant numbers: 16/ERCDC/3854] and Research Motor Neurone [grant number: MRCG-2018-02]. Peter Bede and the neuroimaging aspects of the study were supported by the Health Research Board [grant number: EIA-2017-019], the Irish Institute of Clinical Neuroscience IICN – Novartis Ireland Research (IICN – 2016) and the Iris O'Brien Foundation. The psychology aspects of the study were supported by the Motor Neurone Disease Association [MND, grant number: Hardiman/Oct15/879-792]. Muthuraman Muthuraman was supported by the German Research Foundation [grant number: CRC-1193-B05]. We thank Professor Julie Kelly for critical comments on the manuscript and the Wellcome-HRB Clinical Research Facility at St. James's Hospital in providing a dedicated environment for the conduct of high quality clinical research. Finally, we would like to thank all the patients, participants and their families who volunteered to take part in this study.

Author contributions

R.M., B.N., S.D., M.M, N.P., O.H., P.B., E.L., – Conception and design of the study.

R.M., S.D. B.N., M.P-G, R.C., M.B., K.M., T.B., M.G., B.G., A.C., P.L., T.B., C.S., B.G., M.H., – Acquisition and analysis of data.



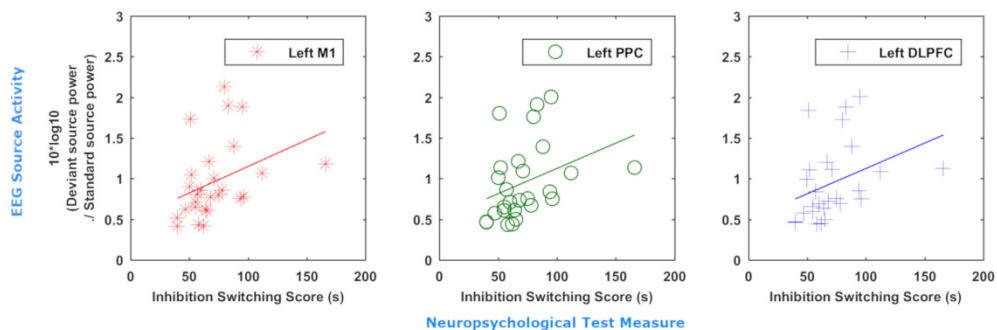


Fig. 6. Increased activity in the posterior parietal and dorsolateral prefrontal cortex correlates to poorer performance in cognitive switching tasks. Correlation of inhibition/switching score (in seconds) for 27 patients with mean power in the left primary motor cortex (red), posterior parietal cortex (PPC, green), and middle and superior frontal gyri (M/SFG, blue) illustrated by scatterplot with line of best fit.

R.M., S.D., B.N., M.M., O.H. - Drafting of manuscript or figures.

#### Potential conflicts of interest

Nothing to report.

#### References

- Agosta, F., Canu, E., Valsassina, P., Riva, N., Prella, A., Comi, G., Filippi, M., 2013. Divergent brain network connectivity in amyotrophic lateral sclerosis. *Neurobiol. Aging* 34, 419–427. <https://doi.org/10.1016/j.neurobiolaging.2012.04.015>.
- Alho, K., 1995. Cerebral generators of mismatch negativity (MMN) and its magnetic counterpart (MMNm) elicited by sound changes. *Ear Hear.* 16, 38–51. <https://doi.org/10.1097/00003446-199502000-00004>.
- Alho, K., Woods, D.L., Algazi, A., Knight, R.T., Näätänen, R., 1994. Lesions of frontal cortex diminish the auditory mismatch negativity. *Electroencephalogr. Clin. Neurophysiol.* 91, 353–362. [https://doi.org/10.1016/0013-4694\(94\)00173-1](https://doi.org/10.1016/0013-4694(94)00173-1).
- Beatty, R.E., Benedek, M., Wilkins, R.W., Jauk, E., Fink, A., Silvia, P.J., Hodges, D.A., Koschutnig, K., Neubauer, A.C., 2014. Creativity and the default network: a functional connectivity analysis of the creative brain at rest. *Neuropsychologia* 64, 92–98. <https://doi.org/10.1016/j.neuropsychologia.2014.09.019>.
- Bede, P., Elamin, M., Byrne, S., McLaughlin, R.L., Kenna, K., Vajda, A., Fagan, A., Bradley, D.G., Hardiman, O., 2015. Patterns of cerebral and cerebellar white matter degeneration in ALS. *J. Neurol. Neurosurg. Psychiatry* 86, 468–470. <https://doi.org/10.1136/jnnp-2014-308172>.
- Bede, P., Omer, T., Finegan, E., Chipika, R.H., Iyer, P.M., Doherty, M.A., Vajda, A., Pender, N., McLaughlin, R.L., Hutchinson, S., Hardiman, O., 2018. Connectivity-based characterisation of subcortical grey matter pathology in frontotemporal dementia and ALS: a multimodal neuroimaging study. *Brain Imaging Behav.* 1–12. <https://doi.org/10.1007/s11682-018-9837-9>.
- Benjamini, Y., 2010. Discovering the false discovery rate. *J. Royal Stat. Soc. Ser. B (Stat. Methodol.)* 72, 405–416. <https://doi.org/10.1111/j.1467-9868.2010.00746.x>.
- Bunge, S.A., Ochsner, K.N., Desmond, J.E., Glover, G.H., Gabrieli, J.D.E., 2001. Prefrontal regions involved in keeping information in and out of mind. *Brain* 124, 2074–2086. <https://doi.org/10.1093/brain/124.10.2074>.
- Burton, M.W., 2001. The role of inferior frontal cortex in phonological processing. *Cogn. Sci.* 25, 695–709. [https://doi.org/10.1207/s15516709cog2505\\_4](https://doi.org/10.1207/s15516709cog2505_4).
- Byrne, S., Elamin, M., Bede, P., Hardiman, O., 2012a. Absence of consensus in diagnostic criteria for familial neurodegenerative diseases. *J. Neurol. Neurosurg. Psychiatry* 83, 365–367. <https://doi.org/10.1136/jnnp-2011-301530>.
- Byrne, S., Elamin, M., Bede, P., Shatunov, A., Walsh, C., Corr, B., Heverin, M., Jordan, N., Kenna, K., Lynch, C., McLaughlin, R.L., Iyer, P.M., O'Brien, C., Phukan, J., Wynne, B., Bokde, A.L., Bradley, D.G., Pender, N., Al-Chalabi, A., Hardiman, O., 2012b. Cognitive and clinical characteristics of patients with amyotrophic lateral sclerosis carrying a C9orf72 repeat expansion: a population-based cohort study. *Lancet Neurol.* 11, 232–240. [https://doi.org/10.1016/S1474-4422\(12\)70014-5](https://doi.org/10.1016/S1474-4422(12)70014-5).
- Cooray, G., Garrido, M.L., Hyllienmark, L., Brisman, T., 2014. A mechanistic model of mismatch negativity in the ageing brain. *Clin. Neurophysiol.* 125, 1774–1782. <https://doi.org/10.1016/j.clinph.2014.01.015>.
- Crockford, C., Newton, J., Loneragan, K., Chivwera, T., Booth, T., Chandran, S., Colville, S., Heverin, M., Mays, I., Pal, S., Pender, N., Pinto-Grau, M., Radakovic, R., Shaw, C.E., Stephenson, L., Swingler, R., Vajda, A., Al-Chalabi, A., Hardiman, O., Abrahams, S., 2018. ALS-specific cognitive and behavior changes associated with advancing disease stage in ALS. *Neurology* 91, e1370–e1380. <https://doi.org/10.1212/WNL.0000000000006317>.
- da Silva, F.L., 2013. EEG and MEG: relevance to neuroscience. *Neuron* 80, 1112–1128.
- Darvas, F., Pantazis, D., Kucukaltun-Yildirim, E., Leahy, R.M., 2004. Mapping human brain function with MEG and EEG: methods and validation. *NeuroImage* 23, S289–S299. <https://doi.org/10.1016/j.neuroimage.2004.07.014>.
- Delis, D.C., Kaplan, E., Kramer, J.H., 2001. Delis-Kaplan Executive Function System (D-KEFS). Psychological Corporation, San Antonio TX.
- Döring, C., Müller, M., Hagenmüller, F., Ajdacic-Gross, V., Haker, H., Kawohl, W., Rössler, W., Heekeren, K., 2016. Mismatch negativity: alterations in adults from the general population who report subclinical psychotic symptoms. *Eur. Psychiatry* 34, 9–16. <https://doi.org/10.1016/j.eurpsy.2016.01.001>.
- Douw, L., Nieboer, D., Stam, C.J., Tewarie, P., Hillebrand, A., 2018. Consistency of magnetoencephalographic functional connectivity and network reconstruction using a template versus native MRI for co-registration. *Hum. Brain Mapp.* 39, 104–119. <https://doi.org/10.1002/hbm.23827>.
- Dukic, S., Iyer, P.M., Mohr, K., Hardiman, O., Lalor, E.C., Nasseroleami, B., 2017. Estimation of coherence using the median is robust against EEG artefacts. *Conf. Proc. IEEE Eng. Med. Biol. Soc.* 2017, 3949–3952. <https://doi.org/10.1109/EMBC.2017.8037720>.
- Efron, B., 2009. Empirical Bayes estimates for large-scale prediction problems. *J. Am. Stat. Assoc.* 104, 1015–1028. <https://doi.org/10.1198/jasa.2009.tm08523>.
- Elamin, M., Pinto-Grau, M., Burke, T., Bede, P., Rooney, J., O'Sullivan, M., Loneragan, K., Kirby, E., Quinlan, E., Breen, N., Vajda, A., Heverin, M., Pender, N., Hardiman, O., 2017. Identifying behavioural changes in ALS: validation of the beamont behavioural inventory (BBI). *Amyotroph. Lateral Scler. Frontotemporal Degener.* 18, 68–73. <https://doi.org/10.1080/21678421.2016.1248976>.
- Erdogan, S.B., Tong, Y., Hocke, L.M., Lindsey, K.P., deB Frederick, B., 2016. Correcting for blood arrival time in global mean regression enhances functional connectivity analysis of resting state (fMRI-BOLD) signals. *Front. Hum. Neurosci.* 10, 311.
- Escera, C., Yago, E., Alho, K., 2001. Electrical responses reveal the temporal dynamics of brain events during involuntary attention switching. *Eur. J. Neurosci.* 14, 877–883.
- Escera, C., Yago, E., Corral, M.-J., Corbera, S., Nuñez, M.L., 2003. Attention capture by auditory significant stimuli: semantic analysis follows attention switching. *Eur. J. Neurosci.* 18, 2406–2412.
- Fonov, V., Evans, A.C., Botteron, K., Almli, C.R., McKinstry, R.C., Collins, D.L., 2011. Unbiased average age-appropriate atlases for pediatric studies. *NeuroImage* 54, 313–327. <https://doi.org/10.1016/j.neuroimage.2010.07.033>.
- Fuchs, M., Kastner, J., Wagner, M., Hawes, S., Ebersole, J.S., 2002. A standardized boundary element method volume conductor model. *Clin. Neurophysiol.* 113, 702–712. [https://doi.org/10.1016/S1388-2457\(02\)00030-5](https://doi.org/10.1016/S1388-2457(02)00030-5).
- Giard, M.-H., Perrin, F., Pernier, J., Bouchet, P., 1990. Brain generators implicated in the processing of auditory stimulus deviance: a topographic event-related potential study. *Psychophysiology* 27, 627–640.
- Grieve, S.M., Menon, P., Korgaonkar, M.S., Gomes, I., Foster, S., Kiernan, M.C., Vucic, S., 2015. Potential structural and functional biomarkers of upper motor neuron dysfunction in ALS. *Amyotroph. Lateral Scler. Frontotemporal Degener.* 17, 85–92. <https://doi.org/10.3109/21678421.2015.1074707>.
- Hajian-Tilaki, K., 2013. Receiver operating characteristic (ROC) curve analysis for medical diagnostic test evaluation. *Caspian J. Intern. Med.* 4, 627–635. <https://doi.org/10.1016/j.ebobygn.2006.01.016>.
- Holmes, C.J., Hoge, R., Collins, L., Woods, R., Toga, A.W., Evans, A.C., 1998. Enhancement of MR images using registration for signal averaging. *J. Comput. Assist. Tomogr.* 22, 324–333. [https://doi.org/10.1016/S1053-8119\(96\)80030-9](https://doi.org/10.1016/S1053-8119(96)80030-9).
- Hopfinger, J.B., Buonocore, M.H., Mangun, G.R., 2000. The neural mechanisms of top-down attentional control. *Nat. Neurosci.* 3, 284–291. <https://doi.org/10.1038/72999>.
- Howard, M.A., Volkov, I.O., Mirsky, R., Garell, P.C., Noh, M.D., Granner, M., Damasio, H., Steinschneider, M., Reale, R.A., Hind, J.E., Brugge, J.F., 2000. Auditory cortex on the human posterior superior temporal gyrus. *J. Comp. Neurol.* 416, 79–92. [https://doi.org/10.1002/\(SICI\)1096-9861\(20000103\)416:1<79::AID-CNE6>3.0.CO;2-2](https://doi.org/10.1002/(SICI)1096-9861(20000103)416:1<79::AID-CNE6>3.0.CO;2-2).
- Iyer, P.M., Mohr, K., Broderick, M., Gavin, B., Burke, T., Bede, P., Pinto-Grau, M., Pender, N.,

- N.P., McLaughlin, R., Vajda, A., 2017. Mismatch negativity as an indicator of cognitive sub-domain dysfunction in amyotrophic lateral sclerosis. *Front. Neurol.* 8, 395. <https://doi.org/10.3389/fneur.2017.00395>.
- Jääskeläinen, I.P., Ahveninen, J., Bonmassar, G., Dale, A.M., Ilmoniemi, R.J., Lövén, S., Lin, F.-H., May, P., Melcher, J., Stufflebeam, S., Tiitinen, H., Belliveau, J.W., 2004. Human posterior auditory cortex gates novel sounds to consciousness. *Proc. Natl. Acad. Sci. U. S. A.* 101, 6809–6814. <https://doi.org/10.1073/pnas.03037610101>.
- Jemel, B., Achenbach, C., Müller, B.W., Röpcke, B., Oades, R.D., 2002. Mismatch negativity results from bilateral asymmetric dipole sources in the frontal and temporal lobes. *Brain Topogr.* 15, 13–27. <https://doi.org/10.1023/A:1019944805499>.
- Katada, E., Sato, K., Ojika, K., Ueda, R., 2004. Cognitive event-related potentials: useful clinical information in Alzheimer's disease. *Curr. Alzheimer Res.* 1, 63–69.
- Kiernan, M.C., Vucic, S., Cheah, B.C., Turner, M.R., Eisen, A., Hardiman, O., Burrell, J.R., Zoing, M.C., 2011. Amyotrophic lateral sclerosis. *Lancet* 377, 942–955. [https://doi.org/10.1016/S0140-6736\(10\)61156-7](https://doi.org/10.1016/S0140-6736(10)61156-7).
- Kujala, T., Leminen, M., 2017. Low-level neural auditory discrimination dysfunctions in specific language impairment—a review on mismatch negativity findings. *Dev. Cogn. Neurosci.* 28, 65–75. <https://doi.org/10.1016/j.dcn.2017.10.005>.
- Lyytinen, H., Blomberg, A.P., Näätänen, R., 1992. Event-related potentials and autonomic responses to a change in unattended auditory stimuli. *Psychophysiology* 29, 523–534.
- MacLean, S.E., Blundon, E.G., Ward, L.M., 2015. Brain regional networks active during the mismatch negativity vary with paradigm. *Neuropsychologia* 75, 242–251. <https://doi.org/10.1016/j.neuropsychologia.2015.06.019>.
- Maess, B., Jacobsen, T., Schröger, E., Friederici, A.D., 2007. Localizing pre-attentive auditory memory-based comparison: magnetic mismatch negativity to pitch change. *NeuroImage* 37, 561–571. <https://doi.org/10.1016/j.neuroimage.2007.05.040>.
- May, P., Tiitinen, H., 2001. Human cortical processing of auditory events over time. *Neuroreport* 12, 573–577.
- May, P.J.C., Tiitinen, H., 2004. The MMN is a derivative of the auditory N100 response. *Neuro. Clin. Neurophysiol.* 2004, 20.
- May, P.J.C., Tiitinen, H., 2010. Mismatch negativity (MMN), the deviance-elicited auditory deflection, explained. *Psychophysiology* 47, 66–122. <https://doi.org/10.1111/j.1469-8986.2009.00856.x>.
- May, P., Tiitinen, H., Ilmoniemi, R.J., Nyman, G., Taylor, J.G., Näätänen, R., 1999. Frequency change detection in human auditory cortex. *J. Comput. Neurosci.* 6, 99–120.
- Menon, V., Uddin, L.Q., 2010. Saliency, switching, attention and control: a network model of insula function. *Brain Struct. Funct.* 214, 655–667. <https://doi.org/10.1007/s00429-010-0262-0>.
- Moeller, F., Muthuraman, M., Stephani, U., Deuschl, G., Raethjen, J., Siniatchkin, M., 2013. Representation and propagation of epileptic activity in absences and generalized photoparoxysmal responses. *Hum. Brain Mapp.* 34, 1896–1909. <https://doi.org/10.1002/hbm.23026>.
- Müller, B.W., Jäppner, M., Jentzen, W., Müller, S.P., 2002. Cortical activation to auditory mismatch elicited by frequency deviant and complex novel sounds: a PET study. *NeuroImage* 17, 231–239. <https://doi.org/10.1006/nimg.2002.1176>.
- Muthuraman, M., Hellriegel, H., Hoogenboom, N., Anwar, A.R., Mideksa, K.G., Krause, H., Schmitzler, A., Deuschl, G., Raethjen, J., 2014. Beamformer source analysis and connectivity on concurrent EEG and MEG data during voluntary movements. *PLoS One* 9, e91441. <https://doi.org/10.1371/journal.pone.0091441>.
- Muthuraman, M., Raethjen, J., Koirala, N., Anwar, A.R., Mideksa, K.G., Elble, R., Groppa, S., Deuschl, G., 2018. Cerebello-cortical network fingerprints differ between essential, Parkinson's and mimicked tremors. *Brain* 141, 1770–1781. <https://doi.org/10.1093/brain/awy098>.
- Naatanen, R., 1995. The mismatch negativity: a powerful tool for cognitive neuroscience. *Ear Hearing* 16, 6–18. <https://doi.org/10.1097/00003446-199502000-00002>.
- Näätänen, R., 1995. The mismatch negativity: a powerful tool for cognitive neuroscience. *Ear Hear.* 16, 6–18.
- Näätänen, R., Michie, P.T., 1979. Early selective-attention effects on the evoked potential: a critical review and reinterpretation. *Biol. Psychol.* 8, 81–136.
- Näätänen, R., Gaillard, A.W.K., Mäntysalo, S., 1978. Early selective-attention effect on evoked potential reinterpreted. *Acta Psychol.* 42, 313–329. [https://doi.org/10.1016/0001-6918\(78\)90006-9](https://doi.org/10.1016/0001-6918(78)90006-9).
- Näätänen, R., Paavilainen, P., Rinne, T., Alho, K., 2007. The mismatch negativity (MMN) in basic research of central auditory processing: a review. *Clin. Neurophysiol.* 118, 2544–2590. <https://doi.org/10.1016/j.clinph.2007.04.026>.
- Näätänen, R., Kujala, T., Escera, C., Baldeeweg, T., Kreegipuu, K., Carlson, S., Ponton, C., 2012. The mismatch negativity (MMN)—a unique window to disturbed central auditory processing in ageing and different clinical conditions. *Clin. Neurophysiol.* 123, 424–458. <https://doi.org/10.1016/j.clinph.2011.09.020>.
- Näätänen, R., Sussman, E.S., Salisbury, D., Shafer, V.L., 2014. Mismatch negativity (MMN) as an index of cognitive dysfunction. *Brain Topogr.* 27, 451–466. <https://doi.org/10.1007/s10548-014-0374-6>.
- Nasserollesami, B., 2018. An implementation of empirical bayesian inference and non-null bootstrapping for threshold selection and power estimation in multiple and single statistical testing. *BioRxiv* 342964. <https://doi.org/10.1101/342964>.
- Nasserollesami, B., Dukie, S., Broderick, M., Mohr, K., Schuster, C., Gavin, B., McLaughlin, R., Heverin, M., Vajda, A., Iyer, P.M., Pender, N., Bede, P., Lalor, E.C., Hardiman, O., 2017. Characteristic increases in EEG connectivity correlate with changes of structural MRI in amyotrophic lateral sclerosis. *Cereb. Cortex* 1–15. <https://doi.org/10.1093/cercor/bhx301>.
- Nekovarova, T., Fajnerova, I., Horacek, J., Spaniel, F., 2014. Bridging disparate symptoms of schizophrenia: a triple network dysfunction theory. *Front. Behav. Neurosci.* 8. <https://doi.org/10.3389/fnbeh.2014.00171>.
- Nixon, P., Lazarova, J., Hodinott-Hill, I., Gough, P., Passingham, R., 2004. The inferior frontal gyrus and phonological processing: an investigation using rTMS. *J. Cogn. Neurosci.* 16, 289–300. <https://doi.org/10.1162/089892904322984571>.
- Oades, R.D., Wild-Wall, N., Juran, S.A., Sachsse, J., Okkina, L.B., Röpcke, B., 2006. Auditory change detection in schizophrenia: sources of activity, related neuropsychological function and symptoms in patients with a first episode in adolescence, and patients 14 years after an adolescent illness-onset. *BMC Psychiatry* 6, 7. <https://doi.org/10.1186/1471-244X-6-7>.
- Okkina, L.B., Wild-Wall, N., Oades, R.D., Juran, S.A., Röpcke, B., Pfueller, U., Weisbrod, M., Chan, E., Chen, E.Y.H., 2005. Frontal and temporal sources of mismatch negativity in healthy controls, patients at onset of schizophrenia in adolescence and others at 15 years after onset. *Schizophr. Res.* 76, 25–41. <https://doi.org/10.1016/j.schres.2004.10.003>.
- Oostenveld, R., Fries, P., Maris, E., Schoffelen, J.-M., 2011. FieldTrip: open source software for advanced analysis of MEG, EEG, and invasive electrophysiological data. *Comput. Intell. Neurosci.* 2011. <https://doi.org/10.1155/2011/156869>.
- Opitz, B., Rinne, T., Mecklinger, A., von Cramon, D.Y., Schröger, E., 2002. Differential contribution of frontal and temporal cortices to auditory change detection: fMRI and ERP results. *NeuroImage* 15, 167–174. <https://doi.org/10.1006/nimg.2001.0970>.
- Pascual-Marqui, R.D., Lehmann, D., Koukoku, M., Kochi, K., Anderer, P., Saletu, B., Tanaka, H., Hirata, K., John, E.R., Prichep, L., Biscay-Lirio, R., Kinoshita, T., 2011. Assessing interactions in the brain with exact low-resolution electromagnetic tomography. *Philos. Trans A Math Phys. Eng. Sci.* 369, 3768–3784. <https://doi.org/10.1098/rsta.2011.0081>.
- Phukan, J., Pender, N.P., Hardiman, O., 2007. Cognitive impairment in amyotrophic lateral sclerosis. *Lancet Neurol.* 6, 994–1003. [https://doi.org/10.1016/S1474-4422\(07\)70265-X](https://doi.org/10.1016/S1474-4422(07)70265-X).
- Pinto-Grau, M., Burke, T., Loneragan, K., McHugh, C., Mays, I., Madden, C., Vajda, A., Heverin, M., Elamin, M., Hardiman, O., Pender, N., 2017. Screening for cognitive dysfunction in ALS: validation of the Edinburgh Cognitive and Behavioural ALS Screen (ECAS) using age and education adjusted normative data. *Amyotroph Lateral Scler Frontotemporal Degener.* 18, 99–106. <https://doi.org/10.1080/21678421.2016.1249887>.
- Proudfoot, M., Colclough, G.L., Quinn, A., Wu, J., Talbot, K., Benatar, M., Nobre, A.C., Woolrich, M.W., Turner, M.R., 2018. Increased cerebral functional connectivity in ALS: a resting-state magnetoencephalography study. *Neurology*. <https://doi.org/10.1212/WNL.0000000000005333>.
- Raichle, M.E., MacLeod, A.M., Snyder, A.Z., Powers, W.J., Gusnard, D.A., Shulman, G.L., 2001. A default mode of brain function. *Proc. Natl. Acad. Sci. U. S. A.* 98, 676–682. <https://doi.org/10.1073/pnas.98.2.676>.
- Reis, P.M.R., Hebenstreit, F., Gabsteiger, F., von Tscharn, V., Lochmann, M., 2014. Methodological aspects of EEG and body dynamics measurements during motion. *Front. Hum. Neurosci.* 8. <https://doi.org/10.3389/fnhum.2014.00156>.
- Rinne, T., Alho, K., Ilmoniemi, R.J., Virtanen, J., Näätänen, R., 2000. Separate time behaviors of the temporal and frontal mismatch negativity sources. *NeuroImage* 12, 14–19. <https://doi.org/10.1006/nimg.2000.0591>.
- Ruusuvirta, T., Huotilainen, M., Fellman, V., Näätänen, R., 2009. Numerical discrimination in newborn infants as revealed by event-related potentials to tone sequences. *Eur. J. Neurosci.* 30, 1620–1624. <https://doi.org/10.1111/j.1460-9568.2009.06938.x>.
- Schall, U., 2016. Is it time to move mismatch negativity into the clinic? *Biol. Psychol.* 116, 41–46. <https://doi.org/10.1016/j.biopsycho.2015.09.001>.
- Scherg, M., Berg, P., 1991. Use of prior knowledge in brain electromagnetic source analysis. *Brain Topogr.* 4, 143–150. <https://doi.org/10.1007/BF01132771>.
- Schreiber, H., Gaigalat, T., Wiedemuth-Catrinescu, U., Graf, M., Utner, I., Mucic, R., Ludolph, A.C., 2005. Cognitive function in bulbar- and spinal-onset amyotrophic lateral sclerosis. A longitudinal study in 52 patients. *J. Neurol.* 252, 772–781. <https://doi.org/10.1007/s00415-005-0739-6>.
- Schröger, E., 1996. A neural mechanism for involuntary attention shifts to changes in auditory stimulation. *J. Cogn. Neurosci.* 8, 527–539. <https://doi.org/10.1162/jocn.1996.8.6.527>.
- Schuster, C., Hardiman, O., Bede, P., 2016. Development of an automated MRI-based diagnostic protocol for amyotrophic lateral sclerosis using disease-specific pathognomonic features: a quantitative diseases-state classification study. *PLoS One* 11, e0167331. <https://doi.org/10.1371/journal.pone.0167331>.
- Seeley, W.W., Menon, V., Schatzberg, A.F., Keller, J., Glover, G.H., Kenna, H., Reiss, A.L., Greicius, M.D., 2007. Dissociable intrinsic connectivity networks for salience processing and executive control. *J. Neurosci.* 27, 2349–2356. <https://doi.org/10.1523/JNEUROSCI.5587-06.2007>.
- Sorrentino, P., Rucco, R., Jacini, F., Trojsi, F., Lardone, A., Basile, F., Femiano, C., Santangelo, G., Granata, C., Vettoliere, A., Monsurro, M.R., Tedeschi, G., Sorrentino, G., 2018. Brain functional networks become more connected as amyotrophic lateral sclerosis progresses: a source level magnetoencephalographic study. *NeuroImage Clin.* 20, 564–571. <https://doi.org/10.1016/j.nicl.2018.08.001>.
- Swanson, J., 2005. The Delis-Kaplan executive function system: a review. *Can. J. Sch. Psychol.* 20, 117–128. <https://doi.org/10.1177/0829573506295469>.
- Teplan, M., 2002. Fundamentals of EEG measurement. *Meas. Sci. Rev.* 2, 1–11.
- Todd, J., Harms, L., Schall, U., Michie, P.T., 2013. Mismatch negativity: translating the potential. *Front. Psychiatry* 4. <https://doi.org/10.3389/fpsy.2013.00171>.
- Tzourio-Mazoyer, N., Landeau, B., Papathanassiou, D., Crivello, F., Etard, O., Delcroix, N., Mazoyer, B., Joliot, M., 2002. Automated anatomical labelling of activations in SPM using a macroscopic anatomical parcellation of the MNI MRI single-subject brain. *NeuroImage* 15, 273–289. <https://doi.org/10.1006/nimg.2001.0978>.
- Ulanovsky, N., Las, L., Nelken, I., 2003. Processing of low-probability sounds by cortical neurons. *Nat. Neurosci.* 6, 391–398. <https://doi.org/10.1038/nn1032>.
- Van Veen, B.D., van Drongelen, W., Uuchtman, M., Suzuki, A., 1997. Localization of brain electrical activity via linearly constrained minimum variance spatial filtering. *IEEE*

- Trans. Biomed. Eng. 44, 867–880. <https://doi.org/10.1109/10.623056>.
- Vucic, S., Kiernan, M.C., 2006. Novel threshold tracking techniques suggest that cortical hyperexcitability is an early feature of motor neuron disease. *Brain* 129, 2436–2446. <https://doi.org/10.1093/brain/awl172>.
- Welsh, R.C., Jelsone-Swain, L.M., Foerster, B.R., 2013. The utility of independent component analysis and machine learning in the identification of the amyotrophic lateral sclerosis diseased brain. *Front. Hum. Neurosci.* 7, 251. <https://doi.org/10.3389/fnhum.2013.00251>.
- Wendel, K., Väisänen, O., Malmivuo, J., Gencer, N.G., Vanrumste, B., Durka, P., Magjarević, R., Supek, S., Pascu, M.L., Fontenelle, H., de Peralta Menendez, R. Grave, 2009. EEG/MEG source imaging: methods, challenges, and open issues. *Comput. Intell. Neurosci.* <https://doi.org/10.1155/2009/656092>.
- Wijnen, V.J.M., van Boxtel, G.J.M., Eilander, H.J., de Gelder, B., 2007. Mismatch negativity predicts recovery from the vegetative state. *Clin. Neurophysiol.* 118, 597–605. <https://doi.org/10.1016/j.clinph.2006.11.020>.
- Winkler, I., Karmos, G., Näätänen, R., 1996. Adaptive modeling of the unattended acoustic environment reflected in the mismatch negativity event-related potential. *Brain Res.* 742, 239–252.
- Yago, E., Escera, C., Alho, K., Giard, M.H., 2001. Cerebral mechanisms underlying orienting of attention towards auditory frequency changes. *Neuroreport* 12, 2583–2587. <https://doi.org/10.1097/00001756-200108080-00058>.



REVIEW

## Measuring network disruption in neurodegenerative diseases: New approaches using signal analysis

Roisin McMackin,<sup>1</sup> Muthuraman Muthuraman,<sup>2</sup> Sergiu Groppa,<sup>2</sup> Claudio Babiloni,<sup>3,4</sup> John-Paul Taylor,<sup>5</sup> Matthew C Kiernan,<sup>6,7</sup> Bahman Nasserroleslami,<sup>1</sup> Orla Hardiman<sup>1,8</sup>

<sup>1</sup>Academic Unit of Neurology, Trinity College Dublin, the University of Dublin, Dublin, Ireland  
<sup>2</sup>Department of Neurology, Universitätsmedizin der Johannes Gutenberg-Universität Mainz, Mainz, Germany  
<sup>3</sup>Dipartimento di Fisiologia e Farmacologia "Vittorio Erspamer", Università degli Studi di Roma "La Sapienza", Roma, Italy  
<sup>4</sup>Istituto di Ricovero e Cura San Raffaele Cassino, Cassino, Italy  
<sup>5</sup>Institute of Neuroscience, Newcastle University, Newcastle upon Tyne, UK  
<sup>6</sup>Brain & Mind Centre, University of Sydney, Sydney, Australia  
<sup>7</sup>Institute of Clinical Neurosciences, Royal Prince Alfred Hospital, Sydney, Australia  
<sup>8</sup>Beaumont Hospital, Dublin, Ireland

**Correspondence to**  
 Professor Orla Hardiman, Academic Unit of Neurology, Room 5.43, Trinity Biomedical Sciences Institute, 152-160 Pearse Street, Trinity College Dublin, the University of Dublin, Dublin D02 R590, Ireland; hardimao@tcd.ie

Received 23 November 2018  
 Revised 21 January 2019  
 Accepted 21 January 2019



© Author(s) (or their employer(s)) 2019. Re-use permitted under CC BY-NC. No commercial re-use. See rights and permissions. Published by BMJ.

**To cite:** McMackin R, Muthuraman M, Groppa S, et al. *J Neurol Neurosurg Psychiatry* Epub ahead of print: [please include Day Month Year]. doi:10.1136/jnnp-2018-319581

### ABSTRACT

Advanced neuroimaging has increased understanding of the pathogenesis and spread of disease, and offered new therapeutic targets. MRI and positron emission tomography have shown that neurodegenerative diseases including Alzheimer's disease (AD), Lewy body dementia (LBD), Parkinson's disease (PD), frontotemporal dementia (FTD), amyotrophic lateral sclerosis (ALS) and multiple sclerosis (MS) are associated with changes in brain networks. However, the underlying neurophysiological pathways driving pathological processes are poorly defined. The gap between what imaging can discern and underlying pathophysiology can now be addressed by advanced techniques that explore the cortical neural synchronisation, excitability and functional connectivity that underpin cognitive, motor, sensory and other functions. Transcranial magnetic stimulation can show changes in focal excitability in cortical and transcortical motor circuits, while electroencephalography and magnetoencephalography can now record cortical neural synchronisation and connectivity with good temporal and spatial resolution. Here we reflect on the most promising new approaches to measuring network disruption in AD, LBD, PD, FTD, MS, and ALS. We consider the most groundbreaking and clinically promising studies in this field. We outline the limitations of these techniques and how they can be tackled and discuss how these novel approaches can assist in clinical trials by predicting and monitoring progression of neurophysiological changes underpinning clinical symptomatology.

### INTRODUCTION

Neurodegenerative diseases including Alzheimer's disease (AD), Lewy body dementia (LBD), Parkinson's disease (PD), frontotemporal dementia (FTD), amyotrophic lateral sclerosis (ALS) and multiple sclerosis (MS) are associated with reproducible neuropathological signatures of neuronal loss, and in most cases, deposition of specific categories of misfolded proteins in anatomic brain regions that correlate with clinical signs. Definitive diagnostic categorisation is correspondingly generally based on clinicopathological correlation, with evidence of characteristic histological changes within specific anatomic regions of the brain.<sup>1</sup>

There is now, however, emerging evidence that the pathogenesis of neurodegeneration is related to widespread and progressive changes in brain networking. This can be defined both in structural

terms, as patterns of focal and tract neural degeneration,<sup>2</sup> and in functional terms, as altered patterns of brain connectivity and neural<sup>3</sup> and neuromotor<sup>4</sup> transmission.

Structural neuroimaging including MRI has provided additional information about patterns of grey matter atrophy<sup>5</sup> and white matter tract degeneration,<sup>2</sup> while functional MRI and fluoro-deoxyglucose positron emission tomography have provided indirect metabolic correlates of network disruption.<sup>6</sup> These techniques have increased our understanding of the pathogenesis and spread of AD, LBD, PD, FTD, ALS and MS, and have offered new therapeutic targets in clinical trials. However, these approaches cannot directly capture abnormal neural transmissions and networking associated with clinical symptoms. This limitation can now be addressed using advanced quantitative electroencephalography and magnetoencephalography (EEG/MEG) and transcranial magnetic stimulation (TMS).

Application of TMS to the motor cortex paired with target muscle electromyography (EMG) can demonstrate changes in excitability in cortical and transcortical motor circuits and offers excellent temporal and good spatial resolution.<sup>7</sup> By contrast, EEG/MEG has traditionally offered excellent (millisecond) temporal resolution counterbalanced by poor spatial resolution and excessive extracerebral (eg, ocular, head, cardiac) artefacts.<sup>8</sup> However, the use of EEG/MEG recording systems with a montage of many (up to 256) sensors, removal of artefacts from the digitised signals<sup>9</sup> and subsequent application of source localisation methods<sup>10</sup> has substantially increased spatial resolution. Additional quantitative EEG/MEG (qEEG/MEG) methods can now be applied to these high spatial and temporal resolution recordings to generate numerical measures of functional brain activity and functional connectivity between brain areas both at rest<sup>11</sup> and during specified tasks.<sup>12 13</sup>

These technological improvements have opened exciting opportunities in the application of neurophysiological measurements to provide localised, real-time recordings of neural networking abnormalities in neurodegeneration.

Here we have considered the most promising TMS and EEG/MEG measurements used to investigate AD, LBD, PD, FTD, ALS and MS network pathology. We discuss the neuronal basis of these measurements, describe examples of measurements

with potential to enable assessment of early preclinical functional changes associated with neurodegenerative conditions, describe the remaining limitations of these technologies and how they can be developed further as inexpensive and informative biomarkers of clinical subphenotype and disease progression.

### Electroencephalography and magnetoencephalography

Electroencephalography (EEG) and magnetoencephalography (MEG) recordings probe (temporal) synchronisation of cortical neuronal activity using sensors placed on (for EEG) or at small distance from (for MEG) the scalp. While the exact mechanisms of the cortical signal generation remains to be understood, there is evidence that scalp-recorded EEG/MEG signals reflect the spatial summation of relatively long-lasting (ten to hundreds of milliseconds) excitatory/inhibitory post-synaptic potentials and dendritic influences of neurons (e.g. the cortical pyramidal neurons), summed together in adjacent regions.<sup>14</sup> In addition to these post-synaptic potentials the EEG/MEG oscillations also originate from the flow of the activity volleys in the longer-range pathways such as thalamo-cortical connections and loops.<sup>15,16</sup> While the fast spiking activity of the cortical neurons are not usually considered to be reflected in EEG/MEG signals due to poor spatial summation processes at a given instant, there is evidence that such activities may also appear at higher EEG/MEG frequencies in the high gamma band (>40 Hz).<sup>17</sup>

EEG can capture activity in cortical sources oriented both tangentially and radially to the scalp surface due to the electric field propagation and electrical conduction in the volume. However, the signals are attenuated by propagation of electric currents through regions of the head with different resistance. By contrast, while MEG signals are captured exclusively by cortical sources oriented tangentially to the scalp surface due to magnetic field propagation, they are not affected by the propagation of electric currents through head tissues with different resistance.<sup>13</sup>

Two main classes of EEG/MEG signals can be derived from experimental recordings. The first class is event-related with most frequent applications developed in time domain. Within this line are evoked or event-related potentials (EPs/ERPs) and the MEG counterparts, evoked or event-related magnetic fields (EFs/ERFs). EPs/ERFs are obtained by the average of hundreds/thousands of short EEG/MEG periods (ten to several hundreds of milliseconds) of activity recorded during repeated sensory stimuli (eg, visual, auditory) with no response required.<sup>18</sup> Likewise, ERPs/ERFs are obtained by the average of many EEG/MEG periods (ten to several hundreds of milliseconds) of activity, however, they are recorded during repeated sensory stimuli and/or voluntary tasks associated with cognitive processes and usually a behavioural response.<sup>19</sup> The analysis of those potentials is typically performed in the time domain, investigating latency and amplitude of a sequence of EEG voltage or magnetic field peaks and the underlying cortical source activity. However, more recent applications are developed by a spectral analysis of oscillatory components at delta, theta, alpha, beta and gamma bands from EPs/ERFs and ERPs/ERFs.<sup>20</sup> Finally, less frequent in the field of neurodegenerative diseases, ongoing EEG and MEG rhythms related to sensory and cognitive motor events are analysed with spectral analysis as “event-related desynchronisation/synchronisation” of those frequency bands.<sup>21</sup>

The second class is that of “resting-state” EEG/MEG signals collected in the absence of event, typically analysed in frequency domain (figure 1). This analysis can be performed by linear (eg, discrete Fourier transformation) or nonlinear techniques to quantify brain neural oscillatory activity<sup>22</sup> in terms of peak frequency,

magnitude (eg, power density) and phase, either at sensory or brain source level. Statistical interrelatedness of cortical sources of EEG/MEG signals provides useful information about functional brain connectivity at rest (figure 1) underpinning vigilance, wake-sleep cycle and cognitive functions.<sup>23</sup> A key benefit of such spectral frequency analysis, particularly at source level, is the ability to relate specific changes in oscillatory EEG/MEG activity (and relative cortical sources) at a given frequency band to specific brain regions, higher functions or neuropathological processes affecting neural or neuromotor transmission.<sup>3,24</sup>

Until recently EEG/MEG recordings have been limited by relatively poor signal-to-noise ratio, excessive artefactual components and low spatial resolution due to a low number of sensors available in acquisition systems.<sup>8</sup> Those limitations have now been addressed by advanced technologies. Careful application of blind source separation, independent component analyses, and non-parametric statistics<sup>25</sup> have now dramatically reduced the level of noise and artefact in the EEG/MEG signals. Additionally, advances in cortical source localisation methods, including low resolution electromagnetic brain tomography, and beamforming have improved the accuracy in source estimation of EEG/MEG signals (figure 2),<sup>40</sup> providing complementary measurements to those derived from functional neuroimaging based on MRI. As a result, abnormalities in such signals due to brain neurodegenerative diseases may be attributed to activation and connectivity in specific cortical (and subcortical) regions.<sup>12,13,24</sup>

### Transcranial magnetic stimulation

With the development of coil designs with high focality<sup>7</sup> and ‘threshold tracking’ methods which provide excellent intra- and inter-day reproducibility,<sup>26</sup> TMS can now provide robust measures of function in a variety of cortical network components.

By delivering magnetic stimuli to the motor cortex, TMS can invoke muscle responses which are measured by EMG. These responses (motor evoked potentials; MEPs) primarily originate from the activation of the upper motor neurons and related cortical interneurons. The descending pathways activate spinal cord networks including lower motor neurons’ connections to associated muscles. The MEP in the target muscles can provide information about the integrity of the corticospinal tract. This is quantified by measures such as the minimum stimulation intensity required to achieve a target MEP amplitude known as motor threshold (figure 3).<sup>27</sup>

TMS can also be used to interrogate additional motor pathways of the brain. The use of precisely-timed ‘conditioning’ magnetic or electrical pulses can activate network components such as interneurons. Measures including short intracortical inhibition (SICI)/long intracortical inhibition (LICI), intracortical-facilitation (ICF), interhemispheric inhibition and facilitation, and short afferent inhibition (SAI)/long afferent inhibition (LAI) can quantify the dysfunction of interneuronal<sup>28</sup> and callosal<sup>29</sup> network components and sensorimotor connections,<sup>30</sup> generating inferences about the excitatory/inhibitory balance across cortical structures and neurotransmitter (e.g. glutamatergic, GABAergic, monoaminergic) function.<sup>31</sup> This technology has already been commercialised for use in diagnostics and clinical outcome measures for neuromuscular disorders.<sup>27</sup>

TMS has other utilities in interrogating cortical network excitability. Conditioning sub- and supra-threshold stimuli over non-primary motor areas, such as the supplementary motor areas, premotor cortices, dorsolateral prefrontal or posterior parietal regions can reveal the connectivity of these regions to the primary motor cortices and the other brain areas.<sup>32</sup> In this

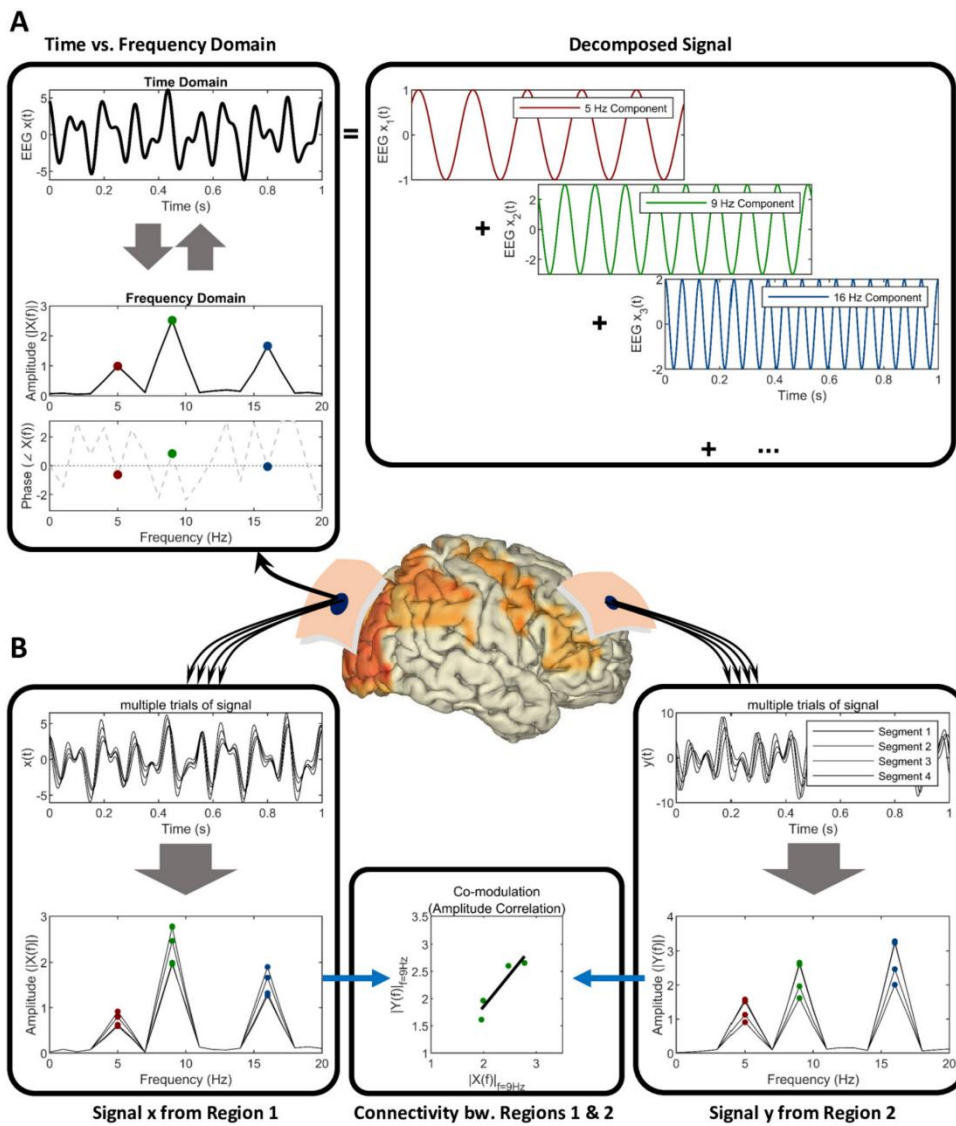


**Figure 1** Schematic of (A) time versus frequency domain representation of electromagnetic neural signals and (B) spectral connectivity between signals from two brain regions. (A) The representation of an exemplary segment of signal as a combination of sinusoidal waveforms. The strengths or amplitudes of the sinusoidal components together with their phase information constitute the frequency domain (spectral) representation of the signal. (B) Multiple epochs, trials or segments of data corresponding to two brain regions can be assessed in specific frequencies to infer and quantify the connectivity.

way, modern TMS can serve much beyond a test for conduction velocity and excitability, but as measures of the integrity and functional connectivity between several cortical regions.<sup>27</sup>

**Interrogation of functional networks in clinical disorders**  
Abnormal brain network function can now be usefully investigated

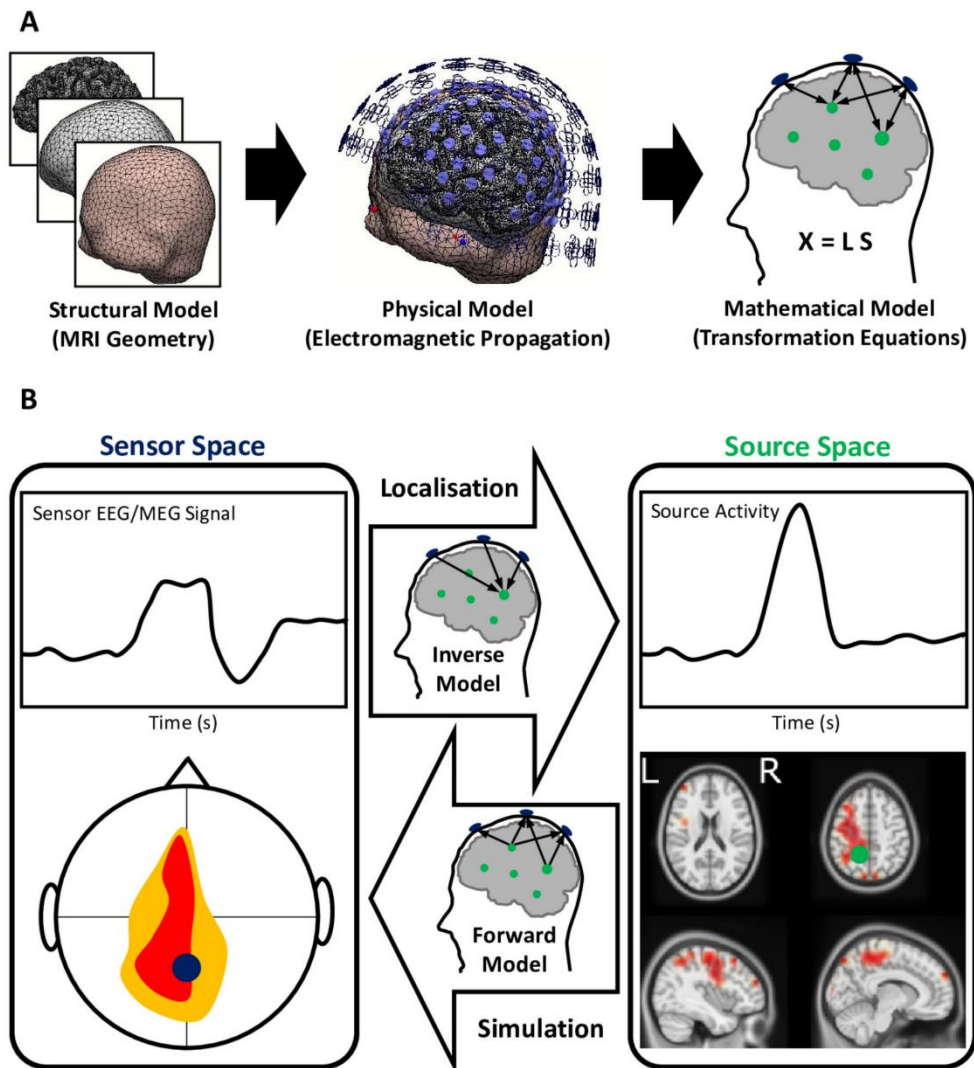


**Figure 2** Electromagnetic source imaging using electroencephalography and magnetoencephalography (EEG/MEG) source localisation (A) building models of source and sensor activity and (B) forward versus inverse transformation of signals between the sensors and brain sources. (A) MRI geometry is used for developing structural models of the brain, corticospinal fluid and scalp (among many layers) that are in-between the brain sources generating the neuroelectric activity and electrodes/sensors. The structural model when used together with physical electromagnetic properties of the tissue materials and the governing equations of electromagnetic propagation forms a physical model. The physical model is solved and formulated for the discrete finite number of the modelled sources of activity in the brain (usually about thousands), as well as the EEG/MEG sensors used during the data acquisition (usually a few hundreds). The mathematical model  $X=LS$  is a multivariate relationship between the sensor activity ( $X$ ), source activity ( $S$ ) and the mathematical model ( $L$ ). (B) This mathematical model can forward-transform the simulated source activities to the sensors, as well as project the recorded sensor activity to localise the underlying brain sources using the constructed inverse model.

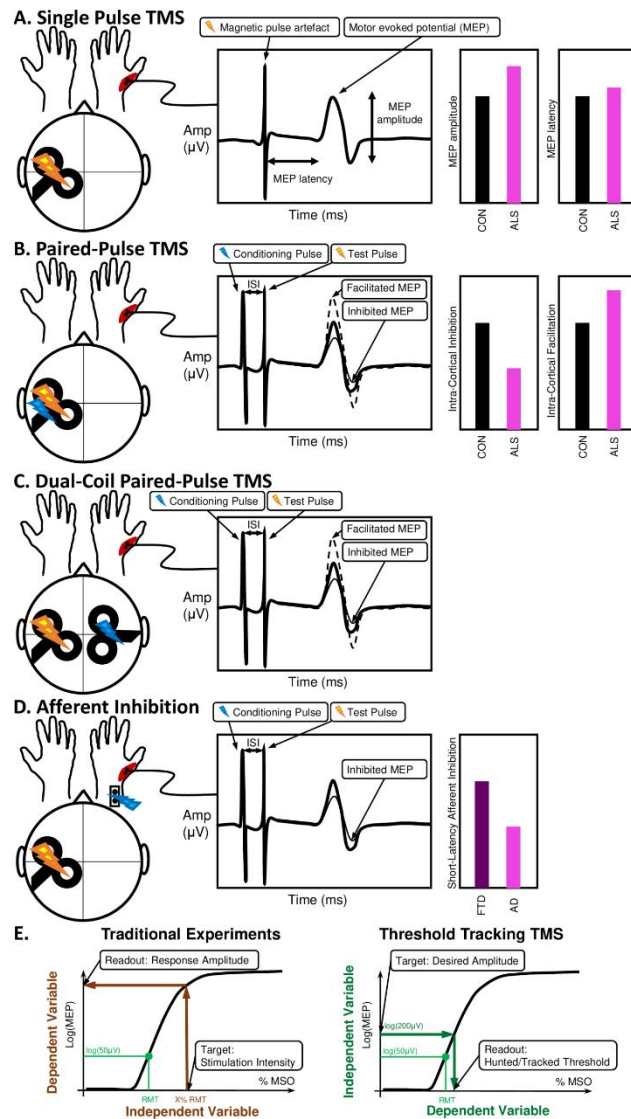


**Figure 3** Transcranial magnetic stimulation (TMS) can provide: (A) single-pulse measures, (B) paired-pulse measures, (C) dual-coil paired pulse measures and (D) afferent inhibition measures that when combined with (E) threshold tracking can quantify network connectivity changes in the motor system. The test pulse generates a motor evoked potential (MEP) whose delay and amplitude can be used for quantifying the excitability and conduction in the motor circuits and pathways. This is usually achieved by conditioning the MEP with sub-maximal or supra-maximal conditioning pulses delivered at specific interstimulus intervals before the main test pulse (either in the same brain region with the same coil, over another brain region with a second coil or by peripheral nerve stimulation). This conditioning may facilitate or inhibit the MEP, depending on the (inter-)neuronal populations engaged in each paradigm, the ISI and stimulation intensities or thresholds used. These measures have been proved useful for diagnosis and response prediction in neurodegeneration, eg, in ALS<sup>9</sup> and AD.<sup>30</sup> The threshold tracking method is used to achieve a less variable quantification of the stimulus-response characteristics by targeting a specific desired amplitude rather than a specific stimulation intensity. AD, Alzheimer’s disease; ALS, amyotrophic lateral sclerosis; MSO, maximum stimulator output; ISI, inter-stimulus interval.



**Table 1** Established neurophysiological changes in neurodegeneration, their clinical utility and discrimination ability

Neurodegeneration	Method	Neurophysiological change	Clinical application	Discrimination statistics	References
Alzheimer's disease Dementia with Lewy bodies	EEG/ MEG	▶ ↓ Posterior $\alpha$ power ▶ ↑ Parietal $\delta$ and $\theta$ power	▶ Prodromal differential diagnosis ▶ Diagnostic biomarker ▶ Differential diagnosis of AD and DLB	▶ Sensitivity – 78.3% ▶ Specificity – 66.7% ▶ AUROC – 72% ▶ AUROC=0.97 (log $\delta$ ) and 0.93 (log $\theta$ ) ▶ AUROC=0.879 (log $\delta$ ) and 0.75 (log $\theta$ )	Andersson <i>et al</i> , Babiloni <i>et al</i> <sup>43</sup>
Frontotemporal dementia	EEG	▶ Combined 25 rsEEG measures	▶ Differential diagnosis between ADD, PDD, DLB and bvFTD	▶ AUROC=100% ▶ Specificity=100% ▶ Selectivity=100%	Garn <i>et al</i> <sup>65</sup>
Parkinson's disease	EEG	▶ ↑ $\beta$ power ▶ ↑300 Hz power	▶ Differential diagnosis ▶ Thresholding of DBS ▶ CT antikinetic measure ▶ CT prokinetic outcome measure	▶ To be determined.	Assenza <i>et al</i> , Little <i>et al</i> , Muthuraman <i>et al</i> , Assenza <i>et al</i> <sup>49,52</sup>
Amyotrophic lateral sclerosis	TMS	▶ ↓Short intracortical inhibition	▶ Differential diagnosis from mimic disorders ▶ Prodromal biomarker ▶ CT outcome measure	▶ Sensitivity - 73.21% ▶ Specificity - 80.88%	Vucic <i>et al</i> , Menon <i>et al</i> , NCT02450552, NCT02781454 <sup>28</sup>
Multiple sclerosis	EEG +TMS	▶ Multimodal ERPs	▶ Prognosis ▶ CT outcome measure	▶ Sensitivity - 56.7% ▶ Specificity - 88.3% ▶ Positive predictive value - 70.8 %	Giffroy <i>et al</i> , NCT01765361 <sup>18</sup>

ADD, Alzheimer's disease dementia; AUROC, area under the receiver operating characteristics curve; CT, clinical trial; DLB, dementia with Lewy bodies; ERP, event-related potential; PDD, Parkinson's disease dementia; bvFTD, behavioural variant frontotemporal dementia; rsEEG, resting state electroencephalography.

by neurophysiological approaches based on EEG/MEG signals and signals from TMS-linked EMG. These measures are particularly helpful in quantifying signature changes in specific brain regions and in detecting patterns of abnormal communication between them. Recognising and defining these patterns can thus inform both the nature of the network impairment in neurodegeneration and its progression over time. They can also proffer quantitative biomarkers of these syndromes to improve diagnosis, differential diagnosis, prognosis and therapeutic testing (table 1). The combination of advanced neurophysiological measures into multidimensional markers can further assist in distinguishing neurodegenerative conditions (eg, AD vs FTD<sup>33</sup>) whose affected networks overlap, but also differ. Substantial progress has already been made in these areas, as outlined below for each of the major neurodegenerative conditions.

#### Mild cognitive impairment and dementias

Alzheimer's disease dementia (AD) accounts for 50%–75% of dementias, while dementia with Lewy bodies (DLB) accounts for an additional 10%–20%<sup>34</sup> of all dementias.

Candidate biomarkers of AD and DLB at clinical (dementia) or prodromal (mild cognitive impairment: MCI) stages have been generated using frequency domain spectral analysis from eyes-closed resting state (rs) EEG/MEG.<sup>35</sup> Such rsEEG/rsMEG markers are cost-effective, non-invasive, suitable in cognitively/physically disabled patients and not susceptible to learning effects. Resting state cortical delta and alpha rhythms in particular reveal compromised network synchronisation and connectivity in AD, Parkinson's disease with dementia (PDD), and DLB at both group and individual levels.<sup>36,37</sup>

Impaired cortical neural synchronisation in AD and DLB is quantified by reduced posterior cortical alpha (8–12 Hz) and beta (13–30 Hz) rsEEG rhythm intensity and diffuse increases in the intensity of cortical delta (<4 Hz) and theta (4–7 Hz) oscillations.<sup>38</sup> These patterns are more marked in DLB.<sup>36</sup> Reduced cortical alpha is also found in PDD but to a lesser degree, while

widespread theta rhythms are greater in PDD than ADD.<sup>37</sup> These rsEEG findings have been cross-validated by rsMEG.<sup>39–41</sup>

The clinical importance of these measures is reflected in their presence in MCI stages of degeneration,<sup>42</sup> their ability to predict progression from MCI to dementia<sup>38</sup> and their power to discriminate between dementias<sup>36</sup> and prodromal MCIs<sup>43</sup> (table 1).

Spectral coherence provides information about cortical network connectivity, which reflects the functional coordination of neural activity. Coherence quantifies the temporal relationship of oscillations in different areas of the brain. This can be measured from rsEEG/rsMEG signals at sensor and cortical source level. In AD, rsEEG coherence is consistently reduced in alpha rhythms. Inconsistent abnormalities in coherence have been reported between electrode pairs in delta and theta rhythms.<sup>38</sup>

These techniques are already in development to measure decline in cognitive status in ADMCI<sup>44</sup> using progressive decrement in frontoparietal alpha rhythm synchronisation. These advances demonstrate the utility of neurophysiologic instruments as non-invasive quantitative biomarkers of clinical progression in early AD.

#### Parkinson's disease

Parkinson's disease (PD) is characterised by progressive degeneration of dopaminergic neurons of the substantia nigra pars compacta (SNpc).<sup>45</sup> The high spatial resolution conferred by source localisation of EEG has established that PD network pathology also extends beyond the basal ganglia, including premotor, supplementary motor regions and cerebellar sources.<sup>12</sup>

Degeneration of the SNpc in PD prevents the intricate basal ganglia network of feedforward and feedback loops which regulate cortical motor output.<sup>45</sup> The dysfunction of this network is captured using spectral EEG by an increase in basal ganglia-cortical beta power, as these oscillations represent the probability of a voluntary movement.<sup>46</sup> Beta oscillations increase longitudinally<sup>47</sup> and differentiate PD from trends in dementia and

stroke.<sup>48</sup> Causation between these oscillations and PD motor symptoms has been established using deep brain stimulation (DBS), as stimulation at 5–20 Hz (but not 30–50 Hz) exacerbates bradykinesia. By contrast, levodopa and DBS of the subthalamic nucleus reduce beta power, correlating with a therapeutic effects on bradykinesia and rigidity.<sup>46,49</sup> Levodopa and apomorphine treatment also elicits high gamma (300 Hz) oscillations. This prokinetic switch from low to high frequency oscillation suggests a clinical utility for excitatory DBS in addition to current inhibitory protocol.<sup>48</sup>

In PD, TMS can detect a reduction in resting motor threshold (RMT) that correlates with poorer Unified Parkinson's Disease Rating Scale motor score, indicative of pathological corticospinal hyperexcitability.<sup>50</sup> Additional TMS studies demonstrate reduced SICI and increased ICF in the off state of PD, pointing to additional abnormalities in intracortical inhibitory and facilitatory cortical network activity<sup>51</sup> as drivers of motor hyperexcitability.

These neurophysiologic measures not only provide information about location and nature of PD pathology, but are also important as potential clinical biomarkers. For example, change in subthalamic nucleus beta power can be used to determine the parameters for closed-loop DBS. Stimulation when beta oscillations rise above a threshold is found to provide better therapeutic effect than continuous or random-intermittent delivery of DBS.<sup>52</sup>

Although further studies are required to determine the diagnostic accuracy and longitudinal change of single and combined rsEEG measures in PD, existing TMS, MEG and EEG based evidence has already pointed to the utility of advanced neurophysiological tools as quantitative measures of networks dysfunction.

#### Frontotemporal dementia

The well-established dysfunction of prefrontal and temporal networks in FTD can be discriminated by spectral EEG measures, providing a basis for the use of EEG in developing quantitative FTD biomarkers. For example, intrahemispheric information sharing is significantly lower between frontal and temporal areas in behavioural variant FTD (bvFTD).<sup>53</sup> Source localisation of EEG further demonstrates changes in the orbitofrontal and temporal cortices with enhanced spatial resolution.<sup>54</sup> While such measures individually have not demonstrated sufficient specificity for use as diagnostic biomarkers alone, the combination of spectral and behavioural measures can reliably discriminate FTD from other types of dementia. For example, a logistic regression model of delta and theta oscillatory activity, combined with cognitive task performance, has demonstrated 93.3% classification accuracy in differentiating AD and FTD patients.<sup>53</sup> A separate study, combining neuropsychological parameters with frontoparietal and frontotemporal EEG functional connectivity measures from multiple electrodes, similarly achieved an 87.4% accuracy in discriminating bvFTD patients from controls.<sup>53</sup>

A recent study expanded this approach, using 25 EEG parameters to train support vector machine classifiers to distinguish between AD, PD or LBD and bvFTD, such that 100% specificity, sensitivity and accuracy was achieved.<sup>55</sup>

The use of such parameters in differential diagnosis has also recently been expanded beyond the dementias, to explore the differentiation of psychiatric and neurodegenerative disorders which overlap clinically. For example, a combination of EEG and imaging parameters has demonstrated 87% accuracy in differentiation of FTD from late-onset bipolar disorder which have overlapping behavioural symptoms.<sup>56</sup> Such

distinction based on network pathology may assist in distinction of solely psychiatric disorders from early manifestations of neurodegeneration.<sup>57</sup>

#### Amyotrophic lateral sclerosis

Amyotrophic lateral sclerosis (ALS) is characterised by progressive degeneration of upper and lower motor neurons.<sup>58</sup> Diagnostic delays of up to 15 months from symptom onset are common in ALS. Access to clinical trials at an early stage of disease is accordingly compromised.<sup>59</sup>

Quantitative measures of brain network dysfunction have the capacity to reduce diagnostic delay and improve diagnostic accuracy. However, while imaging and physiological studies have demonstrated broader patterns of atrophy across ALS, such as in the thalamus,<sup>60</sup> basal ganglia<sup>5</sup> and prefrontal cortex,<sup>61,62</sup> resting state EEG/MEG in ALS can reliably identify increases in intra- and inter-motor cortical functional connectivity.<sup>3,24</sup> This finding is consistent with evidence of motor hyperexcitability as defined by threshold tracking TMS in ALS.

Using TMS, hyperexcitability in ALS is quantified by reduced motor threshold, a measure of corticospinal excitability. SICI, a measure of GABAergic interneuron function, is also consistently reduced in ALS, implying loss of inhibition as a source of network hyperexcitability.<sup>63</sup> This decrease in SICI can distinguish ALS from mimic neuromuscular syndromes with 73–21% sensitivity and 80–88% specificity.<sup>28</sup> Decreased SICI may also be present pre-symptomatically,<sup>4</sup> providing a prodromal biomarker.

The most common extra-motor impairment in ALS is executive dysfunction, occurring in up to 50% of patients.<sup>64,65</sup> In addition to the existence of cognitively impaired (and non-impaired) patient groups<sup>64</sup> the existence of cognitive ALS subphenotypes is supported by a 14.3% genetic correlation between schizophrenia<sup>66</sup> and ALS and the increased risk of psychiatric disorders, FTD and ALS conveyed by *C9orf72* expansions.<sup>67</sup>

Biomarkers of such cognitive network impairment are urgently required for early discrimination of this subphenotype, in addition to providing outcome measures for cognition-targeting clinical trials. As cognitive impairment in ALS correlates with poorer prognosis,<sup>64</sup> subphenotyping based on domains of network impairment has the potential to improve early prognostic accuracy and facilitate recruitment to cognition-targeted therapeutic trials.

Promising work using cognitive ERPs can capture millisecond-by-millisecond differences in executive network activity. Application of quantitative EEG analysis of ERP in ALS patients has shown increased average delay in the mismatch negativity ERP, a measure of involuntary attention switching. This correlates to Stroop task performance, a psychological test of inhibitory control and attention shifting.<sup>19</sup> On source localisation of this EEG signal it is revealed that during this task ALS patients demonstrate excessive left frontoparietal activity which correlates with poorer inhibitory control, in addition to decreased bilateral inferior frontal activity.<sup>12</sup> Such measures have the advantage of providing an objective and quantitative biomarkers of cognitive network dysfunction that are not biased by learning effects or physical disability.

As demonstrated for dementias, combination of such measures of motor, cognitive and broader network dysfunction could further enhance discrimination ability from mimic neuromuscular disorders, providing a non-invasive, low-cost, multidimensional biomarker of ALS, in addition to characterising ALS subphenotypes.

**Multiple sclerosis**

Multiple sclerosis (MS) is a disorder characterised by foci of inflammation and demyelination through the central nervous system, leading to axon loss and grey matter generation<sup>68</sup> with clinical evidence of progressive neurodegeneration. The clinical use of somatosensory, motor and visual evoked potentials to document silent and manifest lesions in MS was commonplace before replacement with MRI scanning.<sup>69</sup>

Neurophysiological tools are now used to objectively characterise connectivity by MEG and EEG measures, such as resting-state network microstate activity measures, which predict total disease duration, annual relapse rate, disability score, depression score and cognitive fatigue measures in relapse-remitting MS.<sup>70</sup>

Advances in event-related EEG/MEG parameters has also captured specific network dysfunction underlying fatigue in MS, with increased P100 visual ERP latency correlating with visual fatigue scores and increased latency in the V component of brainstem auditory ERPs correlating with brainstem fatigue scores.<sup>71</sup> Changes in TMS-evoked motor potentials and central-motor conduction time also show strong correlation to disability score.<sup>72</sup>

These TMS and EEG parameters are now re-emerging as important MS biomarkers, with the realisation that MRI measures can show weak association with clinical presentation, known as the clinical/MRI paradox.<sup>73</sup> A combination of electrophysiological parameters, labelled the 'global evoked potential' score, predicts both annual disability score progression and risk of disability progression and a cut-off has been defined to detect patients at high risk of disability progression at a predictive value of 70%.<sup>18</sup>

**Neurophysiologic signal analysis as biomarkers and outcome measures in clinical trials**

For diagnostic biomarkers, mathematically-defined combinations of neurophysiology based network measures are likely to evolve over the coming years. For *prognostic and stratification* biomarkers, however, the neurophysiological validity and relevance of the network activity is the priority to assure meaningful interpretations.

Standardisation of biomarkers based on neural signals is already well advanced for neuropsychiatric disorders,<sup>74–75</sup> but have not yet been used consistently in neurodegenerative conditions, despite the acknowledged biological overlap between conditions such as ALS and schizophrenia.<sup>66</sup> Biomarker development in neurodegeneration is promising, although verification and validation of the sensitivity and specificity reported for these biomarkers (table 1) will be required within each neurodegenerative disease.

The clinical utility of EEG in resting-state has already been used as a pharmacodynamic marker in a dose-finding study in rodents, and has been successfully translated to a human study of an antidepressant compound.<sup>76</sup> Similarly, a recent retigabine trial in ALS has used the decrease in SICI as a recruitment criterion (NCT02450552) while a trial of mexiletine (NCT02781454) is now using change in RMT and SICI as primary and secondary outcome measures respectively. SAI has also shown promise as a predictor of cholinesterase inhibitor response in AD,<sup>30</sup> warranting further investigation as an electrophysiological outcome measure.

Resting-state EEG has also been utilised as a secondary outcome measure in testing the nutritional aid Souvenaid as a therapy in AD, with change in delta band functional connectivity

showing improved trajectory.<sup>77</sup> A combination of multimodal evoked potentials was also used as an outcome measure in a phase III trial (NCT01765361) of the recently approved drug ocrelizumab for MS.

These early studies point to a move towards therapies based on modulation of network dysfunction, allowing for earlier, and possibly presymptomatic intervention based on early changes in physiological measures.<sup>4</sup>

**CURRENT LIMITATIONS**

While consistent changes in electrophysiological measures have been identified in some neurodegenerative diseases (such as increased beta power in PD<sup>48–49–53</sup>), others require further evaluation and validation (eg, increased motor threshold in Huntington's disease or decreased motor threshold in PD<sup>78</sup>). Furthermore, while single measures may for some diseases provide sufficient specificity and selectivity for diagnosis, such as SICI in ALS,<sup>4–28–63</sup> this has yet to be achieved for other diseases such as AD.<sup>79</sup> In the longer term, it is likely that combinations of multiple measures (including neurophysiological, behavioural and neuroimaging) will be required to capture broader patterns of network disruption. Individual measures are more likely to provide tools for differential diagnosis to enhance patient stratification and provide quantitative measures in clinical trials.<sup>79</sup> Going forward, large multicentre studies will be required to validate all individual and multidimensional physiological measures for use in routine clinical settings.

**CONCLUSION AND FUTURE DIRECTIONS**

The use of physiological methods such as EEG, MEG and TMS permits the interrogation of network function with excellent temporal resolution. These methods are non-invasive, do not depend on intact motor or language function or participant engagement, and are substantially lower in cost, compared with neuroimaging alternatives using MRI or positron emission tomography. With the evolution of EEG/MEG recording techniques, improved preliminary data processing, source estimation techniques and focal TMS coils, the perceived limitations of excess noise and poor spatial resolution have been substantially reduced. As a result, the location, nature and overlap of cortical neural network disruption in the brain neurodegenerative diseases can be directly measured and quantified as a readout reflecting cortical neural excitability, synchronisation and connectivity as relevant underpinning of cognitive and sensorimotor functions.

While underutilised in multicentric clinical trials testing disease-modifying drugs for major neurodegenerative diseases to date, these improved quantitative neurophysiological measures have enhanced the state-of-the-art in clinical neurophysiology research. They have shown that neurodegenerative diseases affect the cortical neural excitability, synchronisation and functional connectivity in relation to cognitive, sensory and motor impairment in AD, DLB, PD, FTD, ALS and MS patients. Future longitudinal, harmonised, multi-centre, cross-validation studies will provide a non-invasive quantification of cortical neural network disruption in the neurodegenerative diseases and can provide neurophysiological predictors of clinical trajectories and correlates of disease progression.

Important future directions will also include the application of such biomarkers for earlier and possibly pre-symptomatic intervention, enhancing the probability of therapeutic success; and the development of physiological parameters as objective, numerical outcome measures that provide sensitive non-invasive

and cost effective tools for detecting therapeutic effects of new medicinal compounds.

### SELECTION CRITERIA

References were accessed using the NCBI Pubmed, Embase and Web of Science databases.

Search criteria used for review of each neurodegenerative disease included combination of methodology terms (“EEG”, “evoked potential”, “event related potential”, “MEG”, “transcranial magnetic stimulation”, “TMS”, “deep brain stimulation”) with disease name terms (“Alzheimers”, “Parkinsons”, “Parkinsonism”, “frontotemporal dementia”, “amyotrophic lateral sclerosis”, “multiple sclerosis”, “Lewy bodies”) in the previous 15 years 2003 to 2018. Papers were chosen so as to highlight those with the best methodology (number of subjects and patients, diagnosis based on biomarkers in line with the international Guidelines, use of advanced EEG/MEG/TMS techniques at the state-of-the art, research groups with high reputation) investigating physiological measures with potential clinical utility. The number of papers accessed per database, search criterion and disease reviewed, is summarised in online supplementary table 1.

Reviews highlighting the limitations of the methods reviewed in the clinical application were also discussed to provide counter-information in order to minimise potential bias. Search criteria for review of the remaining limitations included combination of methodology terms (“EEG”, “MEG”, “transcranial magnetic stimulation”, “TMS”) with the word “problem” or “limitations” and “neurodegenerative” in the previous 5 years 2013 to 2018, so as to restrict review of these limitations to those applicable to the current state of the art.

**Contributors** OH planned the review, convened the expert group, oversaw the project development and had final editorial oversight of the manuscript. OH and RM wrote the introduction, limitations and conclusions. BN, MM, SG and RM wrote the methodology section. All authors reviewed and reported on neurodegenerative disease literature. BN composed the figures. RM composed the tables. All authors edited and revised the manuscript prior to submission. OH and RM submitted the study.

**Funding** OH, BN and RM were supported by the Irish Health Research Board [grant numbers: EIA-2017-019, HRB-MRCG-2018-02, HRB-JPND-2017-1], Science Foundation Ireland [grant number: 16/ERC/D/3854], the Irish Research Council [grant numbers: GOIPG/2017/1014, GOIPD/2015/213], the American ALS Association [grant number: ALS18-CM-396] and Research Motor Neurone. JPT was supported by the National Institute for Health Research (NIHR), Newcastle Biomedical Research Centre based at Newcastle upon Tyne Hospitals NHS Foundation Trust and Newcastle University. The views expressed are those of the authors and not necessarily those of the NHS, the NIHR or the Department of Health. MM and SG were supported by Transregional Collaborative Research Center (CRC) SFB TR-128. MCK was supported by the National Health and Medical Research Council of Australia Program Grant [grant number: 1132524] and Practitioner Fellowship [grant number: 1156093]. Funding sources had no involvement in the writing of this review.

**Competing interests** OH receives personal fees from Taylor and Francis, Cytokinetics and Wave Pharmaceuticals, outside the submitted work.

**Patient consent for publication** Not required.

**Provenance and peer review** Commissioned; externally peer reviewed.

**Open access** This is an open access article distributed in accordance with the Creative Commons Attribution Non Commercial (CC BY-NC 4.0) license, which permits others to distribute, remix, adapt, build upon this work non-commercially, and license their derivative works on different terms, provided the original work is properly cited, appropriate credit is given, any changes made indicated, and the use is non-commercial. See: <http://creativecommons.org/licenses/by-nc/4.0/>.

### REFERENCES

- Love S. Post mortem sampling of the brain and other tissues in neurodegenerative disease. *Histopathol* 2004;44:309–17.
- Müller H-P, Kassubek J. Diffusion tensor magnetic resonance imaging in the analysis of neurodegenerative diseases. *JoVE* (77).

- Nasserollesami B, Dukic S, Broderick M, et al. Characteristic increases in EEG connectivity correlate with changes of structural MRI in amyotrophic lateral sclerosis. *Cereb Cortex* 2017;1–15.
- Vucic S, Nicholson GA, Kiernan MC. Cortical hyperexcitability may precede the onset of familial amyotrophic lateral sclerosis. *Brain* 2008;131:1540–50.
- Bede P, Elamin M, Byrne S, et al. Basal ganglia involvement in amyotrophic lateral sclerosis. *Neurology* 2013;81:2107–15.
- Kepler JS, Conti PS. A cost analysis of positron emission tomography. *AJR Am J Roentgenol* 2001;177:31–40.
- Ueno S, Matsuda T, Fujiki M. Functional mapping of the human motor cortex obtained by focal and vectorial magnetic stimulation of the brain. *IEEE Trans Magn* 1990;26:1539–44.
- Reis PM, Hebenstreit F, Gabsteiger F, et al. Methodological aspects of EEG and body dynamics measurements during motion. *Front Hum Neurosci* 2014;8.
- Mognon A, Jovicich J, Bruzzone L, et al. Adjust: an automatic EEG artifact detector based on the joint use of spatial and temporal features. *Psychophysiology* 2011;48:229–40.
- Darvas F, Pantazis D, Kucukaltun-Yildirim E, et al. Mapping human brain function with MEG and EEG: methods and validation. *Neuroimage* 2004;23(Suppl 1):S289–S299.
- Muthuraman M, Raethjen J, Koirala N, et al. Cerebello-cortical network fingerprints differ between essential, Parkinson's and mimicked tremors. *Brain* 2018;141:1770–81.
- McMackin R, Dukic S, Broderick M, et al. Dysfunction of attention switching networks in amyotrophic lateral sclerosis. *Neuroimage Clin* 2019;22.
- Muthuraman M, Hellriegel H, Hoogenboom N, et al. Beamformer source analysis and connectivity on concurrent EEG and MEG data during voluntary movements. *PLoS One* 2014;9:e91441.
- Murakami S, Okada Y. Contributions of principal neocortical neurons to magnetoencephalography and electroencephalography signals. *J Physiol* 2006;575:925–36.
- Neuper C, Klimesch W. *Event-related dynamics of brain oscillations*. Elsevier, 2006.
- Vuckovic A, Hasan MA, Osuagwu B, et al. The influence of central neuropathic pain in paraplegic patients on performance of a motor imagery based brain computer interface. *Clin Neurophysiol* 2015;126:2170–80.
- Telenczuk B, Baker SN, Kempter R, et al. Correlates of a single cortical action potential in the epidural EEG. *Neuroimage* 2015;109:357–67.
- Giffroy X, Maes N, Albert A, et al. Multimodal evoked potentials for functional quantification and prognosis in multiple sclerosis. *BMC Neurol* 2016;16.
- Iyer PM, Mohr K, Broderick M, et al. Mismatch negativity as an indicator of cognitive sub-domain dysfunction in amyotrophic lateral sclerosis. *Front Neurol* 2017;8.
- Başar E, Femir B, Emek-Savaş DD, et al. Increased long distance event-related gamma band connectivity in Alzheimer's disease. *Neuroimage Clin* 2017;14:580–90.
- Graimann B, Pfurtscheller G. Quantification and visualization of event-related changes in oscillatory brain activity in the time–frequency domain. In: Neuper C, Klimesch W, eds. *Progress in brain research*. Elsevier, 2006: 79–97.
- Siegel M, Donner TH, Engel AK. Spectral fingerprints of large-scale neuronal interactions. *Nat Rev Neurosci* 2012;13:121–34.
- van Diessen E, Numan T, van Dellen E, et al. Opportunities and methodological challenges in EEG and MEG resting state functional brain network research. *Clin Neurophysiol* 2015;126:1468–81.
- Proudford M, Colclough GL, Quinn A, et al. Increased cerebral functional connectivity in ALS: a resting-state magnetoencephalography study. *Neurology* 2018;90.
- Dukic S, Iyer PM, Mohr K, et al. Estimation of coherence using the median is robust against EEG artefacts. *Conf Proc IEEE Eng Med Biol Soc* 2017;2017:3949–52.
- Samusyte G, Bostock H, Rothwell J, et al. P157 reliability of threshold tracking technique for short interval intracortical inhibition. *Clinical Neurophysiology* 2017;128:e93.
- Groppa S, Oliviero A, Eisen A, et al. A practical guide to diagnostic transcranial magnetic stimulation: report of an IFCN Committee. *Clin Neurophysiol* 2012;123:858–82.
- Menon P, Geevasinga N, Yiannikas C, et al. Sensitivity and specificity of threshold tracking transcranial magnetic stimulation for diagnosis of amyotrophic lateral sclerosis: a prospective study. *Lancet Neurol* 2015;14:478–84.
- Ibey RJ, Bolton DA, Buick AR, et al. Interhemispheric inhibition of corticospinal projections to forearm muscles. *Clin Neurophysiol* 2015;126:1934–40.
- Di Lazzaro V, Oliviero A, Pilato F, et al. Neurophysiological predictors of long term response to AChE inhibitors in AD patients. *J Neurol Neurosurg Psychiatry* 2005;76:1064–9.
- Agarwal S, Koch G, Hillis AE, et al. Interrogating cortical function with transcranial magnetic stimulation: insights from neurodegenerative disease and stroke. *J Neurol Neurosurg Psychiatry* 2018.
- Ruddy KL, Leemans A, Woolley DG, et al. Structural and functional cortical connectivity mediating cross education of motor function. *J Neurosci* 2017;37:2555–64.
- Lindau M, Jelic V, Johansson SE, et al. Quantitative EEG abnormalities and cognitive dysfunctions in frontotemporal dementia and Alzheimer's disease. *Dement Geriatr Cogn Disord* 2003;15:106–14.
- Burns A, Iliffe S. Dementia. *BMJ* 2009;338:b75.

- 35 Babiloni C, Lizio R, Marzano N, et al. Brain neural synchronization and functional coupling in Alzheimer's disease as revealed by resting state EEG rhythms. *Int J Psychophysiol Off J Int Organ Psychophysiol* 2016;103:88–102.
- 36 Andersson M, Hansson O, Minthon L, et al. Electroencephalogram variability in dementia with Lewy bodies, Alzheimer's disease and controls. *Dement Geriatr Cogn Disord* 2008;26:284–90.
- 37 Babiloni C, De Pandis MF, Vecchio F, et al. Cortical sources of resting state electroencephalographic rhythms in Parkinson's disease related dementia and Alzheimer's disease. *Clinical Neurophysiology* 2011;122:2355–64.
- 38 Vecchio F, Babiloni C, Lizio R, et al. Resting state cortical EEG rhythms in Alzheimer's disease: toward EEG markers for clinical applications: a review. *Suppl Clin Neurophysiol* 2013;62:223–36.
- 39 Mandal PK, Banerjee A, Tripathi M, et al. A comprehensive review of magnetoencephalography (MEG) studies for brain functionality in healthy aging and Alzheimer's disease (AD). *Front Comput Neurosci* 2018;12.
- 40 Olde Dubbelink KT, Stoffers D, Deijen JB, et al. Cognitive decline in Parkinson's disease is associated with slowing of resting-state brain activity: a longitudinal study. *Neurobiol Aging* 2013;34:408–18.
- 41 Franciotti R, Iacono D, Della Penna S, et al. Cortical rhythms reactivity in AD, LBD and normal subjects: a quantitative MEG study. *Neurobiol Aging* 2006;27:1100–9.
- 42 Babiloni C, Del Percio C, Lizio R, et al. Abnormalities of cortical neural synchronization mechanisms in subjects with mild cognitive impairment due to Alzheimer's and Parkinson's diseases: an EEG study. *J Alzheimers Dis* 2017;59:339–58.
- 43 Babiloni C, Del Percio C, Lizio R, et al. Abnormalities of resting state cortical EEG rhythms in subjects with mild cognitive impairment due to Alzheimer's and Lewy body diseases. *J Alzheimers Dis* 2018;62:247–68.
- 44 Babiloni C, Frisoni G, Steriade M, et al. Frontal white matter volume and delta EEG sources negatively correlate in awake subjects with mild cognitive impairment and Alzheimer's disease. *Clin Neurophysiol* 2006;117:1113–29.
- 45 Surmeier DJ, Obeso JA, Halliday GM. Selective neuronal vulnerability in Parkinson disease. *Nat Rev Neurosci* 2017;18:101–13.
- 46 Jenkinson N, Brown P. New insights into the relationship between dopamine, beta oscillations and motor function. *Trends Neurosci* 2011;34:611–8.
- 47 Caviness JN, Hentz JG, Belden CM, et al. Longitudinal EEG changes correlate with cognitive measure deterioration in Parkinson's disease. *J Park Dis* 2015;5:117–24.
- 48 Assenza G, Capone F, di Biase L, et al. Corrigendum: oscillatory activities in neurological disorders of elderly: biomarkers to target for neuromodulation. *Front Aging Neurosci* 2017;9.
- 49 Muthuraman M, Koirala N, Ciolac D, et al. Deep brain stimulation and L-dopa therapy: concepts of action and clinical applications in Parkinson's disease. *Front Neural* 2018;9.
- 50 Park J, Chang WH, Cho JW, et al. Usefulness of transcranial magnetic stimulation to assess motor function in patients with parkinsonism. *Ann Rehabil Med* 2016;40:81–7.
- 51 Ni Z, Bahl N, Gunraj CA, et al. Increased motor cortical facilitation and decreased inhibition in Parkinson disease. *Neurology* 2013;80:1746–53.
- 52 Little S, Pogosyan A, Neal S, et al. Adaptive deep brain stimulation in advanced Parkinson disease. *Ann Neurol* 2013;74:449–57.
- 53 Dottori M, Sedeño L, Martorell Caro M, et al. Towards affordable biomarkers of frontotemporal dementia: a classification study via network's information sharing. *Sci Rep* 2017;7.
- 54 Nishida K, Yoshimura M, Isotani T, et al. Differences in quantitative EEG between frontotemporal dementia and Alzheimer's disease as revealed by LORETA. *Clin Neurophysiol* 2011;122:1718–25.
- 55 Garn H, Coronel C, Waser M, et al. Differential diagnosis between patients with probable Alzheimer's disease, Parkinson's disease dementia, or dementia with Lewy bodies and frontotemporal dementia, behavioral variant, using quantitative electroencephalographic features. *J Neural Transm* 2017;124:569–81.
- 56 Metin SZ, Erguzel TT, Ertan G, et al. The use of quantitative EEG for differentiating frontotemporal dementia from late-onset bipolar disorder. *Clin EEG Neurosci* 2018;49:171–6.
- 57 Lanata SC, Miller BL. The behavioural variant frontotemporal dementia (bvFTD) syndrome in psychiatry. *J Neural Neurosurg Psychiatry* 2016;87:501–11.
- 58 Ludolph A, Drory V, Hardiman O, et al. A revision of the El Escorial criteria – 2015. *Amyotroph Lateral Scler Frontotemporal Degener* 2015;16:291–2.
- 59 Galvin M, Ryan P, Maguire S, et al. The path to specialist multidisciplinary care in amyotrophic lateral sclerosis: a population-based study of consultations, interventions and costs. *PLoS One* 2017;12.
- 60 Menke RAL, Proudfoot M, Talbot K, et al. The two-year progression of structural and functional cerebral MRI in amyotrophic lateral sclerosis. *NeuroImage: Clinical* 2018;17:953–61.
- 61 Iyer PM, Egan C, Pinto-Grau M, et al. Functional connectivity changes in resting-state EEG as potential biomarker for amyotrophic lateral sclerosis. *PLoS One* 2015;10:e0128682.
- 62 Machts J, Cardenas-Blanco A, Acosta-Cabrero J, et al. Prefrontal cortical thickness in motor neuron disease. *NeuroImage Clin* 2018;18:648–55.
- 63 Grieve SM, Menon P, Korgaonkar MS, et al. Potential structural and functional biomarkers of upper motor neuron dysfunction in ALS. *Amyotroph Lateral Sclerosis and Frontotemporal Degeneration* 2016;17:85–92.
- 64 Elamin M, Phukan J, Bede P, et al. Executive dysfunction is a negative prognostic indicator in patients with ALS without dementia. *Neurology* 2011;76:1263–9.
- 65 Ringholz GM, Appel SH, Bradshaw M, et al. Prevalence and patterns of cognitive impairment in sporadic ALS. *Neurology* 2005;65:586–90.
- 66 McLaughlin RL, Schijven D, van Rheenen W, et al. Genetic correlation between amyotrophic lateral sclerosis and schizophrenia. *Nat Commun* 2017;8.
- 67 Devenney EM, Ahmed RM, Halliday G, et al. Psychiatric disorders in C9orf72 kindreds: study of 1,414 family members. *Neurology* 2018;91:e1498–507.
- 68 Di Filippo M, Portaccio E, Mancini A, et al. Multiple sclerosis and cognition: synaptic failure and network dysfunction. *Nat Rev Neurosci* 2018;19:599–609.
- 69 Hardmeier M, Leocani L, Fuhr P. A new role for evoked potentials in MS? repurposing evoked potentials as biomarkers for clinical trials in MS. *Mult Scler* 2017;23:1309–19.
- 70 Gschwind M, Hardmeier M, Van De Ville D, et al. Fluctuations of spontaneous EEG topographies predict disease state in relapsing-remitting multiple sclerosis. *NeuroImage Clin* 2016;12:466–77.
- 71 Pokryszko-Dragan A, Bilinska M, Gruszka E, et al. Assessment of visual and auditory evoked potentials in multiple sclerosis patients with and without fatigue. *Neuro Sci* 2015;36:235–42.
- 72 Kale N, Agaoglu J, Onder G, et al. Correlation between disability and transcranial magnetic stimulation abnormalities in patients with multiple sclerosis. *J Clin Neurosci* 2009;16:1439–42.
- 73 Krieger SC, Cook K, De Nino S, et al. The topographical model of multiple sclerosis. *Neural Neuroimmunol Neuroinflamm* 2016;3.
- 74 Farzan F, Atluri S, Frehlich M, et al. Standardization of electroencephalography for multi-site, multi-platform and multi-investigator studies: insights from the Canadian biomarker integration network in depression. *Sci Rep* 2017;7.
- 75 Snyder SM, Rugino TA, Hornig M, et al. Integration of an EEG biomarker with a clinician's ADHD evaluation. *Brain Behav* 2015;5:e00330.
- 76 Sanacora G, Smith MA, Pathak S, et al. Lanicemine: a low-trapping NMDA channel blocker produces sustained antidepressant efficacy with minimal psychotomimetic adverse effects. *Mol Psychiatry* 2014;19:978–85.
- 77 Scheltens P, Twisk JWR, Blesa R, et al. Efficacy of Souvenaid in mild Alzheimer's disease: results from a randomized, controlled trial. *JAD* 2012;31:225–36.
- 78 Ljubisavljevic MR, Ismail FY, Filipovic S. Transcranial magnetic stimulation of degenerating brain: a comparison of normal aging, Alzheimer's, Parkinson's and Huntington's disease. *Curr Alzheimer Res* 2013;10:578–96.
- 79 Tsolaki A, Kazis D, Kompatsiaris I, et al. Electroencephalogram and Alzheimer's disease: clinical and research approaches. *Int J Alzheimers Dis* 2014;2014.

## 10.2. Appendix chapter 4

### Appendix 4.1. Ethical approval letter for all TMS and EEG studies performed within this project

THE ADVERSE EFFECTS OF DRUGS FOR  
PROSCRIPTIONS OR WITHDRAWN PRODUCTS

SJH/AMNCH Research Ethics Committee Secretariat  
Claire Hartin Ph: +353 1 4142199  
email: claire.hartin@amnch.ie



**THE ADELAIDE & MEATH  
HOSPITAL, DUBLIN**  
INCORPORATING  
THE NATIONAL CHILDREN'S HOSPITAL

MILLAGATE, DUBLIN 24, IRELAND  
TELEPHONE +353 1 4142000

Ms. Roisin McMackin  
Room 5.43 Trinity Biomedical Sciences Institute  
152-160 Pearse Station  
Dublin 2

28th February 2017

**Re: Characterising Network Disruption in Human Neurodegeneration: A Spectral EEG and TMS based approach in Amyotrophic Lateral Sclerosis**

**REC Reference: 2017-02 Chairman's Action (18)**  
*(Please quote reference on all correspondence)*

Dear Ms Mc Mackin,

The REC is in receipt of your recent request to SJH/AMNCH Research Ethics Committee in which you queried ethical approval for the above named study.

The Chairman, Dr. Peter Lavin, on behalf of the Research Ethics Committee, has reviewed your correspondence and granted ethical approval for this study.

Yours sincerely,



Claire Hartin  
Secretary  
SJH/AMNCH Research Ethics Committee

The SJH/AMNCH Joint Research and Ethics Committee operates in compliance with and is constituted in accordance with the European Communities (Clinical Trials on Medicinal Products for Human Use) Regulations 2004 & ICH GCP guidelines.

### Appendix 4.2. Control consent form for TMS-based study participants.

## CONTROL CONSENT FORM

**Study title: Characterising Network Disruption in Human Neurodegeneration: A Spectral EEG and TMS based Approach in Amyotrophic Lateral Sclerosis – TMS aspect**

I have read and understood the Control Information Leaflet about this research project. The information has been fully explained to me and I have been able to ask questions, all of which have been answered to my satisfaction.	Yes <input type="checkbox"/>	No <input type="checkbox"/>
I understand that I don't have to take part in this study and that I can opt out at any time. I understand that I don't have to give a reason for opting out and I understand that opting out won't affect my future medical care.	Yes <input type="checkbox"/>	No <input type="checkbox"/>
I am aware of the potential risks of this research study.	Yes <input type="checkbox"/>	No <input type="checkbox"/>
I give permission for researchers to look at other data I previously provided to The Academic Unit of Neurology to get information. I have been assured that information about me will be kept private and confidential.	Yes <input type="checkbox"/>	No <input type="checkbox"/>
I have been given a copy of the Information Leaflet and this completed consent form for my records.	Yes <input type="checkbox"/>	No <input type="checkbox"/>
I consent to take part in this research study having been fully informed of the risks.	Yes <input type="checkbox"/>	No <input type="checkbox"/>
I give informed explicit consent to have my data processed as part of this research study.	Yes <input type="checkbox"/>	No <input type="checkbox"/>
I consent to be contacted by researchers as part of this research study to enquire about participation in future sessions of this study.	Yes <input type="checkbox"/>	No <input type="checkbox"/>
I consent to automated processing being performed on my data for the purposes of grouping participants into categories based on the measurements taken.	Yes <input type="checkbox"/>	No <input type="checkbox"/>
I consent to the anonymization of my data in future so that it can no longer be attributed to me.	Yes <input type="checkbox"/>	No <input type="checkbox"/>
I consent to the online publication of fully anonymised data that can no longer be attributed to me.	Yes <input type="checkbox"/>	No <input type="checkbox"/>
<b>FUTURE CONTACT</b>		
I consent to be re-contacted by researchers about possible future research related to the current study for which I may be eligible.	Yes <input type="checkbox"/>	No <input type="checkbox"/>

STORAGE AND FUTURE USE OF INFORMATION		
RETENTION OF RESEARCH MATERIAL IN THE FUTURE		
OPTION 1: I give permission for material/data to be stored for <u>possible future research related</u> to the current study <u>only if consent is obtained</u> at the time of the future research but only if the research is approved by a Research Ethics Committee.	Yes <input type="checkbox"/>	No <input type="checkbox"/>
OPTION 2: I give permission for material/data to be stored for <u>possible future research related</u> to the current study <u>without further consent being required</u> but only if the research is approved by a Research Ethics Committee.	Yes <input type="checkbox"/>	No <input type="checkbox"/>
OPTION 3: I give permission for material/data to be stored for <u>possible future research unrelated*</u> to the current study <u>only if consent is obtained</u> at the time of the future research but only if the research is approved by a Research Ethics Committee.	Yes <input type="checkbox"/>	No <input type="checkbox"/>
OPTION 4: I give permission for material/data to be stored for <u>possible future research unrelated*</u> to the current study <u>without further consent</u> being required but only if the research is approved by a Research Ethics Committee.	Yes <input type="checkbox"/>	No <input type="checkbox"/>
OPTION 5: I agree that some future research projects may be carried out by researchers working for <u>commercial/pharmaceutical companies</u> .	Yes <input type="checkbox"/>	No <input type="checkbox"/>
OPTION 6: I understand <u>I will not be entitled to a share of any profits</u> that may arise from the future use of my material/data or products derived from it.	Yes <input type="checkbox"/>	No <input type="checkbox"/>

*\*See "Consent to Future Uses" section of information leaflet for more information*

---

Control Name (Block Capitals)	Control Signature	Date
-------------------------------	-------------------	------

To be completed by the Principal Investigator or nominee.

I, the undersigned, have taken the time to fully explain to the above patient the nature and purpose of this study in a way that they could understand. I have explained the risks involved as well as the possible benefits. I have invited them to ask questions on any aspect of the study that concerned them.

---

Name (Block Capitals)	Qualifications	Signature	Date
-----------------------	----------------	-----------	------

2 copies to be made: 1 for control and 1 for PI.



**Appendix 4.3. Patient consent form for TMS-based study participants.**

**PATIENT CONSENT FORM**

**Study title: Characterising Network Disruption in Human Neurodegeneration: A Spectral EEG and TMS based Approach in Amyotrophic Lateral Sclerosis – TMS aspect**

I have read and understood the Patient Information Leaflet about this research project. The information has been fully explained to me and I have been able to ask questions, all of which have been answered to my satisfaction.	Yes <input type="checkbox"/>	No <input type="checkbox"/>
I understand that I don't have to take part in this study and that I can opt out at any time. I understand that I don't have to give a reason for opting out and I understand that opting out won't affect my future medical care.	Yes <input type="checkbox"/>	No <input type="checkbox"/>
I am aware of the potential risks of this research study.	Yes <input type="checkbox"/>	No <input type="checkbox"/>
I give permission for researchers to look at other data I previously provided to The Academic Unit of Neurology and/or The National ALS Register to get information. I have been assured that information about me will be kept private and confidential.	Yes <input type="checkbox"/>	No <input type="checkbox"/>
I have been given a copy of the Information Leaflet and this completed consent form for my records.	Yes <input type="checkbox"/>	No <input type="checkbox"/>
I consent to take part in this research study having been fully informed of the risks.	Yes <input type="checkbox"/>	No <input type="checkbox"/>
I give informed explicit consent to have my data processed as part of this research study.	Yes <input type="checkbox"/>	No <input type="checkbox"/>
I consent to be contacted by researchers as part of this research study to enquire about participation in future sessions of this study.	Yes <input type="checkbox"/>	No <input type="checkbox"/>
I consent to automated processing being performed on my data for the purposes of grouping participants into categories based on the measurements taken.	Yes <input type="checkbox"/>	No <input type="checkbox"/>
I consent to the anonymization of my data in future so that it can no longer be attributed to me.	Yes <input type="checkbox"/>	No <input type="checkbox"/>
I consent to the online publication of fully anonymised data that can no longer be attributed to me.	Yes <input type="checkbox"/>	No <input type="checkbox"/>
<b>FUTURE CONTACT</b>		
I consent to be re-contacted by researchers about possible future research related to the current study for which I may be eligible.	Yes <input type="checkbox"/>	No <input type="checkbox"/>

STORAGE AND FUTURE USE OF INFORMATION		
RETENTION OF RESEARCH MATERIAL IN THE FUTURE		
OPTION 1: I give permission for material/data to be stored for <u>possible future research related</u> to the current study <u>only if consent is obtained</u> at the time of the future research but only if the research is approved by a Research Ethics Committee.	Yes <input type="checkbox"/>	No <input type="checkbox"/>
OPTION 2: I give permission for material/data to be stored for <u>possible future research related</u> to the current study <u>without further consent being required</u> but only if the research is approved by a Research Ethics Committee.	Yes <input type="checkbox"/>	No <input type="checkbox"/>
OPTION 3: I give permission for material/data to be stored for <u>possible future research unrelated*</u> to the current study <u>only if consent is obtained</u> at the time of the future research but only if the research is approved by a Research Ethics Committee.	Yes <input type="checkbox"/>	No <input type="checkbox"/>
OPTION 4: I give permission for material/data to be stored for <u>possible future research unrelated*</u> to the current study <u>without further consent</u> being required but only if the research is approved by a Research Ethics Committee.	Yes <input type="checkbox"/>	No <input type="checkbox"/>
OPTION 5: I agree that some future research projects may be carried out by researchers working for <u>commercial/pharmaceutical companies</u> .	Yes <input type="checkbox"/>	No <input type="checkbox"/>
OPTION 6: I understand I <u>will not be entitled to a share of any profits</u> that may arise from the future use of my material/data or products derived from it.	Yes <input type="checkbox"/>	No <input type="checkbox"/>

*\*See "Consent to Future Uses" section of information leaflet for more information*

---

\_\_\_\_\_ | \_\_\_\_\_ | \_\_\_\_\_  
 Patient Name (Block Capitals) | Patient Signature | Date

Where the participant is capable of comprehending the nature, significance and scope of the consent required, but is physically unable to sign written consent, signatures of two witnesses present when consent was given by the participant to Prof. Orla Hardiman or her nominee.

NAME OF FIRST WITNESS: \_\_\_\_\_ SIGNATURE: \_\_\_\_\_

NAME OF SECOND WITNESS: \_\_\_\_\_ SIGNATURE: \_\_\_\_\_

To be completed by the Principal Investigator or nominee.

I, the undersigned, have taken the time to fully explain to the above patient the nature and purpose of this study in a way that they could understand. I have explained the risks involved as well as the possible benefits. I have invited them to ask questions on any aspect of the study that concerned them.

---

\_\_\_\_\_ | \_\_\_\_\_ | \_\_\_\_\_ | \_\_\_\_\_  
 Name (Block Capitals) | Qualifications | Signature | Date

2 copies to be made: 1 for patient and 1 for PI.

**Appendix 4.4. Control consent form for EEG-based study participants.**

**CONTROL CONSENT FORM**

<p><b>Study title: Characterising Network Disruption in Human Neurodegeneration: A Spectral EEG and TMS based Approach in Amyotrophic Lateral Sclerosis – EEG aspect</b></p>
------------------------------------------------------------------------------------------------------------------------------------------------------------------------------

I have read and understood the Control Information Leaflet about this research project. The information has been fully explained to me and I have been able to ask questions, all of which have been answered to my satisfaction.	Yes <input type="checkbox"/>	No <input type="checkbox"/>
I understand that I don't have to take part in this study and that I can opt out at any time. I understand that I don't have to give a reason for opting out and I understand that opting out won't affect my future medical care.	Yes <input type="checkbox"/>	No <input type="checkbox"/>
I am aware of the potential risks of this research study.	Yes <input type="checkbox"/>	No <input type="checkbox"/>
I give permission for researchers to look at other data I previously provided to The Academic Unit of Neurology to get information. I have been assured that information about me will be kept private and confidential.	Yes <input type="checkbox"/>	No <input type="checkbox"/>
I have been given a copy of the Information Leaflet and this completed consent form for my records.	Yes <input type="checkbox"/>	No <input type="checkbox"/>
I consent to take part in this research study having been fully informed of the risks.	Yes <input type="checkbox"/>	No <input type="checkbox"/>
I give informed explicit consent to have my data processed as part of this research study.	Yes <input type="checkbox"/>	No <input type="checkbox"/>
I consent to be contacted by researchers as part of this research study to enquire about participation in future sessions of this study.	Yes <input type="checkbox"/>	No <input type="checkbox"/>
I consent to automated processing being performed on my data for the purposes of grouping participants into categories based on the measurements taken.	Yes <input type="checkbox"/>	No <input type="checkbox"/>
I consent to the anonymization of my data in future so that it can no longer be attributed to me.	Yes <input type="checkbox"/>	No <input type="checkbox"/>
I consent to the online publication of fully anonymised data that can no longer be attributed to me.	Yes <input type="checkbox"/>	No <input type="checkbox"/>

<b>FUTURE CONTACT</b>		
I consent to be re-contacted by researchers about possible future research related to the current study for which I may be eligible.	Yes <input type="checkbox"/>	No <input type="checkbox"/>

STORAGE AND FUTURE USE OF INFORMATION		
RETENTION OF RESEARCH MATERIAL IN THE FUTURE		
OPTION 1: I give permission for material/data to be stored for <u>possible future research related</u> to the current study <u>only if consent is obtained</u> at the time of the future research but only if the research is approved by a Research Ethics Committee.	Yes <input type="checkbox"/>	No <input type="checkbox"/>
OPTION 2: I give permission for material/data to be stored for <u>possible future research related</u> to the current study <u>without further consent being required</u> but only if the research is approved by a Research Ethics Committee.	Yes <input type="checkbox"/>	No <input type="checkbox"/>
OPTION 3: I give permission for material/data to be stored for <u>possible future research unrelated*</u> to the current study <u>only if consent is obtained</u> at the time of the future research but only if the research is approved by a Research Ethics Committee.	Yes <input type="checkbox"/>	No <input type="checkbox"/>
OPTION 4: I give permission for material/data to be stored for <u>possible future research unrelated*</u> to the current study <u>without further consent</u> being required but only if the research is approved by a Research Ethics Committee.	Yes <input type="checkbox"/>	No <input type="checkbox"/>
OPTION 5: I agree that some future research projects may be carried out by researchers working for <u>commercial/pharmaceutical companies</u> .	Yes <input type="checkbox"/>	No <input type="checkbox"/>
OPTION 6: I understand I <u>will not be entitled to a share of any profits</u> that may arise from the future use of my material/data or products derived from it.	Yes <input type="checkbox"/>	No <input type="checkbox"/>

*\*See "Consent to Future Uses" section of information leaflet for more information*

---

Control Name (Block Capitals)	Control Signature	Date
-------------------------------	-------------------	------

**To be completed by the Principal Investigator or nominee.**

I, the undersigned, have taken the time to fully explain to the above patient the nature and purpose of this study in a way that they could understand. I have explained the risks involved as well as the possible benefits. I have invited them to ask questions on any aspect of the study that concerned them.

---

Name (Block Capitals)	Qualifications	Signature	Date
-----------------------	----------------	-----------	------

2 copies to be made: 1 for control and 1 for PI.

Appendix 4.5. Patient consent form for EEG-based study participants.

**PATIENT CONSENT FORM**

<p><b>Study title: Characterising Network Disruption in Human Neurodegeneration: A Spectral EEG and TMS based Approach in Amyotrophic Lateral Sclerosis – EEG aspect</b></p>
------------------------------------------------------------------------------------------------------------------------------------------------------------------------------

I have read and understood the Patient Information Leaflet about this research project. The information has been fully explained to me and I have been able to ask questions, all of which have been answered to my satisfaction.	Yes <input type="checkbox"/>	No <input type="checkbox"/>
I understand that I don't have to take part in this study and that I can opt out at any time. I understand that I don't have to give a reason for opting out and I understand that opting out won't affect my future medical care.	Yes <input type="checkbox"/>	No <input type="checkbox"/>
I am aware of the potential risks of this research study.	Yes <input type="checkbox"/>	No <input type="checkbox"/>
I give permission for researchers to look at other data I previously provided to The Academic Unit of Neurology and/or The National ALS Register to get information. I have been assured that information about me will be kept private and confidential.	Yes <input type="checkbox"/>	No <input type="checkbox"/>
I have been given a copy of the Information Leaflet and this completed consent form for my records.	Yes <input type="checkbox"/>	No <input type="checkbox"/>
I consent to take part in this research study having been fully informed of the risks.	Yes <input type="checkbox"/>	No <input type="checkbox"/>
I give informed explicit consent to have my data processed as part of this research study.	Yes <input type="checkbox"/>	No <input type="checkbox"/>
I consent to be contacted by researchers as part of this research study to enquire about participation in future sessions of this study.	Yes <input type="checkbox"/>	No <input type="checkbox"/>
I consent to automated processing being performed on my data for the purposes of grouping participants into categories based on the measurements taken.	Yes <input type="checkbox"/>	No <input type="checkbox"/>
I consent to the anonymization of my data in future so that it can no longer be attributed to me.	Yes <input type="checkbox"/>	No <input type="checkbox"/>
I consent to the online publication of fully anonymised data that can no longer be attributed to me.	Yes <input type="checkbox"/>	No <input type="checkbox"/>

<b>FUTURE CONTACT</b>		
I consent to be re-contacted by researchers about possible future research related to the current study for which I may be eligible.	Yes <input type="checkbox"/>	No <input type="checkbox"/>

STORAGE AND FUTURE USE OF INFORMATION		
RETENTION OF RESEARCH MATERIAL IN THE FUTURE		
OPTION 1: I give permission for material/data to be stored for <u>possible future research related</u> to the current study <u>only if consent is obtained</u> at the time of the future research but only if the research is approved by a Research Ethics Committee.	Yes <input type="checkbox"/>	No <input type="checkbox"/>
OPTION 2: I give permission for material/data to be stored for <u>possible future research related</u> to the current study <u>without further consent being required</u> but only if the research is approved by a Research Ethics Committee.	Yes <input type="checkbox"/>	No <input type="checkbox"/>
OPTION 3: I give permission for material/data to be stored for <u>possible future research unrelated*</u> to the current study <u>only if consent is obtained</u> at the time of the future research but only if the research is approved by a Research Ethics Committee.	Yes <input type="checkbox"/>	No <input type="checkbox"/>
OPTION 4: I give permission for material/data to be stored for <u>possible future research unrelated*</u> to the current study <u>without further consent</u> being required but only if the research is approved by a Research Ethics Committee.	Yes <input type="checkbox"/>	No <input type="checkbox"/>
OPTION 5: I agree that some future research projects may be carried out by researchers working for <u>commercial/pharmaceutical companies</u> .	Yes <input type="checkbox"/>	No <input type="checkbox"/>
OPTION 6: I understand I <u>will not be entitled to a share of any profits</u> that may arise from the future use of my material/data or products derived from it.	Yes <input type="checkbox"/>	No <input type="checkbox"/>

*\*See "Consent to Future Uses" section of information leaflet for more information*

---

\_\_\_\_\_ | \_\_\_\_\_ | \_\_\_\_\_  
 Patient Name (Block Capitals) | Patient Signature | Date

Where the participant is capable of comprehending the nature, significance and scope of the consent required, but is physically unable to sign written consent, signatures of two witnesses present when consent was given by the participant to Prof. Orla Hardiman or her nominee.

NAME OF FIRST WITNESS: \_\_\_\_\_ SIGNATURE: \_\_\_\_\_

NAME OF SECOND WITNESS: \_\_\_\_\_ SIGNATURE: \_\_\_\_\_

To be completed by the Principal Investigator or nominee.

I, the undersigned, have taken the time to fully explain to the above patient the nature and purpose of this study in a way that they could understand. I have explained the risks involved as well as the possible benefits. I have invited them to ask questions on any aspect of the study that concerned them.

---

\_\_\_\_\_ | \_\_\_\_\_ | \_\_\_\_\_  
 Name (Block Capitals) | Qualifications | Signature | Date

2 copies to be made: 1 for patient and 1 for PI.

### 10.3. Appendix chapter 5

#### Appendix 5.1. Supplementary introduction to section 5.2.

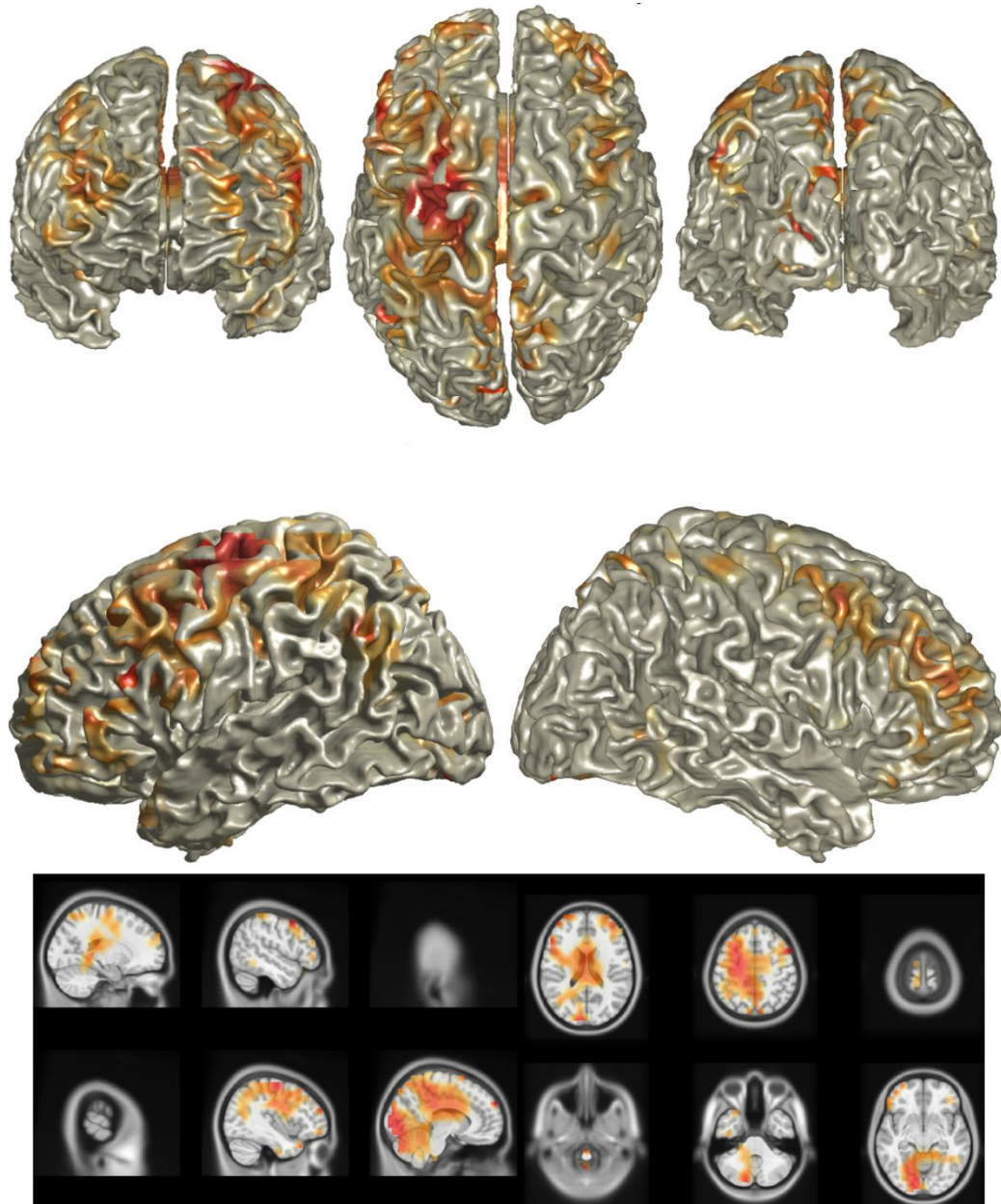
Application of TMS over the scalp to engage motor cortical tissue and measurement of the associated motor evoked potentials in a target muscle can be used to examine changes in motor cortical excitability, inhibition and facilitation in disease<sup>321</sup>. Such protocols have demonstrated early motor cortex hyperexcitability and GABA-ergic interneuron decline in ALS<sup>71</sup>. This methodology is, however, unsuitable for investigating such changes in non-motor regions such as cognitive networks or in patients lacking target muscle function, due to lack of a quantifiable stimulus-associated output measure in the absence of EEG recording. Non-motor cortical function can be interrogated by simultaneous TMS and EEG. However, this methodology presents numerous mechanistic and analytical challenges, including TMS-related EEG artefacts and limitations to coil positioning, although methods to overcome these are in development<sup>683,684</sup>. Alternatively, repetitive TMS can be used to evoke persistent changes in cortical function which can be measured afterward by EEG. This type of TMS is, however, associated with significant discomfort to participants over cognition-associated scalp areas, such as the prefrontal cortex<sup>685</sup>. By comparison, recording EEG during a task designed to engage cortical networks of interest can detect any changes in function of both motor and non-motor cortical regions while avoiding discomfort associated with repetitive stimulation of scalp muscle and nerves overlying the region of interest<sup>686</sup>. Use of dry EEG can also reduce potential discomfort associated with the sensation of wet conductive gel on the scalp. Recently developed dry EEG electrodes are now rivalling signal quality to that of wet EEG in some cases<sup>687</sup>. The unique combination of advantages of EEG are therefore well suited to the detection of early, motor and non-motor cortical pathology in neurodegenerative diseases such as ALS with established, spatially distributed cortical pathology<sup>101</sup>.

## **Appendix 5.2. Discussion on the use of personalised and template MRI scans for head modelling in EEG source analysis.**

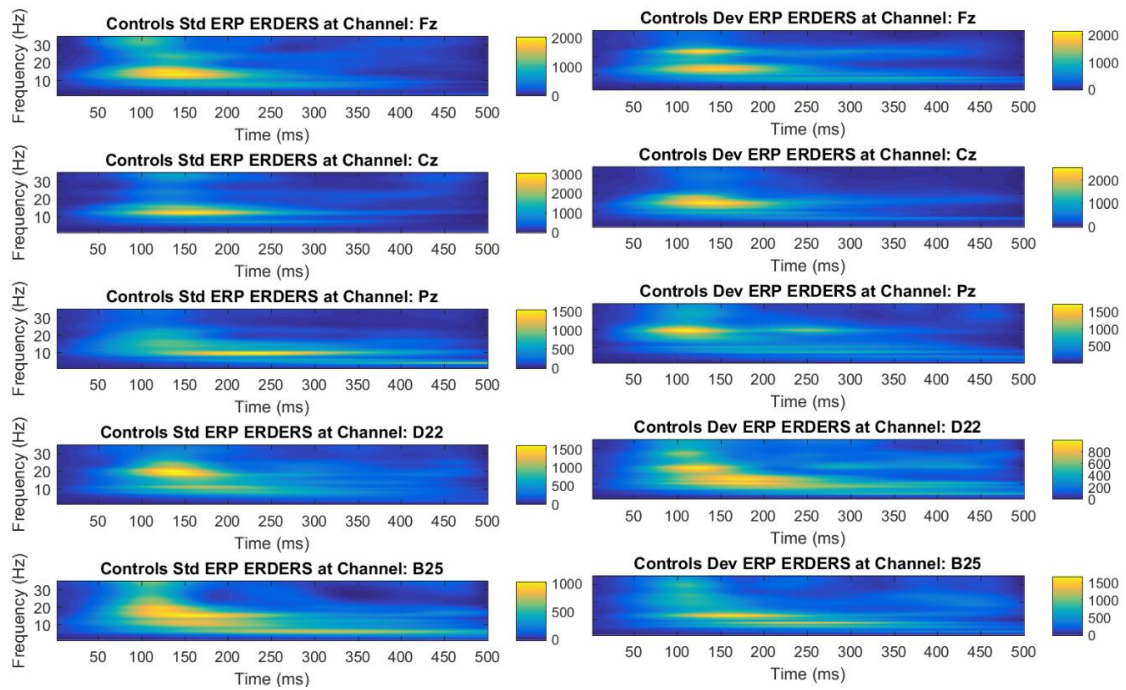
While an individual's MRI scan is optimal for the design of the model of head tissue required for source localisation, this additional cost can be overcome by the design of head models based on openly accessible model MRI scans (e.g. Colin27, ICBM152). Such head models are found to provide comparable localisation accuracy to those based on each individual's own MRI scans

482,484 .



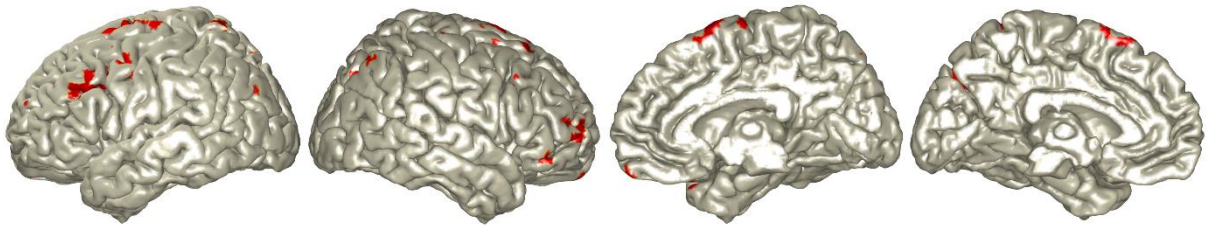


**Appendix 5.3. Statistically significant changes in bilateral dorsolateral prefrontal and left motor, posterior parietal, occipital and midcingulate cortical activity in ALS patients at baseline.** Statistically significance (false discovery rate=10%,  $\beta=0.13$ ,  $P_1=0.079$ ) increases in power in ALS patients relative to healthy controls as determined by LCMV are highlighted in red. No significant decreases in power in ALS were identified. Axial MRI views are from above (i.e. left is left). Top left panel – Frontal view. Top right panel – Occipital view.

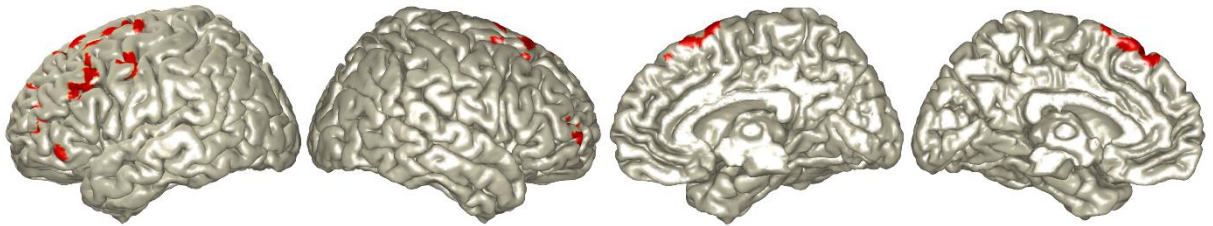


**Appendix 5.4.** Mean standard (left) and deviant (right) auditory evoked potential-associated ERSP (i.e. phase-locked components). Colour bar represents % change in power from baseline.

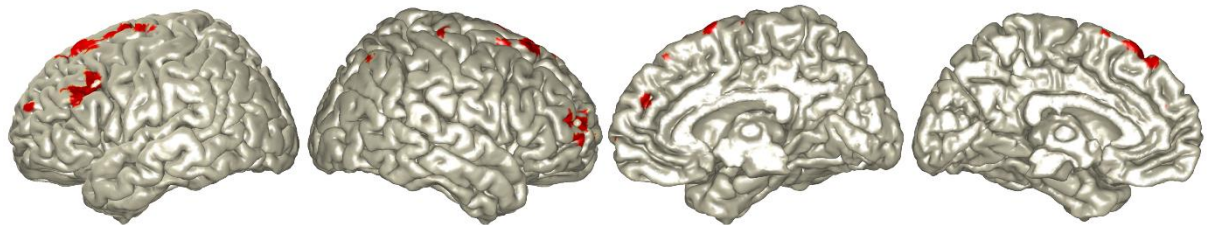
**0-100ms post stimulus**



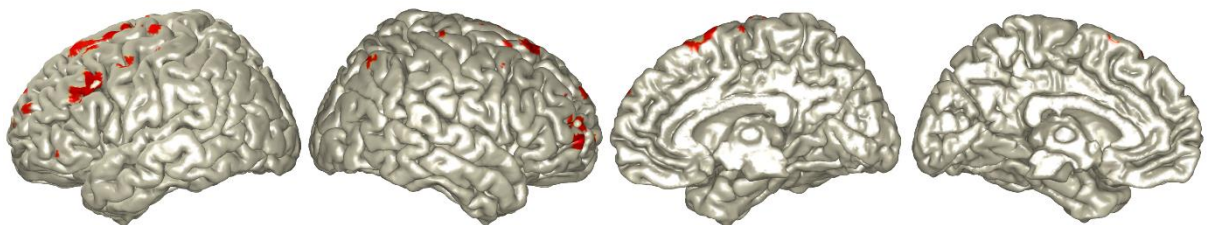
**100-200ms post stimulus**



**200-300ms post stimulus**

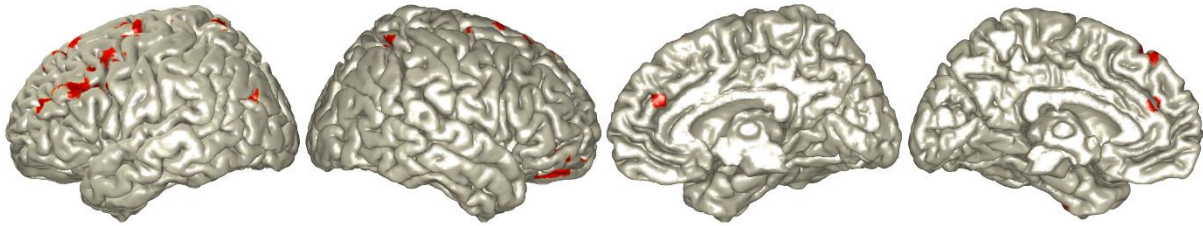


**300-400ms post stimulus**

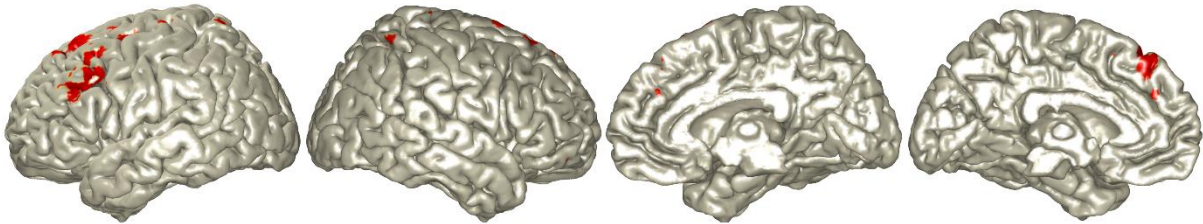


**Appendix 5.5. Top 5% of significantly active control sources of alpha band event-related oscillations for each 100ms WOI analysed after standard tones. All sources highlighted show significant increase in alpha band oscillatory power relative to baseline, determined by sign rank testing at a false discovery rate of 10%.**

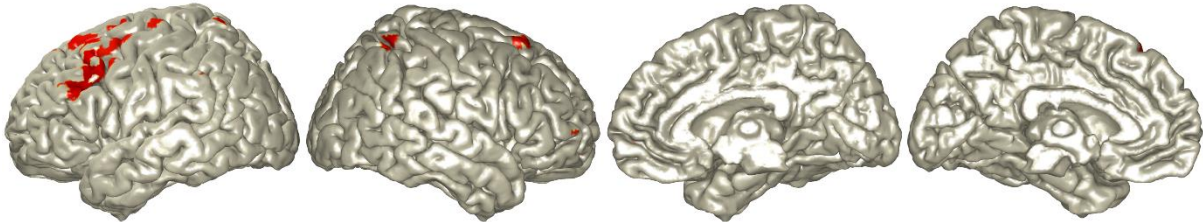
**0-100ms post stimulus**



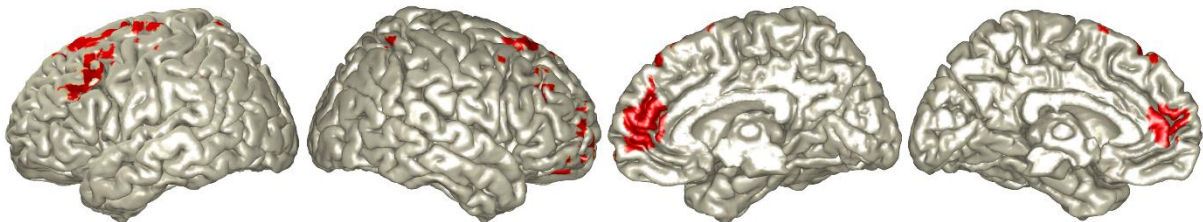
**100-200ms post stimulus**



**200-300ms post stimulus**



**300-400ms post stimulus**



**Appendix 5.6. Top 5% of significantly active control sources of alpha band event-related oscillations for each 100ms WOI analysed after deviant tones. All sources highlighted show significant increase in alpha band oscillatory power relative to baseline, determined by sign rank testing at a false discovery rate of 10%.**

## 10.4. Appendix chapter 6

### Appendix 6.1. McMackin et al., 2020



Cerebral Cortex, September 2020;30: 4834–4846

doi: 10.1093/cercor/bhaa076

Advance Access Publication Date: 21 April 2020  
Original Article

ORIGINAL ARTICLE

## Localization of Brain Networks Engaged by the Sustained Attention to Response Task Provides Quantitative Markers of Executive Impairment in Amyotrophic Lateral Sclerosis

Roisin McMackin<sup>1</sup>, Stefan Dukic<sup>1,2</sup>, Emmet Costello<sup>1</sup>, Marta Pinto-Grau<sup>1,3</sup>, Antonio Fasano<sup>1</sup>, Teresa Buxo<sup>1</sup>, Mark Heverin<sup>1</sup>, Richard Reilly<sup>4,5</sup>, Muthuraman Muthuraman<sup>6</sup>, Niall Pender<sup>1,3</sup>, Orla Hardiman<sup>1,7</sup> and Bahman Nasserroleslami<sup>1</sup>

<sup>1</sup>Academic Unit of Neurology, Trinity College Dublin, The University of Dublin, Dublin, D02 R590, Ireland, <sup>2</sup>Department of Neurology, Brain Center Rudolf Magnus, University Medical Center Utrecht, 3584 CX Utrecht, The Netherlands, <sup>3</sup>Beaumont Hospital Dublin, Department of Psychology, Dublin 9, Dublin, Ireland, <sup>4</sup>Trinity College Institute of Neuroscience, Trinity College Dublin, The University of Dublin, Dublin 2, Dublin, Ireland, <sup>5</sup>Trinity Centre for Biomedical Engineering, Trinity College, The University of Dublin, Dublin 2, Dublin, Ireland, <sup>6</sup>Biomedical Statistics and Multimodal Signal Processing Unit, Department of Neurology, Johannes-Gutenberg-University Hospital, D55131, Mainz, Germany and <sup>7</sup>Department of Neurology, Beaumont Hospital Dublin, Dublin 9, Dublin, Ireland

Address correspondence to Orla Hardiman, Academic Unit of Neurology, Trinity College Dublin, The University of Dublin, Room 5.43, Trinity Biomedical Sciences Institute, 152-160 Pearse Street, Dublin D02 R590, Ireland. Email: hardimao@tcd.ie  
Joint Last Authorship: Orla Hardiman (hardimao@tcd.ie) and Bahman Nasserroleslami (bahman.nasserroleslami@tcd.ie)

### Abstract

**Objective:** To identify cortical regions engaged during the sustained attention to response task (SART) and characterize changes in their activity associated with the neurodegenerative condition amyotrophic lateral sclerosis (ALS). **Methods:** High-density electroencephalography (EEG) was recorded from 33 controls and 23 ALS patients during a SART paradigm. Differences in associated event-related potential peaks were measured for Go and NoGo trials. Sources active during these peaks were localized, and ALS-associated differences were quantified. **Results:** Go and NoGo N2 and P3 peak sources were localized to the left primary motor cortex, bilateral dorsolateral prefrontal cortex (DLPFC), and lateral posterior parietal cortex (PPC). NoGo trials evoked greater bilateral medial PPC activity during N2 and lesser left insular, PPC and DLPFC activity during P3. Widespread cortical hyperactivity was identified in ALS during P3. Changes in the inferior parietal lobule and insular activity provided very good discrimination (AUROC > 0.75) between patients and controls. Activation of the right precuneus during P3 related to greater executive function in ALS, indicative of a compensatory role. **Interpretation:** The SART engages numerous frontal and parietal cortical structures. SART-EEG measures correlate with specific cognitive impairments that can be localized to specific structures, aiding in differential diagnosis.

**Key words:** amyotrophic lateral sclerosis, attention, EEG, hyperactivity, source localization

© The Author(s) 2020. Published by Oxford University Press.

This is an Open Access article distributed under the terms of the Creative Commons Attribution Non-Commercial License (<http://creativecommons.org/licenses/by-nc/4.0/>), which permits non-commercial re-use, distribution, and reproduction in any medium, provided the original work is properly cited. For commercial re-use, please contact journals.permissions@oup.com

Downloaded from <https://academic.oup.com/cercor/article/30/9/4834/5820432> by guest on 11 January 2021

## Introduction

The sustained attention to response task (SART) has been developed to detect clinically relevant lapses in attention. It represents a simple and quantitative task of executive functions that has been used to capture attentional impairments in different neurodegenerative diseases (Robertson et al. 1997; Bellgrove et al. 2006; O'Gráda et al. 2009; Huntley et al. 2017). Drifts in attention are captured by a failure to inhibit motor responses to targets (i.e., commission errors). As the task requires only button press responses, it is suitable for performing during EEG recording with little to no electromyographic artifacts. Recently, SART-generated event-related potentials (ERPs) time-locked to Go and NoGo trials have been interrogated in healthy individuals using quantitative electroencephalography (EEG). These ERPs have individual peaks which relate to sensory detection ("P1" and "N1") (Jin et al. 2019), motor control ("N2"), and attentional engagement ("P3"). The latter two peaks are typically larger during correct response withholding (Zordan et al. 2008). By combining SART with EEG, distinct indices of the neural network activities required for different aspects of task performance can therefore be determined. This facilitates specific interrogation of the sequentially engaged sensory, motor, and cognitive networks on a millisecond-by-millisecond basis in a quantitative, economical manner. Further, by requiring both motor and cognitive performance, the SART is expected to engage networks that bridge cognitive and motor functions, as opposed to tasks that demand only the individual functions. This makes SART a very suitable candidate for interrogating the cortical pathology in neurological conditions which cause both motor and executive decline, including amyotrophic lateral sclerosis (ALS), Huntington's disease, and Parkinson's disease (Gan et al. 2018).

Despite these advantages, the cortical regions engaged by the SART remain unclear. Low-resolution sensor-level topographies have indicated frontoparietal engagement during the task (Zordan et al. 2008; Staub et al. 2015), and dorsolateral prefrontal and anterior cingulate malfunctioning during SART has been reported in Huntington's disease (Beste et al. 2008). However, the sources of the SART ERPs in healthy individuals have yet to be reported in high spatial and temporal resolution.

Such source-resolved measures could provide important insights into and biomarkers of different cognitive and/or motor neurodegenerations, such as occurs in the neurodegenerative condition ALS, for which differential diagnostic markers are urgently required.

ALS is the most common form of motor neuron disease and is characterized by the presence of upper and lower motor neuron degeneration. Clinical (Elamin et al. 2011; Phukan et al. 2012), neuroimaging (Turner et al. 2012), and neuropathological (Gregory et al. 2019) evidence have demonstrated extensive additional nonmotor involvement; however quantitative measurement of this decline in cognition and behavior in ALS remains challenging.

Detailed neuropsychological assessment with appropriate adjustments for motor impairment has provided information on the nature and frequency of different cognitive domain impairments in ALS (Phukan et al. 2012). However, these types of assessments are excessively time-consuming for clinical trials, in some instances are subject to learning effects, and are insensitive to early, presymptomatic network deterioration. Screening tools, such as the Edinburgh cognitive and behavioral screen

(ECAS) for ALS, are useful in a clinical setting but have limited utility in clinical trials and are not sufficiently sensitive for a detailed assessment of cognitive/behavioral change (Pinto-Grau et al. 2017). Function magnetic resonance imaging (fMRI) and positron emission tomography (PET) have been used to measure cortical activity during specific tasks, but these technologies are limited by cost (Lulé et al. 2009), low temporal resolution, and variance across different scanners (McMackin et al. 2019c).

By contrast, we and others have recently demonstrated how the source localization of EEG facilitates spatially and temporally precise functional imaging of ALS cortical pathology (Dukic et al. 2019; McMackin et al. 2019a, 2019b). Therefore, given the motor and cognitive pathology of ALS, measurement of SART-associated ERPs using source-resolved EEG provides an opportunity to simultaneously interrogate motor and cognitive network functions and investigate their relationship to symptomatic impairments.

Here, we have spatially resolved the sources of these cognitive indices in healthy individuals and patients with ALS by linearly constrained minimum variance (LCMV)-based source imaging. We demonstrate how quantifying changes in SART-ERP indices and their relation to cognitive and motor symptoms facilitate the investigation of cortical malfunction relating to cognitive impairment in ALS.

## Materials and Methods

### Ethical Approval

Ethical approval was obtained from the ethics committee of St James's Hospital (REC reference: 2017-02). All participants provided written informed consent before participation. All work was performed in accordance with the Declaration of Helsinki.

### Participants

#### Recruitment

Patients were recruited at the Irish National ALS specialty clinic in Beaumont Hospital. Healthy controls included appropriately consented, neurologically normal, age-matched individuals recruited from an existing population-based control bank.

### Inclusion Criteria

Patients were over 18 years of age and diagnosed within the previous 18 months with possible, probable, or definite ALS in accordance with the El Escorial revised diagnostic criteria (Ludolph et al. 2015).

### Exclusion Criteria

Exclusion criteria included any diagnosed psychological, neurological, or muscular disease other than ALS, use of CNS medications (e.g., antidepressants, antiseizure medication) except riluzole, inability to participate due to ALS-related motor decline (e.g., inability to sit in the chair for the required time or click the mouse to respond), or evidence of significant respiratory insufficiency. Participants were also rescheduled if they slept two or more hours below normal the night before the session and were asked to abstain from consuming alcohol the night before the recording.

**Table 1** Characteristics of ALS patients and controls

	Patients	Controls
n	23	33
Mean age at EEG [range] (years)	63 [32–78]	63.21 [46–82]
Gender (f/m)	3/20	17/16
Site of onset (spinal/bulbar/thoracic)	17/5/1	N/A
Mean disease duration [range] (months)	20.01 [4–42]	N/A
Handedness (right/left/ambidextrous)	22/0/1	31/2/0
C9orf72+	3	Untested
Mean ALSFRS-R score [range]	38.24 [24–43]	N/A
Mean ECAS total score [n abnormal]	105.33 [3]	Untested
Mean ECAS ALS-specific score [n abnormal]	78.47 [3]	Untested
Mean ECAS ALS-nonspecific score [n abnormal]	26.65 [2]	Untested

Handedness was determined by the Edinburgh handedness index. ECAS scores are out of a maximum total score of 136, ALS-nonspecific score of 36, and ALS-specific score of 100. C9orf72+ – carrying a repeat expansion of the C9orf72 gene. ECAS: Edinburgh cognitive and behavioral assessment scale. N abnormal: number of participants scoring below the abnormality cutoff score, accounting for years of education.

### Demographics and Characteristics of Patients and Controls

Patient and control characteristics are summarized in Table 1. None of the participants met the criteria for FTD diagnosis. One patient was using noninvasive ventilation at nighttime but was clinically asymptomatic with respect to respiratory impairment and had ALS functional rating scale revised (ALSFRS-R) orthopnea and dyspnea scores of 3 (out of 4).

### Experimental Paradigm

#### Task Design

EEG was recorded across 128-channels during 4 × 5-min-long consecutive sessions during which participants undertook the SART. Participants were seated 1 ± 0.1 m from a computer monitor where numbers one to nine in single-digit format were appearing in a random order for 250 ms, using Presentation software (Neurobehavioral Systems Inc.). Digits were presented in light gray (RGB code: 250, 250, 250 from 255) on a black background to reduce discomfort associated with the bright light from purely white numbers, reported during protocol testing. Font size was randomized between 100, 120, 140, 160, and 180 points to avoid participants using a perceptual template of the number 3s features for target recognition and to encourage cognitive processing of the numerical value (Robertson et al. 1997). Each stimulus was followed by an interstimulus interval of randomized duration between 1120 and 1220 ms during which time a black screen was presented. Responses were registered by clicking the left button of a computer mouse with the right index finger. Each recording session contained 252 trials of which the number 3 appeared at random in 11% of trials. During these sessions lights were turned off, and experimenters were outside the room to avoid visual/auditory distractions. Online performance and EEG measures were monitored by the experimenter in the neighboring recording room. Appropriate break times

were provided to minimize fatigue. Five behavioral measures of performance were captured: NoGo accuracy (percentage of three-digit stimuli followed by response omission), Go accuracy (percentage of nonthree digit stimuli followed by a response in the permitted time window), total accuracy (combined NoGo and Go accuracy), anticipation (clicking less than 150 ms after a go stimulus), and response time.

### Participant Instructions

At the beginning of the session, the task was explained to participants using the following instructions: Participants were instructed to click the left mouse button every time they saw a number except for the number 3. Participants were requested to equally prioritize speed and accuracy as both were used as measures of performance. They were asked to refrain from lifting their finger away from the mouse button between clicks as this would increase response time measures. Instructions to use their finger only to click the mouse, avoiding tension in the arm and shoulder, and to reduce noise in the EEG signal were also given. Participants were then given one practice round to ensure they understood the task, which had up to 45 trials (without performance being measured), and it was performed under supervision of the experimenter.

### Data Acquisition

#### EEG Data

EEG recordings were conducted in the Clinical Research Facility at St. James's Hospital, Dublin using a BioSemi ActiveTwo system (BioSemi B.V.) within a room electromagnetically shielded as a Faraday cage. Subjects were measured with an appropriately sized 128-channel EEG cap. Data were online filtered to a bandwidth of 0–134 Hz and digitized at 512 Hz. Participant responses and response time were measured and recorded in individual files as well as being marked on the EEG recording to allow for precise time-locking and categorization of EEG data epochs.

### Cognitive and Motor Function Tests

Fifteen patients underwent psychological assessment using the ECAS within 4 weeks of the EEG recording. Additionally, ALSFRS-R was collected longitudinally by neurologists at the Irish national ALS specialty clinic in Beaumont Hospital. Total and ALS-specific ECAS scores within 30 days of EEG data collection were available for 15 patients, while ALS-nonspecific scores were available for 17 patients, and ALSFRS-R scores were available for 14 patients. Three additional patients had ALSFRS-R data within 3 months before and after the EEG recording date. Using the data from these two time points, ALSFRS-R scores for these three patients were estimated by interpolation assuming linear decline such that ALSFRS-R scores were available for 17 patients in total. Scores are summarized in Table 1. Of those patients who performed abnormally in the ECAS, two had abnormal ALS-nonspecific scores but not total or ALS-specific scores, one had an abnormal ALS nonspecific score but could not complete the language, fluency, and spelling tasks to provide remaining scores, and one performed abnormally in total and ALS-specific scores but not in their ALS-nonspecific score.

## Data Analysis

### Signal Preprocessing

Signal preprocessing was performed using custom MATLAB (R2014a and R2016a, Mathworks Inc.) scripts and the EEGLAB (Delorme and Makeig 2004) and FieldTrip (Oostenveld et al. 2011) toolboxes. Data were filtered using a 0.3-Hz dual-pass fifth-order Butterworth high-pass filter and a 30-Hz dual-pass 117th-order equiripple finite impulse response low-pass filter. Highly contaminated and nonstereotyped artifacts were removed by visual inspection before epoching data from 200 before the stimulus to 900-ms poststimulus. In cases where responses occurred 150 ms or less after stimulus onset, trials were rejected and counted as an “anticipation error.” Stereotyped artifacts (e.g., eye blinks, eye movements, and noisy single electrodes) were then removed by independent component analysis (Delorme and Makeig 2004). Data were common average referenced, and mean baseline amplitude was subtracted. Mean correct Go (clicking upon a nonthree digit) and NoGo (not clicking upon a “3” digit), ERPs were calculated for each participant. Due to low error number, there were an insufficient number of clean epochs for incorrect trial-associated ERP analysis. The mean number of included artifact-free correct Go/NoGo trials was 810.13/82.22 for patients and 815.42/82.79 for controls out of a maximum of 897/111.

### Sensor Space Analysis

Electrodes of primary interest were chosen based on established topographic maps of the SART N2 and P3 peaks (Zordan et al. 2008; Staub et al. 2015). Four characteristics of the N2 and P3 peaks of each mean Go and NoGo epoch were measured in Fz, FCz, Cz, and Pz electrodes. Namely, the peak (maximal positive amplitude for P3, maximal negative amplitude for N2) amplitude and latency, mean amplitude, and area of the peak within the 220–350-ms and 350–550-ms time windows associated with N2 and P3, respectively. These time windows were chosen based on visual inspection of group mean ERPs and the existing SART-ERP literature (Zordan et al. 2008; Jurgens et al. 2011; Hart et al. 2012, 2015; Kam et al. 2015). Time windows for quantifying peaks of interest were also limited to a maximum of 200 ms to facilitate baseline correction in source analysis (which required matching baseline and peak time windows) while using the same windows for sensor and source analysis.

For assessment of correlations with cognitive performance measures, where similarly significant correlations existed between performance measures and all peak size measures (peak amplitude, mean amplitude, and mean area), we report  $P$  and  $\rho$  values with respect to peak amplitude where describing peak size (e.g., “smaller” or “larger”).

### Source Space Analysis

Channels with continuously noisy data were excluded (excluded channels mean [range] in controls: 0.18 [0–4] and patients: 0.22 [0–4]), and data from these channels were modeled by spline interpolation of neighboring channels. Source localization was performed using custom MATLAB scripts and LCMV beamforming (Van Veen et al. 1997) as implemented in the FieldTrip toolbox. Boundary element head models (Fuchs et al. 2002) incorporating geometries for the brain, skull, and scalp tissues were generated using the ICBM152 MRI template (Fonov et al. 2011), as template-based and individualized boundary element head

models are found to provide comparable localization accuracy (Fuchs et al. 2002; Douw et al. 2018).

LCMV was used to estimate brain power maps for the Go and NoGo trials during two time windows, 220–350- and 350–550-ms poststimulus onset, to localize sources of the N2 and P3 ERPs, respectively. Localization was performed of Go and NoGo trials, as well as of the corresponding baseline windows of equal duration (N2: –130 to 0 ms, P3: –200 to 0 ms). Source localizations were performed using common spatial filters (estimated separately for Go and NoGo and for N2 and P3) calculated from epoched data spanning the start of the peak’s baseline window to the end of that peak’s time window. These common spatial filters were then used to source localize baseline and peak time windows separately. Covariance matrices, used by LCMV, were calculated for individual trials and mean averaged. Regularization of the covariance matrices was implemented at 5% of the average variance of EEG electrodes for each subject separately. Sources within the brain volume were modeled by a grid with 10-mm resolution. The leadfield matrix was normalized to avoid potential norm artifacts (Jonmohamadi et al. 2014). Go and NoGo source activities are reported with baseline correction as  $10 \cdot \log_{10}(\text{Power}_{\text{peak}}/\text{Power}_{\text{baseline}})$ , with the difference between Go and NoGo source activity reported as  $10 \cdot \log_{10}(\text{Power}_{\text{NoGo}}/\text{Power}_{\text{Go}})$ .

## Statistics

### Behavioral Analysis

Group-level comparisons of performance during the SART were implemented with Mann–Whitney  $U$  test. Adaptive false discovery rate (FDR) of 5% was implemented to correct for multiple comparisons, calculated by the Benjamini–Hochberg method (Benjamini and Hochberg 1995).  $P$  values are reported as uncorrected values were significant (determined by a corrected value of  $< 0.05$ ).

### Sensor Space Analysis

A four-factor ANOVA was performed for each of the four peak characteristics for both N2 and P3, resulting in eight ANOVA. For each ANOVA the variables included were sex (male or female, accounting for nongender imbalance), trial type (Go or NoGo), electrode (Fz, FCz, Cz, or Pz), and group (ALS patient or control). Post hoc analysis was implemented by Tukey’s honestly significant difference (Kim 2015). Adaptive false discovery rate (FDR) of 5% was implemented to correct post hoc  $P$  values for multiple comparisons as described for behavioral analysis.

### Source Space Analysis

A 10-mm grid in the brain volume yields 1726 sources including white matter. To analyze these high-dimensional data, a 10% false discovery rate (Benjamini 2010) was used as a frequentist method for determining significant source activity differences. Discrimination ability between patients and controls is quantified by AUROC (Hajian-Tilaki 2013). Empirical Bayesian inference (Efron 2009) was used to calculate the Bayesian posterior probability and statistical power.

### Neuropsychology correlation

Spearman’s rank correlation was used to test the association of the changes in EEG measures (peak characteristics or mean power within a cortical region) and cognitive and functional measures based on interindividual differences. These measures



were as follows: Performance in the SART task during EEG collection, performance in the Delis–Kaplan color word interference task (CWIT) (Delis et al. 2004), ECAS scores, and ALSFRS-R scores. Multiple comparison correction was implemented using FDR (Benjamini and Hochberg 1995) set to 5%. For source-level correlation analysis, mean power was calculated for brain regions identified as major sources of peak activity, defined by the Automated Anatomical Labelling atlas (Tzourio-Mazoyer et al. 2002). Where significant correlations are reported regarding Go and NoGo combination measures, for example, total (Go and NoGo) performance accuracy or the difference between NoGo and Go ERP measures, the relationship was verified not to be due to only Go or NoGo trials.

## Results

### Performance

Patients ( $n = 23$ ) and controls ( $n = 33$ ) did not differ significantly in response time or accuracy. However, patients committed significantly more anticipation errors (patient mean [standard deviation]: 8.73% [13.85%], control mean [standard deviation]: 1.01% [3.26%],  $P = 0.0031$ ).

### Control Characteristics

#### Sensor Space

Mean patient and control Go and NoGo ERPs in electrodes of interest are shown in Figure 1. ANOVAs did not reveal any significant gender effects on waveform features.

N2: N2 in Cz was significantly smaller in Go trials than NoGo trials in controls (peak area  $P = 0.018$ , peak amplitude  $P = 0.006$ ). This N2 difference significantly correlated with faster response times ( $P = 8.08 \times 10^{-6}$ ,  $\rho = 0.69$ ) and poorer NoGo accuracy ( $P = 0.0086$ ,  $\rho = 0.45$ ) in controls (Fig. 2A).

P3: P3 was significantly smaller for Go trials compared with NoGo trials in all four electrodes of interest (Fig. 1, Tukey's post hoc  $P = 3.50 \times 10^{-5}$ – $8.15 \times 10^{-7}$ ). P3 peak latency in the Pz electrodes was also significantly greater in NoGo trials compared with Go trials ( $P = 5.12 \times 10^{-7}$ ). Controls with later responses had later NoGo P3 peaks in Fz ( $P = 0.0020$ ,  $\rho = 0.52$ ), while those with better NoGo accuracy had smaller Go P3 peaks in Cz ( $P = 0.011$ ,  $\rho = -0.43$ ) and FCz ( $P = 0.0034$ ,  $\rho = -0.50$ ), and those with better Go accuracy had larger NoGo P3 peaks in Pz ( $P = 0.0070$ ,  $\rho = 0.46$ ). Better overall accuracy also correlated significantly with smaller NoGo P3 peaks in Fz ( $P = 1.26 \times 10^{-4}$ ,  $\rho = -0.62$ ). Correlations are illustrated in Fig. 3A–D.

#### Source Space

N2: The left primary motor cortex and bilateral dorsolateral prefrontal cortex (DLPFC) and lateral posterior parietal cortex (PPC) were identified as primary mean sources of both Go and NoGo N2, with greater bilateral precuneus activation during NoGo trials (Fig. 4).

P3: Mean P3 sources were similar to those of N2 for Go and NoGo trials, although controls showed decreased left insular, PPC, and DLPFC activity during NoGo trials relative to Go trials (Fig. 5).

### ALS Patient Differences

Differences in peak and source measures between patients and controls are summarized in Table 2.

### Sensor Space (ERP) Differences

N2: Patients did not show a significant difference in the N2 peak between Go and NoGo trials. Correspondingly, N2 was significantly smaller for NoGo trials in ALS patients compared with controls in FCz ( $P = 5.08 \times 10^{-4}$ ) and Cz ( $P = 0.001$ ). Unlike controls, the difference in N2 between Go and NoGo trials did not correlate with SART performance; however those patients with greater N2 NoGo-Go differences in Cz had higher ECAS total ( $P = 0.0022$ ,  $\rho = -0.73$ , Fig. 2A) and ALS-specific ( $P = 0.017$ ,  $\rho = -0.61$ ) scores, indicating better cognitive performance, particularly in tasks of executive function and language (Fig. 2B).

P3: The P3 peak did not differ significantly between patients and controls for any trial type or characteristic. Patients and control with longer response times had later ( $P = 0.0074$ ,  $\rho = 0.35$ ), smaller ( $P = 2.31 \times 10^{-5}$ ,  $\rho = -0.53$ ) Go P3 peaks in Cz (Fig. 3E,F). Otherwise, patients did not display the correlations between their P3 peak characteristics and task performance that were observed for controls. Overall accuracy was found to significantly correlate with later Go P3 peaks in Cz in patients ( $P = 0.0069$ ,  $\rho = 0.54$ , Fig. 3C).

### Source Space Differences

N2: Patients showed similar patterns of source activity to controls during N2 (Fig. 4).

P3: While similar locations of source activity were observed in patients and controls during Go and NoGo trials, ALS patients showed similar differences between NoGo and Go source differences to N2 during P3 (Fig. 5), unlike controls. Correspondingly, ALS patients displayed widespread, significantly increased activity during NoGo trials relative to Go trials when compared with controls, with the most discriminant differences (AUROC  $> 0.75$ ) being in the left inferior parietal lobule and left insula (Fig. 6).

### Source Space Correlations in ALS Patients

Greater right precuneus power during P3 in NoGo relative to Go trials negatively correlates with CWIT inhibition score ( $P = 0.0015$ ,  $\rho = -0.91$ , Fig. 7). As greater scores in this task indicated poorer behavioral inhibition, this relationship demonstrated that the abnormal activation of this area was associated with greater preservation of this executive function.

## Discussion

This study demonstrates for the first time the specific cortical structures that contribute to performance of the SART and quantifies the relationship between SART performance measures and underlying cognitive performance. Furthermore, we have identified abnormalities in cortical function which strongly correlate with executive impairment in ALS.

### ERP Peak Characteristics

At sensor level, our control findings were consistent with the literature, demonstrating the robustness of SART-associated ERPs. N2 and P3 peaks were present in the anticipated time windows and, as expected, larger for healthy individuals during correct response omission.

#### Central N2

NoGo N2 was maximal in Cz, as previously established. We identified that smaller differences in N2 size between NoGo and Go trials were associated with faster reaction times. We also

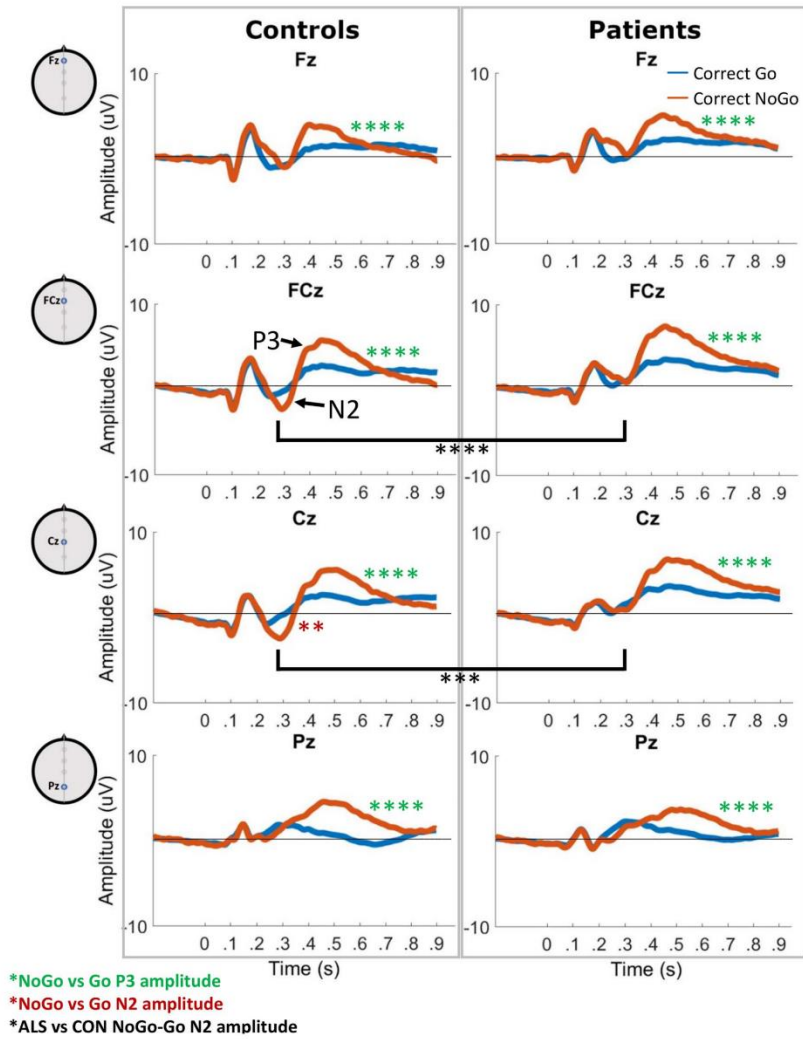


**Figure 1.** Mean Go (blue) and NoGo (red) trial ERPs in controls and ALS patients. N2 peaks are visible in the NoGo trial ERP in Fz and Cz in the 220–350-ms window. P3 peaks are present in the 350–550-ms window in both Go and NoGo trial ERPs in all electrodes. Green asterisks represent significantly larger P3 peak amplitudes in NoGo versus Go trials. Red asterisks represent significantly larger (more negative) N2 peak amplitudes in NoGo versus Go trials. Black asterisks represent significant differences in NoGo-Go N2 peak amplitude between ALS patients and controls. \*\* $P < 0.01$ , \*\*\*\* $P < 0.0001$ . CON: controls.

identified a correlation between smaller NoGo N2 peaks and better NoGo trial accuracy. As the N2 peak has been associated with automated motor response control (Zordan et al. 2008), this may reflect greater ability to withhold and greater response speed where less cortical resources are required to inhibit upper motor neurons.

Notably, these correlations were not present for ALS patients, which may represent the compensatory engagement of alternative cortical resources. Alternatively, the established malfunction of inhibitory cells of the motor system (Menon et al. 2019) in addition to upper motor neurons may lead to reduction in NoGo N2 in combination with slowing reaction times.

Downloaded from https://academic.oup.com/ercor/article/30/9/4834/5820432 by guest on 11 January 2021

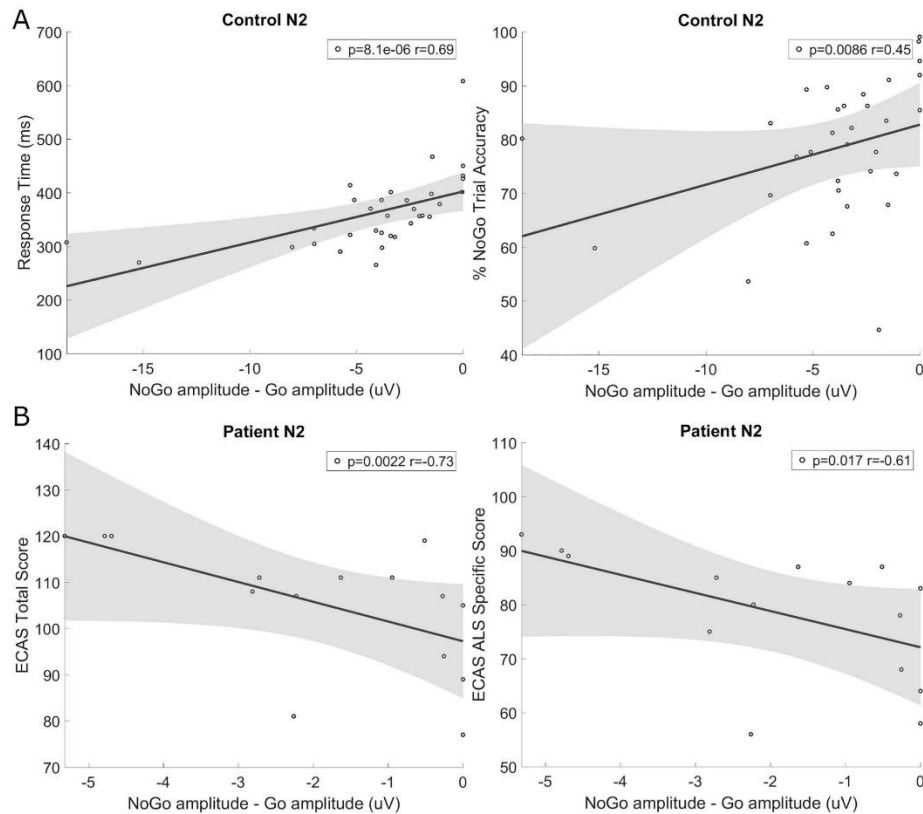


**Figure 2.** Correlations between NoGo minus Go (NoGo-Go) N2 peak amplitude in Cz and cognitive task performance. (A) Correlation with response time and NoGo trial accuracy in controls demonstrates that those with smaller NoGo versus Go N2 peak differences had significantly faster response times and better NoGo accuracy. (B) Correlation with patient ECAS total and ALS-specific score demonstrates that those with smaller (less negative) N2 peak differences had lower ECAS scores.

#### Frontal and Parietal P3

The P3 peak was present across the frontoparietal axis of sensors during NoGo trials in keeping with the SART-ERP literature (Zordan et al. 2008; Hart et al. 2012; Staub et al. 2015). Such spatially distributed P3 peaks associated with other cognitive tasks have been shown to consist of two distinct entities, namely, the frontal and parietal P3. Frontal P3 peaks have been associated with orientation to novel stimuli, declining over task duration although remaining elevated in distractible children (Kilpeläinen et al. 1999) and those with panic disorder (Richard Clark et al. 1996). By contrast, parietal P3 peaks are associated with working memory and attention to target stimuli (Richard Clark et al. 1996; Kilpeläinen et al. 1999).

Here we have identified similarly distinct behaviors in the frontal and parietal SART-associated P3 peaks. In frontocentral electrodes, P3 latency related to response timing and is likely to provide an index of orientation speed. Smaller frontocentral

P3 peaks were associated with more accurate performance in the opposite trial type (i.e., better Go performance with smaller NoGo peaks and vice versa). By contrast, larger NoGo parietal P3 was associated with better Go trial performance. This is in keeping with the cognitive resources required for accurate Go and NoGo SART performance. The engagement of working memory and attentional control was indicated by a large NoGo parietal P3, and quick orientation to the task was indicated by earlier, smaller frontal P3 peaks (Richard Clark et al. 1996; Kilpeläinen et al. 1999).

The orienting frontal P3 is typically earlier than the parietal P3; however, it has been hypothesized that frontal P3 peaks may also encompass compensatory prefrontal engagement due to parietal decline (van Dinteren et al. 2014). This may explain why ALS patients, but not in controls, demonstrated greater Cz P3 peak latencies during Go trials in those with better accuracy.

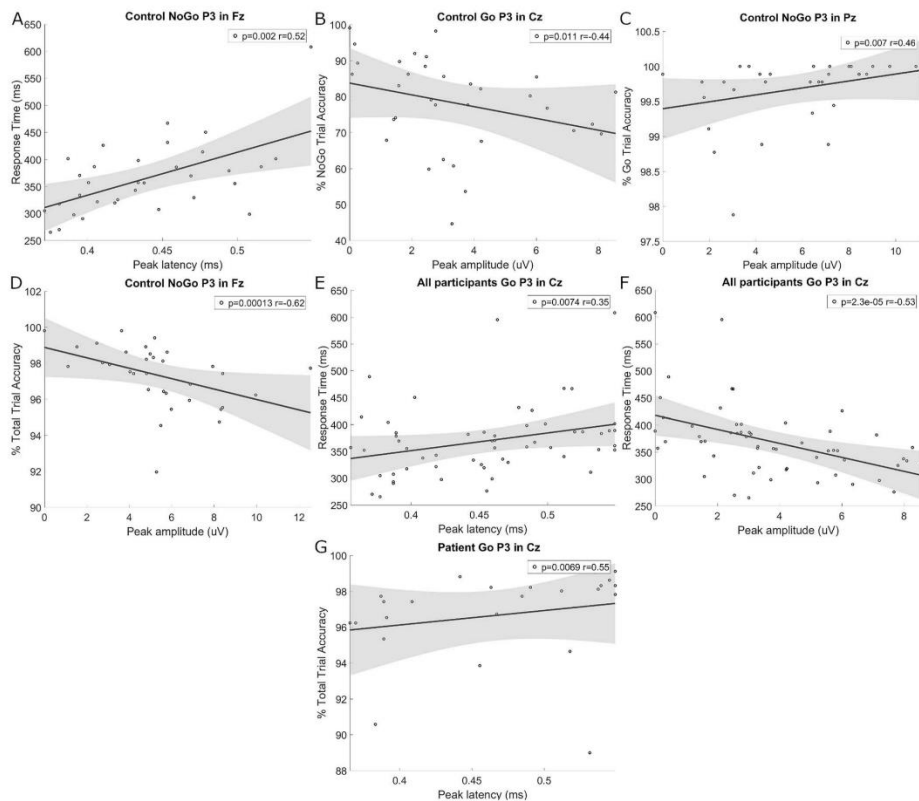


**Figure 3.** Correlations between P3 peak characteristics and SART performance. In controls, (A) later responses correlate with later P3 peaks in Fz during NoGo trials, (B) better NoGo accuracy inversely correlates with Go P3 peak size in Cz, (C) Go accuracy positively correlates with NoGo P3 peak amplitude in Pz, and (D) overall accuracy inversely correlates with NoGo P3 peak amplitude in Fz. In all participants, (E) later responses correlate with longer peak latency and (F) smaller peak amplitude during Go trials in Cz. In patients, (G) greater overall accuracy correlates with longer Go P3 peak latency in Cz.

### Cortical Source Imaging

At source level both Go and NoGo N2 and P3 peaks were associated with extensive prefrontal and motor cortex engagement, particularly in the left cortex, in keeping with the use of the right hand for task performance. Such widespread cortical engagement is expected, given the numerous cognitive and motor domains required for accurate task performance. The medial PPC (i.e., the precuneus) was additionally engaged during NoGo trials relative to Go trials during N2, in keeping with its role in both voluntary attention shifting and movement control (Cavanna and Trimble 2006). By contrast, the left insula and inferior parietal lobule show lower power in NoGo trials relative to Go trials during P3, in keeping with the role of the left insula in the salience network (Uddin et al. 2017) and goal-directed behavior (Varjačić et al. 2018). The left inferior parietal

lobule has been attributed numerous functions, among which are object-directed action (Chen et al. 2018) and expectancy violation (O'Connor et al. 2010). This engagement of numerous cortical structures by different elements of the SART highlights the range of cortical pathologies that could contribute to decline in SART performance measures. While SART-ERP analysis can temporally dissect the cause of such performance decline, it is clear from source imaging that a specific peak abnormality could also result from dysfunction in several different cortical structures. Source imaging can therefore not only inform on source contributing to cognitive and motor symptoms but could also discriminate between psychiatric or neurodegenerative syndromes with similar symptoms driven by differing cortical pathologies.

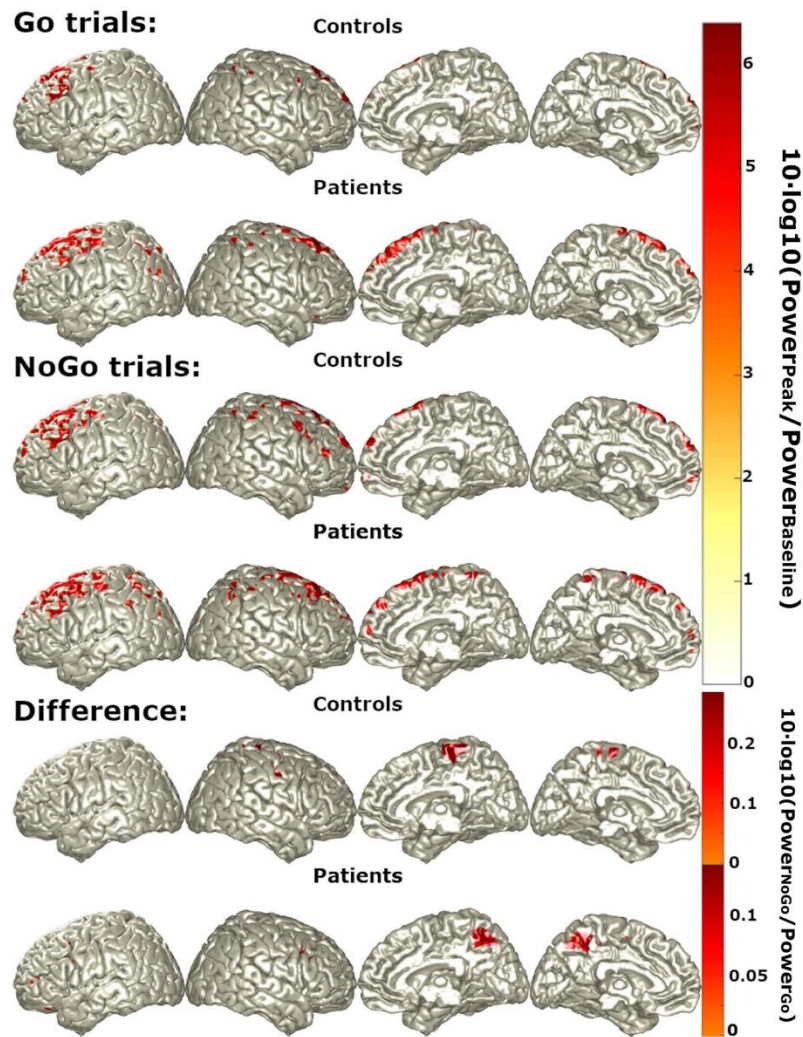


Figure 4. Primary sources (regions with top 5% power) of N2 during Go trials, NoGo trials, and NoGo trials relative to Go trials ("difference") in controls (first rows) and patients (second rows).

**Quantifying Cortical Pathology Driving Cognitive Impairment in ALS**

ALS patients maintained similar Go and NoGo accuracy but were more likely to attempt to complete trials rapidly clicking before cognitively processing the presented digit, resulting in greater anticipation error. Despite sensor-level differences, patients and control activity did not differ significantly at a specific N2 source.

This is likely to be a function of spatially distributed differences in activity which summate in signals captured by individual electrodes at source level. Patients did, however, demonstrate very similar elevation in precuneus activity during NoGo relative to Go trials in both N2 and P3. As this elevation in right precuneus activity during P3 was associated with greater behavioral inhibitory function, this may represent a compensatory recruitment of this region. Indeed, this exemplifies the utility of source

Downloaded from https://academic.oup.com/cercor/article/30/9/4834/5820432 by guest on 11 January 2021

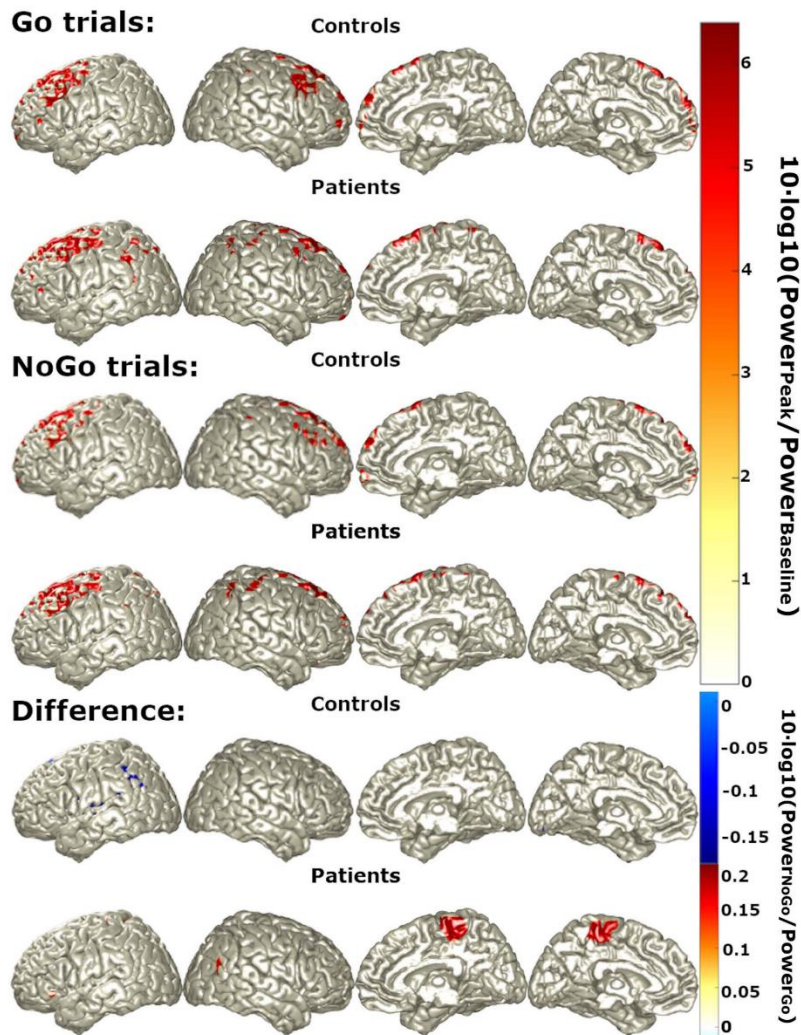


Figure 5. Primary sources (regions with 5% power) of P3 during Go trials, NoGo trials, and NoGo trials relative to Go trials ("difference") in controls (first rows) and patients (second rows).

localized EEG during task performance for quantifying cognitive pathology during presymptomatic phases of compensatory cortical activity that are more amenable to clinical intervention.

ALS patients demonstrated additional widespread cortical activity elevation during NoGo relative to Go trials during P3, particularly in the left insula and inferior parietal lobule, which

showed very good discrimination between patients and controls (AUROC > 0.75). Such posterior parietal hyperengagement has previously been observed during involuntary attention switching (McMackin et al. 2019b, Dukic et al. 2019) and at rest (Proudford et al. 2018; Dukic et al. 2019) and may provide additional discriminatory power in the development of cortical diagnostic

Table 2 Significant differences in ALS sensor-level and source-level measures compared with controls

Sensor level (ERP peaks)			
Peak	Trial	Electrode	Change in ALS
N2	NoGo	Cz	↓ Peak amplitude
		FCz	↓ Peak amplitude
P3	NoGo-Go	Cz	No correlation to task performance
	Go	Cz	Later peak positively correlates with greater overall accuracy, no correlation between peak amplitude and accuracy.
	NoGo	Fz, Pz	No correlation between amplitude or latency to performance
Source level			
Peak	Trial	Source	Change in ALS
P3	NoGo-Go	Left posterior parietal and insular cortex	↑ Activation, area under receivership operating curve > 0.75

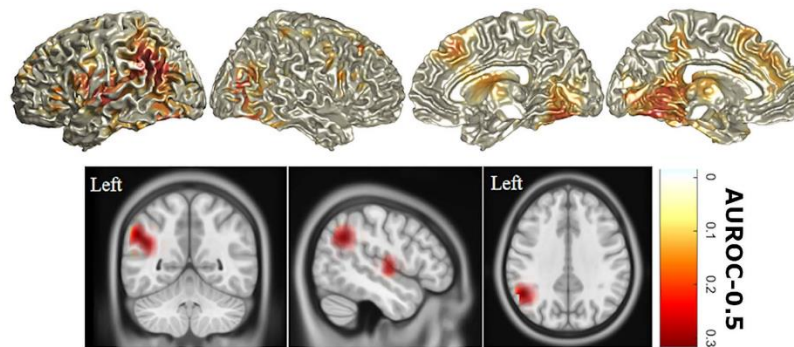


Figure 6. P3 sources with statistically significant differences in activity in ALS compared with controls. Differences between NoGo and Go trial source activity during the P3 peak were compared between ALS patients and controls. All highlighted areas represent significant (FDR = 10%, type II error = 0.38 Bayesian Posterior probability = 0.87) increases in power with heat map values representing AUROC = 0.5 (i.e., perfect discrimination = 0.5). Orthogonal MRI scans show only those differences with an AUROC > 0.75, that is, very good discriminators. AUROC: area under the receivership operating curve.

biomarkers. A previous study in Huntington's disease identified reduced activity in the left DLPFC (Beste et al. 2008), right medial frontal, and anterior cingulate cortex during the NoGo P3, while we find hyperactivity in these areas in ALS, highlighting the ability of this task to identify differing underlying cortical pathologies in neurodegenerations with overlapping cognitive and behavioral symptoms.

We acknowledge that while these cross-sectional data serve well to characterization of ALS disease heterogeneity, these measures demand larger-scale studies for adequately powered subgroup analysis. Additional larger, longitudinal studies will be required to further evaluate the application of this technology in clinical trials and disease prognostics.

In conclusion, here we have provided a spatially and temporally precise description of the cortical activity which underlies the N2 and P3 peaks of the randomized SART-ERP in healthy adults and illustrated the applications of this methodology for interrogating cognitive and motor malfunction in a complex neurodegenerative disease. While larger patient recruitment is required for further investigation of the use of SART as an ALS biomarker, we have established that the SART-ERP and its

underlying source activity can provide objective, quantitative, early markers of cognitive and motor pathology. The localization of EEG recorded during a wider battery of cognitive, motor, and sensory tasks has considerable potential to provide patient-specific profiles of cortical network disturbance which could in turn provide biomarkers that improve patient subgrouping, clinical trial stratification, and prognostic accuracy.

### Funding

Irish Research Council (grant numbers GOIPG/2017/1014, GOIPD/2015/213); the Health Research Board (grant numbers HRA-POR-2013-246, MRCG-2018-02); Science Foundation Ireland (grant number 16/ERC/3854); Research Motor Neurone (MRCG-2018-02); and the Thierry Latran Foundation. The psychology aspects of the study were supported by the Motor Neurone Disease Association (grant number Hardiman/Oct15/879-792). MM was supported by Transregional Collaborative Research Center (grant number SFB TR-128) and Boehringer Ingelheim Fonds (grant number BIF-03).

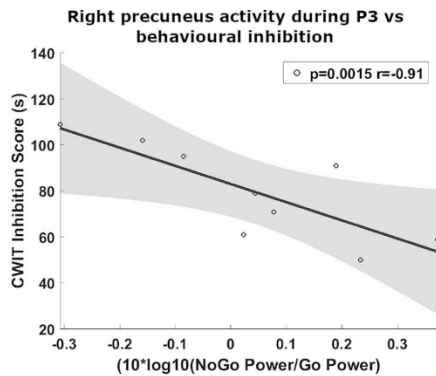


Figure 7. Greater behavioral inhibition in ALS is associated with increased right precuneus activity during NoGo P3 relative to Go P3. Higher CWIT inhibition score indicates poorer behavioral inhibition.

## Notes

The authors thank Ms Orla Keenan for her contribution to experimental setup. We thank the Wellcome-HRB Clinical Research Facility at St James's Hospital in providing a dedicated environment for the conduct of high-quality clinical research.

Conflicts of Interest: None declared.

## Author Contributions

R.M., B.N., S.D., M.M., N.P., O.H.—conception and design of the study; R.M., S.D.—acquisition and analysis of data; and R.M., S.D., B.N., M.M., O.H.—drafting of manuscript or figures.

## References

- Bellgrove MA, Hawi Z, Gill M, Robertson IH. 2006. The cognitive genetics of attention deficit hyperactivity disorder (ADHD): sustained attention as a candidate phenotype. *Cortex*. 42:838–845.
- Benjamini Y. 2010. Discovering the false discovery rate. *Journal of the Royal Statistical Society: series B (Statistical Methodology)*. 72:405–416.
- Benjamini Y, Hochberg Y. 1995. Controlling the false discovery rate: a practical and powerful approach to multiple testing. *Journal of the Royal Statistical Society Series B (Methodological)*. 57:289–300.
- Beste C, Saft C, Andrich J, Gold R, Falkenstein M. 2008. Response inhibition in Huntington's disease—a study using ERPs and sLORETA. *Neuropsychologia*. 46:1290–1297.
- Cavanna AE, Trimble MR. 2006. The precuneus: a review of its functional anatomy and behavioural correlates. *Brain*. 129:564–583.
- Chen Q, Garcea FE, Jacobs RA, Mahon BZ. 2018. Abstract representations of object-directed action in the left inferior parietal lobule. *Cerebral Cortex*. 28:2162–2174.
- Delis DC, Kramer JH, Kaplan E, Holdnack J. 2004. Reliability and validity of the Delis-Kaplan executive function system: an update. *Journal of the International Neuropsychological Society*. 10:301–303.
- Delorme A, Makeig S. 2004. EEGLAB: an open source toolbox for analysis of single-trial EEG dynamics including independent component analysis. *Journal of Neuroscience Methods*. 134:9–21.
- Douw L, Nieboer D, Stam CJ, Tewarie P, Hillebrand A. 2018. Consistency of magnetoencephalographic functional connectivity and network reconstruction using a template versus native MRI for co-registration. *Human Brain Mapping*. 39:104–119.
- Dukic S, McMackin R, Buxo T, Fasano A, Chipika R, Pinto-Grau M, Costello E, Schuster C, Hammond M, Heverin M, et al. 2019. Patterned functional network disruption in amyotrophic lateral sclerosis. *Human Brain Mapping*. 40:4827–4842.
- Efron B. 2009. Empirical Bayes estimates for large-scale prediction problems. *Journal of the American Statistical Association*. 104:1015–1028.
- Elamin M, Phukan J, Bede P, Jordan N, Byrne S, Pender N, Hardiman O. 2011. Executive dysfunction is a negative prognostic indicator in patients with ALS without dementia. *Neurology*. 76:1263–1269.
- Fonov V, Evans AC, Botteron K, Almli CR, McKinstry RC, Collins DL. 2011. Unbiased average age-appropriate atlases for pediatric studies. *Neuroimage*. 54:313–327.
- Fuchs M, Kastner J, Wagner M, Hawes S, Ebersole JS. 2002. A standardized boundary element method volume conductor model. *Clinical Neurophysiology*. 113:702–712.
- Gan L, Cookson MR, Petrucelli L, La Spada AR. 2018. Converging pathways in neurodegeneration, from genetics to mechanisms. *Nature Neuroscience*. 21:1300–1309.
- Gregory JM, McDade K, Bak TH, Pal S, Chandran S, Smith C, Abrahams S. 2019. Executive, language and fluency dysfunction are markers of localised TDP-43 cerebral pathology in non-demented ALS. *Journal of Neurology, Neurosurgery, Psychiatry*.
- Hajian-Tilaki K. 2013. Receiver operating characteristic (ROC) curve analysis for medical diagnostic test evaluation. *Caspian Journal of Internal Medicine*. 4:627–635.
- Hart EP, Dumas EM, Reijntjes R, Van Der Hiele K, Van Den Bogaard SJA, Middelkoop HAM, Roos RAC, Van Dijk JG. 2012. Deficient sustained attention to response task and P300 characteristics in early Huntington's disease. *Journal of Neurology*. 259:1191–1198.
- Hart EP, Dumas EM, van Zwet EW, van der Hiele K, Jurgens CK, Middelkoop HA, van Dijk JG, Roos RA. 2015. Longitudinal pilot-study of sustained attention to response task and P300 in manifest and pre-manifest Huntington's disease. *Journal of Neuropsychology*. 9:10–20.
- Huntley JD, Hampshire A, Bor D, Owen AM, Howard RJ. 2017. The importance of sustained attention in early Alzheimer's disease. *International journal of geriatric psychiatry*. 32:860–867.
- Jin CY, Borst JP, van Vugt MK. 2019. Predicting task-general mind-wandering with EEG. *Cognitive, Affective, & Behavioral Neuroscience*. 19:1059–1073.
- Jonmohamadi Y, Poudel G, Innes C, Weiss D, Krueger R, Jones R. 2014. Comparison of beamformers for EEG source signal reconstruction. *Biomedical Signal Processing and Control*. 14:175–188.
- Jurgens CK, Van Der Hiele K, Reijntjes R, Van De Wiel L, Witjes-Ané MNW, Van Der J, Roos RAC, Middelkoop HAM, van Dijk JG. 2011. Basal ganglia volume is strongly related to P3 event-related potential in premanifest Huntington's disease. *European Journal of Neurology*. 18:1105–1108.



- Kam JW, Mickleborough MJ, Eades C, Handy TC. 2015. Migraine and attention to visual events during mind wandering. *Experimental Brain Research*. 233:1503–1510.
- Kilpeläinen R, Luoma L, Herrgård E, Yppärilä H, Partanen J, Karhu J. 1999. Persistent frontal P300 brain potential suggests abnormal processing of auditory information in distractible children. *Neuroreport*. 10:3405–3410.
- Kim H-Y. 2015. Statistical notes for clinical researchers: post-hoc multiple comparisons. *Restorative Dentistry and Endodontics*. 40:172–176.
- Ludolph A, Drory V, Hardiman O, Nakano I, Ravits J, Robberecht W, Shefner J, WFN Research Group On ALS/MND. 2015. A revision of the El Escorial criteria - 2015. *Amyotroph Lateral Sclerosis and Frontotemporal Degeneration*. 16:291–292.
- Lulé D, Ludolph AC, Kassubek J. 2009. MRI-based functional neuroimaging in ALS: an update. *Amyotroph Lateral Sclerosis*. 10:258–268.
- McMackin R, Bede P, Pender N, Hardiman O, Nasseroleisami B. 2019a. Neurophysiological markers of network dysfunction in neurodegenerative diseases. *Neuroimage Clinical*. 22:101706.
- McMackin R, Dukic S, Broderick M, Iyer PM, Pinto-Grau M, Mohr K, Chipika R, Coffey A, Buxo T, Schuster C, et al. 2019b. Dysfunction of attention switching networks in amyotrophic lateral sclerosis. *Neuroimage Clinical*. 22:101707.
- McMackin R, Muthuraman M, Groppa S, Babiloni C, Taylor J-P, Kiernan MC, Nasseroleisami B, Hardiman O. 2019c. Measuring network disruption in neurodegenerative diseases: new approaches using signal analysis. *Journal of Neurology, Neurosurgery, and Psychiatry*. 90:1011–1020.
- Menon P, Yiannikas C, Kiernan MC, Vucic S. 2019. Regional motor cortex dysfunction in amyotrophic lateral sclerosis. *Annals of Clinical and Translational Neurology*. 6:1373–1382.
- O'Connor AR, Han S, Dobbins IG. 2010. The inferior parietal lobule and recognition memory: expectancy violation or successful retrieval? *Journal of Neuroscience*. 30:2924–2934.
- O'Grada C, Barry S, McGlade N, Behan C, Haq F, Hayden J, O'Donoghue T, Peel R, Morris D.W, O'Callaghan E, et al. 2009. Does the ability to sustain attention underlie symptom severity in schizophrenia? *Schizophrenia research*. 107(2-3):319–323.
- Oostenfeld R, Fries P, Maris E, Schoffelen J-M. 2011. FieldTrip: open source software for advanced analysis of MEG, EEG, and invasive electrophysiological data. *Computational Intelligence and Neuroscience*. 2011:1–9.
- Phukan J, Elamin M, Bede P, Jordan N, Gallagher L, Byrne S, Lynch C, Pender N, Hardiman O. 2012. The syndrome of cognitive impairment in amyotrophic lateral sclerosis: a population-based study. *Journal of Neurology, Neurosurgery, and Psychiatry*. 83:102–108.
- Pinto-Grau M, Burke T, Lonergan K, McHugh C, Mays I, Madden C, Vajda A, Heverin M, Elamin M, Hardiman O, et al. 2017. Screening for cognitive dysfunction in ALS: validation of the Edinburgh cognitive and behavioural ALS screen (ECAS) using age and education adjusted normative data. *Amyotroph Lateral Sclerosis Frontotemporal Degeneration*. 18:99–106.
- Proudfoot M, Colclough GL, Quinn A, Wu J, Talbot K, Benatar M, Nobre AC, Woolrich MW, Turner MR. 2018. Increased cerebral functional connectivity in ALS: a resting-state magnetoencephalography study. *Neurology*. 90:e1418–e1424.
- Richard Clark C, McFarlane AC, Weber DL, Battersby M. 1996. Enlarged frontal P300 to stimulus change in panic disorder. *Biological Psychiatry*. 39:845–856.
- Robertson IH, Manly T, Andrade J, Baddeley BT, Yiend J. 1997. 'oops!': Performance correlates of everyday attentional failures in traumatic brain injured and normal subjects. *Neuropsychologia*. 35:747–758.
- Staub B, Doignon-Camus N, Marques-Carreira JE, Bacon É, Bonfond A. 2015. Age-related differences in the use of automatic and controlled processes in a situation of sustained attention. *Neuropsychologia*. 75:607–616.
- Turner MR, Agosta F, Bede P, Govind V, Lulé D, Verstraete E. 2012. Neuroimaging in amyotrophic lateral sclerosis. *Biomarkers in Medicine*. 6:319–337.
- Tzourio-Mazoyer N, Landeau B, Papathanassiou D, Crivello F, Etard O, Delcroix N, Mazoyer B, Joliot M. 2002. Automated anatomical labeling of activations in SPM using a macroscopic anatomical parcellation of the MNI MRI single-subject brain. *Neuroimage*. 15:273–289.
- Uddin LQ, Nomi JS, Hebert-Seropian B, Ghaziri J, Boucher O. 2017. Structure and function of the human insula. *Journal of Clinical Neurophysiology*. 34:300–306.
- van Dinteren R, Arns M, Jongasma MLA, Kessels RPC. 2014. Combined frontal and parietal P300 amplitudes indicate compensated cognitive processing across the lifespan. *Frontiers in Aging Neuroscience*. 6:294.
- Van Veen BD, van Drongelen W, Yuchtman M, Suzuki A. 1997. Localization of brain electrical activity via linearly constrained minimum variance spatial filtering. *IEEE Transactions on Biomedical Engineering*. 44:867–880.
- Varjačić A, Mantini D, Levenstein J, Slavkova ED, Demeyere N, Gillebert CR. 2018. The role of left insula in executive set-switching: lesion evidence from an acute stroke cohort. *Cortex, In Memory of Professor Glyn Humphreys*. 107:92–101.
- Zordan L, Sarlo M, Stablum F. 2008. ERP components activated by the "GO!" and "WITHHOLD!" conflict in the random sustained attention to response task. *Brain and Cognition*. 66:57–64.



## PAPER

## OPEN ACCESS

## RECEIVED

19 August 2020

## REVISED

13 November 2020

## ACCEPTED FOR PUBLICATION

4 January 2021

## PUBLISHED

25 February 2021

Original content from this work may be used under the terms of the [Creative Commons Attribution 4.0 licence](https://creativecommons.org/licenses/by/4.0/).

Any further distribution of this work must maintain attribution to the author(s) and the title of the work, journal citation and DOI.



## Sustained attention to response task-related beta oscillations relate to performance and provide a functional biomarker in ALS

Roisin McMackin<sup>1</sup>, Stefan Dukic<sup>1,2</sup>, Emmet Costello<sup>1,3</sup>, Marta Pinto-Grau<sup>1,3</sup>, Orla Keenan<sup>1</sup>, Antonio Fasano<sup>1</sup>, Teresa Buxo<sup>1</sup>, Mark Heverin<sup>1</sup>, Richard Reilly<sup>4,5</sup>, Niall Pender<sup>1,3</sup>, Orla Hardiman<sup>1,6,7</sup> and Bahman Nasseroleislami<sup>1,7</sup>

<sup>1</sup> Academic Unit of Neurology, Trinity College Dublin, The University of Dublin, Dublin, Ireland

<sup>2</sup> Department of Neurology, University Medical Centre Utrecht Brain Centre, Utrecht University, Utrecht, The Netherlands

<sup>3</sup> Department of Psychology, Beaumont Hospital Dublin, Dublin, Ireland

<sup>4</sup> Trinity College Institute of Neuroscience, Trinity College Dublin, The University of Dublin, Dublin, Ireland

<sup>5</sup> Trinity Centre for Biomedical Engineering, Trinity College Dublin, The University of Dublin, Dublin, Ireland

<sup>6</sup> Department of Neurology, Beaumont Hospital Dublin, Dublin, Ireland

<sup>7</sup> Joint last authorship.

E-mail: [hardimao@tcd.ie](mailto:hardimao@tcd.ie)

**Keywords:** EEG, oscillations, attention, ALS, executive function, event related synchronization, event related desynchronization

### Abstract

**Objective.** To characterize the cortical oscillations associated with performance of the sustained attention to response task (SART) and their disruptions in the neurodegenerative condition amyotrophic lateral sclerosis (ALS). **Approach.** A randomised SART was undertaken by 24 ALS patients and 33 healthy controls during 128-channel electroencephalography (EEG). Complex Morlet wavelet transform was used to quantify non-phase-locked oscillatory activity in event-related spectral perturbations associated with performing the SART. We investigated the relationships between these perturbations and task performance, and associated motor and cognitive changes in ALS. **Main results.** SART induced theta-band event-related synchronization (ERS) and alpha- and beta-band event-related desynchronization (ERD), followed by rebound beta ERS, in both Go and NoGo trials across the frontoparietal axis, with NoGo trials eliciting greater theta ERS and lesser beta ERS. Controls with greater Go trial beta ERS performed with greater speed and less accuracy. ALS patients exhibited increased anticipation compared to controls but similar reaction times and accuracy. Prefrontal (area under the receiver operating characteristic curve (AUROC) = 0.8, Cohen's  $d$  = 0.97) and parietal (AUROC = 0.82, Cohen's  $d$  = 1.12) beta-band ERD was significantly reduced in ALS but did not relate to performance, while patients with higher Edinburgh Cognitive and Behavioural ALS Screen (ECAS) ALS-specific scores demonstrated greater ERS in beta ( $\rho$  = 0.72) upon successful withholding. **Significance.** EEG measurement of task-related oscillation changes reveals variation in cortical network engagement in relation to speed versus accuracy strategies. Such measures can also capture cognitive and motor network pathophysiology in the absence of task performance decline, which may facilitate development of more sensitive early neurodegenerative disease biomarkers.

### 1. Introduction

The sustained attention to response task (SART) is a widely employed task of ability to sustain overt attention. This subdomain of executive function is probed by requiring the participant to withhold a motor response to a rare target among regular responses to non-target stimuli. While accuracy and response time measures have shown ability to capture impairments

in sustained attention [1], the contribution of a combination of perceptual, planning, motor and attention functions to these task-specific measures makes them relatively non-specific to the dysfunction in different regions of cortical networks. Further, differences in performance may reflect variation in participant approach with respect to the speed-accuracy trade-off (i.e. the extent to which response speed is prioritised over response accuracy) [2].

The functions and neural processes engaged by SART are reflected in the cortical regions it activates, including prefrontal, parietal and motor domains. We have recently demonstrated this cortical activation through the combination of quantitative electroencephalography (EEG) and source analysis, which provides excellent temporal resolution with good spatial resolution. We have also demonstrated that disease-related abnormalities in cortical network activation can be interrogated individually using spatially and temporally specific measures to determine the nature of underlying network disruption, even in the absence of impaired task performance [3].

Functional network communication at short and long range is captured by EEG as sinusoidal oscillations of specific frequencies, typically grouped into delta (<4 Hz), theta (4–7 Hz), alpha (8–12 Hz), beta (13–30 Hz) and gamma (>30 Hz) bands. Changes in the magnitude (power) of these oscillations in relation to task performance are referred to as event-related spectral perturbations (ERSP). ERSP reflect changes in the degree of network communication within and between cortical regions as a task is performed [4, 5]. Relative increase in oscillation magnitude is referred to as event-related synchronization (ERS), while relative decreases are referred to as event-related desynchronization (ERD). These ERSP may be phase-locked (i.e. occurring at the same position along the sinusoidal waveform across trials relative to the stimulus delivery) or non-phase locked (i.e. oscillation magnitude changes consistently, but the position along the sinusoidal waveform relative to stimulus delivery varies across trials) [6]. While phase-locked changes are captured by time domain analysis, such as our previous analysis of event related potentials, non-phase locked changes are lost through averaging across trials. These non-phase locked oscillations can capture important information on cortical network performance and provide valuable information on physiological processes. Additionally, they have highlighted disrupted intracortical motor and cognitive network communication in Parkinson's [7, 8] and Alzheimer's [9] disease, predict cognitive decline in mild cognitive impairment [10], and provide greater diagnostic ability than event-related potential measures in mild cognitive impairment and Alzheimer's disease [11].

Here, we investigated the changes in cortical oscillations during the SART by quantifying non-phase locked ERSP. We sought to establish whether these oscillations are disrupted in amyotrophic lateral sclerosis (ALS) using time-frequency domain EEG analysis, and to determine whether such oscillations predict task performance measures in controls and in ALS patients. We hypothesised that these measures will provide additional insight into the nature of dysfunction in cortical networks which bridge motor and cognitive function in ALS.

## 2. Methods

### 2.1. Participants

#### 2.1.1. Recruitment

Patients were recruited at Ireland's National ALS specialty clinic in Beaumont Hospital. Controls included healthy, age-matched, population-based individuals recruited from an existing cohort established and maintained by the Irish ALS Research Group.

#### 2.1.2. Inclusion criteria

All participants were over 18 years of age and able to give informed written consent, or in the presence of two witnesses, verbal consent. Patients were diagnosed with Possible, Probable or Definite ALS in accordance with the El Escorial Revised Diagnostic Criteria.

#### 2.1.3. Exclusion criteria

Those with neurological functional/structural, psychological or muscular disorders other than ALS (including those with comorbid frontotemporal dementia (FTD)) and those currently taking neuromodulatory or myomodulatory medications (e.g. antidepressants, anti-epileptics, GABA antagonists) that could affect recordings were excluded, except for riluzole.

### 2.2. Experimental paradigm

The experimental paradigm is identical to that described in detail in our previous SART study [3], briefly described here. Participants were seated at a distance of  $1 \pm 0.1$  m in front of a monitor. Individual digits of one to nine were shown in random order for 250 ms with an interstimulus interval randomised between 1120 and 1220 ms during which the screen was black. Responses were captured by clicking the left button of a computer mouse with the right index finger. Four recording sessions of 252 trials, with the number 3 appearing in 11% of trials, were undertaken. The behavioural measures captured were: response time, overall response accuracy, NoGo accuracy (percentage of 3-digit stimuli followed by response omission), Go accuracy (percentage of non-3 digit stimuli followed by a response in the permitted time window) and anticipation rate (clicking less than 150 ms after a go stimulus). Participants were instructed to click every time they saw a number except for the number three, to equally prioritise speed and accuracy and to use only their finger to respond, to reduce EMG artefact in the EEG signal. Participants performed one practice round without performance being measured under supervision of the experimenter.

### 2.3. Data acquisition

#### 2.3.1. EEG

EEG recordings were taken with 128 Ag-AgCl electrodes during the experimental paradigm via

the BioSemi® ActiveTwo system (BioSemi B.V., Amsterdam, The Netherlands). Recordings were performed at St. James's Hospital, Dublin. EEG signals were filtered online from 0 to 134 Hz and digitized at 512 Hz.

**2.3.2. ALS functional rating scale revised (ALSFRS-R)**  
ALSFRS-R data were recorded at the Irish National ALS specialty clinic for each participant. Scores were included in analysis if collected within  $\pm 90$  d of EEG.

**2.3.3. Cognitive and behavioural tests**  
ECAS and Delis–Kaplan Executive Function System Colour-Word Interference Test (CWIT) [12] data were included if collected within  $\pm 90$  d of EEG.

**2.3.4. Disease duration**  
Disease duration was quantified as the number of months between patient-reported date of first symptom onset and date of EEG recording.

## 2.4. Data analysis

### 2.4.1. EEG signal pre-processing

Signal pre-processing procedures are identical to those described in detail in our previous SART study [3]. This includes application of a high pass 0.3 Hz dual-pass 5th order Butterworth filter and a low pass 35 Hz dual-pass 117th order equiripple finite impulse response filter, manual removal of non-stereotyped artefacts, epoching of data from 200 ms pre-stimulus to 900 ms post-stimulus, independent component analysis and removal of noise-specific components, mean baseline amplitude subtraction and common average referencing.

### 2.4.2. Time-frequency analysis

Each trial epoch consisted of 563 data points (i.e. 1100 ms of data recorded at 512 Hz) per channel. A random subset of Go trials followed by correct responses (a click) were chosen to match the number of NoGo trials followed by correct response (no click) for further analysis. Complex Morlet wavelets were chosen for time-frequency analysis as they have a sinusoidal basis with symmetric Gaussian envelopes and their width can be adjusted for the desired number of oscillations. To facilitate the application of the complex Morlet wavelet transform, for each channel, each epoch was data-padded with 563 repetitions of the first data point at the start, and 563 repetitions of the last data point at the end. As data had been low-pass filtered at 35 Hz during pre-processing for a previous time-domain analysis [3], calculation of wavelet moduli was performed for a range of 1–35 Hz. The complex coefficients of transform ( $W$ ) were subsequently re-epoched by removing the padded data. Mean inter-trial phase variance (ITV) across epochs ( $e$ ) was calculated per time point ( $t$ ) and frequency ( $f$ ) to provide a measure specifically of non-phase locked

(i.e. not captured by our previous event related potential (ERP) analysis) oscillatory activity [13] as:

$$\text{ITV}(f, t) = \frac{\sum_1^{N_e} |W_{f,t,e} - \bar{W}_{f,t}|^2}{N_e - 1}$$

where  $\bar{W}$  denotes mean value of  $W$  across all epochs and  $N_e$  denotes the total number of epochs. ITV were calculated for the Fz, Cz and Pz channels. These electrodes were chosen due to their proximity to executive and motor function associated cortical domains. Baseline values for each frequency were calculated as mean ITV across the  $-200$  ms to 0 ms window. Event related spectral perturbation (ERSP) values for each time and frequency was then calculated as:

$$\text{ERSP}(f, t) = 100 \times \frac{\text{ITV}_{f,t} - \overline{\text{ITV}}_{f, \text{baseline}}}{\overline{\text{ITV}}_{f, \text{baseline}}}$$

for  $t = 1-900$  ms. Time–frequency analysis was performed separately for Go and NoGo trials. Analysis of the difference between NoGo and Go trials was performed by subtraction thereafter.

## 2.5. Statistics

### 2.5.1. Oscillation analysis

To check for gender effect, analysis of variance (ANOVA) were performed separately for each Go and NoGo region of interest (ROI), using electrode, gender and group (patient or control) as independent variables, to measure the significance of gender and group effects on ROI power (dependent variable). A false discovery rate (FDR) of 5% was applied to  $p$ -value families across ANOVA, implemented using the Benjamini and Hochberg method [14], to account for multiple comparisons. Tukey's post hoc analysis was also implemented for each ANOVA to identify individual electrodes which significantly differed between groups. For time–frequency plane statistical analysis of each electrode, data were down sampled to 34 Hz (i.e. 1/15 data points). To identify significant (i.e. significantly different from zero) ERSP in controls, Wilcoxon's (paired) Sign-Rank  $W$ -statistic, transformed to  $Z$  scores, was used as a test statistic. To identify significant differences between control and patient ERSP, area under the receiver operating characteristic curve (AUROC) [15] was used as a test statistic. In both cases, a 5% false discovery rate [16] was used as a frequentist method for determining significant power differences amidst these high-dimensional data. Empirical Bayesian inference [17] provided Bayesian posterior probabilities, as well as the achieved statistical power and AUROC.

### 2.5.2. Effect sizes and correlations

Specific time-frequency areas were defined as ROIs based on significant oscillation patterns identified in the control group (without inclusion of, or comparison to the patient group) as ERD/ERS elicited by the

SART in controls has not previously been reported. These ROIs were defined in order to determine effect size of differences between patients and controls and investigate clinical correlations in patients, based on mean ERSP values (without down sampling) within these ROIs. Cohen's  $d$  was used as an index of effect size, where  $d > 0.8$  indicates a large effect size [18].

Spearman's non-parametric rank correlation was used to investigate relationships between mean ERSP values in the ROIs and neuropsychological and motor test scores. Partial correlation was implemented for investigating relationships to CWIT inhibition and inhibition-switching subscores, to control for the effects of decline in speech function (quantified by the ALSFRS-R speech score) at time of CWIT testing. Multiple comparisons were accounted for using a 5% FDR, implemented using the Benjamini and Hochberg method [14].

### 2.5.3. Demographics

Mann-Whitney  $U$ -testing and chi-squared proportion testing were used to compare age and gender respectively between groups, with significant differences determined where  $q = 0.05$  (corresponding to the  $p < 0.05$  for individual testing).

### 2.5.4. Selected measures for reporting the main findings

For reporting the results of statistical analyses, we use the  $p$ -values as a first stage screening for significant findings. We then report the effect sizes (e.g. Cohen's  $d$ ), which reflect how strong the changes in the brain are (as a patho-physiological phenomenon). Finally, to show how much discrimination between controls and ALS patients is afforded by each measure, we use the AUROC as a measure commonly used in medical statistics [19].

## 3. Results

### 3.1. Participant demographics

The same ALS patient and control datasets were employed as in our previous time-domain study [3], with one additional patient dataset analysed here. Therefore, a total of 24 ALS patients (3 female, age median [interquartile range]: 69 [59–72] years) and 33 controls (17 female, age median [interquartile range]: 64 [57–69] years) were included in this analysis. Groups were age-matched but not gender matched, as previous comparison of male and female controls for parameters of interest revealed no gender-related differences [3]. ANOVA found significant group effects for some ROI (described below) but no significant gender effects. The ALS cohort included three patients with a *C9orf72* gene expansion, with the remainder of patients not carrying or not tested for this pathogenic expansion. Site of onset of disease symptoms was spinal in eighteen patients, bulbar in five patients, and thoracic in one patient. Disease duration and time since diagnosis

median [interquartile range] of patients was 17.65 [10.15–23.92] months and 4.42 [2.98–9.71] respectively. ALSFRS-R, ECAS and CWIT scores collected within 90 d of EEG were available for 18, 15 and 9 patients respectively. Survival data were not analysed as only two patients were deceased at time of analysis.

### 3.2. Task performance

Mean response time was 364 ms in controls and 375 ms in patients. Mean  $\pm$  standard deviation trial accuracy (Go and NoGo) was  $99.67 \pm 0.48$  and  $78.31 \pm 12.73\%$  in controls and  $98.96 \pm 1.60$  and  $77.90 \pm 12.53\%$  in patients respectively. Control and patient accuracy and response time measures were not significantly different. Patients had significantly ( $p = 0.0042$ ) greater anticipation errors than controls (patient mean  $\pm$  standard deviation:  $0.084 \pm 0.14\%$ , control:  $0.01 \pm 0.03\%$ ).

### 3.3. Event related spectral perturbations

#### 3.3.1. Go trials

During Go trials, theta-band (4–7 Hz) ERS (i.e. increase in power relative to baseline), alpha-band (8–12 Hz) ERD (i.e. decrease in power relative to baseline) and beta-band (13–30 Hz) ERD were present across the frontoparietal axis. Beta ERD was followed by ERS, predominantly in Fz and Cz. These ERSP patterns in healthy controls, as informed by sign rank statistical analysis, were examined further as ROIs for comparing ALS patients against controls and when performing correlation analyses in 100–700 ms, 250–600 ms, 200–500 ms and 650–850 ms post-stimulus time windows respectively (figure 1(A)).

#### 3.3.2. NoGo trials

Theta-band ERS, alpha-band ERD and beta-band ERD were also present across the frontoparietal axis during NoGo trials. A significant synchronization was also present in upper beta band (20–30 Hz). These ERSP were examined further as ROIs (when comparing ALS patients and controls and when performing correlation analyses) in 100–700 ms, 350–700 ms, 200–600 ms and 750–850 ms post-stimulus time windows respectively (figure 1(B)).

#### 3.3.3. The difference between NoGo and Go trials

NoGo trials differed from Go trials by greater theta band ERS over Fz and Cz, greater alpha ERD (i.e. greater event-related reduction in oscillatory power in NoGo trials relative to Go trials) and reduced slow beta (13–22 Hz) ERS (i.e. less event-related increase in oscillatory power in NoGo trials relative to Go trials) in all three electrodes. These ERSP differences in the control group were in the 150–450 ms, 500–900 ms and 600–850 ms post-stimulus time windows respectively (figure 2), and were defined as additional ROIs (for comparing ALS patients against controls and when performing correlation analyses).

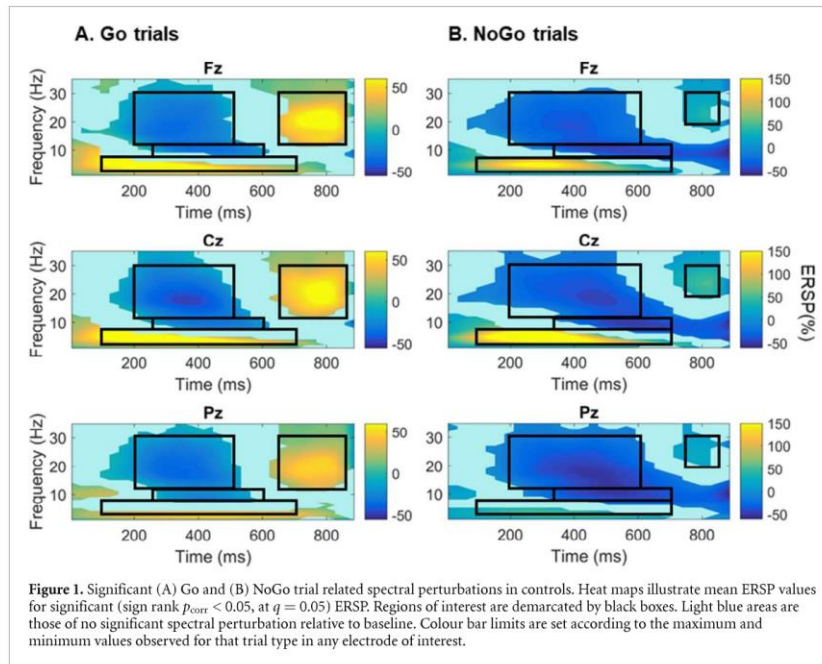


**Figure 1.** Significant (A) Go and (B) NoGo trial related spectral perturbations in controls. Heat maps illustrate mean ERSP values for significant (sign rank  $p_{\text{corr}} < 0.05$ , at  $q = 0.05$ ) ERSP. Regions of interest are demarcated by black boxes. Light blue areas are those of no significant spectral perturbation relative to baseline. Colour bar limits are set according to the maximum and minimum values observed for that trial type in any electrode of interest.

### 3.4. ERSP in ALS compared to controls

Analysis of the entire time-frequency plane identified significantly reduced beta-band ERD in Fz and Pz during Go and NoGo trials in ALS compared to controls (AUROC values illustrated in figure 3, effect sizes and AUROC values listed in table 1). These findings are in keeping with the findings of ANOVA, which identified significant group effect (across electrodes) on beta-band power in this window ( $p$  values listed in table 1). This ANOVA also identified significant reduction in Go trial beta ERS (650–850 ms,  $p = 7.72 \times 10^{-4}$ ) across electrodes, which was predominantly accounted for by Fz, the only individual electrode to show significant difference between groups at post hoc testing (Tukey's  $p = 0.048$ ). No significant differences between patients and controls were found for the difference between NoGo and Go trial ERSP.

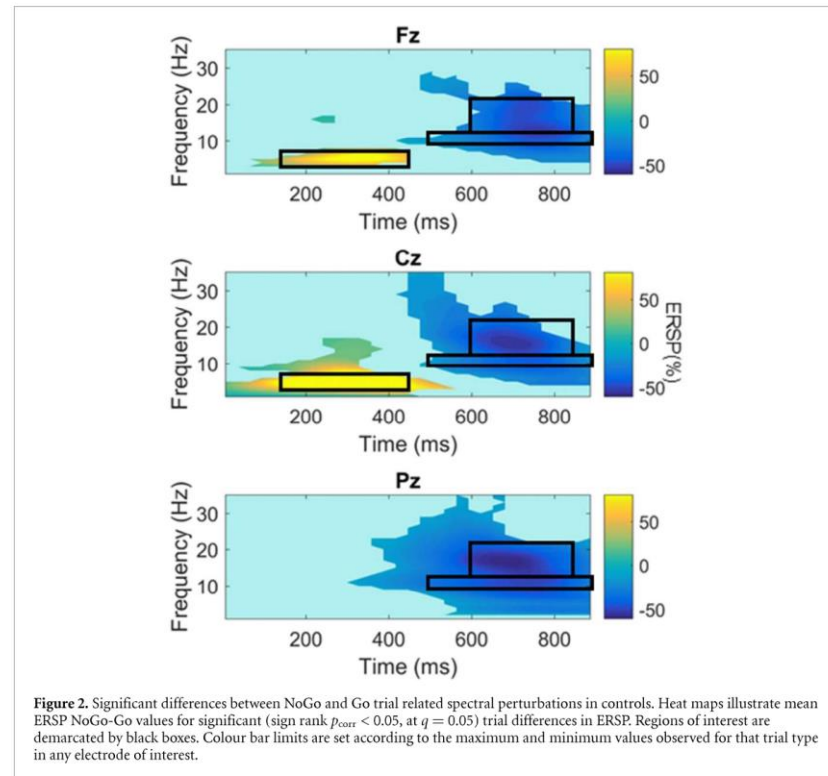
### 3.5. Correlation with task performance

Correlations between late beta-band ERS in Go (650–850 ms post stimulus) and NoGo (750–850 ms post stimulus) trials and task performance measures are summarised in table 2. Significant negative correlation was identified between response accuracy and late beta band ERS in Pz during Go trials (i.e. poorer accuracy with greater beta ERS) for controls but not patients.

Significant negative correlations between response time and beta-band late ERS in patients and the overall group (i.e. faster response time with greater beta ERS) across the electrodes of interest were present in controls alone as a trend but were not significant following multiple comparison correction. Theta band ERS in Pz during Go trials showed significant negative correlation with response time in the total group ( $p = 0.010$ ,  $\rho = -0.34$ ) with similar trends when patients and controls were considered separately (patients:  $p = 0.055$ ,  $\rho = -0.39$ , controls:  $p = 0.052$ ,  $\rho = -0.34$ ). Patient, but not control, response times also negatively correlated with Cz alpha band ERSP in NoGo trials (i.e. greater alpha ERD was associated slower response times,  $p = 0.013$ ,  $\rho = -0.5$ ). Patient ECAS ALS-specific score was correlated with beta ERS (750–850 ms post stimulus,  $p = 0.0024$ ,  $\rho = 0.72$ ) over Cz during NoGo trials (i.e. greater executive performance with greater beta ERS, figure 4). No significant correlations were identified for other ROIs, disease duration or ALSFRS-R or CWIT scores.

## 4. Discussion

We have characterized SART-evoked cortical oscillation changes at sensor level along the frontoparietal axis and have correlated these with task performance. These oscillations relate to the speed and accuracy



with which a participant performs the task, and are disrupted in ALS patients.

#### 4.1. SART related spectral perturbations in controls

Beginning at approximately 150 ms post-stimulus, alpha and beta band ERD were observed during both Go and NoGo trials across the frontoparietal axis, in addition to theta band ERS over the frontal lobe (in Fz and Cz), which was greater during correct response withholding. Beta ERD was followed by ERS, which was significantly reduced during correct response withholding.

#### 4.2. Beta oscillations (13–30 Hz)

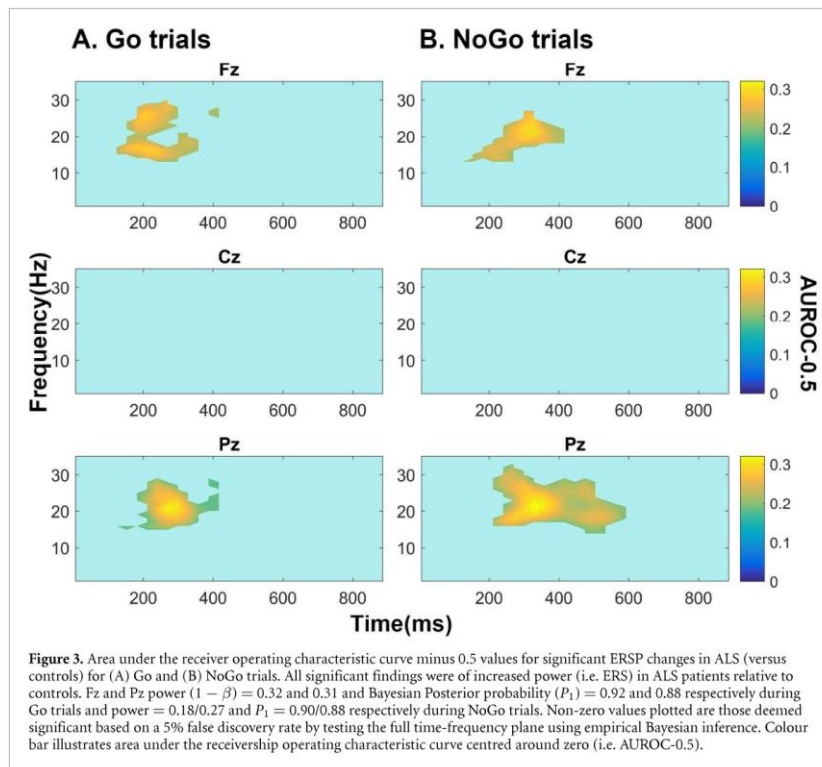
Motor tasks evoke well-characterized movement-related beta desynchronization ( $\beta$ MRD), beginning in the second before movement onset and peaking during movement performance, followed by movement-related synchronization ( $\beta$ MRS) during movement termination [20, 21].  $\beta$ MRD is associated with motor planning and execution, while  $\beta$ MRS reflects inhibition of the motor networks to terminate the motor program [22]. Like SART-related beta

ERS observed here,  $\beta$ MRS is maximal in Cz and larger in Go trials than NoGo trials, and reaches significance at approximately 800 ms post-stimulus [22]. Similar to the SART, a Go/NoGo task not designed to test sustained attention is also found to elicit beta ERD/ERS during Go and NoGo trials, with Go trial ERS inversely correlating with response time [23]. These similarities indicate that the SART captures this measure of motor cortical activation and inactivation in addition to those of attention and response control.

#### 4.3. Alpha oscillations (8–12 Hz)

Alpha ERD/ERS did not correlate with control task performance in this study, such that the ability to determine the role of this ERD in SART performance is limited. Alpha ERD is associated with thalamo-cortical network excitation [24] and release of the task-engaged cortical regions from inhibition [25]. This measure has been captured during a number of other attention and memory tasks, and is considered to reflect retrieval of task-relevant information from one's 'knowledge system' [25, 26].

Peri-movement alpha ERD is also observed in Go/NoGo tasks not designed to test attention or



memory, and represents a general disinhibition of the motor networks to facilitate movement. In keeping with our observations, this movement-related alpha band ERD ( $\alpha$ MRD) generally persists for longer than  $\beta$ MRD and does not typically rebound to synchronization [27]. However,  $\alpha$ MRD is not found to be greater during NoGo trials of these tasks [23, 27, 28], as we observed here, while cognitive alpha ERD increases with task complexity. Therefore, this alpha change may not be a purely motor cortical phenomenon and requires further characterization by larger, source level studies to differentiate potential cognitive and motor underpinnings.

#### 4.4. Theta oscillations (4–7 Hz)

Theta band ERS showed significant correlation with SART response time in the overall group, with similar trends within the individual groups that were probably underpowered to detect this effect in each single group. An  $n$ -back task study, which also identified frontocentral-predominant theta ERS peaking approximately 250 ms after stimulus delivery, demonstrated association of this ERS with attention allocation, rather than working memory [29]. Further, frontal midline theta, a focal increase in theta

power induced by numerous cognitive tasks and localized to the dorsal anterior cingulate and medial prefrontal cortex [30], reflects attentional processing [31]. This is consistent with the presence of theta ERS for all trial types, with greater magnitude during NoGo trials.

#### 4.5. Increasing SART specificity and understanding the speed-accuracy trade-off

Utility of the SART as a test of sustained attention has been criticized due to the extent of performance variation within healthy populations, which has been attributed to the speed-accuracy trade-off [2]. Task performance requires sufficient working memory, attention, response inhibition and motor control, among other functions. Therefore, differences in performance measures such as response time and accuracy may reflect normal or abnormal differences in an array of cortical functions. However, this lack of specificity is advantageous when EEG is recorded simultaneously, as a battery of measures which individually interrogate each of these functions, differentiated by their spatial, temporal and frequency characteristics, can be measured from a single paradigm.



**Table 1.** Summary of statistics for significant changes in SART-associated ERD/ERS in ALS patients compared to controls. ANOVA group effect  $p$  values are the effect of group on this region of interest for this trial type, across electrodes. Difference between ALS and controls pertains to ANOVA and individual electrode analyses. Cohen's  $d$  quantifies effect size ( $>0.8$  denotes large effect size,  $>1$  denotes very large effect size), area under the receiver operating characteristic curve (AUROC) quantifies discrimination between ALS and controls by this measure ( $>0.8$  denotes very good discrimination).

Frequency range (Hz)	Trial	Time range (ms post stimulus)	Difference between ALS and controls	ANOVA group effect $p$	Electrode	AUROC	Cohen's $d$
13–30	Go	200–500	Less ERD in ALS	$5.18 \times 10^{-4}$	Fz	$>0.8$	0.97
					Pz	$>0.82$	0.92
	NoGo	200–600	Less ERD in ALS	$9.71 \times 10^{-4}$	Fz	$>0.8$	0.89
					Pz	$>0.82$	1.12

**Table 2.** Significant correlations between beta-band (13–30 Hz) ERS (%) and SART performance measures. Negative rho values reflect less ERS with larger behavioural measure value (longer reaction time or greater accuracy). Go trials time window—650–850 ms post stimulus, NoGo trials time window—750–850 ms post stimulus. Uncorrected  $p$ -values ( $p$ ) remained significant when corrected at FDR  $q = 0.05$ .

EEG trial	Channel	Behavioural measure	Participant	$p$	rho	
Go	Fz	Response time	All	$1.18 \times 10^{-4}$	-0.49	
			Patient	$1.12 \times 10^{-4}$	-0.72	
	Cz		All	$9.22 \times 10^{-6}$	-0.56	
			Patient	$6.19 \times 10^{-5}$	-0.74	
	Pz		All	$9.30 \times 10^{-4}$	-0.43	
			Patient	$9.97 \times 10^{-5}$	-0.72	
			Total % accuracy	Control	0.011	-0.44
			NoGo % accuracy		0.008	-0.45
NoGo	Cz	Response time	All	0.0036	-0.38	
			Patient	0.0052	-0.56	

We have previously demonstrated how time-domain analysis of SART-EEG provides individual measures of response control and attention, facilitating identification of specific cognitive and motor functions affected in ALS [3]. Here we have extracted non-phase locked cortical oscillatory changes across time and frequency domains, capturing additional measures of specific network activity and communication that were lost through averaging in our previous analysis and which are not frequency-domain reflections of event related potentials. We have demonstrated that individuals who prioritize speed over accuracy display greater beta ERS during Go trials, potentially reflecting greater post-movement motor cortical inhibition in these individuals. While the causative relationship between this measure of motor cortical deactivation and task approach warrants further investigation, the specificity of this correlation to this ROI within the time-frequency plane facilitates separation of this variation in speed-accuracy trade-off observed in healthy cohorts [2] from other, pathological, changes in cortical networking captured at other times and frequencies, such as those we have identified in ALS.

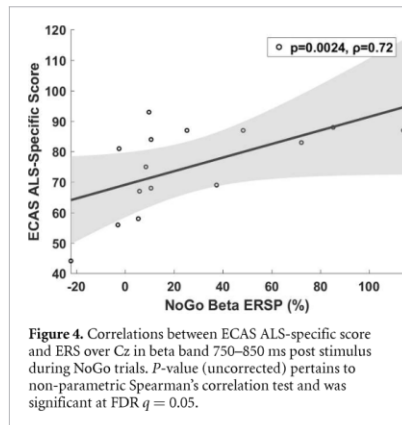
#### 4.6. Dysfunctional network communication in ALS during the SART

ALS patients showed significant reduction in frontal and parietal beta ERD.  $\beta$ MRD elicited by motor preparation-specific paradigms [32] has previously been shown to be reduced in ALS. This has been

proposed to reflect upper motor neurone degeneration, although motor function of the upper extremities does not correlate with  $\beta$ MRD [33, 34]. SART-elicited beta ERD similarly did not correlate with task performance, in alignment with the lack of difference in task response time or accuracy between patients and controls. The lack of significant change in Cz beta ERD in ALS patients observed here also indicates measurement of broader motor network dysfunction beyond the precentral gyrus, such as in the premotor, supplementary motor and posterior parietal cortices. Therefore, while the similarity of this ERD to  $\beta$ MRD suggests that they are of similar (or the same) motor physiological basis, source localisation is required to clarify the specific generators of these oscillations.

Regardless of its physiological origin, the large effect size (Cohen's  $d = 1.12$ ) and good discrimination (AUROC = 0.82) of ALS patients from controls by beta ERD highlights the need for further exploration of this promising measure as a biomarker of ALS and ALS subphenotypes. Further, as the symptoms of neurodegenerative diseases such as ALS can limit the duration of data collection sessions, the ability of SART to simultaneously elicit a number of distinct measures of motor, motor preparatory and executive function could maximise the efficiency with which cognitive and motor networks are interrogated in both research and clinical settings.

As a group, ALS patients also showed reduced Go trial beta ERS, predominantly over the prefrontal cortex. While the correlation between Go trial beta



ERS and poorer response accuracy observed in controls was absent, strong correlations were observed between NoGo trial beta ERS over the motor cortex and executive performance in patients. This correlation, alongside existing literature (described above), may reflect ALS patients with sufficient executive function exerting increased prefrontal control over motor cortex activation to sustain task performance. Patient (but not control) response times were also longer in those with more central alpha ERD in NoGo trials. Together, these findings indicate that sustained performance in patients is achieved through balancing pathological dysfunction with compensatory engagement in cognitive and motor networks. These findings exemplify the utility of EEG in capturing cortical network (dys)function in disease with greater sensitivity and source specificity than task performance measures, which do not emerge until cognitive reserve and alternative neural networks can no longer compensate [35]. However, larger dataset collection is now required to perform comparisons of these measures between clinical, genetic and disease stage ALS subcohorts and facilitate further interrogation of the relationship between this cortical pathophysiology and cognitive and motor symptom severity with higher statistical power. Further, the pathological or compensatory roles of ERS in ALS require further elucidation through longitudinal and source level analyses.

#### 4.7. Limitations

This analysis focussed on three electrodes of interest across the frontoparietal axis in order to simultaneously investigate previously unexamined SART-associated cortical oscillations and perform preliminary screening for potential ALS biomarkers. Spatial resolution of these findings is poor. Therefore, while they capture the activity of important generators of SART response across primary motor, pre-motor and

supplementary motor areas (in the motor domain) and prefrontal and parietal generators (in the cognitive domain), our ability to attribute different ERS to specific cortical regions is limited. Source-localised analysis will be needed in a future study to elucidate the sources of abnormalities in cognitive oscillations across the cortex, informed by a dense electrode montage, and potentially increase the discriminative ability of these measures in detecting ALS. Expansion of the datasets shall facilitate further interrogation of the relationships between these measures of cortical pathophysiology and disease stage, rate of progression and symptom severity.

## 5. Conclusion

Our data demonstrate that time-frequency analysis of EEG during SART, in addition to event related potential analysis, provide measures of cognitive and motor network function that may not be captured by behavioural performance or by other neuropsychological testing. These measures help to dissect the summated complex interactions within and between the cortical networks which regulate task performance, including speed-accuracy trade-off strategy and compensation for pathology. Moreover, we demonstrate that cortical oscillation abnormalities not captured by task performance measures have large effect sizes and show good discrimination between ALS patients and controls. Such discrete measurements may provide informative, sensitive biomarkers of disease-related network dysfunction and warrant further investigation.

## Acknowledgments

The authors report no conflicts of interest which would bias the conduct of this study. This study was funded by the Irish Research Council [IRC, Grant Numbers: GOIPG/2017/1014, GOIPD/2015/213], the Health Research Board [HRB, Grant Numbers: HRA-POR-2013-246, MRCG-2018-02], Science Foundation Ireland [SFI, Grant Number: 16/ERC-D/3854] and Research Motor Neurone [Grant Number: MRCG-2018-02]. Additional psychology data for participants of the study were collected with support of the Motor Neurone Disease Association [MNDA, Grant Number: Hardiman/Oct15/879-792]. We thank the Wellcome-HRB Clinical Research Facility at St. James's Hospital in providing a dedicated environment for the conduct of high-quality clinical research. Finally, we would like to thank all the patients, participants and their families who volunteered to take part in this study.

## Ethical statement

This study was ethically approved by St. James's Hospital (REC reference: 2017-02 Chairman's Action 18).

All participants gave written, informed consent in advance of participation. The study was performed in accordance with the Declaration of Helsinki.

### Author contributions

R M, B N, O H, N P, R R—Conception and design of the study. R M, S D, M P-G, E C, A F, T B, M H, O K—Acquisition of data. R M—Analysis of data. R M, B N, O H—Drafting of manuscript or figures.

### ORCID iDs

Roisin McMackin <https://orcid.org/0000-0002-9223-2241>

Emmet Costello <https://orcid.org/0000-0001-8620-9531>

Richard Reilly <https://orcid.org/0000-0001-8578-1245>

Bahman Nasserolelami <https://orcid.org/0000-0002-2227-2176>

### References

- Robertson I H, Manly T, Andrade J, Baddeley B T and Yiend J 1997 Oops!: performance correlates of everyday attentional failures in traumatic brain injured and normal subjects *Neuropsychologia* **35** 747–58
- Dang J S, Figueroa I J and Helton W S 2018 You are measuring the decision to be fast, not inattention: the sustained attention to response task does not measure sustained attention *Exp. Brain Res.* **236** 2255–62
- McMackin R, Dukic S, Costello E, Pinto-Grau M, Fasano A, Buxo T, Heverin M, Reilly R, Muthuraman M, Pender N, Hardiman O and Nasserolelami B 2020 Localization of brain networks engaged by the sustained attention to response task provides quantitative markers of executive impairment in amyotrophic lateral sclerosis *Cereb. Cortex* **30** 4834–46
- Hummel F C and Gerloff C 2006 Interregional long-range and short-range synchrony: a basis for complex sensorimotor processing *Progress in Brain Research Event-Related Dynamics of Brain Oscillations* vol 159 ed C Neuper and W Klimesch (Amsterdam: Elsevier) pp 223–36
- Donner T H and Siegel M 2011 A framework for local cortical oscillation patterns *Trends Cogn. Sci.* **15** 191–9
- Pfurtscheller G and Lopes da Silva F H 1999 Event-related EEG/MEG synchronization and desynchronization: basic principles *Clin. Neurophysiol.* **110** 1842–57
- Defebvre L, Bourriez J-L, Dujardin K, Derambure P, Destée A and Guieu J-D 1994 Spatiotemporal study of Bereitschaftspotential and event-related desynchronization during voluntary movement in Parkinson's disease *Brain Topography* **6** 237–44
- Dushanova J, Philipova D and Nikolova G 2009 Event-related desynchronization/synchronization during discrimination task conditions in patients with Parkinson's disease *Cell. Mol. Neurobiol.* **29** 971–80
- Babiloni C et al 2000 Movement-related electroencephalographic reactivity in Alzheimer disease *NeuroImage* **12** 139–46
- Missonnier P, Gold G, Herrmann F R, Fazio-Costa L, Michel J-P, Deiber M-P, Michon A and Giannakopoulos P 2006 Decreased theta event-related synchronization during working memory activation is associated with progressive mild cognitive impairment *Dement. Geriatr. Cogn. Disord.* **22** 250–9
- Fraga F J, Ferreira L A, Falk T H, Johns E and Phillips N D 2017 Event-related synchronization responses to N-back memory tasks discriminate between healthy ageing, mild cognitive impairment, and mild Alzheimer's disease 2017 *IEEE Int. Conf. on Acoustics, Speech and Signal Processing (ICASSP)* pp 964–8
- Delis D C, Kaplan E and Kramer J H 2001 *Delis-Kaplan Executive Function System (D-KEFS)* (San Antonio, TX: Psychological Corporation)
- Kalcher J and Pfurtscheller G 1995 Discrimination between phase-locked and non-phase-locked event-related EEG activity *Electroencephalogr. Clin. Neurophysiol.* **94** 381–4
- Benjamini Y and Hochberg Y 1995 Controlling the false discovery rate: a practical and powerful approach to multiple testing *J. R. Stat. Soc.* **57** 289–300
- Hajian-Tilaki K 2013 Receiver operating characteristic (ROC) curve analysis for medical diagnostic test evaluation *Caspian J. Intern. Med.* **4** 627–35
- Benjamini Y 2010 Discovering the false discovery rate *J. R. Stat. Soc.* **72** 405–16
- Efron B 2009 Empirical Bayes estimates for large-scale prediction problems *J. Am. Stat. Assoc.* **104** 1015–28
- Cohen J 1988 *Statistical Power Analysis for the Behavioral Sciences* (New York, NY: Routledge)
- Zhou X-H, McClish D K and Obuchowski N A 2009 *Statistical Methods in Diagnostic Medicine* vol 569 (New York: Wiley)
- Vinding M C, Tsitsi P, Piitulainen H, Waldthaler J, Jousmaki V, Ingvar M, Svenningsson P and Lundqvist D 2019 Attenuated beta rebound to proprioceptive afferent feedback in Parkinson's disease *Sci. Rep.* **9** 1–11
- Alegre M, Gurtubay I G, Labarga A, Iriarte J, Valencia M and Artieda J 2004 Frontal and central oscillatory changes related to different aspects of the motor process: a study in go/no-go paradigms *Exp. Brain Res.* **159** 14–22
- Solis-Escalante T, Müller-Putz G R, Pfurtscheller G and Neuper C 2012 Cue-induced beta rebound during withholding of overt and covert foot movement *Clin. Neurophysiol.* **123** 1182–90
- Wu H-M, Hsiao F-J, Chen R-S, Shan D-E, Hsu W-Y, Chiang M-C and Lin Y-Y 2019 Attenuated NoGo-related beta desynchronization and synchronization in Parkinson's disease revealed by magnetoencephalographic recording *Sci. Rep.* **9** 7235
- Pfurtscheller G 2003 Induced oscillations in the alpha band: functional meaning *Epilepsia* **44** 2–8
- Klimesch W 2012 Alpha-band oscillations, attention, and controlled access to stored information *Trends Cogn. Sci.* **16** 606–17
- Klimesch W 1999 EEG alpha and theta oscillations reflect cognitive and memory performance: a review and analysis *Brain Res. Rev.* **29** 169–95
- Schmiedt-Fehr C, Mathes B, Kedilaya S, Krauss J and Basar-Eroglu C 2016 Aging differentially affects alpha and beta sensorimotor rhythms in a go/no-go task *Clin. Neurophysiol.* **127** 3234–42
- Funderud I, Lindgren M, Lovstad M, Endestad T, Voytek B, Knight R T and Solbakk A-K 2012 Differential Go/NoGo activity in both contingent negative variation and spectral power *PLoS One* **7** e48504
- Missonnier P, Deiber M-P, Gold G, Millet P, Gex-Fabry Pun M, Fazio-Costa L, Giannakopoulos P and Ibáñez V 2006 Frontal theta event-related synchronization: comparison of directed attention and working memory load effects *J. Neural Transm.* **113** 1477–86
- Ishii R, Canuet L, Aoki Y, Ikeda S, Hata M, Iwase M and Takeda M 2013 Non-parametric permutation thresholding for adaptive nonlinear beamformer analysis on MEG revealed oscillatory neuronal dynamics in human brain 2013 *35th Annual Int. Conf. IEEE Engineering in Medicine and Biology Society (EMBC)* pp 4807–10
- Ishii R et al 2014 Frontal midline theta rhythm and gamma power changes during focused attention on mental

- calculation: an MEG beamformer analysis *Front. Hum. Neurosci.* **8** 406
- [32] Neuper C and Pfurtscheller G 2001 Event-related dynamics of cortical rhythms: frequency-specific features and functional correlates *Int. J. Psychophysiol.* **43** 41–58
- [33] Kasahara T, Terasaki K, Ogawa Y, Ushiba J, Aramaki H and Masakado Y 2012 The correlation between motor impairments and event-related desynchronization during motor imagery in ALS patients *BMC Neurosci.* **13** 66
- [34] Bizovičar N, Dreo J, Koritnik B and Zidar J 2014 Decreased movement-related beta desynchronization and impaired post-movement beta rebound in amyotrophic lateral sclerosis *Clin. Neurophysiol.* **125** 1689–99
- [35] Anthony M and Lin F 2018 A systematic review for functional neuroimaging studies of cognitive reserve across the cognitive aging spectrum *Arch. Clin. Neuropsych.* **33** 937–48

## **10.5. Additional publications**

1. Calvert GHM, **McMackin R**, Carson RG. Probing interhemispheric dorsal premotor-primary motor cortex interactions with threshold hunting transcranial magnetic stimulation. *Clinical Neurophysiology* 2020;131(11):2551–2560.
2. Dukic S, **McMackin R**, Buxo T, et al. Patterned functional network disruption in amyotrophic lateral sclerosis. *Human brain mapping* 2019;40(16):4827–4842.